LEABHARLANN CHOLÁISTE NA TRÍONÓIDE, BAILE ÁTHA CLIATH | TRINITY COLLEGE LIBRARY DUBLIN
Ollscoil Átha Cliath | The University of Dublin

Terms and Conditions of Use of Digitised Theses from Trinity College Library Dublin

Copyright statement

All material supplied by Trinity College Library is protected by copyright (under the Copyright and Related Rights Act, 2000 as amended) and other relevant Intellectual Property Rights. By accessing and using a Digitised Thesis from Trinity College Library you acknowledge that all Intellectual Property Rights in any Works supplied are the sole and exclusive property of the copyright and/or other IPR holder. Specific copyright holders may not be explicitly identified. Use of materials from other sources within a thesis should not be construed as a claim over them.

A non-exclusive, non-transferable licence is hereby granted to those using or reproducing, in whole or in part, the material for valid purposes, providing the copyright owners are acknowledged using the normal conventions. Where specific permission to use material is required, this is identified and such permission must be sought from the copyright holder or agency cited.

Liability statement

By using a Digitised Thesis, I accept that Trinity College Dublin bears no legal responsibility for the accuracy, legality or comprehensiveness of materials contained within the thesis, and that Trinity College Dublin accepts no liability for indirect, consequential, or incidental, damages or losses arising from use of the thesis for whatever reason. Information located in a thesis may be subject to specific use constraints, details of which may not be explicitly described. It is the responsibility of potential and actual users to be aware of such constraints and to abide by them. By making use of material from a digitised thesis, you accept these copyright and disclaimer provisions. Where it is brought to the attention of Trinity College Library that there may be a breach of copyright or other restraint, it is the policy to withdraw or take down access to a thesis while the issue is being resolved.

Access Agreement

By using a Digitised Thesis from Trinity College Library you are bound by the following Terms & Conditions. Please read them carefully.

I have read and I understand the following statement: All material supplied via a Digitised Thesis from Trinity College Library is protected by copyright and other intellectual property rights, and duplication or sale of all or part of any of a thesis is not permitted, except that material may be duplicated by you for your research use or for educational purposes in electronic or print form providing the copyright owners are acknowledged using the normal conventions. You must obtain permission for any other use. Electronic or print copies may not be offered, whether for sale or otherwise to anyone. This copy has been supplied on the understanding that it is copyright material and that no quotation from the thesis may be published without proper acknowledgement.

TRINITY COLLEGE
21 NOV 2007
LIBRARY DUBLIN
THESIS
8279

Potential Applications of Halloysite for Improved Topical Drug Delivery

Presented by

Catherine Ryan, B.Sc. (Pharm.), M.P.S.I.

under the direction and supervision of

Professor Patrick B. Deasy, B.Sc. (Pharm.), M.A., Ph.D., F.T.C.D., F.P.S.I.

for a

DOCTOR OF PHILOSOPHY DEGREE

at the

University of Dublin, Trinity College

Research for which was performed in

Pharmaceutics and Pharmaceutical Technology,

THE SCHOOL OF PHARMACY AND PHARMACEUTICAL SCIENCES

December 2006

This thesis has not been submitted as an exercise for a degree at any other university. It is entirely the work of the undersigned author, except where duly acknowledged. The author agrees that the Library may lend or copy this thesis upon request.

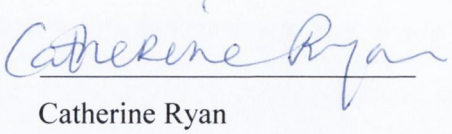

Catherine Ryan

To my parents, sisters and brother

SUMMARY

The aim of this thesis was to evaluate the potential application of halloysite, an aluminosilicate clay material, for use in topical and transdermal drug delivery. Halloysite is a tubular material, the hollow lumen has been used to control the release of active materials for a range of applications. Price *et al.* (2001) investigated the release of tetracycline HCl, for use as an anti-fouling agent in marine applications. Salter (2003) investigated the capacity of the tubules to produce sustained release of pesticides. Halloysite is chemically similar to kaolin, which has an established role in pharmaceutical and topical preparations (Handbook of Pharmaceutical Excipients, 2005). Hence it was considered that halloysite might have applications in the area of topical and transdermal drug delivery.

Two grades of halloysite were initially investigated, Halloysite G from New Zealand and Balekisir Halloysite from Turkey. Halloysite G was chosen as it was available in an extracted form. The Balekisir grade was chosen because it had a pink, flesh-like colour. It was thought this would be cosmetically more acceptable due to its similarity to natural skin tone. However its tubules were shorter than those of the halloysite G grade, therefore the halloysite G grade was chosen for further study because the longer tubule offered a potentially greater entrapment volume. The sample was modified using a number of chemical processes in order to examine the factors affecting the composition and structure of the clay. It was hoped also to purify the clay and enhance qualities that would be desirable in topical and transdermal drug delivery such as the sorptive capacity. The modified grades were examined using a number of techniques including SEM, XRD, ICP-MS, surface area and skeletal density analysis. The Balekisir halloysite had a greater quantity of iron, which most likely accounted for the pink colour. The deferration and acid washing procedures removed a large quantity of iron, a small portion remained which was intrinsic to the structure and had substituted for aluminium in the octahedral sheet. The deferration process caused the samples to more closely align due to the removal of the surface iron oxides. The most significant alteration of the acid washed sample was the increase in surface area. This occurred due to the dissolution of aluminium from the edge, which resulted in tubule splitting.

An organo-halloysite grade was also produced by adsorption of a surfactant to the tubule surface. Preliminary investigations focused on a range of surfactants. Cetrimide, a cationic

surfactant with antiseptic properties was used to modify the hydrophilic clay surface. The nature of the surfactant adsorption on the halloysite surface and various factors which influence adsorption at the solid liquid interface were examined. Factors considered important include surface modification, equilibration time and the presence of an electrolyte in the system. The antiseptic activity of the cetrimide coated halloysite grade was evaluated using an agar plate method.

A range of drugs commonly encountered in topical and transdermal drug delivery was originally considered. Three representative compounds, urea, salicylic acid (SA) and metronidazole were chosen. Drug loaded halloysite samples (halloysite G and the cetrimide coated grade) were prepared using a vacuum loading method. Formulation and process variables impacting on the loading of each active compound were investigated in each case. Release profiles and the quantity of drug encapsulated were used to characterise the loaded samples. The cetrimide coated grade was more efficient at encapsulating the active constituents. No potential for modulated drug release was observed.

Spray-dried halloysite complexes were formulated to produce more uniform particles. The urea halloysite complexes were co-spray dried with lecithin. The quantity of urea in the formulation was the most important variable influencing urea encapsulation. The solvent medium, solid content and lecithin grade were important variables in complex formation. The quantity of lecithin in the formulation affected particle morphology.

Spray-dried salicylic acid complexes prepared with halloysite and cetrimide were incorporated into two common topical cream bases, Aqueous Cream and Cetrimide Cream. The spray dried samples were prepared based on different formulation and processing variables. The spray dried samples incorporated in the topical cream bases represent these varying conditions and formulations. The specific spray dried samples were also selected based on the resultant variances in composite characteristics (surface area and skeletal density). The samples also had varying amounts of SA encapsulated. The spray-dried samples were included in the two topical cream bases at a concentration of 20% w/w. This concentration was judged as suitable based on rheological and texture analysis studies of halloysite and cetrimide coated samples in two ointment bases, white soft paraffin (WSP) and macrogol base. This concentration did not adversely affect the aesthetics of the product and hence the cosmetic appeal to the patient. Cream formulations were chosen because

preliminary studies examining release from the ointment formulations showed negligible release of SA. The cumulative release was greater from the Aqueous Cream base than from the Cetrimide Cream base due to a difference in apparent viscosity between the bases.

Halloysite and metronidazole were included in a calcium alginate bead formulation. Non-drug beads were investigated initially to optimise the formulation. The halloysite content, cetrimide coating and the drying method were important variables. The cetrimide coated grade resulted in samples which disintegrated relatively quickly. The freeze-dried samples had a larger degree of closed porosity, which accounted for their brittle character. The release of metronidazole from the beads was not significantly retarded. The effect of the composition of the gelation medium on drug release was also investigated, however the burst release effect was increased in these approaches. Various coating materials were investigated also. Metronidazole encapsulation was most effective using the calcium chloride gelation medium and the release was most effectively retarded by coating this formulation with chitosan. Metronidazole release from this preparation was equivalent to that observed from an equivalent weight of a proprietary preparation that contains metronidazole.

ACKNOWLEDGEMENTS

First and foremost, I wish to thank my supervisor Professor Patrick Deasy for his guidance and constant support over the years and especially in preparing this text. I would also like to extend my appreciation for giving me the opportunity to investigate and conduct the research presented in this manuscript.

My thanks are extended to the academic and technical staff of Pharmaceutics and Pharmaceutical Technology and in particular, Derek Bell, Brian Canning, Derek Coss, Conan Murphy, Brian O' Reilly and Pat Quinlan, for their assistance and willingness to help during the course of my research. I would like to thank Dr. Anne-Marie Healy for her help with the Texture Analyser. I also wish to thank Neal Leddy of the Centre for Microscopy and Analysis for his help with SEM and EDX.

There are so many people that I wish to thank, however my expressions will not adequately express my sincere gratitude. I would like to thank my fellow post-graduates for their friendship and support over the years (in alphabetical order): Fiona Brennan, Adam Byrne, Rob Byrne, Dave Coughlan, Jenny Coppins, Deirdre D'Arcy, Shadeed Gad, Mark Hanlon, Gillian Hudson, Lene Visdal-Johnsen, Arun Katheri, Emma Lawless, Karl Levis, Anthony McMahon, Des Murphy, Cora Nestor, Fiona Ní Chearúil, Orla Ní Ógáin, Lorraine Nolan, Anne Salter, Almath Spooner, Lidia Tajber, and Martina Whyte. I would like to express my special appreciation to my lab partner Alecia Barry, for her invaluable help and advice. It was a pleasure to share a lab with her and I thank her for all the laughs and chats.

I would like to thank my friends outside of College and all the people I have had the pleasure to work with in my locum jobs.

I would like to thank my parents, Mary and Bill, my sisters, Natasha, Fiona, Monica and Pamela and especially my brother John who was never too far away in Computer Science, TCD and who was always a great support. Finally I would like to thank Des, for always being there.

TABLE OF CONTENTS

Title Page		i
Declaration		ii
Dedication		iii
Summary		iv
Acknowledgements		vii
Table of Contents		viii
Presentations Associated with this Thesis		xxii
Symbols and Abbreviations		xxiii

Introduction

Chapter 1	**Introduction**	**1**
1.1	Origin and Scope of Work	1
1.2	The Structure and Function of Skin	3
	1.2.1 Introduction	3
	1.2.2 Subcutaneous fat layer	4
	1.2.3 Dermis	4
	1.2.4 Epidermis	5
	1.2.4.1 Introduction	5
	1.2.4.2 The viable epidermis	5
	1.2.4.3 Stratum corneum	5
1.3	Permeation Pathways through the Stratum Corneum	6
1.4	Percutaneous Absorption	9
1.5	In-Vitro Studies	11
1.6	Mathematics of Skin Permeation	13
	1.6.1 Introduction	13
	1.6.2 Pseudo-steady state permeation (infinite dosing)	13
	1.6.3 Finite dosing	17
1.7	Influence of Permeant Physicochemical Properties on Route of Absorption	18
	1.7.1 Introduction	18
	1.7.2 Partition coefficient	18
	1.7.3 Molecular size	19

1.7.4 Solubility/melting point 19
1.7.5 Ionisation 20
1.7.6 Other factors 20
1.8 Halloysite 21
1.8.1 Introduction 21
1.8.2 Halloysite morphology 22
1.8.3 Worldwide halloysite resources 22
1.8.4 Formation of halloysite 23
1.8.5 Structure of halloysite 24
1.8.5.1 Previous structural studies 24
1.8.5.2 Present concept and proposed structure 24
1.8.6 Surface charge of halloysite 26
1.8.7 Effect of iron content on halloysite structure 27
1.9 Surfactants 28
1.9.1 Introduction 28
1.9.2 Surfactant classes 30
1.9.2.1 Anionic surfactants 30
1.9.2.2 Cationic surfactants 30
1.9.2.3 Non-ionic surfactants 30
1.9.2.4 Amphoteric surfactants 31
1.9.3 Cetrimide 31
1.9.3.1 Introduction 31
1.9.3.2 Molecular structure 31
1.9.3.3 Physicochemical properties 31
1.9.3.4 Antimicrobial activity 32
1.9.3.5 Incompatibilities 32
1.10 Adsorption Isotherms at Solid Interfaces 32
1.10.1 Adsorption 32
1.10.2 Adsorption isotherms 33
1.11 Semi-Solid Formulations 35
1.11.1 Introduction 35
1.11.2 Ointments 36
1.11.2.1 Introduction 36
1.11.2.2 Hydrocarbon bases 36

1.11.2.3 Fats and fixed oil bases 37
1.10.2.4 Silicones 37
1.10.2.5 Absorption bases 37
1.10.2.6 Emulsifying bases 38
1.10.2.7 Water soluble bases 38
1.11.3 Creams 39
1.11.4 White soft paraffin (WSP) 40
1.11.4.1 Definition 40
1.11.4.2 Description 40
1.11.4.3 Manufacture 40
1.11.4.4 Properties 41
1.11.5 Polyethylene glycol (PEG) 41
1.11.5.1 Introduction 41
1.11.5.2 Molecular structure 41
1.11.5.3 Physicochemical properties 42
1.11.5.4 Applications 42
1.12 Salicylic Acid 43
1.12.1 Molecular structure 43
1.12.2 Physicochemical properties 43
1.12.3 Spectral properties 44
1.12.3.1 UV absorption spectrum 44
1.12.3.2 Infrared (IR) spectrum 44
1.12.4 Uses and adverse effects 45
1.13 Metronidazole 45
1.13.1 Introduction 45
1.14.2 Molecular structure 46
1.13.3 Physicochemical properties 46
1.13.4 Spectral properties 46
1.13.4.1 UV absorption spectrum 46
1.13.4.2 Infrared (IR) spectrum 47
1.13.5 Metronidazole uses 47
1.14 Urea 48
1.14.1 Introduction 48
1.14.2 Characteristics 48

1.14.3 Uses 48

Experimental

Chapter 2 Materials 49

Chapter 3 Methodology 53

3.1 Preparation of Halloysite Powder Samples 53
3.1.1 Cetrimide coated halloysite 53
3.1.2 Extraction of Balekisir halloysite 53
3.1.3 Acid washed Halloysite G 54
3.1.4 Deferration of halloysite G and Balekisir halloysite 54
3.1.5 Thermogravimetric analysis (TGA) 55
3.2 Characterisation of Halloysite Powder Samples 55
3.2.1 X-Ray diffraction (XRD) 55
3.2.2 Scanning electron microscopy (SEM) 55
3.2.3 Fourier transform infrared spectroscopy (FTIR) 55
3.2.4 Density studies 56
3.2.4.1 Bulk and tapped density 56
3.2.4.2 Apparent density 56
3.2.4.3 Helium pycnometry studies 57
3.2.5 Surface area analysis 57
3.2.6 Qualitative energy dispersive X-ray (EDX) microanalysis 59
3.2.7 Inductive coupled plasma-mass spectrometry (ICP-MS) 60
3.2.8 Evaluation of the flow properties of halloysite and cetrimide coated halloysite 60
3.2.8.1 Introduction 60
3.2.8.2 Flowability (Flodex® Tester) of halloysite powders 60
3.2.8.3 Static angle of repose of powder mixes 61
3.3 Characterisation of Surfactant - Halloysite Adsorption Isotherms 62
3.3.1 Critical micelle concentration (CMC) determination 62
3.3.1.1 Introduction 62
3.3.1.2 Surface tension method 62
3.3.1.3 Conductivity method 62

3.3.2 Halloysite adsorption isotherms 63
3.3.2.1 Introduction 63
3.3.2.2 Surfactant isotherms – depletion method 63
3.3.2.3 Trimethylammonium bromide surfactant quantitation using an anionic dye 64
3.3.2.4 Quantitation of trimethylammonium bromide surfactants using a reverse-HPLC method 65
3.3.2.5 HPLC equipment validation 66
3.3.2.6 Factorial study of TTAB - halloysite adsorption isotherms 66
3.3.2.7 Deflocculation studies 67
3.4 Evaluation of the antimicrobial activity of cetrimide in cetrimide - halloysite composites 67
3.4.1 Introduction 67
3.4.2 Nutrient agar medium preparation 68
3.4.3 Disc preparation 68
3.4.4 Agar plate - preliminary study 68
3.4.5 Agar plate - advanced study 69
3.4.6 Colony forming unit (CFU) evaluation 69
3.5 Evaluation of Halloysite – Ointment Systems 69
3.5.1 Formulation of halloysite – ointment systems 69
3.5.1.1 Halloysite white soft paraffin (WSP) physical mixes 69
3.5.1.2 Formulation of macrogol ointment systems containing halloysite or cetrimide coated halloysite 70
3.5.2 Rheological evaluation of halloysite – ointment systems 71
3.5.2.1 Introduction 71
3.5.2.2 Continuous shear studies 71
3.5.2.3 Stepped flow studies 72
3.5.2.4 Dynamic oscillatory studies 72
3.5.3 Texture analysis evaluation of halloysite - ointment systems 73
3.5.3.1 Hardness testing of halloysite - ointment systems 73
3.5.3.2 Adhesive testing of halloysite - ointment systems 73
3.6 Formulation of Urea - Halloysite Complexes 74
3.6.1 Preparation of buffer media 74
3.6.2 Solubility studies 74

3.6.3 Urea quantitation using a Quantichrom® urea assay kit 75
3.6.4 Loading of halloysite G with urea 76
3.6.5 Loading of halloysite G with urea - fractional factorial study 76
3.6.6 Urea, halloysite and lecithin systems 77
3.7 Characterisation of Urea Halloysite Complexes 80
3.7.1 SEM 80
3.7.2 Release studies from urea loaded halloysite 80
3.8 Formulation of Salicylic Acid - Halloysite Complexes 81
3.8.1 Solubility studies 81
3.8.1.1 Saturation solubility studies 81
3.8.1.2 Dynamic solubility study 81
3.8.2 Loading of halloysite G with salicylic acid 81
3.8.3 Loading of halloysite G with salicylic acid - factorial studies 82
3.8.3.1 Introduction 82
3.8.3.2 Preliminary study 82
3.8.3.3 Advanced study 82
3.8.4 Co-spray-dried salicylic acid, halloysite and cetrimide complexes 83
3.9 Characterisation of Salicylic Acid - Halloysite Complexes 85
3.9.1 SEM 85
3.9.2 Skeletal density analysis 85
3.9.3 Surface area analysis 85
3.9.4 Particle size analysis 85
3.9.5 Release studies from salicylic acid - halloysite complexes 85
3.10 Formulation of Salicylic Acid and Co-Spray-Dried Salicylic Acid - Halloysite Topical Preparations 86
3.10.1 Aqueous Cream formulations 86
3.10.2 Cetrimide Cream formulations 86
3.10.3 Salicylic acid formulations 86
3.11 Characterisation of Salicylic acid and Co-Spray-Dried Salicylic Acid - Halloysite Topical Formulations 87
3.11.1 Release studies using Franz cells 87
3.11.2 Rheological evaluation of co-spray dried topical formulations 87
3.12 Formulation of Metronidazole - Halloysite Complexes 88
3.12.1 Solubility studies 88

3.12.1.1 Saturated solubility studies 88
3.12.1.2 Dynamic solubility studies 88
3.12.2 Loading of halloysite G with metronidazole 88
3.12.3 Formulation of metronidazole halloysite chitosan co-spray-dried complex 88
3.13 Metronidazole Release from Halloysite Complexes 89
3.14 Formulation of Non-Drug Beads 89
3.14.1 Formulation of halloysite - alginate beads 89
3.14.2 Modification of halloysite - alginate bead formulations 89
3.14.3 Rheological evaluation of bead formulations 90
3.15 Characterisation of Non-Drug Beads 90
3.15.1 SEM 90
3.15.2 Skeletal density 90
3.15.3 Surface area analysis 90
3.15.4 Swelling Studies 91
3.15.5 Sphericity analysis 91
3.16 Formulation of Halloysite - Alginate Beads Containing Metronidazole 92
3.16.1 Formulation of metronidazole containing beads 92
3.16.2 Formulation variables 92
3.16.2.1 External diameter of the needle 92
3.16.2.2 Metronidazole concentration 92
3.16.3 Coating of bead samples 92
3.16.3.1 Eudragit® E PO 92
3.16.3.2 Chitosan coating 93
3.16.4 Gelation medium 93
3.16.4.1 Concentration of sodium polyphosphate (NaPP) 93
3.16.4.2 Glutaraldehyde 93
3.16.4.3 Chitosan 93
3.17 Metronidazole Release from Bead Formulations 93
3.17.1 Release studies 93
3.17.2 Metronidazole encapsulation 94
3.18 Statistical Methods 94
3.18.1 Two sample t-tests 94
3.18.2 Factorial experimentation 95

3.18.3 Analysis of variance 95
3.18.4 Linear regression analysis 96

Results and Discussion

Chapter 4 Characterisation of Chemically Modified Halloysite 97

4.1 Introduction 97
4.2 SEM Image Analysis 98
4.3 Density Analysis 103
4.3.1 Introduction 103
4.3.2 Bulk density 103
4.3.3 Apparent density 105
4.4.4 True density analysis using helium pycnometry 105
4.4 Surface Area Analysis 106
4.5 Elemental Analysis 109
4.5.1 Introduction 109
4.5.2 EDX Microanalysis 109
4.5.3 Inductive coupled plasma-mass spectrometry (ICP-MS) 113
4.6 FTIR Spectroscopy 114
4.7 X-Ray Diffraction Studies 118
4.8 Flow Properties 121
4.8.1 Introduction 121
4.8.2 Flowability 121
4.8.3 Static angle of repose 123
4.9 Conclusions 123

Chapter 5 Characterisation of Surfactant Halloysite Adsorption Isotherms 127

5.1 Introduction 127
5.2 Critical Micelle Concentration 128
5.2.1 Introduction 128
5.2.2 Critical micelle concentration determination 130

5.2.3 The effect of electrolyte addition 131
5.2.4 Effect of altering the hydrocarbon chain length 133
5.3 Flocculation/Deflocculation Studies 135
5.3.1 Introduction 135
5.3.2 The concepts of flocculation/deflocculation 136
5.3.3 Deflocculation studies involving surfactants 140
5.3.3.1 Introduction 140
5.3.3.2 TTAB 141
5.3.3.3 BAC 142
5.3.3.4 Sodium lauryl sulphate (SLS) 143
5.4 HPLC Validation 144
5.4.1 Definition 144
5.4.2 Parabens 144
5.4.3 Trimethylammonium bromides 145
5.5 Adsorption Isotherms 147
5.5.1 Introduction 147
5.5.2 TTAB adsorption isotherms 150
5.5.2.1 TTAB adsorption - factorial analysis 150
5.5.3 Halloysite G 154
5.5.3.1 Unmodified halloysite 154
5.5.3.2 Equilibration time 156
5.5.3.3 Electrolyte addition 158
5.5.4 Acid modified halloysite 160
5.5.4.1 Introduction 160
5.5.4.2 Adsorption profile - modified halloysite 162
5.5.4.3 Equilibration time 164
5.5.4.4 Electrolyte addition 165
5.6 Increasing Chain length-HTAB 169
5.6.1 HTAB adsorption isotherm 169
5.6.2 Electrolyte addition 171
5.7 Trimethylammonium Bromides - HPLC method 172
5.7.1 TTAB 172
5.7.2 Increasing chain length - HTAB 173
5.8 Other Cationic Surfactant Groups 175

5.8.1 Introduction 175
5.8.2 Alkylbenzyldimethylammonium chloride surfactants 176
5.8.3 Alkylpyridinium Chloride surfactants 177
5.8.3.1 Adsorption isotherm 177
5.8.3.2 Electrolyte addition 178
5.8.3.3 Increasing chain length - CPC 179
5.9 Anionic Surfactants 180
5.9.1 SDBS 180
5.9.2 Varying electrolyte concentration 182
5.10 Microbiological Assessment 183
5.10.1 Preliminary study 183
5.10.2 Calibration 185
5.10.3 Advanced Study 188
5.10.4 Colony Forming Unit (CFU) count 191
5.11 Conclusions 193

Chapter 6 Topical Formulations Incorporating Halloysite 197

6.1 Introduction 197
6.2 Urea 198
6.2.1 Introduction 198
6.2.2 Solubility study 199
6.2.3 Loading study 200
6.2.4 Spray-dried urea/halloysite complexes 203
6.2.4.1 Introduction 203
6.2.4.2 Lecithin 204
6.2.4.3 SEM of spray-dried complexes 205
6.2.4.4 Urea release 211
6.3 Rheological and Textural Evaluations of Halloysite – Ointment Systems 213
6.3.1 Introduction 213
6.3.2 Flow rheology 214
6.3.2.1 Introduction 214
6.3.2.2 Continuous flow rheometry 214
6.3.2.3 Stepped flow rheometry 216

6.3.3 Dynamic oscillatory rheology 219
6.3.3.1 Introduction 219
6.3.3.2 Linear viscoelastic region determination 219
6.3.3.3 Dynamic oscillatory studies on halloysite - WSP systems 220
6.3.3.4 Dynamic oscillatory studies on halloysite - macrogol systems 225
6.3.4 Texture analysis of halloysite - ointment systems 228
6.3.4.1 Introduction 228
6.3.4.2 Texture analysis of halloysite - WSP ointment systems 229
6.3.4.3 Texture analysis of halloysite - macrogol ointment systems 230
6.3.4.4 Evaluation of the adhesive properties of Halloysite - WSP ointment systems 231
6.4 Salicylic Acid 234
6.4.1 Introduction 234
6.4.2 Solubility studies 236
6.4.2.1 Saturation solubility study 236
6.4.2.2 Dynamic solubility studies 237
6.4.3 Halloysite loading with salicylic acid – preliminary study 239
6.4.3.1 Introduction 239
6.4.3.2 Salicylic acid release and factorial analysis 240
6.4.4 Halloysite loading with salicylic acid – advanced study 242
6.4.4.1 Introduction 242
6.4.4.2 Salicylic acid release and factorial analysis 243
6.4.5 Formulation and characterisation of co-spray-dried salicylic acid - halloysite - cetrimide systems 246
6.4.5.1 Formulation of a co-spray dried system containing salicylic acid 246
6.4.5.2 Surface area and skeletal density characterisation 247
6.4.5.3 Particle size analysis 248
6.4.5.4 SEM analysis 249
6.4.6 Salicylic acid encapsulation and release 253
6.4.7 Topical product formulations 256
6.4.7.1 Introduction 256

6.4.7.2 Salicylic acid release – vehicle effect 257
6.4.7.3 Controlled release and kinetics 260
6.4.7.4 Rheological evaluation of formulations 266
6.5 Conclusions 268

Chapter 7 Formulation of Metronidazole – Halloysite Complexes 271

7.1 Introduction 271
7.2 Metronidazole Solubility Studies 272
7.2.1 Metronidazole saturated solubility 272
7.2.2 Dynamic solubility 273
7.3 Halloysite Loading Studies 274
7.4 Spray-Dried Complex 277
7.4.1 Introduction 277
7.4.2 Chitosan 277
7.4.3 Metronidazole release profiles 278
7.5 Bead Formulation 280
7.5.1 Introduction 280
7.5.2 Sodium alginate 281
7.5.3 Non-drug bead formulation 282
7.5.4 Rheological analysis of alginate complexes 283
7.6 Bead Characterisation 289
7.6.1 Introduction 289
7.6.2 Surface area and skeletal density analysis 290
7.6.3 SEM analysis 294
7.6.4 Bead sphericity analysis 298
7.6.5 Swelling studies 299
7.7 Preparation and Characterisation of Metronidazole Beads 302
7.7.1 Introduction 302
7.7.2 Formulation variables 303
7.7.2.1 Introduction 303
7.7.2.2 Needle orifice diameter 304
7.7.2.3 Metronidazole concentration 305
7.7.3 Sample coating 306

7.7.3.1 Introduction 306
7.7.3.2 Eudragit® E PO 307
7.7.3.3 Glutaraldehyde 308
7.7.3.4 Chitosan 309
7.7.4 Gelation Medium 309
7.7.4.1 Introduction 309
7.7.4.2 Incorporation of glutaraldehyde in the gelation medium 310
7.7.4.3 Increasing concentration of sodium polyphosphate (NaPP) in the gelation medium 311
7.7.5 Chitosan containing formulations 312
7.7.5.1 Introduction 312
7.7.5.2 Preliminary studies 312
7.7.5.3 Rheological evaluation of chitosan solutions 313
7.7.5.4 Release profiles 313
7.8 Metronidazole Release from Rozex® Gel 315
7.9 Conclusions 317

Chapter 8 General Discussion 321

References 331

Appendices 373

Appendix 1: Calibration curves used to determine the concentration of drugs in solution. 373

Appendix 2: Chromatogram for parabens standards obtained using UV detection at 254 nm. 378

Appendix 3: Chromatogram for tetradecyltrimethylammonium bromide obtained using UV detection at 205 nm. 379

Appendix 4: Chromatogram for hexadecyltrimethylammonium bromide obtained using UV detection at 205 nm. 380

Appendix 5a: Main effects plot for the loading of halloysite with urea using a fractional factorial, 2^{4-1} design. 381

Appendix 5b: Interaction plot for the loading of halloysite with urea using a fractional factorial, 2^{4-1} design. 382

Appendix 6: Residual plot for release of salicylic acid from halloysite at t = 8 hours – advanced study. 383

PRESENTATIONS ASSOCIATED WITH THIS THESIS

Oral Presentations

Ryan, C., Deasy, P.B., (2004). Modification of Halloysite with the Surfactant, Cetrimide. Socrates Intensive Course on Innovative Therapeutics: from Molecules to Medicines, Parma, 27 June-7 July 2004.

Poster Presentations

Ryan, C., Deasy, P.B., 2004. Rheological Properties of Surface Modified Halloysite. 26th Joint Research Seminar, Queen's University Belfast, April 2004.

Ryan, C., Deasy, P.B., 2003. Topical Drug Delivery using Halloysite as a Novel Excipient. 14th International Symposium on Microencapsulation, National University of Singapore, September 2003.

ABBREVIATIONS AND SYMBOLS

α	alpha
β	beta
δ	delta
ρ	density
η_0	viscosity of the dispersion medium
ε	matrix porosity
τ	tortuosity
θ	theta
μg	micrograms
μL	microlitres
μm	micrometres
μNm	micronewton metres
γ_{SL}	interfacial tension between the liquid medium and solid particles
ΔG	surface free energy
$^\circ$	degrees
$^\circ C$	degrees centigrade
+/-	plus or minus
A	initial loading of substance per unit volume
Al	aluminium
ANOVA	analysis of variance
BAC	benzalkonium chloride
BP	British Pharmacopoeia
Br	bromide
C	carbon (solubility of the substance in the matrix Equation. 6.1, 6.3)
C_0	concentration of the permeant in the first layer of the membrane
C_v	concentration of the permeant in the donor solution
CD	coefficient of determination
Cl	chlorine
cm	centimetres

cm^2	centimetres squared
cm^3	centimetres cubed
CMC	critical micelle concentration
CFU	colony forming unit
CPC	cetylpyridinium chloride
cps	centipoise
Cu	copper
D	diffusion coefficient
dc/dx	concentration gradient
DPC	dodecylpyridinium chloride
df	degrees of freedom
dM/dt	rate of change of cumulative mass of permeant that passes per unit area
EDX	energy dispersive x-ray
Fe	iron
G	gauge
G'	storgage modulus
G"	loss modulus
g	grams (or acceleration due to gravity)
h	membrane thickness
H	hydrogen
HPLC	high performance liquid chromotography
HTAB	hexadecyltrimethylammonium bromide
hr	hour/hours
Hg	mercury
Hz	hertz
ICP-MS	inductive coupled plasma mass spectroscopy
J	flux
K	potassium
k	constant
keV	kiloelectronvolts
L	litres (lag time in Equation 1.6)
log	logarithm to the base 10
M	molar

mM	millimolar
m	metres
mbar	millibars
Mg	magnesium
mg	milligrams
min	minute/minutes
ml	millilitres
mm	millimetres
mmol	millimoles
mN	millinewtons
mNm	millinewton metres
MPa	megapascals
mPa.s	millipascal seconds
Ms	mean square
mtor	millitorr
mV	millivolts
N	newtons
N.mm	newton millimetres
n	number of replicates
Na	sodium
Ni	nickel
nm	nanometres
O	oxygen
P	partition coefficient
Pa	pascal
PEG	poly(ethylene) glycol
pH	minus log of hydrogen ion concentration
pK_a	dissociation exponent for a weak acid
p.s.i.	pounds per square inch
Q	cumulative release per unit area
R^2	correlation coefficient
Rev min^{-1}	revolutions per minute
rpm	revolutions per minute
s	second/seconds

SA	salicylic acid
SC	stratum corneum
S.D.	standard deviation
SDBS	sodium dodecyl benzene sulphate
SEM	scanning electron microscopy/micrograph
Si	silicon
SLS	sodium lauryl sulphate
SS	total sum of squares
t	time
TTAB	tetradecyltrimethlammonium bromide
USP	United States Pharmacopoeia
UV	ultraviolet spectroscopy
V	terminal velocity
v/v	volume per volume
W	pellet width
WSP	white soft paraffin
w/v	weight per volume
w/w	weight per weight
XRD	X-ray diffraction

Chapter 1

INTRODUCTION

1.1 ORIGIN AND SCOPE OF WORK

Effective release is a critical consideration of all drug delivery systems. Equally important in topical drug delivery formulations is patient acceptability. This is judged by appearance and feel of the formulation both in the container and on administration (Smith *et al.*, 1999). Due to the essential need for ease of application and often cosmetic appeal, topical delivery of the active may be compromised. This study focuses on the use of halloysite, an aluminosilicate material that is chemically similar to kaolin. Kaolin is used in oral and topical pharmaceutical formulations (Handbook of Pharmaceutical Excipients, 2005). However the morphology of halloysite is typically that of a hollow tubule, the lumen of which could facilitate improved topical delivery of drugs.

Halloysite has been characterised by Levis and Deasy (2002). Its use in drug delivery has also been investigated (Levis, 2000; Salter, 2003; Kelly *et al.*, 2004). Utilisation of halloysite for controlled drug delivery relies mainly on the internal lumen of the tubule, the potential entrapment volume of which was determined to be approximately 0.25 ml/g for a typical sample (Levis and Deasy, 2002). This novel excipient may facilitate the controlled topical delivery of drugs from both the entrapped lumen or desorption of surface adsorbed drug. Halloysite has a positive charge at the ends of the tubule and a negative surface charge along the tubule length (Tari *et al.*, 1999).

The initial focus of this research was the chemical modification of the halloysite sample in order to determine if it could be made more effective for topical drug delivery. A number of methods were investigated. An organo-clay grade was created by binding cetrimide, a quaternary ammonium cationic surfactant with antiseptic properties (Sweetman, 2005) to the negative surface charge of halloysite.

The drug loading of halloysite with a number of drugs including urea, salicylic acid and metronidazole using a vacuum loading method was investigated. The formation of halloysite drug complexes using spray-drying methods was also performed. The encapsulation of drug in the complexes was characterised using release studies.

The effect of the addition of the clay complexes to topical formulations and the resultant effect on the cosmetic appearance and mechanical properties were elucidated prior to formulation of drug loaded topical products. The effect of formulation on release of active was investigated using an established in-vitro procedure.

The formulation of bead complexes for potential use in wound applications was also considered. Kaolin is used in topical preparations in poultices and as a dusting powder (Handbook of Pharmaceutical Excipients, 2005). It was hoped to exploit similar properties in halloysite, which would be expected to be superior due to a larger surface area (Theng, 1995). Halloysite has displayed a superior adsorption capability for alkaloids compared to kaolin (Evicm and Barr, 1955; Barr and Arnista, 1957). The impact of formulation and process variables on bead morphology and characteristics produced using a gelation technique was assessed to determine an optimum formulation prior to the addition of metronidazole.

1.2 THE STRUCTURE AND FUNCTION OF SKIN

1.2.1 Introduction

The skin is a multilayered organ deliminating the human body that serves several essential roles. As the major protective barrier between the body and the environment, the skin minimises the potentially harmful effects of ultraviolet radiation, temperature extremes, microbial infection, and mechanical, chemical or electrical trauma (McGuire *et al.*, 2000). It is the largest organ of the human body, providing around 10% of the body mass of an average person, and it covers an average area of 1.7 m^2. It would appear that such a large and accessible organ would offer ideal and multiple sites to administer therapeutic agents for both local and systemic actions. However human skin is a highly efficient self-repairing barrier designed to protect the body from the external environment (Williams, 2003). Human skin is a very complex organ (Figure 1.2.1) though in many instances of transdermal drug delivery it is often regarded somewhat simplistically merely as a physical barrier.

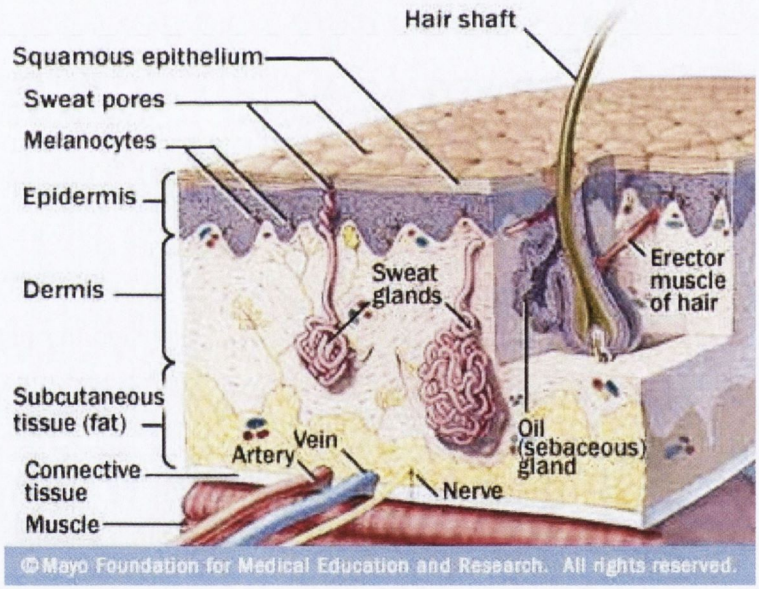

Figure 1.2.1 Anatomy of the skin.

In vivo, skin is in a process of continual regeneration; it has immunological and histological responses to assault (as would be the case if an exogenous chemical, such as a drug was applied to the surface) and is metabolically active. Human skin consists of

discrete layers including the innermost subcutaneous fat layer (hypodermis), the overlying dermis, the viable epidermis and the outermost layer of the tissue, the stratum corneum (a non-viable epidermal layer). Two permeation routes across the skin are possible: annexial (through the annexes of the skin such as the sweat glands) and transepidermal, i.e. across the stratum corneum.

1.2.2 Subcutaneous Fat Layer

The subcutaneous fat layer, or hypodermis, bridges between the overlying dermis and the underlying body constituents. In most areas of the body this layer is relatively thick, typically in the order of several millimetres. However there are regions of the body where the subcutaneous fat layer is absent, such as the eyelids. This layer of adipose tissue principally serves to insulate the body and to provide mechanical protection against physical shock. The subcutaneous fatty layer can also provide a readily available supply of high-energy molecules, whilst the principal blood vessels and nerves are carried to the skin in this layer.

1.2.3 Dermis

The dermis (or corium) is typically 3-5 mm thick and is the major component of human skin. It is composed of a network of connective tissue, predominantly collagen fibrils providing support, and elastic tissue providing flexibility, embedded in a mucopolysaccharide gel (Wilkes *et al.*, 1973). In terms of transdermal drug delivery this layer is often viewed as gelled water and thus provides a minimal barrier to the delivery of most polar drugs, although the dermal barrier may be significant when delivering highly lipophilic molecules. Numerous structures are embedded within the dermis including blood and lymphatic vessels, nerve endings, pilosebaceous units (hair follicles and sebaceous glands) and sweat glands (eccrine and apocrine). For transdermal delivery of most drugs, the blood supply thus maintains a concentration gradient between the applied formulation on the skin surface and the vasculature across the skin membrane. It is this concentration gradient that provides the driving force for drug permeation.

There are three main appendages found on the surface of human skin that originate in the dermis. Hair follicles are found over the entire surface of the skin except for the load-bearing areas (soles of feet, palms of hands) and the lips. The sebaceous gland associated with the hair follicle secretes sebum and help to maintain the surface pH around 5. Eccrine

(sweat) glands and apocrine glands also originate in the dermal tissue. The eccrine glands secrete sweat, a dilute salt solution at a pH of around 5 (Williams, 2003).

1.2.4 Epidermis

1.2.4.1 Introduction

The epidermis is a complex multi-layered membrane that varies in thickness from 0.06 mm on the eyelids to 0.8 mm on the palms and soles of the feet. The epidermis contains no blood vessels; hence nutrients and waste products must diffuse across the dermo-epidermal layer in order to maintain tissue integrity. Similarly molecules permeating across the epidermis must cross the dermo-epidermal layer in order to be cleared into the systemic circulation. The epidermis contains four histologically distinct layers, which are the stratum basale, stratum spinosum, stratum granulosum and the stratum corneum. A fifth layer, the stratum lucidum, is sometime described but is more usually considered to be the lower levels of the stratum corneum. The stratum corneum is considered to be the main barrier to the transdermal delivery of drugs. The viable epidermis is used to describe the underlying layers.

1.2.4.2 The Viable Epidermis

The stratum basale is more commonly referred to as the basal layer. The cells of the basal layer are similar to those of other tissues within the body and they are metabolically active. This layer contains the only cells (keratinocytes) within the epidermis that undergo cell division. On average dividing basal cells replicate once every 200-400 hr. After replication one daughter cell remains in the basal layer whilst the others migrate upwards through the epidermis towards the skin surface. Cells begin to differentiate, synthesise keratin and change morphology as they migrate upwards towards the stratum corneum. In the stratum granulosum the cells begin to flatten and viable cell components are degraded by enzymes in this layer. The cell nucleus disintegrates within the stratum lucidum and an increase in keratinisation occurs.

1.2.4.3 Stratum Corneum

The outermost epidermal layer is the stratum corneum (SC) or horny layer, which acts as the main barrier to skin permeation by dermally applied drug formulations (Nicoli, 2004). The SC is the final product of epidermal cell differentiation, and though it is an epidermal

layer, it is often viewed as a separate membrane in topical and transdermal drug delivery. Typically the SC comprises only 10-15 cell layers and is around 10 μm thick when dry, but it may swell to several times this thickness when wet. The thickness of the SC depends on the site; it is thickest on the soles and palms and is thinnest on the lips. The membrane consists of dead, anucleate, keratinised cells embedded in a lipid matrix. The SC serves to regulate water loss from the body whilst preventing the entry of harmful materials, including microorganisms.

The structure of the SC itself can be explained in terms of the so-called "brick and mortar" model (Elias, 1981) in which horny keratinocytes (corneocytes) represent the bricks while the intercellular lipids and water-retaining natural moisturising factors act as the mortar. Typically it takes 14 days for a daughter cell from the stratum basale to differentiate into a SC cell, the SC cells are typically retained for a further 14 days prior to shedding. The barrier nature of the SC depends critically on its unique constituents; 75-80% is protein, 5-15% is lipid, with 5-10% unidentified on a dry weight basis (Wilkes *et al.*, 1973). The protein is located primarily within the keratinocytes and is predominantly alpha keratin (around 70%) and some beta-keratin (approximately 10%). Enzymes and other proteins account for approximately 15% of the protein component.

The lipid content of the SC varies between individuals and with body site (Lampe *et al.*, 1983) but major components of the domain include ceramides, fatty acids, cholesterol, cholesterol sulphate and sterol wax/esters. In addition to the keratinocytes and lipid lamellae, water plays a key role in maintaining SC barrier integrity. Water may mediate the activity of some hydrolytic enzymes, it is also a plasticiser and thus prevents the SC from cracking due to mechanical assault.

1.3 PERMEATION PATHWAYS THROUGH THE STRATUM CORNEUM

The SC is the rate-limiting barrier to drug delivery for most molecules. There are essentially three pathways by which a molecule can traverse intact SC: via the appendages (shunt routes): through the intercellular lipid domains or by a transcellular route. Figure 1.3 depicts the intercellular and transcellular routes of permeation. It is likely that a molecule may pass through the SC by a number of these routes. The relative contributions of these pathways to the flux depend on the physico-chemical properties of the permeant. However,

for most permeants the fractional area offered by these shunt routes is so small that the predominant pathway to traverse the tissue remains across the bulk of the skin surface.

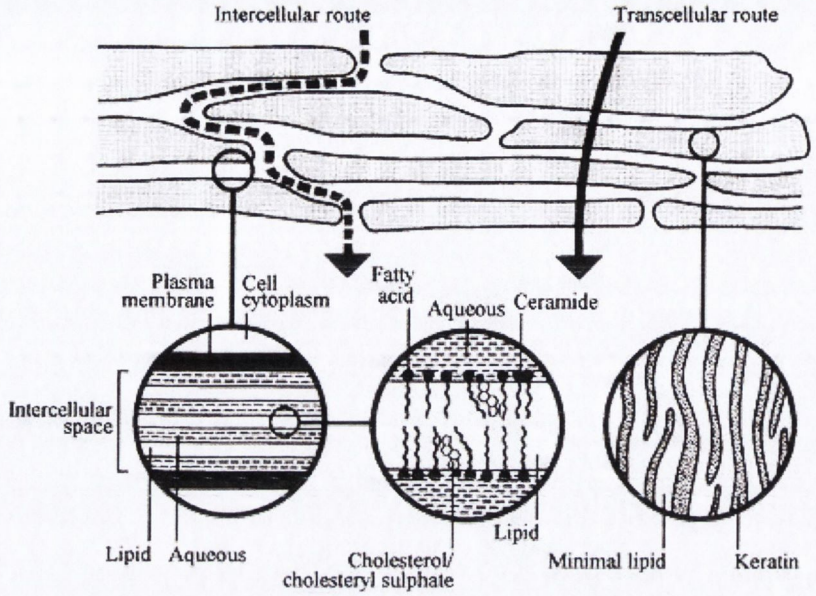

Figure 1.3 A representation of the principal mechanisms and pathways operating during transdermal and topical drug delivery (Bronaugh and Maibach, 1999).

The appendages (hair follicles, sweat ducts) essentially offer pores that bypass the barrier of the SC. However these openings onto the surface occupy only around 0.1% of the total skin surface (Scheuplein, 1967). Eccrine sweat glands may be numerous in several areas of the body (palms and soles), but their openings onto the skin surface are still very small. Also these ducts may be actively secreting sweat that would be expected to diminish the inward diffusion of topically applied drugs. The duct of the sebaceous gland is filled with sebum, which is lipoidal, rather than with aqueous sweat. Transappendageal transport may also be important for large polar molecules and ions that would traverse poorly across the bulk of the SC. Iontophoretic drug delivery largely depends on the presence of shunt routes. The method uses electrical charge to drive molecules into the skin via the path of least resistance. The shunt routes provide less resistance than the SC bulk.

The transcellular route is considered as a polar route through the SC. Solutes diffuse through the hydrated keratin, which provides an essentially aqueous environment. Hence

diffusion of hydrophilic molecules through the keratinocytes is rapid. However the keratin filled cells do not exist in isolation and they are bound to a lipid envelope that connects to the intercellular bi-layered lipid domains. Hence a molecule crossing the SC by this route must first partition into the keratinocyte, followed by diffusion through the hydrated keratin. The keratin also provides potential binding sites for solutes. The nature of the permeant will influence the relative importance of the transcellular route to the observed flux. The rate-limiting barrier for permeation of hydrophilic molecules by this route is the bi-layered lipid that the molecules must traverse between the keratinocytes.

The lipid bilayers comprise around 1% of the SC diffusional area yet provide the only continuous phase. The importance of SC lipids in regulating water loss and controlling the penetration of materials into the skin has been established (Elias, 1981). It is now generally accepted that the intercellular lipid route provides the principal pathway by which most small, uncharged molecules traverse the SC (Roberts *et al.*, 1996). The lipids have a heterogeneous packing that accounts for water loss regulation, whilst permitting sufficient water to enter the tissue to maintain keratinocyte hydration. The intercellular route is highly tortuous because permeants must move through the continuous lipid domains between keratinocytes in contrast to transcellular permeation, which is usually regarded as the thickness of the SC. In the case of intercellular permeation the path length taken is considerably greater than SC thickness. Estimates of the pathlength have ranged from 150 to 500 μm; this is influenced by the physicochemical properties of the permeant.

Localised diseases such as dermatoses, skin cancer and viral infections do not always require systemic delivery. The skin has the advantage that it is accessible. Key factors to consider in the topical bioavailability of compounds include the physicochemical properties of the drug such as solubility, partitioning and its ionisation. The intercellular pathway is the main route by which drugs penetrate into the deeper lying layers of skin. The depth to which a topically applied compound could penetrate the skin depends upon its particular function. Table 1.3.lists some common therapeutic agents and the desired site of activity.

Table 1.3 Drug substances commonly encountered in topical and transdermal drug delivery and the intended site of action (Neubert *et al.*, 1988).

Target region	Category	Example
Surface	Skin cleansers Skin protections	Ethanolic preparations
Stratum corneum	Moisturizers Keratolytic agents	Urea Salicylic acid
Living epidermis	Antiphlogistic agents Antibiotics Diagnostic agents	Glucocorticoids Tetracycline
Systemic circulation	Vasotonic agents Transdermal therapeutic agents	Heparin Estradiol Glycerol trinitrate
Sweat glands	Antiperspirants	Al^{3+} salts
Sebaceous glands	Anti-acne agents Hormones	Erythromycin Anti-androgens

1.4 PERCUTANEOUS ABSORPTION

Topically applied drug often cannot reach disease sites in the epidermis or dermis in sufficiently high concentrations to exert a therapeutic effect (Idson, 1975). The interaction of the SC with the applied drug and vehicle largely determines the rate and extent of percutaneous absorption. The two major processes in percutaneous absorption are intraphase diffusion and interphase partitioning (Ostrenga *et al.*, 1971). They occur consecutively and repeatedly as the drug passively leaves the vehicle and permeates the various layers of the skin. The higher the diffusion and partition coefficients of a drug, the greater are a drug's ability to penetrate the skin. Drugs move from vehicle to viable epidermis primarily through the SC, but as discussed previously the sweat ducts or pilosebaceous follicles may also play a role.

The rate of penetration is also directly proportional to the rate of vehicle release of drug, concentration of applied drug, surface area, duration of application and degree of SC

hydration. Percutaneous absorption is inversely proportional to SC thickness and therefore may vary depending on anatomical site. Transfer of drug from the vehicle to the skin surface, the initial step in percutaneous absorption, is determined by drug diffusion through the vehicle and partitioning into surface skin tissue (e.g. SC or sebum). Solubility is a crucial factor in release of drug from the vehicle. First dissolution of the drug in the vehicle is a pre-requisite for its diffusion through the vehicle to the skin surface. Second, the relative solubility of the drug in the vehicle and skin surface is a major determinant of the partition coefficient between the two phases. The vehicle may be simple, such as an aqueous solution or it may be more complex such as an emulsion. The vehicle – skin surface partition coefficient is an important factor in percutaneous absorption (McGuire *et al.*, 2000). The molecules adjacent to the SC surface will partition into the membrane dependent on their physicochemical properties. In the case of a lipophilic molecule such as estradiol ($\log P_{(octanol/water)} = 2.29$) partitioning into the SC from a saturated aqueous vehicle will be thermodynamically favourable. Obviously when applied in an oily vehicle the driving force will be significantly decreased. Since only molecules adjacent to the skin can partition from the vehicle into the tissue, further drug delivery is dependent upon molecules within the vehicle randomly redistributing to replenish molecules adjacent to the skin surface. Molecular diffusion through the vehicle depends on the nature of the formulation (its viscosity) and in extreme cases the diffusion of the drug through the vehicle can limit the rate of transdermal drug delivery. Additional considerations apply if the vehicle contains suspended particles. For poorly water soluble drugs delivered from an aqueous system, dissolution of drug particles to maintain a saturated solution may be the rate limiting step for transdermal drug delivery (Williams, 2003). After reaching the skin surface, the drug must diffuse across the SC (or through the follicle). Drug diffusion through the SC is generally slow and represents the rate-limiting step in percutaneous absorption. Drug transport is driven by a concentration gradient that is maintained by rapid removal of the drug by the systemic circulation via dermal capillaries. The systemic circulation is often referred to as a "sink" for the drug (McGuire *et al.*, 2000).

Once the permeant has partitioned into the outer layer of the SC, the drug then diffuses through the SC. This may be a multi step pathway depending on the permeant. At the SC/viable epidermis junction there is another partitioning step as the molecules move into the viable tissue before further diffusion through the membrane to the epidermis/dermis junction. Again there is partitioning followed by diffusion through the dermal tissue to the

capillaries, where there is another partitioning step for the molecules to enter the blood vessels before removal in the systemic circulation. In addition to these multiple partitioning and diffusion processes for transdermal drug delivery, there are other potential fates for molecules entering human skin. Permeants may bind with various elements of the skin. For example, drug binding to keratin within the SC could provide a reservoir effect; reservoir formation within the skin for steroids is a well established phenomenon. The skin is also metabolically active. The potential exists for drugs to be degraded (or activated as with prodrugs) at metabolic sites, and they may also bind to receptors within the skin (Williams, 2003).

1.5 IN-VITRO STUDIES

One of the principal benefits of performing *in-vivo* studies is the generation of realistic measures for the amounts of drug that would enter the skin or systemic circulation when the biology of the skin is intact; an active circulation and lymphatic system operate *in-vivo* as do locally active metabolic systems. In practical terms it is extremely difficult to evaluate most drugs using *in-vivo* methods and given the difficulties with in-vivo experimentation, most transdermal drug delivery studies use *in-vitro* techniques. The goal of permeation experiments is to create a kinetic profile, which shows the rate at which an active compound diffuses through the skin. A simple diffusion cell, the well-established Franz cell model, similar to that in Figure 1.5, is usually used for these measurements.

A membrane is selected and placed between the donor and acceptor compartments of the cell where it acts as a diffusion barrier, analogous to the skin. The test substance is applied to the donor side from where it diffuses through the membrane into the acceptor medium. The system is kept at a fixed temperature usually using a water bath to simulate surface skin temperature of 33 ^{o}C as an in-vivo mimic. By sampling and analyzing the acceptor side at different times, the migration of the compound through the skin can be recorded as a concentration-time profile. Important changes in the characteristics of a drug product or in the thermodynamic properties of the drug substance in the dosage form should manifest as a difference in drug release (Shah *et al.,* 1999). The method selected depends on the substance under test and specific factors that are being investigated.

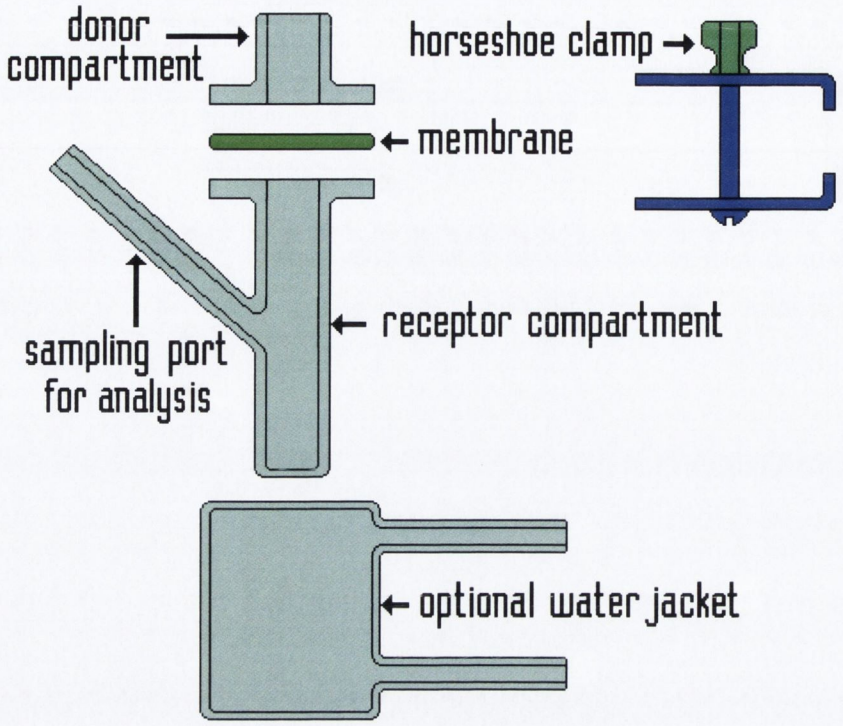

Figure 1.5 Schematic of a Franz cell used for in-vitro transdermal drug evaluations.

Ideally the most appropriate membrane to select for experiments involving topical products intended for human use is viable skin of human origin. There are considerable ethical and legal constraints on obtaining and using human material. Hence the use of alternative models including animal and artificial membranes has been undertaken. However the data obtained from these models does not transfer directly to human skin *in-vitro* or *in-vivo*. Data obtained from animal membranes can be more reproducible that from donated human tissue, as the animal's history is usually controlled whereas that of surgically excised human skin is less controlled because pre-treatment, handling and length of storage can vary. Animal models that have been employed include hairless mouse or rat skin. These models differ from human skin in their lipid contents and thickness, respectively. Hairless mouse tissue also loses its integrity rapidly, whereas the human SC remains intact for longer periods of time (Bond and Barry, 1988). One of the most popular animal membranes used is pig-skin, from the region behind the ear, due to its similarity to human skin (Williams, 2003).

Artificial membranes have also been employed. Simple inert polymer membranes, most commonly, polydimethylsiloxane (PDMS or Silastic®) provide a "non-porous" hydrophobic reproducible barrier. The membrane does allow the passage of water equivalent to transepidermal water loss during permeation studies. The main role of artificial polymer membranes is for quality control purposes or for testing formulation variables. It is usually best to employ the simplest membrane that will discriminate between two formulations or different products (Williams, 2003).

1.6 MATHEMATICS OF SKIN PERMEATION

1.6.1 Introduction

Human skin is a complex, multi-layered heterogeneous biological tissue that varies enormously from species to species, person to person and site to site. Despite the complexities, relatively simple mathematical models can be assigned to data obtained through experimentation involving skin. Drug absorption across human skin is passive (no active transport mechanisms have been reported), with the result that transport can be described in physical terms. Two principal situations are considered:

1. The drug is applied as an infinite dose - it does not deplete over the time of application (e.g. transdermal patches).
2. A finite dose is applied and so pseudo-steady state permeation would not be encountered (e.g. with a cream for local action).

1.6.2 Pseudo-Steady State Permeation (Infinite Dosing)

The amount of material passing through a unit area per unit time is termed the flux (J). The molecules move in response to a thermodynamic force arising from a concentration gradient. Fick's first law of diffusion states that the rate of transfer of the diffusing substance through unit area of a section is proportional to the concentration gradient, measured normal to the section. Fick's first law may be expressed as:

$$J = - D \frac{dc}{dx}$$ **Equation 1.1**

where J, is the flux of the permeant, D is the diffusion coefficient of the permeant and dc/dx is the concentration gradient (c is the concentration and x is the space coordinate measured normal to the section).

Fick's second law of diffusion can be derived from Equation 1.1. When a topically applied permeant enters the skin, it is usually assumed that diffusion is unidirectional. Unidirectional diffusion in an isotropic medium is expressed mathematically by Fick's second law of diffusion, Equation 1.2:

$$\frac{\delta c}{dt} = \frac{D\delta^2 C}{\delta x^2}$$

Equation 1.2

Thus the rate of change in concentration with time at a point within a unidirectional field is proportional to the rate of change in the concentration gradient at that point.

However, the skin membrane is highly complex, hence precise mathematical solutions to permeation data are not possible. Thus, the following solutions to Fick's second law must be treated as approximations that allow comparisons and standardisation of permeation data.

Most in-vitro experimental designs aim to mimic as closely as possible the in-vivo situation. The most common in-vitro design is where a membrane (usually the epidermis) separates two compartments. One compartment contains the permeant in a vehicle possibly a simple aqueous or buffer solution or more complex system such as a cream vehicle (termed the donor medium) and the other compartment contains a receptor (or receiver) solution that provides sink conditions (i.e. essentially zero concentration). After sufficient time steady-state permeation across the membrane is achieved when the concentration gradient of the permeant across the membrane is constant. Under these conditions Equation 1.1 can be simplified to:

$$\frac{dM}{dt} = \frac{DC_0}{h}$$

Equation 1.3

where M is the cumulative mass of permeant that passes through per unit area of the membrane, C_0, is the concentration of the permeant in the first layer of the membrane (at the skin surface in contact with the donor solution) and h is the membrane thickness.

In practical terms it is very difficult to measure C_0, the concentration of permeant in the first layer of the membrane, removal of the outer layer is problematic and contamination from the applied donor solution is almost inevitable. However, the concentration of the permeant in the vehicle (donor solution) bathing the skin membrane (C_v) is usually known or can be determined, since C_0 and C_v are simply related by:

$$P = \frac{C_0}{C_v} \qquad => \qquad C_0 = PC_v \qquad \textbf{Equation 1.4}$$

where P is the partition coefficient of the permeant between the membrane and the vehicle. Substitution of equations leads to Equation 1.5:

$$\frac{dM}{dt} = \frac{DPC_v}{h} \qquad \textbf{Equation 1.5}$$

This is the most widely applied equation in examining transdermal drug delivery data. The lag time can be deduced by extrapolation of the pseudo steady-state portion of the permeation profile to the intercept on the time axis. As a useful approximation, the pseudo steady-state permeation for most drugs is achieved after around 2.7 times the lag time (Barry, 1983). Crank, (1975) showed that the lag time (L) can be related to the diffusion coefficient by:

$$L = \frac{h^2}{6D} \qquad \textbf{Equation 1.6}$$

From Equation 1.6 it is apparent that the diffusion coefficient of a molecule in the membrane can simply be obtained by measuring the lag time. This approach has been used for studies with simple isotropic membranes such as polymers. However, skin is not a simple isotropic membrane. Difficulties are encountered in the determination of the membrane thickness, also it is uncertain if the SC alone or the viable epidermis constitutes the rate determining membrane. It can be seen from Equation 1.6 that membrane thickness

is a squared function, hence any errors are magnified substantially. Additionally, lag times obtained from permeation experiments with human skin tend to be highly variable and strongly influenced by permeant-skin binding. Alternatively the diffusion coefficient for a steady-state profile can be deduced by further manipulation of the preceding equations:

$$D = \frac{dM/dt\ h}{PC_v} = \frac{J\ h}{PC_v} \qquad \textbf{Equation 1.7}$$

where dM/dt is the rate of change of cumulative mass of permeant that passes per unit area through the membrane, usually termed the flux (J) of the permeant.

The expression allows calculation of the apparent diffusion coefficient without requiring an accurate lag time value, but does necessitate some approximation for the membrane thickness (though this function is not squared). The partition coefficient (SC/vehicle) for the permeant may be obtained from separate experimentation. The permeability coefficient (k_p) of a permeant through a membrane can be defined by:

$$k_p = PD/h \qquad \textbf{Equation 1.8}$$

Substitution into Equation 1.5 results in:

$$\frac{dM}{dt} = J = k_p C_v \qquad \textbf{Equation 1.9}$$

The pseudo steady-state flux is simply obtained as the gradient of the linear portion of the permeation profile and if the concentration of the permeant in the applied vehicle is known then the permeability coefficient can be determined. It is this parameter, the permeability coefficient that is often used to characterise the permeation of drugs through the skin, other parameters such as the diffusion coefficient can also be used but are more difficult to calculate accurately due to the difficulty in estimating membrane thickness.

The above equations, though relatively simple and easy to use are based on some important assumptions implied in their derivations. The validity of some of the assumptions is questionable; hence the application of the equations to some experimental designs is questionable.

It is assumed that:

- The SC is the major rate limiting barrier and that the primary rate determining step is permeation through the SC and not partitioning into or out of the membrane. This assumption appears to hold true for many permeants except for very lipophilic or hydrophilic molecules; for these particular molecules, partitioning behaviour may be rate limiting.
- Permeation through the appendages is negligible compared to permeation through the bulk of the SC. However, it should be noted that the shunt routes may be significant for ions and large molecules. The equations describe permeation at steady-state conditions.
- Permeation through the SC is solely by passive diffusion.
- The nature of the SC is not affected by the application of the vehicle. This is unlikely to be true if an aqueous vehicle is applied to a dry or partially hydrated SC membrane.
- The drug dissolves in the SC. This is considered a reasonable assumption considering the varying nature of the tissue.
- The diffusion coefficient of the permeant is independent of concentration, time or distance. However, it is likely that some permeants bind to the tissue to some extent with the result that the diffusion coefficient is dependent on concentration.
- The relationship between lag time and diffusion coefficient is not applicable if the permeant binds to the tissue.
- Fickian diffusion theory was developed for isotropic media. The SC is a heterogeneous membrane, yet it is assumed that it is uniform in character (Williams, 2003).

1.6.3 Finite Dosing

Not every clinical situation includes the application of an infinite dosing form, with the result that pseudo steady-state conditions are unlikely to be achieved with the finite dose form. The permeation profile resulting from a finite dose illustrates that cumulative permeation increases to a plateau beyond which the amount permeated remains constant unless further doses are applied to the membrane surface. If the instantaneous flux values are plotted against time, then a peak in the profile is observed which corresponds with the appearance in the receptor solution of the majority of the applied dose. Several parameters

tend to be reported from instantaneous flux profiles for a finite dose. These parameters include the maximum flux (J_{max}) and the time to maximum flux (T_{max}). The magnitude of J_{max} (Crank, 1975) is given by:

$$J_{max} = \frac{1.85\ D\ C_0\ \delta}{h^2} \qquad \textbf{Equation 1.10}$$

where D is the apparent diffusion coefficient, C_0 is the concentration of the permeant in the first layer of the SC (this is maximal when the solid deposited drug is in contact with the skin surface), h is the thickness of the SC and δ is the thickness of the finite dose layer on the skin surface.

1.7 Influence of Permeant Physico-Chemical Properties on Route of Absorption

1.7.1 Introduction

The physico-chemical properties of the active of interest, exert a vital influence on the ability of the molecule to cross the membrane in question However the properties of the molecule not only have ramifications for its ability to traverse the membrane but also to dissolve and diffuse from the vehicle it is contained in to the membrane of interest.

1.7.2 Partition coefficient

In order to cross the membrane, (detected using the Franz cell set-up), SA must first partition into the membrane. It is considered that this process may be the rate-limiting step in the permeation process. The partition coefficient of a permeant is usually the governing factor in dictating which pathway it will follow through the skin (Barry, 1987). It would be expected that a hydrophilic molecule would partition preferentially into the hydrated keratin filled keratinocytes rather than into the lipid bilayers, whereas lipophilic permeants will preferentially permeate into the lipoidal domains. Therefore, hydrophilic molecules are expected to permeate largely via the intracellular route whereas the intercellular route will dominate for lipophilic molecules. Roberts *et al.* (1995) concluded that a mixed permeation model was possible due to the lipid and polar regions of the bilayers, but the partition coefficient of the permeant would be an important factor in determining if it transverses via this route.

For molecules with intermediate partition coefficients (this would typically encompass most molecules with a log $P_{(octanol/water)}$ of 1 to 3) showing some solubility in both oil and water phases, the intercellular route probably dominates. For more lipophilic molecules (log $P > 3$), the intercellular route will be almost exclusively the pathway. SA has an intermediate log P value of 2.19 (Peña *et al.*, 2006). It is important to note that a molecule must partition out of the stratum corneum into the essentially aqueous viable epidermal tissues. For more hydrophilic molecules (log $P < 1$) the transcellular route increasingly predominates (Williams, 2003).

1.7.3 Molecular Size

The size and shape of a molecule has important consequences for determining its flux through human skin or any other membrane examined. The molecular weight is taken as a convenient measure of permeant bulk volume. It is inherently assumed that the molecule is essentially spherical. It has long been accepted that, in simple isotropic media, molecular weight influences the diffusion coefficient of the molecule with increasingly bulky molecules decreasing in diffusivity (Crank, 1975). Idson, (1975) suggested that an inverse relationship existed between transdermal flux and molecular weight of the permeant despite the heterogeneity within human skin. Scheuplein *et al.* (1969) demonstrated with work on steroids that small molecules cross human skin faster than large molecules. However since the majority of molecules chosen for transdermal drug delivery lie within a narrow range of molecular weights (100-500 Dalton), molecular size is not as crucial as the partition coefficient in determining flux. The impact of molecular weight is more apparent when considering peptides and proteins (Williams, 2003).

1.7.4 Solubility/Melting Point

It is well known that most organic molecules with high melting points and with high enthalpies of melting have relatively low aqueous solubility at normal temperatures and pressures (typical conditions encountered in transdermal drug delivery). As mentioned earlier lipophilic molecules tend to permeate through the skin faster than more hydrophilic molecules. A correlation exists between the partition coefficient (usually describes solubility within the intercellular lipids) and the permeability coefficient for a homologous series of compounds. However whilst lipophilicity is generally a desired characteristic, some aqueous solubility is also required as the vehicle is usually an aqueous based formulation. The steady state flux of the drug crossing the tissue is a product of the

permeability coefficient and the applied concentration. Whilst lipophilic permeants may provide a relatively high permeability coefficient, their aqueous solubility (and hence concentration in an aqueous formulation) will be relatively low, with a consequent impact upon drug flux through the tissue. This concept can be extended further if the permeant has poor water solubility, then the amount of the drug present in the aqueous formulation will be small but owing to its lipophilicity it will enter the stratum corneum relatively quickly, thus possibly resulting in a rapid reduction in concentration in the aqueous vehicle leading to donor depletion. As the thermodynamic activity of the drug in the formulation falls the driving force for diffusion drops and flux decreases rapidly (Williams, 2003). As a result a balance between lipophilicity and aqueous solubility is desirable for drug candidates.

1.7.5 Ionisation

It is a logical assumption that the extent of ionisation of the permeant strongly dictates its permeability considering the role played by the lipid bilayer domains which feature prominently in the intercellular route. It is a strongly held belief that ionisable drugs are poor transdermal permeants. The pH partition hypothesis devised by Shore *et al.* (1957) for the absorption of drugs through the gastrointestinal tract has been extrapolated to consider if weak acid and base candidates are suitable for transdermal drug delivery. However although Shore's hypothesis declares that only the unionised form can permeate in significant amounts, due to the complex nature of human skin, the model cannot be rigidly applied. It is believed that if ionised molecules are to traverse then the shunt route may be a likely route.

As stated above, drug flux is a product of the permeability coefficient and effective drug concentration in the vehicle. The degree of ionisation can affect the relative solubility of the substance in question, hence for an ionised species the permeability coefficient may be low but the solubility may be high. It is possible that the resultant flux may be equivalent to that resulting from the converse situation of an unionised species (Williams, 2003).

1.7.6 Other factors

Due to the implicit heterogeneous nature of the stratum corneum, drug binding to some of the components is a possibility. Interactions can vary from hydrogen bonding to weak van der Waals forces. Binding can alter the lag time significantly. Normally pseudo steady-state flux prevails after approximately 2.7 times the lag time. This is considerable more

important if the drug is applied from a finite dose. The delay and reduced availability from the applied dose due to drug binding may be quite significant.

The influence of hydrogen bonding activity of applied therapeutic agents on drug flux has been investigated by (Pugh, 1999). In earlier studies Pugh *et al.* (1996) concluded that that the stratum corneum was a hydrogen bond acceptor. Contrasting views exist and El Tayar *et al.* (1991) earlier concluded it was predominantly a hydrogen bond donating medium. Du Plessis *et al.* (2002) concluded from the literature that diffusion was not solely dependent on the number of hydrogen bonding groups but also on their distribution with respect to symmetry within the molecule. Therefore by increasing the number of hydrogen bonding groups within the molecule, permeation can be dramatically altered.

1.8 HALLOYSITE

1.8.1 Introduction

Halloysite ($Al_4Si_4O_{10}(OH)_8.4H_2O$) is a naturally occurring aluminosilicate that exhibits a tubular morphology in the hydrated state (Bates *et al*, 1950). It is a 1:1 type layer silicate being a member of the kaolin group of minerals. It may be regarded as being composed of kaolinite layers between which a single layer of water molecules is interposed (Theng, 1974). Halloysite differs from kaolinite in composition, layer stacking sequence and ring configuration (Bailey, 1990). Unlike kaolinite, it is capable of existing in a hydrated (endellite) and dehydrated state (metahalloysite), the empirical formula of each being $Al_2Si_2O_5(OH)_4.2H_2O$ and $Al_2Si_2O_5(OH)_4$, respectively (Levis, 2000). Compared with kaolinite, stacking of successive layers within a single crystal is disordered (Brindley, 1961). According to Yuan and Murray (1997), it may be considered an extremely poor crystalline member of the kaolinite group. Alexander *et al.* (1943) and Bates *et al.* (1971) showed that, unlike the platy structure of kaolinite, halloysite occurs in a number of different morphological forms. Under the microscope kaolinite particles are seen as flat, hexagonal plates whereas those of halloysite are seen as tubes (Grim, 1953; Bates *et al.*, 1950). Halloysite also differs from kaolinite in that it has a higher exchange capability and higher surface area (Harvey, 1996).

1.8.2 Halloysite Morphology

Halloysite occurs in a variety of morphologies and these have been related to their chemical composition (Tazaki, 1981). The most common morphology is that of an elongated hollow tubule, but the occurrence of short tubular, spheroidal and tabular (platy) forms have been widely reported (Carson and Kunze, 1970; Dixon and McKee, 1974; Tazaki, 1981; Churchman and Theng, 1984; Noro, 1986). Kirkman (1977a, 1997b) described squat cylindrical and disk halloysite in rhyolitic tephra of New Zealand. Nagasawa and Karube (1975) reported ribbon-shaped halloysite in altered montmorillonite clay. Tazaki (1979) described that various morphologies of halloysite including spherical, walnut-shaped, acicular, crinkly, platy, tubular and square-tube were observed on the surface of altered plagioclase in volcanic ash. In addition, tabular halloysite was found in Texas soils by Kunze and Bradley (1964) and Carson and Kunze (1970). However, generally the most common morphology is that of the elongated hollow tubules (Dixon and McKee, 1974).

1.8.3 Worldwide Halloysite Resources

The commercial development of high purity halloysite resources is restricted to New Zealand, South Korea, China, Turkey and Japan. Lower grade resources are exploited in Japan, the United States and to a smaller extent in the Czech Republic, France, the Philippines and Morocco. The primary and largest source of halloysite deposits are found in New Zealand, where they are exploited by New Zealand China Clays Ltd. (a subsidiary company of Ceramco Corporation Ltd.). These deposits were first discovered early in the 20th century but it was not until the 1960s that the systematic exploration and development program was carried out over various volcanic areas in the North Island. This led to the confirmation of these large deposits and several smaller deposits in the Coromandel region (Harvey, 1996). New Zealand China Clays Ltd. was established in 1969 to process the halloysite and develop both local and export markets in ceramics and other applications. The development of these resources coincided with a shortage of quality halloysite from the Korean deposits. Three commercially significant halloysite resources were confirmed and developed at Maturi Bay, Mahimahi and Maungaparerua. Currently 100% of the New Zealand halloysite is exported to make the world's finest porcelain and china creations due to its low iron and titanium content.

In Japan there are substantial deposits of halloysite in the Gaerome clays, which occur in Pliocene sediments in Seto (Aiche Prefecture) and Tajimi-Toki (Gifu Prefecture) areas in the vicinity of Nagoya, Central Japan. This area is one of the country's main centres of ceramic production. Other sources of halloysite in Japan are used to produce material for refractories and in the manufacture of paper (Harvey, 1996).

Other sources include the USA where the deposits are located 80 km north of Reno at the Dragon mine in Utah (now closed); halloysite from this source was used as part of initial studies on oil cracking catalysts. French deposits in the Dordogne region are employed in the production of ceramic porcelain. In the Czech Republic, halloysite is exploited from a deposit near Michalovce for the production of heavy clayware, refractories, ceramic insulators, paper and rubber filling. In the Philippines, halloysites of both weathering and hydrothermal origin are common components in many ceramics (Harvey, 1996).

1.8.4 Formation of Halloysite

Halloysite is the product of both subtropical or tropical weathering and hydrothermal alteration (Harvey, 1996). During the weathering of rhyolitic tephras in New Zealand, volcanic glass altered to allophane, which on ageing crystallised to cylindrical halloysite (Kirkman, 1975). The rhyodacites were formed by either partial melting or differentiation of lower crustal material (Harvey, 1996). The volcanic heat has played a significant role in the formation of the halloysite deposits by providing a heat source for hydothermal alteration. Kirkman (1977b) observed that in New Zealand, allophane dominates clay fractions of tephras up to about 13,000 years of age, whereas the clay fractions of tephras between 13,000 and 42,000 years of age contain small but increasing amounts of halloysite. Similarly Aomine and Miyauchi (1963) reported that cylindrical halloysite had formed from allophane after 8000-9000 years in a buried soil on Mount Aso, Japan. Kirkman (1977b) also observed that for rhyolitic tephras, most of the aluminium originally present in the allophane has been incorporated into the 1:1 lattice and that excess silica has been deposited as amorphous flakes. Farmer *et al.* (1979) showed that the extent to which halloysite is formed is dependent on concentration of silica in the soil and soil temperature. Harvey (1996) observed that hydrated halloysite from deposits at Maungaparerua, New Zealand was the dominant weathering product from feldspar in feldspar rich rocks.

1.8.5 Structure of Halloysite

1.8.5.1 Previous Structural Studies

Berthier described and named halloysite (metahalloysite) in 1826; at that time it was considered as an amorphous substance with no characteristic shape (Bates *et al.*, 1950). Early workers (Mellor, 1908; Rogers, 1917) also described it as amorphous. However Shaw and Humbert (1941) observed from electron micrographs that the mineral typically occurred as split rods. Bates *et al.* (1950) concluded that metahalloysite exists in the form of hollow tubes, may of which are split longitudinally or have collapsed to form laths or ribbons.

1.8.5.2 Present Concept and Proposed Structure

Figure 1.8.5.2a gives a diagrammatic picture of the structure of halloysite (endellite) proposed by Hendricks (1938). As in the other kaolin minerals, there is a 1:1 structure in which a modified gibbsite sheet is bonded to a silicon-oxygen sheet. In the mineral gibbsite, the six hydroxyl ions on one side of the unit cell occupy a distance of 8.62 Å, while in the silicon-oxygen sheet in kaolinite the corresponding six oxygen ions occupy a distance of 8.93 Å (Bates *et al.*, 1950). From this Pauling, (1930) pointed out that the two sheets, which make up the structure are not a perfect fit. Water enters the interlayer space in halloysite to minimise cation-cation Coulomb repulsion between adjacent layer surfaces and to coordinate exchangeable cations postulated as present to compensate for Al(IV). The layers roll into tubes due to the lateral misfit between a larger tetrahedral sheet and a smaller octahedral sheet. Tetrahedral rotation, which compensates similar misfit in most layer silicate structures, is blocked in halloysite by dynamic disorder of H-bonds and H_20 molecules so basal oxygens cannot all rotate in the same direction (Bailey, 1990). It is proposed that in a typical unit of endellite halloysite that the b_0 has a dimension of 8.93 Å compatible with the spacing of the oxygen ions on one side and a similar dimension of 8.62 Å typical of the hydroxyl ions on the other. However since adjoining units are less than 3 Å away, the six oxygen ions of one unit stretch the opposing hydroxyl ions to fit the cell dimension of 8.93 Å. Due to the greater distance of 5.74 Å and the presence of water molecules between the 1:1 units, the hydroxyl ions are only slightly subject to "stretching" forces from opposing oxygen layers of neighbouring units. The six hydroxyl ions are therefore free to approach their normal spacing of 8.62 Å, while the six oxygen ions on the opposite side of the same unit occupy a distance of 8.93 Å (Bates *et al.*, 1950).

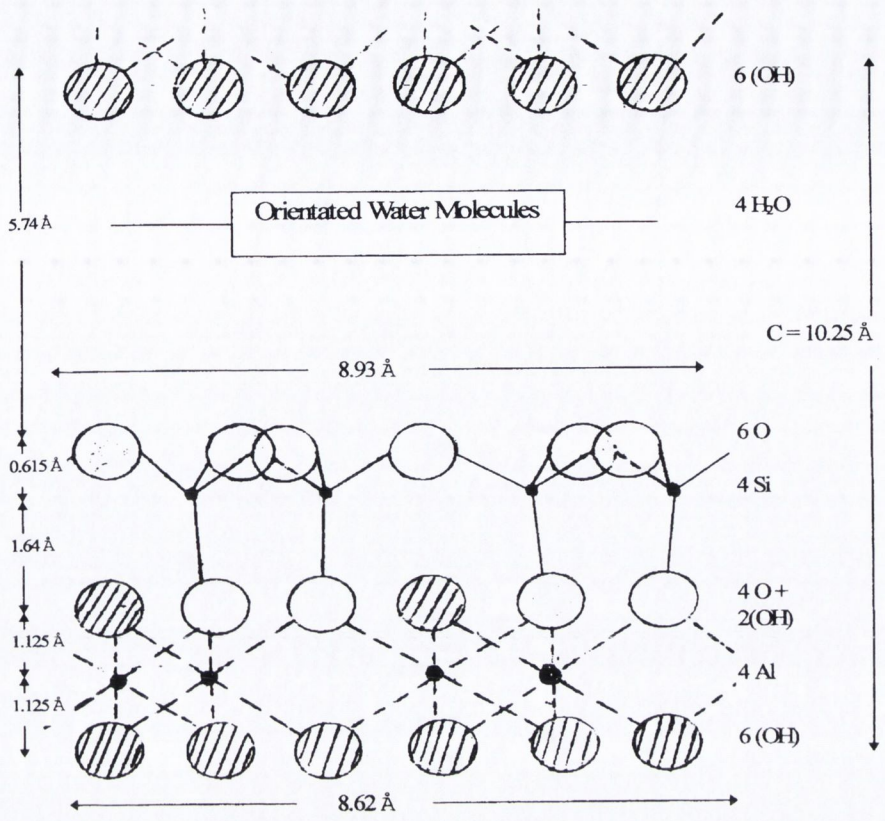

Figure 1.8.5.2a Structure of halloysite (endellite) according to Hendricks (1938).

If it is assumed that the "vertical" bonds within the unit remain of equal length relative to each other, a curvature will occur, as seen in Figure 1.8.5.2b (Bates *et al.*, 1950). When the halloysite dehydrates (metahalloysite), upon loss of the oriented water molecules between the layers, adjoining units come together from a distance of 5.4 Å to approximately 3 Å. The hydroxyl ions, which in the tubular form occupied approximately their normal spacing of 8.62 Å and were under little strain, now become subject to the forces of the closer oxygen ions and are "stretched" to a distance of approximately 8.93 Å (Bates *et al.*, 1950). The resulting strain manifests itself in the form of collapsed or split and partially unrolled tubes of metahalloysite. On the other hand, kaolinite with a similar layer composition to halloysite is almost invariably planar because in this instance the lateral misfit is corrected by the rotation of alternate silica tetrahedral in opposite directions (Radoslovich, 1963). However as previously mentioned, tetrahedral rotation is blocked by the presence of interlayer water in hydrated halloysite.

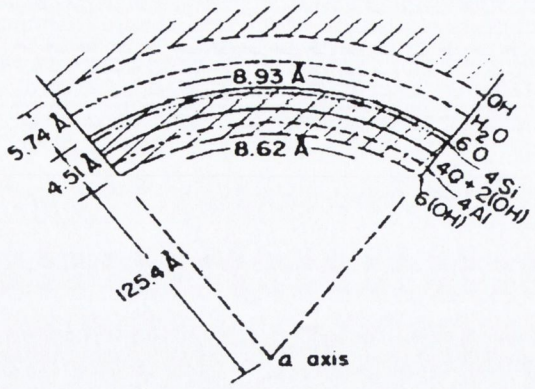

Figure 1.8.5.2b Diagrammatic representation of the structure of proposed curved halloysite (endellite) according to Bates *et al.* (1950).

1.8.6 Surface Charge of Halloysite

The basal or 'face' and 'edge' surfaces of halloysite normally carry a negative and positive charge, respectively but the negative 'face' charges predominate. Therefore halloysite functions as a polyvalent anion (Salter, 2003). Bailey (1990) showed that the cation exchange capacity confirmed the net negative charge of the mineral. This was confirmed by electrophoretic experiments carried out by Tari *et al.* (1999) and Levis and Deasy (2002), using a zetasizer. Tari *et al.* (1999) confirmed that the permanent negative surface charge tends to electrostatically attract cations in order to ensure the electroneutrality of the system.

The exact origin of the negative charge has been attributed to a number of different factors. van Olpen (1977) stated that the clay lattice carries a net negative charge as a result of isomorphous substitutions of certain electropositive elements by elements of lower valency. Soma *et al.* (1992) and Newman *et al.* (1994) confirmed van Olphen's observations. The authors attributed the permanent negative charge to non-stoichiometric substitution of Fe^{3+} for Al^{3+} in the octahedral sheet. The authors also postulated that Al vacancies in the octahedral sheet account for the permanent negative charge. Soma *et al.* (1992) further confirmed by XPS (x-ray photoelectron spectroscopy) that halloysite carries a negative charge on the 'face' surface of the material, occurring from the non-stoichiometric substitution of Al^{3+} by Fe^{3+}. Bailey (1990) proposed that the permanent negative charge in halloysite might originate from the isomorphous substitution of Al^{3+} for

Si^{4+} in the tetrahedral sheet. The presently accepted view is that a combination of the substitution of octahedral Al^{3+} by Fe^{3+} and also the acidic and amphoteric properties of the silica and gibbsite sheets lead to a net negative charge on the mineral's surface. The positive charge at the edge of the tubule can be attributed to the disruption of the tetrahedral silica sheets and the octahedral alumina sheets (van Olpen, 1977).

As outlined above the reasoning for the generation of the net negative charge is that the substitution of Fe^{3+} for Al^{3+} results in a positive layer deficiency (Takahashi *et al.*, 2001). In addition, the silica 1:1 unit is mainly positioned on the outer surface of the tubule whereas the aluminium is present on the inner surface of the tubule, which gives an enhanced negative charge over a wide pH range. Levis and Deasy (2002) explained that surface hydroxyl groups (Sur-OH) are formed on exposure of these oxides to water, which are easily ionised (Equation 1.11):

$$Si-OH_2^+ \xleftarrow{H^+} Si-OH \xrightarrow{OH^-} Si-O^- \qquad \textbf{Equation 1.11}$$

Silica is an acidic oxide; therefore the reaction to the right hand side predominates over a wide pH range. By contrast the net charge on the edges of halloysite, which are composed mainly of gibbsite (alumina) can be positive or negative depending on pH due to the amphoteric nature of alumina (Theng and Wells, 1995a). However as explained earlier since the surface is predominately silica, the net charge on the surface will be negative.

1.8.7 Effect of Iron Content on Halloysite Structure

Studies have shown that the morphology of halloysite mineral is not only affected by the mechanism involved in its generation, but can be influenced by the level of iron that has substituted the aluminium ions within the gibbsite (Levis, 2000). Many authors have reported analyses of halloysite with significant amount of Fe_2O_3 (Kunze and Bradley, 1964; Tazaki, 1981; Wada and Mizota, 1982; Noro, 1986).

The iron content of halloysite appears to affect particle shape. Low structural iron contents are associated with long tubular particles, intermediate contents with short and/or wide tubes, and high contents with spheroidal and other non-tubular forms. It has also been observed that halloysites containing high amounts of extractable (non-structural) iron generally show a low intercalating ability (Churchman and Theng, 1984). The

incorporation of iron in the octahedral sheet is a likely cause for an increase in its lateral dimensions and results in a decrease in the misfit between the tetrahedral and octahedral sheets (Wada and Mizota, 1982). The invariable high iron content of tabular halloysite (Kunze and Bradley 1964; Carson and Kunze, 1970) samples supports this view.

Soma *et al.* (1992) indicated by XPS that Fe^{3+}, substitutes for Al^{3+} in octahedral positions in approximately a 1:2 proportion. ESR (electron spin resonance) and Mossbauer spectra techniques have been used to indicate the presence of Fe^{3+} in the octahedral structural unit (Nagasawa and Noro 1987a,b: Quantin *et al.*, 1984). Further, halloysite layers within a crystal are generally non-homogeneous in composition. Built up like "onion skins", the surface layers would either be enriched or depleted in Fe depending on the chemical environment in which the crystal growth occurs.

Reported values for Fe_2O_3 in samples range from 0.5% to 12.8% w/w. There is evidence that long-tube halloysites contain the least Fe_2O_3 and have the most curvature, and that the amount of Fe_2O_3 increases through short tube and spheroidal halloysites to platy halloysites. Platy halloysites have the most Fe_2O_3 and the least curvature (Bailey, 1990). Noro (1986) attributed the morphological change to the larger size of the iron ion relative to that of aluminium and the resultant increase in the octahedral layer. The length of the crystal layer in the b dimension increases with increasing amounts of the large Fe^{3+} cation. The value of the b dimension for iron deficient long tubular halloysite maybe as small as 8.88 Å, but increases to equal that of kaolinite (8.93-8.94 Å) at 3.5-4.0% weight Fe_2O_3. It surpasses that of kaolinite with increasing quantities of Fe_2O_3 (Noro, 1986). The latter halloysites exhibit a platy morphology. Therefore Soma *et al.* (1992) concluded that when the structural Fe_2O_3 content exceeds 4% weight, the lateral dimension of the octahedral sheet would become so large as to cause it to curl around the tetrahedral sheet.

1.9 SURFACTANTS

1.9.1 Introduction

Surfactants are among the most versatile products used in the chemical industry, appearing in such diverse products as motor oils, pharmaceuticals and detergents. They are also used with drilling muds in the prospecting of petroleum and as flotation agents in the beneficiation of ores. The last couple of decades have seen the extension of surfactant

applications to high-technology areas such as biotechnology, microelectronics and viral research. A surfactant is a substance that when present at low concentrations in a system has the property of adsorbing onto the surfaces or interfaces of the system and of altering to a marked degree the surface or interfacial free energies of the surface (or interface) (Rosen, 1989).

Surface active agents are characterised by the possession of both polar and non-polar regions on the same molecule. The polar or hydrophilic region of the molecule may carry a positive or negative charge, giving rise to cationic or anionic surfactants respectively or may be composed of a non-ionic polyoxyethylene chain. The non-polar or hydrophobic portion of the molecule is most commonly a flexible hydrocarbon chain. A large number of molecules including many of biological interest also contain aromatic hydrophobic groups. The existence in the same molecule of two moieties, both of which have affinities for different solvents types, account for them being termed amphiphiles. This dual nature is responsible for the phenomenon of surface activity, micellization, solubilisation and other properties. Owing to their tendency to become adsorbed at interfaces, they are often called surface active agents or colloidal surfactants (Attwood and Florence, 1983). The amphipathic structure of the surfactant accounts for the concentration of the surfactant at the air-water interface and a reduction of the surface tension of water, but also orientation of the molecule at the surface with its hydrophilic group in the aqueous phase and its hydrophobic group orientated away from it (Rosen, 1989).

The choice of surfactant depends on the desired outcome. Many natural surfaces are negatively charged. Therefore if the surface were to be made hydrophobic (water-repellant) by use of a surfactant, then a cationic surfactant would be the most appropriate choice. The surfactant adsorbs onto the surface with its positively charged hydrophilic head group orientated toward the negatively charged surface due to electrostatic attraction. The hydrophobic group is orientated away from the surface, making the surface water-repellent. The adsorption of the positive surfactant may even reverse the negative charge of the surface. Non-ionics adsorb onto surfaces with either the hydrophilic or the hydrophobic group orientated toward the surface, depending on the nature of the surface. If polar groups capable of hydrogen bonding with the hydrophilic group of the surfactant are present on the surface, then the surfactant will probably be orientated with its hydrophilic group toward the surface making the surface more hydrophobic. Zwitterionic (amphoteric)

surfactant groups carry both positive and negative charges, hence they adsorb onto both negatively and positively charged surfaces without changing the surface charge significantly (Rosen, 1989).

1.9.2 Surfactant Classes

1.9.2.1 Anionic Surfactants

Anionic surfactants as a group are the most widely used surface active agents in personal products and for industrial purposes. Their primary application is in products intended for cleansing and detergency. Anionic surfactants are further sub-categorised. Common sub-types include carboxylates, esters of sulphuric acids, sulphonates and phosphoric acid esters.

1.9.2.2 Cationic Surfactants

Cationic surfactants are compatible with non-ionic and amphoteric surfactants. As a rule they cannot be used together with anionic surfactants because they interact to form water-insoluble complexes. Cationic surfactants are strongly adsorbed by negatively charged substrates, which include skin and hair, glass, ceramics, clays and many types of microorganism. Long chain primary, secondary and tertiary amine salts exhibit surface activity and find numerous industrial applications (ore flotation, corrosion inhibition). On the other hand, quaternary ammonium salts are the major types of cationic surfactant used in pharmaceuticals, cosmetics and toiletries. They are used due to their antimicrobial properties and their capacity to bind to negatively charged surfaces. The quaternary nitrogen atom unlike the primary, secondary and tertiary retains its positive charge regardless of the pH of the medium.

1.9.2.3 Non-ionic Surfactants

Non-ionic surfactants as a group find wide application in pharmaceutical and cosmetic products. They are compatible with the other surfactant classes and retain their utility over a broad range of pH values. Their hydrophilic-lipophilic balance values range from 2 up to 18, depending on the structure. Chemically they include esters, ethers and amides. As a rule, chemicals in this class act as surfactants only if they carry at least one free OH group or an ether grouping, normally derived from ethylene or propylene oxide (Rieger, 1989).

1.9.2.4 Amphoteric Surfactants

The amphoteric surfactant group are commonly used in skin and hair products as relatively mild detergents. They are not particularly useful as emulsifiers and their capacity to bind to substrates exhibits a pH dependency. At high pH values they behave as anionics; at intermediate pH, they exhibit both anionic and cationic properties. They perform as cationic surfactants at low pH values (Rieger, 1989).

1.9.3 Cetrimide

1.9.3.1 Introduction

Cetrimide is a quaternary ammonium cationic surfactant (Rosen, 1989). Cetrimide is now defined to consist primarily of trimethyltetradecylammonium bromide, it may contain smaller amounts of dodecyl- and hexadecyl-trimethylammonium bromides. It contains 96.0 per cent to 101.0 per cent of alkyltrimethylammonium bromides, calculated as $C_{17}H_{38}BrN$ (M_r 336.4) (dried substance) (British Pharmacopoeia, 2007). However, the main component of the original cetrimide specified in the 1953 BP, was hexadecyl-trimethylammonium bromide. It has antiseptic and disinfectant properties.

1.9.3.2 Molecular Structure

The molecular formula of cetrimide is $C_{17}H_{38}BrN$ and its molecular weight is 336.4. The chemical structure of cetrimide is given in Figure 1.9.3.2.

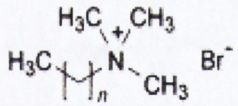

Figure 1.9.3.2 Chemical structure of cetrimide (British Pharmacopoeia, 2007)

1.9.3.3 Physicochemical Properties

Cetrimide is a white to creamy white, free flowing powder, having a faint but characteristic odour and a bitter soapy taste (Handbook of Pharmaceutical Excipients, 2005). It is freely soluble in water and in alcohol (British Pharmacopoeia, 2007). It has a solubility of 1 g in 10 ml of water (product MSDS, Sigma). The pH of a 1% w/v solution is between 5-7.5. Its melting point occurs in the range 232-247 °C. It is hygroscopic and at 40-50% relative humidity and 20 °C, its flow properties are retarded (Handbook of Pharmaceutical

Excipients, 2005). The solubility of cetrimide in a range of solvents is listed in Table 1.9.3.3.

Table 1.9.3.3 Solubility of Cetrimide in various solvents (Handbook of Pharmaceutical Excipients, 2005).

Solvent	Solubility
Water	Soluble
Hot water	Very soluble
Ethanol	Very soluble
Acetone	Sparingly soluble
Ether	Practically insoluble
Benzene	Practically insoluble

1.9.3.4 Antimicrobial Activity

Cetrimide has good bactericidal activity against Gram positive bacteria. The typical minimum inhibitory concentration (MIC) for *Staphylococcus aureus* is 10 μg/ml. It is less active in general towards Gram negative species than Gram positive. Typical MIC values for *Escherichia coli* and *Pseudomonas aeruginosa* are 30 μg/ml and 300 μg/ml, respectively. It is inactive against bacterial spores and relatively ineffective against fungi. It is most effective at neutral or slightly alkaline pH values. Its activity is appreciably reduced in acidic media (Handbook of Pharmaceutical Excipients, 2005).

1.9.3.5 Incompatibilities

Cetrimide is incompatible with alkali soaps, anionic surfactants and non-ionic surfactants in high concentrations. It is also incompatible with iodine, phenyl-mercuric nitrate, alkali hydroxides, acid dyes and bentonite clay (Handbook of Pharmaceutical Excipients, 2005).

1.10 ADSORPTION ISOTHERMS AT SOLID INTERFACES

1.9.1 Adsorption

Adsorption from a dilute aqueous solution onto the walls of the container or onto particulate matter present in suspension may involve specific chemical interaction between adsorbate and adsorbent (chemisorption). The most common interactions of this type

include an ion-exchange process in which the counterions of the substrate are replaced by surfactant ions of similar charge; hydrogen bond formation between adsorbate molecule and substrate and an ion-pairing interaction in which the surfactant ions are adsorbed onto oppositely charged sites unoccupied by counterions. Alternatively the interaction may be less specific as in adsorption through weak van der Waals forces between the adsorbent and adsorbate molecules. Frequently more than one mechanism may be involved in the adsorption process, for example the charged groups of the adsorbate may undergo chemical interaction, whilst the remainder of the molecule is adsorbed by van der Waals attraction (Attwood and Florence, 1983).

1.10.2 Adsorption Isotherms

Adsorption isotherms are traditionally determined by solution depletion methods (Fan *et al.*, 1997). After equilibration the surface excess is determined by change in the solution surfactant concentration. Conventionally the isotherms have been described as simple monolayers or bilayers. However more recent data suggests discrete surface aggregation. Techniques which probe the surface such as atomic force microscopy (AFM), neutron reflectivity and fluorescence measurements have been used to more fully elucidate surface features. However in the pre-aggregation region even the most advanced techniques provide inconclusive information. Adsorption isotherms can provide information concerning electrostatic interactions that occur at low surfactant concentration. They can also be used to monitor the change in surface charge as solution conditions and the amount of surfactant binding are altered.

Interpreting the results is based on discerning the rate of increase of surface excess (Γ) with concentration (c). The "two-step" and "four-region" isotherm models are two approaches employed to interpret results. The models appear to be fundamentally different but have much in common. They differ in their assignment of the initiation of hemimicelle aggregation. Hemimicelles are adsorbed surfactant aggregates on the substrate. The concentration at which a rapid increase in the surface excess occurs, indicating a cooperative adsorption process is referred to as the hemimicelle concentration (hmc). The four-region model predicts it occurs in region two, whilst higher concentrations are expected in the two-step model (Atkin *et al.*, 2003).

Gao *et al.* (1987) in work conducted on alkylpyridinium halides adsorbed to silica, determined two plateau regions in the adsorption isotherm. The plateau regions are depicted in Figure 1.10.2a. Region I is designated as low surface excess where attraction is via electrostatic interaction. The surface excess is primarily determined by the surface charge. Adsorption is sparse in this region so there is little interaction between adsorbed surfactant molecules. Region II is the first plateau region, here the substrate surface charge has been neutralised, however surfactants still adsorb as monomers in this region. Region III is a hydrophobic interaction region, where an abrupt increase in adsorption occurs at the hmc, monomers electrostatically attached in lower regions act as nucleation points for the admicellar structure. Region IV, above the CMC value is a second plateau, where the admicelle structure continues to develop into aggregates that are fully formed.

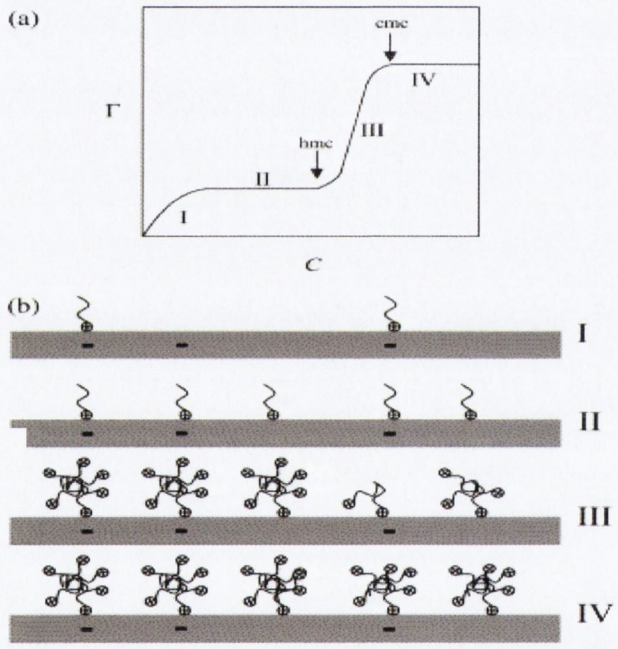

Figure 1.10.2a The "two step model" proposed for the adsorption of cationic surfactants to silica. Adapted from Gao *et al.* (1987).

The four-region or reverse orientation model proposed by Somasundaran and Fuerstenau (1966) for interpretation of surfactant adsorption isotherms when plotted on log-log scales is depicted in Figure 1.10.2b. Log-log plots amplify features at the low surface excess region.

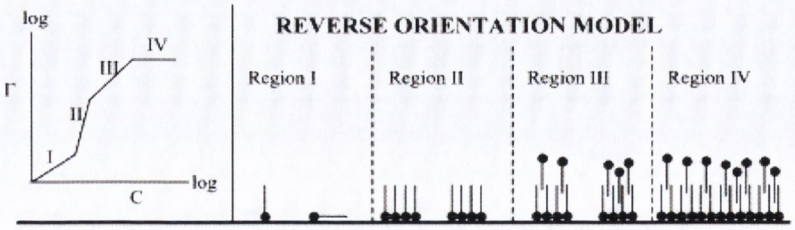

Figure 1.10.2b The four-region or reverse model of adsorption. Proposed adsorption isotherm and surfactant aggregates on solid substrates (Fan *et al.*, 1997).

Electrostatic attraction occurs in region I, the hydrocarbon tails interact with hydrophobic patches on the substrate. Primary aggregates form in region II due to the strong lateral interaction between adsorbed monomers. The hydrocarbon tails face the solution with the result that hydrophobic patches are formed on the surface. In the four-region model this aggregate is known as a hemimicelle. It can be seen from Figure 1.10.2b that an increase in the surface excess occurs in region III without an increase in the number of surface aggregates. The surface becomes hydrophilic again as head groups face into the solution. The transition from region II to region III is thought to be due to surface charge neutralisation. The surface morphology is assumed to be a fully formed bi-layer in region IV. The actual isotherm could be a combination of the two-step and four region models; however the four-region model is more valid as the two-step model does not account for lateral hydrophobic interactions that occur between surfactant structures (Atkin *et al.*, 2003).

1.11 SEMI-SOLID FORMULATIONS

1.11.1 Introduction

The vast majority of topically applied preparations are semi-solids; they have good residence time on the skin and can be used to deliver therapeutic agents over an extended period of time (Williams, 2003). Semi-solids include preparations such as ointments, creams, gels and pastes. Semi-solids are used mainly for topical drug delivery. They differ from other topical dosage forms such as hydroalcoholic solutions, powders and suspensions wherein the latter can be used for other routes of administration (McGuire *et al.*, 2000).

1.11.2 Ointments

1.11.2.1 Introduction

Ointments are usually greasy, semisolid preparations, which are often anhydrous, and which contain the medicament either dissolved or dispersed in the vehicle. Ointments are often mixed with fatty alcohols such as cetyl alcohol or stearyl alcohol or mixtures of these two as so-called matrix builders or bodying agents. The fatty alcohols are only sparingly soluble in paraffin hydrocarbons and crystallise in them at room temperature with an orthorhombic or monoclinic lattice. It is a typical layer lattice with an alternating structure of polar and non-polar levels. This results in the formation of a highly dispersed, three dimensional network. If the crystalline product is a simple, three dimensional network of filliform crystalline threads, then a simple gel matrix is present that merely causes an increase in consistency of the mass, but can scarcely prevent diffusion for the molecular dispersed substances dissolved in the remaining base. On the other hand, a lamellae-like structure of the three dimensional network can in addition to affecting consistency, also lead to an absolute diffusion barrier within the ointment barrier (Führer, 1982). Ointment bases can be classified into hydrocarbons, fats and fixed oils, silicones, adsorption bases, emulsifying and water-soluble bases.

1.11.2.2 Hydrocarbon Bases

Hydrocarbon bases usually consist of soft paraffin, (Vaseline, petroleum jelly or petrolatum) or a mixture of soft paraffin with hard paraffin to produce a suitable consistency. Paraffins deposit a greasy film on the skin surface, which retards moisture loss. This occlusive property improves the hydration of the horny layer in dry, scaly skin conditions. It is widely assumed that petrolatum is pharmacologically inert, but it is believed it may contain some trace compounds as it showed a response in a skin blanching test (Woodford and Barry, 1974). Plastibases® provide a series of hydrocarbon vehicles in which the manufacturing process incorporates polyethylene into mineral oil at high temperatures, followed by rapid cooling. The polyethylene, a large hydrocarbon polymer, forms the structural matrix in a system, which is fluid at the molecular level but is a typical dermatological semisolid at the macroscopic level. This feature suggests that drug release should be favoured from these vehicles compared to petrolatum systems. They are compatible with most medicaments and maintain their consistency even at high concentrations of solids. Plastibases® are soft, smooth, homogeneous, non-sensitising

vehicles, which display little change in apparent viscosity over the normal storage temperature range. The bases are easily applied and spread readily, adhere to the skin imparting a velvety, non-greasy feel and can readily be removed (Barry, 2002).

1.11.2.3 Fats and Fixed Oil Bases

Topical vehicles have frequently contained fixed oils of vegetable origin, which consist essentially of the mono-, di-, and triglycerides of mixtures of saturated and unsaturated fatty acids. The most common oils include peanut, sesame, olive, almond, arachis and maize oils. Such oils are prone to degradation on exposure to light air and high temperatures and they may become rancid. Addition of an antioxidant is usually necessary to minimise this. Trace metal contaminants may catalyse degradation (Barry, 2002).

1.11.2.4 Silicones

Silicones provide formulations with properties similar to hydrocarbon bases. The silicones are a family of polymers with a structure consisting of alternate atoms of silicon and oxygen, with organic groups such as phenyl or methyl bonded to the silicon backbone. Silicones are water repellent, with a low surface tension; they are used in barrier creams to protect the skin from water-soluble irritants (Barry, 2002).

1.11.2.5 Absorption Bases

Absorption bases possess hydrophilic properties so they can soak up water to form water-in-oil (w/o) or oil-in-water (o/w) emulsions yet retain their semisolid character. In general they are anhydrous vehicles composed of a hydrocarbon base and a substance that is miscible with the hydrocarbon but also carries polar and non-polar groups and therefore functions as a water-in-oil or an oil-in-water emulsifier. The polar groups may be hydroxyl, sulphate, sulphonate, carboxyl or an ether linkage. Typical materials include lanolin, cholesterol, lanosterol, acetylated sterols or partial esters of polyhydric alcohols such as sorbitan monostearate. Anhydrous lanolin is commonly known as wool fat, modifications of which include liquid lanolin and hydrogenated wool fat. Simple ointment BP, is a mixture of wool fat, hard paraffin, cetostearyl alcohol and white or yellow soft paraffin, absorbs about 15% of its weight of water to yield a water-in-oil emulsion. Wool Alcohols Ointment BP contains wool alcohols, hard paraffin, and white or yellow soft paraffin. It can absorb an equivalent weight of water. Absorption bases deposit a greasy

film on the skin surface in a manner similar to that of hydrocarbons, but they are not as effective in preventing the transepidermal water loss (Barry, 2002).

1.11.2.6 Emulsifying Bases

Emulsifying bases are somewhat similar to absorption bases but can form an oil-in-water system, for example using a mixture of paraffins with cetostearyl alcohol and a surface active agent (e.g. sodium lauryl sulphate (SLS) or cetrimide). The emulsifying agents thus generate a water-miscible ointment (i.e. they are self-emulsifying), which allows it to be readily washed from the skin, in contrast to the hydrocarbon bases. Differing bases can be prepared and are classified according to the ionic nature of the emulsifying agent. Anionic emulsifying bases contain an anionic emulsifying agent such as emulsifying wax, which contains a mixture of cetostearyl alcohol and SLS. This is the agent that is found in Emulsifying Ointment BP, comprising liquid paraffin (20%), white soft paraffin (50%) and emulsifying wax (30%). An anionic ointment is incompatible with a cationic therapeutic agent, as the structure of the base may be modified. Cationic emulsifying ointments containing for example cetrimide as the emulsifying agent are most suitable for use with cationic drugs, and non-ionic emulsifying bases (such as cetomacrogol as the emulsifier) can also be used with cationic medicaments. The surfactant can also help to solubilise the therapeutic agent and can help to wet the skin surface (Barry, 2002).

1.11.2.7 Water Soluble Bases

Water soluble bases contain mixtures of water soluble high and low molecular weight polyethylene glycols (macrogols). These ethylene glycol polymers are analogous to the paraffins in that they range from mobile liquids to hard waxes and hence can be blended to form an ointment with the desired properties. Water soluble bases have several important advantages over other ointment bases, they mix readily with skin secretions, they are chemically very stable, they soften at skin temperatures allowing them to spread easily (depending on the polymer composition) and therefore can be washed from the skin without difficulty. They are not occlusive. However, they do lose their semi-solid consistency if around 8% water is taken into the ointment and they are incompatible with several classes of compounds, including phenols, iodine and penicillin.

1.11.3 Creams

For pharmaceutical and medical uses, a cream can be defined as a semi-solid emulsion for application to the skin or mucous membranes. Creams are usually more acceptable to patients than ointments as they tend to be less greasy, are easy to apply and usually can be simply washed from the skin surface. However, they tend to be less occlusive than, for example, hydrocarbon base ointments and thus are less effective at hydrating the stratum corneum. An emulsion is a system of two liquid phases, one of which is dispersed as fine globules within the other. The globules can vary in size, typically from 0.25 to 20 μm in diameter, with emulsions containing predominantly large droplets termed "coarse" emulsions and those with a globule size around 5 μm diameter termed "fine" emulsions. Very fine globules with diameters down to 10 nm (i.e. little larger than a micelle) can be prepared; these systems are termed "microemulsions". The liquid droplets or globules form the disperse phase (or internal phase), whilst the liquid in which the droplets are dispersed is termed the continuous phase (or external phase). Typically emulsions appear milky except for microemulsions, which are generally transparent. Some microemulsions form spontaneously but generally an emulsion is an unstable system which requires the addition of an emulsifying agent to improve stability. Without the addition of an emulsifier, the dispersed globules flocculate, collide and coalesce and form even larger globules that would ultimately separate into the oil and water phases; this phenomenon is termed "cracking" or "demulsification". The emulsifier reduces flocculation and coalescence by steric or electrostatic repulsion of the globules. Additionally an emulsion can be stabilised to some extent by increasing the viscosity of the continuous phase, thus reducing the mobility of the droplets and hence reducing the potential for globule collision. Many materials can act as emulsifying agents, including surfactants (anionic, cationic or non-ionic), some proteins, polymeric hydrocarbons or alcohols and some finely divided powders such as bentonite.

Dermatological creams can be w/o emulsions, termed oily creams which tend to act as emollients and are used as cleansers. Since the continuous phase is oily, these creams are more occlusive than o/w systems, and can leave a protective oily layer on the skin surface as the water evaporates. More common are the o/w creams or washable creams with a continuous aqueous phase containing oily globules. Oil-in-water creams do not deposit an oily layer onto the entire skin surface; o/w creams can deliver lipophilic materials to the skin as well as water-soluble molecules from the continuous phase (Williams, 2003).

Describing topical and transdermal delivery from a cream is complex since the system is dynamic; the cream changes as the continuous phase evaporates and as the emulsion cracks (Higuchi, 1982). If a water soluble permeant is applied in an o/w cream, then as the water evaporates from the tissue surface, the degree of saturation of the permeant in the water phase will rise. This could increase drug delivery markedly, especially if the oil phase inhibits drug crystallisation, allowing the formation of a supersaturated state and hence permeation will be promoted. Conversely, if an aqueous permeant is incorporated into an oily w/o cream then the oil can deposit on the skin surface, thus providing an additional barrier to permeation for the hydrophilic permeant. Further, as an emulsion cracks, the micelles formed from the emulsifier can trap the drug within the continuous phase (Williams, 2003).

1.11.4 White Soft Paraffin (WSP)

1.11.4.1 Definition

WSP is a purified mixture of semi-solid hydrocarbons, obtained from petroleum. It may be partially or completely decolourised. It may contain a suitable antioxidant. WSP described in the BP (2007) monograph is not suitable for oral use (British Pharmacopoeia, 2007). It has the general formula, C_nH_{2n+2} in which chain branching is common. Petrolatum may contain some cyclic alkanes and aromatics with paraffin side chains. The average molecular weight is dependent on the source.

1.11.4.2 Description

WSP, also known as petrolatum, is an unctuous, soft mass. White petrolatum is white to faintly yellow in colour, while yellow petrolatum is pale yellow to yellow. Both types are odourless and almost tasteless, transparent in thin layers and not more than slightly fluorescent in daylight, even when melted (Handbook of Pharmaceutical Excipients, 2005).

1.11.4.3 Manufacture

WSP is manufactured from the semi-solid material that is left over from the steam or vacuum distillation of petroleum. The residue is de-waxed and/or blended with stock from other sources and lighter fractions to give the appropriate consistency. Final purification is by a combination of high pressure hydrogenation (or sulphuric acid treatment) and filtration through adsorbents. White petrolatum is more highly refined than the yellow.

Yellow and white soft paraffin differ only in colour, since WSP is bleached. Hard paraffin and microcrystalline waxes are chemically similar to WSP but contain no fluid components.

1.11.4.4 Properties

Petrolatum contains n-paraffins, isoparaffin and cyclic paraffin. The high content of these branched and cyclic components account for its softer character compared to paraffin, thus making it an ideal ointment base (Longworth and French, 1969; Barry and Grace, 1970). Soft paraffins form a two-phase colloidal gel type of structure, which contains liquid, microcrystalline and crystalline hydrocarbons. During preparation, when a molten sample cools, the stiffening wax phase develops into an amorphous, three dimensional network or matrix, which forms a compact structure with voids of molecular dimensions; the liquid phase binds to the matrix by a sorption mechanism. The proportions of the various paraffins vary considerably between batches and grades of petrolatum. Creep testing on pharmacopoeial grades of WSP highlighted that varying results for compliance values were observed. These differences can lead to problems with quality control. The diversity is due to variable sources of crude material, refinement methods and bleaching processes employed (Barry, 1974).

1.11.5 Polyethylene Glycol (PEG)

1.11.5.1 Introduction

PEGs are hydrophilic synthetic polymers. They are condensation polymers of ethylene oxide and water. Their relatively low price, water solubility and favourable toxicity have resulted in their use in a wide variety of pharmaceutical formulations (Handbook of Pharmaceutical Excipients, 2005).

1.11.5.2 Molecular Structure

The accepted chemical name is α-hydroxy-ω-hydroxypoly-(oxy-1, 2-ethanediyl). They have the general formula $HOCH_2(CH_2OCH_2)_nCH_2OH$ where n is the average number of oxyethylene groups. The number, which follows the name, indicates the average molecular weight of the compound. PEG 300 has a molecular weight between 285 and 315, where n is 6.4. In the case of PEG 4000 the molecular weight is in the range 3000 and 4800 and n lies between 69 and 84 (Handbook of Pharmaceutical Excipients, 2005).

1.11.5.3 Physicochemical Properties

Liquid PEGs (grades 200-600) are clear, colourless or slightly yellowish, viscous liquids. The odour is slight but characteristic, and the taste is bitter and slightly burning. PEG 600 can be semi-solid at ambient temperatures. Solid PEGs (grades 1000-2000) are white or off white in colour, and range in consistency between pastes and waxy flakes. A 5% solution has a pH in the range 4.5-7.5. Liquid PEGs have a density in the range 1.11-1.14 g/cm^3, while solid PEGs have a density in the range 1.15-1.21 g/ cm^3. PEGs are very hygroscopic, but this decreases with increasing molecular weight, whereas solid grades of 4000 and above have low hygroscopicity. All grades are soluble in water and miscible in all propotions with other PEGs. The solubility of PEGs in a range of solvents is given in Table 1.11.5.3.

Table 1.11.5.3 Solubility of solid PEGs in various solvents (Handbook of Excipients, 2005).

Solvent	Solubility
Methanol	Soluble
Ethanol	Soluble
Acetone	Soluble
Methylene Chloride	Soluble
Ether	Slightly soluble
Aliphatic Hydrocarbons	Slightly soluble
Liquid Paraffin	Insoluble
Fats	Insoluble
Fixed Oils	Insoluble

1.11.5.4 Applications

These include parenteral, ophthalmic, oral, rectal and topical products. In solid dosage formulations, higher molecular weight PEGs can be used to enhance the effectiveness of tablet binders, to impart plasticity to granules and in film coating as plasticisers. Solid grades are employed in topical ointments with the consistency of the base being adjusted by the addition of liquid grades of PEG (Handbook of Pharmaceutical Excipients, 2005).

1.12 SALICYLIC ACID

1.12.1 Molecular Structure

The accepted chemical name of salicylic acid is 2-hydroxybenzenecarboxylic acid. Its molecular formula is $C_7H_6O_3$ and its molecular weight is 138.1 (British Pharmacopoeia, 2007). The chemical structure is given in Figure 1.12.1.

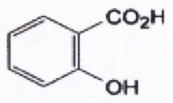

Figure 1.12.1 Chemical structure of salicylic acid (British Pharmacopoeia, 2007).

1.12.2 Physicochemical Properties

Salicylic acid occurs as white, fine needle-like crystals or as a fluffy, white, crystalline powder. Synthetic salicylic acid is white and odourless. The acid prepared from natural salicylate may have a slightly yellow or pink tint and a faint wintergreen-like odour. The acid has a sweetish, afterward acrid, taste. It is stable in the air (Abounassif *et al.*, 2004). Salicylic acid has a melting point in the range 157-159 °C. The pH of a saturated solution is 2.4 (The Merck Index, 1989).

The volume of various solvents required to dissolve 1 g of salicylic acid is given in Table 1.12.2. Salicylic acid has pKa values of 2.97 and 13.4 (Drug Information Full Text, 2006).

Table 1.12.2 The volume of solvent required to dissolve 1 g of salicylic acid (The Merck Index, 1989).

Solvent	Volume (ml)
Water	460
Boiling water	15
Alcohol	2.7
Acetone	3
Chloroform	42
Ether	3
Benzene	135
Glycerol	60
Fats or oils	80

1.12.3 Spectral Properties

1.12.3.1 UV Absorption Spectrum

The UV spectrum of salicylic acid in ethanol (4 mg %) was scanned from 200-400 nm, it was characterised by maxima at 210, 234 and 303 nm (Abounassif *et al.*, 2004).

1.12.3.2 Infrared (IR) Spectrum

Structural assignments of salicylic acid were correlated with band frequencies and are given in Table 1.12.3.2.

Table 1.12.3.2 IR characteristics of salicylic acid (Abounassif *et al.*, 2004).

Wavenumber (cm^{-1})	Assignments
3220	-OH
3050	Aromatic C – H stretch
1650	- C = O (carboxylic)
1440	C = C stretch
690	Aromatic C – H bending

1.12.4 Uses and Adverse Effects

Salicylic acid is not employed internally as an analgesic due to its local irritating effect on the gastrointestinal tract. It is employed externally on the skin, where it exerts a slight antiseptic action and a marked keratolytic action. The latter action makes salicylic acid a beneficial agent in the local treatment of warts, corns, fungus infections and certain forms of eczematoid dermatitis. Tissue cells swell, soften and ultimately desquamate. Salicylic acid is applied as a 2 to 20% concentration in lotions or ointments and as a 10 to 40% concentration in plasters. Salicylic acid plaster is used for the destructive effect of salicylic acid on hardened, keratinised tissue (Drug Information Full Text, 2006).

Salicylic acid has keratolytic properties (Sweetman, 2005) and is applied topically in the treatment of hyperkeratic and scaling skin conditions such as dandruff, ichthyosis and psoriasis. Initially a concentration of about 2% is used, increased to about 5% if necessary. It is often used in conjunction with other agents such as benzoic acid, coal tar, resorcinol and sulphur. Salicylic acid also possesses fungicidal properties and is used topically in the treatment of such fungal skin infections such as tinea. Salicylic acid is a mild irritant and application of preparations containing it to the skin may cause dermatitis.

Salicylic acid is further applied in the treatment of acne and psoriasis in various concentrations depending on the desired amount of keratolysis. Its keratolytic mechanism is not fully elucidated, but salicylic acid's dermatopharmacological effect may be related to its impact on the SC structure affecting intercorneocyte cohesion and sequamation (Bashir *et al.*, 2005).

1.13 METRONIDAZOLE

1.13.1 Introduction

Metronidazole is an antibacterial agent with activity against protozoa and anaerobic bacteria. It has a wide range of uses including amoebiasis, giardiasis, trichomoniasis vaginosis, antibiotic-associated colitis, surgical infection prophylaxis, peptic ulcer, inflammatory bowel disease and rosacea (Sweetman, 2005).

1.13.2 Molecular Structure

Metronidazole is defined chemically as 2-(2-methyl-5-nitro-1H-imadazol-1-yl)ethanol. Its molecular formula is $C_6H_9N_3O_3$ and its molecular weight is 171.2 (British Pharmacopoeia, 2007). The chemical structure of metronidazole is given in Figure 1.13.2.

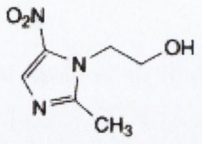

Figure 1.13.2 Chemical structure of metronidazole (British Pharmacopoeia, 2007).

1.13.3 Physicochemical Properties

Metronidazole is a white to pale yellow, odourless crystalline powder. It has a melting point in the range 159 to 163 °C (British Pharmacopoeia, 2007). A saturated solution has a pH of 5.8 (The Pharmaceutical Codex, 1994). The solubility of metronidazole in various solvents at 25 °C is given in Table 1.13.3. Metronidazole is soluble in dilute acids (The Pharmaceutical Codex, 1994).

Table 1.13.3 Solubility of metronidazole in various solvents at 25 °C (Wearley and Anthony, 1976).

Solvent	Solubility (mg/ml)
Water	10.5
Methanol	32.5
Ethanol	15.4
Chloroform	3.8
Heptane	<0.01

1.13.4 Spectral Properties

1.13.4.1 UV Absorption Spectrum

Metronidazole exhibits an absorption maximum at about 274 nm using 0.1 N sulphuric acid in methanol as a solvent (Wearley and Anthony, 1976).

1.13.4.2 Infrared (IR) Spectrum

Structural assignments of metronidazole were correlated with band frequencies and are given in Table 1.13.4.2.

Table 1.13.4.2 IR characteristics of metronidazole (Wearley and Anthony, 1976).

Wavenumber (cm^{-1})	Assignments
3230	-OH stretch
3105	C = CH; C – H stretch
1538 & 1375	NO_2; N-O stretch
1078	C – OH; C – O stretch
830	C – NO_2; C – N Stretch

1.13.5 Metronidazole Uses

Metronidazole may be effective in the management of ulceration of the skin including pressure sores and fungating tumours. Metronidazole 200 mg three times daily successfully reduced the smell of an ulcerating tumour in a woman with breast cancer (Ashford, 1980).

A topical gel formulation of metronidazole has been developed which can be applied to fungating tumours and other severe skin lesions to control offensive odour. Once daily application has proved effective. Treatment is supplemented by metronidazole irrigation for wound cleansing large or deep cavities (Allwood, 1988).

Several double blind studies have indicted metronidazole is effective in the treatment of rosacea. Metronidazole 200 mg twice daily by mouth was significantly better than placebo (Pye and Burton, 1976) and was as effective as oxytetracycline by mouth (Saihan and Burton, 1980). Similarly, topical application of a 1% cream was found to be as effective as oxytetracycline by mouth (Nielsen, 1983). A 0.75% metronidazole gel also proved effective when compared with placebo in patients with acne rosacea, although the mode of action is still unknown (Sweetman, 2005).

1.14 UREA

1.14.1 Introduction

Urea is a defined by the BP (2007) as a carbamide. Its molecular formula is CH_4N_2O and the molecular weight is 60.1. The chemical structure is given in Figure 1.14.1.

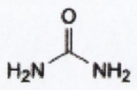

Figure 1.14.1 Chemical structure of urea (British Pharmacopoeia, 2007).

1.14.2 Characteristics

Urea is a white crystalline powder or transparent crystals. It is slightly hygroscopic. It is very soluble in water, soluble in alcohol and practically insoluble in methylene chloride (British Pharmacopoeia, 2007). Urea may gradually develop a slight odour of ammonia on prolonged standing (USP online). It is fairly rapidly absorbed from the gastrointestinal tract and causes irritation. It is distributed into extracellular and intracellular fluids including lymph, bile, cerebrospinal fluid and blood. It is reported to cross the placenta and penetrate the eye. It is excreted unchanged in the urine (Sweetman, 2005).

1.14.3 Uses

Urea is an osmotic agent similar to mannitol. However it is mainly applied topically in the treatment of icthyosis and hyperkeratotic skin disorders (Sweetman, 2005). The BP (2007) defines the use of urea as that of a keratolytic. In the management of icthyosis and other dry skin conditions it is applied in creams or lotions containing 5 to 25% urea. A preparation containing 40% urea may be used for nail destruction. Topical preparations may be irritant to sensitive skin (Sweetman, 2005). It is also used for its humectant properties (Clarke, 2004; McGuire *et al.*, 2000). Urea labelled with carbon – 13 is used in the *in-vivo* diagnosis of *Helicobacter pylori* infection. A single dose of ^{13}C urea is taken by mouth and a breath or blood sample is taken 30 minutes later. The bacteria produces urease, which hydrolyses the urea to carbon dioxide and ammonia, therefore an excess of carbon-13-labelled carbon dioxide in the sample, compared with a baseline sample indicates that an infection is present.

Chapter 2

MATERIALS

In general, except where otherwise stated, reagent grade chemicals were used. The qualities or grades of materials listed here are those quoted by the manufacturer. Most of these correspond in quality, though not by name, to either the General Purpose Reagent (GPR) or Analar Grade used by BDH Chemicals (UK).

Description	Lot/Batch Number	Supplier
Acetic acid, glacial	K28440836052	BDH Laboratory Supplies, UK
Acetonitrile		Solvent stores, TCD-BDH
Aqueous Cream	37270	Pinewood Healthcare, Ireland
Benzalkonium chloride	110K2503	Sigma Chemical Co., USA
Calcium chloride dihydrate	A609382526	Merck KGaA, Germany
Cetostearyl alcohol	CD60800002	Cognis GMBH, Germany
Chitosan	Low molecular weight, 4075681	Fluka Chemicals
Chloroform		Solvent stores, TCD
Citric acid	F1375138	BDH
Diprosalic® ointment	03E1414	Schering – Plough, England
Disodium hydrogen phosphate dodecahydrate	A484279344	Merck KGaA, Germany
Dodecylpyridinium chloride hydrate	08809MS-245	Sigma Chemical Co., USA
Ethanol		Solvent stores, TCD-BDH
Glutaraldehyde	6840099	Sigma Chemical Co., USA

Description	Lot/Batch Number	Supplier
Halloysite Balekisir		Central Anatolia, Turkey
Halloysite G	Batch No.: 12/98	NZ China Clays Ltd.
Hexadecylpyridinium chloride	664K0039	Sigma Chemical Co., USA
Hexadecyltriemethylammonium bromide	JF06730H1	Aldrich
Hexane		Solvent stores, TCD
Hydrochloric acid (37% w/w; 1.18 g/ml)	3211599-114	A.C.S. Reagent, Aldrich
Liquid paraffin		BDH Laboratory Supplies, UK
L-ascorbic acid	57H1246	Sigma Chemical Co., USA
Lipoid® S75		Lipoid GmBH, Germany
Lipoid® S100		Lipoid GmBH, Germany
2-methyl-5-nitro-1-imadazole ethanol	455161/1	Fluka Chemicals
1-Octanesulfonic acid sodium salt	54051/1, 1171408	Fluka Chemicals
PEG 300	442747/1	Fluka Chemicals
PEG 4000	445230/1	Fluka Chemicals
Perchloric acid	36080	Riedel-de Haen, Germany
Petroleum jelly		Lennox chemicals
Potassium bromide	50K3691	Sigma Chemical Co., USA
Potassium chloride	TA928037	BDH Laboratory Supplies, UK
Rozex® Gel 0.75%	5079006	Galderma, United Kingdom
Salicylic acid	K34847660532	BDH Laboratory Supplies, UK
Silastic® Membrane 7-4107	2252981	Dow Corning Corp., USA.
Sodium alginate	Lot: 89H0178	Sigma Chemical Co., USA
Sodium bicarbonate	81K0247	Sigma Chemical Co., USA
Sodium bromide	440459/1	Fluka Chemicals

Description	Lot/Batch Number	Supplier
Sodium chloride	K9405432	BDH Laboratory Supplies, UK
Sodium citrate dihydrate	073K0082	Sigma-Aldrich Chemical Co., USA
Sodium dihydrogen phosphate dihydrate	K91867448324	Merck KGaA, Germany
Sodium hydroxide pellets	13260	Riedel-de Haen, Germany
Sodium lauryl sulphate	39H0077	Sigma Chemical Co., USA
Sodium polyphosphate	JR01112ER	Aldrich Chemicals, USA
Sodium dithionite	1105341	Fluka Chemicals
Sodium dodecylbenzene sulphate	455609/1	Fluka Chemicals
Tetradecyltrimethylammonium bromide	459903/1	Fluka Chemicals
Tropaeolin 000 No. 2	304250/1	Fluka Chemicals
Urea	32270	Riedel-de Haen, Germany
Water	HPLC grade and deionised	

Chapter 3

METHODOLOGY

3.1 PREPARATION OF HALLOYSITE POWDER SAMPLES

3.1.1 Cetrimide Coated Halloysite

A 0.2% w/v solution of cetrimide was prepared by dissolving cetrimide (2.0 g) in HPLC grade water (1 litre). Halloysite (10 g) was dispersed in this solution with the aid of an Ultra Turrax® stirrer. The contents were stirred for 8 hr using a stirring plate (Stuart Scientific). The contents were left to equilibrate over night. The cetrimide coated halloysite was removed by vacuum filtration and then dried in an oven at 40 °C for 24 hr. The material was then ground in a pestle and mortar. It was sieved using an apperture size of 125 μm.

3.1.2 Extraction of Balekisir Halloysite

A sample of the crude Balekisir halloysite rock (approximately 50 g) was weighed out. The rock was broken up into peanut size pieces using a hammer; 20 g was weighed out and placed in a metallic beaker. HPLC grade water (100 ml) was added. The mixture was agitated using a multi-blade Heidolph® stirrer for 30 min. The stirrer speed was arbitrarily set at dial no. 6 in order that adequate agitation was achieved. The water quantity was sufficient to allow the pieces of rock to be further size reduced via autogenous grinding. This is a process whereby the particles impact off each other, resulting in size reduction. Size reduction is also achieved by impaction with the blade of the stirrer and the container walls. At the end of the grinding process, the material was sieved using a sieve with an aperture size of 125 μm. The container was washed with some HPLC grade water and the washings were added to the sieved material. The contents were then transferred to a graduated cylinder (100 ml) and brought back to the original volume of 100 ml, and labelled sample A. The solids remaining on the sieve were then subject to the above autogenous grinding procedure again and the material recovered was labelled sample B. The samples were left to settle for 24 hr. Following the 24 hr settling period, the

supernatant and the top layer of sediment from sample A was removed, and left to settle for a further 24 hr, it was then dried to constant weight at 50 °C for 48 hr in an oven. This was labelled sample C. The remainder of sample A was then agitated for 30 min, made up to 100 ml and then left to settle for 24 hr prior to drying. The top layer of sediment was labelled sample D and the remainder sample E. The original sample was sub-divided into a number of samples labelled A-E, in order to determine if a purer sample could be obtained using the extraction process as outlined above.

3.1.3 Acid Washed Halloysite G

Halloysite G (20 g) was added to a graduated cylinder. 50 ml of Hydrochloric Acid (37% w/w) was added to the contents. The cylinder was capped and gently inverted, to ensure all the halloysite was in contact with the acid. The lid was removed after each inversion, to relieve the pressure build up due to the evolution of heat and any gases that formed. The contents were left to settle overnight. The supernatant was removed and the halloysite was washed with HPLC grade water until the pH of the contents was at least 5. The treated clay was dried at 50 °C in a forced air circulation oven for 24 hr. The clay was ground down to a powder using a pestle and mortar and sieved using an aperture size 125 μm.

3.1.4 Deferration of Halloysite G and Balekisir Halloysite

Halloysite (10 g) was added to a large glass beaker and 125 ml of 0.3 M solution of sodium citrate was added to the clay. A 12.5 ml volume of 1.0 M sodium bicarbonate solution was also added. The contents were heated to 75 °C and stirred for 15 min, at which point 25 ml of 0.54 M sodium dithionite solution was added. The contents were heated for a further 15 min at 75 °C, they were then left to cool to room temperature. Excess liquid was removed and the clay was centrifuged at 3000 rpm for 30 min. The deferration process was repeated. The content appeared grey after the first deferration process and the supernatant had a slight yellow appearance. After the second deferration process the samples appeared whiter, the supernatant did not appear yellow. The contents were left to dry at ambient temperature and were sieved using an aperture size of 125 μm. The pink colour of the Balekisir sample was removed by the deferration process.

3.1.5 Thermogravimetric Analysis (TGA)

Halloysite G, Balekisir halloysite and deferrated samples of each clay were heated to 800 ^{o}C using a Mettler Toledo (TC 15) thermogravimetric analysis apparatus. Powder samples in the weight range 7-10 mg were accurately weighed into an alumina (70 µl) sample pan and placed on an analytical pan in the sample furnace. The sample was heated at a rate of 10 ^{o}C per minute and the resultant weight loss was determined using Star^{e} software®.

3.2 CHARACTERISATION OF HALLOYSITE POWDER SAMPLES

3.2.1 X-Ray Diffraction (XRD)

X-ray diffraction (XRD) patterns were obtained using a Siemens D500 X-ray powder diffractometer. Powdered samples were studied by placing a thin layer of the powder in conventional cavity mounts. The samples were scanned in all cases from 5 to 75° 2θ. A 1.00^{o} dispersion slit, a 1.00^{o} antiscatter slit and a 0.15^{o} receiving slit were used. The Cu anode X-ray was operated at 40 kV and 20 mA in combination with a Ni filter to give monochromatic Cu Kα X-rays, λ=1.5056 Å.

3.2.2 Scanning Electron Microscopy (SEM)

SEM was used to evaluate halloysite powder samples. The samples were mounted on aluminium stubs using double-sided sticky tape. The samples were coated with a thin film of gold in a Polaron SC500 sputter coater (UK) and examined using a field emission Hitachi S4300 scanning electron microscope (Japan). The analysis allowed an examination of the size and surface appearance of the particles in the powder samples. The effects of the chemical modification procedures and of coating halloysite with cetrimide on the appearance of the halloysite particles could be observed. Spray-dried complexes and beads formulations were analysed in the same manner. Estimations of particle dimensions due to the various processes and also the presence of debris could be determined.

3.2.3 Fourier Transform Infrared Spectroscopy (FTIR)

FTIR was carried out using a Perkin Elmer paragon 1000 fourier transform infra-red spectrometer. Potassium Bromide (KBr) discs were prepared using sample loadings of 0.1% w/w in the case of cetrimide and a 0.03% w/w loading in the case of samples containing halloysite. A more dilute KBr disc containing halloysite was prepared due to the high spectral absorption of silica, a constituent of the halloysite mineral. Discs were

prepared by grinding the sample with KBr in an agate mortar and pestle. The sample mixture was then placed in an evacuated KBr punch and die set. Eight tonnes of pressure were applied to the sample in a Graseby Specac IR press. Two FTIR spectra were obtained for each sample system.

3.2.4 Density Studies

3.2.4.1 Bulk and Tapped Density

A 100 g of sample was introduced into a dry graduated cylinder (250 ml) without compacting it. The sample volume was noted. The cylinder was placed in the holder of a settling apparatus (Copley Scientific, UK). The test was carried out in accordance with Appendix XVII D of the British Pharmacopoeia, 2007. The sample was tapped and the volume was noted after the specified number of taps (10, 500 and 1250 times). It was not necessary to carry out a further 1250 taps (final tap amount 2500) as the resultant change in sample volume after 1250 taps was not observed to change by 2 ml or more compared to the volume after 500 taps. The bulk density is the density of the poured material. The tapped density is the density of the sample after it has been tapped 1250 times. Each sample was examined in triplicate.

3.2.4.2 Apparent Density

The apparent density of halloysite, cetrimide coated halloysite and acid washed halloysite was determined using a liquid displacement method. The liquid chosen was hexane. The pre-weighed sample was placed in a density bottle (BS733, Jay Tec, UK). The volume of the bottle was calculated using a fixed weight of water. The density of water was known; hence the corresponding volume was calculated. It was possible to calculate the density of hexane because the container volume had been calculated. A fixed weight of each sample specified was placed in the bottle and hexane was added. The contents were maintained at 25 ^{o}C in a water bath until hexane ceased to emerge from the stoppered bottle. The bottle was re-weighed. Subtraction of the powder weight from the content weight gives rise to the weight of the hexane, the density of which has already been calculated. The volume occupied by the powder sample is equivalent to the displaced hexane volume; this can be used to calculate the density of the powder sample.

3.2.4.3 Helium Pycnometry Studies

Helium pycnometry was used to obtain the skeletal density of materials. It was carried out using a calibrated AccuPyc 1330 (Micromeritics, USA). The calibration standard had a volume of 0.718463 cm^3 (Micromeritics, USA). Prior to analysis, the samples were dried overnight to a constant weight in a vacuum oven at 50 °C with a vacuum pressure of 600 mbar. These storage conditions were considered to be adequate for all samples after the weight of a test sample stored as outlined was determined at appropriate intervals using an electronic balance (Sartorius®). Powdered halloysite samples were analysed, with their mass being accurately determined prior to analysis using an MT5 microbalance (Mettler Toledo, Switzerland). Each sample was analysed in duplicate using the run parameters given in Table 3.2.4.3. Following analysis the sample was re-weighed. Where the mass differed from that prior to the run, this mass was used to calculate sample density. This difference can occur if contaminating gases or water were present in the sample prior to analysis. These would be removed by purging during analysis making the post analysis mass a more accurate measure of the sample mass.

Table 3.2.4.3 Run parameters used in helium pycnometry analysis.

Volume of sample cup (cm^3)	1
Number of purges	10
Purge pressure (p.s.i.)	19.5
Number of runs	50
Run fill pressure (p.s.i.)	19.5
Equilibration rate (p.s.i./min)	0.0050
Run precision	Yes
Percent full scale	0.05

3.2.5 Surface Area Analysis

Surface area analysis was performed using a Micromeritics Gemini 2370 Surface Area Analyser with nitrogen as the adsorptive gas. The Gemini system is a balanced adsorption apparatus, which uses a technique known as SMART (a sorption method using adaptive rate technology) i.e. adsorbate gas is supplied to the sample at exactly the rate that the sample can adsorb it (Camp and Stanley, 1991). Moisture was removed from the samples using a vacuum oven set at 50 °C for 24 hr prior to analysis. Subsequently, samples were

degassed for 24 hr using a Micrometrics FlowPrep 060 Degasser. The FlowPrep uses a flowing gas (helium), which is passed over a heated sample (50 ^{o}C) to remove moisture and other contaminants. Following degassing the sample mass was determined. The mass used was sufficient to ensure that the surface area available for analysis was greater than 1 m^2, as this gives greatest accuracy.

The Gemini analyser consists of two tubes of matched internal volume; one of these tubes contains the sample while the other is empty. The tubes are either classed as small tubes or large-bulb tubes, the latter being used for samples, which have a low surface area. The tubes contain filler rods, these filler rods (hollow glass rods) reduce the amount of gas above the sample and hence act to minimise the pressure 'noise' caused by the boiling of the liquid nitrogen and lead to more precise measurement. The filler rods achieve and improve baseline performance by reducing the random pressure fluctuations caused by slight temperature variations at or near the liquid nitrogen surface. By displacing most of the gas from this gradient region, the filler rods leave less gas to expand and contract in response to temperature changes. Without the random pressure fluctuations, the Gemini system can achieve a much closer balance of pressures and precise gas uptake measurement. However the importance and necessity to use the filler rods is diminished when samples with large surface areas, such as the clay samples examined in this study. However the filler rods were nonetheless used to maximise accuracy and precision.

A powdered halloysite sample (sieved through an aperture size of 125 μm) was added to a small sample tube to a depth of approximately one inch. An equal volume of inert material having negligible surface area was added to the balance tube (3 mm solid glass beads were used) in the case of the bead samples, in order to provide a more accurate result as the bead formulations had a smaller surface area than the halloysite powder. Approximate volume balance was attained, confirmed by the ΔFree Space value being –0.5 to +0.5 cm^3 in all cases. A short filler rod was inserted into the tube containing the sample and a long filler rod was placed in the other small glass tube. Helium was used for free space measurement, while nitrogen was used as the adsorptive gas. The saturation pressure (P_o) was measured each day. The operating conditions used in the determination of the BET surface area of the samples were an evacuation rate of 500 mm Hg/min and an evacuation time of 3 min with an equilibration time of 10 sec.

BET multipoint surface areas were determined. The volume of nitrogen adsorbed at six relative pressure points between 0.05 and 0.3 units was measured. This is the range to which the linearity of the BET plot is usually restricted (Sing *et al.*, 1985). The BET multipoint area was calculated using either five or six of the measured points (i.e. the surface area was calculated with all six points and then recalculated omitting the first point or the last point; whichever result gave the highest correlation coefficient for the fit of the BET plot was selected). Analyses were performed at least in duplicate. The relative pressures listed in Table 3.2.5 were used to determine an adsorption isotherm for halloysite G.

Table 3.2.5 Relative pressures at which the volume of nitrogen adsorbed on the halloysite G sample were determined.

Point number	Relative pressure	Point number	Relative pressure	Point number	Relative pressure
1	0.0010	**10**	0.1250	**19**	0.5000
2	0.0025	**11**	0.1500	**20**	0.5500
3	0.0050	**12**	0.1750	**21**	0.6000
4	0.0075	**13**	0.2000	**22**	0.6500
5	0.0100	**14**	0.2500	**23**	0.7000
6	0.0250	**15**	0.3000	**24**	0.7500
7	0.0500	**16**	0.3500	**25**	0.8000
8	0.0750	**17**	0.4000	**26**	0.8500
9	0.1000	**18**	0.4500	**27**	0.9000

3.2.6 Qualitative Energy Dispersive X-ray (EDX) Microanalysis

Qualitative EDX microanalysis was carried out on halloysite and chemically treated halloysite samples. A qualitative and semi-quantitative analysis was conducted on samples. The samples were mounted on aluminium stubs using adhesive carbon tape. This method of analysis applies to products containing an element with an atomic number ranging from 11 to 62 in the periodic table. The powder samples were coated using a carbon rope in a Polaron E6300 vacuum evaporator (UK). The samples were then examined using a variable pressure scanning electron microscope (Hitachi S-3500N, Japan) and an X-ray

detector (Princeton Gamma Tech). The elemental analysis was performed at different spots on the samples so that the elemental content could be obtained.

3.2.7 Inductive Coupled Plasma-Mass Spectrometry (ICP-MS)

A known weight of each halloysite powder sample was digested with concentrated hydrochloric acid (HCl) and hydrogen peroxide (H_2O_2) with heat prior to analysis. The digested material was diluted with deionised water to a known final volume. A dilution of this digest was analysed. The instrument used was an Agilent 7500a ICP-MS in quantitative mode. Semi-quantitative analysis was initially carried out to determine the levels of the various elements present. The elements were then analysed quantitatively using six different standard curves with at least five individual standards per curve. The levels of aluminium and silicon in the samples were not determined due to i) their very high levels in the sample and ii) silicon would not be digested fully by the technique used. The above work was conducted by the Centre for Microscopy and Analysis, Trinity College Dublin.

3.2.8 Evaluation of the Flow Properties of Halloysite and Cetrimide Coated Halloysite

3.2.8.1 Introduction

The flow properties of halloysite and cetrimide coated halloysite were investigated in order to quantitatively assess any improvement in flow as a result of coating with the cationic surfactant.

3.2.8.2 Flowability (Flodex® Tester) of Halloysite Powders

The flodex determination of intrinsic flowability is based upon the ability of a powder to fall freely through a hole in a plate. For convenience the flowabilty index is given in millimeter diameter of the smallest hole the powder falls through freely on three successive attempts. This type of unit may be used to establish dry powder flow characteristics prior to using the powders in large scale production processes.

The test apparatus is comprised of a stainless steel cylinder with an approximate capacity of 200 ml. Also supplied was a series of stainless steel discs each with a precision drilled hole in the centre (covering a range from 4 to 32 mm diameter). Each disc was attached to

form a bottom for the cylinder. A shutter covered the hole during the filling operation. This could be removed smoothly, without vibration to allow powder to flow through the hole.

The test was started with the 16 mm hole or aperture. Once the disc was in position and the shutter closed, 50 g of halloysite sample or cetrimide coated halloysite was introduced into the cylinder. The shutter was opened after approximately 30 sec.

The test was positive if the powder flowed through the hole leaving a residue in the cylinder in the form of an upside-down truncated cone. A powder that flocculates in bulk will fall abruptly forming a cylindrical cavity. If the powder did not flow through the hole, the test was negative. In the case of a positive result the test was repeated with smaller apertures until the result was negative. For negative results, the size of the apertures was increased until the test was positive. The procedure was repeated for cetrimide coated halloysite.

3.2.8.3 Static Angle of Repose of Powder Mixes

The static angle of repose is the angle between the horizontal and the slope of a cone of material. It is formed when excess feed material falls away from a cone of material supported on a stand. The apparatus comprised of a stainless steel cylinder with an approximate capacity of 1 L mounted, which is open at both ends. This cylinder was mounted on a stand, which covered the bottom of the cylinder. Approximately 100 g of a powdered halloysite or cetrimide coated halloysite sample was introduced into the cylinder. After approximately 30 sec the cylinder was slowly lifted off the powder sample. The powder sample formed a cone shape on the stand. The height of the cone was carefully measured. The static angle of repose of a powder sample was determined using Equation 3.1.

$$\text{Static angle of repose } (\tan^{-1} \text{ degrees}) = \frac{2h}{D} \qquad \textbf{Equation 3.1}$$

where h = axial height of cone (cm)

D = diameter of platform (cm)

The angle of repose quoted was an average of six determinations. The angle of repose is a direct indication of the potential flowability of a material. The lower the angle of repose of a dry material, the more flowable it is.

3.3 CHARACTERISATION OF SURFACTANT - HALLOYSITE ADSORPTION ISOTHEMS

3.3.1 Critical Micelle Concentration (CMC) Determination

3.3.1.1 Introduction

The CMC value of a range of surfactants was determined using the surface tension method. The effect of the electrolytes, potassium chloride (KCl) and sodium bromide (NaBr) on the CMC value of specific systems was also investigated. The CMC of trimethyltetradecylammonium bromide (TTAB) grade of cetrimide was also determined using conductivity measurements.

3.3.1.2 Surface Tension Method

Solutions of surfactants in the concentration range 0.001-0.4% w/v were prepared by making serial dilutions of a stock aqueous solution of each surfactant. The glassware was rinsed thoroughly with deionised water in order that the CMC value was not influenced by contaminants from external sources. The surface tension of each concentration was determined using a Lauda® TD1 tensiometer. A plot of surface tension versus surfactant concentration was plotted. The CMC value occurs at the point of inflection of the plot.

3.3.1.3 Conductivity Method

The conductivity of the TTAB solutions prepared as outlined in Section 3.3.1.2 was determined using a Cyberscan 500® conductivity meter. A plot of conductivity against concentration was plotted. The CMC value occurs at the point of inflection of the conductivity plot.

3.3.2 Halloysite Adsorption Isotherm

3.3.2.1 Introduction

The adsorption of a range of surfactants on halloysite was determined using a depletion method. Halloysite G was the adsorbent used in all cases. UV spectrophotometery was used to determine the unbound surfactant concentration except in the case of quaternary ammonium surfactants. A dye method in conjunction with UV spectrophotometery was used to quantify quaternary ammonium surfactants. A HPLC method was also investigated. A factorial study was conducted on the adsorption of TTAB on halloysite G. The effect of chemically modifying halloysite with concentrated hydrochloric acid was investigated. The equilibration contact time of the surfactant with the adsorbent was also examined.

3.3.2.2 Surfactant Isotherms - Depletion Method

The depletion method was employed to determine the extent of surfactant adsorption on halloysite. The adsorbed surfactant is the difference between that detected after the equilibration process and the original quantity added. An equal quantity of the adsorbent material was added to screw capped tubes. Varying quantities surfactant solutions were added to each tube. The contents were made up to final volume (40 ml) with deionised water. If electrolyte was included in the system, an equal quantity was added to each tube at this stage. The samples were inverted end over end in a Turbula tumbler mixer (Switzerland) for a period of 24 hr or otherwise where indicated. After the inversion period the samples were allowed to settle. A 10 ml volume of supernatant was centrifuged at 5000 rpm. A portion of the resultant supernatant was then filtered through a 0.45 μm membrane filter (Millex®-HV PVDF). Samples were diluted where appropriate. The filtrate was examined for surfactant content using UV spectrophotometery (Heλios, Thermo Spectronic, Electron Corporation) at an appropriate wavelength for all surfactant groups except for the trimethylammonium bromide compounds. The surfactant quantity was determined using an appropriate calibration equation, Appendix 1. The quaternary ammonium compounds were quantified using two methods, a dye method and a high performance liquid chromatography method (HPLC) method. Table 3.3.2.2 depicts the surfactant adsorption isotherm systems examined, the method of surfactant quantitation and the appropriate wavelength.

Table 3.3.2.2 Surfactant adsorption systems examined and the method of detection used for each system.

Surfactant	Electrolyte (mM)	Detection Method (wavelength, λ - nm)
Tetradecyltrimethylammonium bromide (TTAB)	-	Dye method - UV 486 nm HPLC method - UV 205 nm
TTAB	NaBr (150)	Dye method - UV 486 nm
Hexadecyltrimethylammonium bromide (HTAB)	-	Dye method - UV 486 nm HPLC method - UV 205 nm
HTAB	NaBr (150)	Dye method - UV 486 nm
Benzalkonium chloride (BAC)	-	UV - 262 nm
Cetylpyridinium chloride (CPC)	-	UV - 259 nm
Dodecylpyridinium chloride (DPC)	-	UV - 259 nm
DPC	KCl (10)	UV - 259 nm
Sodium dodecyl benzene sulphate (SDBS)	-	UV - 224 nm
SDBS	KCl (10)	UV- 224 nm

3.3.2.3 Trimethylammonium Bromide Surfactant Quantitation Using an Anionic Dye

In order to quantitatively determine the amount of trimethylammonium surfactants remaining unbound in the surfactant halloysite systems after equilibration, complexation of the unbound dye with an anionic dye was undertaken. The samples were prepared as outlined in Section 3.3.2.2. It is not possible to quantify the sample using UV without complexing the unbound surfactant with a dye. A slight excess of the dye, Tropaeolin 000 No. 2 (4-(hydroxyl-1-Naphthylazo)benzene sulfonic acid Sodium salt), was added to the

supernatant and the resulting 1:1 complex was extracted using chloroform. The complex concentration was analysed at 486 nm using a spectrometer (Genesys 5, Spectronic). The quantity of unbound surfactant was determined using an appropriate calibration equation, Appendix 1.

3.3.2.4 Quantitation of Trimethylammonium Bromide Surfactants using a Reverse Phase HPLC Method

The concentration of quaternary ammonium surfactants was determined by a reverse phase HPLC method. The method was received from Phenomenox, UK. The HPLC system used was a Shimadzu liquid chromatograph, LC-10 ATVP system (Shimadzu Corp., Japan) equipped with a UV-VIS SPD-10AVP detector operated at 35 ^{o}C. The temperature was maintained at 35 ^{o}C using a column block heater (Jones Chromatography, Wales, UK). The column used was a Luna C18, 5 μm, 250 x 4.6 mm.

The mobile phase consisted of 75% acetonitrile (HPLC grade), 25% 0.1M perchloric acid solution and octanesulfonic acid sodium salt (0.2% w/v). The mobile phase was filtered through a Gelman® membrane filter (0.2 μm pore size) using a vacuum filter apparatus (Millipore Corp., USA). The mobile phase was degassed using a DGU-14A Shimadzu degasser. The column was equilibrated with mobile phase until a stable baseline was obtained. Samples were filtered firstly using 0.45 μm filters (Gelman filtration); they were then filtered using 0.2 μm filters (Gelman filtration). 10 μl samples were injected onto the column using SiL-10 ADVP Shimadzu autoinjector. The flow rate was 1.0 ml/min. Absorbance readings were made at 205 nm. The retention time was 3.12 min.

A calibration curve of cetrimide concentration vs. area under the peak was prepared daily from stock solutions. Stock solutions (300 mg/10 ml) were prepared by dissolving the surfactant in HPLC grade water, with the aid of a sonicator (Bransonic 220, USA). The stock solution was diluted to give concentrations in the range 0.003-3.0% w/v. A blank solution was also prepared. The absorbance vs. their respective concentrations were subject to linear least square regression analysis, resulting in a linear calibration equation. The appropriate calibration equation for each system is depicted in Appendix 1; this equation was used to calculate the cetrimide concentration in the unknown samples. By subtraction of the amount detected from that, which was added, the amount bound was calculated. Samples were prepared in duplicate and each was analysed in duplicate.

The assay was validated for linearity, repeatability and intermediate precision. The inter-day and intra-day accuracy and precision were assessed by preparing and injecting six concentrations over a range of 0.001-0.25% w/v in duplicate each day on three consecutive days. The resulting plots of peak area against concentration were assessed for linearity. Each sample was analysed in triplicate. Robustness, specificity and interference were also investigated.

3.3.2.5 HPLC Equipment Validation

A parabens (10 µl) sample was injected into the HPLC apparatus outlined in Section 3.3.2.5. The mobile phase was a mixture of acetonitrile and water in a ratio of 60:40. Absorbance readings were made at 254 nm. Repeated injection was conducted over a period of three consecutive days. The method was assessed for the % relative standard deviation (RSD) for each of the peaks produced each day on the three consecutive days.

3.3.2.6 Factorial Study of TTAB - Halloysite Adsorption Isotherm

A 2^3 factorial experiment was designed to assess the effect of altering the cetrimide halloysite environment conditions and the resultant effect on the binding curve achieved. The experimental factors examined were chosen, as they are prevalent in the literature in the analysis of other substrates such as silica. (Goloub *et al.*, 1996). These included the duration of sample equilibration (24 or 48 hr). The addition of NaBr salt increases the adsorption of the surfactant and maintains a constant thermodynamic activity in the system (Cherkaoui *et al.*, 1998). The alteration of the surface microclimate as a result of washing the clay with acid was also investigated. The factors investigated are given in Table 3.3.2.6. The experiment was carried out as described in Section 3.3.2.2. All sample runs were replicated. A dye method was used to measure the quantity of unbound surfactant. The isotherms were assessed by evaluation of the amount bound using analysis of variance (ANOVA). Quantity adsorbed was the model response factor used.

Table 3.3.2.6 Design components of the cetrimide halloysite binding curve, 2^3 factorial study.

Variable	Type	Low	High
Clay	Formulation	Unwashed	Acid washed
Time	Process	24 hr	48 hr
NaBr Salt	Formulation	0	150 mM

3.3.2.7 Deflocculation Studies

Deflocculation studies were performed on halloysite G. All of the equipment used in this experiment was carefully washed with HPLC grade water to avoid ion contamination of the samples. Stock solutions of surfactant systems in the range of 0-2.0% w/v were prepared; the contents were sonicated to aid dissolution. Halloysite (1.0 g) was weighed out and added to a volumetric flask. The requisite amount of surfactant stock solution was added in order to produce a range of final concentrations in the order of 0-0.2% w/v for TTAB, 0-0.25% for BAC and 0-0.5% w/v for sodium lauryl sulphate (SLS). A blank sample was prepared in each case. HPLC grade water was added in order to produce a final volume of 100 ml. The contents in the cylinders were inverted a number of times and the systems were observed over a period of 72 hr.

3.4 EVALUATION OF THE ANTIBACTERIAL ACTIVITY OF CETRIMIDE IN CETRIMIDE-HALLOYSITE COMPOSITES

3.4.1 Introduction

The study was intended to demonstrate the extent of antimicrobial activity, if any, pertaining to the cetrimide treated halloysite grade. Free cetrimide has antimicrobial activity (Handbook of Pharmaceutical Excipients, 2005). The study was designed to show if the activity was altered by being bound to the halloysite clay sample. Two strains of the gram-positive organism *Staphylococcal aureus* (*S. aureus*), Oxford and Cowan, were used to examine the antimicrobial properties of the surface modified clay. The Cowan strain is a more sensitive strain than the Oxford strain. The bacterial strains were received on slants from Dr. Russell in the Department of Microbiology, Moyne Institute, TCD. The samples were stored in the fridge prior to use. They were placed in an incubator (Astell Hearson) at

37 °C overnight prior to use to encourage growth. The bacterial strains were grown in nutrient medium on agar plates. Clay samples compressed into discs were placed on the seeded agar plates and incubated for 24 hr in the incubator at 37 °C. The cetrimide grade examined was TTAB.

3.4.2 Nutrient Agar Medium Preparation

Nutrient agar medium was prepared by dissolving a known quantity in a requisite volume of deionised water. The sample was boiled using a hot plate (Stuart Scientific) in order to fully dissolve the nutrient agar. The sample was sterilised by autoclaving at 121 °C for 15 min. The agar medium was retained in its molten state by maintaining it at 55 °C in a water bath (Thermomix® BU Braun) prior to pouring into the plates.

3.4.3 Disc Preparation

Compressed discs of halloysite G, cetrimide, cetrimide coated halloysite and physical mixes of halloysite G with cetrimide were prepared using a 13 mm punch and die assembly. 300 mg of each sample were placed in the die assembly. Eight tonnes of pressure were applied to the sample using a Graseby Specac IR press for a duration of 2 min. In the case of the halloysite G samples, the pressure was applied for longer (3 minutes) as the samples proved excessively brittle when subjected to compression for a 2 min time period.

3.4.4 Agar Plate - Preliminary Study

Nutrient agar medium was prepared as outlined above in Section 3.4.2. Three loopfuls of cells from the Oxford strain of bacteria were suspended in sterile water. The water was previously sterilised using an autoclave at 121 °C for 15 min. A designated volume of the bacterial suspension was added to each plate. Agar medium (20 ml) was added to the petri dishes using a tilt measure (Quickfit, UK). The contents were gently agitated using a swirling motion. The agar plate contents were allowed to solidify prior to use for a period of approximately 1 hr. Compressed discs of each sample prepared according to Section 3.4.3 were placed on the agar surface. Each agar plate contained two discs. The samples were left for 1 hr at room temperature prior to incubation at 37 °C for 24 hr in an incubator. After 24 hr the samples were removed and the zone of inhibition if any was noted. The zone of inhibition was measured in two directions at right angles using callipers. The samples were also photographed. The experiment was repeated for the Cowan strain.

3.4.5 Agar Plate - Advanced Study

The advanced study was repeated as for the preliminary study above but the cells from each bacterial strain were suspended in Tryptone Soy Broth (TSB) rather than sterile water. The TSB was prepared by dissolving the requisite quantity in a known volume of water. The medium was sterilised by autoclaving at 121 °C for 15 min.

3.4.6 Colony Forming Unit (CFU) Evaluation

Three loopfuls of the Oxford strain were aseptically transferred to a test-tube containing TSB (10 ml) using the flame sterilisation technique. The TSB was prepared as outlined in Section 3.4.5. Serial dilutions of this stock suspension were made using sterile water. 0.2 ml samples from the tubes, which were equivalent to serial dilutions of 1×10^{-4}, 1×10^{-5}, 1×10^{-6} and 1×10^{-7} were each added to a separate petri dish. 20 ml of nutrient agar medium was added to each petri dish and the contents were swirled gently to aid in homogeneous dispersion of the bacteria. The plates were allowed to set and were then stored inverted in an incubator at 37 °C for 24 hr. After 24 hr the petri dishes were removed from the incubator and a grid was marked on the rear of each plate. The number of CFUs in each section of the grid was counted and the overall total number of CFUs per plate calculated. Only plates with counts greater than 30 CFUs and less than 300 CFUs were considered. The plates, which had CFU counts within the designated range, were used to calculate the number of CFU in the original stock suspension. The experiment was repeated for the Cowan strain. Each sample was replicated.

3.5 EVALUATION OF HALLOYSITE-OINTMENT SYSTEMS

3.5.1 Formulation of Halloysite-Ointment systems

3.5.1.1 Halloysite White Soft Parafffin (WSP) Physical Mixes

Physical mixes at three concentrations levels (10% w/w, 20% w/w and 40% w/w) of halloysite and cetrimide coated halloysite in White Soft Paraffin (WSP) ointment were prepared. The ointment base was melted using a hotplate (Stuart Scientific). Prolonged heating of WSP is not advised. The halloysite was added gradually to the molten ointment base with stirring over a three min period. It was stirred for a further two min after the final addition. It was stirred at a speed of 8000 rpm initially; this was increased to 9500 rpm for the final two min. An Ultra Turrax® T25 (Labortechnik) stirrer was used. The mixture was

gently stirred with a spatula as it cooled to prevent sedimentation. As the quantities of the physical mixes containing cetrimide-coated halloysite prepared were smaller, the above method was not employed in their production. The cetrimide coated halloysite was added to the molten base and then stirred with a spatula until it had solidified.

3.5.1.2 Formulation of Macrogol Ointment Systems Containing Halloysite or Cetrimide Coated Halloysite

Macrogol ointment was prepared according to a BP method (British Pharmacopoeia, 1998). Poly(ethylene) glycol (PEG) 4000 was added to the liquid PEG 300 and was warmed using a hotplate (Stuart Scientific). The halloysite grades were added at this stage over a 5 min period. Macrogol ointment was also prepared without the addition of halloysite. Table 3.5.2.2 outlines the requisite quantities of halloysite and cetrimide coated halloysite grades and each of the PEG components that were used to formulate each system. The contents were stirred with a spatula until cool.

Table 3.5.1.2 Quantities of halloysite, cetrimide coated halloysite and PEG components used to prepare the various halloysite/cetrimide coated halloysite macrogol ointment systems.

System	Halloysite/cetrimide coated halloysite (g)	PEG 300 (g) (65%)	PEG 4000 (g) (35%)
Macrogol ointment	-	65.00	35.00
Halloysite/cetrimide coated halloysite 10%	10.00	58.50	31.50
Halloysite/cetrimide coated halloysite 20%	20.00	52.00	28.00
Halloysite/cetrimide coated halloysite 40%	40.00	39.00	21.00

3.5.2 Rheological Evaluation of Halloysite - Ointment Systems

3.5.2.1 Introduction

Rheological properties of various ointment systems were evaluated using a Carri-Med CSL^2 500 (TA Instruments, UK), which is a controlled stress/controlled rate rheometer. Geometries of various types and sizes including the cone and plate attachment can be used to analyse a wide array of samples. Virtually friction free application of torque is accomplished using an air bearing. Air is used as a lubricating medium resulting in movement under the smallest of forces. The pressurised air is passed through a coarse filter dessicant dryer system and a double filter regulator assembly, to remove particulate matter and ensure a sufficiently pure dry air supply. The air pressure is controlled at 37.5 psi using a valve mechanism. A peltier plate is temperature controlled using a constant circulating water supply and this enables rapid and accurate heating and cooling of samples. The instrument determined an automatic gap of 52 μm. The automatic gap setting mechanism was used in order to minimise manual operating errors and reduce operating time. All experiments were conducted using cone and plate geometry (angle 4°). The geometry also dictates the sample size used. It must spread to the edges of the geometry but not over or under fill in order to avoid any drag effect. Positioning of the sample on the plate plays a crucial role also. Equilibration of the sample on the plate prior to analysis is vital in order that the shear history and internal stresses caused by sample loading dissipate. An equilibrium time of 3 min was employed. It also ensures that a uniform temperature permeates throughout the sample. Each experiment was replicated at least in triplicate, with a fresh sample loaded for each run.

3.5.2.2 Continuous Shear Studies

Continuous shear measurements were used to evaluate sample flow and apparent viscosity characteristics of WSP and WSP ointment systems containing uncoated halloysite at concentrations of 10%, 20% and 40% w/w. Flow curves were conducted over a time period of 3 min at 25 ^{o}C. The time for flow is important as if it is too long or short it can distort the real effects of the systems and the resultant rheograms produced (Barnes *et al.*, 1989). Preliminary flow studies were performed to determine the region at which structural breakdown occurs. The flow tests were then performed at a shear range below the destructive shear stress value for the particular sample.

3.5.2.3 Stepped Flow Studies

Stepped flow rheology analysis was conducted also. Forty points of analysis were chosen. At each time point the stress was ramped between two extremes and the sample was allowed to gain equilibrium at each point hence providing a better indication of the sample's viscosity. Stepped flow studies were conducted on the WSP and uncoated halloysite in WSP samples. Macrogol ointment and macrogol ointment - halloysite systems at concentrations of 10% and 20% w/w were also evaluated.

3.5.2.4 Dynamic Oscillatory Studies

The oscillatory technique is theoretically a non-destructive test, which measures the viscous and elastic behaviour of the sample simultaneously. When performing oscillatory frequency sweeps, the linear viscoelastic region (LVR) of the system must be first evaluated using a manual torque sweep. The LVR region is used to determine where the samples bonds are stretched but not broken. An oscillatory torque value within this region is used to perform dynamic oscillatory studies. Oscillatory measurements were performed on the systems outlined in Table 3.5.2.4. All systems were examined over a frequency range of 0.01-10 Hz.

Table 3.5.2.4 The oscillatory torque values (μN.m) at which each system was examined using dynamic oscillatory rheology.

Halloysite-Ointment System	Halloysite (μN.m)	Cetrimide halloysite (μN.m)
WSP		
Ointment base	1000	
10%	100	70
20%	100	35
40%	2000	200
Macrogol		
Ointment base	50	
10%	50	200
20%	100	400
40%	600	-

3.5.3 Texture Analysis Evaluation of Halloysite - Ointment Systems

3.5.3.1 Hardness Testing of Halloysite - Ointment Systems

Hardness testing was performed on halloysite and cetrimide coated halloysite ointment systems. Both WSP and macrogol ointment systems were investigated. The concentrations of the halloysite grades in the ointment systems were 10%, 20% and 40% w/w. Hardness testing was conducted using a Stable Micro Systems Texture Analyser (TA-XT2) in texture profile analysis (TPA) mode. The ointment systems were carefully poured into beakers in a semi-molten state with light agitation to prevent sedimentation in order to reduce the entrapment of air. The samples were stored in a dessicator prior to use. The beakers were placed beneath the sample probe, which was calibrated to a specific height above the sample. The beakers were held in place with adhesive tape. The sample probe (25 mm) was twice compressed into the sample at pre-test, test and post-test speeds of 1 mm/s. The probe was compressed to a depth of 10 mm into each sample. It was important that the sample height was sufficient to avoid interference from the container as the probe is compressed to its fixed depth. A delay period of 15 s between the end of the first and the beginning of the second compression was allowed. At least four replicate analyses were performed for each sample formulation; a fresh sample was used each time. The hardness is a measure of the force required to cause sample deformation as the probe is compressed into the formulation on the first occasion. The hardness was measured in g.

3.5.3.2 Adhesive Testing of Halloysite - Ointment Systems

Adhesive testing was performed on halloysite and cetrimide coated halloysite ointment systems. Both WSP and macrogol ointment systems were investigated. The concentrations of the halloysite grades in the ointment systems were 10%, 20% and 40% w/w. Hardness testing was conducted using a Stable Micro Systems Texture Analyser (model TA-XT2) in adhesive mode. A piece of pig hide was adhered to a probe (diameter 25 mm, surface area 490.63 mm^2) using double-sided adhesive tape. The probe was placed in contact with each ointment system at a pre-test speed of 1 mm/s. On contact, a force of 2.5 N was applied at a test speed of 0.5 mm/s for 15 s. The post-test speed used was 1 mm/s. The samples were characterised using the peak detachment force and the work of adhesion. All samples were measured at least in quadruplicate and a fresh sample and piece of pig hide was used in each case.

3.6 FORMULATION OF UREA - HALLOYSITE COMPLEXES

3.6.1 Preparation of Buffer Media

Specific buffer solutions were prepared by dissolving the requisite quantity of each of the buffer components in deionised water. The samples were made up to volume using deionised water and were left to equilibrate prior to the determination of the pH of the system using an Orion pH meter. The samples were adjusted to the final pH value +/- 0.05 units with 0.1 M sodium hydroxide or 0.1M HCl solutions.

Table 3.6.1 Constituents and quantities used to prepare buffer media

Buffer System	*Citric acid (g/litre)*	*Sodium hydrogen phosphate (g/litre)*	*Sodium acid phosphate (g/litre)*	*Sodium chloride (g/litre)*
McIlvaine 2.5	19.7	4.4		
McIlvaine 5.5	9.3	39.9		
McIlvaine 6.8	4.8	55.3		
McIlvaine 8.0	0.58	69.7		
Phosphate buffer solution (PBS) 6.8		11.9	5.2	4.8
PBS 7.4		19.1	2.1	4.4

3.6.2 Solubility Studies

The saturation solubility of urea in various media was determined. An indication of solubility was obtained primarily from the United States Pharmacopoeia (USP 29-NF24) and British Pharmacopoeia (2007) references. A known quantity of the active, which exceeded the reference solubility in 5 ml of medium, was placed in a 10 ml ampoule, to

which 5 ml of the dissolution medium was then added. The ampoule was then flame sealed and placed in a shaker bath (Model 25, Precision Scientific, USA) and set to shake at 50 cycles per min for either 24 or 48 hr at temperatures of 20 or 33 °C. The samples were then filtered using 0.45 μm membrane filters (Gelman Supor-450, USA). In the case of samples examined at 33 °C the syringes, filters, sample holders and dilution medium were pre-heated in an oven (Gallenkamp) to approximately 40 °C prior to being used so that recrystallisation of the active from the saturated solution was minimised due to a reduction in the temperature of the environment. Samples were diluted where required with the appropriate medium. All sample determinations were replicated. In order to quantify the amount of urea dissolved a QuantiChrom® urea assay kit was employed.

3.6.3 Urea Quantitation Using a QuantiChrom® Urea Assay Kit

A quantitative colorimetric determination of urea in samples was conducted using a QuantiChrom™ urea assay kit (DIUR-01K), (BioAssay Systems, USA). It is based on an improved Jung method, which utilses a chromogenic reagent that forms a coloured complex specifically with urea. The intensity of the colour measured at 520 nm (optimum wavelength), is directly proportional to the urea concentration in the sample. The formulation substantially reduces interference by substances in the raw sample. The kit contains two reagents, A and B, which are stored at 4 °C. They are equilibrated at room temperature prior to use. Equal volumes of each reagent are combined and added to the sample within 20 min of their mixing. The absorbance of the samples is read within an optimum period of time using a plate reader at a wavelength in the range 470-550 nm. Maximum absorbance occurs at 520 nm. The kit also contains a urea standard 100 mg/dL. The linear detection range is 0.006 mg/dL to 100 mg/dL urea in a 96-well plate (QuantiChrom™ urea assay kit (DIUR-01K), Product information leaflet BioAssay Systems, USA).

5 μL of the standard, blank and of each sample removed during the release studies were each transferred to a separate well in a clear bottom 96-well plate. 200 μL of working reagent (reagents A and B combined) was added to each well. The plate was tapped lightly to mix the samples. The samples were incubated for 15 min prior to the absorbance being read at 492 nm using a plate reader (FLUOstar OPTIMA, BMG Lab Tech, UK). Standard samples of urea in both McIlvaine buffer pH 5.5 and in water media were included in each

plate in order that the linearity of the reading was assessed. The urea quantity is measured by multiplying the concentration of the standard by the ratio of sample absorbance to the absorbance of the standard.

3.6.4 Loading of Halloysite G with Urea

5.0 g of the halloysite G sample (sieved through 125 μm mesh beforehand) was weighed out. A specified volume of the urea loading solution was measured out and mixed thoroughly with the halloysite on a stirrer plate (Stuart Scientific). The halloysite and drug loading solution was placed in a sealed desiccator vessel and a vacuum applied (vacuum suction pressure approx. 30 mm Hg) for 15 min until all the air bubbles were removed. The loading set up is illustrated in Figure 3.6.4. The vacuum was removed and the contents were stirred. The vacuum was reapplied once more as above, to ensure that the drug solution had fully displaced all the air present in the mineral tubules. The urea loaded samples were dried at room temperature for 24 hr. The dried powders were ground gently with a mortar and pestle and sieved through a 125 μm mesh to separate any large agglomerates. The loading apparatus was covered in order that any photodegradation was minimised.

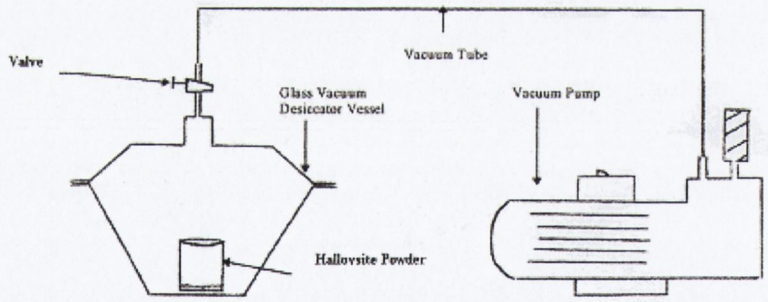

Figure 3.6.4 Illustration of apparatus used to load the halloysite powder with urea.

3.6.5 Loading of Halloysite G with Urea - Fractional Factorial Study

A fractional factorial design, 2^{4-1} was carried out in order to assess the extent of the effect of four variables, namely, the pH of the loading medium, loading solution volume, halloysite coated with cetrimide or non-coated halloysite and also single versus double loading on the amount of urea loaded and the effect if any on the subsequent rate of urea

release from the loaded halloysite sample. Table 3.6.5 lists the factors and the specific levels at which the samples were prepared. A fractional factorial analysis 2^{4-1}, with design generator ABC was used to dictate the levels of each factor used in each run. Eight runs were conducted and each run was replicated. A total of 16 samples were prepared and analysed.

Table 3.6.5 Variables used in the 2^{4-1} fractional factorial design to examine the optimum loading conditions of urea into halloysite.

Variable	Low level (-)	High level (+)
Loading Solution pH	McIlvaine Buffer pH 2.5	McIlvaine Buffer pH 8.0
Loading Solution Volume	28 ml	56 ml
Halloysite	Non-coated	Cetrimide coated
Loading	Single	Double

Each of the formulation variables was examined at two levels. The samples were loaded as detailed in Section 3.6.4. The amount of urea released from each of the samples was determined using release studies (Section 3.7.2). The amount released at specific time intervals was evaluated using an analysis of variance (ANOVA).

3.6.6 Urea, Halloysite and Lecithin Systems

The aim of these experiments was to determine if the release profile of urea from halloysite could be modified to any extent by the non-ionic emulsifier, lecithin. Two grades of lecithin were used, Lipoid S75® and Lipoid S100®. Designated quantities of lecithin as outlined in Table 3.6.6 were either dispersed or dissolved in the vehicle. The requisite quantity of urea was then added. The contents were stirred using a stirrer plate (Stuart Scientific) prior to the addition of the halloysite sample. The system was then stirred for 1 hr prior to being spray-dried.

The systems were spray-dried using a Buchi–191 mini spray-drier (Buchi, Switzerland). The equipment was first washed through with water (50 ml). The inlet temperature was 135 °C and the corresponding outlet temperature was 101 °C. The pump rate was 3%. The aspirator was initially set at 95% but was then increased to 100% for the duration of the

experiment. The system was then left run dry prior to the inlet temperature being lowered to that specified in the experimental run as detailed in Table 3.6.6. In the all cases except for sample 1, the new inlet temperature was set to 95 ^{o}C and the pump rate was also altered accordingly as specified in Table 3.6.6. The system was equilibrated with the same vehicle prior to the sample being spray-dried. It was found that an increased sample yield was recovered from the ethanol containing systems.

Table 3.6.6 Process and Formulation Components of Co-Spray-Dried Systems of Urea, Halloysite and Lecithin.

Sample	Vehicle	Halloysite (% w/v)	Urea (% w/v)	Lecithin – grade and quantity (% w/v)	Pump Rate	Inlet/Outlet °C
1	Water - 100 %	2.0	2.0	Lipoid S75 - 1%	5.0 %	140/110
2	Ethanol:water; 60:40	2.0	2.0	Lipoid S75 -1%	3.0%	95/77
3	Ethanol:water; 60:40	2.0	2.0	Lipoid S100 -1%	3.0%	95/77
4	Ethanol:water; 60:40	1.0	1.0	Lipoid S100 - 0.5%	3.0%	95/77
5	Ethanol:water; 60:40	1.0	1.0	Lipoid S75 - 0.5%	3.0%	95/77
6	Ethanol:water; 60:40	1.0	1.0	Lipoid S75 - 0.5%	5.0%	95/77
7	Ethanol:water; 60:40	2.0	2.0	Lipoid S75 - 0.2%	3.0%	95/77
8	Ethanol:water; 60:40	2.0	2.0	Lipoid S100 - 0.2%	3.0%	95/77
9	Ethanol:water; 60:40	1.0	1.0	Lipoid S75 - 0.1%	3.0%	95/77

3.7 CHARACTERISATION OF UREA - HALLOYSITE COMPLEXES

3.7.1 SEM

SEM analysis was conducted on spray-dried halloysite/urea/lecithin complexes in exactly the same manner as outlined in Section 3.2.2.

3.7.2 Release Studies from Urea Loaded Halloysite

Release studies were carried out using an Erweka DT6 (Germany) dissolution tester fitted with paddles. Dissolution medium (900 ml) was placed in each dissolution vessel. McIlvaine buffer pH 5.5 was used in the study, it was prepared as outlined in Section 3.6.1 The medium was equilibrated to 33 ^{o}C prior to addition of the drug loaded halloysite or spray-dried halloysite complexes. A sample weight of 1 g was added for each analysis. The sample weight was chosen to ensure that sink conditions would be maintained. Each vessel was covered with a Perspex lid throughout the experiment. The temperature was monitored intermittently using a thermometer. The samples were stirred at a rate of 50 rpm.

Samples (5 ml) were withdrawn at 0.25, 0.5, 1, 2, 3, 4, 5, 6, 7 and 8 hr intervals. Some samples were also withdrawn at 24 hr time periods. Each sample withdrawn was replaced with 5 ml of fresh medium that was maintained at 33 ^{o}C. The sample was taken from a zone midway between the surface of the dissolution medium and the top of the rotating paddle. This zone was not less than 1 cm from the vessel wall (British Pharmacopoeia, 2007).

The samples were then filtered through a 0.45 μm membrane filter (Gelman Supor-450, USA) and diluted as required with the appropriate medium. The quantity of urea in the sample was determined as outlined in Section 3.6.3 using a QuantiChrom^{TM} urea assay kit (DIUR-01K, BioAssay Systems, USA). The effect of repeated sampling on resultant drug concentration was accounted for in subsequent calculations. Release studies were carried out at least in triplicate on each sample.

3.8 FORMULATION OF SALICYLIC ACID - HALLOYSITE COMPLEXES

3.8.1 Solubility Studies

3.8.1.1 Saturation Solubility Studies

The saturated solubility of SA in a range of media was determined in a similar manner to that described in Section 3.6.2. The study was conducted at 25 °C. The quantity of SA in the samples was determined using UV spectrophotometery at a wavelength of 296 nm (Heλios, Thermo Spectronic, Electron Corporation). The quantity of SA in the samples was determined using an appropriate calibration equation.

3.8.1.2 Dynamic Solubility Study

The dynamic solubilities of salicylic acid in water and ethanol were also examined. A quantity of drug exceeding its pre-determined saturation solubility in 50 ml of medium was placed in a jacketed vessel containing 50 ml of the relevant medium, which was equilibrated to room temperature, 25 °C. An overhead stirrer blade (Heidolph stirrer-RZR-1) was placed in the water bath and the contents were stirred at a rate of 50 rpm for an appropriate period of time. The vessels were covered with aluminium foil to minimise possible drug degradation in the case of photosensitive actives. The temperature was monitored at intermittent periods using a thermometer. Samples were withdrawn at 0.25, 0.5, 1, 2, 3, 4, 5, 6 and 7 hr intervals and filtered through a 0.45 μm membrane filter (Gelman Supor-450, USA). The samples were diluted using the appropriate medium and the absorbance of the solution was determined using UV spectroscopy ((Heλios, Thermo Spectronic Electron Corporation). The quantity of drug dissolved in the medium was calculated. Each sample was run in duplicate.

3.8.2 Loading of Halloysite G with Salicylic Acid

Halloysite G was loaded with solutions of SA using the method outlined in Section 3.6.4. However in this study ethanol was used as the drug-loading vehicle. 25 ml of the loading solutions were added to halloysite samples (5 g).

3.8.3 Loading of Halloysite G with Salicylic Acid – Factorial Studies

3.8.3.1 Introduction

Halloysite G was loaded with SA according to the procedures outlined in Sections 3.6.4 and 3.8.2. However some of the factors thought to influence SA encapsulation and release were varied. Two factorial studies were conducted. An advanced study was conducted based on preliminary studies.

3.8.3.2 Preliminary Study

The factors examined in the preliminary study included the halloysite grade and the concentration of SA in the loading solution. The effect of singly loading the samples or loading them on a repeated occasion was investigated also. Table 3.8.3.2 depicts the factors and the levels of each factor examined in the preliminary study. The model response factor was SA release and the quantity of SA released at 8 hr was analysed using ANOVA.

Table 3.8.3.2 Factorial study, 2^3 of the variables influencing SA loading in halloysite G – Preliminary study.

Variable	Low Level (-)	High level (+)
Halloysite	Non-coated	Cetrimide coated
Loading Solution Concentration	10 %w/v	20 %w/v
Loading	Single	Double

3.8.3.3 Advanced Study

An advanced study was conducted into the factors affecting SA encapsulation based on the results of the preliminary study. Table 3.8.3.3 lists the pertinent factors and the respective levels of each investigated. The halloysite grade was again investigated as was loading solution concentration. However the solution concentrations were lower. The impact of drying method on SA encapsulation was considered. The conventional air drying method was compared to that of freeze drying. The samples were freeze dried at a pressure of 100 mTorr and an initial temperature of –80 ^{0}C using a Virtis Benchtop 6K freeze drying apparatus (New York, USA) for a period of 24 hr.

Table 3.8.3.3 Factorial study, 2^3 of the variables influencing SA loading in halloysite G – Advanced study.

Variable	Low level (-)	High level (+)
Halloysite	Non-coated	Cetrimide coated
Loading Solution Concentration	1.5% w/v	3.0% w/v
Drying	Air-dry	Freeze-dry

3.8.4 Co-Spray-Dried Salicylic Acid, Halloysite and Cetrimide Complexes

The method of preparation and spray-drying of the salicylic acid/halloysite/cetrimide systems using the Buchi-191 mini spray dryer (Buchi, Switzerland) is the same as that outlined in Section 3.6.6 above for urea/lecithin/halloysite systems. The specific details pertaining to each sample run are outlined in Table 3.8.4.

Table 3.8.4 Process and Formulation Components of Co-Spray-Dried Systems of Salicylic Acid, Halloysite and Cetrimide.

Sample	Vehicle	Halloysite (% w/v)	Salicylic Acid (% w/v)	Cetrimide (% w/v)	Pump Rate (%)	Inlet/Outlet ^{o}C
1	Ethanol:water; 10:90	2.0	0.2	0.2	5.0	95/75
2	Water - 100 %	2.0	0.2	0.2	5.0	143/111
3	Ethanol:water; 40:60	2.0	0.2	0.2	5.0	95/77
4	Ethanol:water; 60:40	2.0	0.2	0.2	5.0	95/77
5	Ethanol:water; 60:40	5.0	0.5	0.5	5.0	95/77
6	Ethanol:water; 60:40	5.0	0.5	0.2	5.0	95/77
7	Ethanol:water; 60:40	5.0	0.5	0.05	5.0	95/77
8	Ethanol:water; 60:40	5.0	0.5	-	5.0	95/77

3.9 CHARACTERISATION OF SALICYLIC ACID – HALLOYSITE COMPLEXES

3.9.1 SEM

SEM analysis was conducted on spray-dried halloysite/SA/cetrimide complexes in exactly the same manner as outlined in Section 3.2.2.

3.9.2 Skeletal Density Analysis

The skeletal density of the spray-dried SA complexes was determined as outlined in Section 3.2.4.

3.9.3 Surface Area Analysis

The surface area of the spray-dried SA complexes was determined as outlined in Section 3.2.5.

3.9.4 Particle Size Analysis

The particle size distribution of raw SA and the spray-dried sample 4 was determined using a Malvern 2600c (Malvern, USA) laser diffraction particle size analyser. The analyser was fitted with a 300 mm lens. The lens is capable of measuring particles in the size range 5.8 to 564 μm. The samples were placed in the feed tray of a dry powder feeder (PS64, Malvern, USA). The feed rate was controlled in order to distribute the powder into a dispersing air jet, which was sucked across the path of the laser beam by a vacuum. The resultant scattering of the particles in the beam gave a measurement of the particle size distribution, which was calculated by the sizer software using Fraunhofer theory (Byrne, 2004). All measurements were repeated and the result was averaged. The results were expressed as cumulative % undersize.

3.9.5 Release Studies from Salicylic Acid - Halloysite Complexes

SA release from halloysite loaded and spray-dried complexes was carried out in the same manner as that outlined in Section 3.7.2. A sample weight of 1 g was again used for analysis of the vacuum loaded samples, however 0.5 g was used in the case of the spray dried samples due to sample shortages. The quantity of SA in the samples was determined using UV spectrophotometery at a wavelength of 296 nm (Heλios, Thermo Spectronic Electron Corporation). The sample at 24 hr was representative of the total amount of SA

encapsulated in the samples. The quantity of SA in the samples was determined using an appropriate calibration equation.

3.10 FORMUALTION OF SALICYLIC ACID AND CO-SPRAY-DRIED SALICYLIC ACID – HALLOYSITE TOPICAL PREPARATIONS

3.10.1 Aqueous Cream Formulations

Spray-dried samples 4, 5 and 7 as detailed in Section 3.8.4 were added to Aqueous Cream base at a concentration of 20% w/w. Aqueous Cream base was weighed out and placed on a glass slab. The spray-dried sample was incorporated in increments with a spatula. The sample was mixed thoroughly and was placed in a sealed container overnight prior to use. The procedure was repeated for each sample.

3.10.2 Cetrimide Cream Formulations

The Cetrimide Cream was prepared according to the BP (2007) method. Spray-dried samples 4, 5 and 7 were incorporated in the base. The cetostearyl alcohol was melted and heated with the liquid paraffin to about 60° using a hotplate (Stuart Scientific). Deionised water was heated to a similar temperature; the spray-dried sample was added at this stage, no extra cetrimide was added to the system. The aqueous containing spray-dried clay suspension was added to the oily phase when both were approximately 60° in a pre-heated mortar and the components were mixed. It was stirred until cool and made up to final weight using deionised water. The sample was placed in a sealed container overnight prior to use. The procedure was repeated for each spray dried sample.

3.10.3 Salicylic Acid Formulations

SA was incorporated in a number of vehicles at a concentration of 3% w/w. The vehicles included WSP, WSP with 10% liquid paraffin added and Aqueous Cream. The raw material was incorporated into the bases gradually using a spatula and a glass slab.

3.11 CHARACTERISATION OF SALICYLIC ACID AND CO-SPRAY-DRIED SALICYLIC ACID - HALLOYSITE TOPICAL FORMULATIONS

3.11.1 Release studies using Franz cells

Release studies of SA from formulated topical products through a silicon membrane, Silastic® (donated from Dow Corning, USA) was assessed using a Franz cell apparatus (AGB, Ireland). The membrane was used as a simulation of transdermal barriers. The membrane was soaked prior to use in PBS (phosphate buffer solution) pH 7.4 for a period of 1 hr. It was then placed over the jacketed Franz cell apparatus, which had been previously filled with PBS pH, 7.4. The membrane was secured with the aid of an elastic band and the donor compartment attachment. Care was taken in order that the entrainment of air bubbles at the interface between the membrane and the acceptor solution surface was prevented. The system was left to equilibrate for 1 hr prior to use. The jacketed system was maintained at 37 °C using a circulation pump (Vanderkamp, VK 6000, USA). The jacketed Franz cell system was clamped in place on a magnetic stirrer box.

1 g of sample was applied to the donor compartment at t = 0 min and spread evenly over the surface. The donor compartment containing the sample was then covered with a glass slide. The acceptor solution was stirred with a magnetic stirrer bar at a rate sufficient to ensure that the point below the membrane surface was not stagnant. Samples (3 ml) were removed at appropriate intervals, t = 0.5, 1, 2, 3, 4, 5 and 6 hr. Some systems were also sampled at 24 hr. The removed sample was replaced with fresh medium, which was maintained at 33 °C. The absorbance of the removed samples was determined using a UV spectrophotometer (Shimadzu 1700 Pharma Spec) at a wavelength of 295.5 nm. Samples were run in triplicate. Consideration was given to the effect on the resultant concentration of samples being withdrawn and appropriate adjustment was made to the calculations.

3.11.2 Rheological Evaluation of Co-Spray-Dried Topical Formulations

Aqueous Cream and Cetrimide Cream topical formulations containing spray-dried samples 5 and 7 were examined using continuous flow rheometry as outlined in Section 3.5.2.2.

3.12 FORMULATION OF METRONIDAZOLE - HALLOYSITE COMPLEXES

3.12.1 Solubility Studies

3.12.1.1 Saturated Solubility Studies

The saturated solubilities of metronidazole in water and in an ethanol-water (25:75) co-solvent system were determined as described in Section 3.6.2. The solubilities were determined at 25 °C after 24 hr. The quantity of metronidazole in solution was determined using UV spectrophotometery (Heλios, Thermo Spectronic, Electron Corporation) at 320 nm.

3.12.1.2 Dynamic Solubility Studies

The dynamic solubility study of metronidazole in water and McIlvaine buffer pH 5.5 was determined over a period of 6 hr according to the method described in Section 3.8.1.2. The quantity of metronidazole in solution was determined using UV spectrophotometery (Heλios, Thermo Spectronic, Electron Corporation) at 320 nm.

3.12.2 Loading of Halloysite G with Metronidazole

Halloysite was loaded with metronidazole using the method outlined in 3.6.4. Both the halloysite and cetrimide coated halloysite grades were investigated. Two loading vehicles were used. Firstly an ethanol-water (25:75) co-solvent system was investigated. The other vehicle consisted of water with ascorbic acid (0.001% w/v) added. The samples were covered because metronidazole is subject to photodegradation.

3.12.3 Formulation of Metronidazole Halloysite Chitosan Co-Spray-Dried Complex

Metronidazole was formulated with halloysite and chitosan in a spray-dried formulation in a manner similar to that outlined in Section 3.6.6. The ratio of metronidazole to halloysite and chitosan was 0.3:1:0.1. The chitosan was first dissolved in acetic acid (1% v/v) and a sufficient quantity was added in order that there was 0.1 parts of chitosan on a weight basis for each part of halloysite. The liquid medium used was an ethanol-water co-solvent system (60:40). The inlet and outlet temperatures for the system were 95 and 78 °C respectively. The pump rate was 5%.

3.13 METRONIDAZOLE RELEASE FROM HALLOYSITE COMPLEXES

Metronidazole release studies were conducted in a similar manner to that outlined in Section 3.7.2. Again sample weights of 1 g were used except in the case of the spray dried samples were 0.25 g was used. The release medium used to examine vacuum loaded samples was McIlvaine buffer 5.5. However the spray-dried sample was examined at two pH levels, 4 and 7.4. The quantity of metronidazole in solution was determined using UV spectrophotometery (Helios, Thermo Spectronic, Electron Corporation) at 320nm.

3.14 FORMULATION OF NON-DRUG BEADS

3.14.1 Formulation of Halloysite-Alginate Beads

Sodium alginate 2% w/w was added to deionised water and left to hydrate for 3 hr. Sodium polyphosphate (NaPP) 0.5% w/w was also added. The halloysite sample was then added and the contents were homogenised using an Ultra Turrax® T-25 (Labortechnik) at 13,500 rev min^{-1}. The sample was placed in a 5 ml syringe and was clamped at a fixed height above the gelation medium. A needle of external diameter 0.8 mm was used to extrude the samples. The halloysite alginate mixture was dropped at a constant rate into a continuously agitated solution of calcium chloride di-hydrate ($CaCl_2.2H_2O$) (25% w/v). The beads were then left to stir for a further 20 min prior to the cross-linking solution being removed by decanting. The samples were washed with two portions of deionised water (50 ml). The beads were then separated by filtration. The beads were air dried over night and then dried in an oven (Gallenkamp) for 24 hr at 40 °C.

3.14.2 Modification of Halloysite - Alginate Bead Formulations

Beads were produced according to the method outlined above in Section 3.14.1. Other bead formulations were produced with changes in formulation variables such as the quantity and grade of halloysite used as outlined in Table 3.14.2. The drying method was also investigated. The conventional method outlined in Section 3.14.1 above was compared to a freeze-drying method. All samples were dried at room temperature for 2 hr prior to being placed in an oven (Gallenkamp) at 40 °C for 24 hr. Alternatively samples were dried at room temperature for 2 hr and then they were placed in a flask and were submerged in liquid nitrogen. The samples were then freeze-dried using a freeze-drying apparatus

(Virtis, USA) for 24 hr at 200 mTorr and –80 °C. The different batches of beads were characterised visually and physically.

Table 3.14.2 Investigation of the factors affecting the morphology and physical characteristics of halloysite-alginate beads.

Variable	Low (-)	High (+)
Halloysite conc (% w/w)	7.5	15.0
Halloysite grade	Halloysite G	Cetrimide-halloysite.
Drying	Oven dry at 40 °C	Freeze Dry

3.14.3 Rheological Evaluation of Bead Formulations

The flow properties of the various excipients used to produce the beads were examined as it was observed that all samples did not flow equally well through the needle orifice on production. The samples were evaluated using continuous flow shear rheometry as outlined in Section 3.5.2.2. The shear rate variable was held constant and the shear stress values were determined in order to examine the sample over an appropriate shear stress range. Halloysite and cetrimide coated halloysite-alginate systems at 7.5 and 15% w/w concentrations were examined. Sodium alginate 2% w/w was also investigated. Rheological evaluation of chitosan solution at 0.2, 0.6 and 0.8% w/v was also undertaken.

3.15 CHARACTERISATION OF NON-DRUG BEADS

3.15.1 SEM

The beads samples were characterised according to the method in Section 3.2.2.

3.15.2 Skeletal Density

The skeletal density of the beads samples were characterised according to the method in Section 3.2.4.

3.15.3 Surface Area Analysis

The surface area of the beads samples was characterised according to the method in Section 3.2.5. Large bulb tubes were used in the analysis of the bead samples rather than

narrow tubes as the bead samples had a smaller surface area per unit weight. Two long filler rods were used in conjunction with these tubes rather than one long and one short rod as was employed in the analysis of the halloysite samples. Also in the case of the bead samples they were degassed for a period of at least 48 hr and at a temperature of 40 °C.

3.15.4 Swelling Studies

Bead samples (0.2 g) were weighed out and added to a screw cap container. 10 ml of McIlvaine buffer pH 5.5 which had been pre-equilibrated to 33 °C, was added to each container. The samples were placed in a water bath (Thermomix BU® Braun) at 33 °C. The samples were removed periodically and were blotted dry using filter paper. The weight of the sample was noted and it was then replaced in the container, 10 ml of fresh buffer was added and it was replaced in the water bath. The weight of the sample was determined at 1, 2, 3, 4, 5 and 6 hr. The swelling ratio was calculated using Equation 3.2 and the weight versus time was plotted.

Swelling Ratio:

$$\frac{W_t - W_0}{W_0} \times 100\% \qquad \textbf{Equation 3.2}$$

where W_t is the weight at time t, and W_0 is the original weight at time t = 0 min.

3.15.5 Sphericity Analysis

A measure of the sphericity of the beads was obtained using bead parameters measured by an image analysis system (WinSEEDLE v5.1a, Regent Instruments, Inc., Canada). The system analyses a digitised image of beads obtained using a flat bed scanner. At least 400 beads of each sample were analysed. Care was taken to separate the beads in order that a cluster of beads was not analysed. The grey level, which defines what the system considered background was manually set at 70 in order to distinguish the beads from the background (Byrne, 2004). The ratio of the pellet length to its width was taken as an indication of sphericity.

3.16 FORMULATION OF HALLOYSITE - ALGINATE BEADS CONTAINING METRONIDAZOLE

3.16.1 Formulation of Metronidazole Containing Beads

The beads were generally produced using the method outlined in Section 3.14.1 above. Only one concentration of halloysite was employed, 7.5% w/w. Also the cetrimide coated grade was not considered in the further study of bead production because the samples disintegrated relatively quickly. Metronidazole was included with the sodium alginate at the hydration stage at a concentration of 2.0% w/w. This was in excess of its saturation solubility. Other process and formulation variables were examined.

3.16.2 Formulation Variables

3.16.2.1 External Diameter of the Needle

The external diameter of the needle used to produce the beads was 0.8 mm. The effect of preparing beads with a needle of external diameter 0.5 mm was investigated.

3.16.2.2 Metronidazole Concentration

Beads were produced as outlined in Section 3.16.1 but the concentration of metronidazole in the halloysite-alginate complex was reduced to 1% w/w. However it was also added to the gelation medium at a concentration of 1.2% w/w.

3.16.3 Coating of Bead Samples

3.16.3.1 Eudragit® E PO

Bead samples prepared according to the method in Section 3.16.1 were coated with a 6% w/v ethanolic solution of Eudragit® E PO. The beads were dried with warm air from a hair-dryer after coating. Three coats of Eudragit® E PO were applied. The coated samples were stored in a tightly closed container prior to analysis.

3.16.3.2 Chitosan Coating

Bead samples prepared according to the method in Section 3.16.1 were coated with a chitosan solution (0.8% w/v) by stirring the beads in the coating medium. The excess was decanted. The beads were then placed on a wire mesh to air-dry prior to further drying in an oven at 40 °C.

3.16.4 Gelation Medium

3.16.4.1 Concentration of Sodium Polyphosphate (NaPP)

Beads were produced as outlined in Section 3.16.1 but the concentration of NaPP in the halloysite-alginate system was increased from 0.5 to 2.5% w/w.

3.16.4.2 Glutaraldehyde

Beads were produced as outlined in Section 3.16.1 but the cross-linking agent glutaraldehyde was added to the gelation medium at a concentration of 10% w/v.

3.16.4.3 Chitosan

The concentration of $CaCl_2.2H_2O$ was reduced from 25 to 3% w/v and chitosan was included at concentrations of 0.6 and 0.8% w/v. The chitosan was first dissolved in deionised water using glacial acetic acid (2% v/v). The pH of this solution was 4.0. It was left for approximately 6 hr after which any undissolved particles were filtered off with nylon mesh. Appropriate dilution of the chitosan solution was made prior to the addition of the $CaCl_2.2H_2O$. The beads were washed with a solution of NaPP after they were prepared and two portions of deionised water.

3.17 METRONIDAZOLE RELEASE FROM BEAD FORMULATIONS

3.17.1 Release Studies

Release studies were carried out using a Vankel basket apparatus VK 6000 (Vankel Industries). Dissolution medium (900 ml) was placed in each dissolution vessel. McIlvaine buffer pH 5.5 was used in the study, it was prepared as outlined in Section 3.6.1. The medium was equilibrated to 33 °C prior to addition of the bead samples. Each vessel was covered with a Perspex lid throughout the experiment. The temperature was monitored intermittently using a thermometer. The samples were stirred at a rate of 50 rpm.

Samples (5 ml) were withdrawn at 0.25, 0.5, 1, 2, 3, 4, 5 and 6 hr intervals. Some samples were also withdrawn at 24 hr time periods. Each sample withdrawn was replaced with 5 ml of fresh medium that was maintained at 33 °C. The sample was taken from a zone midway between the surface of the dissolution medium and the top of the rotating basket. The samples were then filtered through a 0.45 μm membrane filter (Gelman Supor-450, USA) and diluted as required with the appropriate medium. The quantity of metronidazole in the beads was determined using a UV spectrophotometer (Shimadzu UV 1700 Pharma Spec) at 320 nm. The quantity was determined using a suitable calibration equation.

3.17.2 Metronidazole Encapsulation

The total quantity of metronidazole in the beads was determined by placing a known weight of fractured beads in a specified volume of McIlvaine buffer pH 5.5. The beads were fractured by grinding in a pestle and mortar for approximately 1 min. The samples were sonicated for 3 hr (Bransonic 220, USA). The samples were then stored overnight in an oven (Gallenkamp) at 40 °C. The quantity released from the samples was determined by appropriate dilution and analysis using UV spectrophotometery (Shimadzu UV 1700 Pharma Spec) at 320 nm.

3.18 STATISTICAL METHODS

3.18.1 Two Sample t-Tests

The statistical analyses were carried out using the statistical computer program, Minitab v13.1 (Minitab Inc., USA). Two sample t-tests were used to compare the means of two independent samples. The test procedure involved defining a null and alternative hypothesis. The null hypothesis was that the sample means were equal, while the alternative hypothesis was that that they were not equal. The tests were carried out at a significance level of 0.05. The critical value at this significance level was obtained from a student's t-distribution with n-1 degrees of freedom. The null hypothesis was rejected when the t-ratio exceeded the critical value. This ratio was calculated using Equation 3.3.

$$t = \frac{\overline{X}_2 - \overline{X}_1}{S_D} \qquad \textbf{Equation 3.3}$$

where $\overline{X}_1$ is the mean of sample 1, $\overline{X}_2$ is the mean of sample 2 and S_D is the standard error of the mean difference. In these tests the variances of each sample were not assumed to be equal.

3.18.2 Factorial Experimentation

Full factorial experiments were designated by the following nomenclature:

$N = L^K$

Where K is the number of variables,

L is the number of variable levels and

N is the number of experiment runs.

The experiments allowed the determination of the main effects of each variable and interaction between factors.

In the case of fractional factorial experiments, the number of sample runs, N was dictated by L^{K-1} and the design generator for each run was ABC, where A, B and C refer to the levels of each factor. In all cases the variables were examined at two levels, low (-) or high (+).

3.18.3 Analysis of Variance

The use of t-tests to compare the means of two independent samples was discussed. ANOVA is an extension of the t-test and was used to compare the means of more than two independent samples. The null hypothesis was that all the means are equal and the alternative was that they are not. ANOVA was carried out by dividing the total sum of squares (SS) and degrees of freedom (df) of the data into components associated with each source of variation in the data. From these values, an adjusted mean square was calculated for each source of variation. The ratio of any two adjusted mean squares gave an F-statistic. Where this exceeded the critical value for the test, the difference between the adjusted mean squares was significant. The critical value was calculated using Tukey's 'Honestly Significant Method' at a family significance level of 0.05. This was more appropriate than using an individual significance level of 0.05, as multiple comparisons of means were being made. The results of ANOVA were expressed as p-values. A result was significant if its p-value was less than the significance level, 0.05. In all cases, ANOVA

was used only if the residuals of the data were normally distributed and had a constant variance, which was not dependent on run order or any one factor (Byrne, 2004).

3.18.4 Linear Regression Analysis

Linear regression analysis was used to determine if a linear relationship existed between two variables. This linear relationship can be represented by the following Equation 3.4:

$$Y = mX + C \qquad \textbf{Equation 3.4}$$

where X is the independent variable, Y is the dependent variable and C is the value of Y when X = 0, i.e. the Y-axis intercept. The equation of the line was fitted to the data using the method of least squares. This method gave the equation of the line, which best fitted the data. The adequacy of the fit was assessed from the R^2 value. The closer this value was to 1 the better the fit.

Chapter 4

CHARACTERISATION OF CHEMICALLY MODIFIED HALLOYSITE

4.1 INTRODUCTION

Halloysite is an aluminosilicate clay mineral with a tubular structure. Its use for the oral and periodontal delivery of drugs and the controlled release of pesticides has been previously investigated (Levis, 2002; Kelly, 2002; Salter, 2003). Halloysite is chemically similar to kaolin but differs morphologically because kaolin has a plate-like structure. Kaolin has been used in pharmaceutical formulation including topical products due to its adsorbent character. It was hoped that halloysite would display similar characteristics but have the added advantage of modifying drug release by virtue of the ability of the tubular lumen to entrap drug substances.

The aim of this Chapter was to produce a halloysite grade with enhanced properties for particular exploitation in topical drug delivery. Typical desirable qualities would be improved particle flow because the charging characteristics of halloysite result in aggregation of tubule structures, this has implications for particle flow and may also be prohibitive to the loading of drug solutions into the tubular lumen. An improvement in encapsulation and adsorption characteristics would also be advantageous. Firstly the impact of the adsorption of a cationic surfactant, cetrimide on the tubule surface, which resulted in the creation of an organo-grade of halloysite was investigated. The combination of the established antiseptic properties of cetrimide (Handbook of Pharmaceutical Excipients, 2005) and the clay mineral was intended to be exploited in topical formulations as unmodified clay minerals such as bentonite, kaolin and talc have been employed in topical and cosmetic formulations (Viseras *et al.*, 2006). The second chemical modification process included the removal of free iron (Fe) oxides using a commonly employed procedure (Soil Survey, 1984). An increase in the structural iron content has been associated with a decrease in the tubular morphology and an increase in a tabular

morphology (Tazaki *et al.*, 1981). Finally the sample was washed with concentrated HCl as it was expected that the highly acidic medium would alter the sample structure. An acid treatment process has presently been used to purify kaolin to render it suitable for pharmaceutical use (O' Connor *et al.*, 2005).

The halloysite and chemically modified grades were characterised using a number of techniques including Scanning Electron Microscopy (SEM) image analysis, surface area and density studies. The crystalline structure was assessed using X-ray diffraction (XRD) studies. Fourier transform infrared spectroscopy (FTIR) studies were used to detect compositional and crystalline structural changes. Elemental composition was investigated using energy dispersive x-ray analysis (EDX) and quantitatively using inductive coupled plasma mass spectroscopy analysis (ICP-MS). The techniques elucidated structural and compositional changes.

4.2 SEM IMAGE ANALYSIS

Macroscopically the appearance of the clays was not altered after chemical treatment such as the deferration procedure, conducted to remove Fe_2O_3. The organo-modified halloysite also had a similar appearance. However the acid washed halloysite sample was whiter in appearance, this is attributable to removal of surface contaminants (van Olphen, 1977). It was expected, as outlined in Section 4.1, that any alteration might be visible at the structural level due to the nature of the chemical treatments. SEM was used to detect any structural modification at the microscopic level.

Figure 4.2a shows the halloysite G sample. The sample has a tubular appearance. The tubule diameter is approximately 0.1 μm. The dimension of the tubule length is approximately 0.5 μm in length but was observed to be up to 1 μm. The tubules appear aggregated in the SEM image; intermittent between the tubules is the presence of tubule fragments and debris. The presence of the debris reduces the potential for drug encapsulation. Fragmentation of tubules most likely occurred during pre-treatment procedures as the clay mineral was received in an extracted form. Attrition forces during the extraction from the crude material resulted in size reduction of the tubules.

Deferration of the sample results in the tubules appearing fused together, Figure 4.2b. The tubules are aligned with the surface of one tubule closely approximated with the end of

another. It is postulated that this arises because the deferration procedure results in the loss of Fe oxide coatings and divalent cations such as calcium. This is more clearly elucidated in Section 4.5. The loss of the positive cations, which act like a buffer between the attractive forces of the positive ends and negative surface of the tubules, results in the traditional house of card structure, such as that observed in Figure 4.2b, predominating.

Figures 4.2c and 4.2d are depictions of halloysite G that has been heated to 800 ^{o}C using thermogravimetric analysis (TGA) instrumentation. The halloysite tubules assume a fused appearance with a uniform pore distribution on the sample surface. Salter (2003) noted a sintered appearance in halloysite pellets after they were heated to 1200 ^{o}C. However, the fused appearance of the sample does not resemble that observed by the Salter (2003). The appearance of the halloysite tubules is still distinct.

Figures 4.2e and 4.2f are SEM images of deferrated halloysite G heated to 800 ^{o}C using a TGA instrument. The fused appearance of the deferrated clay is maintained, magnification of the image in Figure 4.2f highlights the fused appearance of the deferrated sample. Large fissures appear between tubule sheets, Figure 4.2e.

Electron micrographs for Balekisir halloysite are shown in Figures 4.2g-l. The tubule length is shorter than the halloysite G sample; it is less than 0.5 μm. The diameter of a tubule is highlighted in Figure 4.2g, the external dimensions are approximately 0.1 μm. This is less than a value of 0.3 μm determined by Levis and Deasy, 2002. However the authors did state that the dimensions varied both within samples and depending on the region in which the material was sourced. The tubule lumen is significantly less. Some debris is also apparent; this is not surprising as the halloysite sample was extracted from crude rock using an autogenous grinding procedure. The relative weight difference of each fraction including contaminants and hence their settling rates was used to separate the halloysite tubules. There is no apparent difference in the Balekisir sample as a resulting of the deferration process, Figure 4.2h.

SEM images of Balekisir halloysite heated to 800 ^{o}C using TGA are shown in Figures 4.2i and 4.2j. The tubules have a clustered arrangement with large pores interspersed. The clusters of tubules are not densely packed, discrete openings are evident between the clusters of tubules. These openings between the tubule clusters are 1-2 μm in size. It is

postulated that the sample would fuse together and assume a sintered appearance if the temperature was increased further.

Heat treatment of the deferrated sample is illustrated in Figures 4.2j and 4.2k. The fused appearance observed with the deferrated halloysite sample after heat treatment is evident with the similarly treated Balekisir sample. There is a stratified and compact appearance to the sample in Figure 4.2j. Magnification of the sample highlights the presence of some tubule fragments and possibly some adulteration form the crude rock source.

Figure 4.2a Halloysite G (Magnification x 45,000)

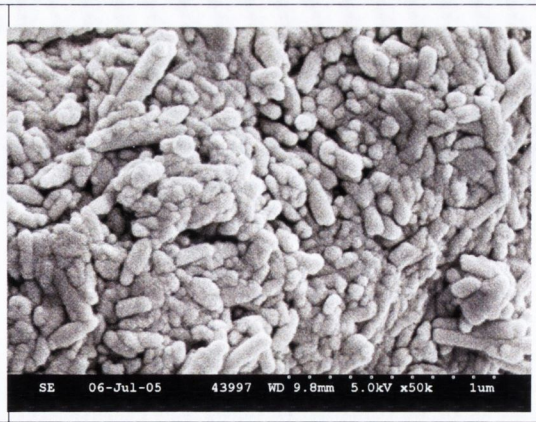

Figure 4.2b Deferrated halloysite G (Magnification x 50,000)

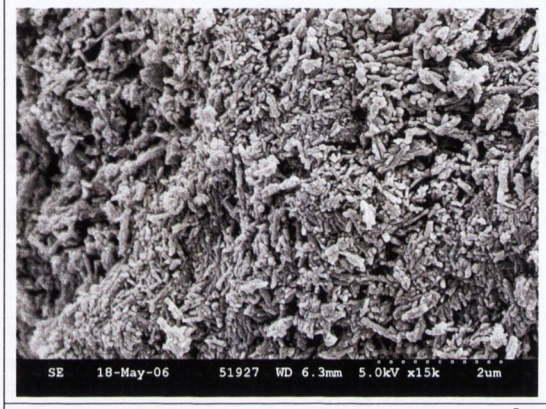

Figure 4.2c Halloysite G heated to 800 °C. (Magnification x 15,000)

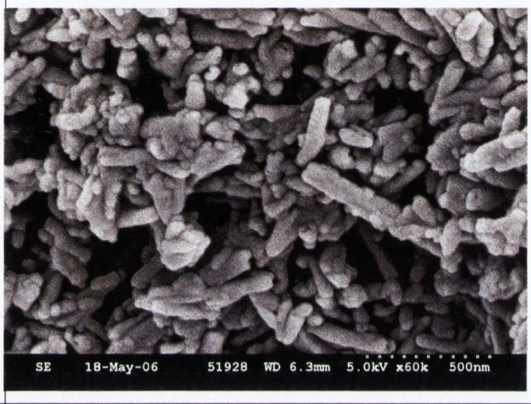

Figure 4.2d Halloysite G heated to 800 °C. (Magnification x 60,000)

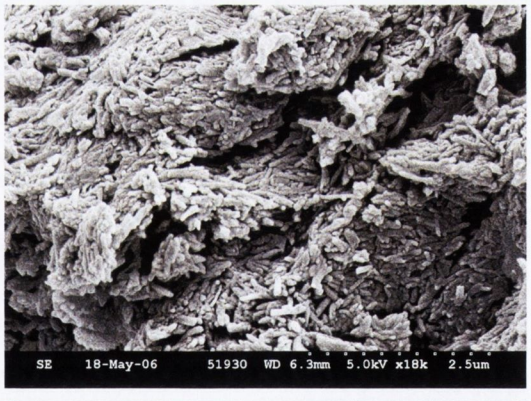

Figure 4.2e Deferrated halloysite G heated to 800 °C. (Magnification x 15,000)

Figure 4.2f Deferrated halloysite G heated to 800 °C. (Magnification x 50,000)

Figure 4.2g Balekisir halloysite. (Magnification x 60,000)

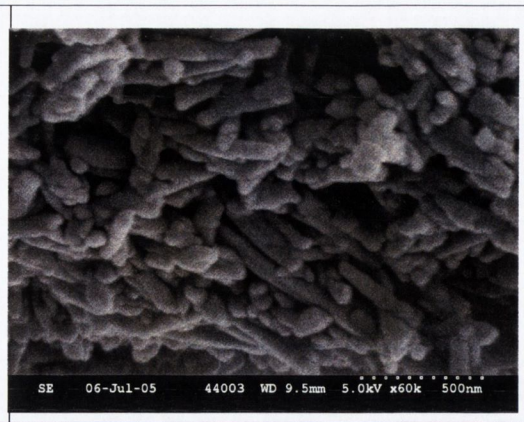

Figure 4.2h Deferrated Balekisir halloysite. (Magnification x 60,000)

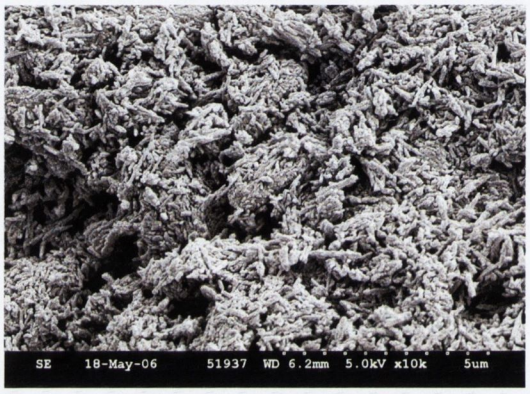

Figure 4.2i Balekisir halloysite heated to 800 °C. (Magnification x 10,000)

Figure 4.2j Balekisir halloysite heated to 800 °C. (Magnification x 30,000)

Figure 4.2k Deferrated Balekisir heated to 800 °C. (Magnification x 35,000).

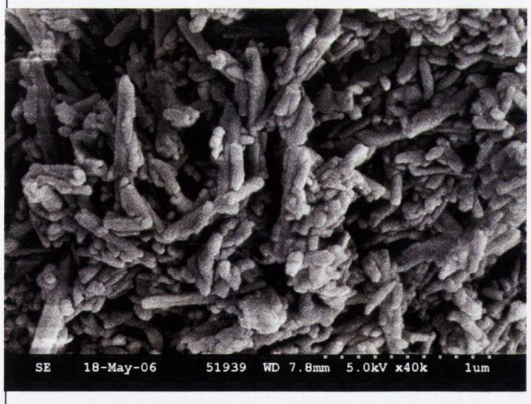

Figure 4.2l Deferrated Balekisir halloysite heated to 800 °C. (Magnification x 40,000)

4.3 DENSITY ANALYSIS

4.3.1 Introduction

Density is universally defined as weight per unit volume, however the difficulty arises when one attempts to determine the volume of particles containing microscopic cracks, internal pores and capillary spaces (Martin, 1993). In light of this, three types of densities may be defined (Gregg and Singh, 1982), bulk density, apparent density and true density. The application and distinction for each category is discussed below.

4.3.2 Bulk Density

The volume occupied by the solid plus the volume of voids when divided into the powder mass yields the bulk density. Therefore, when powder is poured into a graduated cylinder, the bulk density is the mass divided by the volume of the powder bed (Lowell and Shields, 1991). The bulk and tapped density were calculated according to a BP (2007) method. The bulk volume is equivalent to the poured sample volume, that is the volume of the sample after addition to a graduated cylinder. The tapped density value was calculated using the reduced sample volume after the sample was tapped for 1250 strokes using a settling apparatus.

Table 4.3.2 indicates the bulk and tapped densities for the samples. Halloysite from two sources, New Zealand (halloysite G) and Turkey (Balekisir) and cetrimide coated versions of these grades were assessed. In all cases the density of the sample increased after it was subject to the tapping motion. This indicates that interparticulate void space existed between the tubules. The increase in powder bed packing resulted in more particles packing per unit volume. The increase in density as a result of coating halloysite G with cetrimide is modest. This is possibly due to more efficient particle packing as a result of the coating process.

The halloysite G has higher bulk and tapped density values than the Balekisir sample because it has longer tubules (1.0 compared to 0.5 μm), which enables the tubule fragments to pack more efficiently between the tubule framework. There is less of a difference in size between the Balekisir halloysite tubules and the debris. This may account for the small change in bulk and tapped density values. The coating process did not result in a significant difference in density values for the samples and there was a slight decrease in

the case of the bulk density of Balekisir but it was too small to be significant. Hence the particle packing seems to be unchanged as a result of the coating process.

Milling the sample caused a breakdown of aggregate structure into individual units, hence an equivalent volume contained less tubules. It can be seen from Table 4.3.2 that this manifests as a decrease in sample tapped density.

Table 4.3.2 also illustrates indices of particle flow, Carr's compressibility index and the Hausner ratio. Carr's compressibility index is an indirect measure of particle flow. The difference between the tapped and bulk densities of the powder is divided by the tapped density of the powder and is expressed as a percentage. The Carr's index assigned a range between 5-15% as indicative of excellent free flow (Wells, 2002). All the samples examined have values in this range, confirming that they have good flowability. The Hausner index is a ratio of the tapped density to the bulk density (Hausner, 1967). The author found that the ratio depends on interparticulate friction and could be used to predict powder flow properties. The ratios for the samples lie between 1.06 and 1.14. These values represent good powder flow because Hausner designated values less than 1.25 as indicative of good powder flow whilst samples with indices greater than this value had poor flow. The flow properties of the samples are further examined in Section 4.8.

Table 4.3.2 Density and flow indices of halloysite samples.

Sample	**Bulk Density (g/cm^3) (m/v_0)**	**Tapped Density (g/cm^3) (m/v_{1250})**	**Carr's Index (%)**	**Hausner Ratio**
Halloysite G	0.6818	0.7759	12.12	1.14
Halloysite G/cet	0.7482	0.7898	5.26	1.06
Balekisir	0.5330	0.5822	8.45	1.09
Balekisir/cet	0.5149	0.5848	11.94	1.14
Mill-med	0.6944	0.7634	9.03	1.10
Mill-high	0.6757	0.7547	10.47	1.12

4.3.3 Apparent Density

The granule density is determined by the displacement of mercury, which does not penetrate at ordinary pressures into pores smaller than approximately 10 μm (Gregg and Singh, 1982). This is analogous to the apparent density study conducted in this section. The displacement of a volume of hexane equivalent to the known mass of a clay sample introduced into the organic medium is used to calculate the apparent sample density. The density of hexane was calculated to be in the range 0.6642-0.6687 g/cm^3. When the fluid displaced by powder does not penetrate all the pores, the measured density will be less than the true density. However when densities are determined by liquid displacement, an apparent density is obtained which can differ according to the liquid used due to differing capacities to penetrate small pores. Hence it is important to quote the liquid used (Lowell and Shields, 1991).

Table 4.3.3 lists the apparent density of halloysite and chemically modified samples. The density values are significantly greater than the tapped density values. The bulk density of the halloysite G sample was calculated to be 0.7759 g/cm^3 in Section 4.3.2; it increased to 2.2507 g/cm^3 using the liquid displacement method. The cetrimide coated grade has a decreased density because the adsorbed surfactant prohibits intrusion of the hexane, hence the density appears lower.

Table 4.3.3 Apparent density values for halloysite and chemically modified samples determined using hexane.

Sample	Apparent Density (g/cm^3)	St. dev.
Halloysite G	2.2507	0.1064
Acid Washed halloysite G	2.1013	0.092
Cetrimide coated halloysite (0.2 % w/v)	1.7498	0.5660

4.3.4 True Density Analysis Using Helium Pycnometry

The skeletal density of the samples listed in Table 4.3.4 was determined using helium pycnometry. Since helium penetrates into the smallest pores and crevices, it is generally accepted that the helium method gives the closest approximation to true density. Liquids such as water, ethanol and hexane are denied entrance into the smallest pores; liquid

displacement accordingly gives a density somewhat smaller than the true value. The true density is defined as the ratio of the mass to the volume occupied by that mass. Therefore, the contribution to the volume made by pores or internal voids must be neglected when measuring the true density (Lowell and Shields, 1991).

An increase in the density of the sample is observed using this technique compared to the apparent density method outlined above in Section 4.3.3. The skeletal density of halloysite is seen to increase to 2.4833 g/cm^3; the increase is attributable to the smaller inert helium molecule intruding into pores with diameters smaller than the organic hexane molecule. The difference in density values equates to a volume difference of 4.3 cm^3/g, which is due to pores with a diameter smaller than the hexane molecule. The cetrimide coated sample displayed the most prominent change in density value. This is attributable to the surfactant structure occluding the access of the larger hexane molecule to the pore network and interior of the aggregate and tubule structure. However the smaller helium atom has the ability to access these regions.

Table 4.3.4 Skeletal density measurements of halloysite samples using a helium pycnometer.

Sample	Skeletal Density (g/cm^3)	St. dev.
Halloysite G	2.4833	0.0098
Acid washed halloysite G	2.4710	0.0048
Deferrated halloysite G	2.3982	0.0096
Balekisir	2.4809	0.0085
Deferrated Balekisir	2.4549	0.003
Cetrimide	1.1436	0.0043
Cetrimide coated halloysite (0.2 % w/v)	2.2450	0.0037

4.4 SURFACE AREA ANALYSIS

The surface area of the halloysite samples outlined in Table 4.4a was determined using a nitrogen adsorption technique. The amount of a gas or liquid solute that is adsorbed onto

the sample of a powder to form a monolayer is a direct function of the surface area of the sample. Particles with a large specific surface area are good adsorbents for the adsorption of gases and solutes from solution (Martin, 1993). Hence the determination of the surface area is a good indicator of the potential of halloysite to have an adsorbent role in topical formulations.

The surface area value for halloysite G was determined to be 55.98 m^2/g, this is similar to the surface area value of 57.28 m^2/g reported by Levis (2002) for a similar sample of halloysite G. It is also similar to a value of 56.2 m^2/g reported by Churchman *et al.,* (1995) for a tubular material from Jarrahdle, Western Australia. The surface area of Halloysite G is considerably higher than that obtained for some other halloysite samples. Salter (2003) reported a value of 15.34 m^2/g for halloysite from the Goushan region of China. The author noted that this halloysite had longer tubules, which would account for the decrease in surface area.

The concept of size reduction resulting in an increased surface area is the explanation for the higher surface area of Balekisir halloysite. It can be seen from Table 4.4 that it has a value of 64.87 m^2/g. It was noted using SEM analysis in Section 4.2 that Balekisir halloysite is composed of smaller tubules; therefore there is an increased surface area per unit weight of sample.

The deferration procedure resulted in a significant decrease in the surface area of halloysite (Table 4.4). The decrease from 55.98 to 38.21 m^2/g may be a result of the removal of small tubular debris, which would inflate the surface area value, rather than the removal of calcium and Fe salts, which would have smaller surface areas. However it was observed using SEM image analysis in Section 4.2 that the deferrated tubules assumed a fused appearance, this resulted in a decrease in the effective surface area for nitrogen adsorption.

A similar reasoning could be used to explain the decrease in specific surface area as a result of coating the clay with cetrimide. As the cationic surfactant binds to the tubule surface, access to the internal surface area via the pore network may be obstructed. The available surface area for adsorption is effectively reduced. The surface area may have also decreased as a result of surfactant binding which results in less of the tubule material being

packed per gram of material resulting in a decreased surface area. Also the presence of unbound surfactant would compound this.

Table 4.4 Surface area of halloysite samples using a nitrogen adsorption technique.

Sample	Surface Area (m^2/g)	(+/-) St. dev.
Halloysite G	55.98	0.46
Deferrated halloysite G	38.21	0.56
Cetrimide coated halloysite	34.87	1.00
Acid washed halloysite	104.84	1.80
Balekisir halloysite	64.87	0.80
Deferrated Balekisir halloysite	67.43	1.17

The most prominent change in surface area occurs in the sample that was subject to washing with concentrated HCl. The surface area increased by almost 50 m^2/g. This is due to two factors namely acid dissolution of edge Al from the octahedral sheet, which leads to a wedge-like splitting of the clay crystals (Fahn, 1979) and the formation of colloidal silica resulted in an increase in surface area. This has important consequences for halloysite applications. Theng and Wells (1995b) noted an increase of the capacity of halloysite to act as a decolourising agent after it was treated with 1M HCl.

Figure 4.4 depicts a nitrogen adsorption isotherm for halloysite G. The isotherm approximates either a Type II or Type IV isotherm. Type IV isotherms are typical of adsorption onto porous solids (Martin, 1993). Type II isotherms are most frequently encountered when adsorption occurs on non-porous powders or on powders with pore diameters larger than micropores (0-2 nm) (Lowell and Shields, 1991). A Type II isotherm is a normal form of isotherm obtained with macroporous (pore width exceeding 50 nm) adsorbents (Sing *et al.*, 1985; Byrne, 2004). However halloysite undoubtedly has pores within the mesopore range (2-50 nm). Levis (2000) observed using mercury intrusion studies that halloysite G had pores in the range 6-100 nm, with an average size of approximately 50 nm.

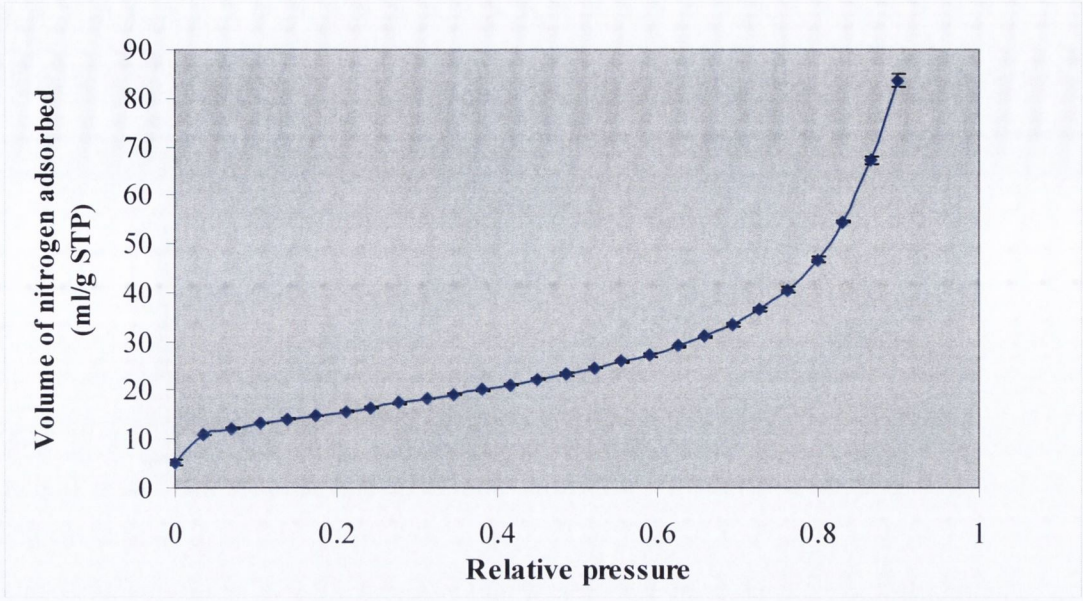

Figure 4.4a Nitrogen adsorption isotherm of halloysite G.

4.5 ELEMENTAL ANALYSIS

4.5.1 Introduction

Halloysite is a 1:1 layer silicate. The structural unit is composed of an octahedral gibbsite sheet bonded to a tetrahedral silicon oxygen sheet. Hence it is expected that the major elemental components are aluminium (Al) and silicon (Si). However, it is accepted that the non-stoichiometric substitution of Fe^{3+} for Al^{3+} in the octahedral sheet occurs (Soma *et al.*, 1992; Newman *et al.*, 1994) and that contaminants including calcium and Fe salts may be present on the surface (Takahasi *et al.*, 2001). The elemental analysis of the samples was determined using two methods, EDX microanalysis and ICP-MS.

4.5.2 EDX Microanalysis

EDX studies confirmed the principal elements in halloysite to be Al and Si, Figure 4.5.2a. Al and Si are present in approximately equal proportions. In addition to these elements low levels of calcium and Fe were detected. The Fe in the sample may be as a consequence of substitution for Al in the octahedral sheet or the presence of Fe in the form of oxides on the surface of the tubule. The deferration process resulted in a reduction of the Fe content from 2.7% to 0.27%. However a rise in the sulphur and sodium content was evident, Figure 4.5.2b. This is not surprising as the deferration process involves treatment with sodium

bicarbonate, sodium citrate and sodium dithionite as outlined in the methodology section. However it must be noted that the technique is only semi-quantitative and the values stated are a guide to the effect of the chemical modifications.

The EDX microanalysis pattern of Balekisir halloysite is portrayed in Figure 4.5.2c. Again Si and Al are the dominant elements. Calcium is present at a level of 0.35%; this is lower than that seen for the halloysite G grade, 9.69% in Figure 4.5.2a. There are low levels of potassium and sulphur in the Balekisir sample, which are not evident in the halloysite G sample. Takahashi *et al.* (2001) observed large amounts of potassium in halloysite deposits in volcanic regions in northern California. The Balekisir sample also has a higher Fe content, 3.56%, than the halloysite G grade. Deferration of the Balekisir sample resulted in a reduction in the Fe content by a factor of ten, Figure 4.5.2d. A small quantity remains; this is attributable to Fe intrinsic to the structure as distinct from free Fe oxides that are removed by the deferration method (Takahashi *et al.*, 2001).

The acid washing procedure resulted in a reduction in the ratio of Al to Si in the modified halloysite G sample examined; this is due to a leaching of Al from the tubule edge. Fe and sulphur have a very low presence, 0.03% and 0.38% respectively, Figure 4.5.2e. The Fe concentration is approximately equivalent to the Fe concentration after the deferration of halloysite G. The acid washing process has resulted in a total removal of calcium from the sample, which was most likely confined to the surface of the halloysite tubule. Charge repulsion would make access of divalent cations such as Ca^{2+} to the interior more difficult (Takahashi *et al.*, 2001). The calcium may be present in the oxide form (Technical information, New Zealand China Clay, 2001), but the carbonate form is also a possibility.

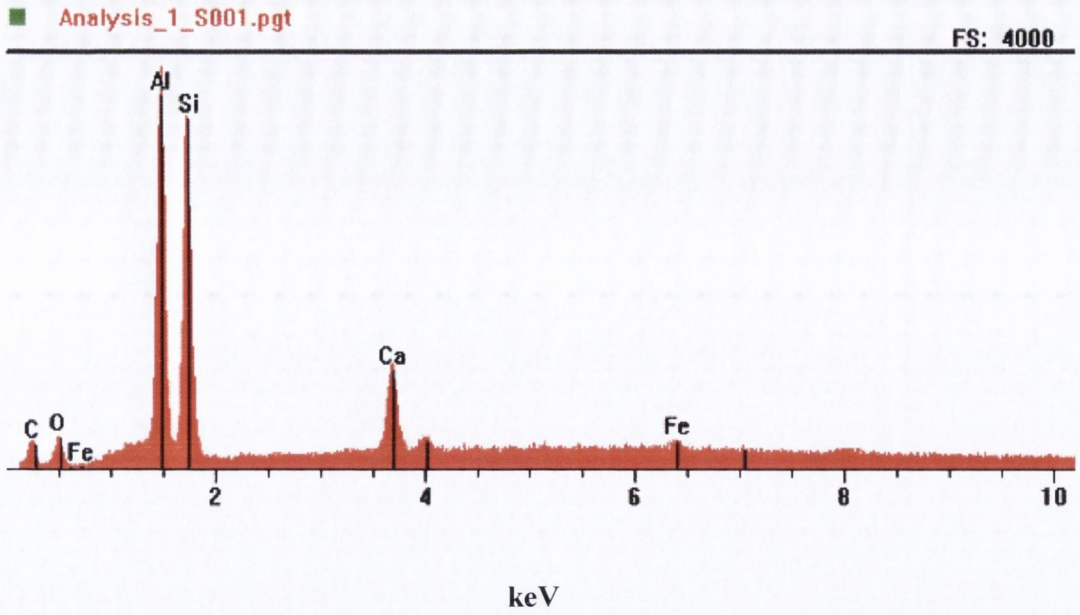

Figure 4.5.2.a EDX microanalysis of halloysite G.

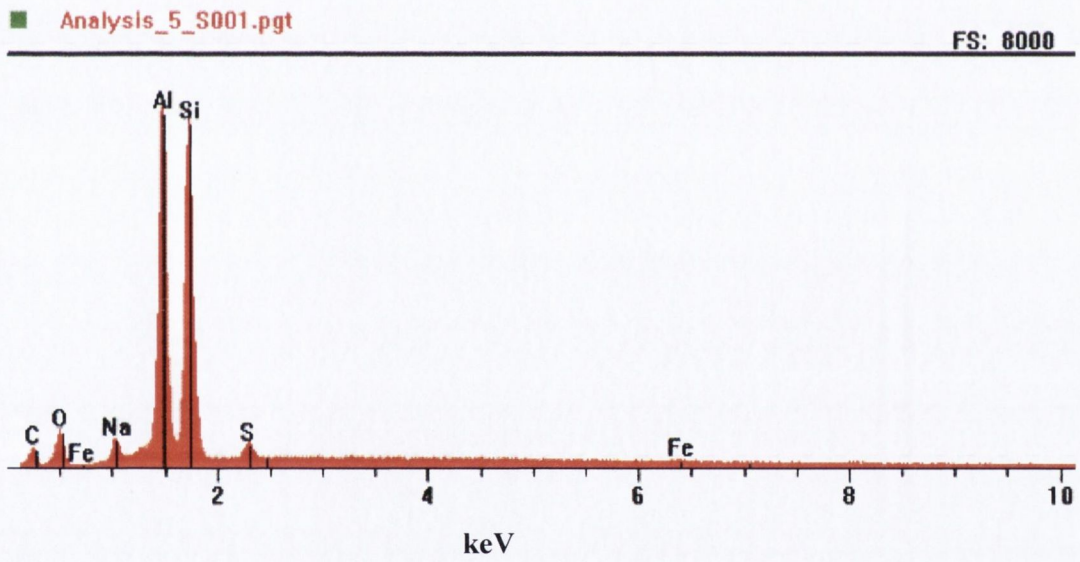

Figure 4.5.2.b EDX microanalysis of deferrated halloysite G.

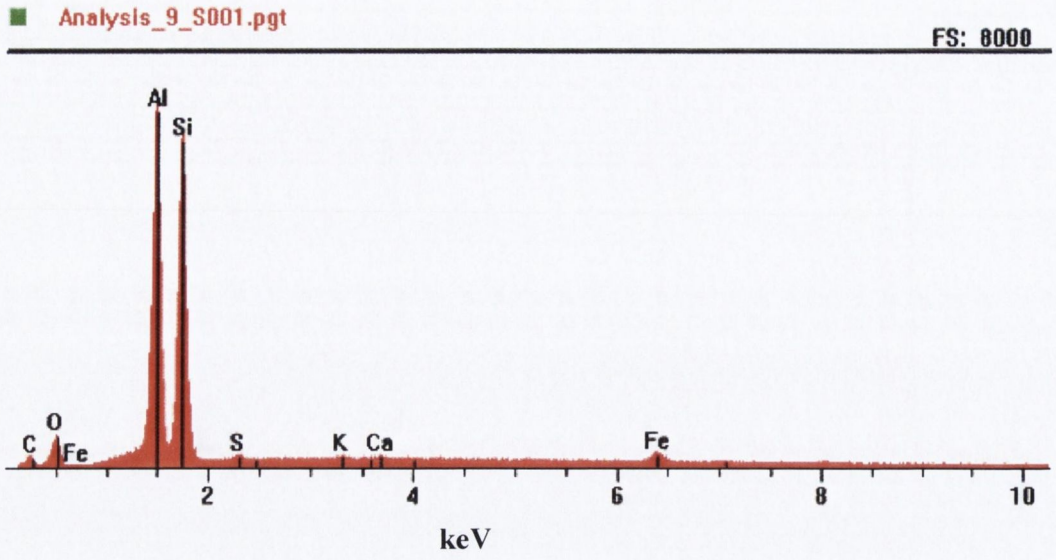

Figure 4.5.2.c EDX microanalysis of Balekisir halloysite.

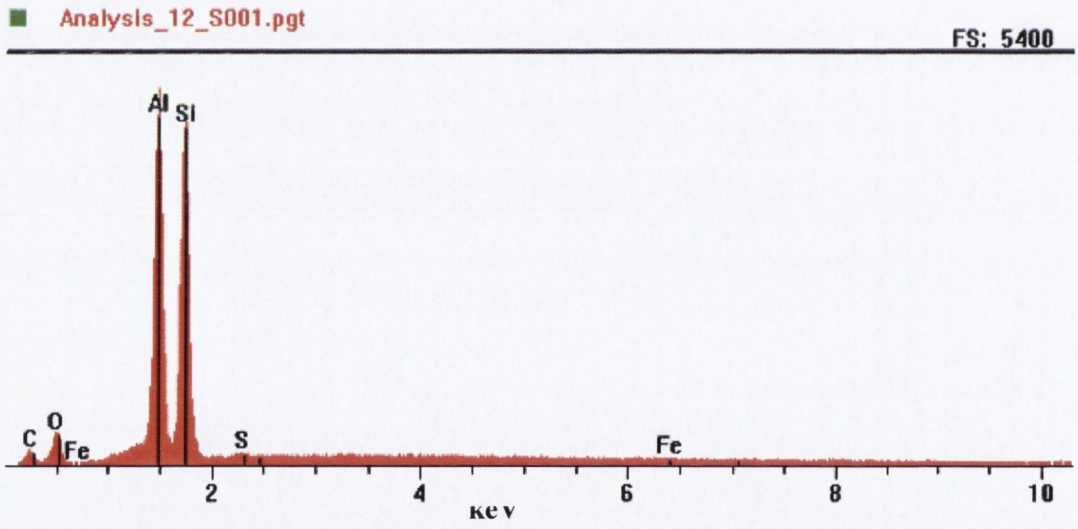

Figure 4.5.2d EDX microanalysis of deferrated Balekisir halloysite.

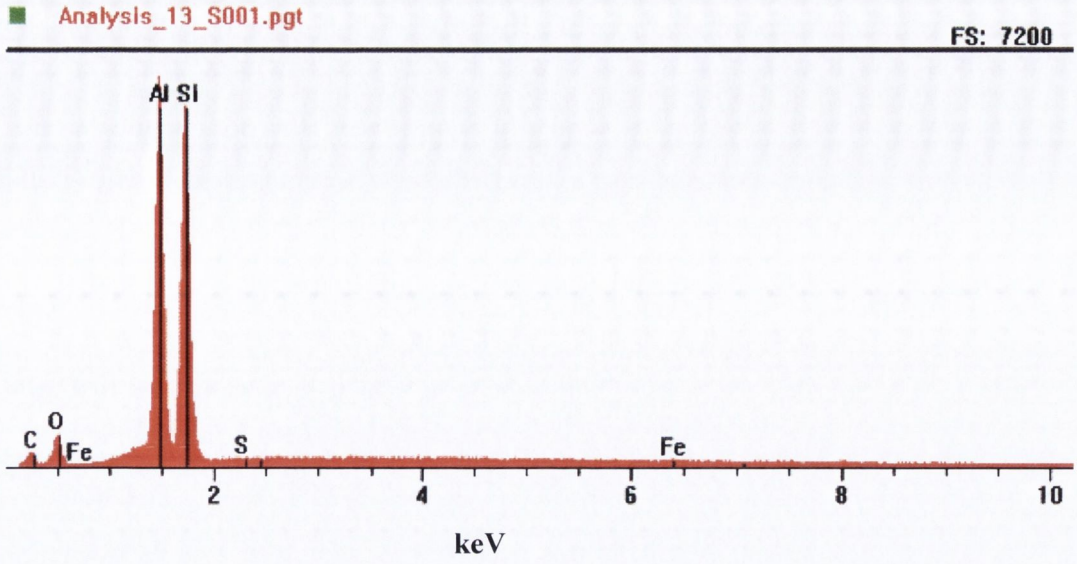

Figure 4.5.2e EDX microanalysis of acid washed halloysite G.

4.5.3 Inductive Coupled Plasma Mass Spectroscopy (ICP-MS)

The trace elements in the halloysite and chemically modified samples were determined quantitatively using ICP-MS analysis. The levels of Al and Si in the sample were not determined due to their very high levels in halloysite and because of the inability of the method to digest Si. Although the EDX microanalysis study in Section 4.5.2 above was a semi-quantitative method it did roughly quantitate the Al and Si content, hence the studies are useful in tandem. Table 4.5.3 depicts the major trace elements of halloysite samples. The ICP-MS results confirm the observations made in the EDX microanalysis study. However it expands this study by the inclusion of other trace elements including copper, barium, magnesium and manganese, which form part of the halloysite elemental composition. Deferration of halloysite G and Balekisir resulted in a decrease in the Fe content in both samples, Table 4.5.3. The Balekisir sample had a significantly higher quantity of Fe. It was thought this was the reason for the pink/flesh coloured appearance of the sample. This attribute was considered advantageous in the use of halloysite clays in topical and transdermal delivery due to the similarity to natural skin tone. Hence it would be expected to be cosmetically more acceptable. The deferration process caused the sample to turn a grey white colour, supporting the hypothesis that the large Fe content was responsible for the colour.

The acid washing procedure also caused a similar reduction in the Fe content of halloysite G. The chemical treatments likewise caused a reduction in other elements including calcium, potassium, barium, magnesium and manganese. This study highlights the very low level of unwanted elements such as lead. The acid washing of halloysite G affects a greater reduction in all elements compared to the deferration procedure. This accounts for the whiter appearance of the acid washed clay compared to the deferrated sample.

Table 4.5.3 Major trace elements of halloysite samples and chemically modified halloysite samples.

Sample	Halloysite G (ppm*)	Deferrated halloysite G (ppm)	Acid washed (ppm)	Balekisir (ppm)	Deferrated Balekisir (ppm)
Potassium	342	139	101	819	446
Sodium	408	18315	156	714	3168
Barium	474	158	35	165	35
Calcium	28,560	257	2	1201	15
Copper	107	68	55	13	14
Iron	2045	260	262	9569	340
Lead	<1	<1	<1	<1	<1
Magnesium	447	35	20	57	13
Manganese	779	2	3	35	<1

*ppm = parts per million.

4.6 FTIR SPECTROSCOPY

The absorption of infrared radiation by clay minerals depends critically on atomic mass and the length, strength and force constants of interatomic bonds in the structures of these minerals. It is also controlled by the constraints of the overall symmetry of the unit cell, and the local site symmetry of each atom within the unit cell. The infrared spectrum of a clay mineral is sensitive to chemical composition, isomorphous substitution and crystallinity, and provides fundamental information not only on mineral identification, but also on surface properties and reactions of minerals with chemicals in their environment

(Wilson, 1994). The importance of the size and shape of mineral particles has been described in detail (Farmer and Russell, 1966; Rendon and Serna, 1981; Serna *et al.*, 1982). Samples with particle sizes much greater than 2 μm must be pre-ground thoroughly in order to minimise scattering of incident IR radiation and the broadening and distortion of absorption bands. The absorption of infrared radiation is also strongly influenced by the degree of crystalline order (Lazarev, 1974). Broadening, loss of intensity and decrease of frequency are caused by isomorphous random substitutions and poor crystallinity (van der Marcel and Beutelspacher, 1976).

Spectra of all members of the kaolinite family show a strong resemblance particularly over the 1200-250 cm^{-1} range, with variations in the absorption pattern in the 1150-1100 cm^{-1} range arising from effects of particle size and shape (Farmer and Russell, 1966; Rendon and Serna, 1981). It can be seen from Figure 4.6a that the acid washing process results in an alteration in this region at 1100 cm^{-1}. The shoulder appearance of the band in the halloysite sample is more intense and defined after chemical treatment with concentrated HCl. A useful spectral region to help to distinguish between well-crystallized kaolinite and halloysite is between 750 cm^{-1} and 800 cm^{-1}. Work conducted on the kaolinite family of minerals showed that two weak bands found at 795 cm^{-1} and 758 cm^{-1} were of approximate equal intensity for kaolin, whereas for halloysite the 795 cm^{-1} band was reduced to a very weak inflection. The spectra of halloysite show wide variations in their intensities, especially in the higher wave numbers. Halloysite samples from sedimental origin, which are less ordered according to X-ray analysis, have also the weakest bands (van der Marcel and Beutelspacher, 1976.

A weak inflection at 3600 cm^{-1} and a corresponding weak feature near 880 cm^{-1} have been interpreted by Mendelovici *et al.* (1979) as arising from OH stretching and bending vibrations of $AlFe^{3+}$ OH groupings resulting from Fe^{3+} substitution for Al in the octahedral sheet of the kaolinite structure. The presence of these inflections in the FTIR spectrum in Figure 4.6a is quite faint and barely distinguishable. Mendelovici *et al.* 1979 further concluded that the use of the more exotic alkali halides CsBr or CsI were necessary before the $AlFe^{3+}$ OH bands were fully exhibited. Tari *et al.* (1999) attributed absorption bands at 1200-900 cm^{-1} to the Si-O-Si and/or Si-O-Al stretching region.

The complete assignment of bands to halloysite spectra is still disputed, however it is generally accepted that the band near 3620 cm^{-1} arises from internal hydroxyl (OH) groups, and that near 3700 cm^{-1}arises from surface OH groups. Halloysite shows significant broadening of bands throughout its spectrum, particularly for the 3700 cm^{-1} and 3620 cm^{-1} OH-stretching bands because of structural distortion caused by variable hydration (Theng *et al.*, 1982). The presence of both of these bands is observed as in both samples in Figure 4.6a. No alteration in the intensity or relative intensities between the two peaks was observed. A potential method for assessing the crystallinity of kaolinites was developed by Neal and Worrall (1977). It is based on the ratio of the 3700 and 915 cm^{-1} hydroxyl band absorbencies. An inverse relationship exists between the magnitude of this ratio and crystallinity. The ratio is approximately equal for both the halloysite and acid washed sample indicating that no change in sample crystalinity has occurred due to the acid washing process. The acid washing process does result in the loss of a band at 1470 cm^{-1}, this may have resulted from a distortion in Al bonding as the acid caused a dissolution of Al (and Fe) from the edge of the tubule (Fahn, 1979). An inflated value of the crystallinity can be derived if substantial adulteration with fine-grained dioctahedral illite or smectite occurs. The presence of these minerals would make a significant contribution to the OH bending at 915 cm^{-1} but relatively little to the 3700 OH cm^{-1} stretching, hence an alteration of the ratio. A weak band found near 3550 cm^{-1} is not found in all halloysites and may arise from H-bonding between surface OH-groups and interlayer water (Kodama and Oinuma, 1963).

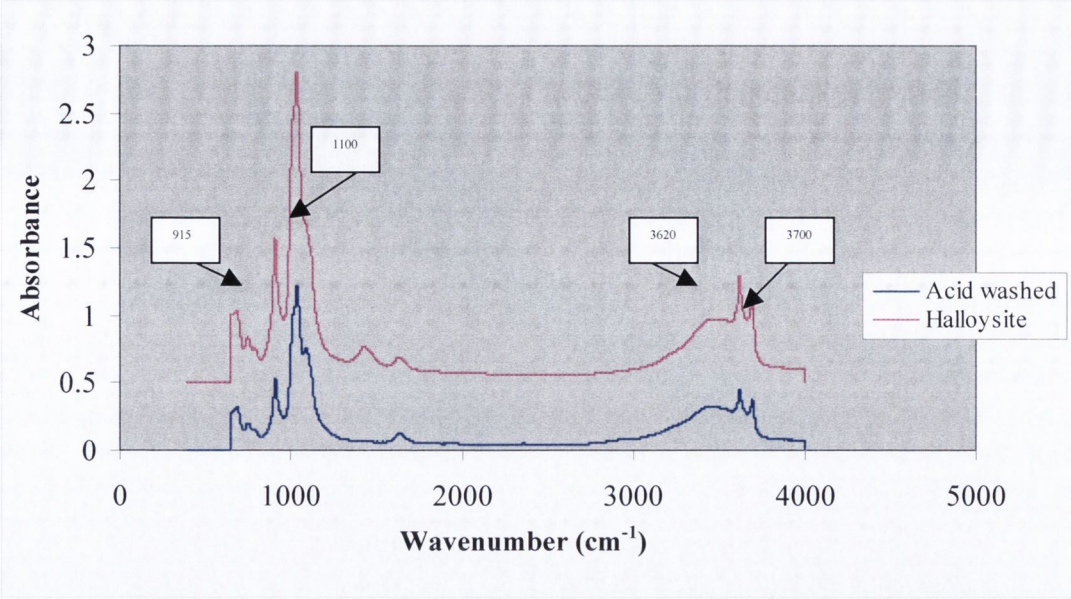

Figure 4.6a FTIR spectra of halloysite and acid washed halloysite.

Figure 4.6b depicts the FTIR spectra for halloysite and cetrimide coated sample. The adsorption of the surfactant does not result in any significant change in the spectrum. Again the broadness of the absorption band at 1100 cm^{-1} is decreased and it is more prominent. The appearance of absorption bands at 2860 and 2940 cm^{-1} is the most prominent difference between the samples. They arise due to stretching and vibrational bonds associated with the interaction of the surfactant and the surface hydroxyl groups. The slight alteration in the absorption bands at 3620 and 3700 cm^{-1} is indicative of the involvement of surface hydroxyl groups.

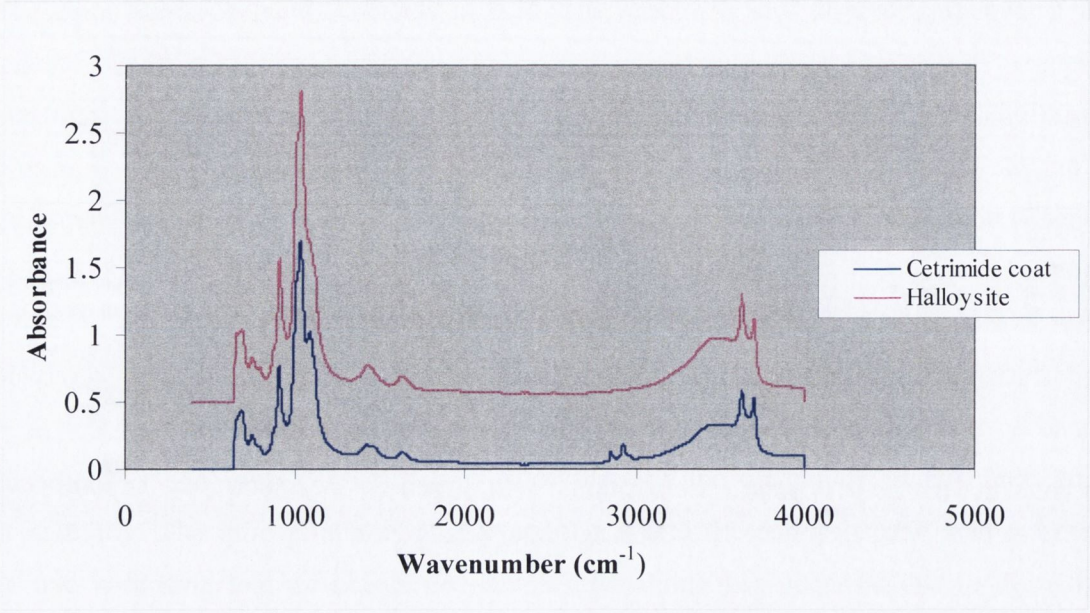

Figure 4.6b FTIR spectra of halloysite and cetrimide coated halloysite.

FTIR in conjunction with XRD can be used to identify and differentiate clay minerals. X-rays of oriented aggregates after heating to 550 °C can be used to identify halloysite. The same heating cycle results in a sharp decrease in IR intensities. The technique can distinguish halloysite from dickite because a comparatively greater decrease in the intensity of the outer vibration (3700 cm^{-1}) than that of the inner O-H vibrations (3650 cm^{-1} and 3620 cm^{-1}) occurs on heating to 550 °C. The opposite effect happens for the inner O-H band of halloysite at approximately 3620 cm^{-1} (van der Marcel and Beutelspacher, 1976).

4.7 X-RAY DIFFRACTION STUDIES

The aim of this section was to conduct XRD studies to determine the crystallographic structure of halloysite and any alteration of this as a result of chemical modification. The crystallographic structure can have a profound impact on both chemical and physical properties. The diffraction angle of the x-rays is governed by the spacing between atomic planes within a crystal (Brittain, 2003). Halloysite is a member of the kaolinite group of minerals; it has a layer of water between each of the repeating layers. It is the presence of this interlayer water that differentiates it from kaolin, which does not possess any water intrinsic to its structure. The gradual loss of the interlayer water at various stages

influences its structure. The impact of atomic substitutions in the octahedral and tetrahedral sheets on the structure was also discussed in Chapter 1.

Figure 4.7a depicts XRD patterns of halloysite G and a sample of halloysite G that was subject to a deferration procedure. The halloysite grade used was a dehydrated form; this is confirmed by the 001 and 002 basal spacing reflections that indicate peaks at 12.30° 2θ and 24.55° 2θ, respectively. This translates to d spacings of 7.35 and 3.63 Å, respectively. This, in conjunction with the absence of a peak at 8.76° 2θ indicative of the 10 Å form, confirms that the halloysite was in a dehydrated form (Levis and Deasy, 2002). Frost *et al.* (1997) observed that the interlayer spacing of a fully hydrated halloysite decreased to 7.2 Å from 10.1 Å. Wada and Mizota (1982) observed that the hydrated form (10 Å) collapsed to the 7.2 Å form after heating at 300 °C. Brindley and Brown (1980) made similar observations, however they noted that the collapse to the 7.2 Å form occurred after heating to 100 °C for an hour. The absence of interlayer water is not surprising because Hughes *et al.* (1966) observed a rapid dehydration of the hydrated form in the 70-30% relative humidity region. Harrison and Greenberg (1962) noted that fully hydrated halloysite underwent some dehydration, even at relative humidities of 90%. It has also been suggested that the stability of the interlayer water may be related to the age of formation (Nagasawa and Noro, 1987b).

The XRD patterns for the halloysite and deferrated sample are similar except for some essential features. The intensity and breadth of the peak at 12.30° 2θ in the deferrated sample is greater than the corresponding peak in the untreated sample. This implies that there is a difference in crystallinity between the samples. Sharp peaks are indicative of a more crystalline material. The presence of the broad diffuse portion in the halloysite spectrum between 15-20° 2θ, which is absent in the deferrated sample, may represent some amorphous material that was removed by the deferration process. The peak at 29.70° 2θ due to crystalline material has been removed by the deferration procedure. This indicates that this peak is due to iron.

Figure 4.7b depicts XRD patterns for Balekisir halloysite and a sample of Baleksir halloysite that was subject to the deferration procedure. The Balekisir halloysite is also present in a dehydrated state due to the reasons outlined above. There are no additional crystalline features in the XRD pattern to explain the pink colour of the Balekisir sample.

The presence of the peak at 29.70° 2θ in the halloysite pattern is not evident in the Balekisir XRD pattern. Deferration of the Balekisir sample results in a decrease in the intensity of the peak at 12.30° 2θ, the base is also not as broad. The peak due to the deferrated sample at this value is still sharp indicating it is crystalline. Therefore it may be concluded there has been some structural alteration as the intensity of x-rays is determined by atom types within a solid and their arrangement within a crystalline material (Brittain, 2003).

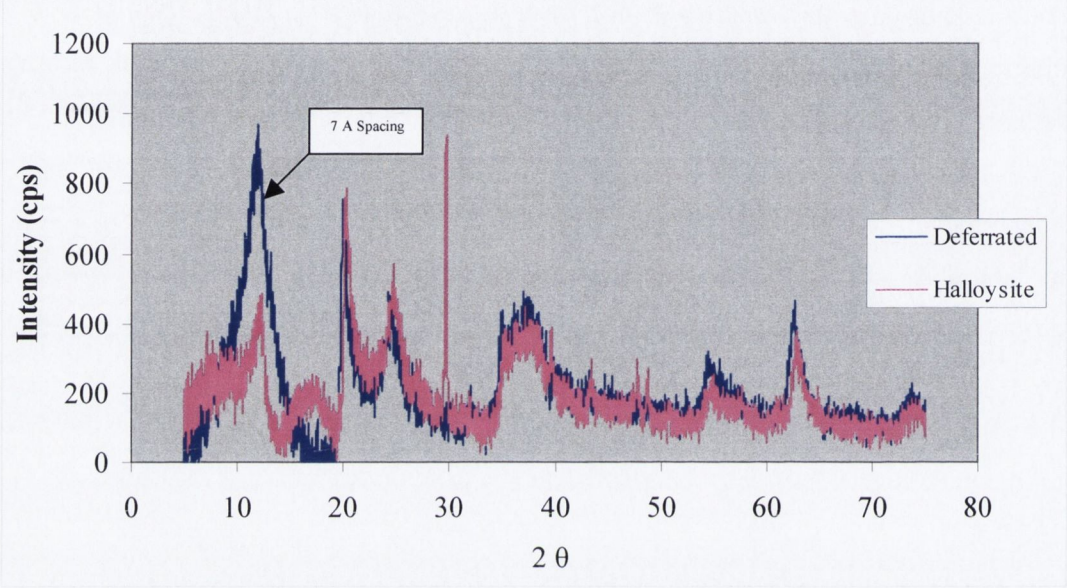

Figure 4.7a XRD pattern of a halloysite G and a sample of halloysite G that was subject to the deferration process.

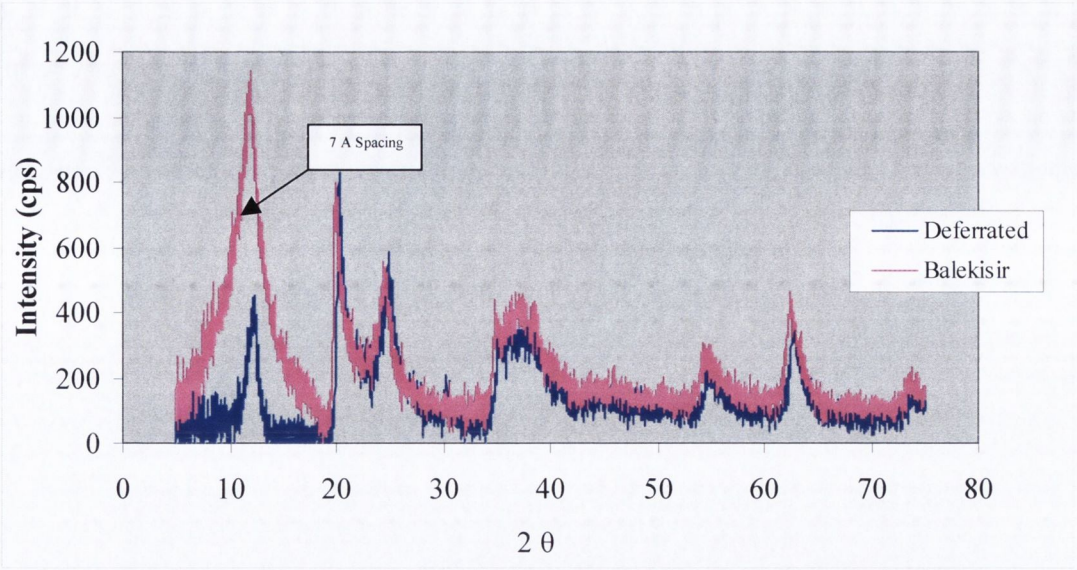

Figure 4.7b XRD pattern of a Balekisir halloysite and a sample of Balekisir halloysite, which was subject to the deferration process.

4.8 FLOW PROPERTIES

4.8.1 Introduction

The aim of this section was to examine the particular flow properties of halloysite and cetrimide coated halloysite. It is an extension of the Hausner ratio and Carr's compressibility index concepts elucidated in Section 4.3.2. The flow properties of halloysite and cetrimide coated halloysite were assessed using the flowability index (Flodex®) and static angle of repose measurements. The experiments were conducted to assess the effect of coating halloysite with the quaternary ammonium surfactant, cetrimide.

4.8.2 Flowability

The test for flowability is intended to determine the ability of divided solids (for example, powders and granules) to flow vertically under defined conditions (British Pharmacopoeia, 2007). The flowability index gives a determination of intrinsic flowability, which is based upon the ability of a powder to fall freely through a hole in a plate. It is a direct indication of the potential flowability of powder mixes i.e. the lower the flowability index the more flowable the material will be (Salter, 2003). The results can depend on the storage conditions of the sample. Neither halloysite nor cetrimide coated halloysite produced a positive result. They did not fall through the aperture at any diameter range. The results are

illustrative of materials with poor flow properties, this is in contrast to the results calculated using the Hausner ratio and Carr's index. The poor flow is attributable to the cohesive forces causing the sample to settle in the holder prior to the test being performed. The variance in results for this test and that determined using bulk and tapped density analysis; Section 4.3.2 may be attributed to test methodology. The Hausner ratio and Carr's index are based on sample consolidation, which cohesive forces could enhance resulting in ratios, which would infer an improved flowability.

Table 4.8.2 Flowability index results for halloysite and cetrimide coated halloysite

Diameter of Disc	Halloysite	Cetrimide coated halloysite
4-32 mm	Negative	Negative

The results for the BP test for flowability may also be expressed in seconds and tenths of seconds related to 100 g of a sample. The results can be presented in a number of formats (a) the mean of the determinations, if none of the determinations deviate from the mean by more than 10 per cent: (b) as a range if deviation by more than 10 per cent occurs: (c) as a plot of the mass against the flow time or (d) as an infinite time, if the entire sample fails to flow through (British Pharmacopoeia, 2007), which was the case with both of the samples studied. However, it was not possible to use this method with the samples examined as they failed to flow through the discs as outlined in Section 3.2.8.2. It would have been expected that the flow properties of the cetrimide coated grade would have been superior as with all other similar test conducted the cetrimide coated grade appeared to flow and settle better than halloysite alone. From the results of tapped density tests in Section 4.3.2, it can be seen that the settling ability of cetrimide coated halloysite is quite different to that of halloysite alone. It may be postulated that the hydrophobic surfactant chains that extend from the cetrimide coated grade might become entangled to reduce the interfacial tension resulting in cohesive forces between particles. A slight compaction force may result when the sample is placed in the funnel, hence accentuating potential cohesive forces, which results in inhibition of sample flow.

4.8.3 Static Angle of Repose

In order to further delineate the flow properties of the two samples, the static angle of repose was investigated. The angle of repose is a measure of the frictional forces in a loose powder. This is the maximum angle possible between the surface of a pile of powder and the horizontal plane. The tangent of the angle of repose is equal to the coefficient of friction μ between the particles (Martin, 1993). The angle of repose like the flowability index, gives a direct indication of the flowability of a material i.e. the lower the angle of a dry material, the more flowable a material will be (Carr, 1965). The angle of repose for halloysite based on an average of six determinations was found to be 44.82°. The equivalent value for the cetrimide coated halloysite was 30.96°.

As discussed in Chapters 1 and 5, halloysite particles are electrically charged with a predominantly anionic charge along the surface and a positive charge at the ends. Therefore this strong electrostatic attraction between the particles would directly result in a tendency for the particles to bridge together and therefore reduce flowability. Coating of the particle with cetrimide reduces this as the cationic head group binds to the negative surface and the "house of cards" structures do not form as readily. This was exemplified by the decrease in the static angle of repose value. The lower the flow angles the better the flow properties. Carr (1965) considered a value of 25° as optimum and indicative of excellent flow properties. This highlights that the cetrimide coating resulted in enhanced flow, however the addition of excipients such as a glidant would be required to obtain optimum flow conditions

Table 4.8.3 Static angle of repose values for halloysite and cetrimide coated halloysite indicating the flowability of each of the samples.

Sample	Cone height (cm)	Angle
Halloysite	4.97	44.82
Cetrimide halloysite	3.0	30.96

4.9 CONCLUSIONS

Halloysite was chemically modified using three procedures. An organo-grade was produced through the electrostatic binding of the surfactant cetrimide to the surface of the

halloysite G tubules. Two grades of halloysite, halloysite G and Balekisir were subject to a deferration process to remove free Fe oxides (Takahashi *et al.*, 2001). Finally halloysite G was washed with concentrated HCl. Microscopic examination of the halloysite and deferrated samples using SEM analysis showed that the typical tubular length of halloysite G (up to 1 μm) was greater than the tubule length of Balekisir halloysite (approximately 0.5 μm). The presence of debris and fractured tubules was evident in both halloysite samples. Heating of the samples to 800 ^{o}C using TGA resulted in the tubules forming clusters with large pores (1-2 μm) in the tubular aggregate matrix. The deferration procedure resulted in the tubules assuming a fused appearance. This was not altered as a result of the heating process.

The closest approximation to true density was obtained using helium pycnometry. The skeletal density for halloysite G was 2.4833 g/cm^3. The skeletal density method resulted in an increase in value as expected due to the ability of the smaller helium atom to intrude into the smaller pores compared to the larger hexane molecule that was used in the apparent density method. The increase in density values using the hexane and helium indicate the presence on intraparticulate pores and interparticulate void spaces between tubule aggregates. The bulk and tapped density values were used to calculate the Carr's compressibility and Hausner ratio flow indices. All the samples examined displayed good flow properties. Analysis of the flow properties was assessed using a Flodex® tester, this indicated that halloysite and cetrimide coated halloysite displayed poor flow. However, the static angle of repose method indicated that cetrimide coated halloysite had superior flow properties to the uncoated grade. The variance in results is explained by the method of determination. The sample consolidated in the Flodex® test apparatus which resulted in a negative outcome; however the ability of the sample to consolidate after tapping results in improved values for the Hausner and Carr's indicies.

The surface area of the samples is an important indicator of the adsorbent capacity of the clay minerals and their potential use in topical formulations for drug loading and wound exudate adsorption. The results of the study highlighted if sample modification could enhance the potential for adsorption. The deferration procedure resulted in an appreciable decrease in the surface area of halloysite G from 55.98 to 38.21 m^2/g. This is attributed to the decrease in the available surface area for adsorption as a result of the fused appearance of the tubular structures. This was depicted in SEM image analysis studies. The acid

washing procedure had a contrasting effect, the surface area increased by almost 50 m^2/g. The acid induced splitting of the clay crystal (Fahn, 1979) and the formation of colloidal silica (Theng and Wells, 1995b), which manifested as an increase in surface area. The surface area of the organo-halloysite grade was 34.87 m^2/g. The reduction is probably due to a decrease in the available surface for nitrogen adsorption caused by the surfactant obscuring pores leading to the interior of the tubule.

Semi-quantitative analysis using EDX microanalysis confirmed the presence of Al and Si as the prominent elemental components. The other obvious elemental components are calcium, potassium, sulphur and iron. The elemental composition was altered as a result of the deferration and acid washing procedures. Quantitative analysis using ICP-MS showed that the acid washing procedure caused a greater reduction of the elemental components than the deferrration procedure except in the case of Fe content. The Fe content was decreased in halloysite G from 2045 to 262 ppm using the acid washing procedure but it was reduced to 260 ppm as a result of the deferration procedure. The Balekisir had a greater Fe content, 9569 ppm compared to the halloysite G sample, 2045 ppm. The halloysite G had a very high level of Ca, 28,560 ppm whilst the Balekisir sample had a high level of potassium, 819 ppm.

The crystallinity of the sample was assessed using XRD studies. The XRD patterns confirmed the halloysite G and Balekisir grades were in the dehydrated state due to the presence of peaks at 12.32° and 24.32° 2θ. These particular angles correspond to d-spacings of 7 and 3.63 Å respectively; they are intrinsic features of dehydrated halloysite. This is confirmed by the absence of a peak characteristic of the hydrated form (10 Å) at 8.76° 2θ. FTIR studies highlighted that chemical treatment of the halloysite G grade did not appreciably alter the FTIR pattern of vibrational and stretching bands of the sample. Washing halloysite with concentrated HCl caused an absorbance band at 1470 cm^{-1} to be removed. It is likely this is attributable to the removal of Al or colloidal silica formation, which are directly attributable to the acid washing procedure. The coating of halloysite with cetrimide results in the formation of bands at 2860 and 2940 cm^{-1}. The formation of the bands is ascribed to the presence of the surfactant and the interplay between it and surface hydroxyl groups.

The characterisation study highlighted that the halloysite samples contained low levels of unwanted elements such as lead (< 1 ppm in all samples) and that purification could be performed by removal of free Fe oxides and calcium salts. It also highlighted the potential of the acid modified grade to be used as an adsorbent due to its increased surface area and its adsorbent capacity as will be further elucidated in Chapter 5. The cetrimide modified clay had enhanced flow properties which may be important in the formulation of topical products. The impact of this grade on the flow properties of ointment bases is discussed in Chapter 6.

Chapter 5

CHARACTERISATION OF SURFACTANT TREATED HALLOYSITE

5.1 INTRODUCTION

The adsorption of cationic surfactants on mineral or inorganic substrates is important from two points of view. First in a practical sense, cationic surfactants are employed in various processes in which adsorption or interaction with inorganic substrates achieves desired results. These applications include, for example, flotation or beneficiation of ores, sedimentation, coagulation, corrosion, detergency, sanitisation and the processing of fertilizers. The second reason is that these substrates may provide well defined systems which permit the development of models for the adsorption process of surfactants (Ginn, 1970).

The aim of this section of work was to describe the adsorption isotherms of various surfactants on the clay mineral, halloysite. Controlling the adsorption of surfactants is a vital parameter in dictating the hydrophilic-hydrophobic character of the material. Halloysite and chemically modified halloysite grades were characterised in Chapter 4. Initially, the behaviour of surfactants at the solution-air interface was investigated by determining the critical micelle concentration (CMC). The effect of electrolyte (sodium bromide (NaBr) and potassium chloride (KCl) addition on the solution CMC was also elucidated. Deflocculating halloysite with surfactants was used as a preliminary study to assess the adsorption behaviour of halloysite. It was also used as a guide to determine the ability of surfactants to extract and isolate enriched tubular material from crude sources such as the Balekisir grade examined in Chapter 4.

The primary group of surfactants examined in this Chapter was the cationic quaternary ammonium compounds. The focus centered on cetrimide because it possesses antiseptic properties and is widely used in topical preparations. The British Pharmacopoeia (2007) defines cetrimide as consisting of trimethyltetradecylammonium bromide (TTAB), and that

it may contain smaller amounts of dodecyl- and hexadecyl-trimethylyammonium bromides (HTAB). However between 96 and 101% of alkyltrimethylammonium bromides must be calculated as $C_{17}H_{38}BrN$ (TTAB). This definition did not always apply. Previously the primary constituent of cetrimide was considered to be the 16 carbon constituent, HTAB. Since cetrimide is principally composed of the 14 carbon constituent, this was the component of primary focus in the study and is referred to as TTAB for distinction. The concept of increasing hydrophobicity as the chain length increased was investigated using hexadecyltrimethylammonium bromide (HTAB), which possesses 16 carbons in its hydrocarbon tail. The HTAB molecule is more hydrophobic than the TTAB molecule because it contains two extra CH_2 units in its hydrocarbon chain structure.

Other cationic surfactants including benzalkonium chloride (BAC) and pyridinium surfactants (dodecylpyridinium chloride (DPC) and cetylpyridinium chloride (CPC)) were investigated, as they possess a benzene ring as part of their strucure, which has ramifications for the nature of binding. The anionic surfactants, sodium lauryl sulphate (SLS) and sodium dodecyl benzene sulphate (SDBS) were also investigated. However, adsorption isotherms with SLS were not examined because a detection method was not readily available. Binding isotherms were elucidated using a solution depletion approach. A 2^3 factorial analysis of primary factors influencing TTAB adsorption was undertaken to determine optimal binding conditions.

The integrity of the antibacterial character of cetrimide on complexation with halloysite was assayed using an agar plate study. The efficacy of the samples to inhibit bacterial growth was determined by measuring the zone of inhibition of bacterial growth around the sample. Two strains of *Staphlococcal aureus* (*S. aureus*) with differing sensitivities were used.

5.2 CRITICAL MICELLE CONCENTRATION (CMC)

5.2.1 Introduction

Cetrimide is an example of an amphiphile; it has two distinct regions of opposing solution affinities within the same molecule. Depending on the number and nature of the polar and non-polar groups present the amphiphile may be predominantly hydrophilic or lipophilic or reasonably well balanced between these two extremes. When present in a liquid medium at

low concentrations, amphiphiles exist separately and are of such a size as to be subcolloidal. Below the CMC the amphiphile exists as monomers at the air water interface. As the concentration increases, aggregation occurs over a narrow concentration range. The addition of further surface-active agent results in aggregate formation, these aggregates are termed micelles. The CMC occurs when the concentration of the monomer at the air water interface and in the bulk reaches saturation. Micellar formation decreases the free energy of the system. The diameter of micelles is of the order of 50 Å, micelles lie in the colloidal size range (Martin, 1993).

The addition of a surfactant to a system reduces the surface tension of the liquid. The surface tension reduces to a particular point, which corresponds to micelle formation; after micelle formation the surface tension plateaus. The interfacial free energy is the minimum amount of work required to create an interface. In measuring the surface tension of a liquid, the interfacial free energy per unit area of the boundary between the liquid and air above it is being calculated (Rosen, 1989). Gibbs adsorption equation (Equation 5.1) may be used to calculate the surface concentration in excess of that in the bulk of the liquid ($\acute{\Gamma}$). It relates the bulk concentration and the interfacial tension. Above the CMC the surface tension remains essentially constant, indicative that the interface is saturated and micelle formation has taken place in the bulk phase. This implies that increasing interfacial adsorption occurs.

$$\acute{\Gamma} = - \frac{c}{RT} \frac{d\gamma}{dc} \qquad \textbf{Equation 5.1}$$

where $\acute{\Gamma}$ is the surface excess or surface concentration, the amount of surfactant per unit area of surface in excess of that in the bulk of the liquid, c is the concentration of amphiphiles in the liquid bulk, R is the gas constant, T is the absolute temperature, and $d\gamma/dc$ is the change in the surface tension of the solution with change of bulk concentration of the substance (Martin, 1993).

5.2.2 Critical Micelle Concentration (CMC) Determination

It can be seen from Fig.5.2.2 that the point of inflection for the plot of surface tension against concentration for TTAB occurs at 0.1% w/v. The CMC is regarded as the surfactant concentration at which the minimum plateau value of surface tension occurs (Ryu and Free, 2003). The CMC value calculated for the surfactant system without any electrolyte was 2.98 mM. This value was determined from surface tension measurements at an air-water interface. The CMC was also calculated using conductivity studies. The same value for the CMC of TTAB was obtained with this method. This supports the conclusion that the CMC value for TTAB is 2.98 mM. It is higher than the value of 2.6 mM determined by Barry *et al.* (1970). However the authors experimented with cetrimide and did not make a distinction based on the exact nature of the hydrocarbon chain lengths in the sample. The difference between the calculated value and that determined by Barry *et al.* (1970) is most likely due to the presence of longer chain surfactants, which have an increased hydrophobic effect and cause the CMC to decrease. Other authors determined higher values for TTAB. Attwood and Patel (1989) calculated a value of 3.08 mM and Atkin *et al.* (2003c) stated that the value for TTAB was 3.6 mM.

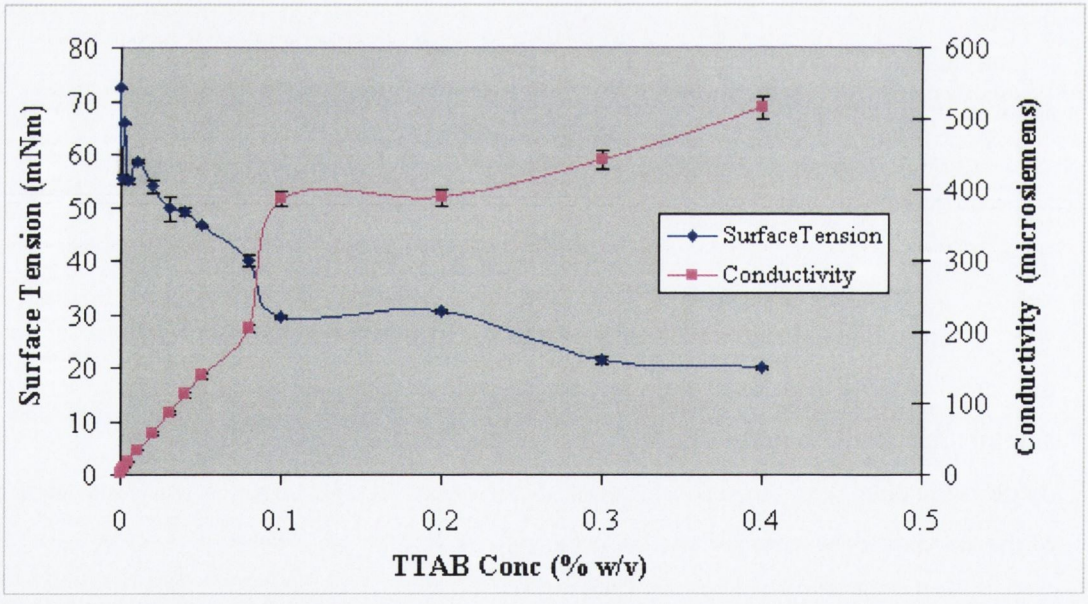

Figure 5.2.2 Plot of the surface tension and conductivity of TTAB solutions against their concentration.

Another cationic surfactant, DPC was examined. There is some divergence in the literature with regard to the CMC for DPC. The CMC value of DPC was calculated as 10.57 mM. It

is similar to the value of 10.1 mM, determined by Koopal *et al.* (2004). However it is considerably lower than the literature values of 14.7 mM and 16.5 mM quoted by Atkin *et al.* (2003c) and Goloub *et al.* (1996) respectively. The value stated by Goloub contained KCl, 10 mM. This would imply that the value for DPC alone was even higher. However, the DPC used in the studies outlined here was only 98% pure (Sigma-Aldrich product information). From the product labeling the quantity of water in the sample was not known. Therefore prior to the determination of the CMC value the amount of water in the sample was quantified using Karl-Fischer titrations. It was concluded that the sample contained one water molecule per DPC molecule.

The CMC values of two anionic surfactants SLS and SDBS were also elucidated and are depicted in Table 5.2.4. The values for SLS and SDBS were determined to be 6.94 mM and 1.5 mM respectively. The value for SLS agrees with that of 6.93 mM, determined by van Doorne (1990), as it lies within the calculated standard deviation. It is less than a value of 8 mM estimated by Greenwood *et al.* (1968). Differences may be attributed to the presence of impurities or surfactants of different chain lengths. SLS like cetrimide, is not composed of a single chain length. The BP (2007) defines SLS as a mixture of sodium alkyl sulphates consisting chiefly of sodium dodecyl sulphate, $C_{12}H_{25}NaO_4S$ (M_r 288.4). It contains not less than 85.0 per cent of sodium alkyl sulphates, calculated as $C_{12}H_{25}NaO_4S$. It can be seen from this definition that SLS is more variable as the purity level is only designated as 85%.

5.2.3 The Effect of Electrolyte Addition

The extent of adsorption of ionic surfactants is greatly affected by addition of electrolyte. It is presumed that the electrolyte exerts its influence by decreasing the repulsion between the orientated ionic head groups allowing a closer packing in the surface layer as the ionic strength is increased (Attwood and Florence, 1983). Monticone and Treiner (1995) examined the addition of the electrolyte, NaBr to surfactant systems. They concluded that the presence of the electrolyte resulted in an increased hydrophobic type effect, which favours micelle formation in the bulk, consequently decreasing the CMC. This may be explained by that attributed to Attwood and Florence above. The addition of the electrolyte allows the surfactant monomers to pack tighter and form aggregates at lower concentrations analogous to that which occurs when the surfactant has increased

hydrophobic moiety as part of its structure. Their observations explain the addition of NaBr to the system in Figure 5.2.3. The plot of surface tension against concentration essentially follows the same trend in both systems, however the system containing the electrolyte NaBr is displaced to lower surfactant concentrations. The point of inflection occurs at a lower concentration, indicating that the driving force for micelle formation in the bulk is altered. It can be seen from Table 5.2.4 that the CMC value decreased to 1.49 mM on addition of NaBr 10 mM. This value deviates from a value of 2.1 mM cited by Atkins *et al.* (2003c). This value was for TTAB, with the addition of 10 mM of salt. However, the type of electrolyte salt added was not stated. The presence of a different salt or surfactant impurities could account for the difference in observed values. Table 5.2.4 also lists the CMC of TTAB in the presence of a higher NaBr concentration (150 mM). The value decreases to 0.89 mM. It can be seen that the decrease is more substantial for 10 mM of electrolyte and that increasing additions do not result in a proportional reduction in the CMC of the system. This highlights that small additions of electrolytes can have a profound effect on the CMC value.

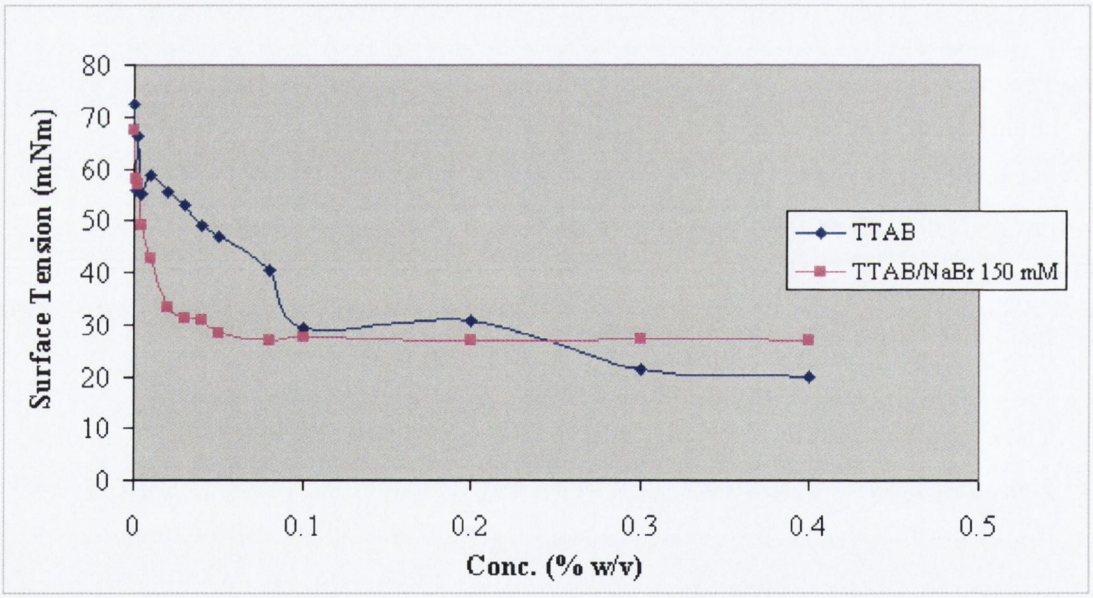

Figure 5.2.3 Plot of the surface tension against concentration for TTAB and TTAB with NaBr 150 mM systems.

Only the plot of the addition of the higher electrolyte concentration, NaBr 150 mM is depicted graphically in Figure 5.2.3, because the shift of the CMC value is more

pronounced. As already stated above it can be seen from Figure 5.2.3 that the point of inflection for the plot of surface tension against concentration occurs at lower values with the addition and increased concentration of NaBr. The decrease in CMC points towards an increased thermodynamic stability in the system with the addition of the NaBr electrolyte.

The effect of electrolyte addition on the CMC value of the anionic surfactant SDBS was also examined, KCl rather than NaBr was used in this system. KCl was chosen for use in conjunction with this particular surfactant as the majority of the literature employed this electrolyte and it would be expected that comparison of values would be more appropriate. The CMC value of SDBS in the presence of KCl, 10 mM was determined to be 0.75 mM. This value is half that obtained for the SDBS surfactant with no added electrolyte. This is in close agreement with the literature value of 0.7 mM obtained by Torn *et al.* (2003) for SDBS in the presence of NaCl, 10 mM.

5.2.4 Effect of Altering the Hydrocarbon Chain Length

The surface activity of a particular surfactant depends on the balance between its hydrophilic and hydrophobic properties. The relationship between increasing surface activity with increasing chain length is expressed by Traube's rule. It states that "in dilute aqueous solutions of surfactants belonging to any one homologous series, the molar concentration required to produce equal lowering of the surface tension of water decreases three fold for each additional CH_2 group in the hydrocarbon chain of the solute" (Attwood and Florence, 1983). This is attributed to the increased hydrophobicity favouring micelle formation in order to shield the hydrocarbon tail portion from the hydrophilic environment. Barry *et al.* (1970) also noted the importance of the length of the hydrocarbon chain. The authors stated that the CMC of alkyltrimethylammonium bromides decreased logarithmically with the number of carbon atoms in the alkyl chain.

Attwood and Florence, (1983) considered it practical to consider that surfactants are usually present as mixtures of several surfactants rather than as single species. They further noted that when dealing with single surfactants the surface properties may easily be affected by minute amounts of highly surface active contaminants or by other members of the same homologous series present as impurities. However, Rosen (1989) regarded the effect of hydrocarbon chain length as not being significant unless the number of carbon

atoms in the hydrocarbon surfactant exceeded 16. He observed a significant decrease in surface saturation at that point possibly due to coiling of the chain. He believed that the most pronounced influence on surface saturation was due to the nature of the hydrophilic head group. Perhaps Rosen's observations are applicable to the relative influences of each of the structural components. It cannot be doubted from the wealth of literature that the length of the surfactant chain does contribute to the extent of surface saturation (Atkin *et al.*, 2003c; Fuerstenau *et al.*, 2004).

As alluded to in section 5.1, the BP (2007) defines cetrimide as consisting primarily of alkylammonium bromides that contain 14 CH_2 units in the hydrocarbon chain. The presence and the quantity of other alkyltrimethylammonium bromides can affect this value, as can adulterants. Therefore it was considered essential to examine the change in the CMC value as the hydrocarbon chain length is increased. HTAB, which contains 16 CH_2 units in the hydrocarbon chain, was examined using surface tension experiments. It can be seen from Table 5.2.4 that the CMC value for the 16 carbon chain alkyltrimethylammonium bromide, HTAB was established to be 1.1 mM. This is in close agreement with the literature value of 0.9 mM as reviewed by Atkin *et al.* (2003c). This value is 17 times smaller than the CMC value for the corresponding 12 carbon chain, dodecyltrimethylammonium bromide (DTAB), as determined by Atkin *et al.* (2003c).

The relationship with increasing chain length can again be seen with the pyridinium chloride surfactants. The CMC value for DPC, which has a hydrocarbon chain length of 12, is shown in Table 5.2.4. The value was calculated as 10.57 mM. As discussed earlier this value was lower than that stated in literature sources. The value for the 16 carbon chain structure, CPC was not determined experimentally but was found in literature to have a value of 0.1 mM (Koopal *et al.*, 2004). This concurs with the expectation that the CMC value would decrease as the hydrocarbon chain length increased.

Table 5.2.4 Experimentally determined CMC values for surfactant systems.

Surfactant System	CMC value (mM)
TTAB	2.98
TTAB/NaBr 10 mM	1.49
TTAB/NaBr 150 mM	0.89
HTAB	1.1
SDBS	1.5
SDBS/KCl 10 mM	0.75
DPC	10.57
SLS	6.94

5.3 FLOCCULATION / DEFLOCCULATION STUDIES

5.3.1 Introduction

The aim of this study was to carry out preliminary work on deflocculating halloysite particles in suspension using the cationic surfactants, TTAB and BAC. The cationic surfactants might be expected to improve the flow properties of halloysite, which can often form large aggregated structures. It was hoped that the surfactants might also result in a separation of the halloysite tubules from any contamination in the system. This is especially true in the case of the autogenously extracted grade, Balekisir halloysite. These specific surfactants were chosen due to their pharmaceutical acceptance and also because they possess innate antiseptic properties. Extensive investigation has not been conducted on the deflocculation of halloysite with surfactants. Most of the research to-date has involved deflocculating kaolin, due to its more widespread use in the ceramic and paper industry (Andreola *et al.*, 2004). Kaolin is chemically similar to halloysite and they also exhibit similar surface charging properties, however they differ morphologically. Halloysite is tubular in structure; it is negatively charged along the tubule ('face') and positively charged at the ends of the tubules ('edge'), where kaolin is negatively charged along the flat surface and positively charged on the 'edges' of its plate-like structure.

5.3.2 The Concepts of Flocculation and Deflocculation

Pharmaceutical suspensions tend to be coarse dispersions rather than true colloids in which insoluble solid particles are dispersed in a liquid medium (Florence and Attwood, 2006). The particles have diameters primarily greater than 0.5 μm and some particles are observed microscopically to exhibit Brownian movement if the dispersion has a low viscosity. In order to approach a stable state the system tends to reduce the surface free energy (ΔG). Equilibrium is reached when $\Delta G = 0$. It can be seen from Equation 5.2 that surface free energy is dependent on two variables, γ_{SL} interfacial tension between the liquid medium and the solid particles and ΔA, the total surface area. Hence, reducing the interfacial tension or the interfacial area may decrease the surface free energy. It is the latter phenomenon, which explains flocculation of particulate suspensions. The large surface area of particles is associated with a surface free energy that makes the system thermodynamically unstable. The highly energetic particles tend to group in such a way, so as to reduce the total surface area and the hence the surface free energy.

$$\Delta G = \gamma_{SL} \cdot \Delta A \qquad \textbf{Equation 5.2}$$

The forces at the surface of a particle affect the degree of flocculation and agglomeration in a suspension. Forces of attraction are of the London - van der Waals type; the repulsive forces arise from the interaction of the electric double layers surrounding each particle. When the repulsion energy is high, the potential barrier is also high and collision of the particles is opposed. The particles remain as discrete units and so the system remains deflocculated. For particles having a diameter of between 2 and 5 μm (depending on the density of the particles and the density and viscosity of the suspending medium), Brownian motion counteracts sedimentation to a measurable extent at room temperature by keeping the dispersed material in random motion (Martin, 1993). The resistance to coagulation or the stability of the dispersion depends on the relative magnitudes of the attractive van der Waals forces between the particles and the repulsive force, which in a system involving charged particles may be associated with the overlapping of their electrical double layers. The stability of a colloidal dispersion may be predicated by the Deryaguain-Landau-Verwey-Overbeek (DLVO) theory (Verwey, 1948).

The particles in a liquid suspension therefore tend to flocculate to reduce surface free energy. They form light fluffy agglomerates that are held together by weak van der Waals

forces, approaching particles are attracted in the secondary minimum so loosely formed flocs are created but the distance between the particles is still sufficient (1000-2000 Å) to avoid caking because the potential energy barrier is still too large to be overcome. This aggregation of the particles in a flocculated system will lead to an increased rate of sedimentation, which can be explained by Stokes law. The factors, which govern the rate of sedimentation, are depicted in Equation 5.3. However, the law holds for dilute suspensions as hindered settling occurs in concentrated suspensions, due to the high concentration particles interfering with one another as they fall.

$$V=\frac{d^2(\rho_s-\rho_0)g}{18\eta_0} \qquad \textbf{Equation 5.3}$$

where v = terminal velocity in cm/sec, d is the diameter of the particle in cm, ρ_s and ρ_0 are the densities of the dispersed phase and the dispersion medium respectively. g is the acceleration due to gravity and η_0, is the viscosity of the dispersion medium in poise.

As can be seen from Equation 5.3, the diameter of the particle is an extremely important determinant as it is the square of this function, which is proportional to the sedimentation velocity.

Figure 5.3.2a graphically depicts the events that occur within both flocculated and deflocculated systems at progressive stages of each process. It can be seen for a flocculated system from Figure 5.3.2a part (i) that there is some clear supernatant with a distinct boundary between the sediment. After some time scenario (ii) becomes apparent, the volume of clear supernatant increases and a relatively large volume of porous sediment is evident which does not alter appreciably with time. However, with the passing of time, the supernatant does become clearer (part iii).

The light fluffy aggregates in a flocculated system are composed of many individual particles, which form porous clumps through which the dispersion medium can flow as the aggregate sediments. This porous structure is retained after settling retaining large volumes of the liquid phase. This manifests as a large volume of sediment. Also a distinct feature of flocculated systems is the ease at which this sediment layer can be re-dispersed with

moderate agitation, due to the incorporation of this large fluid volume throughout the sediment.

Figure 5.3.2a also highlights the suspension characteristics for a deflocculated system. As discussed above particle size has a significant impact on the velocity of sedimentation. Therefore particles that do not agglomerate settle at a slower rate preventing the entrapment of liquid in the sediment. Due to this very slow settling the supernatant of the deflocculated system will remain cloudy for an appreciable time after shaking. This is evident from point (ii) for a deflocculated system. When sedimentation is complete the particles form a close packed arrangement with the smaller particles filling the voids between the larger ones. The particles lowest in the sediment are gradually pressed together by the weight of those above and the energy barrier that arises due to the electric double layer is overcome. It is evident from Figure 5.3.2a, part (iii) that this allows the particles to come in close contact with each other resulting in the sediment being more compacted compared to the flocculated system. In order to re-suspend or re-disperse these particles it is necessary to overcome the high energy barrier, this is not easily done by agitation. The particles remain strongly attracted to each other and form a hard cake (Martin, 1993).

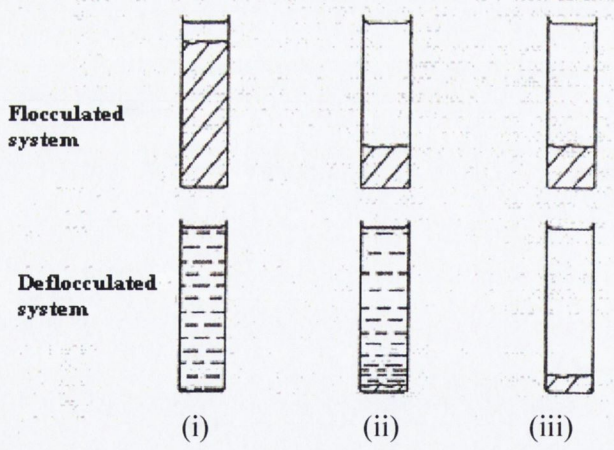

Figure 5.3.2a Diagram depicting the sediment and supernatant in flocculated and deflocculated systems (Billany, 2002).

The theory of flocculated and deflocculated systems as applied to halloysite suspension systems is further complicated by the non-uniform particle charge distribution on the

tubule surface. The appearance and compositional formation of aggregate types frequently encountered in clay suspensions elucidated by van Olphen (1977) can be seen in Figure 5.3.2b. Such aggregates frequently arise due to the electrostatic attraction between sections of clay particles with opposing charge characteristics. The morphology of the tubule is also an important variable. The result is aggregates of varying morphologies and sizes. Halloysite normally tends to form what van Olphen (1977) classically termed a "house of card structure". It is depicted in Figure 5.3.2b (iii). This results from the positive ends of the tubules binding to the negative tubule surface, with the consequence that structural build-up results in the clay suspension ultimately with flocculation occurring.

The adsorption of the surface active agent at the solid liquid interface is an important prerequisite to the process associated with dispersibility. The adsorption of charged ionic surfactants alters the electrical potential. Importantly adsorption also lowers the interfacial tension (Tamamushi, 1963). A reduction in the interfacial tension potentially results in a more thermodynamically stable system. As a result the driving force towards an increase in surface area to reduce this interfacial tension may be diminished and the particles may remain deflocculated for an extended period of time. Surfactant adsorption may have important consequences for the wetting of the clay mineral by the liquid, which has direct implications for the dispersibility of the clay also. Therefore it was considered important that the impact of surfactants on the flocculation characteristics of clay suspensions would be investigated.

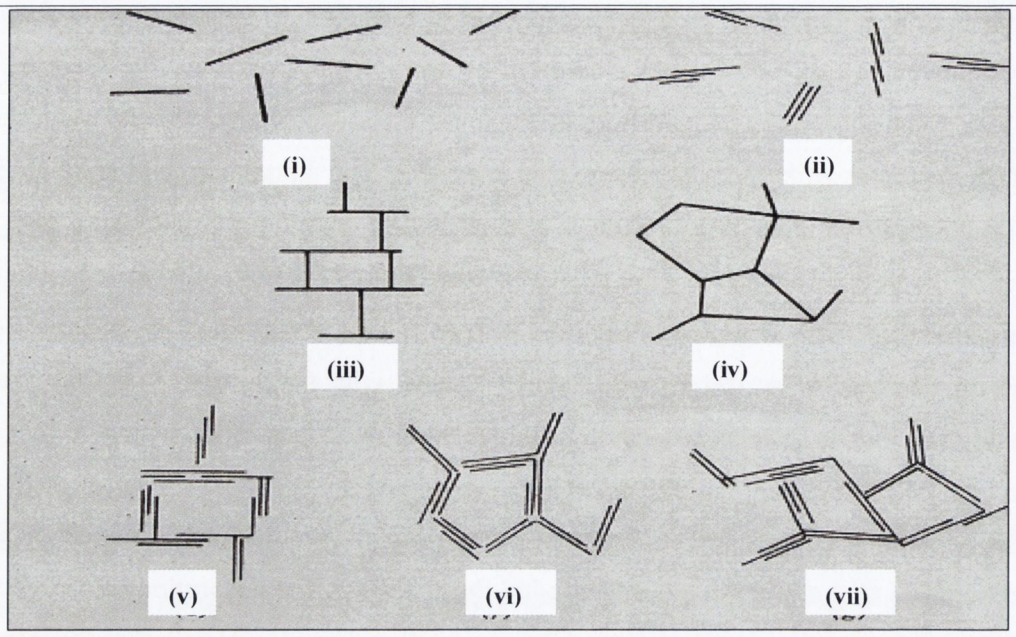

Modes of particle association in clay suspensions and terminology (i) "Dispersed" and "deflocculated". (ii) "Aggregated" but "deflocculated" (face-to-face association, or parallel or oriented aggregation). (iii) Edge-to-face flocculated but "dispersed" (iv) Edge-to-edge flocculated but "dispersed" (v) Edge-to-face flocculated and "aggregated" (vi) Edge-to-edge flocculated and "aggregated" (vii) Edge-to-face and edge-to-edge flocculated and "aggregated".

Figure 5.3.2b Depiction of aggregated clay particles (van Olphen, 1977).

5.3.3 Deflocculation Studies Involving Surfactants

5.3.3.1 Introduction

Surfactants can play a significant role in controlling the degree of flocculation, deflocculation and aggregation occurring in a suspension (Fox, 1985). Surface-active agents that cause flocculation in aqueous media at small concentrations will frequently act as deflocculating agents if the concentration is greatly increased. Initially the charged portion of the surfactant is attracted to the opposite charge on the clay particle. It is proposed that the adsorption neutralises the charge on the particle, lowers the zeta potential and causes flocculation to occur. When the concentration of surfactant is increased, a second layer forms in which the polar groups of this second layer are oriented outwards towards the aqueous phase causing particle repulsion and deflocculation (Napper, 1971). However, Moriyama (1975a, 1975b) found that the deflocculating power of surfactants declined with the addition of very high concentrations. He attributed the marked decrease

in suspension stability observed at high concentrations to the decrease in the electrical repulsion owing to a compression of the double layer thickness. This, in conjunction with the absolute value of the zeta potential forms the basis of the DLVO theory as discussed previously in Section 5.3.2. These two factors dictate the electrical repulsion, which retards the coagulation of particles.

5.3.3.2 TTAB

It can be seen from Table 5.3.3.2 that the addition of TTAB to a 1% w/v halloysite suspension causes flocculation at lower concentrations but at a concentration in the region of the bulk solution CMC the samples becomes deflocculated. The CMC of TTAB in solution was calculated in Section 5.2.2 using both surface tension and conductivity studies to be 0.1% w/v and it is in this concentration region that the sample changes from being flocculated to deflocculated. The surfactant range examined was not sufficiently high for the suspension to destabilise and for flocculation to re-occur. The samples are essentially unchanged after a forty-eight hour period. The region of hemi-micellar formation discussed in Chapter 1 occurred in this region and is thought to correspond to charge neutralization.

The halloysite blank sample is seen to flocculate due to the build-up of the "house of card" structure as described in Section 5.3.2. The particles have a large interfacial energy, which is minimised by the formation of large light fluffy agglomerates, which have a reduced surface area. The drive towards agglomerate formation is compounded by the presence of the negative charge along the tubule surface and the positive charge at the ends, resulting in edge to face association. The presence of the negative charge over a wide pH range was confirmed by Levis and Deasy (2002) using zeta potential measurements. The authors noted the surface charge of the mineral is only slightly negative below a pH value of 2, but as the pH increases from 2 to 6 that a sharp decrease in surface charge to a plateau of -27 mV was observed, before dropping further at pH values greater than 10. The tubule surface was negatively charged as the pH of the samples was in the region of 7 (dependent on the exact concentration of the particular surfactant). Hence the cationic surfactant structure binds to the negative surface charge. This reduces the build-up of particles, as the positive edges no longer bind to the tubule surface forming aggregates and the sample appears as deflocculated.

Table 5.3.3.2 Deflocculation study results for TTAB at time = 0 and 48 hours.

Sample	Surfactant concentration (% w/v)	Time = 0 hr.	Time = 48 hr.
BLANK	0	Flocculated	Flocculated
1	0.025	Flocculated	Flocculated
2	0.05	Flocculated	Flocculated
3	0.10	Deflocculated	Deflocculated / Flocculated
4	0.15	Deflocculated	Deflocculated
5	0.20	Deflocculated	Deflocculated

5.3.3.3 BAC

Another cationic surfactant, BAC was also examined. BAC is an alkylbenzyldimethylammonium chloride. Adsorption is complicated by the presence of a bulky benzene ring in its structure. Table 5.3.3.3 illustrates the results for the deflocculation of halloysite using BAC, a similar trend is observed on addition of BAC to 1% w/v halloysite suspensions as that observed with TTAB. At lower concentrations the surfactant halloysite systems are flocculated similar to the blank sample. At a critical concentration the system is deflocculated. This corresponds to a solution value of 3.53 mM; which correlates with the CMC literature value of 3.6 mM for BAC (Ward *et al.*, 1998). Again the point where the sample becomes deflocculated corresponds to this bulk solution CMC value. The samples are again largely unchanged after a twenty-four hour period, indicative of the ability of the surfactant to maintain stability in the system over the time period examined. Moriyama, (1995a, 1995b) also noted the stability of titanium dioxide suspensions increased remarkably as the concentration of surfactant approached the CMC and stability appeared to be better when surfactants with a low CMC were used.

Table 5.3.3.3 Deflocculation study results for BAC at time = 0.5 and 24 hours.

Sample	Surfactant concentration (% w/v)	Time = 0.5 hr.	Time = 24 hr.
Blank	0	Flocculated	Flocculated
1	0.0125	Flocculated	Flocculated
2	0.025	Flocculated	Flocculated
3	0.075	Flocculated	Flocculated
4	0.125	Deflocculated/ Flocculated	Deflocculated
5	0.15	Deflocculated	Deflocculated
6	0.20	Deflocculated	Deflocculated
7	0.25	Deflocculated	Deflocculated

5.3.3.4 Sodium Lauryl Sulphate (SLS)

Both TTAB and BAC are cationic surfactants but it was thought that the potential of an anionic surfactant could also be exploited. The ability of SLS to stabilise halloysite suspensions was examined at the concentrations outlined in Table 5.3.3.4. The bulk solution CMC value for SLS was calculated in Section 5.2.4 to be 6.94 mM; this corresponds to a concentration of 0.2% w/v. In a similar manner to the cationic surfactants it was expected that the SLS would electrostatically bind to the clay particle, but to the positive edges. The surface area of the edges is significantly less than that of the tubule surface. This might account for the fact that the halloysite suspensions were deflocculated at all SLS concentrations. However, even though the concentrations examined were quite high, destabilisation of the suspensions was not observed. The samples were observed for a seventy-two hr period and no change in suspension appearance occurred. It is interesting to note that economically speaking, use of an anionic surfactant would be more favourable to cause deflocculation of halloysite clay tubules in order to purify the sample because in equivalent weight terms less would be required to cause suspension deflocculation. This assumes of course that the materials would have similar retail value per weight basis.

Table 5.3.3.4 Deflocculation study results for the anionic surfactant SLS at time = 1.5, 48 and 72 hr.

Sample	Surfactant Concentration (% w/v)	Time = 1.5 hr	Time = 24 hr	Time = 72 hr
Blank	0	Flocculated	Flocculated	Flocculated
1	0.025	Deflocculated	Deflocculated **	Deflocculated
2	0.05	Deflocculated	Deflocculated	Deflocculated
3	0.15	Deflocculated	Deflocculated	Deflocculated
4	0.25	Deflocculated	Deflocculated	Deflocculated
5	0.3	Deflocculated	Deflocculated	Deflocculated
6	0.4	Deflocculated	Deflocculated	Deflocculated
7	0.5	Deflocculated	Deflocculated	Deflocculated

** Starting to clear in the top 10 ml of supernatant.

5.4 HPLC VALIDATION

5.4.1. Definition

Validation is the process by which it is established by laboratory studies, that the performance characteristics of the procedure meet the requirements for the intended analytical applications (USP 29NF24).

5.4.2 Parabens

(a) Inter-day and Intra-day precision

Prior to assessment and validation of the HPLC method for trimethylammonium bromides, an established method was run using the equipment and procedure outlined in Chapter 3. The parabens sample elutes three distinct peaks with retention times of 3.553, 3.992 and 4.489 min. They correspond to methyl hydroxyparabens, propyl hydroxparabens and sodium ethyl parabens. A sample chromatogram is depicted in Appendix 2. Inter-day and intra-day precision was assessed by repeat injection of a standard volume of the sample. The % relative standard deviation (% RSD) on day one for the three peaks was between

0.3-0.37%, on day two the values lay between 0.11-0.13% and on the final day the values were in the range 0.1-0.13%. The % RSD for each peak after multiple injection (n=8 on each day) on three consecutive days was 1.73, 1.88 and 1.84%. The values are quoted for peaks as the retention time increases. These values were acceptable indicating that the equipment produced repeatable readings. It showed that the validation of new methodologies was possible with the apparatus.

5.4.3 Trimethylammonium Bromide

(a) Inter-day accuracy and linearity

The USP defines the accuracy of the analytical procedure as the closeness of the test results obtained by that procedure to the true value. The accuracy of an analytical procedure should be established across its range (USP online). The International Conference on Harmonisation (ICH) recommends that accuracy should be assessed using a minimum of nine determinations over a minimum of three concentration levels, covering the specified range (i.e. three concentrations and three replicates of each concentration).

In order to assess the accuracy of the method, a calibration curve was prepared from six concentrations covering the range 0.001-0.25% w/v, which were injected in duplicate. Two calibration curves were independently prepared daily for three consecutive days. Assessment of the accuracy was undertaken by evaluating the linearity of the relationship between estimated and actual concentrations. The resulting R^2 value was 0.9704.

(b) Intra-day and Inter-day precision

The precision of an analytical procedure is determined by assaying a sufficient number of aliquots of a homogeneous sample to be able to calculate statistically valid estimates of standard deviation or relative standard deviation. Assays in this context are independent analyses of samples that have been carried through the complete analytical procedure from sample preparation to final test result (Mullins, 2003). Precision may be a measure of the degree of reproducibility or of repeatability of the procedure under normal operating conditions (USP online). The inter-day precision of the method was determined by assessing the average linearity of calibration curves of peak area against concentration. Each curve was prepared from six concentrations covering the range 0.001-0.25% w/v; each sample was injected in duplicate. Six concentrations were chosen as the ICH

recommends that at least five concentrations be used for the establishment of linearity, a concept that is incorporated in the validation of method precision. Two calibration curves were independently prepared daily for three consecutive days. The resulting R^2 value was 0.9794. This value may be indicative of the repeatability of the method.

Intra-day precision was assessed following repeat injection; the percentage relative standard deviations of the 50 μg/ml, 100 μg/ml and 2500 μg/ml samples were 3.28, 2.29 and 2.07% respectively (n=10). Three concentrations were assessed over the range as the ICH recommends using a minimum of six determinations at 100% of the test concentration.

(c) Robustness

The robustness of the analytical procedure is a measure of its capacity to remain unaffected by small but deliberate variations in procedural parameters listed in the method and provides an indication of its suitability during normal usage (USP online). The sample flow rate was decreased from 1 ml/min to 0.8 ml/min. A corresponding increase in retention time was noted. Changing the temperature at which the samples were run from 35 °C to ambient room temperature did not appear to alter the chromatogram profile or alter the amount eluted.

(d) Specificity and Interference

The ICH defines specificity as the ability to assess unequivocally the analyte in the presence of components that may be expected to be present, such as impurities, degradation products and matrix components. The analysis was specific for trimethylammonium bromides and no interfering peaks were observed from blank mobile phase or from the supernatant from halloysite and water suspensions.

(e) Limit of Detection

The limit of detection for the method was determined to be 0.5 μg/ml.

(f) Limit of Quantitation

The limit of quantitation for the system was 5 μg/ml.

5.5 ADSORPTION ISOTHERMS

5.5.1 Introduction

The adsorption of ionic surfactants at the solid solution interface is of major technological and commercial importance. Broadly speaking the surfactant is used to perform one or sometimes both of two major functions, namely the control of colloid stability and the control of wetting behaviour. Colloid stability is of interest, for example, in relation to detergency and anti-redeposition mechanisms, the formulation of pigment and pharmaceutical dispersions, agricultural soil conditioning, emulsion polymerization, flotation and other mineral separation processes. Wetting is important for example, in detergency, dispersibility of powders, dyeing, flotation, the application of pesticides and herbicides, printing and tertiary oil recovery (Hough and Rendall, 1983). Some surfactants adsorb at solid/water interfaces thereby modifying considerably the properties of the solid surface. This phenomenon has been extensively studied for dispersed particles, in particular with reference to processes such as the flotation of materials, soil remediation or the formation of thin films on solids (O'Haver *et al.*, 1995).

Applications have also been found in the pharmaceutical industry. The importance of the modification of solid substrate surfaces by surfactants for the incorporation of various drugs such as codeine (Strnadova *et al.*, 1995), propantheline bromide (Daniels and Rupprecht, 1985) has been studied. Daniels *et al.* 1986 examined the adsorption of acetylsalicylic acid at silica/water interfaces. Silica has been studied extensively due to its negligible physiological and interesting physiochemical properties. Zimmer *et al.* (1994) have investigated other drugs such as hydrocortisone. Other investigations concerning substrate/surfactant systems include the retention of antibiotic and antithrombic agents on vascular grafts (Yao and Strauss, 1992).

The aim of this section of work was to assess the nature and extent of the adsorption isotherm occurring between a range of surfactants and the substrate halloysite. In order to quantitatively assess surfactant binding a depletion approach was employed. Hough and Rendell, (1983) designated the depletion method as the most widely used approach to the direct determination of adsorption. It is based on the depletion of the species of interest from the solution in equilibrium with the adsorbent. However this method relies on the adsorbent having sufficient interface per unit volume to cause a measurable change in

concentration. In the present study the surface area of halloysite was sufficient, 55.596 m^2/g. Hough and Rendall (1983) stress that only an apparent adsorption isotherm is obtained by these direct measurements. In the simplest concept the difference between the concentration added and the final concentration detected in the supernatant is equivalent to that adsorbed to the clay surface.

When an amine salt or, as in the cases examined below, a quaternary ammonium salt or base is added to a clay-water suspension, the organic cation replaces the cations which were originally present on the clay surfaces. van Olphen (1977) termed this exchange adsorption. He noted that there appeared to be a strong preference by the clay for the organic cation, which is often practically quantitatively adsorbed until all the exchange positions are occupied by the organic cation. The amino groups become strongly attached to the clay surface. Simultaneously, the hydrocarbon chains may attach themselves to the clay surface and displace the previously adsorbed water molecules. It is assumed that sufficient space is available on the clay surface to accommodate the hydrocarbon chains. This is also dependant on the extent of surface hydrophobicity. If the chains are too long to lie flat on the available surface they may tilt. This is one of the possible explanations for different surfactant morphology at the substrate surface especially for a homologous series such as the quaternary ammonium compounds.

The isotherms are depicted as plots of the amount adsorbed against the equilibrium concentration. The majority of the surfactants investigated were cationic as a greater surface area of the halloysite tubule is negatively charged, therefore a greater potential for depletion of the original concentration existed. It would be expected that electrostatic interaction between the two would be the primary foundation for adsorption isotherm formation. The anionic surfactant SDBS was also investigated, as the ends of the tubule possess a positive charge, the extent of which depends on solution pH.

The primary body of the work examines the binding of the 14 carbon chain trimethylammonium bromide to halloysite as this is the main constituent of cetrimide (British Pharmacopoeia, 2007). However, increased hydrophobicity was examined with the 16 carbon homologue also. A wealth of literature exists detailing factors such as pH and ionic strength, which dictate isotherm character (Atkin *et al.*, 2003c; Koopal *et al.*, 1999).

The effect of a number of factors on isotherm formation including equilibrium time, electrolyte addition and substrate modification were investigated.

Other surfactant families were also included in the study. Two surfactants, DPC and CPC belonging to the alkylpyridinium chloride family were examined, again to assess the effect of increasing hydrophobicity with increasing surfactant chain length.

BAC was also examined, as it possesses a benzene ring moiety as part of its hydrocarbon tail. This would have ramifications on hydrophobicity and surfactant packing density. It was thought that these surfactants would provide interesting comparisons.

The anionic surfactant SDBS was included to determine if a significant decrease in adsorption would occur compared to cationic surfactants due to the source for electrostatic attraction being confined to the positive ends of the tubule. The edge charge density would be less than the surface due to the relative differences in surface area. Also electrostatic repulsion between the negative surface of the halloysite tubule and the negatively charged SDB^- ion would be expected to influence adsorption.

Where quantitation of the adsorbed surfactant by direct UV spectrophotometry was not possible, alternative methods were sought. This was the case for the trimethylammonium bromide surfactants. Two methods to measure adsorption were investigated. Firstly, the use of an anionic dye, which readily formed a complex with the unbound surfactant, was employed. This is one of a number of techniques that have been developed, which rely on the extraction into a solvent (e.g. chloroform) layer of an electroneutral complex of the surfactant with the dye molecule of opposite charge. The concentration is deduced visually in a titration experiment or spectrophotometrically after a suitable extraction procedure (Epton, 1948; Longwell and Maniece, 1955; Few and Ottewill, 1956). The methods are relatively rapid and simple, however not highly specific. A second method employed, involved the use of reverse HPLC as described in the methodology section.

Anionic and cationic surfactants react together to form salts, which are almost without exception insoluble or only sparingly soluble in water, but soluble in and therefore extractable by chloroform (Cullum, 1994). In an analogous situation, end-point detection of cationic surfactants depends on their reaction with an anionic dyestuff and extraction of

the insoluble complex with chloroform. The anionic dyestuff used was Orange II sodium salt. The end-point is disclosed by the migration of coloured complex from water to chloroform. The resultant complex was measured using UV spectrophotometery at a wavelength in the visible region. Orange II has been used (Zografi *et al.*, 1964) in the spectophotometric determination of quaternary ammonium salts and non-quaternary materials. Zografi and co-workers (1964) showed that four different quaternary compounds gave 1:1 complexes with Orange II up to pH 12.91. The orange dye was added to the surfactant clay system in a ratio, which was slightly in excess of molar parity with the surfactant in order that complex formation was ensured. The Orange II dye displays an intense colour and it was considered that this rather than complex formation might dictate isotherm characteristics. This was evaluated with the addition of a large excess of dye to varying surfactant concentrations, no anomalies in isotherm formation were observed.

5.5.2 TTAB Adsorption Isotherms

5.5.2.1 TTAB Adsorption - Factorial Analysis

Surfactants may adsorb at solid/water interfaces forming various types of aggregates depending on the characteristics of the solid and of the surfactant as well as the physiochemical conditions of the chemical system in terms of pH and ionic strength (Cherkaoui *et al.*, 2000). This was the basis for a factorial analysis of the binding profile of TTAB to halloysite under various conditions. Three factors were considered, each at two different levels. Firstly the time of equilibrium was examined. The samples were examined at 24 and 48 hr. The second factor considered was the presence of an electrolyte, NaBr. NaBr increases the adsorption of the surfactant and maintains a constant thermodynamic activity of the system (Cherkaoui *et al.*, 1998). The resultant effect of the electrolyte on the adsorption isotherm shape was investigated. Lastly, the nature of the adsorbent was examined. Halloysite was the substrate of interest. It was modified by washing with concentrated HCl and was characterised in Chapter 4. Adsorption of the quaternary ammonium bromide surfactant, TTAB on these substrates was examined at 24 and 48 hr periods both with and without the presence of NaBr electrolyte. HTAB was considered separately.

ANOVA of the amount of TTAB bound on the substrates at two surfactant concentrations, 0.05 and 0.15% w/v was conducted. ANOVA was conducted at a value above and below the bulk solution CMC to ascertain if the factors, which potentially influence TTAB adsorption in turn, were influenced by surfactant concentration. Table 5.5.2.1a depicts the results for the analysis of the samples at a TTAB concentration of 0.05% w/v. ANOVA of the isotherms at a concentration level less than the solution CMC reveal comparable main effect and interaction effects. The results of the ANOVA study for TTAB at a concentration level of 0.05% w/v are displayed in Table 5.5.2.1a. Only the statistics for the main effects are listed. It can be seen from Table 5.5.2.1a that at a TTAB concentration level of 0.05% w/v neither halloysite substrate nor equilibration time have a significant impact on TTAB adsorption. The main effects have p values of 0.348 and 0.214 for halloysite substrate and equilibration time respectively. The presence of NaBr at a concentration of 150 mM is significant ($p < 0.05$).

Table 5.5.2.1a Summary of ANOVA analysis of 2^3 factorial study of TTAB adsorption isotherms on halloysite substrates at a TTAB concentration of 0.05% w/v.

Source	DF	SS	MS	F	p
Halloysite	1	0.0000939	0.0000939	0.95	0.348
Time	1	0.000170	0.000170	1.72	0.214
NaBr	1	0.0010244	0.0010244	10.39	0.007
Error	8	0.0011834	0.0011834		
Total	15	0.0024718			

Table 5.5.2.1b depicts the summary statistics for the ANOVA study at a concentration level of 0.15% w/v. The statistical significance of both the main effects and the interactions of the factors are elucidated. The significance of the factors resembles those noted above for TTAB at a concentration of 0.05% w/v, with the exception of halloysite substrate. The modification of the substrate with concentrated HCl has a significant effect on TTAB adsorption; it has a p value of 0.002. The significance of the other main effects is unchanged compared to the previous ANOVA study. The p value for equilibration time is greater than the significance level of 0.05, indicating it is not significant. The p value for electrolyte addition is again less than 0.05, the significance level ($p = 0.00$).

The significance of the interaction of the factors is also addressed in Table 5.5.2.1b. The single three factor interaction and all the two factor interactions have p values > 0.05, indicating they are not significant. This implies that the change in level of one factor does not impact significantly on the model response factor, adsorption due to another factor. Hence the primary influences on adsorption are attributed to the main effects.

Table 5.5.2.1b Summary of ANOVA analysis of 2^3 factorial study of TTAB adsorption isotherms on halloysite substrates at a concentration of 0.15% w/v.

Source	DF	SS	MS	F	p
Halloysite	1	0.0025528	0.0025528	19.34	0.002
Time	1	0.0001412	0.0001412	1.07	0.331
NaBr	1	0.0106687	0.0106687	80.81	0.000
Halloysite*Time	1	0.0002362	0.0002362	1.79	0.218
Halloysite*NaBr	1	0.0000464	0.0000464	0.35	0.570
Time*NaBr	1	0.0000848	0.0000848	0.64	0.446
Halloysite*Time*NaBr	1	0.0000034	0.0000034	0.03	0.876
Error	8	0.0010562	0.0001320		
Total	15	0.0147897			

Figure 5.5.2.1a below graphically depicts the change in TTAB adsorption at each level of the factors. TTAB adsorption is greater for the acid washed substrate compared to the unmodified sample. The p value for the substrate listed in Figure 5.5.2.1b is less than 0.05, indicating the change in adsorption as the substance is modified is significant. A flatter line, indicating that a large variation in adsorption does not occur, as experimental equilibration time is altered represents the change in adsorption. The p value (p = 0.331) for the factor indicates that changing the equilibration time does not cause a significant alteration in TTAB adsorption. The most profound change in adsorption is obtained in the system examining electrolyte addition. It can be seen from Figure 5.5.2.1a that adsorption increases as NaBr is added to the system. The electrolyte exerts its influence by decreasing the repulsion between the orientated ionic head groups allowing a closer packing in the surface layer as the ionic strength is increased (Attwood and Florence, 1983). This effect is significant (p = 0.000). Figure 5.5.2.1.b below portrays the adsorption of TTAB for each

factor as the change in level of another factor occurs. None of the two factor interactions are significant.

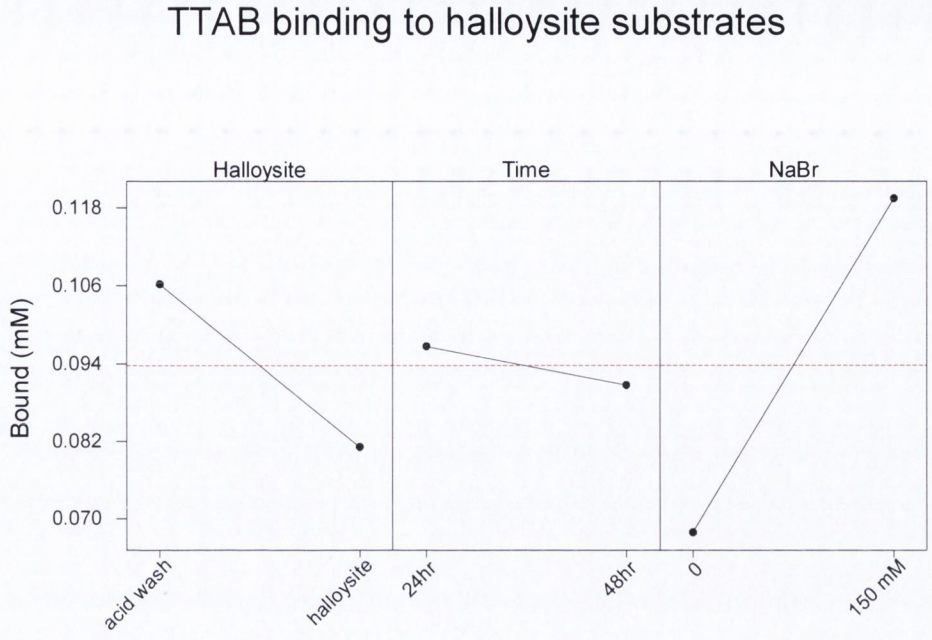

Figure 5.5.2.1a Main effects plot for ANOVA of 2^3 factorial experiment of factors affecting TTAB adsorption on halloysite.

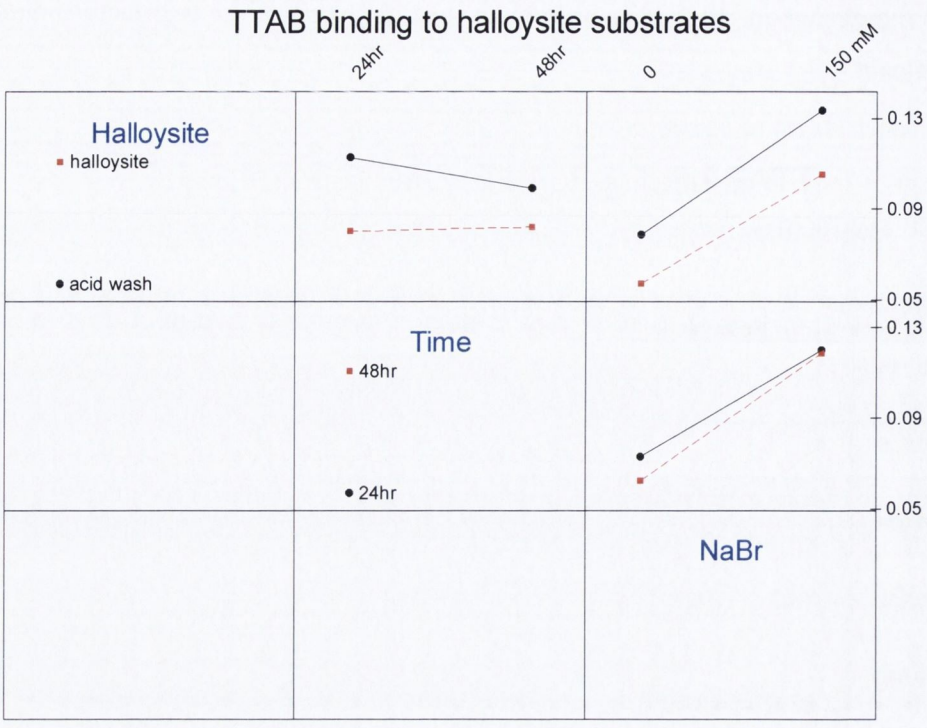

Figure 5.5.2.1b Interaction plot for ANOVA of 2^3 factorial experiment of factors affecting TTAB adsorption on halloysite.

5.5.3 Halloysite G

5.5.3.1 Unmodified Halloysite

The adsorption of organic cations is usually not limited to an amount equivalent to the cation exchange capacity of the clay. van Olphen (1977) noted that adsorption of a quaternary ammonium compound with a long chain and three methyl groups (similar to that used in the present experiment) on a montmorillonite clay was about 2.5 times the cation exchange capacity. The excess was thought to be physically adsorbed by van der Waals linking of the hydrocarbon chains of the exchange-adsorbed cations and those of the excess molecules. It is suggested that rather than just simple monolayer formation, the surfactant continues to adsorb perhaps as suggested by van Olphen above, but that the "exchange adsorbed" surfactant acts as an anchor point for further adsorption, resulting in hemimicelle and micelle formation on the clay surface in the region of the CMC value. It is now well accepted that surfactants self-assemble into structured aggregates at solid-liquid interfaces (Fuerestenau and Wakamatsu, 1975; Somasundaran and Fuerstenau, 1966; Gao *et al.*, 1987; Gaudin *et al.*, 1955). It has been demonstrated that the aggregate structure can

profoundly influence the surfactant adsorption density (Velegol *et al.*, 2000) and the adsorption kinetics (Atkin *et al.*, 2001).

Figure 5.5.3.1 is a plot TTAB adsorption against the equilibrium surfactant concentration. The resultant surfactant isotherm resembles those with constant charge surfaces. The isotherm shows an adsorption plateau at an adsorption level corresponding to surface charge density. Approaching concentrations close to the CMC the adsorption increases again. It would be expected that the isotherm would reach a final plateau in the region of the CMC value (Koopal *et al.*, 1995). As discussed in Chapter 1 different isotherm appearances have been proposed by various authors. Gao *et al.* (1987) proposed a "two-step model" for surfactant adsorption on silica. Somasundaran and Fuerstenau (1966) proposed the four region model for adsorption on solid substrates. The isotherms on halloysite do not conform strictly to either theory but resemble more closely the two-step model. Although halloysite contains silica, it is invariably more complicated. It has a constant surface charge due to non-stoichiometric substitution, but the charge of the tubule ends can vary with solution pH (van Olphen, 1977). Figure 5.5.3.1 portrays an increase in surfactant adsorption with increasing surfactant concentration. The increase corresponding to electrostatic attraction at low surfactant equilibrium concentrations is designated as Region I. It is possible that Region I of the isotherm may represent an overestimation of TTAB adsorption. This occurs at very low concentrations and may lie outside the limits for accuracy and precision. The first plateau region, the formation of which is indicative of charge neutralisation, appears to be evident from the isotherm.

It is postulated that hydrophobic chain interactions corresponding to region III, account for the substantial rise in adsorption. Finally micellar structural formation corresponds to Region IV. As previously noted a plateau occurs in the region of the surfactant CMC, however in Figure 5.5.3.1 an increase in surfactant adsorption just beyond the equilibrium concentration corresponding to the bulk solution CMC (2.98 mM) is observed, presumably corresponding to region III and just prior to plateau formation. It is postulated that the CMC is shifted upwards in concentration by the presence of halloysite in the system. Other authors have also noted the concept. Koopal *et al.* (2004) noted that the micellisation of ionic surfactants might occur at a value other than the CMC because of an alteration in the Gibb's free energy due to the presence of humic acid in the system. Hough and Rendall (1983) also made similar observations. They noted that depending on strength of

monolayer-substrate interaction, the equilibrium surfactant concentration could occur below, at or above the surfactant CMC.

Ryu and Free (2003) determined two very different values for the CMC of CPC using two methods. The difference was attributed to adsorption behaviour at liquid-air interfaces for a surface tension method and those at the liquid-solid interface when they employed an electrochemical quartz crystal microbalance. This might explain variations in the CMC value in an aqueous system and that at a solid-liquid interface.

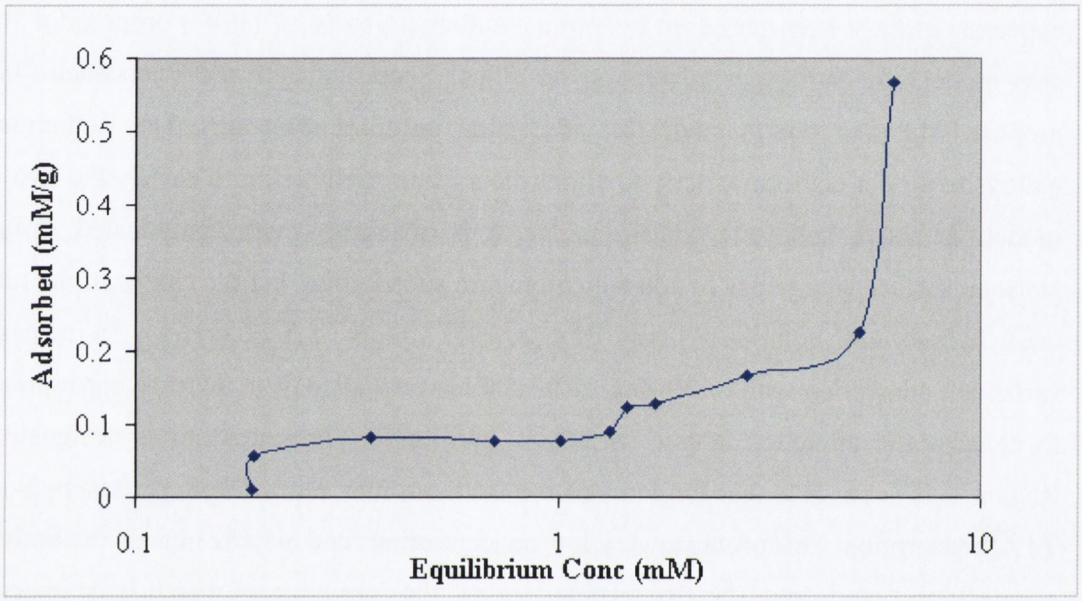

Figure 5.5.3.1 Adsorption isotherm of TTAB on the substrate halloysite. A linear-log plot of the amount adsorbed against the equilibrium concentration after an equilibration time of 24 hr.

5.5.3.2 Equilibration Time

The effect of equilibration time on surfactant adsorption was considered. Although equilibrium is attained in most solutions almost immediately after preparation, its establishment may require hours when surfactants are present in the system (Nash, 1959; Becher and Clifton, 1959; Peper and Taylor, 1963). Cherkaoui *et al.* (1998) used an equilibration time of at least 24 hr for co-adsorption studies of steroids using the cationic surfactant cetyltrimethylammonium bromide onto hydrophilic silica. Monticone and Treiner (1995) used an equilibration time of 12 hr for the co-adsorption of phenoxypropanol at a silica/water interface using cetylpyridinium chloride. However,

Goloub *et al.* (1996) used inversion periods of two hours until a stabilisation in pH occurred in systems, when examining the adsorption of cationic surfactants on silica. Rossi *et al.* (2002) examined non-ionic polymer adsorption on Na+- montmorillionite using an equilibrium time scale of between 18 and 24 hr. Greenwood *et al.* (1968) examined the adsorption of two surfactants, SDS and DTAB at the solid liquid interface using Graphon solid. The authors used inversion periods of at least twelve hours although they had established that equilibrium had been achieved in a much shorter time.

Parfitt and Rochester, (1983) proposed that the strength of the solute-surface bond varies over a wide range from the weakest (van der Waals forces) to the strongest (chemical adsorption), and all types have been observed in studies of adsorption from solution. Of obvious importance to the discussion here is that the proposed the time taken to reach equilibrium is normally indicative of the type of interaction, although this may be ambiguous in the case of porous adsorbents for which pore filling might be slow. At room temperature chemisorption is usually a much slower process than physical adsorption. However physical adsorption is very common, the specific nature of the interaction is usually implied from the chemical nature of the materials involved. The shape of the adsorption isotherm also provides qualitiative information on the nature of solute-surface interaction.

The time points of 24 and 48 hr were chosen for conventional reasons but also as literature references were found to cite varying equilibration times. It can be seen from Figure 5.5.3.2 that there is no essential difference in the adsorption isotherms after 24 and 48 hr equilibration. The adsorption isotherms for TTAB on halloysite were equilibrated for 24 hr and 48 hr. Results of surfactant binding at these points were subject to statistical interpretation using ANOVA. The equilibration time did not prove statistically significant nor did any of the interactions with which the time variable was confounded. It may be concluded that equilibrium would have been reached by the 24 hr period. It is graphically depicted from the main effects plot in Figure 5.5.2.1a that the amount absorbed appears to decrease when equilibrated for the increased time period. However the effects are more clearly illustrated in the interaction plot in Figure 5.5.2.1b. There is a slight variance depending on whether the substrate is untreated or acid-modified. However it can only be concluded based on the statistical analysis that the equilibration time variable has no effect.

Preliminary experimental runs did examine the time point of 72 hr but this did not prove conclusively different.

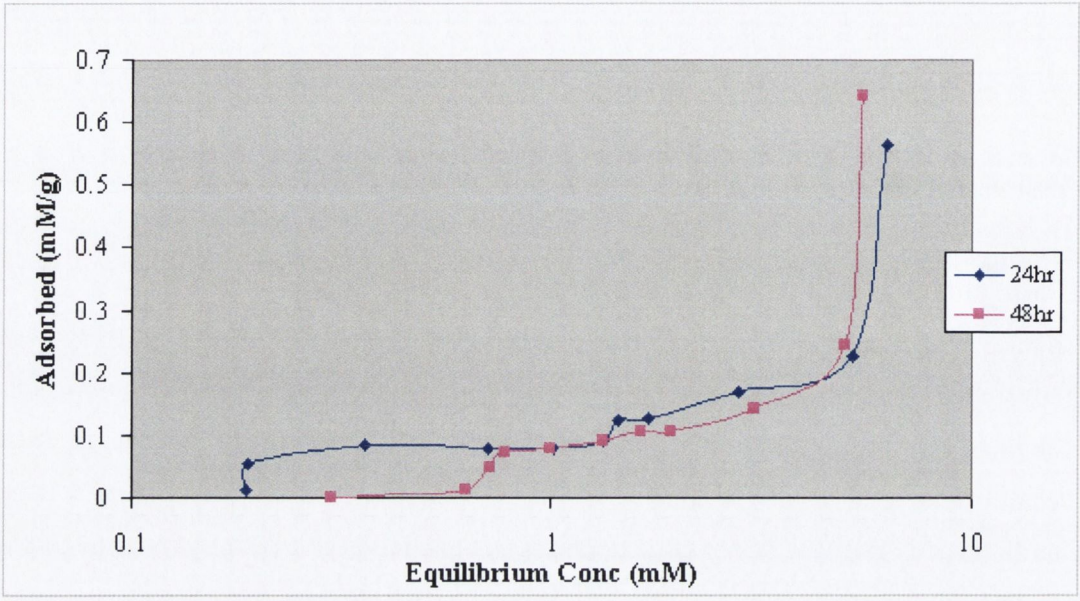

Figure 5.5.3.2 Adsorption isotherms of TTAB on the substrate halloysite after equilibration times of 24 and 48 hr. A linear-log plot of the amount adsorbed against the equilibrium concentration.

5.5.3.3 Electrolyte addition

NaBr was used in this study; KCl was used in later studies in section 5.8.3 with the pyridinium chlorides. Addition of neutral electrolytes to a solid affects adsorption at the solid liquid interface as distinct from that at the liquid air interface. The electrolyte causes an increase in the adsorption of an ionic surfactant to a similarly charged surface, owing to a reduction in the repulsive electrostatic interaction, and a decrease when the surface is of opposite charge (Attwood and Florence, 1983; Rosen, 1989). The presence of salt in the system has a number of other effects; firstly, it increases the hydrophobic effect, which favours micelle formation in the bulk and aggregates at the substrate/solution interface. Secondly it decreases the CMC and consequently shifts the onset of the adsorption plateau to lower surfactant concentrations (Monticone and Treiner, 1995). Determinations of the CMC of TTAB using surface tension methods previously discussed in section 5.2.3 noted a decrease in the CMC concentration with the addition of NaBr to surfactant solutions.

It can be seen from Figure 5.5.3.3 that the addition of NaBr 150 mM results in a similarly shaped isotherm to the system which does not contain electrolyte. However at equivalent equilibrium concentrations of surfactant, increasing amounts are bound to the surface for the system, which contains the NaBr electrolyte. The addition of NaBr does not appear to result in reduced surfactant adsorption at very low concentrations, it does however shift the isotherm to lower equilibrium concentrations relative to the isotherm which does not contain NaBr. This confirms the observations of other investigators. The addition of electrolyte not only shifts the isotherm to lower surfactant concentrations but also results in a significant increase in the maximal surface excess at equivalent concentrations. It would be expected that adsorption in the presence of the electrolyte would be reduced in region I, but the quantity of TTAB adsorbed is equivalent for both isotherms in this region.

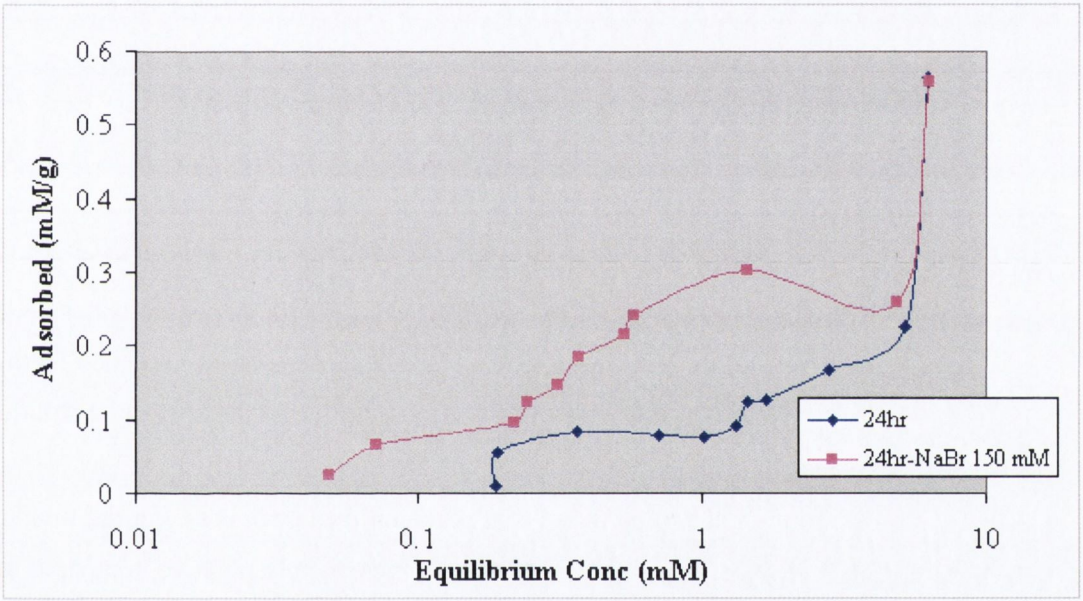

Figure 5.5.3.3 Comparison of adsorption isotherms of TTAB on halloysite after equilibration times of 24 hr with and without the presence of the electrolyte, NaBr 150 mM. A linear-log plot of the amount adsorbed against the equilibrium concentration.

In region I adsorption occurs by primarily head on adsorption and ionic strength of the bulk medium can reduce the attraction of the surface and surfactant by screening the electrostatic attraction. However in region III chain-chain interaction is a dominant mechanism of adsorption as Columbic interaction with the surface has diminished. The presence of the electrolyte may increase adsorption; this is attributed to a reduction in mutual headgroup repulsion between charges and an increased level of counter ion binding

(Koopal *et al.*, 1995; Lee and Koopal 1996). The resultant effect is closer packing of surfactant monomers into surface aggregates and an increase in surface excess.

The addition of the electrolyte to a clay system is quite different from other systems, as the electrolyte does not affect the charge. The clay particle is an example in which an electric double layer originates from crystal imperfections. This fact is responsible for certain unusual properties of clay sols and suspensions that may not be encountered in hydrophobic colloids (van Olphen, 1977). The clay crystal possesses a net negative charge due to the non-stoichiometric substitutions, which is primarily independent of solution conditions. However the edges of the clay particles exhibit a pH dependent surface charge similar to that on the oxide surfaces as discussed previously. This is due to hydroxylation and subsequent ionization of broken Si-O and Al-O bonds (van Olphen, 1977).

5.5.4 Acid Modified Halloysite

5.5.4.1 Introduction

Halloysite was modified for use here as outlined in Section 3.1.4 by washing it with concentrated HCl. The resultant material was then washed with deionised water until the suspension pH was greater than 5. The pH of a 1% w/v suspension of untreated halloysite has an approximate value of 8.3. It was noted that on addition of the surfactant solution to the treated halloysite samples that the resultant pH was approximately 3. At low pH values Levis and Deasy (2002), confirmed using zeta potential measurements that the tubule had very little negative charge. Therefore the edges are increasingly positive compared to the unmodified halloysite.

Many inorganic solids are negatively charged in water. Examples of some negatively charge solids are silica, glass, rutile, zinc oxide and montmorillionite. However, the charge does depend on the pH of the media and the isoelectric point of the surface of the inorganic solid. Thus, above the pH for zero charge inorganic surfaces are negatively charged, while at lower pH values, net positive charges result. This is only partly relevant in the case of halloysite. There is a negative charge along the halloysite tubule surface. Soma *et al.* (1992) concluded that the negative charge arose from the non-stoichiometric replacement of Al^{3+} by Fe^{3+} in the octahedral sheet. The charge is intrinsic to the layer structure; its sign and magnitude are independent of the pH of ambient solution, it is viewed as a permanent

charge. However, the charge on the crystal edges varies with pH; the amphoteric nature of the edge surface results from protonation and deprotonation of hydroxyl groups under acidic and alkaline conditions respectively. Therefore at acidic conditions the edge is positively charged. As discussed above, the aluminium hydroxyl groups become positively charged under acidic conditions (Equation 5.4) and deprotonated under alkaline conditions (Equation 5.5) (van Olphen, 1977; Tombácz *et al.*, 2004). However, in contrast to silica, these groups show more amphoteric behaviour (van Olphen, 1987).

$$Al-OH+H^{+} \Leftrightarrow Al-OH_2^{+} \qquad \textbf{Equation 5.4}$$

$$Al-OH \Leftrightarrow Al-O^{-}+H^{+} \text{ or } Al-OH+OH^{-} \Leftrightarrow Al-O^{-}+H_2O \qquad \textbf{Equation 5.5}$$

Under acidic conditions, protonation of the silicon hydroxyl groups is enhanced (Equation 5.6), while deprotonation is promoted in alkaline solutions (Equation 5.7) (van Olphen, 1977; Tombácz *et al.*, 2004). As silica is an acidic oxide, the reaction shown in Equation 5.7 predominates over a wide pH range (Byrne, 2004).

$$Si-OH+H^{+} \Leftrightarrow Si-OH_2^{+} \qquad \textbf{Equation 5.6}$$

$$Si-OH \Leftrightarrow Si-O^{-}+H^{+} \text{ or } Si-OH+OH^{-} \Leftrightarrow Si-O^{-}+H_2O \qquad \textbf{Equation 5.7}$$

The head group charge present on ionic surfactants results in a more complicated adsorption process when compared to non-ionic amphiphiles. Ionic surfactant adsorption is particularly sensitive to the interactions of counter and co-ions with the charged groups of the surface. If the affinity of co-ions for surface groups is sufficiently high, then the co-ions can compete for adsorption sites at the surface. These factors influence the surface excess and morphology of aggregates formed.

Adjustment of the solution pH can also affect several factors in the surfactant substrate system. These include the level of dissociation of surface groups, the degree of counter ion binding to micelles and the overall ionic strength. Goloub *et al.* (1996) concluded from a literature review that pH was one of the most important experimental features of cationic surfactant adsorption on silica, the others being surface charge density, surfactant structure

and the electrolyte concentration. Goloub pointedly highlights the need to maintain a constant pH, as failure to control the variable would have a profound affect on binding at a particular point and throughout the isotherm. This is a crucial factor in systems containing variable charge substrates.

Adsorbents may be heterogeneous in the sense that they contain a wide range of high to low energy sites, which may be polar or non-polar, as well as associated impurities. This is the case for mineral surfaces (Luckham and Rossi, 1999). The presence of impurities in halloysite was evident when comparing the white appearance of the acid washed and the pale grey appearance of the untreated halloysite. van Olphen (1977) attributed the colour variation to organic and inorganic impurities, but noted that certain ion constituents of the clays themselves were also responsible. The shape of the isotherm largely depends on the interaction between the surface and the adsorbed species. The type of interaction may be chemical or physical, depending on the functional groups on the surface and of those belonging to the surfactant. Several types of bonding can be identified (i) chemisorption; (ii) hydrogen bonding; (iii) hydrophobic bonding and (iv) van der Waals forces. It is likely that the nature of the bond and hence isotherm formation may be influenced by surface heterogeneity Koopal *et al.* (1995) acknowledged the presence of surface heterogeneity for most substances but validly argued that as soon as the lateral attractions between surfactant molecules dominated behaviour, that surface properties became less important.

The above explanation accounts for the adsorption that occurs in systems that are pH adjusted to acidic conditions. In the case of an acid washed clay, there is an intrinsic negative charge irrespective of the pH. However pH dependent charge, such as that ascribed to the hydroxyl groups on silica alters in acidic conditions and the charge would be positive.

5.5.4.2 Adsorption Profile - Modified Halloysite

Chorro *et al.* (1999) found that acid treatment of silica prior to adsorption could reduce the maximum surface excess by almost 50%. It was suggested that the difference was due to different charging properties of the surface. There is less adsorption because of weaker electrostatic attraction, due to a deficiency of negative charge. In the present case this discussion is partly relevant as indicated above. As mentioned earlier the surfactant-modified halloysite systems have pH values in the range of 3. As discussed above, in light

of zeta potential studies conducted on halloysite by Levis (2000) it would be expected that the resultant negative charge on halloysite would be reduced, with a consequent reduction in cationic surfactant binding. This would correlate closely with the observations of Chorro *et al.* (1999) above.

Halloysite will retain some negative charge irrespective of solution pH, but this cannot account for the adsorption profiles depicted in Figure 5.5.4.2. It can be seen that the profiles at 24 hr for both modified and non-modified halloysite predominantly overlap each other. It does appear that the acid modified substrate profile broadly resembles the non-modified substrate but that the features appear to be shifted to slightly lower concentrations. The extent of TTAB binding on both substrates is similar. A 50% reduction in TTAB adsorption on the acid modified substrate compared to the unmodified halloysite is not observed. The isotherm can be explained by virtue of the fact that the surface area of halloysite is seen to increase with acid treatment. The surface area of all clay grades was examined and discussed in Chapter 4. The values attained for halloysite and the acid modified grade were 55.98 and 104.84 m^2/g respectively.

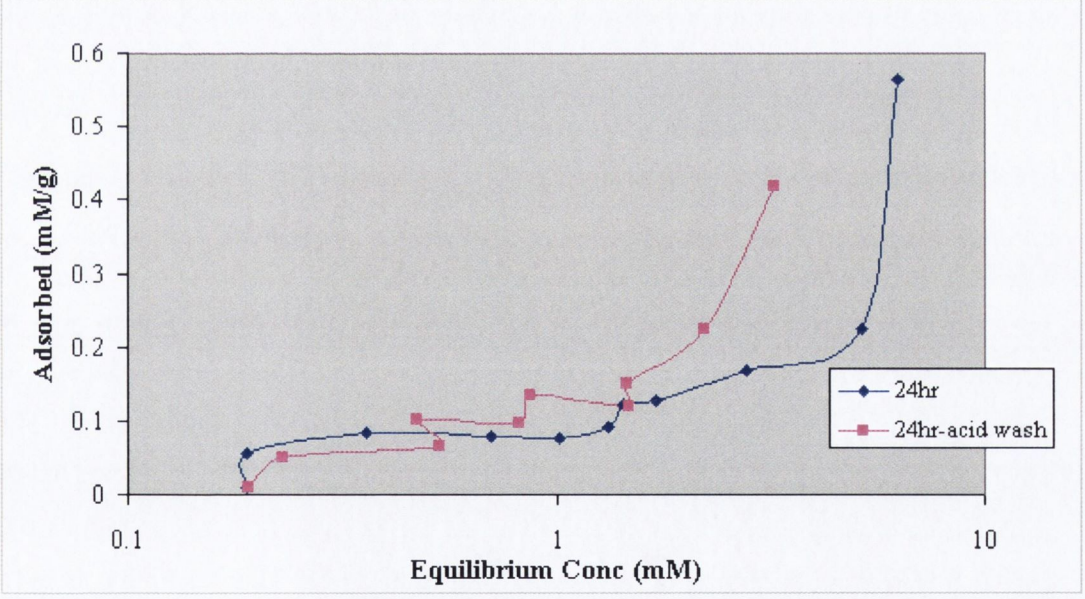

Figure 5.5.4.2 Comparison of adsorption isotherms of TTAB on halloysite and the acid modified substrate after an equilibration time of 24 hr. A linear-log plot of amount adsorbed against the equilibrium concentration.

An increase in specific surface area, mesopore volume and surface activity of clay samples, together with the formation of amorphous colloidal silica due to acid treatment of clays with inorganic acids was noted by several authors (Fahn, 1979; Morgan *et al.*, 1985). Fahn ascribed the changes in surface properties following acid activation of clays to the acid-induced dissolution of edge Al (and Fe) from the octahedral sheet, which resulted in a wedge-like splitting of the clay crystals. It is suggested that colloidal silica forms during acid treatment (Gozalez *et al.*, 1984; Aglietti *et al.*, 1988). It is postulated that the amorphous material provides additional surface area for adsorption. Considerable work has been conducted on clays that are naturally acidic, which can serve as effective decolourizing agents (Takeshi and Kato, 1969; Clarke, 1985). Theng and Wells (1995b) examined halloysite for its potential to act as a bleaching agent. They found that clays that had been severely leached during their formation showed a relatively high propensity for decolorizing oil and butterfat and only required minor treatment with HCl to optimize performance. They found that halloysite rich clay from the bay of Islands, New Zealand, which was acidified to pH 1.5, closely matched that of Tonsil Optimum FF, a standard acid activated clay based on montmorillionite. It should be noted that the surface area of halloysite almost doubled as a result of modification with concentrated HCl. This may be attributable to pore formation; however long chain surfactants may not be able to intrude some of the micropores (de Keizer et al., 1998). Therefore the isotherm may not be an exact representation of surface area of the sample, as the surface may not be exclusively available for adsorption.

5.5.4.3 Equilibration Time

As discussed previously in section 5.5.2.1 the equilibration time element was not a statistically significant factor ($p = 0.331$) for adsorption of TTAB on halloysite substrates, hence doubling the equilibration time has no effect on TTAB adsorption. This is substantiated by the isotherms in Figure 5.5.4.3. The profiles for the acid washed halloysite grade are essentially similar after 24 and 48 hr. At higher surfactant concentrations slightly greater adsorption appears to occur for the profile at 24 hr. The adsorption is noted to decrease at 48 hr. The main effects plot for the time factor in Figure 5.5.2.1a mirrors this observation, however as it is not significant, it can only be said that the main effect, time has no effect. The time factor was examined at two levels, the lower level $t = 24$ hr and at the higher level, $t = 48$ hr. It is considered that time has no effect because sample

equilibration was reached by the 24 hr period. Hence no change was observed as the experimental time was increased.

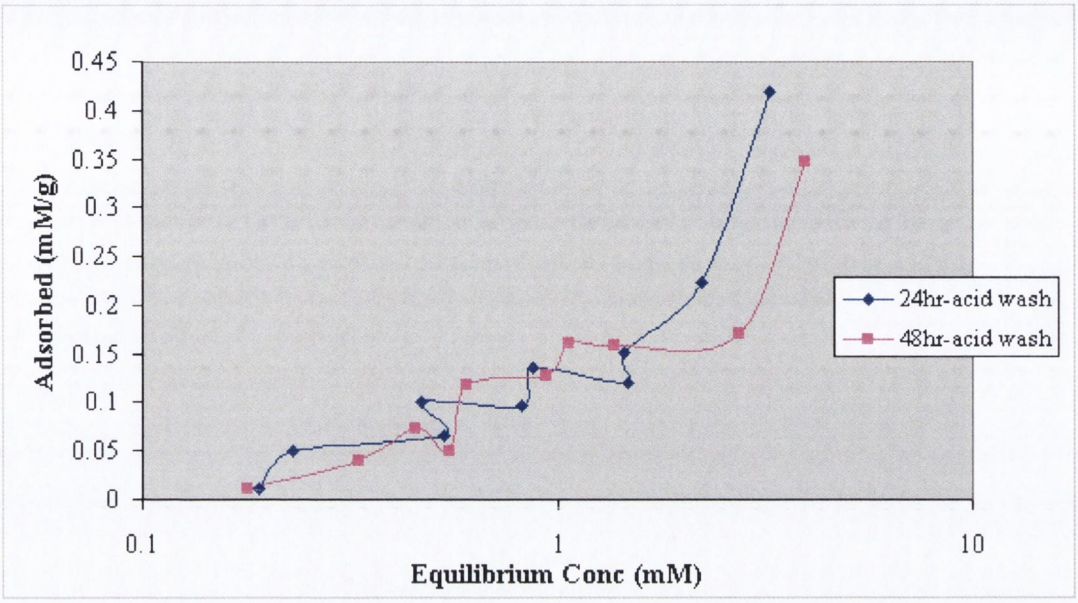

Figure 5.5.4.3a Comparison of adsorption isotherms of TTAB on acid modified halloysite after equilibration times of 24 and 48 hr. A linear-log plot of the amount adsorbed against the equilibrium concentration.

The interaction plots of time with the other variables show that for the unmodified halloysite almost no change in adsorption profile is observed when the equilibrium time is doubled. However, it is interesting to note that a decrease in the amount adsorbed is evident for the acid washed substrate. The interaction of time and substrate is not a statistically significant effect ($p = 0.218$) even though the substrate main effect is significant ($p = 0.002$), this phenomenon is often observed in complex systems.

5.5.4.4 Electrolyte Addition

The addition of the electrolyte NaBr, to the surfactant-substrate system resulted in a significant increase in adsorption of TTAB to the substrate ($p < 0.05$). The p value for the effect is listed in Table 5.5.2.1b ($p = 0.000$). It is obvious from the profiles in Figure 5.5.4.4a that over the 24 hr equilibrium period, NaBr impacts on the adsorption. It was originally thought this might be due to an alteration in pH of the system resulting in an alteration of the surface charge and hence increasing the adsorption but van Olphen (1977)

concluded for substrates such as halloysite that they had primarily a constant surface charge.

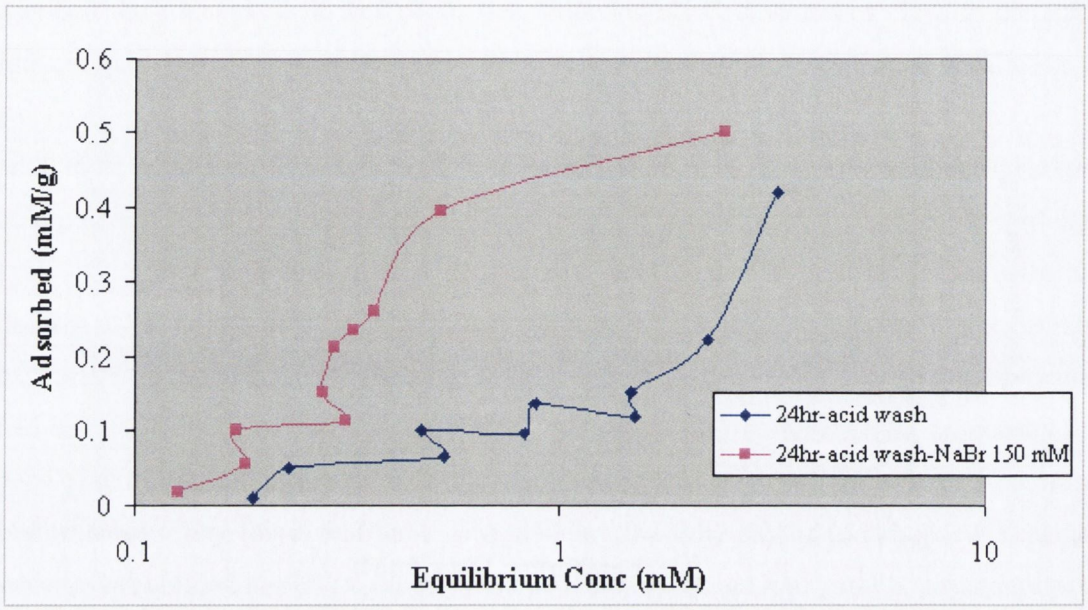

Figure 5.5.4.4a Comparison of adsorption isotherms of TTAB on acid modified halloysite with and without the presence of the electrolyte NaBr (150 mM). A linear-log plot of the amount adsorbed against the equilibrium concentration.

Preliminary experiments examined the addition of NaBr, 1 mM to the system but substantial differences in adsorption were not observed. The concentration of electrolyte added to surfactant substrate systems varies in the literature. Fan *et al.* (1997) used sodium chloride (NaCl) at a concentration of 30 mM in alkyltrimetylammonium bromide adsorption on alumina whereas Fuerstenau and Jia (2004) used NaCl at a concentration of 1 mM in surfactant quartz adsorption studies.

The electric double layer consists of a surface charge and a compensating counter-ion charge, which is accumulated in the liquid in the neighbourhood of the surface of the particles. The presence of an electric double layer is comparatively rare in hydrophobic colloids, the clay particle being an example in which an electric double layer originates from crystal imperfections. Consequently, the electric double layer on the layer surfaces has a constant charge, which is solely determined by the type and degree of isomorphous substitutions (the replacement of one atom by another of similar size in the crystal lattice

without disrupting or changing the crystal structure of the mineral). Therefore, the layer surface charge density is independent of the presence of electrolytes in the suspension. The presence of the electrolyte in the systems examined compressed the electric double layer and decreased surface potential. An inverse relationship exists between electrolyte concentration and surface potential. The extent of compression is governed by the concentration of the electrolyte and the valencies of ions of opposite sign (van Olphen, 1977). The double layer structure of the halloysite particle is complicated by the fact that two crystallographically different surfaces are exposed by plate-like particles (Hofmann *et al.*, 1956; Fripiat, 1957).

It is believed the existence of a constant charge in the particle structure has important ramifications for the shape of the adsorption isotherm. If the surface has a constant potential at a given pH the isotherm displays a characteristic four region behaviour (Koopal, 1993). For constant surface charge surfaces (predominantly the case observed for halloysite) the isotherm displays an adsorption plateau at an adsorption level corresponding to the surface charge density. Approaching concentrations close to the CMC the adsorption increases again and reaches a final plateau value at the CMC. These features are apparent in the surfactant halloysite adsorption isotherms depicted in this section. Some surfactant isotherms on silica (Rupprecht, 1972; Bijesterbosch, 1974) resemble the constant charge case, although the surface charge of silica may change upon surfactant adsorption (Wangnerud and Olofsson, 1992). Koopal *et al.* (1995) discussed metal hydroxides and the existence of constant potential on their surfaces but classified the silica surface in principle as neither constant potential nor constant charge. It has also been noted that the presence of an electrolyte can impact on the intraparticulate mass transfer and hence on adsorption kinetics due to the electrical potential induced by counter diffusing ions (Smith, 1968).

The vast majority of the literature examines the adsorption of cationic surfactants on model surfaces such as silica (Ball and Fuerstenau, 1971; Rennie *et al.*, 1990) and the adsorption of anionic surfactants is mostly studied on positive metal oxide surfaces such as aluminium oxide or titanium dioxide (Chander *et al.*, 1983; Scamehorn, 1982). The charging characteristics of silica are quite different from that of metal oxides (Hiemstra *et al.*, 1989; Hiemstra and van Riemsdijk, 1991; Koopal, 1993) as discussed above, hence surfactant adsorption did not follow the same trends on the two substrate types. This is explained by the existence of constant surface charge and surface potential as mentioned already.

Clays and silicates are fundamentally more complex, heterogeneous systems and are not ideal test substrates for examining theories of adsorption. However they have been widely used due to their technical and commercial importance (Hough and Rendall, 1983). Halloysite possesses a constant surface charge due to isomorphous substitutions but the edges of the clay exhibit a pH dependent surface charge similar to that on oxide surfaces as alluded to previously. Therefore adsorption isotherms on halloysite are the result of a more complex situation than that observed in the majority of the literature.

Figure 5.5.4.4a, depicts the shift of the isotherm for the acid washed substrate containing the NaBr electrolyte to lower concentrations as expected. The presence of an adsorption plateau is also evident; this feature was not evident for the unmodified halloysite isotherms although the isotherms were shifted to lower concentrations. This occurs at a value less than the bulk solution CMC. Quaternary ammonium surfactants are unaffected by changes in solution pH (Koopal, 1994). This is further evidence that other factors such as the presence of the halloysite clay could account for the existence of the CMC at an altered value. An increase in the surface excess is apparent for both scenarios. Adsorption profiles after an equilibrium time of 48 hr (not shown) displayed similar characteristics, the magnitude of surface excess was slightly greater for the isotherm containing the electrolyte compared to the surfactant-acid washed halloysite system.

Figure 5.5.4.4b, below depicts the variation in the pH of the systems with alteration in surfactant concentration. It shows that the electrolyte profile is displaced to higher values. Electrolyte addition does affect the surface potential of halloysite systems. At low surfactant values the pH of the profile, which contains electrolyte, is seen to decrease. This may be explained by the desorption of proton ions as surfactant adsorption progresses through an ion exchange mechanism. After compensation of the surface charge by surfactant the surface charge becomes almost independent of the surfactant adsorption. This indicated that adsorption of surfactant in a second layer with its head group pointed toward the solution had occurred (Goloub *et al.*, 1996). It can be seen that the profile levels off at a concentration below the solution CMC indicating that charge neutralization had occurred. In earlier studies Goloub *et al.* (1992) concluded that the adsorption of surfactants varied with pH but the ionisation of surface groups on silica increased upon adsorption of the ionic surfactant. This would result in pH variation with different isotherms and along the isotherm as the pH changed.

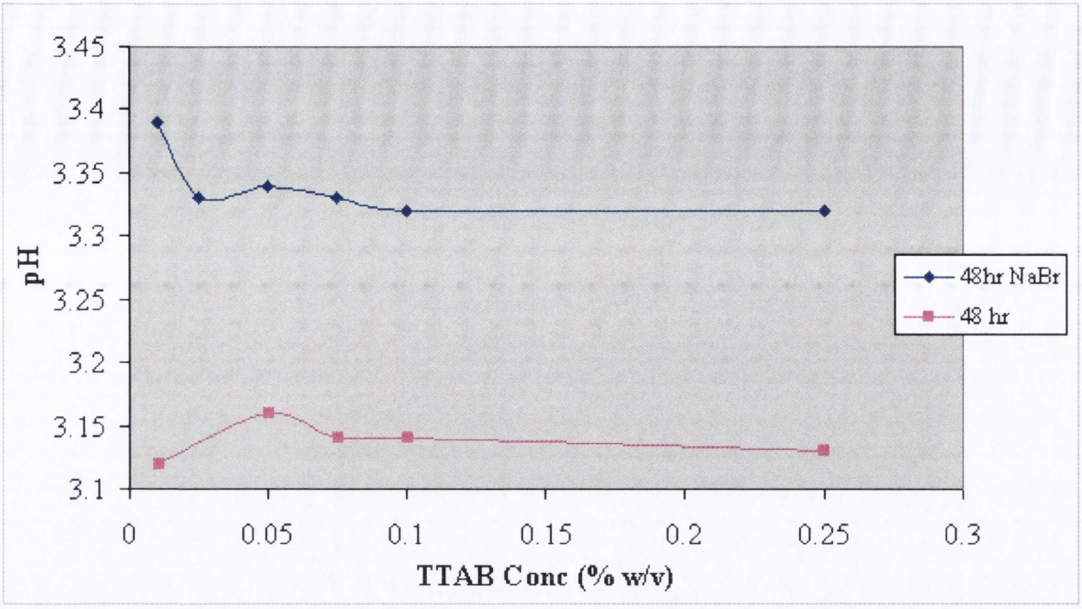

Figure 5.5.4.4b pH profiles for surfactant-acid washed halloysite systems at 48 hr both with and without the electrolyte sodium bromide (150 mM).

The pH profile of the system, which does not contain electrolyte, displays a profile, which is almost a mirror image of the electrolyte containing profile. It may be postulated that the charge compensating ions are such that they increase bulk solution pH as they are exchanged for surfactant that becomes adsorbed. It is also possible that the surfactant altered surface group ionisation as it adsorbed and caused charge neutralisation.

5.6 INCREASING CHAIN LENGTH - HTAB

5.6.1 HTAB adsorption isotherm

The hydrocarbon chain length is of critical importance in determining the adsorption behaviour of a surfactant (Atkin *et al.*, 2003a). Goloub and Koopal (1997) demonstrated that for adsorption to porous silica, increasing the chain length of the monomer by four methylene units, from C_{12} to C_{16}, lowers the concentration at which the characteristic features of the isotherm occur by approximately an order of magnitude. Atkin *et al.* (2003b) investigated the adsorption kinetics for dodecyltrimethylammonium bromide (DTAB) and the corresponding 16 carbon chain surfactant, HTAB on a negatively charged polymer. They found that the rate of adsorption of HTAB is significantly higher than that of DTAB at all concentrations. They also found that the slope of the adsorption isotherm

for HTAB exceeded that of the DTAB isotherm. They concluded this was a direct consequence of the greater hydrophobicity of the HTAB surfactant chain compared to that of the shorter 12-carbon chain. Somasundaran *et al.* (1964) examined the adsorption process of alkyl ammonium acetate surfactants on quartz. They noted that with increasing surfactant concentrations the zeta potential became positive, this effect was noted to occur at lower concentrations as the surfactant chain length increased. They also noted however, that the electrostatic contribution to the energy of adsorption is located entirely within the charged polar head of the surfactant ion and is not affected by hydrocarbon chain association.

Figure 5.6.1 compares the adsorption isotherms for TTAB and HTAB. The HTAB isotherm occurs at lower concentrations relative to the TTAB isotherm. The increased hydrophobicity as a result of 2 extra methylene groups in the HTAB structure compared to TTAB results in an increased driving force towards micelle formation. Aggregate formation improves the thermodynamic stability of the aqueous system, hence monomers tend to aggregate at lower concentrations and the characteristic features of the isotherm such as those observed in Figure 5.6.1 are shifted to lower equilibrium concentrations.

The surface excess is greater for the HTAB surfactant system at all equilibrium concentrations. This may be explained by extrapolation of the idea of hydrophobicity and thermodynamic stability of hydrocarbons in aqueous media. The increase in hydrophobicity is an added driving force for monomers to aggregate, but they also form denser, more tightly packed structures with increasing diameters. This manifests as increased adsorption.

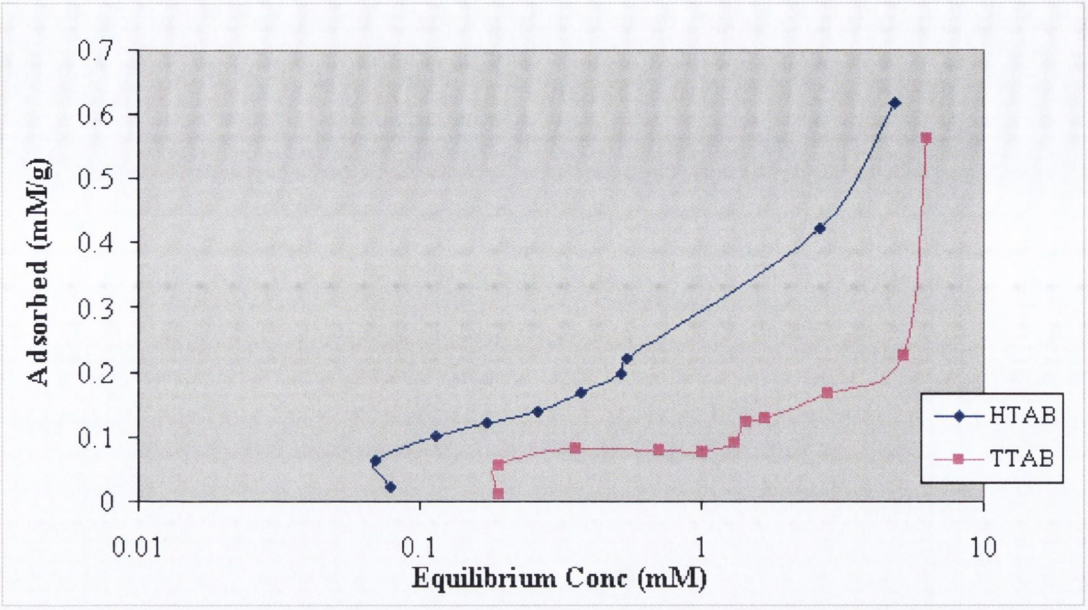

Figure 5.6.1a Adsorption isotherms of TTAB and HTAB on the substrate halloysite after equilibration times of 24 hr. A linear-log plot of the amount adsorbed against the equilibrium concentration.

5.6.2 Electrolyte addition

As already discussed in Section 5.2.3, the addition of a neutral electrolyte (NaCl or KBr) to an aqueous solution of an ionic surfactant containing no electrolyte results in an increased adsorption at the aqueous solution-air interface because of the decrease in repulsion between the orientated ionic heads at the interface (Rosen, 1989). However, as already discussed, the situation at the solid-solution interface may be complicated if the substrate and surfactant are opposite in charge. This is especially relevant at low concentrations when binding is primarily by electrostatic attraction and the presence of electrolyte can decrease binding (Hesselink, 1983).

It can be seen from Figure 5.6.2 that at low concentrations the extent of adsorption was similar in both isotherms, the presence of the electrolyte did not adversely affect the quantity of HTAB adsorbed. It is possible that the prohibitive effect of the electrolyte is evident at lower equilibrium concentrations. However the positive impact on adsorption, and surface excess at increased concentrations is apparent, owing to closer packing of the surfactant ions. A sharp increase in adsorption for the system containing NaBr occurs over a very narrow concentration range. It is expected that this corresponds to region III. A

distinct plateau is not obvious but it is expected that it would manifest at slightly greater concentrations. The appearances of the HTAB isotherms resemble those depicted for TTAB in Section 5.5.3.

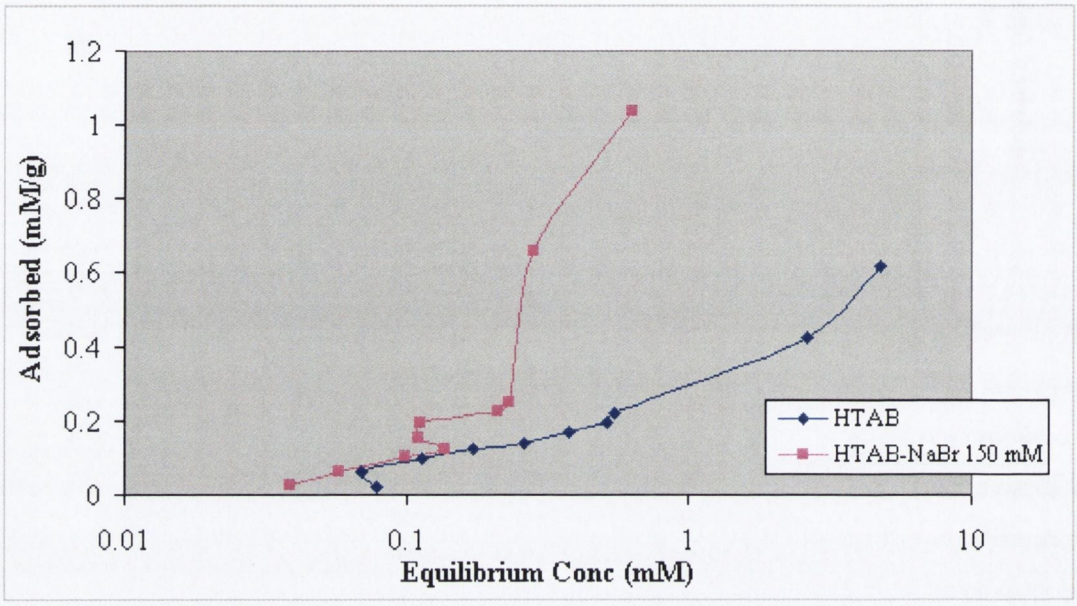

Figure 5.6.2 Comparison of adsorption isotherms of HTAB on halloysite after equilibration times of 24 hr with and without the presence of the electrolyte NaBr (150 mM). A linear-log plot of the amount adsorbed against the equilibrium concentration.

5.7 TRIMETYLAMMONIUM BROMIDES - HPLC METHOD

5.7.1 TTAB

The previously discussed factorial analysis study of TTAB adsorption on halloysite substrates involved the quantitation of unbound surfactant using a dye method. Although the features of the subsequent isotherms correlate closely with literature results, it is possible that the dye method may introduce variation into the samples, as it is not considered highly specific (Hough and Rendall, 1983). It was decided that another method would be used to ascertain if the features remained constant. More recent literature focuses on the elucidation of surfactant adsorption features using more modern technology. Electron spin resonance, Raman and luminescence spectroscopy have been used to study the micropolarity and microviscosity of surfactant layers (Chandar, *et al.*, 1987; Esumi *et al.*, 1992). Neutron reflection and small angle scattering have been used to give an insight

into head group and tail distribution (McDermott *et al.,* 1992). Dijt *et al.* (1994) used optical reflectometry to study adsorption onto a substrate.

HPLC was the second method employed to quantify the unbound surfactant. Liquid chromatography and HPLC have the advantages of not requiring volatile materials, normally not decomposing high-molecular weight substances, easy quantitation and relatively fast separations (Deem, 1985). The isotherm constructed for TTAB using HPLC as a method of quantitation is depicted in Figure 5.7.1. It does not resemble those arrived at using the dye method. Very little adsorption occurs over the majority of surfactant concentrations. Adsorption is only seen to increase at elevated levels. Binding is greater than observed for the dye method at elevated concentrations whilst the converse is true at reduced concentrations. For adsorption studies based on the HPLC quantitation method, binding appears to drop to extremely low levels prior to the CMC in the equilibrium solution. The isotherm does not plateau at the concentrations in excess of the CMC.

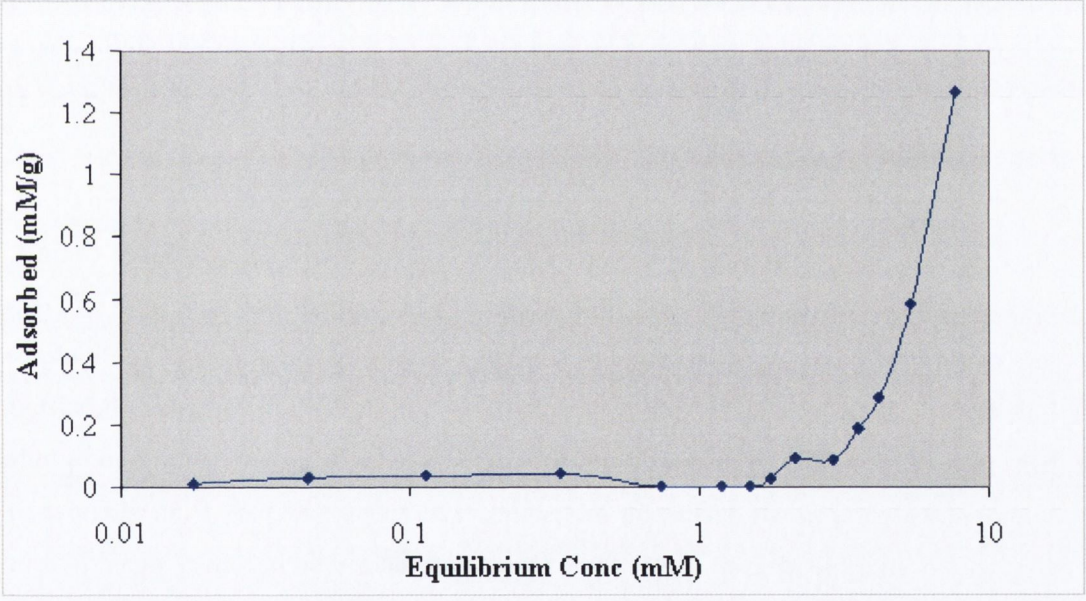

Figure 5.7.1 Adsorption profile of TTAB on halloysite after an equilibration time of 24 hours. A linear-log plot of amount adsorbed against equilibrium concentration.

5.7.2 Increasing Chain Length - HTAB

There is an increase in the maximal surface excess with chain length and the adsorption isotherms are displaced to lower concentrations as the chain length is increased. This has also been noted in the literature (Goloub *at al.*, 1997). It is attributed to the increased

hydrophobicity imparted by the progressively longer hydrocarbon tail groups, which promotes surface aggregate formation at lower surfactant concentrations. As previously elucidated in Chapter 1, the shape of the adsorption isotherm is governed by 4 discrete steps irrespective of model, with each step defined by a separate phenomenon. After the initial ion exchange process, governing step 1 and with increasing adsorption densities, adsorbed surfactants can associate at the interface through hydrocarbon chain-chain interaction. The formation of these aggregates, termed hemimicelles, depends on the hydrocarbon chain length (Fuerstenau, 1956). Typically, the hydrocarbon chain must contain at least eight carbon atoms for chain association to play a role in the physisorption of ionic surfactants (Wakamatsu and Fuerstenau, 1968). As can be seen from Figure 5.7.2 the isotherm depicted does not display the innate isotherm features attributable to surfactant adsorption as observed with the dye method. The isotherm is however shifted to lower surfactant concentrations and an increase in the surface excess is observed. The isotherm does not display a plateau value at the concentrations examined. The isotherms depicted using the HPLC method of quantitation do not display characteristic isotherms features, similar to those noted in Sections 5.5.3 and 5.5.4. It is considered that there may have been a separation problem because cetrimide is often used in reversed phase HPLC because it binds to the column and aids in the separation of compounds.

As noted earlier the alteration in hydrophobicity associated with increasing chain length encourages surfactant molecules to form micelles in aqueous solution. The size of these submicronic aggregates is determined to a large extent by the length of the hydrocarbon chain. Typical micelle sizes range from 5 nm to approximately 100 nm. The shape of a micelle is determined by the ratio of the hydrodynamic volumes of the hydrophilic and hydrophobic parts of the surfactant molecules. The shape will vary from globular to rod-like to an unstable disc-like morphology as the surfactant becomes more hydrophilic (Broze, 1995). HTAB is more hydrophobic than TTAB, hence there is an increased impetus towards micelle formation. Velegol *et al.* (2000) demonstrated using atomic force microscopy and optical reflectometry that the morphology of CTAB micelles altered from short rods to cylindrical micelles when the concentration of CTAB was increased from 0.9 x cmc to 10 x cmc.

It is also worth considering that the impact of chain length depends on the substrate; if the surface were a non-polar solid then chain length would have an added importance. In this

case a primary focus of attachment would be the bonding of the hydrocarbon tail lying along the non-polar substrate (Wakamatsu and Fuerstenau, 1968). However the adsorption of the hydrocarbon tail is not purely of interest in the case of non-polar substrates. Some materials are heterogeneous due to the nature of their formation and others are altered due to treatment processes resulting in substrate modification. Hence the attraction of the hydrocarbon chain to potential non-polar sites may influence the adsorption isotherms of these substrates.

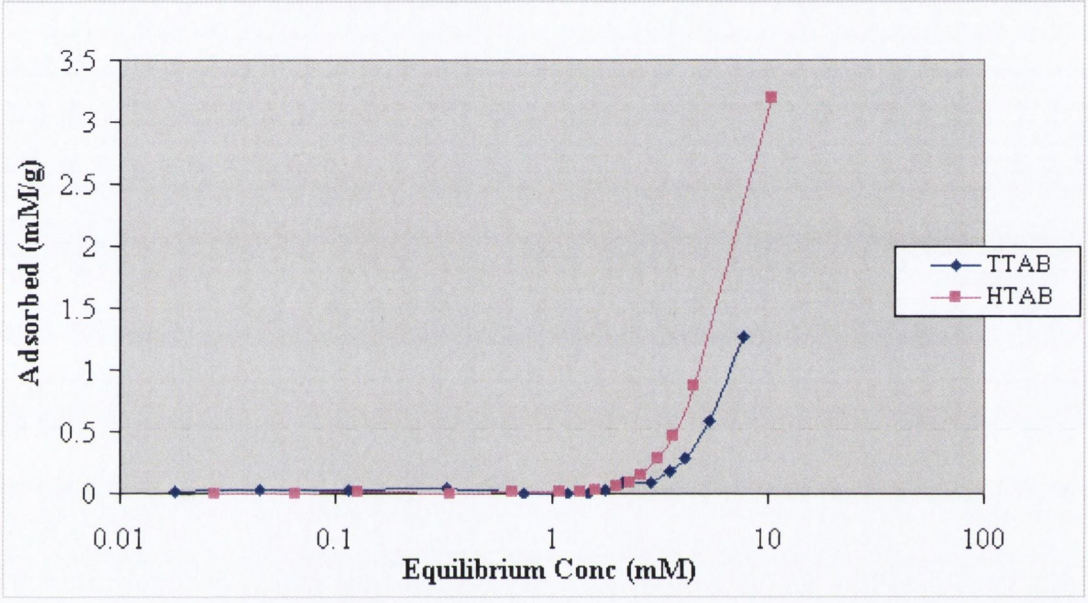

Figure 5.7.2 Adsorption profiles of TTAB and HTAB on halloysite after an equilibration time of 24 hr. A linear-log plot of amount adsorbed against equilibrium concentration.

5.8 OTHER CATIONIC SURFACTANT GROUPS

5.8.1 Introduction

The quaternary ammonium surfactants examined are examples of straight chain monoalkyl quaternary compounds. The effect of an alteration of surfactant structure was investigated using two other surfactant families. BAC is a mixture of alkylbenzyldimethylammonium chlorides, the alkyl groups having chain lengths of C_8 to C_{18}. It is used as an antiseptic detergent (British Pharmacopoeia, 2007). It contains a benzene ring, which is removed from the charged ammonium group by just one methyl group. The pyridinium group of surfactants was also investigated. They like TTAB and BAC possess antiseptic properties.

The pyridinium surfactants (DPC and CPC) contain a benzene ring, however, the charged head-group is part of this structure. DPC contains 12 carbons as part of its hydrocarbon chain and CPC contains 16. The presence of the benzene ring makes it possible to quantify theses surfactants by a UV spectrophotometric method. The pyridinium surfactants contain a suitable chromophore and may be determined by spectrophotometric measurements (Rosen and Nakamura, 1977; Greenland and Quirk, 1963).

5.8.2 Alkylbenzyldimethylammonium Chloride Surfactants

Figure 5.8.2a depicts the isotherm of BAC adsorption on halloysite. It displays a similar shape to TTAB adsorption except that the isotherm profile portrays a gradual increase in adsorption over the concentration range examined. It is devoid of sharp changes in adsorption and it is more difficult to attribute distinct adsorption regions. It is considered that the concentration range examined was not sufficient, as the isotherm does not appear to plateau. The highest equilibrium concentration is above the bulk solution CMC, 3.6 mM (Ward *et al.*, 1998). Due to a number of factors previously discussed a larger range of analysis would have been more appropriate as it is likely that the upper range examined was in the region of the CMC. However, concentration ranges similar to those used for the examination of TTAB were used for comparison purposes. The amount bound per gram of substance at equivalent equilibrium concentrations is less for BAC compared to TTAB. It is considered that the presence of the bulky benzene ring moiety adversely impacted on monomer packing density resulting in decreased BAC binding.

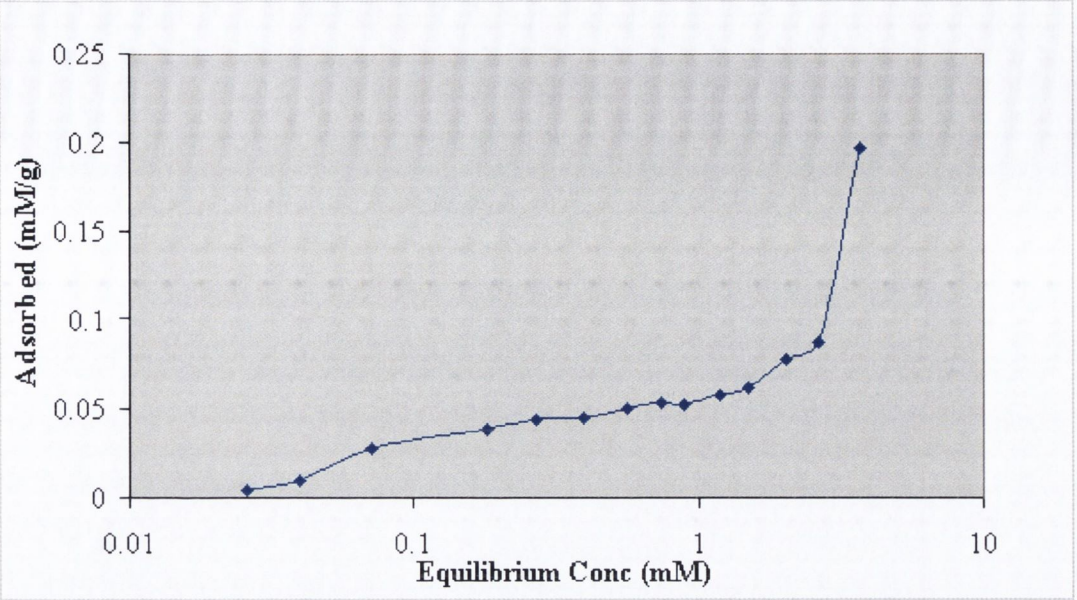

Figure 5.8.2 Adsorption profiles of BAC on halloysite after an equilibration time of 24 hr. A linear-log plot of amount adsorbed against equilibrium concentration.

5.8.3 Alkylpyridinium Chloride Surfactants

5.8.3.1 Adsorption Isotherm

The alkylpyridinium surfactants like BAC contain a benzene ring as part of their structure. The charged pyridinium head group on the molecule is a nitrogen atom in a six-membered ring containing five carbon atoms with three double bonds in their linkage, the head group itself may complicate the adsorption process (Fuerstenau and Jia, 2004). The adsoption profile of DPC in Figure 5.8.3.1 is analogous to the four region model. A log-log plot would highlight the features at low surfactant concentration but the conventional method of data presentation appears to be in the linear-log format, therefore this approach was adopted. The isotherm appears to plateau in the region of the CMC. The solution CMC, determined in Section 5.2.2 was 10.57 mM. Again, as with BAC the amount bound is less than that observed at equilibrium surfactant concentrations of TTAB. Especially in the case of the pyridinium surfactants, this can be attributable to the bulky benzene ring. The bulky ring may obstruct potential binding sites as the charged head group is located in this structure. Somasundaran and Fuerstenau, (1964) confirmed the importance of the head group in adsorption studies. The authors concluded that the electrostatic contribution to the

energy of adsorption is located entirely within the charged polar head of the surfactant ion and is not affected by the hydrocarbon chain association.

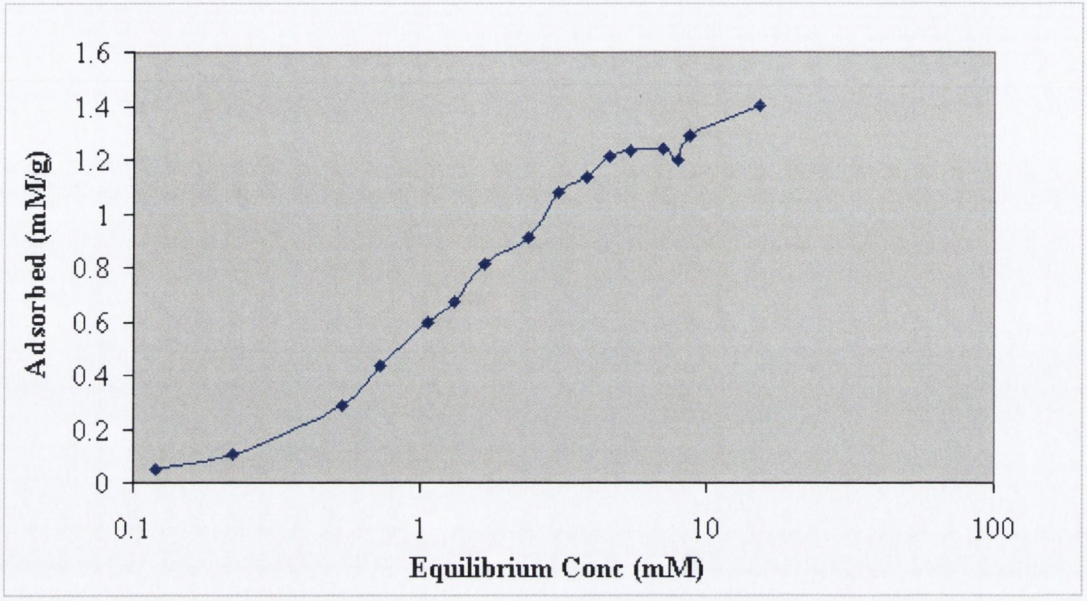

Figure 5.8.3.1 Adsorption profiles of DPC on halloysite after an equilibration time of 24 hr. A linear-log plot of amount adsorbed against equilibrium concentration.

5.8.3.2 Electrolyte Addition

The presence of the electrolyte, KCl in the halloysite - DPC system is portrayed in Figure 5.8.3.2. KCl was also used by Goloub and Koopal, (1997) in surfactant adsorption studies. The isotherms with and without KCl in the system overlap each other over most of the equlibrium concentration range. The addition of KCl did not shift the isotherm to lower concentrations, as observed with the quaternary ammonium group. Reduced surfactant adsorption is not observed at lower surfactant concentrations in the system containing KCl. It would be expected that the electrolyte would buffer the electrostatic attraction. Electrostatic attraction accounts for binding at the beginning of isotherms when the substrate and adsorbate are opposite in charge. This reduction in Region I was not observed for any of the surfactant electrolyte systems examined. It is postulated that it is visible at lower concentrations. An increase in surface excess was only observed in the upper concentration range. In the median range it appears that adsorption was reduced in the presence of the electrolyte, although not significantly. At higher equilibrium concentrations, the KCl system displays increased surface excess. This feature was observed with the trimethylammonium bromide surfactants, however the isotherms and

maximal surface excesses occurred at lower equilibrium concentrations when an electrolyte was present. However it must be noted, although not equivalent, a higher concentration of NaBr electrolyte (150 mM) was used.

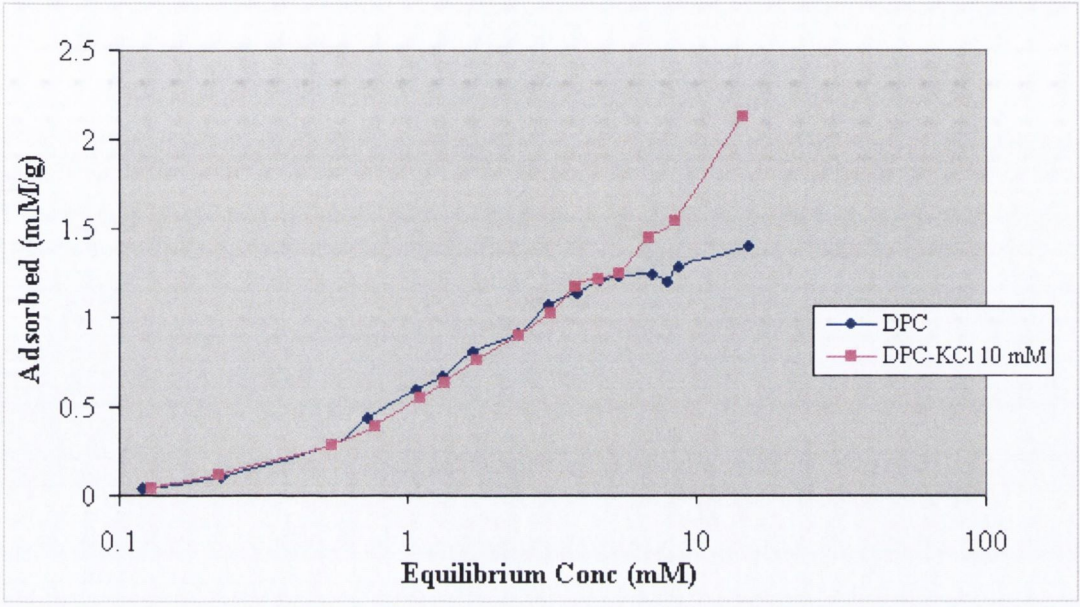

Figure 5.8.3.2 Comparison of adsorption profiles of DPC on halloysite after an equilibration time of 24 hr with and without the addition of KCl electrolyte (10 mM). A linear-log plot of amount adsorbed against equilibrium concentration.

5.8.3.3 Increasing Chain Length - CPC

The increase in hydrophobicity with increasing chain length was again assessed using the pyridinium group of surfactants. Figure 5.8.3.3 shows that the adsorption isotherm for CPC is only slightly displaced to lower concentrations from the DPC isotherm and surface excess is only greater at elevated concentrations. It does not display a plateau but was only evaluated at a concentration slightly above the equilibrium CMC. The isotherm increases with increasing concentration. However specific discernible plateau phases are absent.

The presence of the hydrophobic moiety also has ramifications. For micellization (Shinoda *et al.*, 1963) and for adsorption both at hydrophobic interfaces (Rendall *et al.*, 1979) and hydrophilic surfaces (Dick *et al.*, 1971) the benzene ring gives a contribution equivalent to 3-4 CH_2 groups. This is important when surface modification of a substance is required. It is crucial to note that modification can be achieved with increasingly lower concentrations,

but control of the modification is also increasingly more challenging as the adjustment occurs at such reduced concentrations. Addition of surfactants beyond the monolayer coverage results in the charged surfactant head facing outward again, thus increasing hydrophilic character. The hydrophobic to hydrophilic change occurs at the zeta potential reversal (Fuerstenau, 1970).

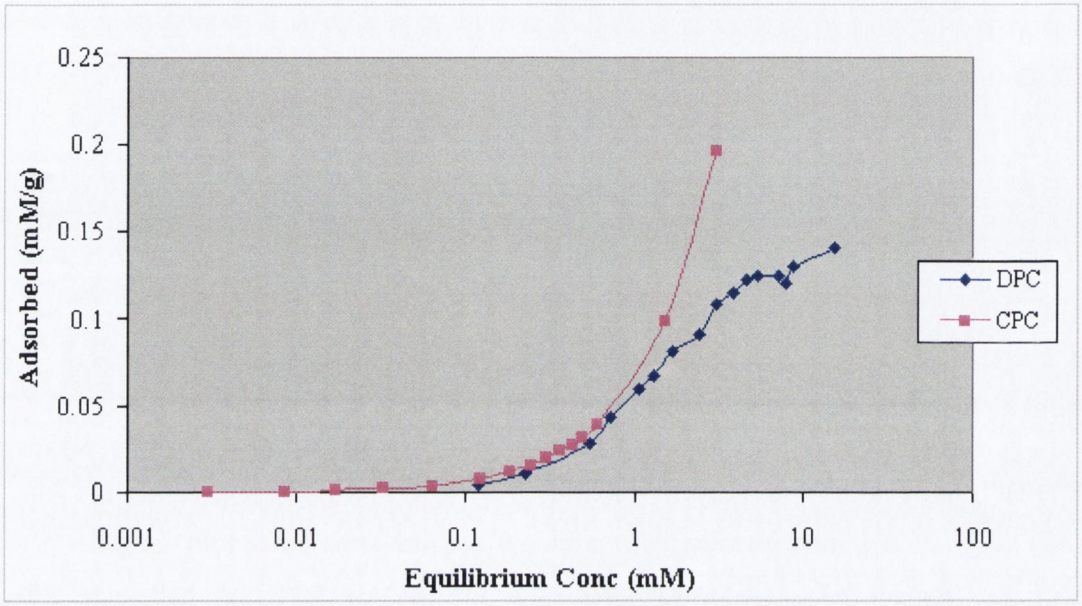

Figure 5.8.3.3a Comparison of adsorption profiles of DPC and CPC on halloysite after an equilibration time of 24 hr. A linear-log plot of amount adsorbed against equilibrium concentration.

5.9 ANIONIC SURFACTANTS

5.9.1 SDBS

The previous adsorption isotherm studies focused on the binding of cationic surfactants to the halloysite tubule surface, initially utilising the negative charge. It is also recognized that other non-electrostatic mechanisms are prevalent. The rationale for examining the anionic surfactant, SDBS, lies in the existence of a positive charge at the ends of the tubule. However, the surface area pertaining to the tubule edges is significantly less than that of the tubule face hence the area for adsorption is considerably less. Another mitigating factor against adsorption is the potential electrostatic repulsion between the negative tubule surface and the SDB^- ion.

Figure 5.9.1 shows the adsorption profile for SDBS on halloysite. A profile of SDBS containing KCl is also displayed. The isotherms are broadly similar to those observed for the cationic surfactant, DPC. However some critical differences must be noted. The isotherm is seen to plateau at elevated concentrations but prior to this a depression in the isotherm is observed. The addition of KCl produced a similar profile but the depression is not as pronounced. As with the addition of electrolyte to other systems the surface excess is increased and the isotherm is displaced to lower concentrations.

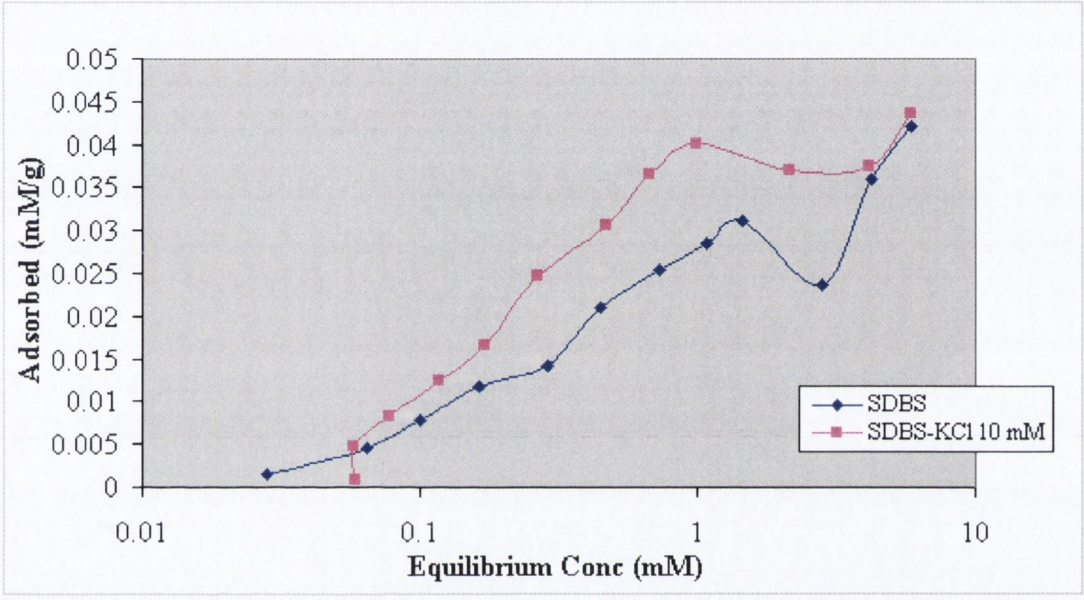

Figure 5.9.1 Comparison of adsorption profiles of SDBS on halloysite after an equilibration time of 24 hr with and without the addition of electrolyte, KCl 10 mM. A linear-log plot of amount adsorbed against equilibrium concentration.

The amount adsorbed is appreciably less than the quantity of cationic surfactants adsorbed by approximately a factor of ten. Torn *et al.* (2003) examined the adsorption of SDBS on kaolinite at 3 pH levels. The adsorption increased from 0.0072 mM to 0.011 mM as the pH decreased from 7.9 to 6.9. Peak adsorption was noted at pH 4.85. This correlates with the existence of positive charge under acidic conditions and an increasing negative charge under alkaline conditions. The amount adsorbed equates extremely well with that adsorbed by halloysite on a surface area basis. They calculated the surface area of the kaolinite sample to be 17.7 m^2/g. They also attributed patchwise heterogeneous clay character to explain differences in isotherms for mixed surfactant systems and acknowledged that the overall adsorption process was sensitive to pH and electrolyte concentration. Wakamatsu

and Fuerstenau (1968) examined the adsorption of the alkylsulfonate surfactants with varying alkyl chain lengths on the positive substrate, alumina, which is similar to the adsorbing material on the edges of the halloysite tubule. The adsorption isotherms had the same general characteristics but the occurrence of specific effects depended on the alkyl chain length as observed previously with other surfactants.

5.9.2 Varying Electrolyte Concentration

The effect of varying the electrolyte concentration while maintaining adsorbent concentration at 2.5% w/v and the concentration of SDBS at 1.5 mM was examined. SDBS adsorption was seen to increase with increasing KCl concentration, and it was seen to begin to plateau at considerably higher concentrations of KCl, Figure 5.9.2. The impact of KCl on adsorption is relatively small as the difference in contribution between the lowest and highest concentrations of KCl is of the order of 0.0014 mM/g of adsorbent. The experiment was also repeated with an adsorbent concentration of 0.5% w/v and SDBS concentration of 0.54 mM. The KCl concentration range was increased to 400 mM. The amount adsorbed began to plateau in a similar fashion to that observed in Figure 5.9.2. Although the amount adsorbed per gram was seen to increase to a maximum of 0.098 mM/g at a KCl concentration of 400 mM, the addition of electrolyte did not have a dramatic impact on SDBS adsorption because SDBS adsorption at 4.5 mM of KCl was 0.077 mM/g. However it can be seen from Figure 5.9.2 that this was still greater than the maximum of 0.056 mM/g adsorbed when the experimental halloysite concentration was 2.5% w/w. Although an exact adsorbate, adsorbent ratio was not maintained, the importance of the adsorbate, adsorbent-solution ratio is highlighted.

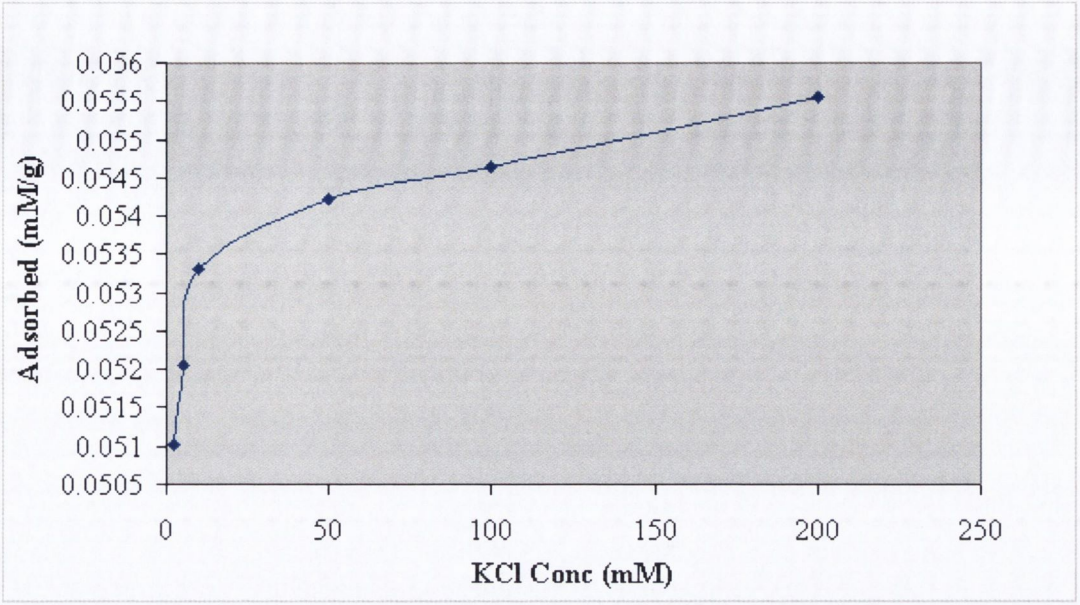

Figure 5.9.2 Adsorption of SDBS on halloysite (2.5% w/v) after an equilibration time of 24 hr as a function of varying KCl concentration.

5.10 MICROBIOLOGICAL ASSESSMENT

5.10.1 Preliminary Study

It is postulated that monolayer surfactant adsorption on halloysite occurs initially by an ion-exchange adsorption process, with the positive cationic surfactant head binding to the negative clay surface. However, it is well known that most types of cationic surfactants are incompatible with anionic surfactants (Rosen, 1989). The aim of this experimental section was to assess if the antimicrobial effect of TTAB was diminished in any respect by the presence of halloysite or if the antimicrobial properties were retained by the TTAB bound halloysite grade. The potential for halloysite to inhibit bacterial growth was also of interest. It was considered that halloysite might exhibit some bacteriostatic or bactericidal properties owing to its adsorptive properties. This was particularly of interest as halloysite was intended to be incorporated with the antimicrobial, metronidazole as described in Chapter 7.

A preliminary study to assess the effect of the surfactant-treated grade of halloysite examined in this body of work on the growth of two strains of the gram-positive organism *S. aureus* was carried out. Two different strains, Cowan and Oxford were provided by the

Department of Microbiology, Trinity College Dublin. The Cowan strain is a more sensitive strain than the Oxford variety. Cetrimide possesses innate antiseptic activity; minimum inhibitory concentrations required to stop growth of susceptible organisms including *Pseudomonas aeroginosa* (*P. aeroginosa*), and *S. aureus* and *Escherichia coli* (*E. coli*) are 300, 10 and 30 μg/ml respectively (Handbook of Pharmaceutical Excipients, 2005). *S. aureus* was chosen for this study due to its availability and also it was relatively less pathogenic compared to *E. coli* or *P. aeroginosa.* Also it is more susceptible to the effect of cetrimide. *S. aureus* was also chosen because it exists on the surface of the skin, hence it is pertinent in the study of topical and transdermal drug delivery. Again TTAB is chosen as the representative chain length for cetrimide.

The zones of non-bacterial growth surrounding the sample disc were measured in two directions. The zone of inhibition is a measure of the samples ability to halt bacterial growth either through a bactericidal or bacteriostatic effect. It can be seen from Table 5.10.1a that the halloysite sample had no effect on bacterial growth. The pure TTAB disc was the most effective at inhibiting bacterial growth. This was expected in light of the absence of any synergistic contribution from the halloysite sample. A consistent difference exists between the physical mix sample and the cetrimide-halloysite grade. The physical mix sample was prepared with the same ratio of surfactant to clay as the surfactant bound grade. The physical mix is more efficient at inhibiting bacterial growth. However, the ability of the cetrimide bound grade to comprehensively stop growth confirms that its activity is still present but has been diminished by the complexation procedure. The interaction between preservatives and natural suspending agents has been examined on a number of occasions with particular attention focusing on natural clays and hydrocolloids. Smith *et al.* (1975) studied eight preservatives and found that only chlorhexidine was adsorbed to a great extent by tragacanth. The authors also classified materials into four classes depending on their antagonistic effect on antimicrobial activity. Kaolin, the most chemically similar material to halloysite was classed as moderately antagonistic, whilst bentonite was classed as highly antagonistic.

Table 5.10.1a Zones of inhibition - Oxford Strain

Sample	Zone of Inhibition (mm)
Halloysite	0
Physical Mix	22
TTAB/Halloysite	18
TTAB	29

It can be seen from Table 5.10.1b that the pattern of values for zones of inhibition for the Cowan strain of *S. aureus* are quite similar to those of the Oxford strain, detailed in Table 5.10.1a. As expected larger zones of inhibition are noted for the Cowan strain, as it is a more sensitive strain than the Oxford variety. However, the zone of inhibition is smaller for the pure TTAB disc. It is 29 mm for the Oxford strain but only 27 mm for the Cowan strain. This may be attributable to the manner in which the cetrimide dissolves and diffuses in the agar medium and may not be adequately indicative of the susceptibility of the strain type. Two strains were examined in order to elucidate if subtle differences existed between the samples, as it can be seen from the study above with the Oxford variety there is a fundamental difference in the zones of inhibition evident for each sample.

Table 5.10.1b Cowan Strain

Sample	Zone of Inhibition (mm)
Halloysite	0
Physical Mix	24
TTAB/Halloysite	19
TTAB	27

5.10.2 Calibration

The TTAB bound grade was prepared with a surfactant concentration in excess of the bulk solution CMC in order to maximise potential binding. However owing to the method of preparation surfactant loss was inevitable when the solution was decanted after equilibrium. Using the surfactant adsorption isotherm, an approximate measure of surfactant adsorption may be obtained. In order to further estimate the amount bound,

physical mix samples were prepared which incorporated varying amounts of TTAB. The corresponding zones of inhibition were measured and are detailed in Table 5.10.2. The concentration of TTAB in the physical mix was plotted against the respective zone of inhibition for the sample, Figure 5.10.2a. A poor linear relationship exists between TTAB concentration in the physical mix and the resultant zone of inhibition. The resultant R^2 value for the plot of zone of inhibition against cetrimide concentration (% w/w) in Figure 5.10.2a was 0.8621. It is proposed that if the pure cetrimide disc did not dissolve into the agar medium in such a diffuse manner, a more uniform zone would have been achieved, hence a better correlation would have been attained. The relationship appears more linear at lower concentrations. However it is more likely that this there is not a linear relationship between concentration and zone of inhibition. The zone of inhibition is clearly evident from the photographs of the agar plates and samples discs. It can be seen to increase as the TTAB concentration is increased in the physical mix. Using the physical mix calibration plot, it was deduced, using the zone of inhibition for TTAB bound halloysite grade (18 mm), that this sample contains an approximate TTAB concentration of 10% w/w. This is less than the 16.67% w/w originally added and is to be expected.

Table 5.10.2 The concentration of TTAB halloysite physical-mix samples and the equivalent zones of inhibition for each sample. The strain of *S. aureus* used was the Oxford variety.

TTAB Conc. (% w/w)	Zone of Inhibition (mm)
0.12	3.38
0.99	9.5
4.76	15
16.67	20
100	36.5

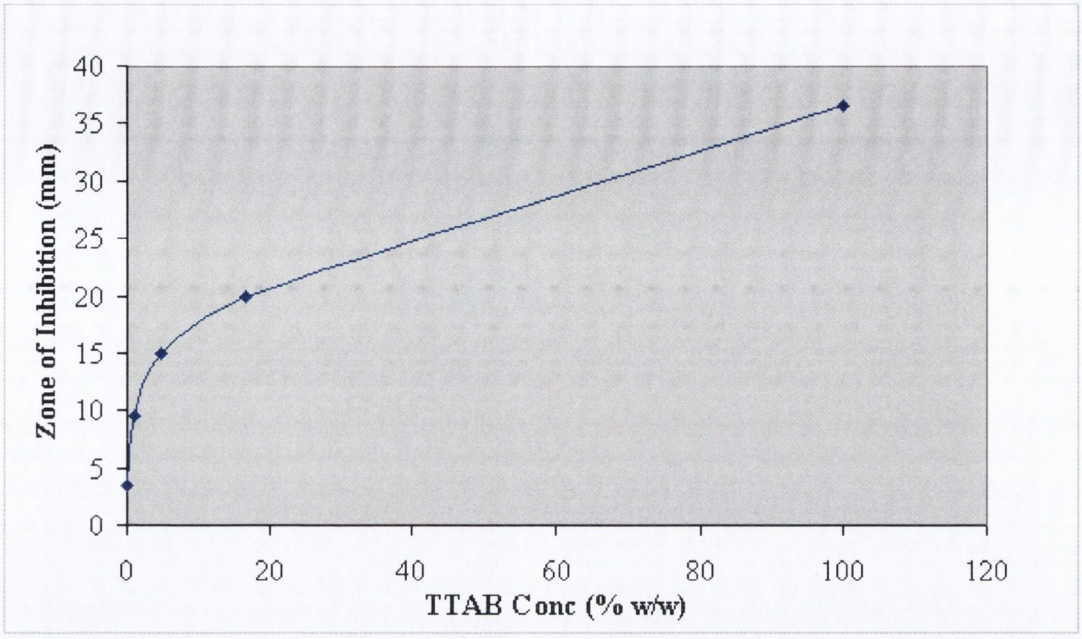

Figure 5.10.2a Plot of the zone of inhibition of TTAB halloysite physical mix samples against the concentration of cetrimide in the physical-mix.

Photographs of the increasing zones of inhibition as the concentration of TTAB in the physical mix samples is increased are depicted in Figures 5.10.2b-5.10.2e. The zone of inhibition for the lowest TTAB concentration (0.12% w/w) is not as obvious in the depictions as the zones observed at higher concentrations. With increasing TTAB concentration, the zones, which appear transparent, become very clear as they are framed by the turbid appearance of the bacterial growth.

Figure 5.10.2b TTAB concentration 0.12% w/w

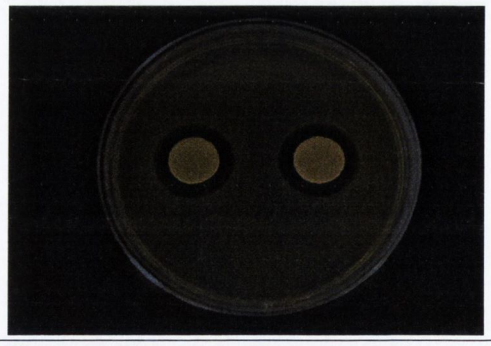

Figure 5.10.2c TTAB concentration 0.99% w/w

Figure 5.10.2d TTAB concentration 4.76% w/w

Figure 5.10.2e TTAB concentration 16.67% w/w

5.10.3 Advanced Study

The above experiment was repeated as above but the bacterial strains were suspended overnight in Tryptone Soy Broth (TSB) rather than in distilled water prior to use in order to encourage development (The Pharmaceutical Codex, 1994). The zones of inhibition for the advanced study are listed in Table 5.10.3a. The zones of inhibition for equivalent samples for the preliminary and advanced study are different. The zones are reduced in the repeat study. This might point towards bacterial growth being more confluent in the advanced study and that cetrimide is relatively less effective. The exception is the pure cetrimide discs for both strains of *S. aureus*. The zone of inhibition for the TTAB disc increases from 29 to 36.5 mm for the preliminary and advanced studies respectively using the Oxford strain. The corresponding values for the Cowan strain are 27 and 52 mm, Tables 5.10.1b and 5.10.3b respectively. The zone of inhibition almost doubled for the TTAB disc for the more sensitive strain when the advanced study was conducted.

However the zones of inhibition for the physical mix and TTAB bound halloysite samples reduced in the advanced study for both strains of *S. aureus*. It could be suggested that the halloysite may have retarded release of the surfactant or created a more tortuous path for diffusion of the surfactant with the result that the confluent bacterial growth was more opportunistic.

Table 5.10.3a Zones of inhibition of the growth of *S. aureus*, Oxford Strain.

Sample	Zone of Inhibition (mm)
Halloysite	0
Physical Mix	20
TTAB/Halloysite	16.5
TTAB	36.5

Table 5.10.3b Zones of inhibition of the growth of *S. aureus*, Cowan Strain.

Sample	Zone of Inhibition (mm)
Halloysite	1
Physical Mix	21.5
TTAB/Halloysite	15.5
TTAB	52

It can be seen from the photographs of the discs on the agar plates that clear zones of inhibition of bacterial growth are evident in Figure 5.10.3b-Figure 5.10.3d. It is interesting to note that there is a halo effect visible in Figure 5.10.3d around the physical mix disc. This is attributed to the TTAB dissolving in the agar medium and the halloysite, which was in intimate contact with the TTAB in the disc then diffusing into the agar medium below the disc resulting in the darker zone surrounding the original sample. This effect was not visible in the photographs of any of the other physical mix samples of lower TTAB concentration, it was observed in Figure 5.10.2e for the physical mix sample at a TTAB concentration of 16.67% w/w. It is considered that the dissolution of the surfactant into the surrounding agar medium has a more profound impact on disc structure as the concentration of TTAB is increased. Hence at the higher concentration of surfactant disc

deformity is more evident. The dissolution of the TTAB in the agar medium at higher concentrations may have affected the solidity of the agar; as a result the halloysite seeped into the agar. The zone of inhibition for the pure TTAB disc is diffuse and uneven settling of the agar medium that occurred as it solidified may have exacerbated this.

Figure 5.10.3a Halloysite disc - Oxford strain

Figure 5.10.3b TTAB disc - Oxford strain

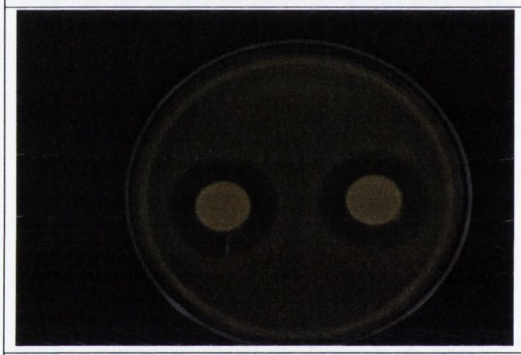

Figure 5.10.3c TTAB bound halloysite- Oxford strain

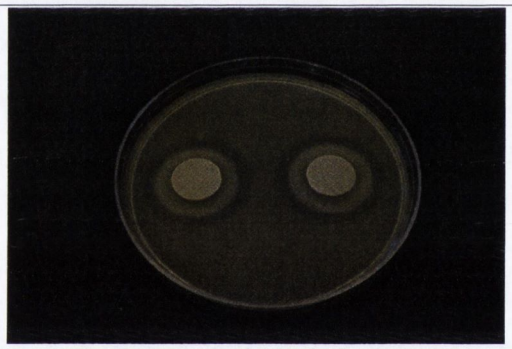

Figure 5.10.3d TTAB halloysite physical mix- Oxford strain

The photographs for the samples evaluated using the Cowan strain (Figures 5.10.3e-5.10.3h) depict features broadly similar to those already viewed above. However, it can be seen from Figure 5.10.3f that a very small zone of inhibition is evident for the halloysite disc. This is in contrast to the Oxford strain, Figure 5.10.3a that did not display a zone of inhibition and may be due to the Cowan strain being a more sensitive strain of *S. aureus*. This might point towards the evidence of some very slight antimicrobial activity due to the halloysite. Halloysite has displayed an adsorptive capacity, which might account for its ability to inhibit bacterial growth through disruption of the bacterial cell wall, through dehydration or adsorption of essential bacterial cell contents.

Figure 5.10.3e TTAB disc- Cowan strain

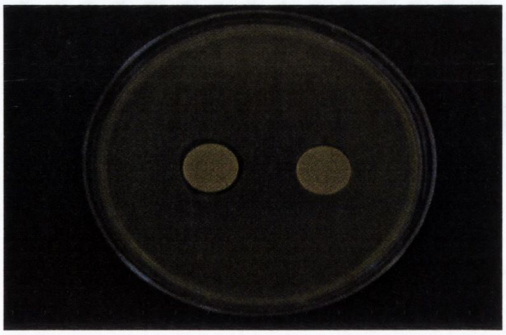

Figure 5.10.3f Halloysite disc- Cowan strain

Figure 5.10.3g TTAB bound halloysite- Cowan strain

Figure 5.10.3h TTAB halloysite physical mix- Cowan strain

5.10.4 Colony Forming Unit (CFU) Count

In order to quantitatively assess the effect of the cetrimide containing disc samples, an assessment of the amount of bacteria in the suspensions using the plating technique was undertaken. Plating techniques are simple, sensitive and widely used for viable counts of bacteria and other microorganisms in samples of food, water and soil. As detailed in the methodology Section the stock suspensions of each strain were diluted several times using a serial dilution scheme to reduce the microbial population sufficiently to obtain separate colonies when mixed with Nutrient Agar in a petri dish. After the agar has hardened each cell is fixed in place and forms an individual colony. The total number of colonies equals the numbers of viable microorganisms in the diluted sample (Prescott *et al*, 2005). The colony count (in CFU) is only a picture at a single instant in time, which records the situation at the moment the CFU count is made (Wallhauser, 1995).

Colonies per plate rather than the number of microorganisms were counted for two reasons, firstly; it is not possible to be absolutely certain that each colony arose from an individual cell. Secondly, some cells including *S. aureus* frequently clump or grow as aggregates. Plates containing between 30 and 300 colonies are counted. Plates with CFU count exceeding 300 are not counted and are designated "Too many to Count" (TMTC), whereas plates where the number was less than 30 were termed "Too few to count" (TFTC). Counts in excess of 300 are not considered as the colonies become very small and some may be missed. Counts below 30 are not considered as small variations introduce high percentage errors, therefore the count for this dilution is considered unreliable (Aulton, 2002).

It can be seen from Table 5.10.4a that the CFU count for the Oxford strain was too high to be counted in all dilutions except for the lowest dilution. A total of 242 CFU was counted, by extrapolation it was deduced that the original bacterial suspension contained 2.42×10^{10} CFUs/ml. A similar situation was evident for the Cowan strain; it had approximately a 15% lower CFU count. This may account in part for the observation of larger zones of inhibition for the samples tested using the Cowan strain. The concentration of CFUs/ml was 2.08×10^{10}, this was extrapolated from the CFU count for TTAB in Table 5.10.4b and the sample dilution. Only TTAB rather than HTAB was used to evaluate the antimicrobial efficacy of the samples. Smith et al., (1975) noted a more significant decrease in the turbidity of *E. coli* cultures treated with low concentrations of cetrimide B.P. compared with equivalent concentrations of HTAB. They attributed the difference to the tendency of HTAB to cause cell aggregation whereas cetrimide caused cell lysis due to the presence of impurities.

Table 5.10.4a Mean CFU counts for each dilution after incubation for 24 hr at 37 °C, Oxford strain of *S. aureus*.

Dilution	Average CFUs
1 x 10 $^{-4}$	TMTC
1 x 10 $^{-5}$	TMTC
1 x 10 $^{-6}$	TMTC
1 x 10 $^{-7}$	242

TMTC: Too many to count

Table 5.10.4b Mean CFU counts for each dilution after incubation for 24 hr at 37 °C, Cowan strain of *S. aureus*.

Dilution	Average CFUs
1 x 10 $^{-4}$	TMTC
1 x 10 $^{-5}$	TMTC
1 x 10 $^{-6}$	TMTC
1 x 10 $^{-7}$	208

TMTC: Too many to count.

5.11 CONCLUSIONS

Cetrimide was chosen as the primary surfactant to examine, as it had an established profile in topical products as an anti-bacterial agent and emulgent. The other cationic surfactants examined have similar uses. TTAB was chosen as the cetrimide form to be used in experiments because this is the constituent that the BP (2007) defines to be the primary constituent in cetrimide BP. The anionic surfactant SDBS was also examined.

The characterisation of the surfactants examined at the solution–air interface using surface tension studies produced values which largely agreed with those in the literature. It verified that the surfactants were pure in origin and that the systems were not contaminated with any electrolytes, which can easily occur. The primary surfactant examined, TTAB, had a solution CMC value of 2.98 mM. This is quite plausible as previously the constituent make-up was not so rigorously defined and it contained other quaternary ammonium

surfactants with varying alkyl chain lengths. The addition of electrolytes (NaBr, KCl) to the surfactant systems resulted in reduced CMC values. These values also adhered to the referenced values. Deflocculation/flocculation studies using cationic surfactants, BAC and TTAB highlighted their efficacy in suspending the halloysite material over periods of twenty-four and forty-eight hours respectively. The quantity required to deflocculate the 1% w/v halloysite suspensions was in the region of the solution CMC. This was indicative of charge neutralisation, with the result that flocculation was avoided by prevention of the "house of cards" structural build-up. The use of an anionic surfactant was also evaluated. SLS caused deflocculation at very low concentrations, which lasted in excess of seventy-two hours. A small quantity was required as the positive edge charge density is significantly less than that of the surface. This could be important economically. The preceding comments underline the ability to use surfactants to extract and obtain highly tubular halloysite from its crude source and hence reduce adulteration.

In Chapter 4, the new surfactant modified halloysite grade was characterised physically and chemically. The nature and extent of the adsorption was examined in detail in this Chapter. It is essential that the nature of the adsorption be characterised, in order that the surface character could be dictated. The 2^3 factorial study of TTAB on halloysite substrates produced some interesting findings. The nature of the halloysite substrate and electrolyte addition were statistically significant factors while equilibration time was not. The surface area of the modified sample almost doubled as a result of the acid washing process. The presence of NaBr shifted isotherms to lower concentrations and increased surface excess. However at lower concentrations it did not appear to negatively impact on adsorption as expected due to the screening of the electrostatic charge. The isotherms did not display an adsorption plateau at the exact position of equilibrium CMC. It is thought that this would occur just above the upper concentration depicted. It is believed that the TTAB isotherms conform to that expected with samples which have a constant surface charge. They appear to conform to the two-step model proposed by Gao *et al.* (1987). The increase in hydrophobicity with increasing chain length produced isotherms, which occurred at lower surfactant concentrations. This is analogous to that observed with the decrease in solution CMC with increasing chain length due to the increased driving force for micelle formation. The shift in position would be more evident if the difference in chain length was greater.

The dye method although not considered highly specific (Hough and Rendall, 1983) produced isotherms, which conformed to those observed in literature sources. The use of the HPLC method although considered more accurate did not result in conventional isotherms. The method resulted in a depression in the region of the equilibrium solution CMC. This may have been a separation issue because cetrimide is often used in reversed phase HPLC because it binds to the column and aids in the separation of compounds.

Isotherms of other cationic surfactants showed that less surfactant bound to the halloysite surface, this is most likely due to the presence of a bulky benzene moiety, which may have hindered adsorption, perhaps by obstructing potential binding sites. This must be considered in tandem with the increased hydrophobicity due to the contribution of the benzene ring. It is difficult however to make comparisons between different surfactant families (Hough and Rendall, 1983). A dramatic decrease in binding was observed for the anionic surfactant, SDBS. This was anticipated as the surface area of positive charge available and hence for electrostatic binding is considerably less as it exists only at the tubule ends. The presence of electrolyte increased the amount of SDBS bound, the compression of the double layer would impact greatly on the ability of the SDB^- ion to approach the tubule and reduce the repulsion between it and the negative tubule surface. Complementary studies indicated that adsorbent surfactant solution ratios were important.

Microbiological assessment confirmed that complexation of TTAB with halloysite did not eradicate the antimicrobial activity. The TTAB halloysite grade produced smaller zones of inhibition compared to the physical mix, which was prepared in the same ratio as the TTAB bound sample. It was estimated that the concentration of cetrimide adsorbed to halloysite was approximately 10% w/w, implying that 6.67% was lost or did not adsorb in the production process. It was observed that the halloysite sample inhibited growth of the more sensitive strain of *S. aureus,* which indicated some potential antimicrobial capacity. The bacterial suspension used for the advanced study had approximate concentrations of 2.42×10^{10} and 2.08×10^{10} CFU/ml for the Oxford and more sensitive Cowan strain, respectively.

Chapter 6

TOPICAL FORMULATIONS INCORPORATING HALLOYSITE

6.1 INTRODUCTION

Clay minerals are incorporated in several health care formulations. In particular they are present in many semi-solid preparations with different functions including stabilisation of suspensions and emulsions, viscosity modification and other special rheological tasks, protection against environmental agents, adhesion to the skin, adsorption of greases and control of heat release. These functions are possible because of the special disposition of clay mineral particles when dispersed in polar solvents, due to their high surface areas and colloidal dimensions. Clays may also be modified to augment or alter some properties and new clay-like materials with special features are also formulated. Clays are frequently used concomitantly with other rheological modifiers to obtain synergistic effects, including the stability or other technical properties of health care products (Viseras *et al.*, 2006). In Chapters 4 and 5 chemical modification of halloysite was examined and characterised. A cetrimide modified grade of halloysite was produced. It is the intention in this Chapter to examine the incorporation of halloysite and modified halloysite with active constituents in topical products. The Chapter examines two actives frequently encountered in topical products, urea and salicylic acid.

The initial focus centered on urea. It was chosen as the first candidate due to its small, simple carbamide structure and its high water solubility which would facilitate its inclusion into the tubular lumen. The British Pharmacopoeia (2007) defines its function as a keratolytic, but it is frequently employed in topical products for its humectant properties. Urea has the ability to draw moisture up from below the dermis into the epidermis (Clarke, 2004) and to improve the moisture content in dry, dehydrated skin. The goal of formulation with halloysite was to examine the ability of halloysite to encapsulate and control the release of this very water soluble component. From a formulation viewpoint the production of this urea halloysite composite could focus on the keratolytic activity of urea or the

hydration aspect. The role of halloysite might be to augment the keratolytic activity of urea, enhance the rheological properties and adhesion to the skin. In its function as a hydrating agent, halloysite could have a barrier function and help to maintain the hydration similar to the role of kaolin for protective purposes (Sweetman, 2005). The texture and rheological properties of halloysite are outlined in this Chapter in order to determine an appropriate concentration at which halloysite could be used in topical preparations.

Formulation of halloysite with another keratolytic, salicylic acid was also investigated. It was intended that this formulation would also concentrate on other properties of halloysite. As elucidated in Chapter 1, halloysite is chemically similar to kaolin. The use of kaolin in topical products is established, it is used in preparations for its absorption and adhesive properties (Alexander, 1973). Halloysite has a greater surface area and cation exchange capacity than kaolin, which is indicative that it could at least equal the adsorptive capacity of kaolin. The potential complex could be used to combat acne through the keratolytic properties of salicylic acid and the insoluble solid content of the halloysite. Halloysite could absorb grease and excess sebum as well as bacterial cell components, hence reducing exacerbation. The latter role is analogous to that of a poultice. Adhesion of the formulation to the skin might also be enhanced.

6.2 UREA

6.2.1 Introduction

The aim of this section was to formulate a urea halloysite complex for potential incorporation into topical products. The solubility of urea was assessed in a number of media and at varying pH levels. The first approach to complex formation utilized the loading of halloysite using a vacuum method employed previously by Levis (2000), Kelly (2002) and Salter (2003). A fractional factorial experimental design (2^{4-1}) was used. The impact of the cetrimide modified grade was also considered. An alternate method for composite formulation involved the use of spray-drying technology. The effect of lecithin addition to the system was also investigated because it was hoped to incorporate the complex into an emulsion, which the presence of lecithin would aid in the stabilization of, due to its inherent emulsifying properties. However due to time constraints emulsion preparation were not formulated. Samples were characterised by SEM image analysis and urea release from the composite systems.

6.2.2 Solubility Study

The British Pharmacopoeia (2007) defines urea as very soluble in water and soluble in alcohol. The extent of urea solubility in a range of vehicles was examined. The vehicles chosen include deionised water, ethanol, McIlvaine buffer, pH 5 and phosphate buffered saline (PBS), pH 6.8. Solubility studies were examined at two temperatures, room temperature (20 °C) and that which approximates to skin temperature (33 °C) (Williams, 2003). The saturation solubilities for the urea in different media at the two temperature values are depicted in Tables 6.2.2a and 6.2.2b. The sample's saturation at 20 °C is significantly lower than that at 33 °C. There is a substantial increase in urea saturation in all vehicles as the temperature is increased.

The samples examined at higher temperatures had higher standard deviations, representative of the problems associated with sampling and dilution. Samples were prepared using urea concentrations well in excess of reference saturation solubilities; hence a large quantity of undissolved urea remained. This in conjunction with the elevated analysis temperature complicated removal of a portion of saturated solution using a needle and syringe. It was found that the standard deviations of the samples were reduced when the needles, syringes and filters were pre-warmed in an oven. The pre-warming procedure reduced the recrystalisation that occurred when urea solutions contacted a surface at a lower temperature.

Table 6.2.2a Saturated solubility of urea in different media at 20 °C, sampled after 24 hours.

Medium	Solubility (% w/v)	(+/-) St. dev.
McIlvaine Buffer pH 5.0	27.23	4.43
PBS pH 6.8	43.78	5.83
Deionised Water	35.66	2.62
Ethanol	11.29	0.01

Table 6.2.2b Saturated solubility of urea in different media at 33 °C, sampled after 24 hours.

Medium	Solubility (% w/v)	(+/-) St. dev.
McIlvaine Buffer pH 5.0	73.54	1.51
PBS pH 6.8	66.88	5.96
Deionised Water	47.27	5.42
Ethanol	18.91	6.29

6.2.3 Loading Study

The intention of this study was to examine the effect of various factors on the loading efficiency of halloysite with the highly water-soluble molecule, urea. The variables examined were the pH of the loading medium (pH 2.5 or 8.0), loading solution volume (28 ml or 56 ml), halloysite grade (halloysite G or cetrimide coated halloysite) and finally the effect of single or double loading of the samples were again analysed. It should be noted that the amount of urea was constant in both loading solutions.

The factors analysed in this study were subject to fractional factorial design, 2^{4-1}, and the design generator was ABC. Eight sample runs were conducted; a true replicate at each design point was also prepared. It was decided to examine loading medium pH because preliminary release studies conducted in McIlvaine buffer at pH levels 5.5 and 6.8 showed an increased release for the higher pH. As pH 5.5 is more physiologically relevant to skin this was chosen for further release studies. Also urea is a weak base and has a pK_b value of 13.82 (Martin 1993). It was hoped that some ionisation of the molecule might result in it binding to the halloysite surface. Loading solution volume was examined as previous loading studies conducted by Levis (2000) used a ratio of loading solution volume to halloysite of 1:1. It was felt that a larger volume might result in more efficiently loaded samples after the application of the vacuum as described in the methodology Section. However a balance must also be considered as too large a volume may result in some of the urea being lost when the excess solution is decanted. The effect of modifying the halloysite surface with the surfactant, cetrimide and its implications for drug release were also explored here. The process of single or double loading of samples was the final variable considered. The model response factor was the amount of urea encapsulated.

The loading efficiency was determined by quantifying the amount of urea released from the loaded samples over a time period of 24 hr. Figure 6.2.3 depicts the quantity of urea released per gram of drug loaded sample after 7 hr. The 7 hr time point was chosen as there was a small decline in urea concentrations at the 24 hr time point. It is likely that there is some urea remaining in the complex and this is not an absolute representation. This may be attributed to the instability of urea in solution at prolonged periods. The quantity of urea released varies from 0.20 g for sample run 11 to 0.44 g for sample 6. The levels for each factor for sample 6 are as follows; the pH of the loading medium was 8, the loading solution volume was 28 ml, the sample used was the cetrimide coated grade and it was loaded on a single occasion. It is interesting to note that the levels of each factor for sample run 11, which had the lowest encapsulation, were exactly opposite to those for sample run 6. The uncoated sample was double-loaded with a greater volume of loading medium, 56 ml at a lower pH of 2.5.

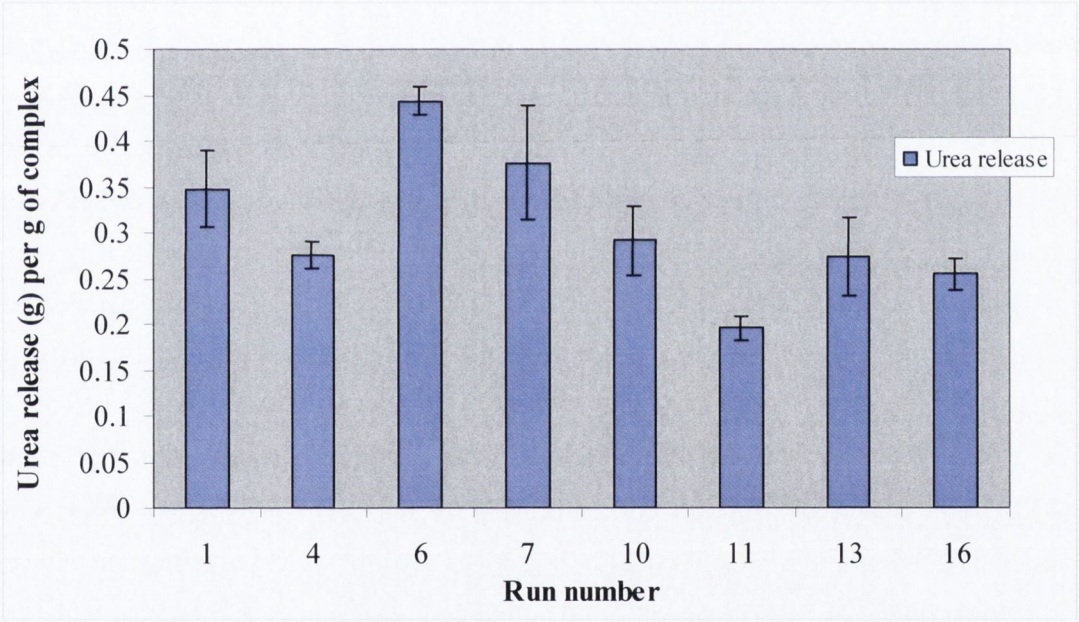

Figure 6.2.3 Comparison of the amount of urea released from halloysite loaded according to conditions designated by fractional factorial design, 2^{4-1}.

Some interesting aspects are highlighted from the main effects plot for each of the factors in Appendix 5. A decrease in the amount released for the lower pH loading medium might indicate that the sample is not ionised to an extent which results in it binding to the halloysite surface, hence less of the sample is loaded under these conditions. A similar

decrease in release is observed for samples loaded using the larger volume. As outlined above this is most likely due to urea loss as a larger volume of solution is removed by decanting, hence a larger amount is lost, resulting in a decreased efficiency of loading. The most notable main effect difference is that attributable to the effect of coating the halloysite with cetrimide. It is possible that micelle formation at the bulk surface has the ability to entrap urea resulting in a higher quantity being encapsulated. It was noted during the loading process that the surfactant coated samples seemed to foam quite extensively. However, some foaming would be expected as the vacuum removed air from the tubules facilitating entry of drug solution. It is postulated that the increased agitation during foaming enhanced sample loading.

Double loading the samples appears to have an insignificant effect on the amount of urea released. The corresponding F-statistic for loading is not statistically significant. This may be due to the fact that the loading solutions are extremely concentrated. The rational for using such high concentrations was based on mercury porosimetry studies conducted by Levis (2000). Levis concluded that the bulk density of sieved halloysite was 0.671 g/ml and that the total mercury intrusion volume into pores less than 0.1 μm was 0.246 ml/g. There is considerable difference between this bulk density value and the skeletal density value of 2.4833 +/- 0.0098 g/cm^3 calculated using helium pycnometry. The difference is likely due to the inability of the larger mercury molecule to intrude the smaller pores, which would be accessible to the much smaller helium atom. The skeletal density of urea (1.333 g/cm^3) and the potential volume available for loading which is approximately 0.25 ml/g (Levis, 2000) were considered prior to loading solution preparation. These values were used to prepare solution concentrations for the preliminary study based on the theoretical amount of urea that could be entrapped per unit weight of halloysite. However, potential volume of 0.25 ml/g considered both the intraparticulate and interparticulate void space and hence very concentrated solutions were prepared that saturated the halloysite sample and masked any modified release potential.

The interaction profiles in Appendix 5 show that the majority of factors do not appear to interact. The F-statistics for the 2-factor interaction of buffer pH and halloysite and also buffer pH with loading volume are not statistically significant (p values of 0.441 and 0.568 respectively). Obvious interactions for the grades of halloysite and loading solution volume and also for buffer pH and frequency of loading are apparent.

Cetrimide coated halloysite was significantly more effective in encapsulating urea than the uncoated grade. This may be due to the nature of the interaction between the components of the system. Urea crystallises in a channel-like structure permitting the enclosure of other compounds, the molecules pack in an orderly manner and are held together by hydrogen bonds between nitrogen and oxygen atoms (Brown, J.F., 1962 as cited in Martin, 1993). The hexagonal channels that form are approximately 5 Å in diameter and can provide room for guest molecules such as long chain hydrocarbons. The study highlights that a large quantity of urea can be encapsulated in the halloysite loaded samples. However due to the high quantity it may not be possible to adequately control the release as the urea saturates the tubule interior and exterior.

6.2.4 Spray-Dried Urea/Halloysite Complexes

6.2.4.1 Introduction

The vacuum drug loading method employed in the previous Section, 6.2.3 resulted in a halloysite urea complex with similar quantities of each component. The sample from run 6 liberated the largest quantity of urea (0.44g per g of the urea-loaded complex). This proved to be an ideal method for complex formation but the high loading solution resulted in saturation of the halloysite structure, which in turn had negligible impact on control of urea release. It would be expected that the surfactant might contribute to release because it aids in the wetting of the sample but the cetrimide adsorption on the clay surface modifies it from hydrophilic to hydrophobic, hence it might alter the wettability of the sample after it is dried. A progression on this study involved the formulation of spray-dried complexes composed of halloysite tubules; between and within which the urea would be entrapped. Production of the urea halloysite complexes using the spray-drying method was employed to produce uniform particles. The atomization step of the spray-drying process produces spherical droplets that ideally dry to form spherical particles (Oakley, 1997).

As stated above the aim of this section was to produce urea halloysite spray-dried complexes. As a further modification it was decided to incorporate, lecithin, which is a complex mixture of phospholipids and other materials (Handbook of Pharmaceutical Excipients, 2005) within the complex during the spray-drying procedure. The spray-drying method has the advantage that multiple solid substances can be incorporated into individual particles at a fixed composition (O'Connor *et al.*, 2005). Lecithin is included in

a number of topical products, including soaps and emulsions as a stabilizer, in creams as an emollient and viscosity modifier (Anonymous, 1974 as cited in Handbook of Excipients, 2005). The multifunctional capacity of lecithin may enable the stabilization of the halloysite clay in cream and emulsion formulations and it will augment the hydrating capacity of the urea. It was hoped that uniform particles in terms of size, morphology and constitution would be produced in order that release from the product would be consistent.

Table 6.2.4.1 outlines the proportion of each constituent used in each sample. A co-solvent system of water and ethanol in a ratio of 40:60 was used in all systems except for sample 1; the solvent was water in this case. Two grades of lecithin were employed, Lipoid S75 and Lipoid S100 at concentrations between 0.1 and 1.0% w/v. Both are unsaturated phospholipids of soybean origin. They differ from each other in terms of the phosphatidylcholine content and are named accordingly. Therefore Lipoid S75 has a phosphatidylcholine content of approximately 75% and Lipoid S100 has an approximate content of 100% (Lipoid Product Information).

Table 6.2.4.1 Quantities and constituents of spray-dried urea halloysite complexes.

Sample	Halloysite (% w/v)	Urea (% w/v)	Lecithin - grade and quantity (% w/v)
1	2.0	2.0	Lipoid S75 - 1%
2	2.0	2.0	Lipoid S75 -1%
3	2.0	2.0	Lipoid S100 -1%
4	1.0	1.0	Lipoid S100 - 0.5%
5*	1.0	1.0	Lipoid S75 - 0.5%
6**	1.0	1.0	Lipoid S75 - 0.5%
7	2.0	2.0	Lipoid S75 - 0.2%
8	2.0	2.0	Lipoid S100 - 0.2%
9	1.0	1.0	Lipoid S75 - 0.1%

*Pump rate 3%, **Pump rate 5%

6.2.4.2 Lecithin

Lecithins are used in a variety of applications including pharmaceutical, food products and cosmetics (Anonymous (1974), Handbook of Pharmaceutical Excipients, 2005). Lecithins

are mainly used in pharmaceutical products as dispersing, emulsifying and stabilizing agents and are included in intramuscular and intraveneous injections, parenteral nutrition formulations and topical products such as creams and ointments. Lecithins are used also used in suppository bases (Novak *et al.*, 1991) to reduce the brittleness of suppositories and have also been investigated for their absorption enhancing properties in an intranasal insulin formulation (Anonymous, 1991 as cited in Handbook of Excipients, 2005). The potential of novel drug delivery systems containing liposomes in which lecithin is included as a component of the bilayer structure to encapsulate drug substances have been investigated (Grit *et al.*, 1993). Glycerophospholipids are the predominant group of substances found in commercially available lecithin. The typical structure is depicted in Figure 6.2.4.2. The trivalent alcohol glycerol forms the backbone of the structure. Glycerophospholipids contain a polar (hydrophilic) region and a non-polar (lipophilic) region.

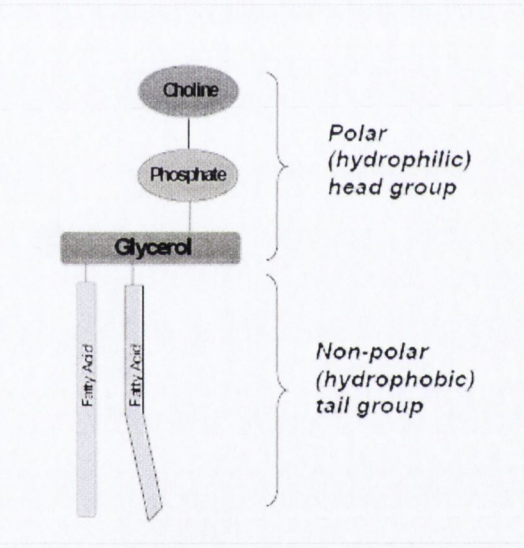

Figure 6.2.4.2 Schematic presentation of a phosphatidylcholine molecule (Lipoid GMBH).

6.2.4.3 SEM of Spray-Dried Complexes

The appearance of the spray-dried complexes was examined by SEM analysis. Macroscopically the spray-dried samples have the appearance of a fine powder that is slightly yellowish in appearance. It can be seen from the SEM image for sample 1 in Figure 6.2.4.3a, that there is a variation in particle size distribution. The particles have a diameter in the range of 5-30 μm. Figure 6.2.4.3b shows a particle from the centre of

Figure 6.2.4.3a at a higher magnification (x 20,000). The particle is approximately 5 μm in diameter and the distinct presence of the halloysite tubule is evident on its surface. The presence of macropores (pore width exceeding 50 nm, Sing *et al.*, 1985) on the surface is also distinguishable. The SEM images for sample 1 depicts particles with a wide size distribution, this is attributable to the liquid feed medium, water. Lecithin dissolves in ethanol but not water. It is however dispersible in water, therefore there is an enhanced possibility of larger, non-uniform particles forming.

Figure 6.2.4.3c depicts sample 3. It is composed of highly porous, non-spherical particles. There is an extensive presence of pores on the surface of the particles, the diameter of the pores is up to 1 μm. The particle has a gelatinous sponge-like appearance. Lipoid S100 seems to act as a matrix in which particles of urea and halloysite are embedded. The concentration of the lecithin is 1% and it is present in a ratio of 1 part lecithin, and 2 parts each of halloysite and urea. Figure 6.2.4.3d is a magnification of a portion of this sample. The halloysite tubules are obvious at this increased magnification and the lecithin material appears to coat them.

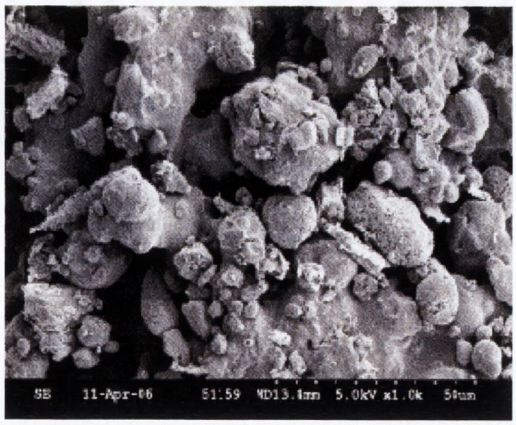

Figure 6.2.4.3a Spray-dried urea complex sample 1. (Magnification x 1,000)

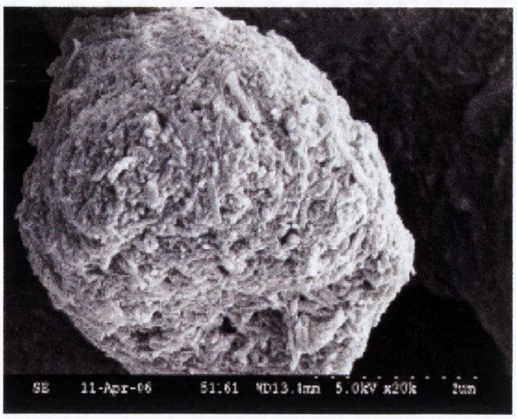

Figure 6.2.4.3b Spray-dried urea complex sample 1. (Magnification x 20,000)

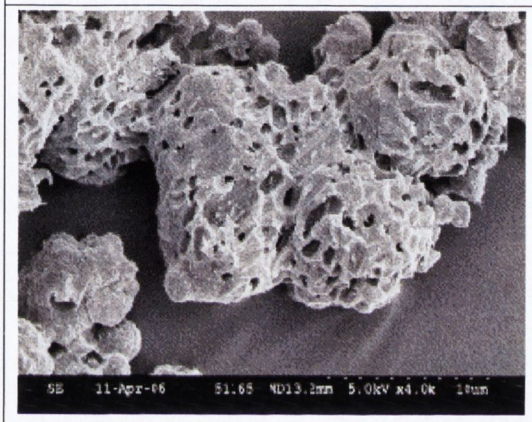

Figure 6.2.4.3c Spray-dried urea complex sample 3. (Magnification x 4,000)

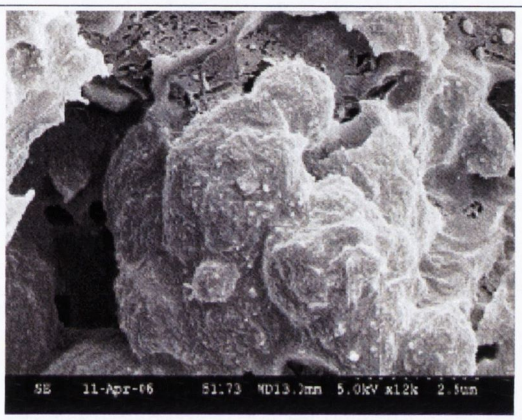

Figure 6.2.4.3d Spray-dried urea complex sample 3. (Magnification x 12,000)

Figure 6.2.4.3e shows sample 4. It, like sample 3, contains the Lipoid S100 grade, the ratio of the lecithin to halloysite and urea components is maintained but the lecithin concentration is reduced to 0.5% w/v. The gelatinous appearance of lecithin is consistent with SEM images of other samples. However, there is an increased presence of more spherical uniform particles. Two distinct particle types are evident in Figure 6.2.4.3e. Firstly, there is a completely spherical particle with a blowhole on the surface. Also present is a fractured sphere, which appears to have a hollow interior. Internal pressure or attrition may have caused the fracture. Magnification of this image results in the electron micrograph of Figure 6.2.4.3f, which confirms the presence of the halloysite tubules embedded on the particle surface. The presence of solids on the surface is a characteristic

feature of the spray-drying process. As the particle dries and depending on the rate, solids come out of solution first on the droplet surface leading to crust formation (Oakley, 1997).

SEM images of sample 5 are illustrated in Figures 6.2.4.3g and Figure 6.2.4.3h. It can be seen from Table 6.2.4.1a that sample 5 contains Lipoid S75 rather than S100 at a concentration of 0.5% w/v. It is identical to the constituents and concentrations of sample 4 in all other respects. Spherical particles with diameters in the range of 5-12 μm are depicted in Figure 6.2.4.3g. The presence of pores with a diameter of up to 0.5 μm on the intact spheres is also highlighted. The larger particles may have a different density than the smaller spheres owing to the presence of occluded or absorbed gases in the feed liquid (Oakley, 1997). This is likely as the tubular and void volume of the halloysite lumen may entrap air, which contributes to porosity and particle fracture during the drying process. The pore network is magnified in Figure 6.2.4.3h. The pores extend from the surface to the interior of the particle, which has implications for particle wetting and the rate of release of the active. The presence of the halloysite tubules enmeshed in the lecithin is discernable from this SEM image also.

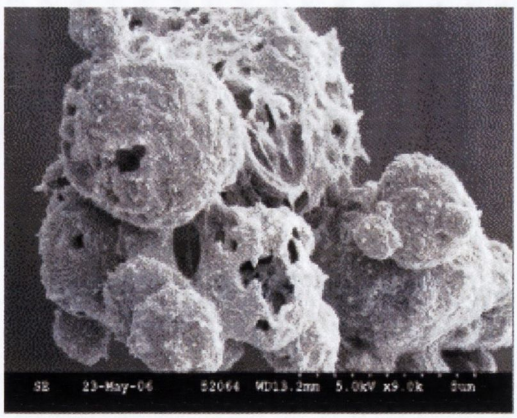

Figure 6.2.4.3e Spray-dried urea complex sample 4. (Magnification x 15,000)

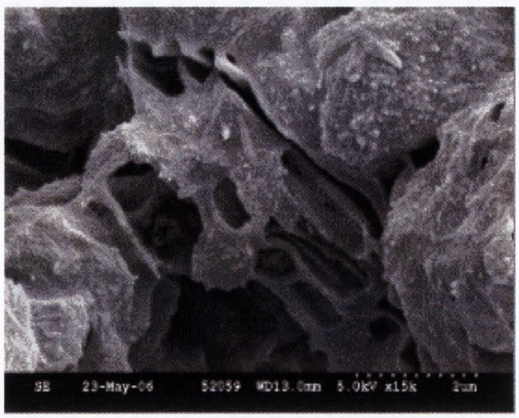

Figure 6.2.4.3f Spray-dried urea complex sample 4. (Magnification x 15,000)

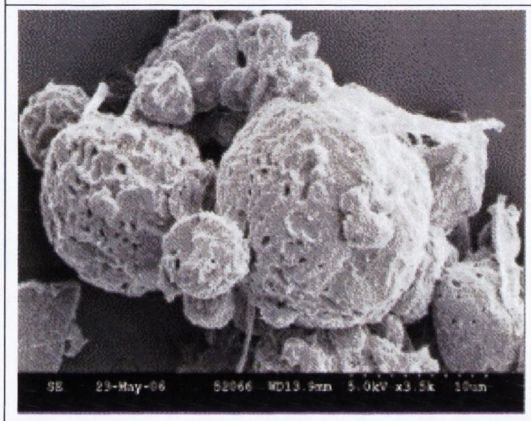

Figure 6.2.4.3g Spray-dried urea complex sample 5. (Magnification x 3,500)

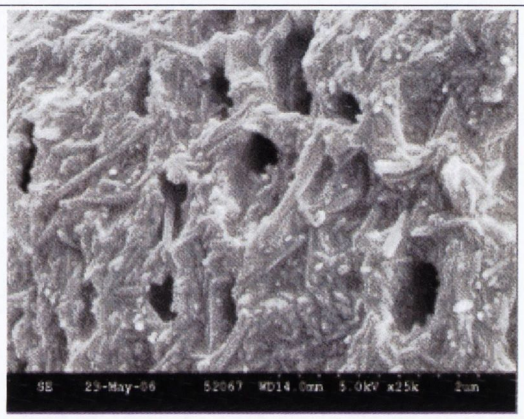

Figure 6.2.4.3h Spray dried urea complex sample 5. (Magnification x 25,000)

Figures 6.2.4.3i and 6.2.4.3j are SEM images of spray-dried complex 7. The Lipoid S75 grade of lecithin was used to produce sample 7. The main difference here is the absence of the gelatinous lecithin appearance. The presence of the halloysite tubules is again discernable but they do not appear coated in lecithin. This is due to the reduction in the overall ratio of lecithin to the other components of the system and the relatively low concentration of lecithin in the formulation. The ratio of lecithin:halloysite:urea for the other systems was 0.5:1:1, in this case it is 0.1:1:1. The regular pore structure is retained. Figures 6.2.4.3k and 6.2.4.3l are images of sample 8. The formulation of sample 8 is identical to 7 except for the grade of lecithin used is Lipoid S100. The particle examined is less spherical than that in Figure 6.2.4.3i and has a rougher surface appearance. At higher concentrations there appears to be some loosely adhered flaky material. This is probably an

incompletely formed lecithin coat. Lipoid S100 has a higher concentration of the polar alcohol group, phosphatidylcholine. This might have affected the drying rate and morphology of the particle. No apparent differences were evident at higher concentrations of lecithin between the samples formulated with the two different grades.

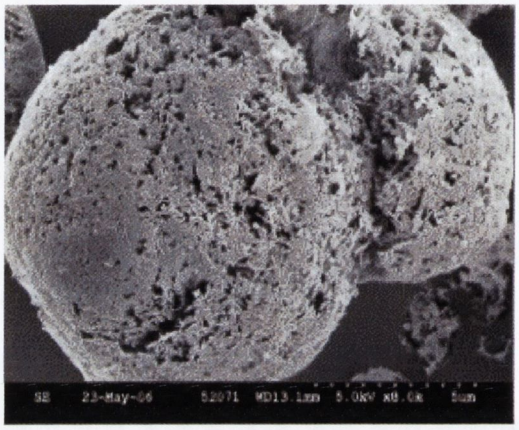

Figure 6.2.4.3i Spray-dried urea complex sample 7. (Magnification x 8,000)

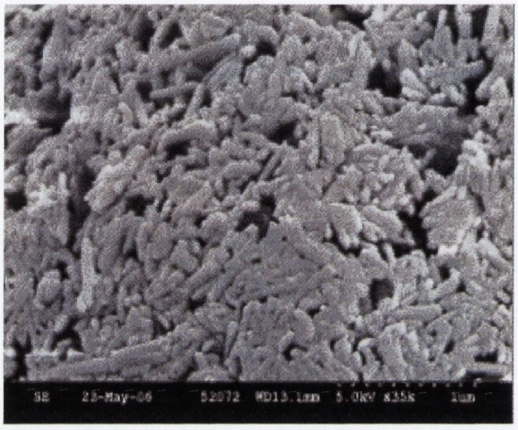

Figure 6.2.4.3j Spray-dried urea complex sample 7. (Magnification x 35,000)

Figure 6.2.4.3k Spray-dried urea complex sample 8. (Magnification x 6,000)

Figure 6.2.4.3l Spray-dried urea complex sample 8. (Magnification x 18,000)

6.2.4.4 Urea Release

The release of urea from the spray-dried complexes examined in the previous Section using SEM analysis is outlined here. The aim of determining the quantity released is to ascertain whether constituent ratio, concentration and lecithin grade employed impacted on the encapsulation of urea during the spray-drying process. Figure 6.2.4.4a illustrates the quantity of urea released per gram of spray-dried material assessed after 7 hr. Samples, 1, 8 and 9 were not examined as there was insufficient sample available for these particular formulations. Sample 2 results in the highest release of urea, 33.5% w/w. It is closely followed by sample 3, which has a release of 32.61% w/w. The third highest releasing formulation was sample 7. Table 6.2.4.1 illustrates the components for each of these systems. They contain urea at a concentration of 2% w/v. It is not surprising that they would have the greatest quantitative release as the remaining systems had a urea concentration of only 1% w/v. Sample 7 encapsulated 25.75% w/w, this is lower than that for samples 2 and 3 despite a urea concentration of 2% w/v. This is due to the reduced ratio of lecithin in the formulation.

Samples 4 and 5 released 23.82% and 17.9% urea respectively. They again had the same ratio of constituents as samples 2 and 3 but the concentrations were halved. From the % encapsulations quoted it is clear that reduction of concentration by half did not imply a 50% reduction in urea release. This indicates that the lower solids concentration resulted in improved encapsulation. Lipoid S100 was used to produce sample 4 and the S75 was used to produce sample 5. The Lipoid S100 was more efficient probably due to its more polar nature. The superiority of the more polar substance was not repeated with samples 2 and 3, but as the urea concentration was higher in the latter case, this may have reduced the importance of lecithin in the formulation.

Samples 5 and 6 had identical constituents but they had different pump rates. Sample 6 was produced at a higher rate of 5% compared to 3% for sample 5. The release from these samples was not significantly different. The t-test had a p value >0.05 (0.375). Despite the differences in % urea released, the release profiles for samples 2, 4, 6 and 7 shown in Figure 6.2.4.4b are very similar. Release is almost complete (84-92%) in all cases by the 1 hr time period. The total amount released was considered as the maximum value released within 24 hr.

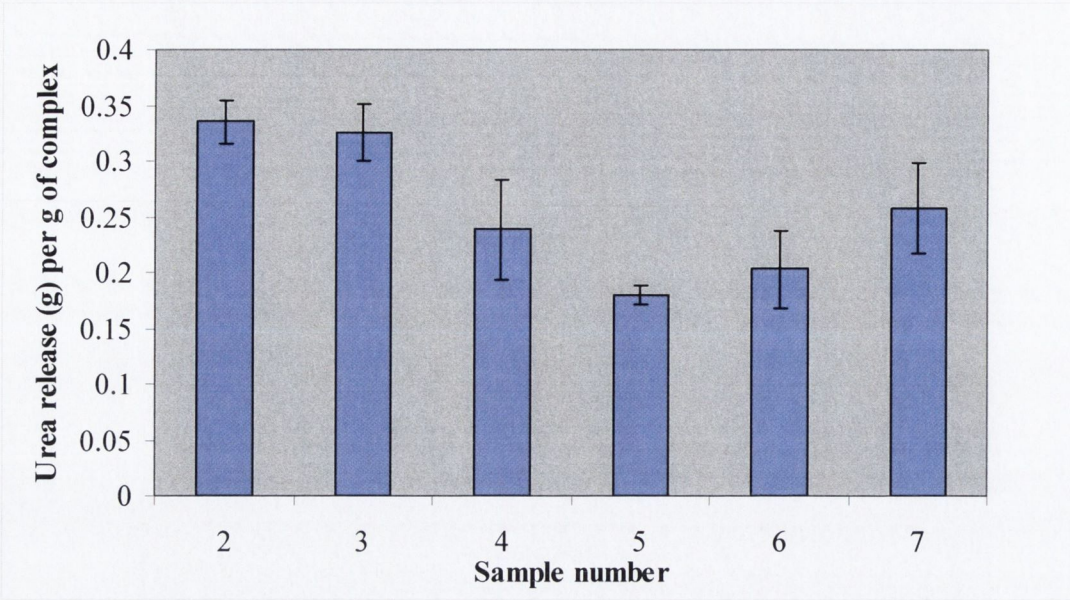

Figure 6.2.4.4a Comparison of the amount of urea released per gram of the halloysite, lecithin and urea co-spray-dried systems after 7 hr. Two grades of lecithin, Lipoid S75 and Lipoid S100 were employed.

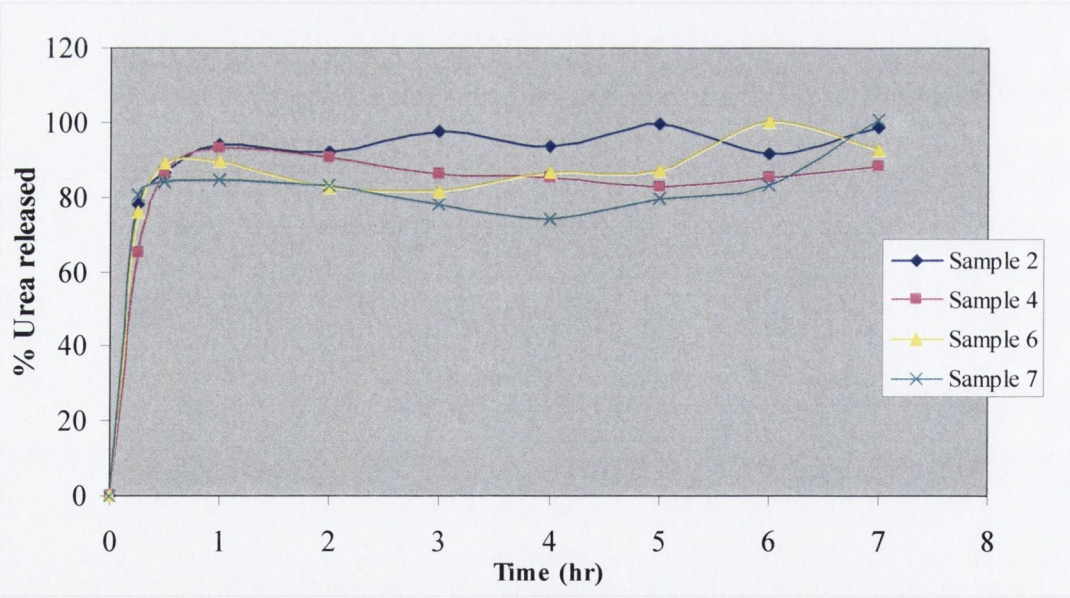

Figure 6.2.4.4b Release profiles of urea from co-spray-dried systems of halloysite, urea and lecithin. Two grades of lecithin, Lipoid S75 and Lipoid S100 were employed.

6.3 RHEOLOGICAL AND TEXTURAL EVALUATIONS OF HALLOYSITE - OINTMENT SYSTEMS

6.3.1 Introduction

Rheology is the science or study of flow. The subject looks at how materials deform and flow under the influence of external forces (IFSCC monograph, 1997). It is a method of classifying a gel, emulsion or semi-solid by providing information on their structure. Pharmaceutical, medical and cosmetic materials range in consistency from fluid to solid. An important category is the semi-solids which are the most difficult to characterize rheologically because they combine both liquid and solid properties within the same material. Pharmaceutical examples of these include ointments, creams, pastes, gels and ingredients such as lanolin and soft paraffin (Radebaugh, 1996). Rheological measurements are conducted on these materials in order to gain an insight into the innate nature of the system. Rheology is also used as an important quality control tool, it is used to assess raw materials, final products and products of manufacturing processes such as mixing, pumping and filling. It can also be used to assess sedimentation and flocculation in emulsions and suspensions. Fundamental changes in a product due to formulation changes, temperature alteration and storage time can be ascertained from rheological evaluation (Barry, 1974).

The aim of this section is to examine the rheological character of two ointment bases, white soft paraffin (WSP) and a water-soluble polyethylene glycol base, Macrogol Ointment BP using shear and dynamic oscillatory rheology techniques. The techniques were further used to characterise the ointment bases with varying quantities of added halloysite. The effect of coating the halloysite grade with cetrimide on rheological properties is also elucidated. The study aims to highlight the concentration of halloysite, which will improve retention of the halloysite-ointment system on the surface of the skin without adversely affecting the formulation of the product. However equally important is patient acceptability from an aesthetic and functional point of view. The texture analysis method of evaluation was used in tandem with rheological assessment to determine product characteristics, which are representative of its firmness and spreadability. Considerable work has been conducted in the field of texture profiling by Sherman, (1970); Barry and Grace (1972); Barry and Meyer (1973). They examined aspects with regard to product usage such as removal from a jar or tube and spreading and adherence to the skin.

During product development key rheological characteristics must be designed into the product so as to provide optimal flow character during processing, packaging, transport, storage and consumer use.

6.3.2 Flow Rheology

6.3.2.1 Introduction

One of the primary techniques used is that of flow rheology. The flow response of a sample is measured as it experiences a changing shearing force. A flow curve is generated by measuring shear rate under a ramped or continuous shear stress. The data provides information on yield stress, viscosity, shear thinning and thixotropy as well as correlations to everyday processes such as pumping, stirring and extrusion. A Newtonian fluid is one, which gives a linear plot for increasing shear stress against shear rate, examples of which include water. If however a viscosity response is experienced with an increase in shear, the material is non-Newtonian. Non-Newtonian flow can be sub-divided into a number of different categories including plastic and pseudoplastic flow. Plastic flow is characterised by a decrease in viscosity after a critical level known as the *yield value* is exceeded (IFSCC Monograph, 1997). A yield value, which is high enough to maintain the product on the skin after application, is necessary (Barry, 1983). Pseudoplastic flow is similar to plastic, except it does not include a yield value. Dilatant systems show an increase in viscosity with increasing shear stress. The importance of flow in any formulation is that from one experiment a large amount of information can be gained that simulates a wide range of application processes and performance properties (TA Instruments, 2002).

6.3.2.2 Continuous Flow Rheometry

Figure 6.3.2.2 displays a conventional flow rheogram for halloysite-WSP ointment systems. It can be seen from the flow curve profiles (arrow indicative of direction of flow) that flow did not occur prior to a yield value being reached, this is indicative of plastic flow behaviour. The apparent yield value increased when halloysite was added to the ointment base and continued to increase with increasing solid content. The WSP ointment base alone has the lowest apparent viscosity. It would be expected that with the addition of solids the viscosity behaviour of the sample would increase. The increase in the viscosity is attributable to the tubular shape of the halloysite material. The thickening power of particles, which have the shape of rods, is superior to those, which have spherical

morphologies. This is as a result of the decreased packing efficiency of the particles (Barnes, 2000). The flow curves for the ointment systems containing halloysite at concentrations of 20 and 40% are very similar displaying a high resistance to flow over the shear stress values examined. The test is destructive at the shear stresses examined. At shear stress values in excess of approximately 450 Pa, structural breakdown occurs in the WSP ointment, the presence of halloysite prevents structural breakdown of the ointment at stress values in excess of 500 Pa.. Hendersen *et al.* (1961) made the first major attempt to establish shear rates corresponding to pharmaceutical use. The authors attributed a shear rate range of 100-10,000 s^{-1} to rubbing into skin (it was dependent on the degree of rubbing). It is important that a balance exists, as an excessively viscous sample will require a high degree of shear or rubbing action.

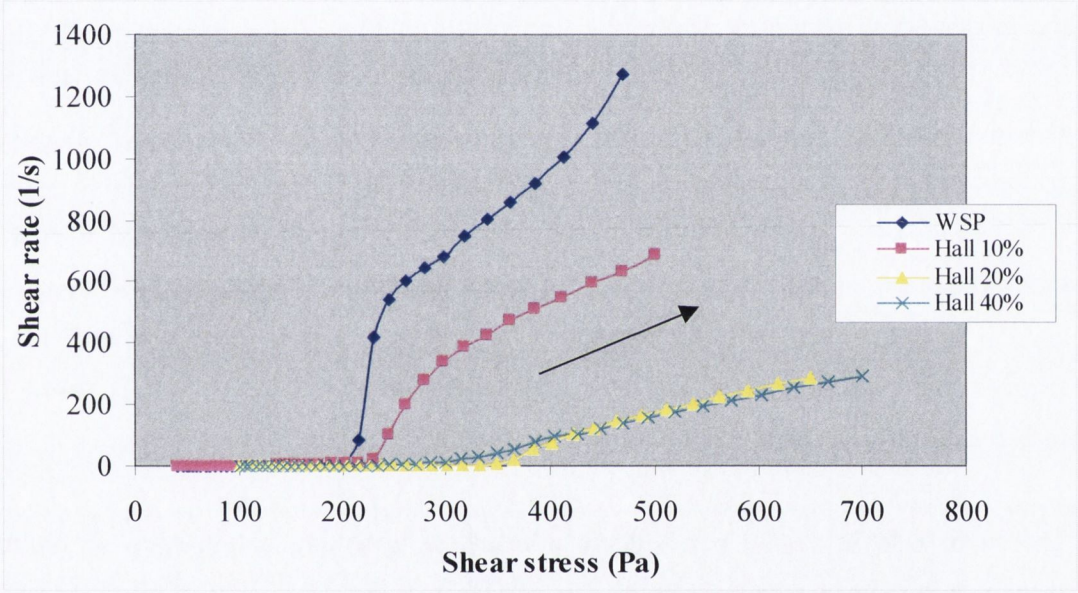

Key: WSP = white soft paraffin; Hall = halloysite.

Figure 6.3.2.2 Flow rheograms for WSP and halloysite-WSP systems with different concentrations of halloysite.

Figure 6.3.2.2 shows the presence of a spur point in the profile of WSP and that containing halloysite 10%. It is a characteristic feature in many rheograms, however the cause of bulges or spurs is not certain. When they occur in rheograms of time-dependent materials and are not due to instrumental artefacts, they are thought to be due to the presence of a three dimensional gel-like structure (Martin *et al.*, 1964). The spur may be taken as a

measure of the strength of a system in which the structure must be broken down before significant flow can occur. The presence of spurs in soft paraffins has been described by Davis, (1969), Barry and Grace, (1970, 1971a, 1971b). They have been attributed to the 3-D framework, which forms due the presence of microcrystalline waxes.

6.3.2.3 Stepped Flow Rheometry

The traditional method of analysis involves continuous flow rheology. The shear stress or shear rate is ramped from one extreme to another, usually low to high in a defined time period. The test is useful as a quick investigation of the sample, but as the test is a rapid ramp, the time dependency of the sample is not eliminated and so for shear thinning materials the viscosities obtained are not the most accurate. Since there is a rapid and continuous change in the force applied to the sample, it does not have time to respond to the lowest shearing forces. There is a loss of information in the low shear region. An alternative technique was employed to improve the quality of information; the flow rheology technique used is called stepped flow. The shearing force is ramped between two extremes as in the continuous flow technique but the force is increased in defined steps. At each step the shear rate was applied for a defined interval and the viscosity was noted at the end. The shear stress is then incremented to the next step. The number of discreet steps and the time at each is also defined. There is an increased chance of the sample reaching its steady state equilibrium for each particular shear stress as more time is given (TA Instruments, 2002). However, the sample run time is longer.

The rheograms in Figure 6.3.2.3a are a result of analysing halloysite-WSP ointment systems using stepped flow rheology. The curves are logarithmic plots of viscosity against shear stress. The zero-rate shear and infinite rate shear plateaus are separated by the power law region. This is where sample structure is seen to breakdown. Sample structure is seen to breakdown in the region of 100 Pa for WSP and the WSP system containing 10% halloysite. It increases to approximately 600 Pa for the 20% loading. A significant increase in the shear stress value is observed for the 40% system, aggregate formation and the large solid content accounted for the increase. The viscosity of dispersions is influenced by the continuous phase, which may be Newtonian or non-Newtonian and the added dispersed phase where the size, shape, amount and deformability of the particles of the material can vary considerably as can the interaction between the individual dispersed particles (Barnes, 2000).

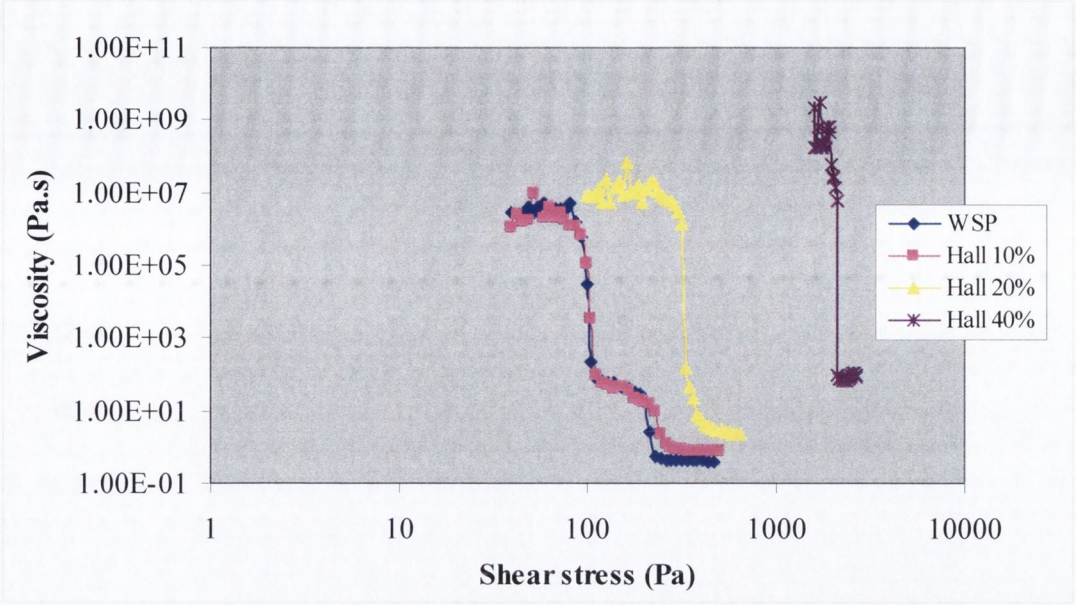

Figure 6.3.2.3a Stepped flow rheogram for WSP and halloysite-WSP ointment systems with varying concentrations of halloysite.

At the zero shear stresses, predictions about the in-container appearance of the sample can be made, as well as its stability as sedimentation, leveling and other similar processes that occur under very small gravitational forces. Therefore the higher the value the more likely that the sample will not suffer from sedimentation but if the value is too high, ease of handling may become a concern. Information on sample breakdown can lead to important changes in the manufacture process. The point at which the sample starts to shear thin (enters the power law region) dictates the energy needed to make the sample flow easier. This can affect the pump ability and the type of packaging used (TA Instruments, 2002).

At the infinite shear viscosity, this usually represents the final application viscosity, which corresponds to the easiest state for pumping, spraying, brushing, etc. Too high a value and the sample may be difficult to apply, too low and the final appearance is more likely to be messy (TA Instruments, 2002). The shape of the flow curve is important in understanding and predicting product performance. It is also important to make measurements in the relevant part of the flow curve, otherwise erroneous assumptions can lead to inaccurate formulation alteration.

Figure 6.3.2.3b illustrates rheograms of macrogol and halloysite-macrogol ointment systems. It highlights that higher shear stresses are required to cause shear thinning for the macrogol ointment base and halloysite-macrogol compared to the equivalent loadings in WSP, Figure 6.3.2.3a. Halloysite at a concentration of 40% proved extremely difficult to examine and the results were not consistent. The power law regions for macrogol, halloysite 10% and halloysite 20% in macrogol ointment are approximately 650, 300 and 800 Pa, respectively. The rheograms depicts that an increased shear stress value is required to cause shear thinning in the macrogol ointment compared to that which had 10% halloysite added. The presence of halloysite particles results in a decreased entanglement of the polymer components of the ointment resulting in a decreased resistance to flow. However with increasing halloysite concentration, solid concentration is a more dominant factor in dictating the viscosity at which the sample flows.

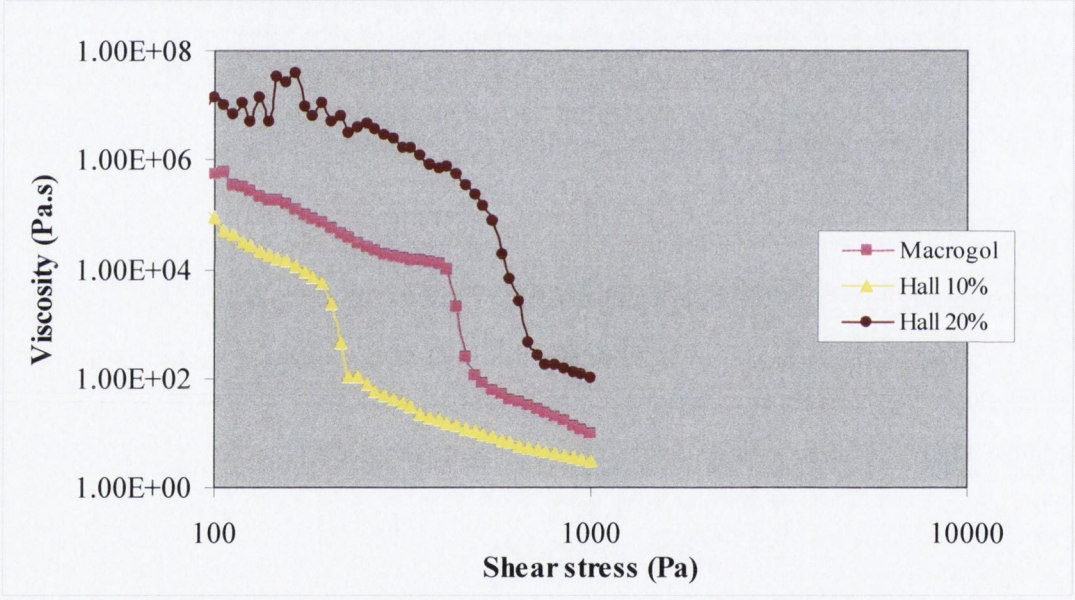

Key: Hall = halloysite; macrogol = macrogol ointment.

Figure 6.3.2.3b Stepped flow rheogram for macrogol and halloysite-macrogol ointment systems with varying concentrations of halloysite.

6.3.3 Dynamic Oscillatory Rheology

6.3.3.1 Introduction

Many materials do not respond in a simple manner to changes in shear rates and cannot be fully defined by a single type of flow. Samples which have a viscous and elastic component are termed viscoelastic and this accounts for their non-ideal behaviour. Most dermatological vehicles show this degree of complexity (Barry, 1983). If the material is viscous all external forces acting on it are lost after the deformation takes place. Conversely an elastic material stores any external forces acting on it and releases them after the external force is removed. Dynamic and kinetic measurements are required to more fully characterise the viscoelasticity of these systems. One of the primary methods of analysis is an oscillation sweep curve. A constant strain is applied to the sample and the oscillatory frequency is increased. The parameters measured from this application are the storage (G') and loss (G") moduli. Structure and stability comparisons can be made easily using oscillatory stress sweeps. Key viscoelastic parameters (G', G" and tan delta) can be measured in oscillation as a function of stress (torque), strain, frequency, temperature or time. The storage modulus is a measure of the energy stored and recovered per cycle of deformation and reflects the solid-like or elastic component of the viscoelastic sample. The loss modulus (G") is a measure of the energy lost; it reflects the liquid-like component of the system. The ratio of G" to G' is known as tan delta (δ), it is a measure of the viscoelasticity of the system. In a completely elastic system, the stress curve during an oscillation study is fully synchronous with the strain curve, while in a completely viscous system the strain and stress curves are 90° out of phase. The closer the value of tan δ for the material is to 0°, the more elastic-like it behaves, while the closer the tan δ is to 90° the more viscous the sample is. The first step to study the viscoelastic structure of a sample is to determine the Linear Viscoelastic Region (LVR) of the sample (IFSCC monograph, 1997).

6.3.3.2 Linear Viscoelastic Region Determination

The LVR of the sample is the range of stresses (or displacements) in which the samples structure is only stretched but not destroyed. This value can also be useful in flow rheometry applications. In order to accurately examine the thixotropic nature of a sample the dynamic stress to be applied during regain should be within the LVR of the original sample, since this would minimise the amount of destruction of any structure regaining.

Modern techniques enable the study of a sample's viscoelasticity and its frequency (and therefore timescale) dependence by dynamic measurements. A dynamic test, if performed correctly, is non-destructive and so the sample is gently probed and its viscoelastic responses noted (TA Instruments, 2002).

This type of experiment involves the oscillatory stress / strain being increased, usually in a logarithmic ramp, at a fixed frequency and temperature. The experiment is performed to define a linear region (LVR), where the sample's interactions are increasingly stretched until they are broken and this results in a drop in the elastic component G'. Figure 6.3.3.2 depicts the LVR for WSP and halloysite-WSP ointment systems.

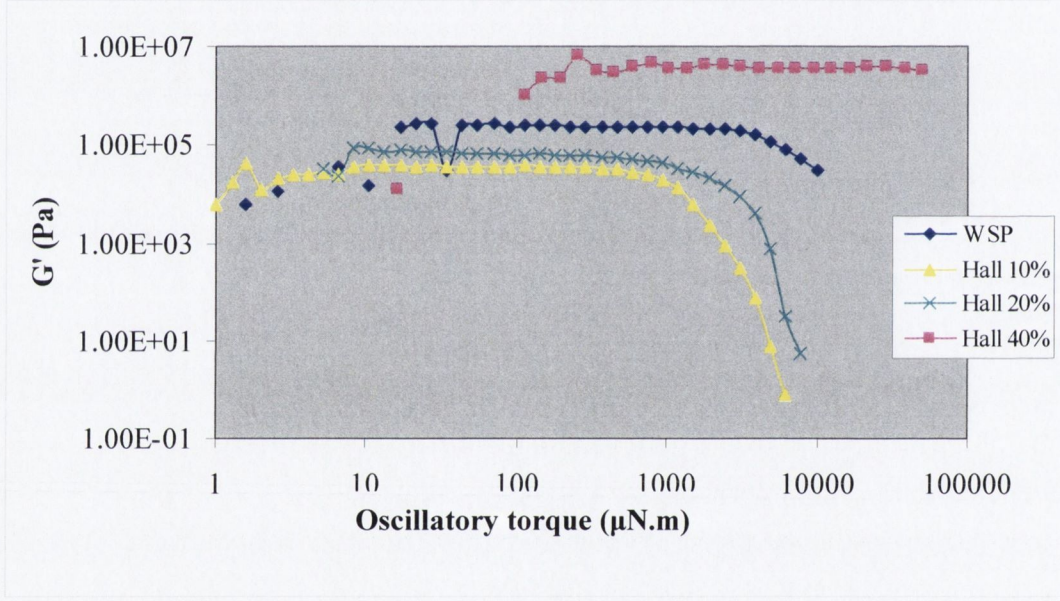

Key: WSP = white soft paraffin; Hall = halloysite.

Figure 6.3.3.2 Rheograms displaying the LVR for WSP and halloysite-WSP ointment systems with varying concentrations of halloysite.

6.3.3.3 Dynamic Oscillatory Studies on Halloysite - WSP Systems

WSP could be classified as a viscoelastic system as it shows frequency dependence; its response varies with frequency of oscillation. The examination of samples at varying frequencies is important. At low frequencies the energy imparted to the sample has time to dissipate. It may do so in the form of heat energy. Whereas at higher frequencies the

frequency of oscillation is increased per unit time, it has less time to dissipate so the elastic nature of the sample predominates in the majority of cases (Tadros, 1995). In Figure 6.3.3.3a the rheogram depicts the storage and loss moduli of WSP. The storage modulus (G') is dominant over almost the entire frequency range. It is possible that at very low frequencies the loss modulus (G") predominates. There is an approximate two-fold difference in the values of G' and G". The value of tan δ is 30° at a frequency of 10 Hz, it is closer to 0° than 90°, indicating the ointment base is more elastic than viscous. It would appear that at lower frequency values G" would predominate because the energy would have more time to dissipate in the form of viscous energy.

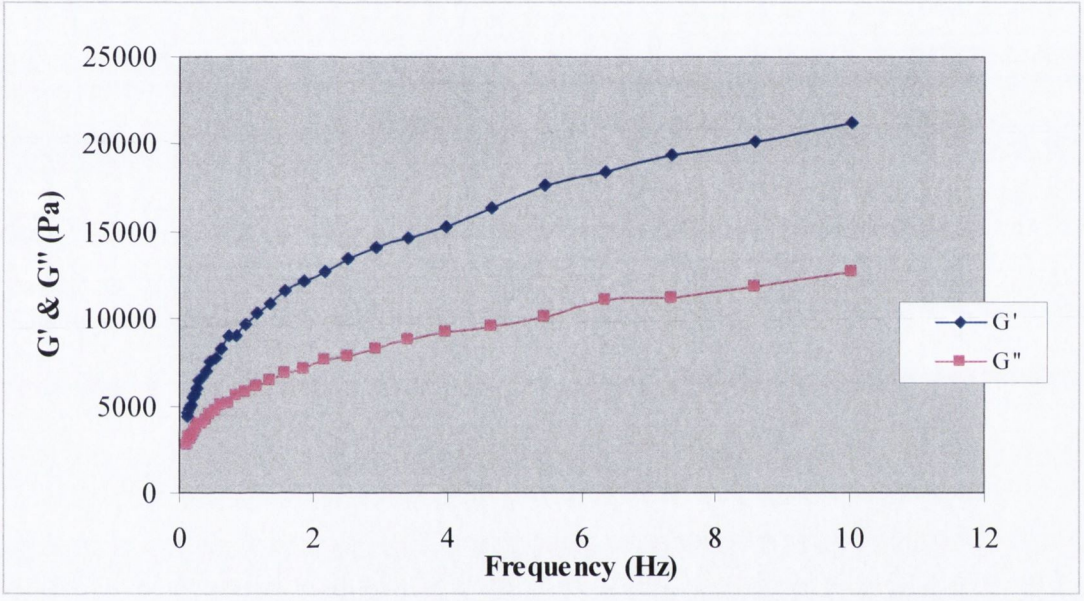

Figure 6.3.3.3a Dynamic oscillatory study of WSP ointment base.

Figure 6.3.3.3b depicts oscillatory rheograms for WSP systems containing halloysite and cetrimide coated halloysite at a concentration of 10%. As can be seen from the rheograms containing surfactant modified halloysite, the G' and G" are decreased with respect to the uncoated clay mineral systems. The effect of coating halloysite with cetrimide results in the positive head of the surfactant binding to the surface of the halloysite tubule, which has a negative charge (Tari *et al.*, 1999). As a consequence a decrease in edge to face association of halloysite tubules occurs because of the decrease in the electrostatic attraction between the tubule surface and the pH dependent positive charge of the tubule ends. This phenomenon was investigated by van Olphen (1977) and was discussed in

Chapter 5. It would be expected that an improvement in the flow property of the ointment system containing the coated halloysite would be experienced. However a decrease in aggregate size structure occurs as the house of card structures do not form, consequently an effective increase in surface area per unit weight occurs which contributes positively to viscosity (Barnes, 2000). However the decrease in G' and G" is attributable to the hydrophobic effect imparted to the hydrophilic clay mineral as a result of the coating process, hence there is a decreased resistance to sample flow.

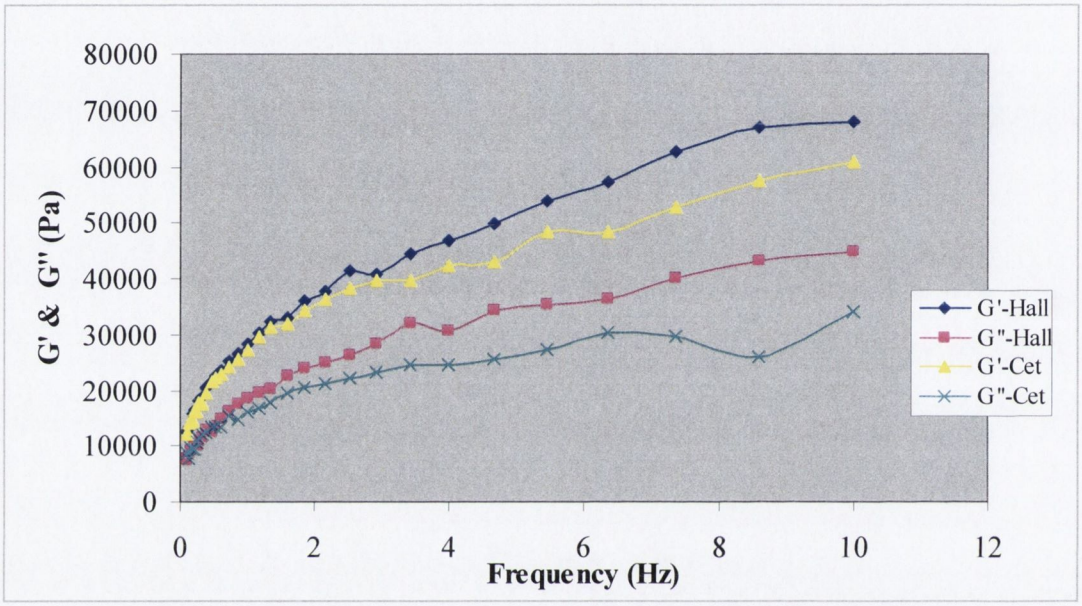

Figure 6.3.3.3b Dynamic oscillatory study of WSP ointment base containing halloysite and cetrimide coated halloysite at a concentration of 10% w/w.

However as the surfactant is used in quantities that exceed its critical micelle concentration it would be expected that multilayers of it would form on the surface of the halloysite tubule having various morphologies ranging from hemimicelles to bilayers. This implies that the hydrophilic surfactant head groups would be exposed to the surface altering the surface properties of the halloysite. However as the cetrimide coated halloysite sample is removed from the aqueous phase after preparation, any admicellar structures will be reduced to a monolayer on drying. About half of the surfactant desorbs in the process of transport through the air-water interface, resulting in monolayer coverage (Wanless, 2004). The clay is hydrophobic along the surface as the hydrophobic tails of the surfactant

monolayer are exposed and impart this character to the clay mineral surface on addition to the ointment base.

In conjunction with the above explanation the evidence for the presence of a monolayer of surfactant on the halloysite surface is also compounded by the differing behaviour of surfactants in water and in oil. A bilayer structure exists on the surface of the halloysite in aqueous solution. However on addition to an oil phase, such as WSP, the outer surfactant molecules of the bilayer desorb to a monolayer leaving the hydrocarbon chains facing the oil phase (Atkin, 2004). The surfactant is seen to work as a dispersant due it is thought to stearic repulsion effects of the hydrocarbon chains of the surfactant (Wanless, 2004).

Despite a reduction in the storage and elastic moduli for the cetrimide coated sample, the ratio of G" to G' is essentially similar compared to the uncoated sample. Tan δ values at a frequency of 10 Hz are 33.50^{o} and 30.65^{o} for the uncoated and coated samples respectively. The corresponding value for the ointment base without the addition of halloysite is 33°; this indicates that the viscoelsticity of the systems is essentially constant because no distinct shift in tan δ is apparent.

Figure 6.3.3.3c depicts dynamic oscillatory rheograms for halloysite-WSP ointment systems containing halloysite and cetrimide coated halloysite at a concentration of 20%. Again G' and G" are greater in the case of the uncoated sample. The ratio of G" to G' is approximately equivalent, the tan δ values at 10 Hz are 29.28^{o} and 27.22^{o} for the uncoated and coated samples respectively. The values are similar to the tan δ for the samples containing 10% halloysite. Therefore increasing sample concentration results in a very small decrease in tan δ values. This highlights a slight increase in the elastic solid component of the sample.

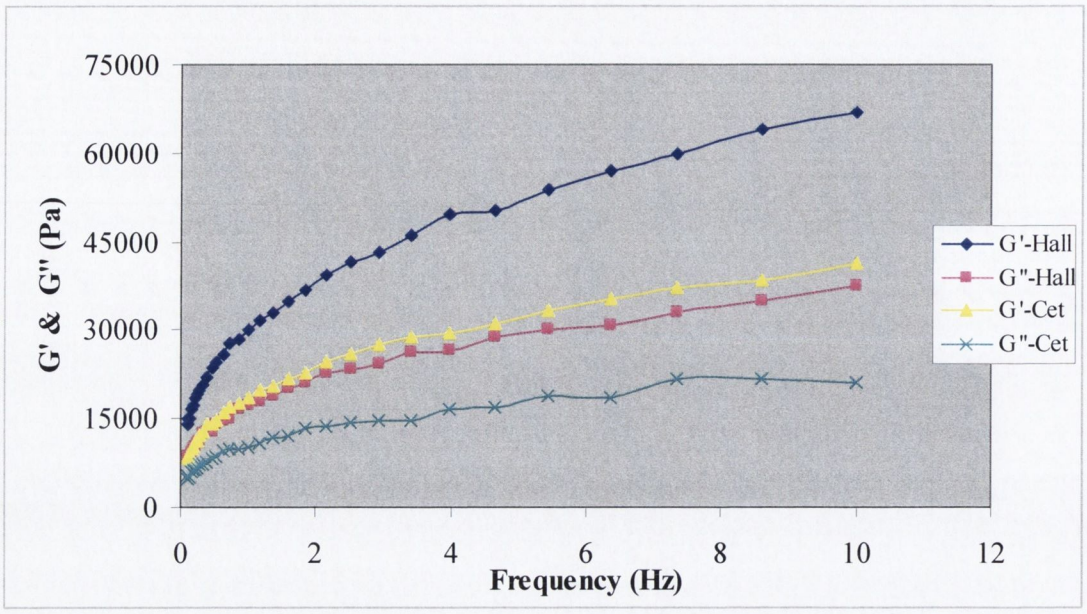

Key: Hall = halloysite ointment systems; Cet = cetrimide coated halloysite systems.

Figure 6.3.3.3c Dynamic oscillatory study of WSP ointment base containing halloysite and cetrimide coated halloysite at a concentration of 20% w/w.

Figure 6.3.3.3d depicts dynamic oscillatory rheograms for halloysite-WSP ointment systems containing halloysite and cetrimide coated halloysite at an increased concentration of 40%. Unlike the lower concentrations there is a noticeable difference in the ratio of G'' to G' between the coated and uncoated samples. The values for tan δ at 10 Hz for the coated and uncoated sample are 29.11° and 15.16°. There is a considerable increase in the solid component of the sample due to increasing the halloysite content to 40% w/w. The viscoelasticity has altered and the sample is more solid like, this is characterised by a tan δ values value closer to 0. The coated sample had a tan δ value equivalent to the lower sample loadings and ointment base.

Coating of halloysite has important ramifications. It allows higher concentrations of halloysite to be used while yet maintaining product stability, as the elastic component is not compromised to such an extent that gravitational effects would be significantly more damaging compared to the lower sample loadings. It improves product flow. This is important as the 40% concentration of halloysite in WSP can have a rough texture, this is especially true if the halloysite is not properly dispersed.

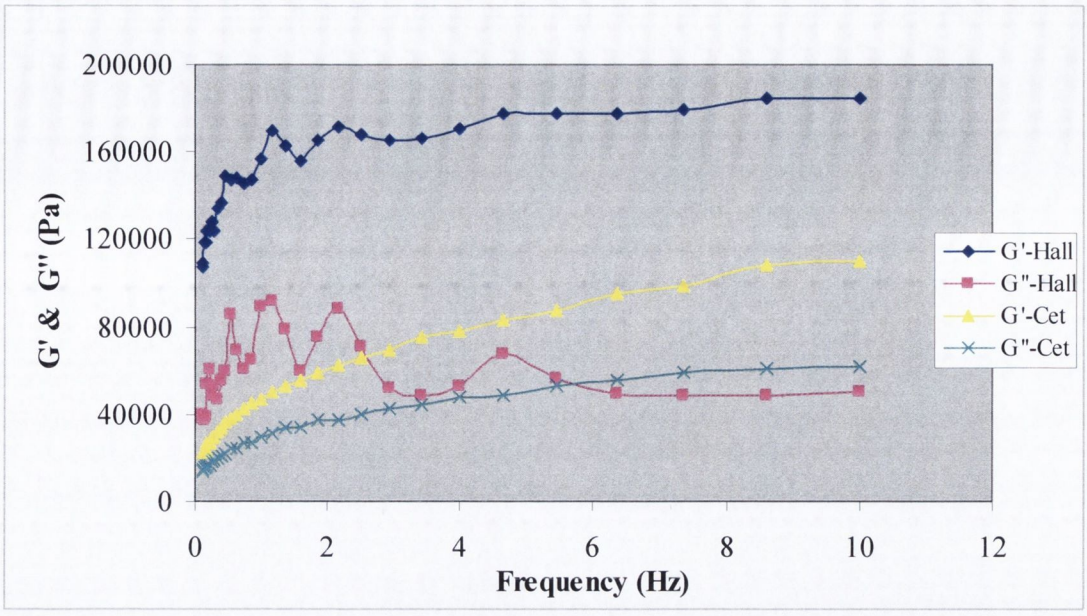

Key: Hall = halloysite ointment systems; Cet = cetrimide coated halloysite systems.

Figure 6.3.3.3d Dynamic oscillatory study of WSP ointment base containing halloysite and cetrimide coated halloysite at a concentration of 40% w/w.

6.3.3.4 Dynamic Oscillatory Studies on Halloysite - Macrogol Systems

The dynamic oscillatory rheogram of macrogol ointment is illustrated in Figure 6.3.3.4a. Profiles, G' and G" have a flattened appearance and share many features, which are characteristic of gel-like substances. The storage modulus of weak gel systems is greater than the loss modulus. The moduli run almost parallel with each other. Strong gels also exhibit G' > G", however the storage modulus has a slope of approximately 0 and G" displays a minimum at intermediate frequencies. Macrogol ointment is composed of a mixture of two polymers, poly(ethylene glycols), PEG 3000 and PEG 400. Cross-linked gel systems exhibit behaviour independent of the frequency of oscillation, whilst a physically entangled gel network shows a substantial decline in G' at low frequencies. A low storage modulus is observed at low frequencies as macromolecules have time to untangle and move past each other at low frequencies exhibiting viscous behaviour. They are confined to more elastic type behaviour at higher frequencies (Mortazavi *et al.*, 1993).

The tan δ value for macrogol ointment at 10 Hz is 16°. The macrogol ointment base displays a more solid-like character compared to WSP, which has a tan δ value of 33°.

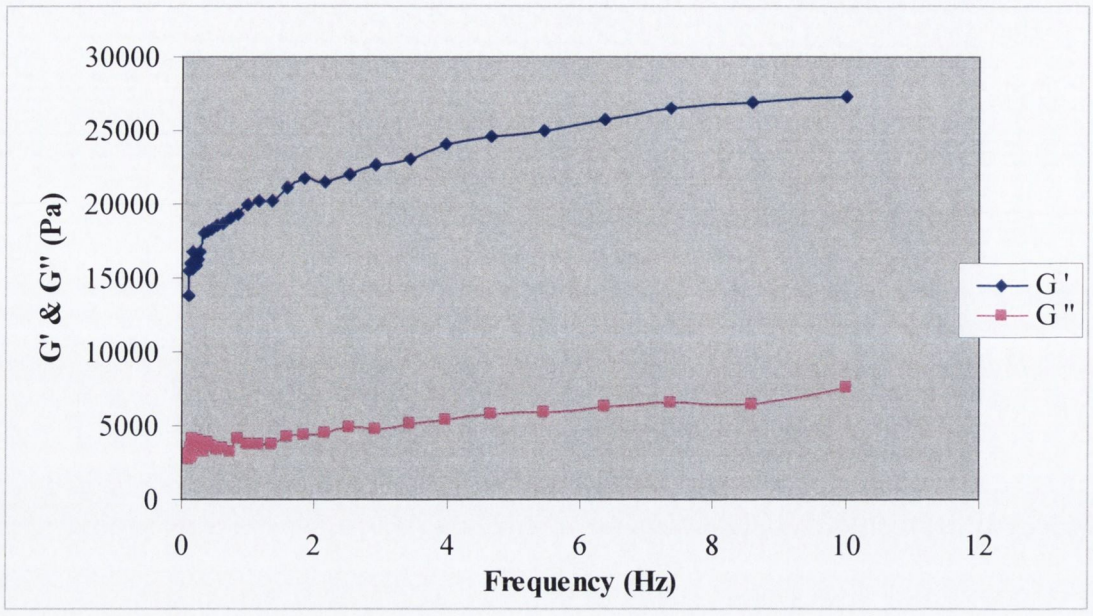

Figure 6.3.3.4a. Dynamic oscillatory rheology profile of macrogol ointment base.

It can be seen from Figure 6.3.3.4b that the addition of the coated halloysite sample to macrogol ointment results in opposite effect to that observed in the WSP systems. The storage and loss moduli curves for the uncoated halloysite exhibit almost linear plots. This could be a scaling factor or could be due to what Craig *et al.* (1994) described as an indication of cross-linking or entanglement within gel networks, which prevents any substantial re-arrangement of molecules. The width of the plateau reflects the degree of association within the gel network. There is an increase in the values of G' to G" for the coated compared to the uncoated systems. This effect is the complete antithesis to that observed for similar sample loadings in the WSP systems. The tan δ values at a frequency of 10 Hz for the coated and uncoated samples are 14.26° and 18.15°, respectively. This indicates an increase in sample elasticity due to coating with cetrimide.

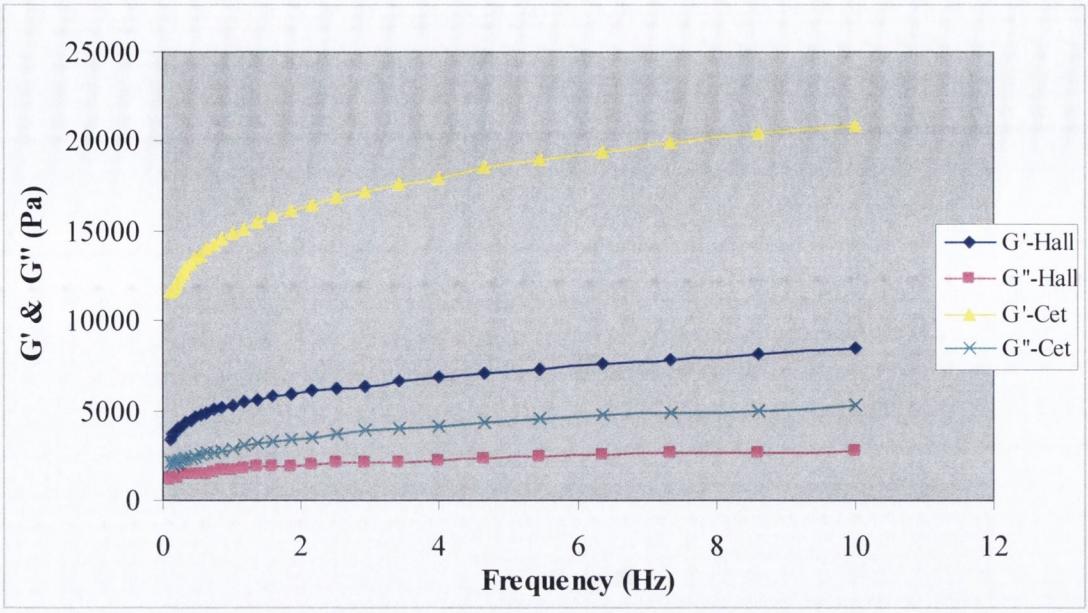

Key: Hall = halloysite ointment systems; Cet = cetrimide coated halloysite ointment systems.

Figure 6.3.3.4b Dynamic oscillatory study of macrogol ointment base containing halloysite and cetrimide coated halloysite at a concentration of 10% w/w.

Figure 6.3.3.4c displays the rheograms of the 20% halloysite samples. The shapes of the curves are very similar to those observed in Figure 6.3.3.4b. There is a considerable rise in the storage modulus of the surfactant-coated sample. However the tan δ values are similar. The values for the uncoated and coated sample are 11.45 and 11.95° respectively. The increase in solid content is accompanied by an increase in the elastic component of both systems, but a difference is not apparent between the two systems at the 20% halloysite concentration. The increase in the elastic component in the surfactant systems occurs because the surfactant interacts strongly with the poly (ethylene glycol) polymer. This occurs in solutions and at the surface. If micelles occur at the surface, the PEG could be incorporated into the micelle interior (this phenomenon is more likely in solution because as described monolayer formation is likely on drying of the substrate at the air water interface). It is also possible for the PEG to form bridges between surfaces (Atkin, 2004). The molecular weight of the PEG plays an important role in determining sample viscosity. The surfactant modified halloysite has a hydrophobicity imparted on it by the hydrocarbon

chains of the surfactant, this can result in interactions with the PEG (Wanless, 2004). It is possible that it might interact with the positively charged ends also.

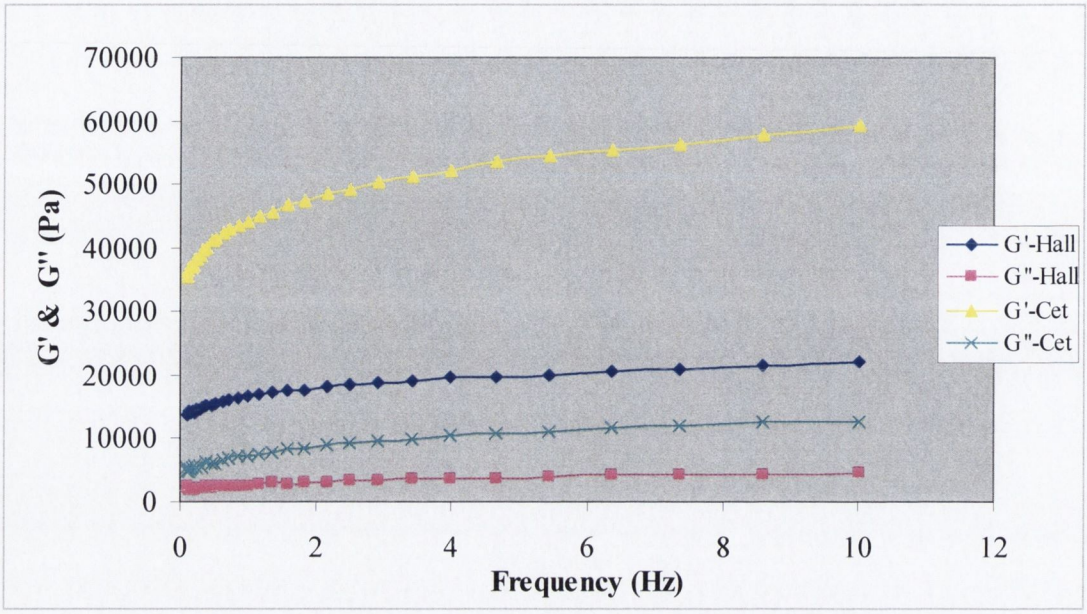

Key: Hall = halloysite ointment systems; Cet = cetrimide coated halloysite ointment systems.

Figure 6.3.3.4c Dynamic oscillatory study of macrogol ointment base containing halloysite and cetrimide coated halloysite at a concentration of 20% w/w.

6.3.4 Texture Analysis of Halloysite-Ointment Systems

6.3.4.1 Introduction

Semi-solid preparations are primarily designed for application to the skin or mucous membranes. To ensure optimal patient acceptability and clinical efficacy, several physical attributes may be identified. These include suitable mechanical properties (eg ease of removal from the container, ease of application/spreading onto the chosen substrate), good retention on the skin/mucous membranes (bioadhesion), the ability to reform structural properties following application and suitable drug release/absorption properties (Jones *et al*, 1997). One method by which the mechanical properties of topical systems may be conveniently determined is texture profile analysis (TPA) (Jones *et al*., 1996).

6.3.4.2 Texture Analysis of Halloysite - WSP Ointment Systems

Sample hardness is defined as the force required to obtain a given deformation (Jones *et al.*, 1997). The hardness of WSP and halloysite-WSP systems was determined using a texture analyser, TA-XT2; the sample probe was twice compressed to a specified depth into the samples. The force required to cause the probe to enter the samples was recorded and is used as an index of sample hardness. The sample is allowed to recover between the end of the first and the beginning of the second compression; this period is termed the delay period. This duration was arbitrarily chosen, however as the duration of the delay period is increased the extent of structural recovery of thixotropic samples is increased following the destructive effects of the first probe compression.

The hardness is also used as an indication of the spreadability of the sample, however spreadability is a more dynamic property. Samples may work-soften when spread to different degrees but display similar hardness values. Despite this, apparent yield values calculated for probe penetration have been correlated with sensory estimates of spreadability (TA-XT2 Application study, 2000).

Figure 6.3.4.2 depicts the hardness of the WSP ointment systems containing halloysite and cetrimide coated halloysite. The force to cause the probe to penetrate into the sample to a defined depth remains essentially unchanged when halloysite at a concentration of 10% is added to the system, irrespective of the presence of surfactant coating. As expected the largest increase is seen with the highest halloysite concentration (40% w/w). The force required to cause a given deformation for this sample is 2975 g compared to 688 g for the WSP ointment base. However the value for the cetrimide coated grade is considerably lower than the uncoated sample, 1169 g because the cetrimide ensures that the halloysite is dispersed more readily in the ointment. Also the hydrophobic coating on the clay ensures that the samples deforms more readily in the ointment when the probe is introduced into the sample. The results reflect those observed in the dynamic rheology study, Section 6.3.3.3, where an increased in the elastic component was seen for the 40% uncoated halloysite sample. The other samples had similar tan δ values. Stepped flow rheological evaluation (Section 6.3.2.3) showed that the sample shear thinned at approximately 3000 Pa. The samples with a 20% concentration of halloysite or coated halloysite require a force in the region of 960 g to cause the probe to penetrate to a defined depth. This process requires less energy input than the sample shear-thinning process. The force required to

cause this deformation is higher than that for the ointment base but is not too high to warrant undue difficulties for the patient in application.

The hardness value for the uncoated halloysite sample at a concentration of 40% is very high and indicates that ointment samples containing uncoated halloysite at this concentration would be very difficult to process and would have little patient acceptability. It is appropriate to consider the rheological evaluation in tandem with texture analysis because the information on the mechanical properties of the systems, which aid in the determination of the formulation, is influenced by rheological properties such as viscosity. In the present study the choice of probe and the rate of probe compression influences the shearing forces exerted on the sample and dictates the sample's flow behaviour.

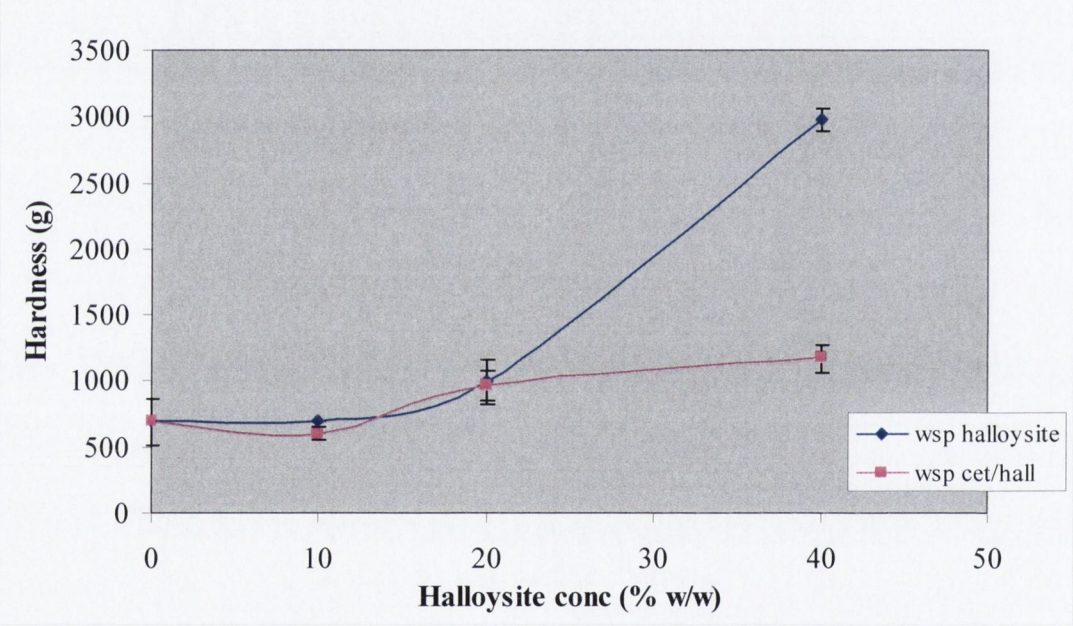

Key: wsp = white soft paraffin; cet/hall = cetrimide coated halloysite.

Figure 6.3.4.2 Hardness values for WSP and halloysite-WSP systems at varying concentrations of halloysite and cetrimide coated halloysite.

6.3.4.3 Texture Analysis of Halloysite - Macrogol Ointment Systems

Figure 6.3.4.2 depicts the hardness of the macrogol ointment systems containing halloysite and cetrimide coated halloysite. The increase in hardness values with increasing solid concentration is more gradual than that observed for the WSP systems in Section 6.3.4.2.

However the hardness values are substantially higher. This is due to the compositional difference. The macrogol ointment is a mixture of PEG polymers which form an entangled gel network but the WSP is composed of paraffins, which can have lubricity effects (Handbook of Pharmaceutical Excipients, 2005). The hardness is seen to increase with the cetrimide coated grade due to the interaction of the PEG polymers and the hydrocarbon chains of the surfactant. However it is lower in the case of the 10% addition, this highlights that manipulation of the concentrations of added halloysite could result in an optimum formulation. Evaluation of the samples was difficult, which highlights that problems would exist with these formulations and that modification with additives would be required to improve processing.

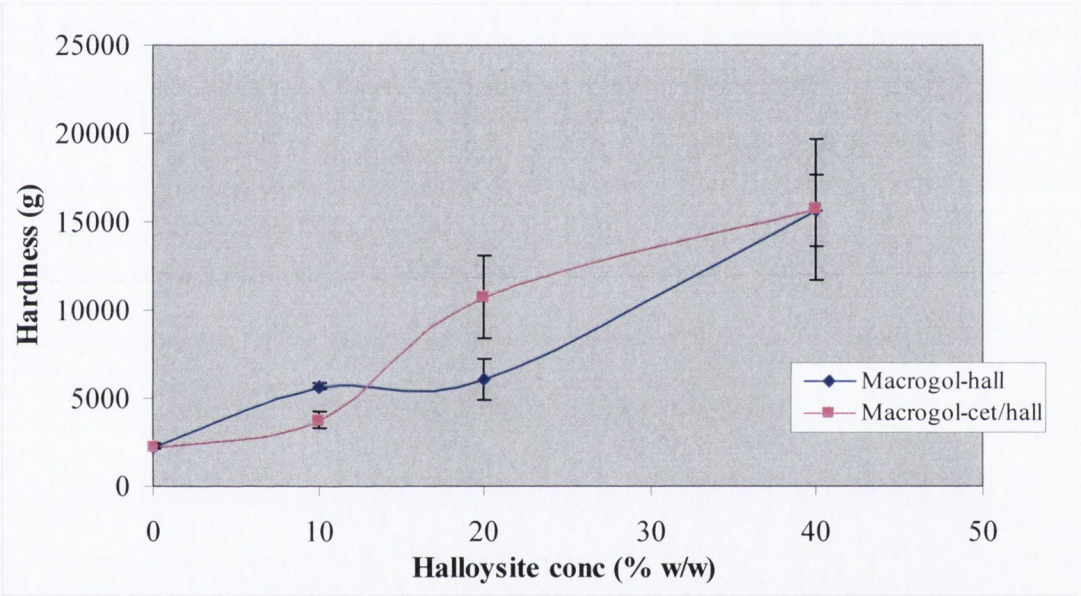

Key: macrogol = macrogol ointment base; cet/hall = cetrimide coated halloysite; hall = halloysite.

Figure 6.3.4.3 Hardness values for macrogol and halloysite-macrogol systems at varying concentrations of halloysite and cetrimide coated halloysite.

6.3.4.4 Evaluation of the Adhesive Properties of Halloysite - WSP Ointment Systems

The adhesiveness is defined as the work required to overcome the attractive forces between the surface of the sample and the surface of the probe, it has been reported to be related to bioadhesion (Jones *et al.*, 1996). However the definition was expanded and defined as the

work required to remove the probe from the sample, inferring for some samples that the probe may be removed following cleavage of both internal bonds within the sample (cohesive bonds) and also bonds occurring between the sample and the surface of the probe (adhesive bonds) (Jones *et al.*, 1997).

Two measures of adhesion are displayed in Figures 6.3.4.4a and 6.3.4.4b. The force required to detach the probe from the halloysite/WSP samples after contact at a specified force for a defined period of time is given in Figure 6.3.4.4a. A higher peak detachment force is required to detach the probe from the cetrimide coated samples. Clinically as the adhesiveness of the formulation increases, so should the expected retention time at the site of application (Jones *et al.*, 1996). This may be due to an enhanced entanglement between the hydrocarbon chains and the substrate. The peak detachment force values for the uncoated samples are less than the ointment substrate. This implies that the addition of the solid halloysite does not appear to enhance adhesion of these samples to the pig hide membrane. The values for the 40% halloysite samples were lower because the substrate did not appear to contact sufficiently with the formulations. This is attributable to the greater hardness of these samples.

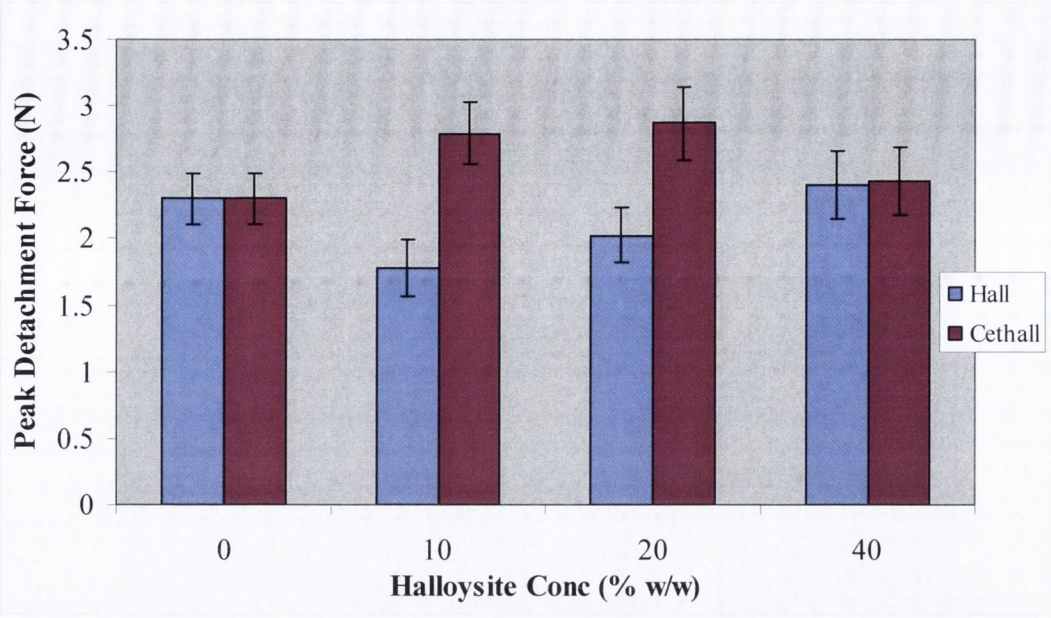

Key: Hall = halloysite; Cet/hall = cetrimide coated halloysite in WSP

Figure 6.3.4.4a The adhesive properties of halloysite-WSP ointment systems with varying concentrations of halloysite and cetrimide coated halloysite represented as the peak detachment force (N).

It can be seen from Figure 6.3.4.4b that the work of adhesion is greater for the uncoated samples compared to the coated samples. The work of adhesion is a direct measure of the area under the force distance curve. This value represents the cohesive and adhesive forces in a sample. Since the coated samples had a higher peak detachment force but a smaller work of adhesion, this implies that the cohesive and adhesive forces in the coated sample were less than those in the uncoated sample. This is due to the cetrimide coating imparting a hydrophobic quality to the clay hence the coated sample was more miscible in the ointment base and the viscosity of the sample decreased. The samples had decreased hardness values also and this was especially evident at the highest (40% w/w) concentration. Therefore more work would be required to work soften the halloysite samples, this was observed in preliminary flow rheometry studies of both halloysite and uncoated halloysite in WSP ointment.

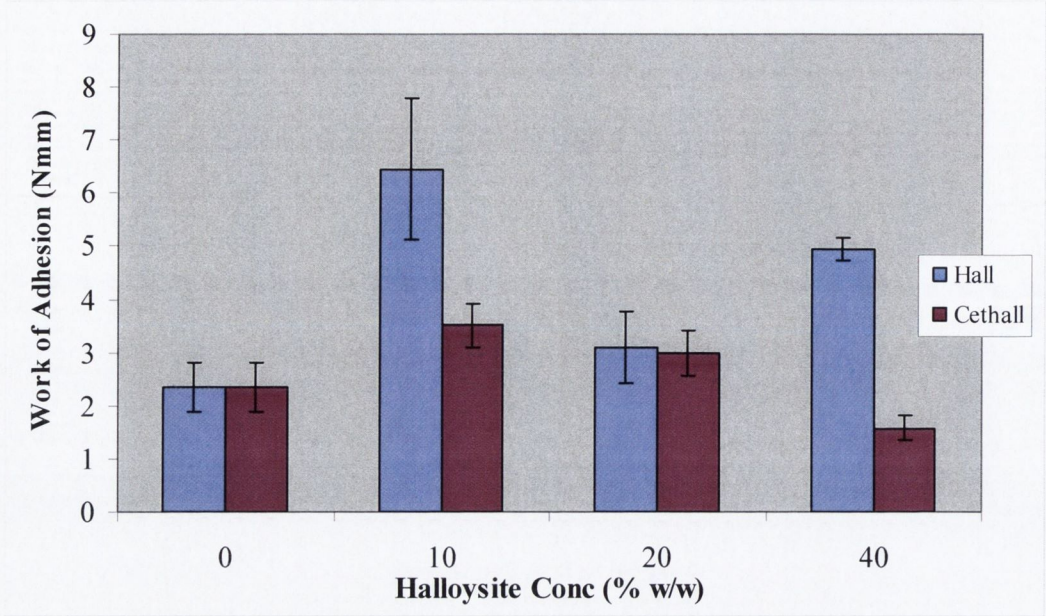

Key: Hall = halloysite; Cet/hall = cetrimide coated halloysite in WSP

Figure 6.3.4.4b Work of adhesion of halloysite-WSP ointment systems with varying concentrations of halloysite and cetrimide coated halloysite.

6.4 SALICYLIC ACID

6.4.1 Introduction

The aim of this section was to formulate salicylic acid (SA) and halloysite composite systems to examine the incorporation of these systems and in topical vehicles such as ointments and creams. It was hoped that this complex could be incorporated into a topical formulation, which could be used in the improved treatment of skin disorders such as acne and excess sebum production though the keratolytic action of SA and the adsorbent contribution of halloysite, halloysite may also act as an exfoliant. Halloysite is chemically similar to kaolin, which has established uses in oral and topical pharmaceutical formulations. In topical preparations kaolin has been used in poultices and as a dusting powder (Handbook of Pharmaceutical Excipients, 2005). Therapeutically, kaolin has been used in oral anti-diarrhoeal preparations (Bergman, 1999; Sweetman, 2005). It was hoped that the adsorbent properties inherent in kaolin would be present in halloysite and this could also be exploited.

In order to produce halloysite-salicylic acid complexes a number of methods were assessed. The conventional method of vacuum loading employed previously to load urea was again investigated for SA, but the factors involved in the procedure were altered. The intention of the preliminary studies to load halloysite with very high SA concentrations was hampered by its poor water solubility. SA is freely soluble in ethanol but only slightly soluble in water (British Pharmacopoeia, 2007). The solubility of SA in different media was assessed to ascertain alternative loading vehicles. Also it was important to establish the solubility of SA in release media to ensure that the dissolution of SA from the complexes is not the rate limiting process. Dynamic solubility studies were also performed.

Preliminary loading studies examined factors such as halloysite grade, loading solution concentration and frequency of loading. Based on the initial experiments an advanced study was undertaken which again examined halloysite grade and concentration but with an additional factor, sample drying method. It was hoped that manipulation of the factors and levels of each factor could highlight an optimum process to encapsulate SA in the halloysite and hence modify its release character with the final aim of incorporation in a topical formulation. Halloysite was also formulated with cetrimide and SA using spray-drying methodology with the aim of producing uniform composites. The resultant samples were characterised using several methods including, particle size analysis, SEM, release studies, skeletal density and surface area analysis. Rheological and textural studies were conducted on halloysite and cetrimide coated halloysite in two ointment bases, WSP and macrogol in order to characterize the impact of the clay on the flow and cosmetic properties of the clay – ointment samples. Preliminary studies were conducted on formulations containing spray-dried complexes in WSP ointment, however very little SA release was observed. Three of the spray-dried samples produced were incorporated into two common cream bases, Aqueous Cream BP and Cetrimide Cream BP. In-vitro testing of the samples was conducted using Franz cells. A comparative study investigating the effects of vehicle choice on the release of SA was also conducted. The samples were further characterised rheologically to more fully understand the factors impacting on release of SA from the cream bases.

6.4.2 Solubility Studies

6.4.2.1 Saturation Solubility Study

The solubility of SA in various solvent systems was undertaken to determine the rate and extent of dissolution as the medium was changed. The solubility of SA varied greatly depending on the medium, 1 g of the substance dissolved in 2.7 ml of alcohol but required 460 ml of water to dissolve the same amount (The Merck Index, 1989). The solubility of SA had consequences for the choice of loading medium because the loading solution volumes used would be too small in the case of water to prepare sufficiently concentrate loading solutions of SA. The solubility also had important implications on the choice of release media. It was essential that the rate-limiting step for SA release be not dictated by the limiting solubility of SA in the medium.

Table 6.4.2.1 shows the solubility of SA in different media at two time points, 24 and 48 hr. SA is a weak acid and has a pK_a value of 2.97. The OH group cannot contribute to the solubility since it is involved in an intramolecular hydrogen bond (Martin, 1993), this is especially important in the context of the solubility studies, especially of SA in water. The pH of a saturated solution of SA in water was 2.45, this agrees closely with a literature value of 2.4 (The Merck Index, 1989). The pH of the saturated solution lies slightly below the pK_a value, the pH value at which 50% of the substance is ionised. These factors account for the poor solubility of SA in water. After a period of 24 hr, it was observed that the saturation solubility was 0.31% w/v. It is accepted that increasing ionisation can increase solubility in a polar solvent. It is possible to alter ionisation by changing the solution pH within specified limits.

It is clear from Table 6.4.2.1 that solution pH impacts considerably on the % solubility of SA. As the pH of the medium is increased the amount in solution increases to 1.29% w/v after a 24 hr time period. However an anomaly appears evident in the data. A further increase in medium pH affected a relative decrease in solubility. This is attributable to the buffering capacity being lost. The pH of saturated solutions of SA in McIlvaine buffer pH 5.5 and 6.8 were 3.8 and 3.42 respectively. It was noted that the pH of the sample in McIlvaine buffer pH 5.5 actually had a higher pH than the McIlvaine 6.8 sample resulting in overall increased saturation solubility. The solubility of SA in ethanol was greater as expected, 27.39% w/v after 24 hr.

Table 6.4.2.1 The solubility (% w/v) of salicylic acid in various media after equilibration time of 24 and 48 hours respectively.

Dissolution Medium	Solubility (% w/v)	(+/-) St. dev.
Water		
24 hr	0.31	0.03
48 hr	0.28	0.01
McIlvaine pH 5.5		
24 hr	1.29	0.05
48 hr	1.23	0.02
McIlvaine pH 6.8		
24 hr	0.70	0.06
48 hr	0.72	0.03
Ethanol		
24 hr	27.39	3.696
48 hr	29.81	2.18

Salicylic acid was added to the specified media at a quantity which exceeded reference solubility by at least a factor of two. This ensured that the thermodynamics of the system resulted in saturated solubilities being determined. The sample solubility was determined after equilibration times of 24 and 48 hr. The experimentally determined values were statistically analysed using a paired t-test, 95% confidence interval was employed. No statistically significant difference occurred between the solubility of the samples for each medium at the 24 and 48 hr time points. This would indicate that the media were saturated by the 24 hr time point.

6.4.2.2 Dynamic Solubility Studies

Dynamic solubility studies were also conducted in order that the dissolution of the salicylic acid over the initial time course could be determined. Analysis was conducted in both water and ethanol. The dynamic study utilising the water medium displayed maximum solubility after three hours (0.28 +/- 0.04 g/100ml), although this value was less than the solubility derived from the saturated studies (0.31 +/- 0.03 g/100ml), it falls within the error limits. From Figure 6.4.2.2a it can be seen that the solubility appeared constant after t

= 3 hr. The dynamic solubility of salicylic acid in ethanol is presented in Figure 6.4.2.2b. Ethanol is a less polar solvent than water, as expected a substantially greater amount is dissolved in ethanol. The time to maximum solubility is achieved after only one hour.

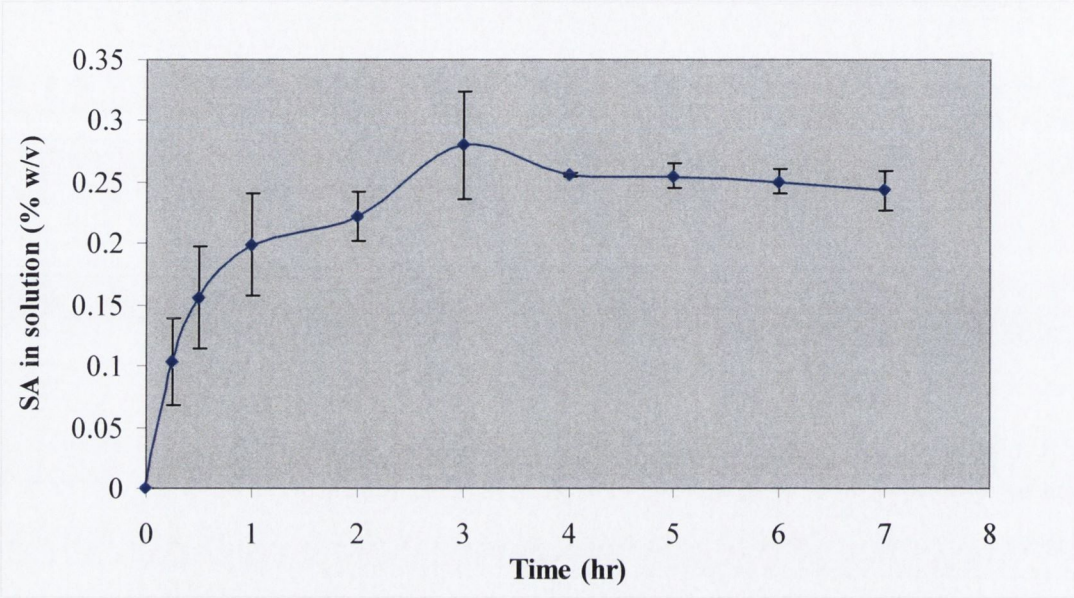

Figure 6.4.2.2a Dynamic solubility study of SA in water.

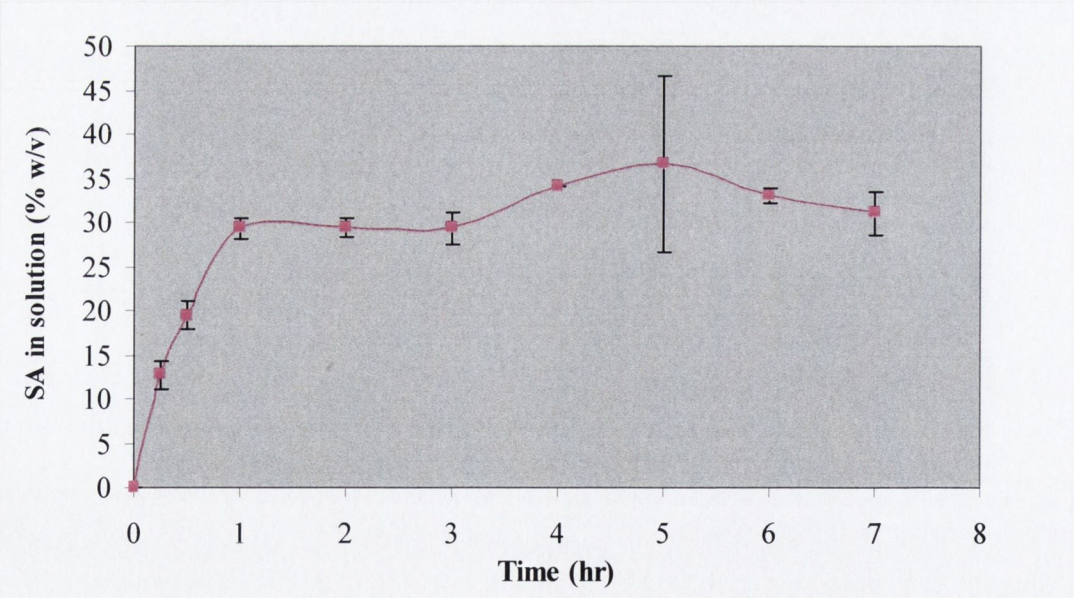

Figure 6.4.2.2b Dynamic solubility study of SA in ethanol.

6.4.3 Halloysite Loading with Salicylic Acid - Preliminary Study

6.4.3.1 Introduction

The aim of this preliminary study was to examine the effect of loading halloysite with the keratolytic salicylic acid. Previous work has been conducted on the possibility of loading halloysite with various drugs with the aim of forming controlled release preparations. Levis (2000) examined loading halloysite with diltiazem hydrochloride, a cationic, calcium channel blocker, which belongs to the benzothiazepine class of compounds (Mazzo *et al.*, 1994) and also with propranolol, a beta-blocker. Levis concluded that the release of diltiazem HCl could not be adequately retarded without further process modification such as coating with cationic polymers. However, in the case of propranolol HCl, a matrix release model aptly described modified release of 90% over an 8 hr period. Salter (2003) confirmed the potential of halloysite to extend the release of pesticides such as cypermethrin and chlorpyrifos.

Examination of the factors affecting the loading of halloysite with salicylic acid was conducted using a 2^3 factorial design experiment in order to optimise the quantity of drug loaded per gram of product. The resulting data was analysed using ANOVA, with the model response being total quantity of SA released. The factors chosen for the preliminary experiment were halloysite grade (halloysite G or cetrimide modified halloysite G), loading solution concentration (SA, 10% w/v or 20% w/v in ethanol) and finally single or double loading procedures. Single loading and double loading procedures were considered because Kelly (2002) found that double loading halloysite with tetracycline base produced statistically significant higher loadings compared to loading the sample on a single occasion.

Table 6.4.3.1 The levels of each factor as they pertain to a particular sample run in the factorial analysis (2^3) of halloysite loading with SA - preliminary study.

Sample	Halloysite	Conc (% w/v)	Loading
1	Halloysite	10	Single
2	Cetrimide coated	10	Single
3	Halloysite	20	Single
4	Cetrimide coated	20	Single
5	Halloysite	10	Double
6	Cetrimide coated	10	Double
7	Halloysite	20	Double
8	Cetrimide coated	20	Double

6.4.3.2 Salicylic Acid Release and Factorial Analysis

Figure 6.4.3.2a displays the quantities of SA released per gram of drug loaded material after 7 hr, this value was chosen to complement that used in previous studies. This is not an absolute quantity, it is postulated that some remains in the complex after this time. Increased amounts of SA were released; however it was not substantially greater than that shown in Figure 6.4.3.2a. Figure 6.4.3.2 shows that SA accounted for 7.9-16.7% of the total weight of the drug loaded complex. Sink conditions were maintained during the study because the amount of SA released was less than 10% of the saturated solubility of SA in the release medium. Sample 4 resulted in the highest SA release (0.167 g/900 ml). The solubility of SA in the release medium was 1.29% w/v (Table 6.4.2.1). The highest sample loading (sample run 8) results in a ratio of 1 part of salicylic acid per 5 parts of halloysite, this ratio alters to 1 part SA per 11.5 parts of halloysite for the sample with the lowest encapsulation (sample run 2). Table 6.4.3.1 depicts the levels of each factor for run 8; they included double loading cetrimide coated halloysite with the higher solution concentration. However it should be noted that the factor levels employed for sample 4 were those used for sample 8, except it was loaded on a single occasion. It resulted in similar release, 15.9% w/w. The common factor amongst the four samples with the highest encapsulation is the use of the loading solution at a concentration of 20% w/v, irrespective of loading frequency. The sample with the lowest encapsulation was an uncoated halloysite sample. It was loaded with the lower solution concentration on a single occasion. Examination of the

release profiles over 24 hr highlighted that release appeared to be complete by t = 8 hr. The release profiles from the double loaded samples exhibited an appearance very similar to the samples loaded using higher solution concentrations.

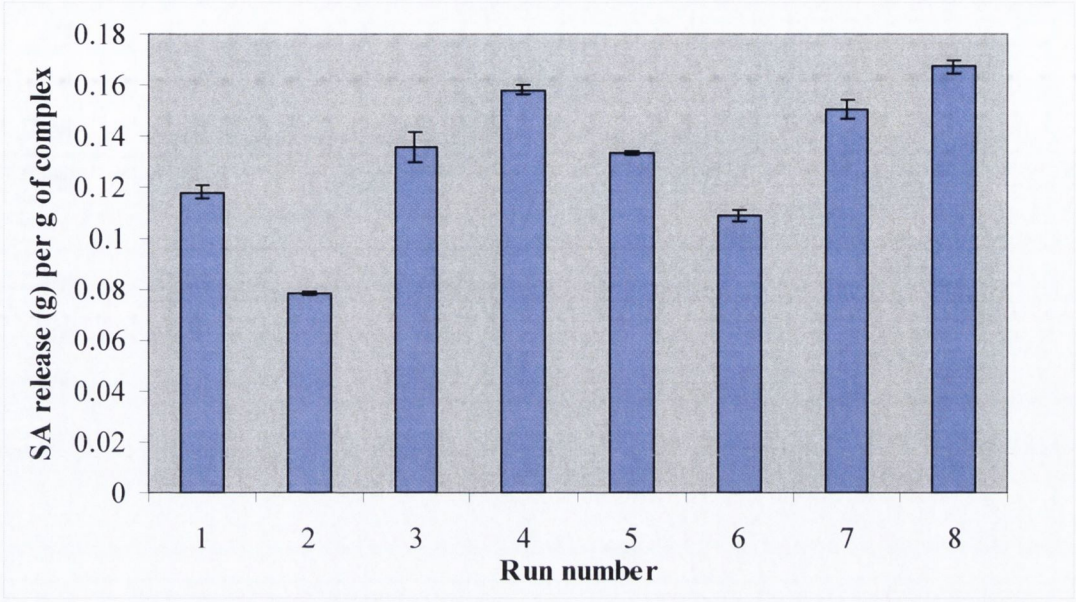

Figure 6.4.3.2 SA release from vacuum loaded halloysite, preliminary loading study.

Table 6.4.3.2 illustrates the results of an ANOVA study of the factors affecting SA release from halloysite. Statistical analysis using ANOVA determines the nature of statistical importance of each of the factors based on their F and p values. The test is conducted with a 95% confidence interval. All main effects, 2-factor and 3-factor interactions are significant ($p < 0.05$) except for one of the 2-factor interactions, halloysite and loading ($p > 0.05$).

The 3 factor interaction is significant, therefore the factors must be examined in conjunction with each other. However, it is more likely that when the samples are loaded for a second time it causes displacement of some of the material loaded initially. For the halloysite grade double loaded with the lower concentration, a release of 13.34% w/w was observed (run no. 5), which mirrors the almost 13.35% w/w released from a halloysite sample (run no. 3) loaded on a single occasion with the higher concentration. However when the sample is coated with cetrimide, the release for the corresponding samples increases from 10.9% w/w (10% w/v concentration, double loading) to 15.8% w/w (single

loading of higher concentration). This again highlights the important contribution made by cetrimide coated halloysite.

Table 6.4.3.2 Summary of ANOVA analysis of 2^3 factorial study of halloysite loaded with salicylic acid – preliminary study.

Source	DF	SS	MS	F	p
Halloysite	1	0.0002241	0.0002241	25.44	0.000
Concentration	1	0.0111012	0.0111012	1260.49	0.000
Loading	1	0.0018051	0.0018051	204.96	0.000
Halloysite*Conc.	1	0.0040033	0.0040033	454.56	0.000
Halloysite*loading	1	0.0000316	0.0000316	3.58	0.077
Conc.*loading	1	0.0001812	0.0001812	20.58	0.000
Halloysite*conc.*loading	1	0.0001531	0.0001531	17.39	0.001
Error	16	0.0001409	0.0000088		
Total	23	0.0176405			

It was concluded that the drug solutions used in this study were too concentrated, hence the tubular lumen and surface was saturated which accounted for the excessive instantaneous release of SA. Also the process of double loading the halloysite was thought to result in the same effect.

6.4.4 Halloysite Loading with Salicylic Acid - Advanced Study

6.4.4.1 Introduction

As stated above the results of the preliminary study indicated that halloysite loaded complexes could encapsulate substantial quantities of SA, but no potential was offered by halloysite to sustain the release of SA. It was the intention to conduct another factorial analysis of halloysite loading with SA, but this time considering the results of the preliminary study. Again, halloysite and the cetrimide modified grade were examined. Substantially lower loading solution concentrations were considered, 1.5% and 2.5% w/v in order to determine if modified SA release from halloysite was possible. The concentrations were arbitrarily chosen to be approximately 10% of those used in the

preliminary study, Section 6.4.3. The volume of loading solution per unit weight of halloysite was maintained. Use of concentrated loading solutions in the preliminary study saturated the intraparticulate and interparticulate tubule surfaces hence it was not possible to determine the role of halloysite in SA release. However, in this study the effect of drying was investigated. The conventional oven drying method and the use of freeze-drying were investigated. As described in the methodology Section the loading procedure involves vacuum application, the aim of which was to remove the air in the tubular lumen and replace this void with SA solution. It was hoped the high vacuum pressures associated with freeze-drying might enhance tubular loading. The levels of each factor for the runs are outlined in Table 6.4.4.1.

Table 6.4.4.1 The levels of each factor as they pertain to a particular sample run in the factorial analysis (2^3) of halloysite loading with SA - advanced study.

Sample	Halloysite	Conc. (% w/v)	Drying
1	Halloysite	1.5	Air
2	Cetrimide coated	1.5	Air
3	Halloysite	2.5	Air
4	Cetrimide coated	2.5	Air
5	Halloysite	1.5	Freeze
6	Cetrimide coated	1.5	Freeze
7	Halloysite	2.5	Freeze
8	Cetrimide coated	2.5	Freeze

6.4.4.2 Salicylic Acid Release and Factorial Analysis

Figure 6.4.4.2 depicts the amount of SA released at t = 1 hr and 8 hr. There does not seem to be a major difference between the amounts released at the two time points for all of the samples. In order to ascertain if the amount of SA release at the t = 1 hr and 8 hr time points was significantly different, paired t-test comparisons with a 95% confidence interval were conducted using the Minitab® statistical package between the amount released for each sample at the two time points. SA release at the two time points was significantly different for samples 1, 2, 4, 6 and 8 ($p < 0.05$). The p values for samples 3, 5, and 7 were 0.095, 0.595 and 0.221 respectively and hence were not statistically significantly different

($p > 0.05$). Reference to Table 6.4.4.1 highlights the common factor between samples 3, 5 and 7 is the use of uncoated halloysite. This is indicative that the cetrimide coated grade impacts on SA release.

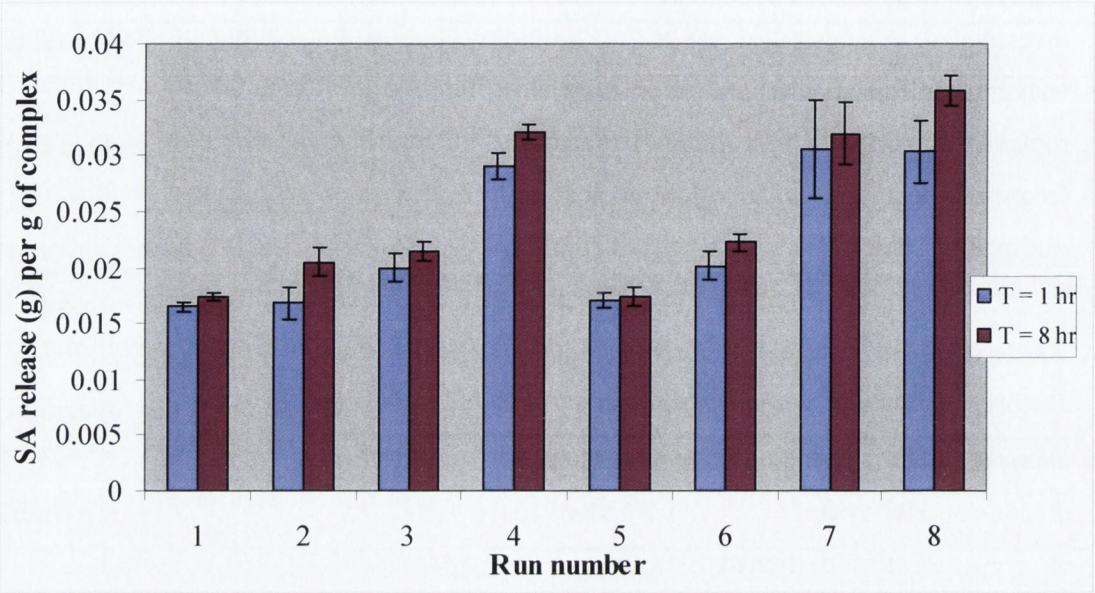

Figure 6.4.4.2 SA release from vacuum loaded halloysite samples, advanced study.

It is evident that the amount of SA release is appreciably reduced compared to the preliminary study. However, the highest amount is 0.0364 g, which is 4.6 times lower than the highest amount released in the preliminary study even though the loading solution concentration is 8 times lower and the sample is only loaded once. Therefore it can be concluded that the essential difference is that the freeze-drying method accounts for the increased efficiency of loading or that loading can be optimized using a lower concentration. It is likely that the latter case is a better explanation. Inspection of Table 6.4.4.1 indicates that sample 8 was produced by freeze-drying of a cetrimide coated halloysite sample loaded with the higher concentration of SA.

SA release from the samples was analysed using ANOVA, the results of the analysis are portrayed in Table 6.4.4.2. In this study all the main effects and interactions are significant ($p < 0.05$). The 3 factor interaction between all the factors is significant ($p = 0.000$), the highest order interaction must be considered. Therefore the factors must be considered in tandem. The increased loading efficiency may be due to the more hydrophobic character of

the surfactant coated grade, which can entrap a relatively greater proportion of salicylic acid which has a partition coefficient value of log P = 2.19 (Peña *et al.*, 2006). The method of drying appears to have very little influence on the quantity of SA released from samples loaded with the 1.5% w/v concentration, its effect is more apparent when the higher concentration is used.

Table 6.4.4.2 Summary of ANOVA analysis of 2^3 factorial study of halloysite loaded with salicylic acid – advanced study.

Source	DF	SS	MS	F	P
Halloysite	1	0.0002527	0.0002527	145.58	0.000
Concentration	1	0.0009604	0.0009604	553.33	0.000
Drying	1	0.0001285	0.0001285	74.03	0.000
Halloysite*Conc.	1	0.0000211	0.0000211	12.14	0.002
Halloysite*drying	1	0.0000135	0.0000135	7.8	0.010
Conc.*drying	1	0.0000775	0.0000775	44.65	0.000
Halloysite*conc.*drying	1	0.0000368	0.0000368	21.22	0.000
Error	24	0.0000417	0.0000017		
Total	31	0.0015322			

In both studies loading solution volumes were maintained constant at 25 ml per 5 g of halloysite. This is a marked departure from the procedure employed by Levis (2000), who employed a 1:1 ratio of loading solution volume to halloysite. It was thought an increased loading solution volume would have an enhanced ability to intrude the tubular lumen especially during vacuum application as opposed to merely wetting the surface due to the adsorbent nature of the halloysite clay. The use of ethanol as the loading solution was invariably more advantageous due to the poor solubility of salicylic acid in water; the poor water solubility would be prohibitive in preparing drug solutions with a concentration greater than 0.28% w/v (the saturation solubility for salicylic acid in water). The saturation solubility of SA in ethanol was determined to be 29.81% w/v after 48 hr, Section 6.4.2.1. Ethanol is a more viscous liquid than water (Waters Guide); this may impact on the manner which it permeates the halloysite tubule and hence the loading efficiency of the drug solutions. The different physiochemical character of the less polar solvent ethanol

will also affect the wettability of the halloysite tubule to different extents depending on the grade of halloysite used.

As discussed in Chapter 5 it would be expected that the cetrimide coated grade would be more hydrophobic due to the surfactant binding to the halloysite surface by ion exchange or ion-pairing mechanisms. Essentially the ionic head of the surfactant would bind with the negative tubule surface and the hydrocarbon chain would extend from the surface imparting its hydrophobic character. Based on this innate difference between the two halloysite grades it would be expected that a profound difference in release and encapsulation profiles might be observed. The role of the surfactant may extend beyond surface modification. The ability of surfactants to adsorb chemical entities at a solid interface has been examined by Monticone and Treiner (1995).

ANOVA analysis of SA release at t = 1 hr revealed broadly similar main effects and interaction plots as those depicted for t = 8 hr. The residuals for the model response factor, SA release are normally distributed, Appendix 6. Maximal release was almost complete by the 1 hr time period for the samples prepared, indicating that complexation was possible but significant controlled release did not occur.

6.4.5 Formulation and Characterisation of Co-Spray-Dried Salicylic Acid-Halloysite-Cetrimide Systems

6.4.5.1 Formulation of a Co-Spray-Dried System Containing Salicylic Acid

An extrapolation of the vacuum loading studies investigating the loading of halloysite with SA is the production of co-spray-dried systems of halloysite, cetrimide and SA. Vacuum loaded studies highlighted that it was possible to produce samples which encapsulated SA. The aim of the current study is to formulate an encapsulated complex, ideally capable of modifying release. The systems were prepared by changing the ratios of each of the constituents present as outlined in Table 6.4.5.1. The systems were left to equilibrate prior to be being spray-dried in order that the cetrimide could adsorb onto the clay surface. The study examines the effect of a constant constituent ratio and alteration in concentration. Formulation variables outlined in Table 6.4.5.1 and also process variables including pump rate were considered. The liquid medium was ethanol and water in a ratio of 60:40 in all cases except where indicated. The solvent type was also altered, which had a direct impact

on inlet/outlet temperature. The selection of the inlet temperature is considered in tandem with the boiling point of the solvent.

Table 6.4.5.1 Formulation variables for SA co-spray dried complexes

Sample	Halloysite (% w/v)	Salicylic Acid (% w/v)	Cetrimide (% w/v)
1[a]	2.0	0.2	0.2
2[b]	2.0	0.2	0.2
3[c]	2.0	0.2	0.2
4	2.0	0.2	0.2
5	5.0	0.5	0.5
6	5.0	0.5	0.2
7	5.0	0.5	0.05
8	5.0	0.5	-

Key: a = ethanol and water medium in a ratio of 10:90; b = water medium, 100%; c = ethanol and water medium in a ratio of 40:60.

6.4.5.2 Surface Area and Skeletal Density Characterisation

The surface area of the spray-dried composites was assessed using nitrogen adsorption. The calculated value is plotted together with its skeletal density in Figure 6.4.5.2. The skeletal density is generally seen to increase in association with the surface area. There is an obvious difference between samples 1-5 and 6-8. Table 6.4.5.1 depicts that the common factor for samples 6-8 is the absence of cetrimide (sample 8) or an increase in the ratio of halloysite and SA to cetrimide. The reduced concentration or absence of cetrimide relative to the other components results in an increased surface area because the surface area of cetrimide would be considerably smaller than halloysite. Hence the increased presence of halloysite in the particle will dictate the surface area and density. The ratio of components is maintained between samples 4 and 5 but the solid concentration is increased by a factor of 2.5 in the liquid feed of sample 5. However it results in a decreased surface area. The increased solid concentration resulted in a denser particle in the case of samples 6, 7 and 8 but not in the case of sample 5. Sample 5 has an increased cetrimide concentration relative to samples 6, 7 and 8. This contributes to the formation of closed pores, which accounts for

the decrease in surface area and density. The difference between samples 3 and 4 is the ratio of liquid medium, sample 3 has a lower % of ethanol (40%) and has lower surface area and skeletal density values also.

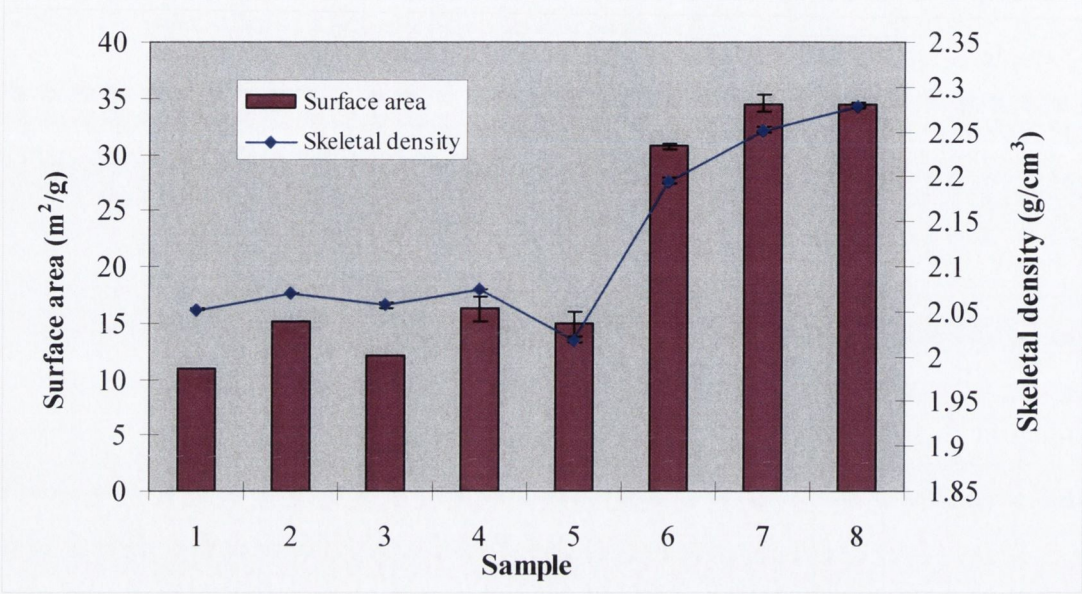

Figure 6.4.5.2 Surface area and skeletal density of halloysite, cetrimide and salicylic acid co-spray dried systems.

6.4.5.3 Particle Size Analysis

It would be expected that the spray-dried composite would be suspended in the topical vehicle; therefore the particle size is undoubtedly a key regulator of flux. This is especially true if the solubility of SA in the vehicle is low, as dissolution of the active is thus rate limiting to flux. Decreasing the particle size will increase the drug dissolution rate in the vehicle and hence promote transdermal delivery (Williams, 2003). It can be seen in Section 6.4.7 that raw SA drug dispersed has a higher flux than the spray-dried systems. Obviously this can be accounted for by the fact that SA is incorporated with halloysite and cetrimide in a co-spray-dried system and is not readily diffusible from this system unlike the free drug form. However, another important consideration is the particle size of the samples. Particle size analysis was conducted on the raw drug and co-spray-dried sample 4. Sample 4 was examined as a representative of the spray-dried formulations. The particle size of the raw drug was significantly smaller. Table 6.4.5.3 depicts the cumulative % undersize for the raw SA material and spray-dried sample 4. The particle size and distribution of the SA

is smaller than the spray-dried sample, 90% of the particles are 42.48 μm or less. The corresponding particle size for the spray-dried sample is almost 4 times bigger, 167.91 μm.

The 10% and 50% values for both samples are similar. The variance in particle distribution has implications for SA dissolution and release studies. The contribution of particle size will be examined in this context in Section 6.4.7.

Table 6.4.5.3 Particle size analysis of salicylic acid and co-spray dried sample 4.

Sample	d(0.1) (μm)	d(0.5) (μm)	d(0.9) (μm)
SA	2.99	13.69	42.48
Spray Dry 4	2.78	12.21	167.91

6.4.5.4 SEM Analysis

SEM studies were conducted on the spray-dried systems in order to elucidate the microscopic features. An overview of the sample and general impression of particle size and morphology was obtained at low magnification. Specific sample detail and character were then obtained using higher magnification values. Sample 1 was spray- dried using water and ethanol in a 10:90 ratio as the solvent medium. The spray-dried composite systems are roughly spherical and have a particle diameter in the range of 8-20 μm. It is obvious from the SEM images in Figures 6.4.5.4a and 6.4.5.4b for sample 1 that some spray-dried particles of SA, cetrimide and also SA/cetrimide composites exist. Their appearance is that of a collapsed or dehydrated sphere and they have a particle size of approximately 2 μm. Figure 6.4.5.4a primarily displays the fissured appearance of a spray-dried sphere. The thickness of the crust is clearly evident when magnified (x 18,000) in Figure 6.4.5.4d and is of the order of approximately 0.3 μm. It is filled with smaller spray-dried composites, the nature of which is unclear. The drying rate, internal pressure, solid content or attrition may be responsible for the fractured appearance.

Figure 6.4.5.4b depicts a spray-dried composite, the surface character of which is typical of a predominant proportion of sample 1. The particle diameter is in the region of 16 μm. The presence of the tubular structure of halloysite is easily distinguishable, this highlights that the procedure was not destructive of the clay. The halloysite scaffold network appears to

be coated by one of the other spray-dried materials, the surface morphology is smooth in places analogous to a brick and mortar appearance. However, both SA and cetrimide seem to be in the interlayer spaces between the halloysite tubules also. The extensive presence of pores on the surface is evident but more clearly defined in Figures 6.4.5.4c and 6.4.5.4d. The pore size and distribution appears uniform in Figure 6.4.5.4d, the deviation in size seems attributable to the presence of tubule clusters that are aligned longitudinally.

Figure 6.4.5.4a Spray-dried salicylic acid complex sample 1-magnification x 3,000

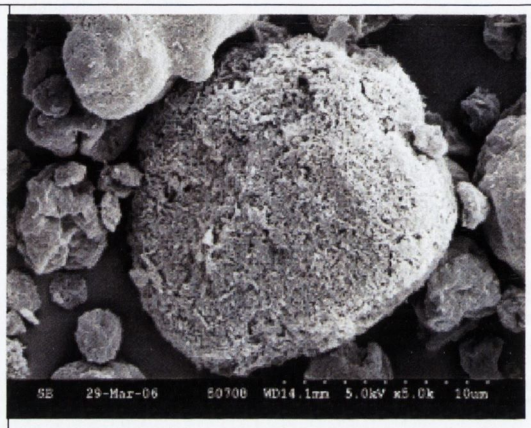

Figure 6.4.5.4b Spray-dried salicylic acid complex sample 1-magnification x 5,000

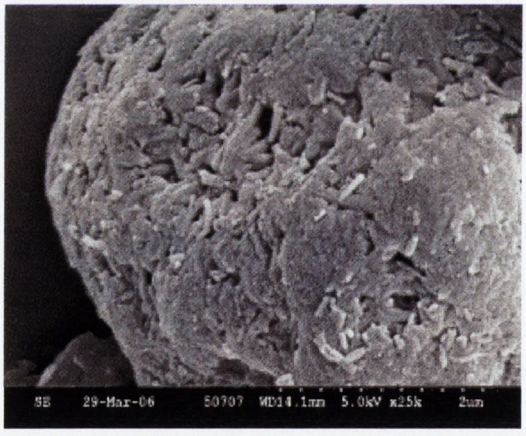

Figure 6.4.5.4c Spray-dried salicylic acid complex sample 1-magnification x 25,000

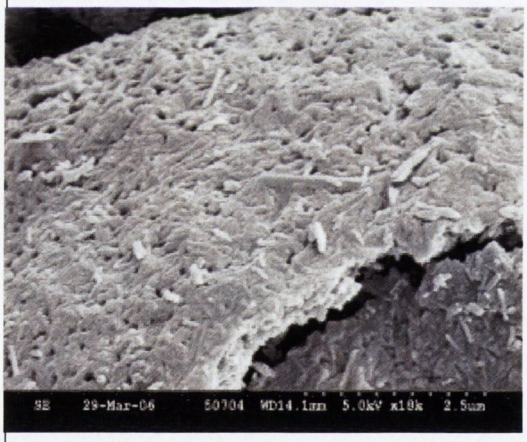

Figure 6.4.5.4d Spray-dried salicylic acid complex sample 1-magnification x 18,000

The SEM depictions for sample 2 in Figures 6.4.5.4f and 6.4.5.4g display similar features to those of sample 1 at low magnification. There are particles of two distinct sizes. The small collapsed spheres observed in sample 1 are again observed here, the size range being

2-5 μm. The other distinct particle is bigger and the size for these larger spray-dried composites lies in the range 12.5-20 μm. Again the presence of pores and halloysite tubules are evident on the surface in Figure 6.4.5.4f. The morphology of some of the larger pores observed in sample 3 are depicted in Figures 6.4.5.4g and 6.4.5.4h. The images show that the pores are not just confined to the surface, they permeate to the interior. The presence of the halloysite tubules protrudes into the void space, increasing the available surface area for nitrogen adsorption during surface area studies.

Figure 6.3.5.4e Spray-dried salicylic acid complex sample 2-magnification x 1,600

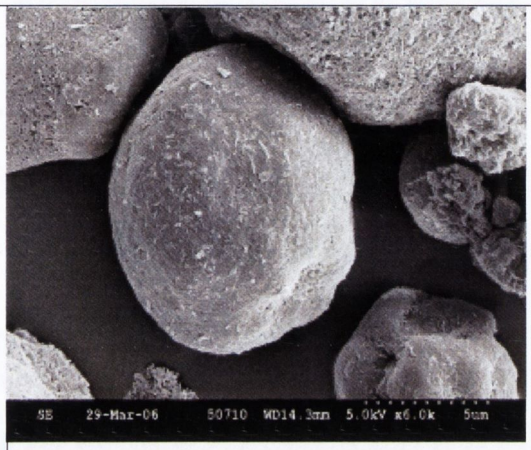

Figure 6.3.5.4f Spray-dried salicylic acid complex sample 2-magnification x 6,000

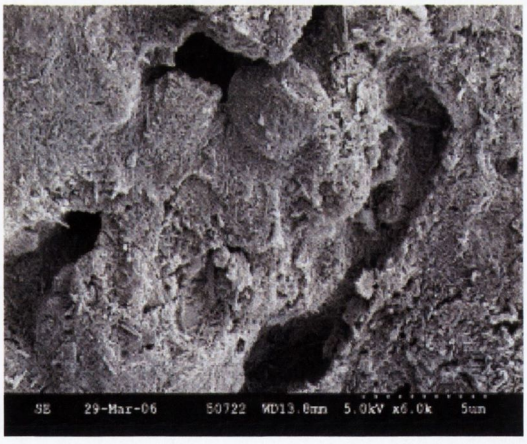

Figure 6.3.5.4g Spray-dried salicylic acid complex sample 3-magnification x 6,000

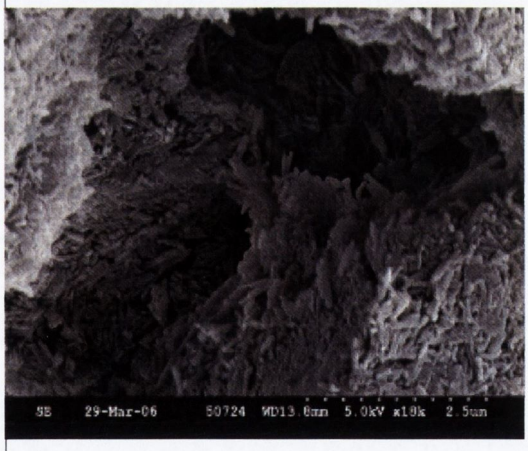

Figure 6.3.5.4h Spray-dried salicylic acid complex sample 3-magnification x 18,000

Figures 6.4.5.4i-k display images of sample 6, it was produced using a reduced concentration of cetrimide relative to the other samples. The ratio of components is

1:0.1:0.04 (halloysite, SA, cetrimide) rather than 1:0.1:0.1. The morphology of the samples is more varied and particles up to 40 μm in diameter are evident. A spherical, hollow particle with a blow-hole is depicted in Figure 6.4.5.4k. This may have occurred due to a disparity in air pressure as the sample dried between the inside and outside of the particle. Characteristic features associated with other samples such as the appearance of pores and halloysite tubules on the particle surface are witnessed again with sample 8 in Figure 6.4.5.4l.

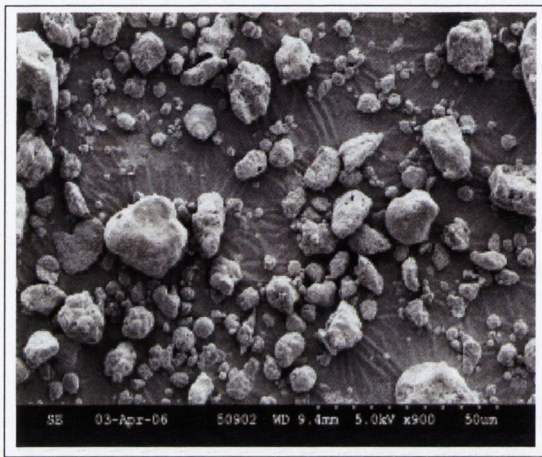

Figure 6.4.5.4i Spray-dried salicylic acid complex sample 6-magnification x 900

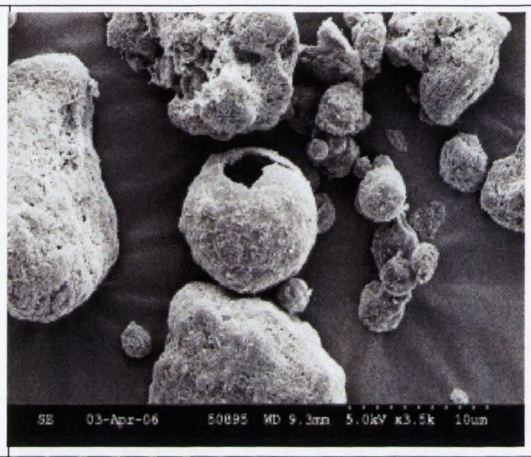

Figure 6.4.5.4j Spray-dried salicylic acid complex sample 6-magnification x 3,500

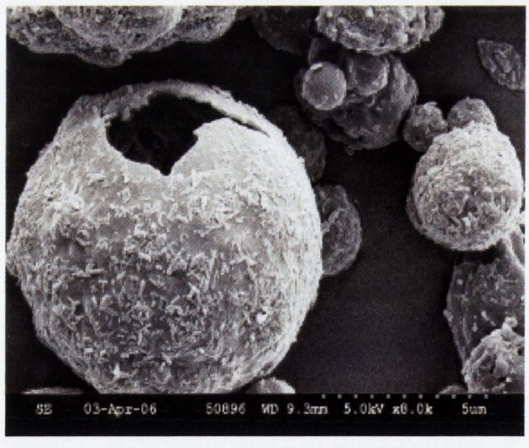

Figure 6.4.5.4k Spray-dried salicylic acid complex sample 6-magnification x 8,000

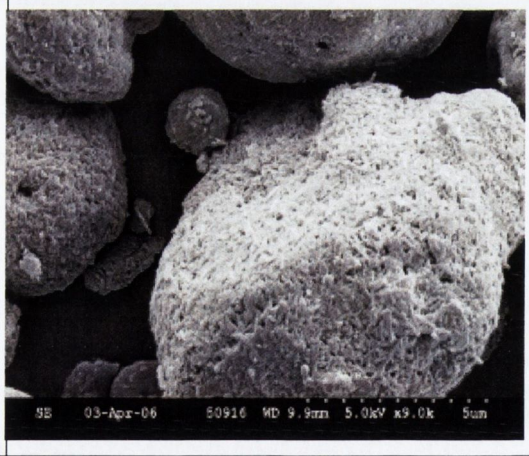

Figure 6.4.5.4l Spray-dried salicylic acid complex sample 8-magnification x 9,000

SEM images of samples 4 and 7 are represented in Figures 6.4.5.4m-p. These samples will be incorporated in topical formulations in Section 6.4.7. They were chosen as they

exemplify from a qualitative point the characteristics of the spray-dried samples produced. Their preparation also employs a diversity of formulation variables. From a qualitative viewpoint the particles from these samples are more spherical and uniform. The presence of macropores interspersed over the surface between irregularly aligned halloysite tubules are clearly evident in the SEM images for both samples.

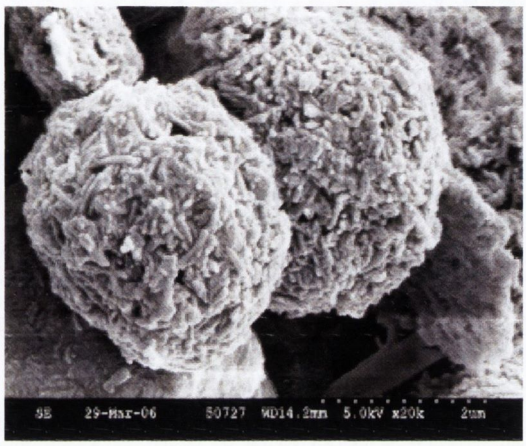

Figure 6.4.5.4m Spray-dried salicylic acid complex sample 4-magnification x 20,000

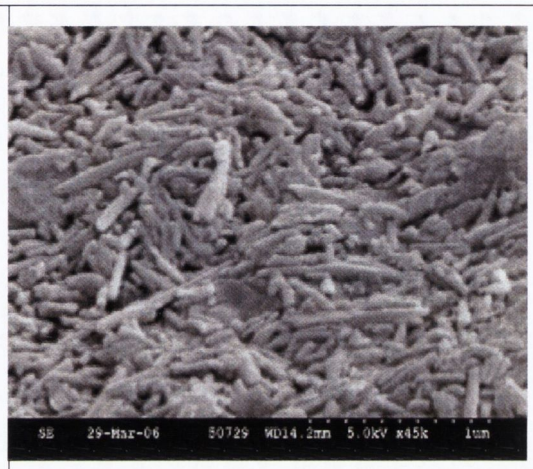

Figure 6.4.5.4n Spray-dried salicylic acid complex sample 4-magnification x 45,000

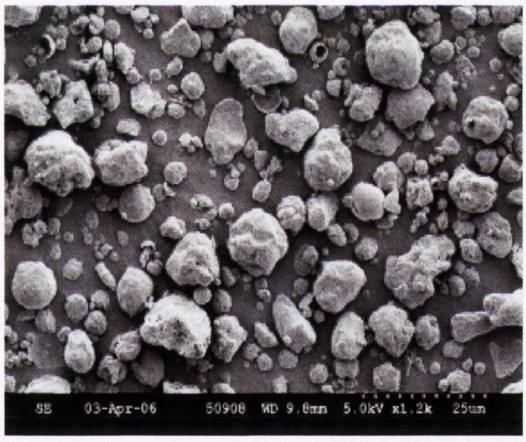

Figure 6.4.5.4o Spray-dried salicylic acid complex sample 7-magnification x 1,200

Figure 6.4.5.4p Spray-dried salicylic acid complex sample 7-magnification x 8,000

6.4.6 Salicylic Acid Encapsulation and Release

The release of SA from the spray-dried complexes is examined in this section. The quantity released per 0.5 g of complex is illustrated in Figure 6.4.6a. 0.5 g were used for

the release studies due to less sample being available for this study because the spray-dried samples were employed in topical formulations. An approximate equivalent SA quantity is released from samples 1, 2 and 7. Reference to Table 6.4.5.1 indicates that in the case of sample 7, it has a high concentration of SA, 0.5% w/v similar to samples 5 and 6. Hence it would be expected that SA release would be higher. Also the concentration of cetrimide in this complex is the lowest, this results in a higher quantity of the other components per unit weight examined, this manifests as a higher SA release. The higher SA concentration (0.5% w/v) was also added to the formulations of samples 5 and 6.

However, only a concentration of 0.2% w/v was added to samples 1 and 2 and they produced higher SA release. It is likely that encapsulation is superior in formulations with lower solid contents. However samples 1 and 2 were formulated with liquid media with a water content of 90 and 100% respectively. In these formulations SA is close to its saturated solubility. The saturated solubility of SA in water was determined to be 0.31 +/- 0.01% w/v in Section 6.4.2.1 after a period of 24 hr. The complexes were not equilibrated for this period prior to spray-drying, therefore it is possible some undissolved SA was present in the release studies. It was evident in Figures 6.4.5.4a and 6.4.5.4b that spray-dried particles of cetrimide and / or SA were present. They had a more collapsed shrivelled appearance and have a diameter of up to 2 μm. This resulted in a higher SA concentration in the samples. SA release from samples 3 and 8 was not examined due to insufficient sample quantities.

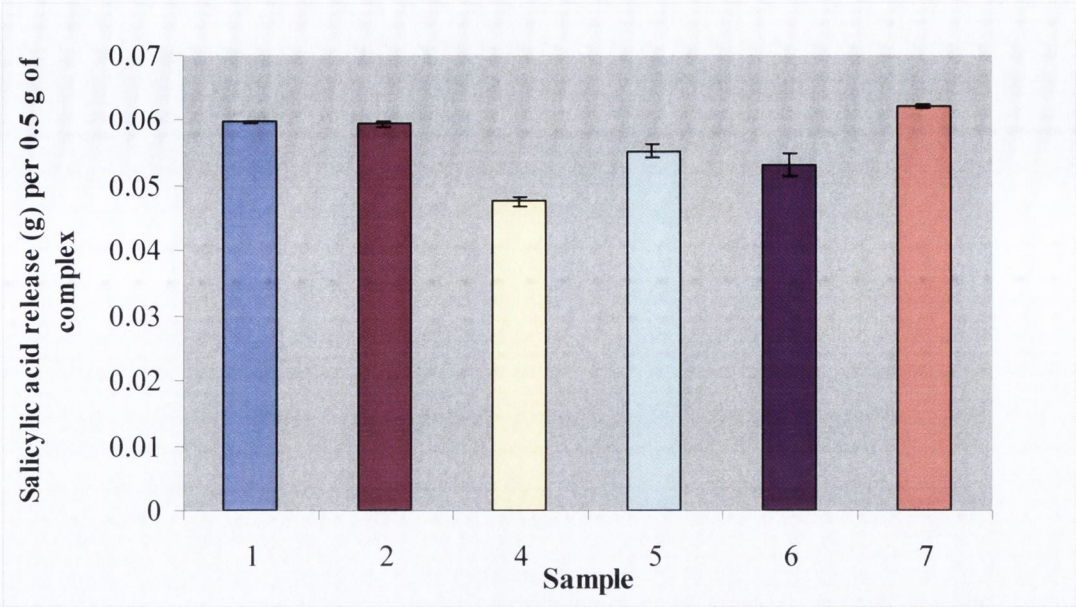

Figure 6.4.6 Amount of salicylic acid released per 0.5 g of halloysite, cetrimide and salicylic acid co-spray dried products.

It is important to determine the aqueous release of these samples prior to incorporation in topical vehicles where release rate is an important factor. However this is not an exact predictor of SA release in topical systems as they are undoubtedly more complex. Figure 6.4.6b illustrates the release profiles for the samples examined. SA release is complete after 1 hr in samples 1, 2, 6 and 7. It is complete after 5 hr in the case of samples 4 and 5. The release rate was faster for the former samples, they also resulted in the highest SA release, Figure 6.4.6a. It would be expected that the release rate from samples 4 and 5 would be greater than sample 7 as they contained a higher concentration of cetrimide which would aid in the wettability of the spray-dried composite.

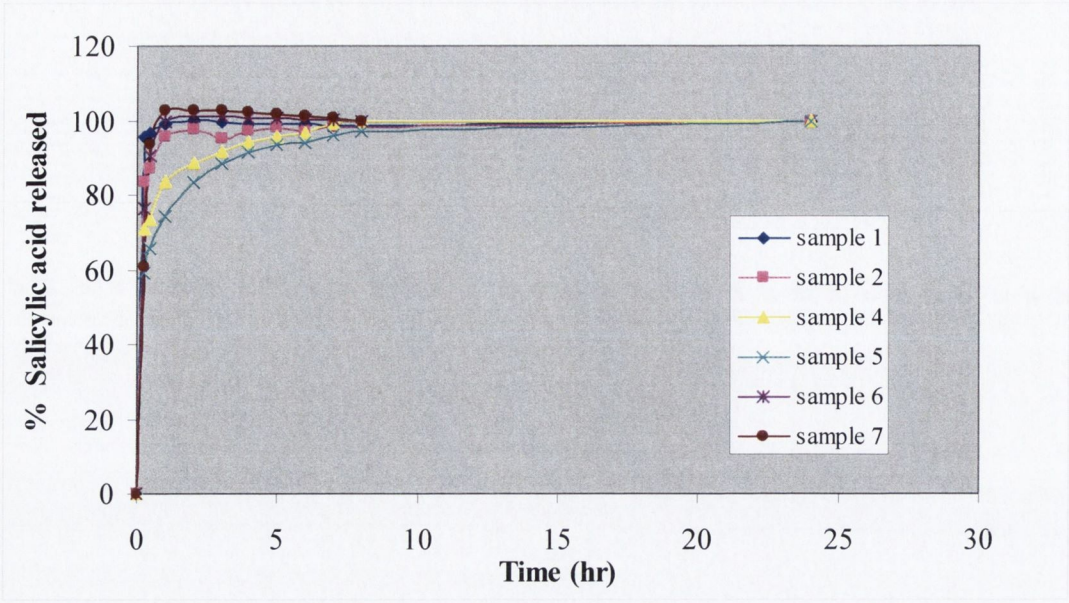

Figure 6.4.6b Release profiles of salicylic acid from halloysite, cetrimide and salicylic acid co-spray-dried systems.

6.4.7 Topical Product Formulations

6.4.7.1 Introduction

The aim of this Section was to examine the incorporation of spray-dried halloysite, SA and cetrimide composite systems in two common topical bases, Aqueous Cream BP and Cetrimide Cream BP. Originally it was intended to examine the release from ointment formulations but preliminary studies showed that very little SA was released, hence the spray-dried complexes were incorporated in topical cream formulations. A pertinent factor to this study is particle size (Williams, 2003). In the preparations analysed SA has poor solubility. In the present study SA is incorporated as a co-spray-dried system, this will impact on the solubility of SA as the particle size may vary between the complexes owing to different conditions it was prepared uinder. Hence the particle size of the co-spray-dried complex will be an important criterion in dictating the flux. If a significant difference in particle size exists between the samples then this could radically alter the flux rates between samples. The release of SA from the formulations was assessed using a Franz cell apparatus. A silicone based membrane Silastic® was employed in this study. The release kinetics were examined using the Higuchi square root of time release model. The

rheological profiles of cream formulations containing spray-dried composites 5 and 7 are also assessed.

6.4.7.2 Salicylic Acid Release - Vehicle Effect

There have been a number of reports on the in-vitro release of drugs from ointments (Foreman *et al.*, 1978; Higuchi, 1961). The choice of vehicle in which to apply the drug can vary depending on the experimental rationale. However, it is clearly preferable to mimic as closely as possible the in-vivo conditions (Williams, 2003). Hence, prior to the incorporation of the spray-dried halloysite-SA composites in cream bases the release of raw active, SA from topical vehicles was examined. The vehicles examined included WSP, WSP incorporating liquid paraffin and Aqueous Cream BP. A proprietary preparation, Diprosalic® ointment was also examined. The release of SA from various vehicles has been studied (Hadgraft, 1983; Nakano and Patel, 1970; Cooper, 1984). The rheological and textural characteristics of WSP were elucidated in Section 6.3. WSP was chosen, as it is one of the formulation components of the proprietary preparation examined. The rationale for the incorporation of liquid paraffin is justified on the same grounds. Aqueous Cream BP was chosen for comparison purposes because of the presence of water in its composition.

The release of SA from Diprosalic®, a proprietary preparation which contains SA 3% w/w and Betamethasone Dipropionate 0.064% w/w in a WSP and liquid paraffin base was examined. The exact concentrations of each component in the ointment base were unspecified. The release profile in Figure 6.4.7.2 is a plot of cumulative SA released per unit area of the Silastic® membrane against time. The plot can be used to calculate the flux (J) of SA, which is the amount of material passing through unit area of the membrane per unit time from a specific vehicle. The theory of flux was outlined in Chapter 1. The Diprosalic® system effected the lowest release; its release profile being approximately linear. This indicates that there is a constant thermodynamic gradient over the time period examined and the concentration of SA did not appear to be depleted.

The impact of the membrane on SA flux using a SA (3% w/v) solution in ethanol was investigated to show that the membrane was not substantially rate limiting. After a period of 2 hr, the cumulative release of SA was 500 $\mu g/cm^2$. This is substantially greater than the SA released from the formulations graphically depicted in Figure 6.4.7.2. Over a similar

time period the SA release from these formulations was between 70-140 μg/cm^2, except in the case of Aqueous Cream BP, which had an approximate release of 320 μg/cm^2. However it must be noted that the ethanol solution is not a saturated solution, hence the thermodynamics for SA release from this vehicle are much less favourable compared to the other vehicles were SA is present at a saturated concentration.

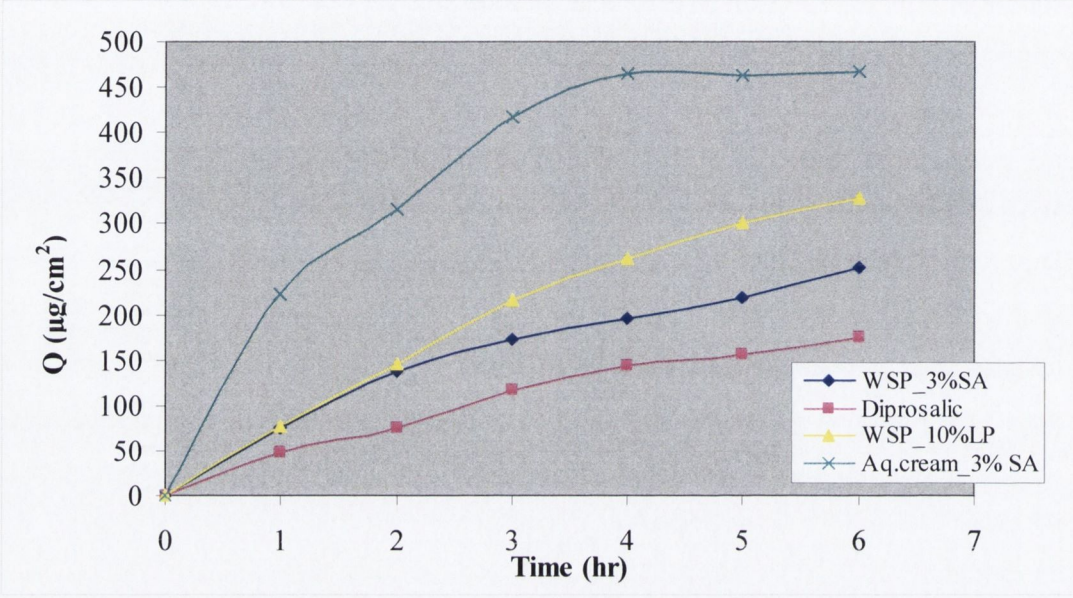

Key: WSP = white soft paraffin; LP = liquid paraffin; Aq. Cream = aqueous cream; SA = salicylic acid.

Figure 6.4.7.2 Cumulative release of SA per unit area (Q, μg/cm^2) from various topical vehicles using a Franz cell apparatus.

A similar quantity of SA (3%), equivalent to that in the Diprosalic® ointment preparation was added to WSP ointment. The release profiles obtained were similar except that the amount released from the WSP system was higher compared to the proprietary preparation, Diprosalic® at each time point, Figure 6.4.7.2. Again the profile did not appear to plateau over the time course of investigation. A similar system was prepared except that liquid paraffin (10% w/w) was added. The liquid paraffin concentration was arbitrary as the concentration in the proprietary preparation was unknown. Again a linear profile, with increased release was obtained.

The difference in cumulative release for the proprietary preparation and that of the simulated products may be attributed to the effect of the type of WSP used in the formulation. White petrolatum is a frequently used vehicle in dermatology. It is a heterogeneous product consisting of various alkanes and cycloalkanes, and it may also contain unsaturated and aromatic hydrocarbons. The properties of the various paraffins vary considerably between different batches of petrolatum. This complexity is reflected in the specifications for petrolatum in various pharmacopoeias. The wide limits of acceptance can lead to difficulties in the production and the quality control of ointments and creams, resulting in products with varying biopharmaceutical properties on the market. The amount of crystalline material in WSP has been found to impact on the flux. Kneczke *et al.* (1996) compared two grades of WSP and noted that the grade with the highest crystallinity content resulted in a slower release of SA. The presence of the steroid active in the Diprosalic® proprietary preparation, albeit at a low concentration, could impact on the flux.

The addition of SA to an aqueous cream base resulted in a substantial increase in drug release. The profile was linear up to the t = 4 hr time point, after which it was seen to level off. This is attributed to sample depletion in the system. As the SA is depleted the driving force for sample dissolution and diffusion in the system is decreased. Sink conditions are maintained, as the concentration of SA in the release medium did not approach saturation solubility. Near the saturation solubility the release rate would no longer be exclusively diffusion controlled but would also have an element of dissolution control. Ideally the concentration in the sink should not exceed one tenth of the saturation solubility (Malcolm, 1995).

Table 6.4.7.2 depicts the quantity of SA released from each formulation as a percentage of the initial concentration. Each formulation contained SA at a concentration level of 3% w/w. It was noted over the time period examined that the concentration of SA in the samples did not fall below 10% of its original concentration. The solubility of salicylic acid in white petrolatum is very low. Loth *et al.* (1984) reported it to be 0.048%, Horsch (1984) reported it to be 0.06%, whilst Knezcke *et al.* (1986) reported a value intermediate between those stated, based on microscopic investigations at 32 ^{o}C. Due to the low solubility, the authors declared that SA/petrolatum preparations are usually suspensions.

Table 6.4.7.2 Release of SA from different formulations as a % of the original sample content.

Sample	SA release (μg/g) of formulation	% SA Release
WSP_3% SA	603	2.01
Diprosalic®	418	1.39
3%SA_WSP/10%LP	789	2.63
Aq. cream_3%SA	1119	3.73

Key: WSP = white soft paraffin; SA = salicylic acid; LP = liquid paraffin; Aq. cream = aqueous cream.

Also the concentration in the sink did not approach 10% of the saturation solubility for the SA in the buffer medium. For this reason it was decided that buffer medium at a physiological pH could be used rather than the necessity for using a vehicle in which SA had an increased solubility profile.

6.4.7.3 Controlled Release and Kinetics

The release of SA in the topical bases was explained by the Higuchi equation, which describes controlled release. The Higuchi model is based on the cumulative release of the sample versus the square root of time. Assessing the linearity of the profile using the regression coefficient, R^2, confirms controlled release kinetics using the Higuchi model. The equation is used to describe the diffusion-controlled release of dispersed substances from insoluble, non-swellable, non-biodegradable matrices (the external geometry remains essentially unchanged during the period of release) under sink conditions. The equation applies to a number of drug delivery matrices including ointments, tablets and polymer systems (Malcolm, 1995). The form of the equation depends on the homogeneity of the matrix (Higuchi, 1961). The simplest form describes release of a dispersed substance, which Higuchi termed a "planar system having a homogeneous matrix" (Higuchi, 1963). Equation 6.1 describes the relationship of the parameters; it is simplified in Equation 6.2.

$$Q = (DC\,(2A-C)\,t)^{0.5} \qquad \textbf{Equation 6.1}$$

$$Q = k\,t^{0.5} \qquad \textbf{Equation 6.2}$$

Key: Q is the cumulative release per unit area (mg/cm^2), D is the diffusion coefficient of substance in the matrix, C is the solubility of substance in the matrix, A is the initial loading of substance per unit volume, t is time and k is a release constant.

Plots of Q versus the square root of time are depicted in Figures 6.4.7.3a and 6.4.7.3b, linear profiles are evident. The cumulative release should maintain a square root of time dependence. The linearity of the profiles, which confirms the $t^{0.5}$ kinetics, is affirmed by the R^2 values, listed in Table 6.4.7.3c. Deviation from square root of time dependence occurs when the concentration of the active falls below saturation (Heller, 1987). However, this did not occur as it can be seen Table 6.4.7.3b that the % SA release over the period examined was extremely low compared to the concentration in the formulation. The spray-dried samples were assessed in two topical bases, Aqueous Cream and Cetrimide Cream BP. It is important to note that two major assumptions hold true in order that release conforms to the mechanism described for homogeneous systems. Firstly, the drug loading (A) is much larger than the matrix solubility (C) and secondly, that sink conditions apply (Malcolm, 1995).

If release is from a heterogeneous matrix, Equation 6.1 must be modified to account for perhaps the presence of material that might impede the diffusion and subsequent release of the substance through the matrix, Equation 6.3. The modifications take account of the tortuosity (τ) of the system and matrix porosity (ε) (Higuchi, 1963). This is likely to be the case for the systems examined due to the presence of the halloysite in the complex. Levis (2000) observed that the diffusion coefficient of Diltiazem HCl in solid lipid particles containing halloysite was approximately half that of comparable particles which did not contain halloysite. The author ascribed this difference to a physical hindrance created by halloysite within the matrix, which increased the tortuosity thereby retarding drug diffusion.

$$Q = \left(\frac{D\varepsilon}{\tau} C\,(2A - \varepsilon C)\,t\right)^{0.5} \qquad \textbf{Equation 6.3}$$

Figure 6.4.7.3a depicts the square root of time release profiles for spray-dried composites in an aqueous cream base. The profiles represent a very poor fit to Equation 6.2. The formulation containing spray-dried sample 5 has the highest rate of release followed by

sample 7, with the lowest rate of release attributable to spray dried sample 4. The concentrations of SA in topical formulations containing spray-dried samples 4 and 7 are 1.9% and 2.49% respectively, Table 6.4.7.3a. It would be expected that sample 7 which has the highest concentration of SA, 2.49% w/w, would have the highest release rate. However as the concentration of SA exceeds its saturated solubility in all formulations, this highlights the importance of other factors such as particle formulation, size, density and surface area. Figure 6.4.5.2 depicts surface area and skeletal density analysis results. Sample 7 has the highest surface area and skeletal density values. The increased surface area has important ramifications for solubility, however the size of pores on the particle surface may dictate the ability of the cream formulations to access the interior particle and hence affect SA release.

The spray-dried sample 5 has the highest rate of release. This sample has the second highest SA concentration (2.21% w/w) but more importantly with reference to Table 6.4.5.1, it has the highest concentration of cetrimide in its spray-dried formulation, 0.5% w/w. This has important implications for wettability of the complex and hence SA release. The rate of release is also attributable to its surface area and skeletal density values. It was observed in Section 6.4.5.2 that sample 5 has lower surface area and skeletal density values than samples 4 and 7. This is due to a large closed pore network which impacts on the SA release. This implies that the low skeletal density is as a result of a high degree of porosity in the sample. The surface area is a reflection of external surface area and open pores. It does not account for closed pores, which contribute to the lower skeletal density value.

It can be seen from Figure 6.4.7.3a that the Aqueous Cream formulation containing spray-dried sample 4 has the lowest SA rate of release; it also has the lowest SA concentration, 1.9% w/w. It is evident from Table 6.4.5.1 that preparation of spray-dried complex 4 incorporated a cetrimide concentration of 0.2% w/v; this is four times higher than that used to produce spray-dried sample 7, 0.05% w/w. It would be expected that an increased cetrimide concentration would increase wettability of the particles and result in greater SA release. However as mentioned above, sample 7 has a higher percentage of SA in the spray-dried formulation, hence it appears that SA concentration has a dominant role in dictating the rate of SA release. The release data was fitted to a Higuchi model, which describes controlled release kinetics in terms of a square root of time plot. The data shown

in Figure 6.4.7.3a deviates from linearity, which indicates it poorly fits the model for controlled release. The correlation coefficients for the data are displayed in Figure 6.4.7.3c.

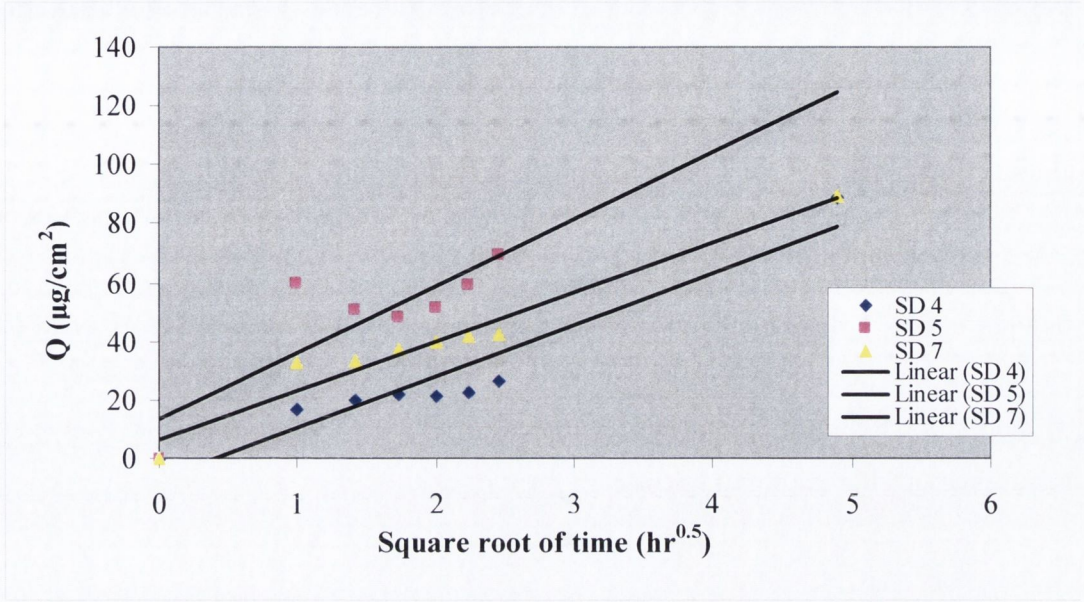

Figure 6.4.7.4a Cumulative release of SA from spray-dried SA/halloysite/cetrimide composites in Aqueous Cream base as a function of $t^{0.5}$.

Figure 6.4.7.3b shows the square root of time release of SA from spray-dried composite systems incorporated in Cetrimide Cream BP base. The order of the rate of SA release from Aqueous Cream formulations is maintained in the case of Cetrimide Cream BP formulations. However the cumulative release from the samples incorporated in the Cetrimide Cream formulations is reduced relative to that from the Aqueous Cream base. The release is greater from the Aqueous Cream formulation for all of the spray-dried samples examined. The cumulative release of SA per cm^2 of membrane from the Cetrimide Cream formulation containing spray-dried sample 4 was 22.21 $\mu g/cm^2$, this increased to 26.21 $\mu g/cm^2$ in the case of release from the Aqueous Cream formulation. The difference was greater in the case of formulation containing spray-dried sample 5, the cumulative release increased from 46.78 to 69.58 $\mu g/cm^2$ from the Aqueous Cream base. The differences are explained by topical base composition. Aqueous Cream has a water content of approximately 70% w/w compared to a 45% w/w content in the Cetrimide Cream base. Aqueous Cream also contains an overall liquid paraffin content of 6% w/v compared to a 50% w/v content in Cetrimide Cream. The modification in the cream bases has

implications for SA solubility. The saturation solubility of SA in water was determined in Section 6.3.2.1 to be 0.31% w/v. It was determined to be approximately 0.05% w/w in petrolatum (Knezcke *et al.*, 1986); therefore the solubility in liquid paraffin would be expected to be less than that in water. The viscosity of the bases is also likely to be different; this factor is examined in Section 6.4.7.4.

Both cream bases contain cetostearyl alcohol which contributes to the viscosity of the systems. In topical pharmaceutical formulations, cetostearyl alcohol will increase the viscosity and impart body in both water-in-oil and oil-in-water emulsions (Handbook of Pharmaceutical Excipients, 2005). Some authors have examined the role of cetostearyl alcohol in slowing the dissolution of water-soluble drugs (Lashmar and Beesley, 1993; Wong *et al.*, 1992; Ahmed and Enever, 1981). These factors resulted in retarded SA release through the increased viscosity of the formulation.

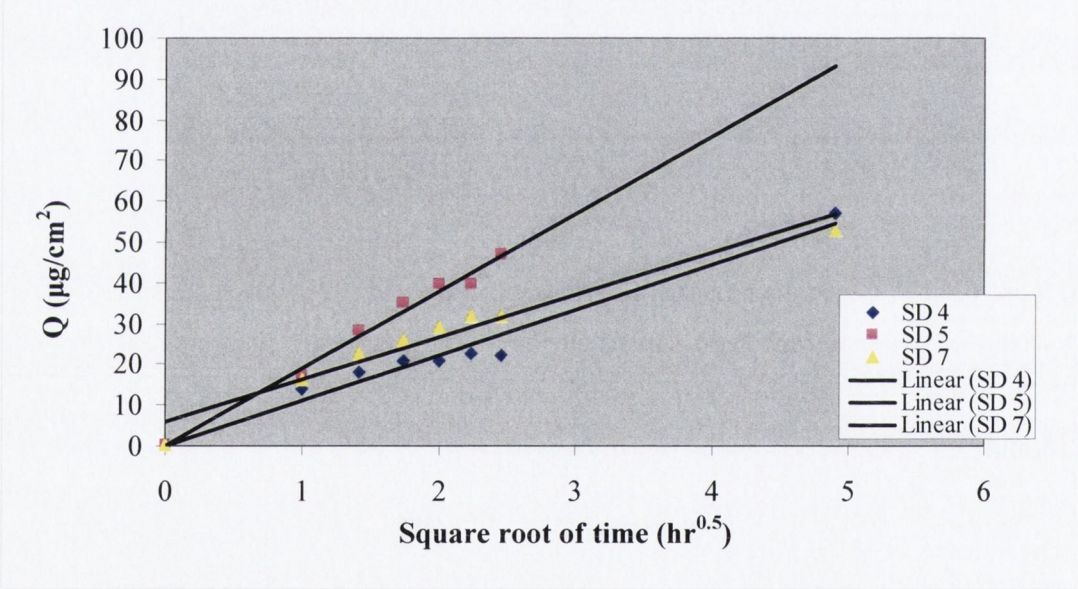

Figure 6.4.7.4b Cumulative release of SA from spray-dried SA/halloysite/cetrimide composites in Cetrimide Cream BP base as a function of $t^{0.5}$.

Table 6.4.7.3a depicts the content of SA in each of the formulations. The concentration range varies from 1.90-2.49% w/w. It was calculated based on studies in Section 6.4.6 that examined the quantity of SA released from the spray-dried composites and the overall concentration of the spray-dried composites in the final formulations.

Table 6.4.7.3a SA content (% w/w) in test formulations.

Sample	SA rel. (g) per g of SD product	SA conc. per g of formulation	% Conc. of SA in topical bases
Spray-dried 4	0.0952	0.0190	1.90
Spray-dried 5	0.1106	0.0221	2.21
Spray-dried 7	0.1244	0.0249	2.49

Table 6.4.7.3b depicts the release of SA as a % of SA present in the formulations. The release is greater from the Aqueous Cream base in all cases. This is due to differences in composition as discussed previously which impact on the viscosity of the base and hence on the diffusivity of the active in the formulation.

Table 6.4.7.3b SA release as a % of SA concentration in topical formulations after a period of 6 hr.

Sample	Aqueous Cream (% w/w)	Cetrimide Cream (% w/w)
Spray-Dried 4	1.211	0.719
Spray-Dried 5	0.756	0.508
Spray-Dried 7	0.861	0.509

Table 6.4.7.3c depicts the correlation coefficients when the release data is investigated using the Higuchi square root of time model. Cetrimide Cream formulations are more uniform and adhere to the model better than the Aqueous Cream formulations. This is highlighted by approximation of the profiles to linearity. The correlation coefficients R^2, indicate the linearity, the values for which are between 0.9568-0.9881. The range for the composites formulated using the Aqueous Cream base was broader, 0.7210-0.9572 and deviate from linearity and the model as the values depart from unity. SA release from the spray-dried formulations in the Aqueous Cream base show a poor fit to the Higuchi model. The profiles in Figures 6.4.7.3a and 6.4.7.3b show that the samples formulated in the

Cetrimide Cream base appear more linear than the corresponding spray-dried formulations in the Aqueous Cream base.

Table 6.4.7.3c Correlation coefficients (fit to Equation 6.2) for SA release from spray-dried systems in different topical bases.

Sample	Aqueous Cream (R^2)	Cetrimide Cream (R^2)
Spray-Dried 4	0.9115	0.9710
Spray-Dried 5	0.7210	0.9881
Spray-Dried 7	0.9572	0.9568

6.4.7.4 Rheological Evaluation of Formulations

The aim of this study was to assess if the difference in cumulative release could be attributed to the existence of differences in the rheological properties. Based on the differences in the components present and differences between constituents common to both vehicles it would be expected that a difference in rheological profiles would be observed. The rheology of the vehicle plays a crucial role in the transport of the drug to the skin surface. For a drug molecule to be released from a vehicle across membrane, it first has to reach the membrane. Mass transport in a formulation occurs either by diffusion of the molecules or by diffusion and convection of the particles (in a suspension). The apparent viscosity of the formulation influences the particle movement (Welin-Berger *et al.*, 2001).

Figure 6.4.7.4a depicts the flow profiles of Cetrimide Cream bases containing spray-dried samples 5 and 7. Spray-dried sample 4 was not investigated due to insufficient sample being available. The spray-dried sample 5 formulation is less viscous than sample 7 over the shear stress range examined. The profile for sample 5 also exhibits some specific features such as spurs and bulges. The nature of these structural features was elucidated in Section 1.7 and are attributable to sample microstructure flow and structural breakdown. Over the shear stress range examined sample 5 displays a hysteresis loop with a greater area, indicative of a greater degree of thixotropy shown by this system.

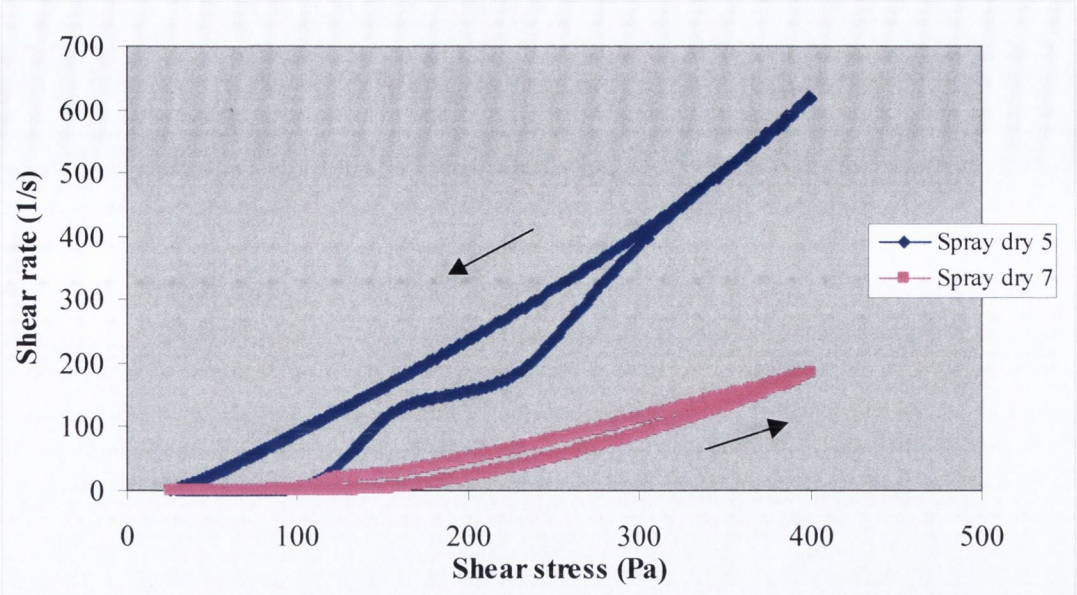

Figure 6.4.7.5a Rheological evaluation of spray-dried SA complexes 5 and 7 in Cetrimide Cream base.

The viscosity trend is reversed in Figure 6.4.7.4b, a depiction of the rheological profiles of spray-dried samples 5 and 7 in Aqueous Cream. The hysteresis area is greater in the case of the samples analysed in the Aqueous Cream formulation. The apparent viscosity for sample 5 reduces from 290 mPa.s during the upward flow curve (flow curves depicted by arrows) to 210 mPa.s on the downward flow curve at a shear stress value of 100 Pa. The downward shear profiles are displaced to the left in all samples. The change in apparent viscosity for sample 7 at an equivalent shear stress value was from 115 mPa.s to 97.8 mPa.s. The apparent viscosity of spray-dried samples, 5 and 7 in Cetrimide Cream base at a shear stress value of 200 Pa is 650 mPa.s and 2190 mPa.s respectively. The apparent viscosity values for both topical formulations were not calculated at equivalent shear stress values because the flow properties were different, shear stress values were chosen at equivalent points prior to structural breakdown. The Cetrimide Cream base was undoubtedly more viscous. It has been observed that in combination with primary emulgents, cetostearyl alcohol forms emulsions with very complex microstructures (Handbook of Pharmaceutical Excipients, 2005). This complex microstructure in conjuction with the increased liquid paraffin and decreased water content relative to the Aqueous Cream base resulted in a decrease in SA release from the Cetrimide Cream formulation relative to the Aqueous Cream formulation.

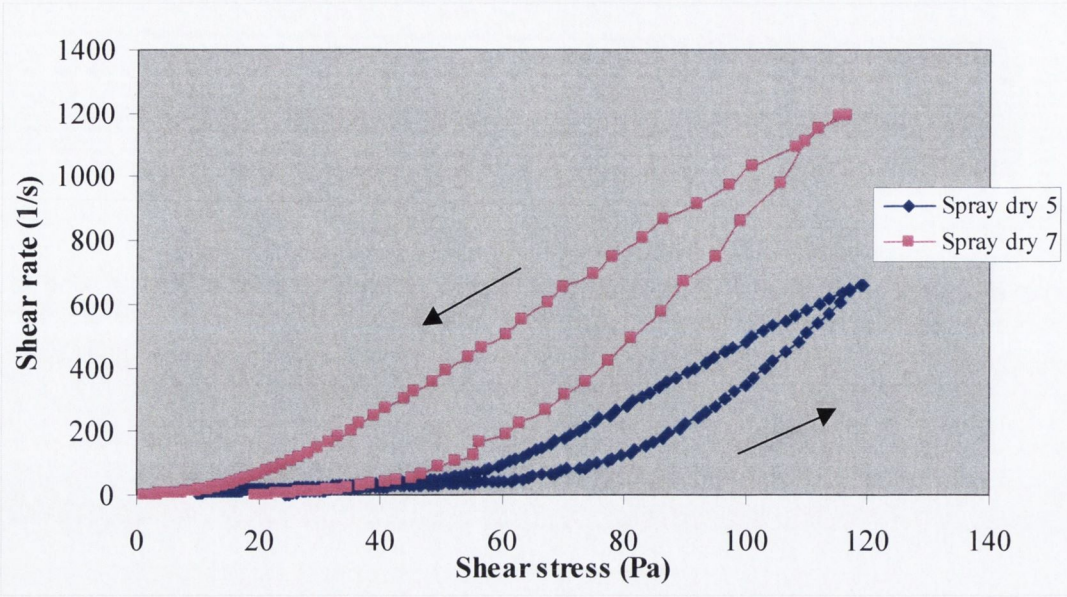

Figure 6.4.7.4b Rheological evaluation of spray-dried SA complexes, 5 and 7 in Aqueous Cream base.

6.5 CONCLUSIONS

The formulation of topical products is a complex process. The essential features which must be addressed include the delivery of the active from the vehicle to the site of action. The active must be dissolved and diffuse through the vehicle to the site of delivery. At the site of delivery the active must partition from the vehicle into the first layer of the SC prior to traversing the SC to the particular site of action. It can be seen that there is a multitude of steps in the process; however it is made more complicated by physicochemical characteristics of the active molecule and the topical vehicle. The work carried out in this section involved the formulation of halloysite complexes involving urea and SA for use in topical drug delivery. The complexes were characterised in order to fully elucidate their properties and their effect on the release profiles of SA in topical formulations.

Urea has an established role in topical products (Clarke, 2004). The molecule was investigated as a model agent due to its small size and high water solubility (British Pharmacopoeia, 2007). Its incorporation in complexes with halloysite was investigated using a 2^{4-1} factorial study. The presence of the cetrimide coating on the halloysite surface had the greatest influence on urea encapsulation. This was due to a number of consequences including the possibility of the cetrimide co-adsorbing the urea. Secondly the

urea crystallises in channel-like formations, which can enclose molecules such as hydrocarbons (Martin, 1993). Hence an increase in encapsulation occurs. The increased volume caused a reduction in encapsulation due to the urea being removed by filtration. However the complexes did not modify urea release. An alternative approach involved the formulation of co-spray-dried complexes. Two grades of lecithin were incorporated, Lipoid S75 and S100. SEM analysis showed that the ratio of lecithin to halloysite in the formulation dictates the morphology. The increased lecithin ratio resulted in a gelatinous structure with halloysite tubules embedded in it. Macropores on the surface were evident. The choice of the spray-dry medium is also important because lecithin dissolves in ethanol but is only dispersed in water. Urea encapsulation and release is dictated by the ratio of the components in the formulation and the overall solid content in the system. A reduction in solid content did not result in a greater % encapsulation, but resulted in comparatively better encapsulation efficiency.

Prior to incorporation of halloysite complexes in topical formulations, rheological and textural analysis studies were conducted to determine the impact of the clay on the flow properties of the halloysite samples. Flow rheological studies showed that an increased level of shear was required to shear thin samples as the concentration of halloysite was increased. Non-destructive dynamic oscillatory studies highlighted that the uncoated halloysite – WSP at the highest concentration displayed the most solid-like character. A surfactant monolayer is present on the halloysite surface in WSP ointment systems, resulting in a decreased resistance to flow. The macrogol systems containing coated and uncoated halloysite had greater values of hardness. The macrogol ointment systems containing 10% halloysite (both coated and uncoated) had a hardness value greater than the halloysite – WSP system which displayed the greatest hardness. This is due to the interaction of the surfactant hydrocarbon chains and the PEG polymers. The adhesive studies were conducted using WSP systems only. The coated samples displayed greater adhesion, this manifested as an increased peak detachment force compared to the uncoated samples. However the uncoated samples had greater values for work of adhesion indicating that they had greater cohesive and adhesive forces. The 40% halloysite samples (coated and uncoated) were not comparable because they were too hard.

SA/halloysite complexes were prepared using the vacuum loading method. The preliminary study highlighted that the cetrimide coated grade resulted in an enhanced

encapsulation. The use of the more concentrated loading solution in a single loading process had a significant impact on encapsulation. However release was instantaneous due to the highly concentrate solutions used. This prompted lower concentrations to be considered in the advanced study. Again the cetrimide grade displayed a superior encapsulation potential. The encapsulation in the advanced study was reduced by a factor of 5, despite the loading solution concentration being reduced by a factor of 8. This highlights that there is an optimum solution concentration.

Co-spray-dried SA complexes were prepared in order to produce uniform particles. The samples were characterised using a number of techniques. The surface area and skeletal density was influenced by halloysite concentration and the ratio of the surfactant in the sample. Particle size analysis conducted on raw SA and the spray-dried sample 4 highlighted that 50% of particles in both samples were approximately equivalent in size but overall the particle and size distribution was greater in the spray-dried sample. The particle size and surface area had important consequences for SA release from topical products. An increase in SA concentration resulted in an increase in the rate of release but the sample porosity also influences this substantially. The difference in cumulative release is influenced by the topical base composition. The Cetrimide Cream composition resulted in a more viscous formulation compared to the use of Aqueous Cream, which decreased diffusion of SA in the base. The halloysite complex confers a controlled release character on the formulations this is confirmed using the Higuchi controlled release kinetics model. The Aqueous Cream formulations demonstrated a poorer fit to the model than the Cetrimide Cream formulations. This in conjunction with the innate characteristics of halloysite affirms the potential of the formulation for topical drug delivery.

Chapter 7

FORMULATION OF METRONIDAZOLE – HALLOYSITE COMPLEXES

7.1 INTRODUCTION

The aim of this section was to develop a topical formulation containing metronidazole and halloysite, for use in the treatment of exudating wounds associated with bacterial infection. It was hoped that metronidazole could be combined with halloysite so that release of the antibacterial could be controlled by encapsulation both within and between the tubular network. It was also hoped to exploit the sorptive capacity of the clay both for the adsorption of toxins and excess wound exudate. The complex would be incorporated in a dressing to prevent the shedding of particles into the wound environment.

The preparation of a metronidazole halloysite complex was first investigated using a vacuum loading procedure. Preparation of a complex with a sufficiently high concentration of metronidazole was hindered by the poor aqueous solubility of metronidazole (The Pharmaceutical Codex, 1994). Hence loading studies were conducted using different vehicles in order that the encapsulation could be optimised using more concentrated solutions. Two different vehicles including an ethanol/water co-solvent system and an ascorbic acid containing vehicle were investigated. The extent of encapsulation and subsequent release from formulations loaded using these vehicles was investigated. Preparation of a spray-dried complex incorporating chitosan with the halloysite/metronidazole complex was investigated to enhance the controlled release of metronidazole. The % release and encapsulation were also assessed for this complex.

Halloysite, alginate and metronidazole complexes were also prepared as a bead formulation. Firstly the beads were produced without the incorporation of metronidazole. The beads were characterised using a number of techniques, including surface area and skeletal density analysis, swelling studies and Winseedle® analysis. Rheological

examination of the halloysite/alginate complexes at various loadings of halloysite was also conducted. The formulation of metronidazole containing beads was also investigated to determine the optimum bead formulation for controlled release of metronidazole. Modification of bead samples were characterised in terms of % release and encapsulation. Formulation components including the diameter of the needle used to produce the beads and the concentration of metronidazole in the overall formulation were investigated. Further formulation manipulation was assessed by modification of the bead core through alteration of the cross-linking components of the gelation medium. Cross-linking agents such as chitosan, glutaraldehyde and sodium polyphosphate (NaPP) were examined as alternatives to calcium chloride ($CaCl_2$). The concept of modified metronidazole release was investigated by encasing the bead formulation within coating materials. Coating substances examined include Eudragit® E PO and chitosan. The bead formulation was also added to a glutaraldehyde solution in order to examine if the bead could be reinforced with the cross-linking agent. The release of metronidazole from the proprietary gel preparation, Rozex® using a Franz cell was also investigated.

7.2 Metronidazole Solubility Studies

7.2.1 Metonidazole Saturated Solubility

The saturated solubility of metronidazole was determined in water and a water/ethanol co-solvent system, the results are presented in Table 7.2.1. The saturated solubility in water was experimentally determined to be 1.0084 +/- 0.1268% w/v, this agreed closely with reference values of 1.00% w/v (The Pharmaceutical Codex, 1994). The solubility in water is quite low and this posed a problem for the preparation of a metronidazole loaded halloysite due to the limitation on drug quantity in loading solution as a result of poor solubility. An alternative solvent system was examined as a means of improving solubility. Chien (1984) found that the aqueous solubility of metronidazole was improved by the addition of one or more water soluble co-solvents. Hence a co-solvent system composed of ethanol and water in a ratio of 25:75 was evaluated. A co-solvent system was used, as this was more reflective of the system employed in the preparation of spray-dried samples. The solubility of metronidazole in the ethanol-water system was more than double the solubility in water.

Table 7.2.1 Solubilities of metronidazole in water and ethanol/water media at 25 °C after equilibration for 24 hr.

Medium	Solubility (% w/v)	St. dev. (+/-)
Water	1.0084	0.1268
Ethanol/water (25:75)	2.2092	0.1964

7.2.2 Dynamic Solubility

A dynamic solubility study of metronidazole in water and McIlvaine buffer pH 5.5 was undertaken to depict the instantaneous solubility profile of a saturated drug system. From Figure 7.2.2 it is clear that in both media the maximum solubility is achieved within 15 min. There is a difference in the solubility for the two media, the concentration being higher for the water medium. The dynamic solubility is approximately 0.9% w/v and 1.0% w/v in McIlvaine buffer, pH 5.5 and water respectively. A saturated aqueous solution of metronidazole has a pH of 5.8 (The Pharmaceutical Codex, 1994). The study is also useful in determining the appropriate quantity of formulation to examine in order that solubility is not the rate-limiting step in metronidazole release from particular formulations prepared later in this Chapter.

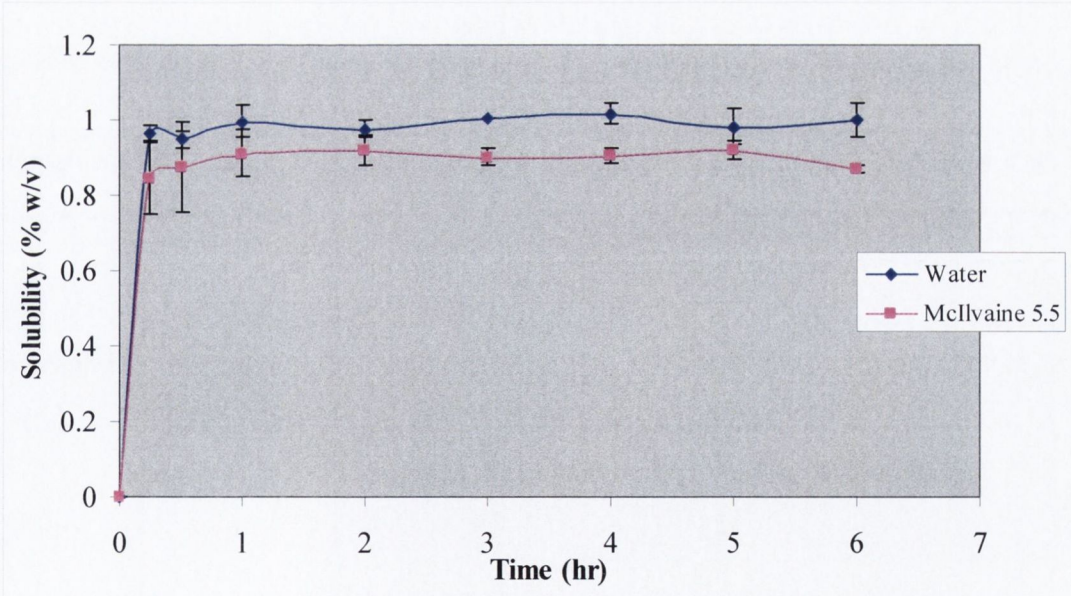

Figure 7.2.2 Dynamic solubility profile of metronidazole in water and in McIlvaine buffer pH 5.5.

7.3 Halloysite Loading Studies

The aim was to examine the entrapment capacity of metronidazole within halloysite and cetrimide coated halloysite. A vacuum loading method was employed in order to achieve both intra-tubular and inter-tubular loading of metronidazole. The nature of the vehicle used to load the metronidazole was also examined. The poor water solubility of metronidazole, discussed in Section 7.2.1 is not conducive to the production of concentrate metronidazole loading solutions. Hence an ethanol/water co-solvent system was employed. The influence of ascorbic acid on the loading of metronidazole was also examined. Previous work conducted by Chien, (1984) found that the presence of the antioxidant substance, ascorbic acid played a role in increasing the solubility. This is due to an alteration in solution pH because metronidazole is more soluble in dilute acids (The Pharmaceutical Codex, 1994). The pH of a 1% w/v solution of ascorbic acid had a value of 2.8; hence this reduces the effective pH of the metronidazole-ascorbic acid system and increases metronidazole solubility. Ascorbic acid was employed at a concentration of 0.001% w/v in the study; this solution had a pH value of 4.93. Ascorbic acid has good solubility in water, 1 part dissolves in 3.5 parts of water (Handbook of Pharmaceutical Excipients, 2005). The concentration of ascorbic acid was reduced from a higher initial concentration of 0.5% w/v because the pH has important consequences for the stability of metronidazole. Maximum stability occurs at a pH value of 5 (Baveja and Rao, 1973).

Therefore the focus of the study was centred on the use of different loading vehicles, with the aim of increasing the concentration of metronidazole in the loading solution and hence encapsulation of metronidazole in the halloysite samples. The extent of encapsulation was determined using release studies, which are depicted in Figure 7.3. There is almost instantaneous release of metronidazole from the samples loaded with the ascorbic acid containing vehicle. Release from the halloysite sample loaded using the ethanol-water vehicle is complete within 2 hr. At the equivalent time point 88% of the metronidazole is released from the cetrimide coated halloysite sample. The release profiles show that halloysite alone does not significantly modify drug release.

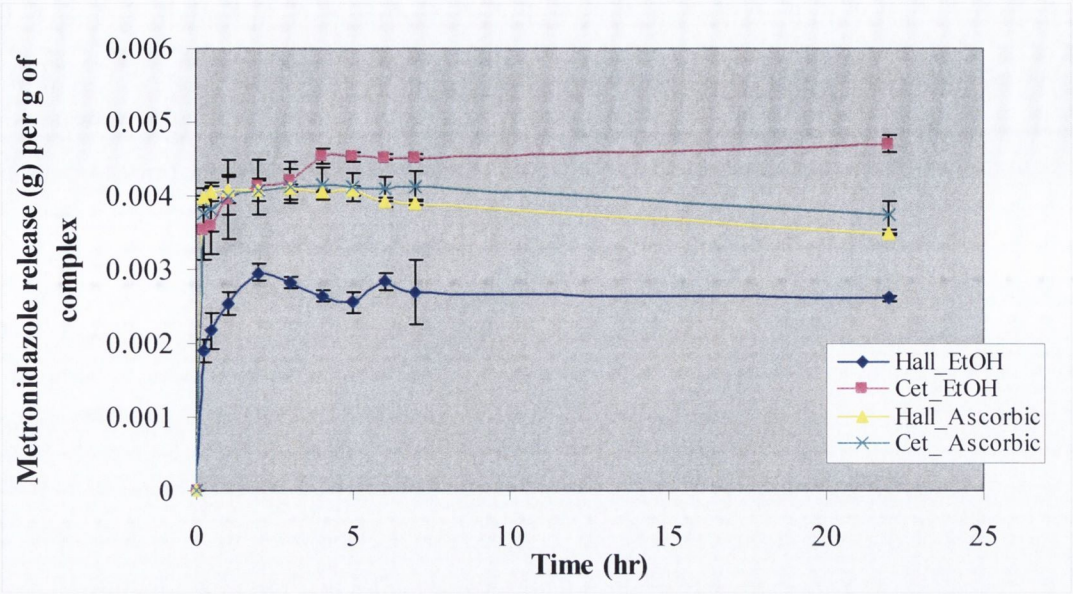

Key: hall = halloysite; cet = cetrimide coated halloysite; EtOH = ethanol/water vehicle; Ascorbic = vehicle containing ascorbic acid (0.001% w/v).

Figure 7.3 Release profiles depicting the release of metronidazole from halloysite samples vacuum loaded with different media.

Tables 7.3a and 7.3b illustrate metronidazole encapsulation, i.e. the amount of metronidazole captured both within and between the tubules per 100 g of drug loaded product. The encapsulation varies from 0.27 to 0.47% w/w. The concentration of metronidazole in the loading solution was 1% w/v and the ratio of metronidazole to halloysite in the study was 0.05:1. Therefore, there was 50 mg of metronidazole for every g of halloysite in the loading experiment. The potential encapsulation was 5% w/w. Tables 7.3a and 7.3b also display the resultant encapsulation efficiency, the values are in the range 5.4-9.4% of the total metronidazole quantity present. The amount of metronidazole confined by the clay mineral is extremely low, highlighting the inability of halloysite to entrap the antibacterial under the present experimental conditions.

It is obvious from Figure 7.3 that there is a difference between the amount encapsulated by the halloysite and cetrimide coated halloysite samples loaded with the ethanol/water vehicle, but no difference was observed between these samples when the ascorbic acid vehicle was used. Statistical significance was determined using a t-test with a 95%

confidence interval for differences. The test confirmed that a significant difference existed between the encapsulation of metronidazole by the two halloysite grades using the ethanol/water vehicle. The difference is attributable to the surfactant conferring a hydrophobic property on the clay surface. Therefore it is possible for the imidazole structure, which has a log P value of –0.01 (The Pharmaceutical Codex, 1994) to associate more intimately with the cetrimide coated sample compared to the uncoated sample resulting in increased encapsulation. Also it is possible that the metronidazole has become co-adsorbed by surface surfactant structures, which causes more to be encapsulated and modulates the release also. Cherkaoui *et al.*, (1998, 2000) examined the co-adsorption of steroids at a silica interface using cationic surfactants. They observed that at surfactant equilibrium concentrations above the critical micelle concentration (CMC) the drug molecules are distributed between the adsorbed aggregates and the free micelles.

The presence of the cetrimide coating does not affect the amount released from the two halloysite grades when the loading vehicle has ascorbic acid present. It can be seen from Figure 7.3 that the release profiles for the samples overlap each other. The similar encapsulation capacity may be a result of the dihydroxyfuran-2-one structure of the ascorbic acid, through an impact on the ionisation of metronidazole. Metronidazole has a pK_a value of 2.5, the ascorbic acid causes a relative decrease in pH and hence an increase in the proportion ionised. Ionisation of metronidazole would minimise the importance of the hydrophobic effect of the surfactant on the clay surface. This manifests as similar release profiles irrespective of the presence of cetrimide.

Table 7.3a Encapsulation (expressed as a percentage of drug loaded product) and encapsulation efficiency (expressed as a percentage of total drug added) of metronidazole within halloysite using different vehicles, expressed as a percentage of drug loaded product.

Loading Medium	Encapsulation (% w/w)	Encapsulation efficiency (%)
Ethanol/water (25:75)	0.27	5.4
Ascorbic acid (0.001% w/v)/water	0.39	7.8

Table 7.3b Encapsulation (expressed as a percentage of drug loaded product) and encapsulation efficiency (expressed as a percentage of total drug added) of metronidazole within cetrimide coated halloysite using different vehicles.

Loading Medium	Encapsulation (% w/w)	Encapsulation efficiency (%)
Ethanol/water (25:75)	0.47	9.4
Ascorbic acid (0.001% w/v)/water	0.41	8.2

7.4 SPRAY-DRIED COMPLEX

7.4.1 Introduction

It is evident from the loading study in Section 7.3 above that the encapsulation of metronidazole is extremely poor with 2.7-4.7 mg of metronidazole encapsulated per gram of sample. Hence it was decided to use an alternative method to produce metronidazole/halloysite complexes. Halloysite was spray-dried with metronidazole and chitosan using a mixed water/ethanol vehicle as outlined in Section 3.12.3. The components in the formulation are chitosan, metronidazole and halloysite. The ratio of constituents is 0.1:0.3:2.0, the metronidazole quantity in the formulation is 150 mg per gram of halloysite. This is increased by a factor of 3 compared to that used in the vacuum loading studies. Chitosan was incorporated in order to control the release of metronidazole from the complex. The intention was to encapsulate metronidazole in a complex between a halloysite and chitosan network entanglement. Halloysite has a polyanionic charge, this electrostatically attaches to the polycationic chitosan structure entrapping the active in the meshwork.

7.4.2 Chitosan

Partial deacetylation of chitin results in the production of chitosan, which is a polysaccharide comprising of copolymers of glucosamine and N-acetylglucosamine. Chitosan is the term applied to deacetylated chitins in various stages of deacetylation and depolymerisation and is therefore not easily defined in terms of its exact chemical composition (Handbook of Pharmaceutical Excipients, 2005). Chitosan is chitin sufficiently deacetylated to form soluble amine salts. The degree of deacetylation

necessary to form a soluble product must be greater than 80-85%. Chitosan is commercially available in several types and grades that vary in molecular weight from 10,000-1,000,000, and vary in degree of deacetylation and viscosity (Genta *et al.*, 1998). Chitosan is a cationic polyelectrolyte and has been shown to be biocompatible and biodegradable (Hirano *et al.*, 1988; Orienti *et al.*, 1996). Hence it has been widely investigated in the context of drug delivery. Henriksen *et al.* (1994) examined the role of chitosan as a stabilising component in liposomes. Chitosan has also been investigated for its ability to control drug release in oral formulations (Denkbas *et al.*, 1999), microencapsulation of enzymes, proteins and cells (Heller *et al.*, 1996) and for its bioadhesive properties (Yamamoto *et al.*, 2000).

7.4.3 Metronidazole Release Profiles

The release of metronidazole from the spray-dried complex was assessed at two pH levels, pH 4 and 7.4. Physiological pH is 7.4 but that of the wound environment can differ depending on the oxygen and lactic acid concentrations (Cundell *et al.*, 2002). The acid pH that arises during the early stages of wound healing due to wound exudate and cell debris shifts through neutral to alkaline as the healing progresses (Liu *et al.*, 2002). The amount of metronidazole released from the spray-dried complex at the two different pHs is illustrated in Figure 7.4.3. The rate and extent of metronidazole release is greater in the pH 7.4 buffer. As mentioned previously in Section 7.2.1 metronidazole is soluble in dilute acids, hence it would be expected that the release rate in the lower pH system would be greater. This should not affect the overall release as sink conditions are maintained in both systems.

There is also a difference in the extent of metronidazole release as the medium pH is changed. Even though the alteration in the polyanionic surface charge of halloysite at low pH results in fewer sites for the possible polyionic complexation between halloysite and the polycationic compound chitosan, the neutral pH resulted in an increased release. The change in pH alters the surface charge of the halloysite structure. Zeta potential studies conducted on halloysite by Levis (2000) indicated that the negative charge increased as the pH was increased. From these studies the zeta potential alters from approximately -16 mV at pH 4 to -28 mV at pH 7. However, chitosan is increasingly positively charged at reduced pH levels. Despite the reduction of negative charge associated with halloysite, it is not sufficient to cause a weakening of the polyelectrolyte complex. The difference in the rate

of release is also compounded by the insolubility of chitosan at neutral pH. The decreased availability of the positive charge on the chitosan results in a decrease in complexation between halloysite and the chitosan. Hence the encapsulation matrix breaks down and the active is released. The system examined using McIlvaine buffer pH 7.4 displayed an approximate release of 0.88% w/w after 5 hr which decreased to 0.66% w/w at an equivalent time point when the medium pH was reduced to 4. Hence release at the lower pH is modified compared to that at neutral pH.

The role of chitosan in retarding drug release at neutral pH was examined by a number of authors (Singh and Ray, 1999; Ganza-González *et al.*, 1999). Ganza-González *et al.* (1999) observed that the medium pH had little effect on the release of metoclopramide from chitosan microspheres even though the % release was greater as the pH of the system increased.

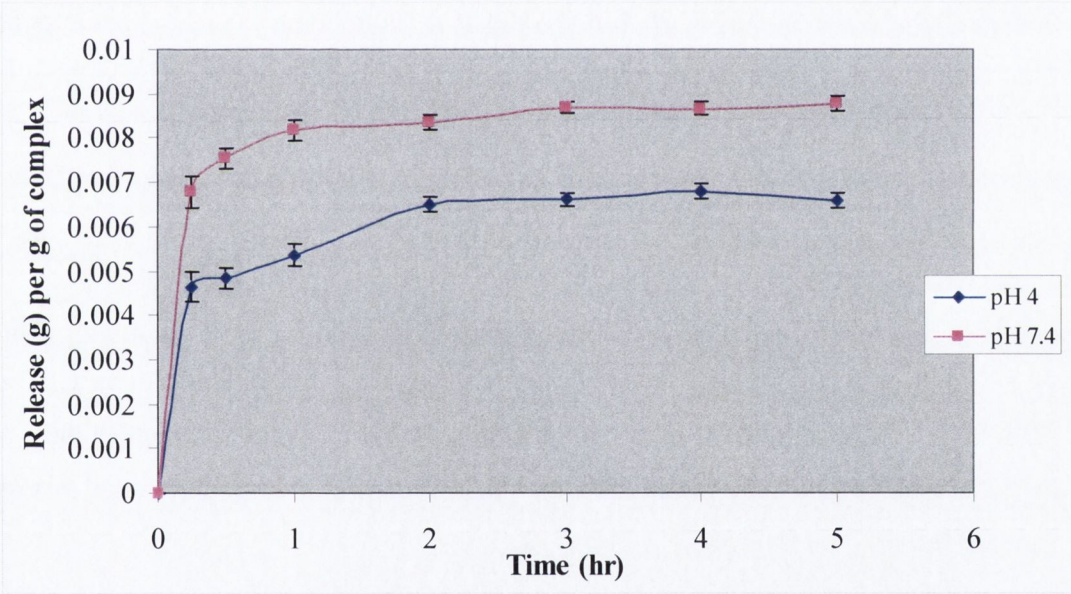

Figure 7.4.3 Metronidazole release (g) per gram of co-spray dried halloysite/metronidazole/chitosan composite.

Release is complete in both systems by two hours. The spray-dried complex had a powder appearance prior to its addition to the sampling vessel. The material was seen to swell and the gelatinous appearance characteristic of hydrated chitosan was evident. The appearance of the spray-dried complex was similar at pH 4 and pH 7.4. The spray-drying process

results in an increased encapsulation of metronidazole relative to the vacuum loading studies but considering the increased addition of metronidazole to the system, the entrapment and release characteristics of the spray-dried complex are still insufficient.

7.5 BEAD FORMULATION

7.5.1 Introduction

The aim of this section was to incorporate halloysite and metronidazole in a bead formulation with the aim of using it topically for the treatment of cutaneous conditions requiring antibacterial therapy. A bead formulation was decided upon as the release of the active could be modulated, quantified and characterised. The preceding spray-drying approach did not result in adequate encapsulation and modification of metronidazole release. It was hoped that the spray-dried material could be encased within a dressing formulation analogous to charcoal dressings such as CarboFlex® and Actisorb®. The intention is to formulate the beads inside a dressing formulation to prevent particles being shed into the wound. Release would be influenced by diffusion and erosion of the swellable device. It would be expected that after disintegration the bead formulation would form a gel and this would also continue to be involved in the absorption of exudate and release of metronidazole.

It was decided that the halloysite and metronidazole would be formulated with alginate. Preliminary studies examined cross-linking the complex with calcium. Each calcium ion binds with two alginate molecules (Handbook of Pharmaceutical Excipients, 2005). It is expected that the halloysite would integrate electrostatically in this complex and this would enhance the network formed.

The presence of halloysite confers a number of advantages. The role of clays in topical products is well established. The presence of halloysite enhances the complex network between alginate and calcium; it also has a similar role in formulations containing the polycation, chitosan which is examined in later studies. It also imparts improved mechanical strength to the beads. The sorptive capacity of the clay is also vital in absorbing exudate and possibly also bacteria and toxins. Studies conducted on *S. aureus* in Chapter 5 highlighted some potential on the part of halloysite to inhibit bacterial growth.

Much attention has focused on the role of calcium alginate beads for the controlled delivery of proteins (Gombotz and Wee, 1998; Rasmussen *et al.*, 2003), drug molecules (Bodmeier and Paeratakul, 1989; Sezer and Akbuğa, 1999; Fernandez-Hervas *et al.*, 1998) or for ophthalmic delivery (Cohen *et al.*, 1997). The alginate matrix, which consists of an open lattice structure, forms porous beads. However, alginates have a low retention capacity for encapsulating low molecular weight and water soluble drugs (Aslani and Kennedy, 1996; Sezer and Akbuğa, 1999), hence one of the aims was to incorporate halloysite in the matrix structure to improve drug delivery.

The method of incorporation of halloysite in an alginate bead was outlined in Chapter 3, in order to produce a formulation for the treatment of infection associated with the wound environment. The incorporation of halloysite and metronidazole is the extension of the established concept of alginate wound dressings. Calcium alginate hydrogels are widely used as wound dressings (Kneafsey *et al.*, 1996). The gelling characteristics of alginate dressings vary according to the product used. Some products only gel to a limited extent to form a partially gelled sheet that can be lifted off, others form an amorphous gel that can be rinsed off with water or physiological saline. A secondary covering is needed. Alginate dressings are highly adsorbent and are therefore suitable for moderately or heavily exudating wounds, but not for eschars or dry wounds. A decrease in pain and reduction in healing time is achieved to a marked extent with alginate, hydrogel and hydrocolloid dressings (British National Formulary, 2004).

7.5.2 Sodium Alginate

The BP (2007) describes sodium alginate as consisting mainly of the sodium salt of alginic acid, which is a mixture of polyuronic acids $(C_6H_8O_6)_n$. It is composed of residues of d-mannuronic acid and l-guluronic acid, and is obtained mainly from algae belonging to the Phaeophyceae. It is a white or pale yellowish-brown powder, slowly soluble in water forming a viscous, colloidal solution, practically insoluble in alcohol. Alginic acid swells in water but does not dissolve; it is capable of absorbing 200-300 times its own weight of water. The molecular weight is typically 20,000-240,000 and has a density of 1.601 g/cm^3. The pH of a 3% w/v aqueous dispersion lies in the range 1.5-3.5 (Handbook of Pharmaceutical Excipients, 2005).

Various grades of alginic acid are available that vary in their molecular weight and hence viscosity. Viscosity increases considerably with increasing concentration, typically a 0.5% aqueous dispersion will have a viscosity of approximately 20 mPa.s, while 2% w/v dispersion will have a viscosity of 2000 mPa.s. Alginic acid hydrolyses slowly at warm temperatures producing a material with a lower molecular weight and lower dispersion viscosity (Handbook of Pharmaceutical Excipients, 2005). The polymer is known to form a physical gel by hydrogen bonding at low pH (acid gel) and by ionic interactions with polyvalent cations (King, 1983; Haug, 1964). Addition of a calcium salt, such as calcium citrate or calcium chloride causes cross-linking of the alginic acid polymer resulting in an apparent increase in molecular weight. The viscosity and primary structure of the polymer are important features determining its swelling and gelling properties, the primary structure is often designated by the length and fraction of the hexuronic acid residues in the alginate (Handbook of Pharmaceutical Excipients, 2005).

The ability of alginates to interact differently with varying chemical environments makes it a very interesting polymer in several pharmaceutical applications (Tonnesen and Karlsen, 2002). Alginic acid is used in a variety of oral and topical pharmaceutical formulations. In tablet and capsule formulations, alginic acid is used as both a binder and a disintegrating agent at concentrations of 1-5% w/w (Shotton and Leonard, 1976; Esezobo, 1989). Alginic acid is used widely as a thickening and suspending agent in a variety of pastes, creams and gels; and as a stabilizing agent for oil-in-water emulsions. Therapeutically it has been used as an antacid (Vatier *et al.*, 1996). Alginic acid has been investigated extensively in the area of controlled release. Formulations including sustained release microparticles containing indomethacin (Joseph and Venkataram, 1995), encapsulated alginic acid coated liposomes (Machluf *et al.*, 1997) and floating alginate beads for gastrointestinal delivery (Murata *et al.*, 2000) have been investigated.

7.5.3 Non-Drug Bead Formulation

In order to optimise the formulation of halloysite/metronidazole/alginate bead complexes a preliminary investigation was conducted to determine the effect of varying formulation conditions on bead morphology and characteristics. Early studies examined the effect of the height and stirring speed of the gelation medium. In order to determine a suitable bead formulation non-drug alginate-halloysite beads were produced using the gelation medium $CaCl_2$ solution. An investigation into three formulation and process parameters was

undertaken in order to determine the optimum levels of each factor. Halloysite or cetrimide coated halloysite was incorporated at a level of 7.5% w/w or 15.0% w/w. The clay levels were arbitrary. Two methods of drying were also examined. Conventional air-drying for 24 hr at room temperature followed by drying in an oven at 50 °C was employed, as was a freeze-drying procedure. Table 7.5.3 lists the samples produced, their formulation and method of drying.

The cetrimide grade was used even though it was expected that the surfactant might increase wetting due to the alteration in contact angle between any liquid and the bead surface. It was expected that this might increase the rate of sample disintegration. It was hoped that if a controlled release formulation was produced that a mixture of bead types including those produced using the cetrimide grade of halloysite might be included in order that the overall release profile would incorporate an immediate release component. Also it was thought that the antimicrobial effect of the cetrimide would be beneficial.

Table 7.5.3 Non-drug halloysite–alginate beads produced using different formulations and process conditions.

Sample	Halloysite	Concentration (% w/w)	Drying method
1	Halloysite	7.5	Air-Oven Dry
2	Cetrimide-halloysite	7.5	Air-Oven Dry
3	Halloysite	15.0	Air-Oven Dry
4	Cetrimide-halloysite	15.0	Air-Oven Dry
5	Halloysite	7.5	Freeze Dry
6	Cetrimide-halloysite	7.5	Freeze Dry
7	Halloysite	15.0	Freeze Dry
8	Cetrimide-halloysite	15.0	Freeze Dry

7.5.4 Rheological Analysis of Alginate Complexes

Rheological evaluation of systems for bead formulation was conducted because it was noted that bead production proved more difficult with some of the formulations. An alteration in viscosity would be expected especially with an increase in solid content; hence it was decided to examine the shear flow properties of the formulations. Firstly, the

flow property of the alginate base at specified intervals after preparation was assessed using stepped ramp shear rheology. Stepped ramp rheology was used rather than continuous flow rheology for the same reasons as those outlined in Chapter 6. The sample has more time to reach an equilibrium shear rate at a specified shear stress value prior to applying an increased shear stress value; hence a more realistic sample profile is produced.

Figure 7.5.4a illustrates the flow profile for sodium alginate dispersion at a concentration of 2% w/w. The up and down flow curves overlap each other, no hysteresis is evident. This is indicative that the integrity of the sample structure is retained. The flow profile approximates to linearity suggesting Newtonian flow; the viscosity of the system is constant irrespective of the shear stress applied. However examination of the apparent viscosity of the system reveals that it undergoes shear thinning as the shear stress is increased. The apparent viscosity reduces from 135 mPa.s at a shear stress value of 38.93 Pa to 113.6 mPa.s at a shear stress value of 79.64 Pa. The calculated apparent viscosity value lies between the reference values of 20 mPa.s and 2000 mPa.s quoted in Section 7.5.2 for dispersions with concentrations of 0.5 and 2.0% w/v respectively. This indicates that a linear relationship does not exist between apparent viscosity and concentration.

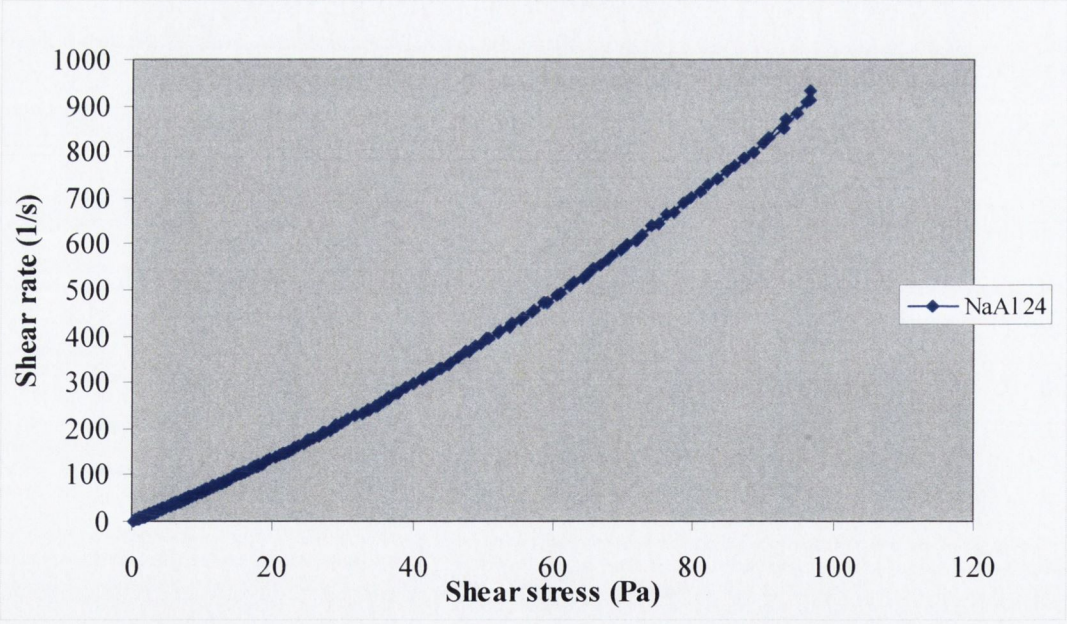

Figure 7.5.4a Rheological profile of sodium alginate 24 hr after preparation.

The rheology of the alginate halloysite complexes was also examined for a number of reasons. The alginate material was hydrated prior to the addition of the halloysite, NaPP and metronidazole. The time intervals between additions and duration prior to mixing and extrusion were maintained constant. Firstly the nature of increased concentration was addressed. It can be seen from Figure 7.5.4b that an increase in viscosity is observed as the concentration of cetrimide halloysite in the system was doubled. At lower levels of shear stress the profiles for samples overlap each other but they diverge as the shear stress value increases. The increased level of cetrimide halloysite resulted in the sample being able to withstand higher shearing forces. The upper limit for the shear stress range for the samples containing cetrimide halloysite 15% was in excess of 150 Pa. The sample containing cetrimide halloysite 7.5% w/w displayed structural breakdown at the increased shearing forces, the upper limit on the range of examination for this sample was 115 Pa. The initial portions of the profiles for all the samples in Figure 7.5.4b display a linear appearance. The linearity is reflected by the regression coefficients, R^2 for the samples which lie between 0.9822-0.9872. This is interesting as it indicates that the samples are Newtonian-like, i.e. the viscosity of the sample is essentially constant. However it should be noticed that although similar graphical features were observed with the sodium alginate dispersion, the apparent viscosity decreased as the shear stress was increased. The up and down curves for the sample with a cetrimide halloysite 7.5% w/w concentration overlap each other. There is no indication of thixotropic features. However, the sample which had a 15% concentration of cetrimide halloysite, resulted in a slight displacement between the up and down curves.

The effect of holding the sample on the peltier plate prior to analysis was investigated. It was found during sample preparation that it was more difficult to extrude the last remaining sample from the syringe. The final portion of the sample in the syringe undergoes an increased shearing force and over a prolonged period of time compared to the sample that is passed through the needle first. Holding the sample in position prior to analysis primarily examined the nature of time difference rather than simulating the exact increased forces exerted on the final portion of sample adjacent to the plunger.

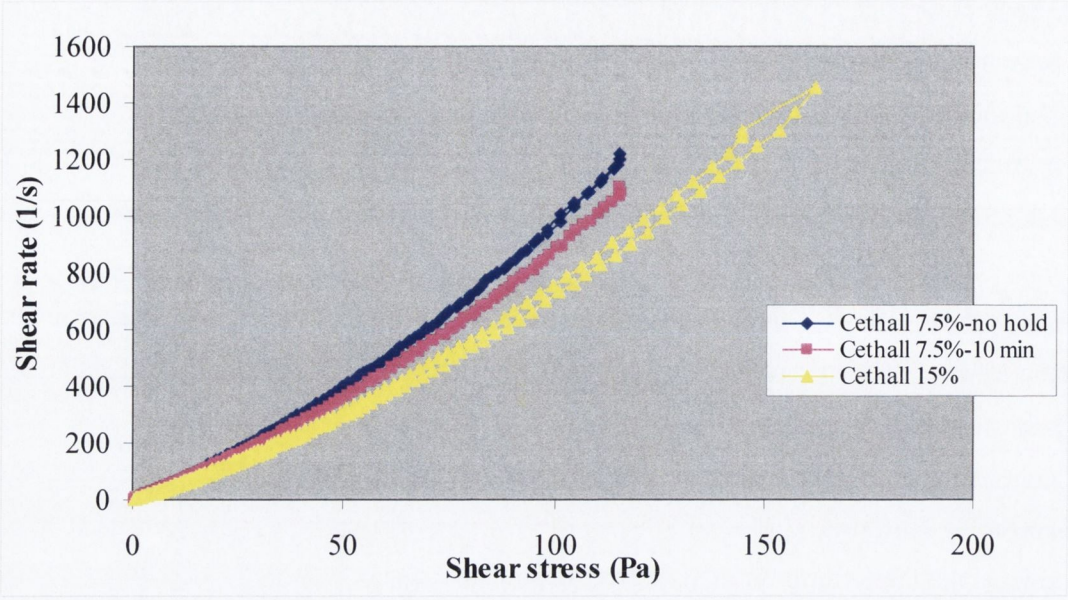

Key: cethall refers to cetrimide coated halloysite at concentrations of 7.5% or 15% w/w.

Figure 7.5.4b Rheological examination of formulations for pellets and the effect of the time duration elapsed prior to evaluation.

It can be seen from Figure 7.5.4b that the profile for the sample, which was held on the peltier plate for 10 min prior to analysis was more viscous. It had an apparent viscosity of 109.3 mPa.s at a shear stress value of 111.5 Pa. The sample which was analysed immediately had an apparent viscosity value of 98.4 mPa.s at an equivalent shear stress value. This change may be attributable to the gel structure forming an enhanced network. It is unlikely that the application of the sample to the plate caused sufficient structural breakdown, which manifested as a decrease in apparent viscosity compared to the sample which was allowed to equilibrate prior to analysis. This is proposed by again looking at the sample profiles. The samples undergo shearing forces in excess of 100 Pa but the samples over the evaluation period do not display any time dependent structural reformation. The up and down curves overlap each other.

Figure 7.5.4c depicts the difference in flow properties between samples that contain halloysite and cetrimide coated halloysite. It can be seen that the profiles containing the halloysite grades at the lower concentration are essentially similar. However, structural breakdown was evident in the cetrimide halloysite sample beyond a shear stress value of

120 Pa. It was possible to examine the halloysite sample at values in excess of this. The upper limit shear stress range for this sample is 135 Pa.

Figure 7.5.4c displays a more drastic change in the profiles produced as a result of doubling the concentration of halloysite from 7.5% to 15% w/w compared to that observed in Figure 7.5.4b when the cetrimide halloysite in equivalent systems was doubled. Again the profiles display a linear appearance. The 15% concentration profile is shifted upwards, more considerably than that observed in Figure 7.5.4b for the cetrimide halloysite samples. The up and down curves are almost superimposable.

From Figure 7.5.4c an increased concentration of halloysite results in a reduction of the slope of the sample profile. As the apparent viscosity is equal to the reciprocal of the slope, this is indicative of an increase in sample viscosity. Figure 7.5.4d illustrates the change in apparent viscosity as a function of applied stress. It confirms that the halloysite 15% sample has the greatest viscosity. It is interesting to note that the profiles for remaining samples resemble each other, including both cetrimide samples. There is a sharp reduction in the viscosity of each sample over a very small change in shear stress; thereafter the reduction in apparent viscosity is more gradual with increase in shear stress. This points to shear thinning behaviour rather than Newtonian as suggested by the shear stress-shear rate profiles in Figures 7.5.4b and 7.5.4c.

The reason for the cetrimide free sample effecting such a change with increase in concentration is based on the existence of a polyanionic negative charge on the halloysite surface and on the alginate polysaccharide (Wong *et al.*, 2002). Increasing the solid concentration results in an increase in viscosity due to the repulsion between like charges. Coating the halloysite with the cationic surfactant causes a neutralisation of the negative charge on the clay mineral surface. Consequently a reduction in particle repulsion allows the sample to flow more easily, the resulting rheological profile shape being dictated by the presence of the surfactant rather than solid content as is the case for the halloysite containing sample.

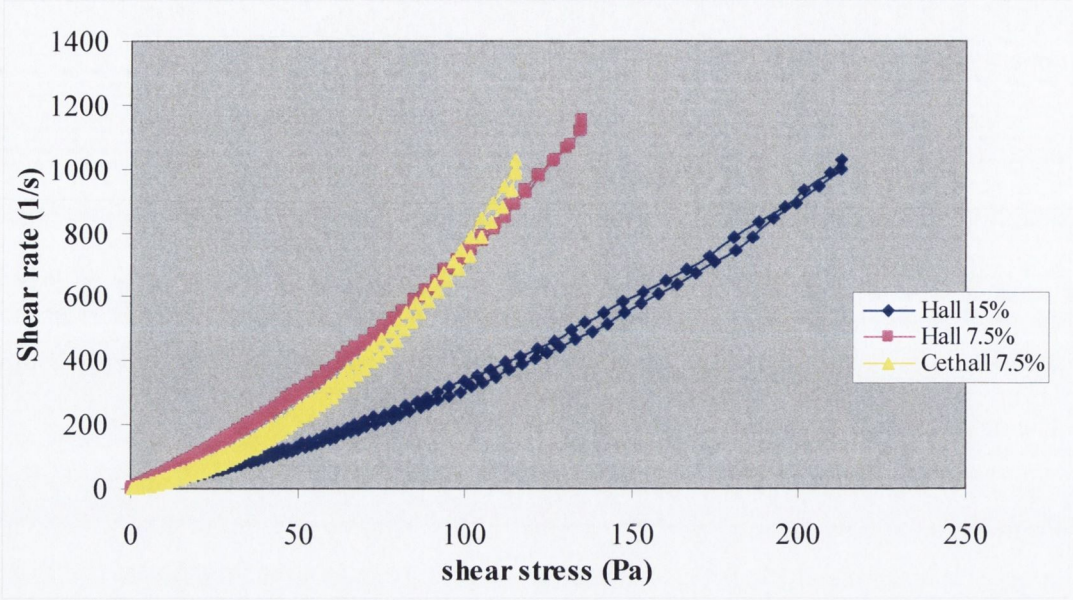

Key: hall= halloysite; cethall=cetrimide coated halloysite.

Figure 7.5.4c Rheological examination of formulations for pellets containing halloysite at a concentration of 7.5% or 15% w/w and also of cetrimide halloysite, 7.5% w/w.

As noted earlier, it was increasingly difficult to extrude the final portion of the sample from the syringe. This was especially so in the case of the cetrimide coated sample. However, as the viscosity was lower compared to the uncoated halloysite samples, the difficulty was attributed to the entrainment of air in the sample during the shearing process due to the presence of the surfactant. The air bubbles could cause an increase in apparent viscosity analogous to the effect of increased phase volume in an emulsion. This would manifest as an increased resistance to flow.

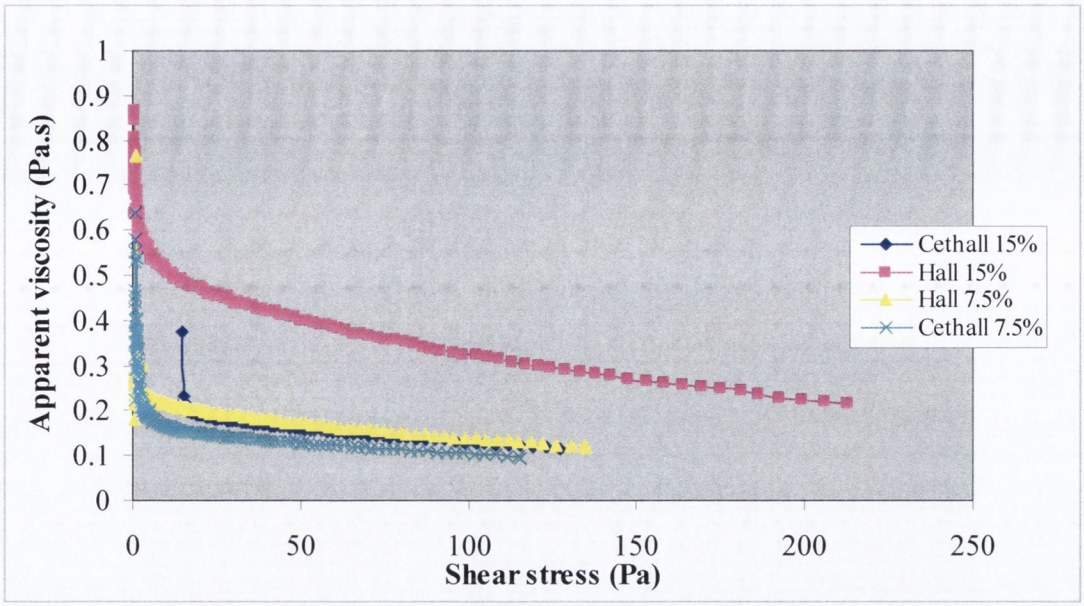

Key: cethall = cetrimide coated halloysite; hall = halloysite.

Figure 7.5.4d Apparent viscosity of formulations for pellets containing halloysite and cetrimide coated halloysite at concentrations of 7.5% and 15% w/w.

7.6 BEAD CHARACTERISATION

7.6.1 Introduction

The morphology and the characteristics of non-drug beads produced in the study were investigated using a number of techniques. The aim was to find an optimum formulation in order that metronidazole could be incorporated in the formulation. It was hoped that the optimum formulation would produce spherical beads that were uniform in size and shape. It was also desirable that the beads would display a highly absorbable capacity and not disintegrate too readily. The beads prepared using the specific formulations outlined in Table 7.5.3 were examined qualitatively and quantitatively using a number of techniques. The bead surface and size was examined using SEM analysis. The sphericity was investigated using Winseedle® software. The physical nature of the beads was analysed using skeletal density, surface area studies and swelling studies.

7.6.2 Surface Area and Skeletal Density Analysis

A wealth of literature exists on the production of calcium alginate pellets using various modifications of the basic procedure of sol-gel transformation of alginate (Wong *et al.*, 2002). This is brought about by the cross-linking of the polyanionic alginate with divalent cations, such as Ca^{2+} and Zn^{2+} (Aslani and Kennedy, 1996). The linear polycationic copolymer, chitosan, has also been used for ionotropic gelation. The resulting beads are characterised primarily using drug release, encapsulation and swelling studies (Murata *et al.*, 1996). Other techniques such as DSC and FTIR have been used also (Kulkarni *et al.*, 2001). Little focus has been placed on bead density and surface area despite the importance of the concepts. Surface area calculation is important in this study for a number of reasons. It provides information on bead structure (porosity) in tandem with other techniques such as skeletal density and qualitative methods like SEM. Also it is an indication of the potential of the sample to adsorb toxins and absorb exudate from a wound.

Figure 7.6.2a is a depiction of the surface area and skeletal density of the samples outlined in Table 7.5.3a. The standard deviations were too small to be displayed in Figure 7.6.2a. As outlined in Section 3.15.3, the surface area of the beads was determined based on the volume of nitrogen adsorbed per unit weight of beads at varying pressures. The characteristics for cetrimide halloysite 7.5% prepared by air-drying were not determined due to a lack of adequate resolution in the instrument used. Despite a degassing period of 6 days, it was not possible to calculate the surface area because the sample did not reach equilibrium. If the surface area of the formulations is firstly considered, it is quite obvious that the surface area of the halloysite 7.5% beads irrespective of drying method is considerably lower than that of other formulations. This is due to the relative decrease in halloysite concentration, which has a high surface area of 55.98 +/- 0.46 m^2/g as determined in Chapter 4. Each formulation was brought to final weight using water. However this cannot account for the fact that the cetrimide coated halloysite sample did not have a similarly low surface area. The surface area of pellets produced using this formulation is 14.42 +/- 0.02 m^2/g, this value is approximately 38 times that of the equivalent uncoated sample, which has a value of 0.40 m^2/g and it is approximately 11 times the value of the oven dried, uncoated sample (1.26 m^2/g). The presence of the surfactant in the system reduces the surface tension and increases particle wetting of the formulation. This helps to provide a better entanglement of formulation components. It may also be responsible for air entrainment in the formulation during the homogenization

step. This air entrainment leads to the development of an extensive pore network formation throughout the bead as the samples are dried. This is especially true in the freeze-dried sample because it is likely that water will fill some of the air pockets. This water turns to ice during the immersion step in liquid nitrogen, it is then removed during the freeze-drying process.

The extent of the differences between samples at the higher halloysite concentrations was considerably reduced. This highlights the importance of solid concentration on the surface area of the bead. The surface area of the uncoated bead dried using the freeze-drying method is greater than that prepared using the air-oven drying method. However this observation is reversed in the case of the samples which were prepared using cetrimide coated halloysite. It is not surprising that the uncoated halloysite 15% sample had the highest surface area. It too was the most viscous formulation, Section 7.5.4. This was explained due to the repulsion between the polyanionic charges of the respective components. This repulsion may be responsible also for the development of pores between the components resulting in an increased surface area value.

The importance of drying method is depicted in Figure 7.6.2a. The uncoated sample at higher solid concentrations has a higher surface area due to the freeze-drying method. Prior to drying the sample is frozen using liquid nitrogen, this causes the water in the sample to turn to ice. During the freeze-drying process the ice is removed by sublimation and voids in the sample remain. The result is reversed for the cetrimide coated sample, as perhaps the drying method is not as crucial to pore formation because the surfactant plays this role. This is evident for the sample prepared using halloysite and cetrimide coated sample prepared at concentrations of 7.5% w/w and dried using the freeze-drying procedure. However as the concentration is increased, the contribution of the solid halloysite to surface area is greater. As the surface area is reflective of the external surface and the surface due to open pores but not closed pores, any deviations might be accounted for by a relative difference between open and closed porosity.

Figure 7.6.2a also depicts the skeletal density of the bead samples. The skeletal density of the beads was determined using helium pycnometry. The values reflect the compositional and closed porosity of the samples (Byrne, 2004). The trend observed for skeletal density is similar to that for surface area with a couple of exceptions. It would be expected that

formulations containing an increased quantity of halloysite would have a higher density value. The magnitude of the differences between samples is not mirrored. The range of values for samples was 1.1692-2.2753 g/cm^3. The freeze-dried halloysite 15% w/w sample also has the largest skeletal density, whilst the sample with the lowest surface area also had the lowest skeletal density.

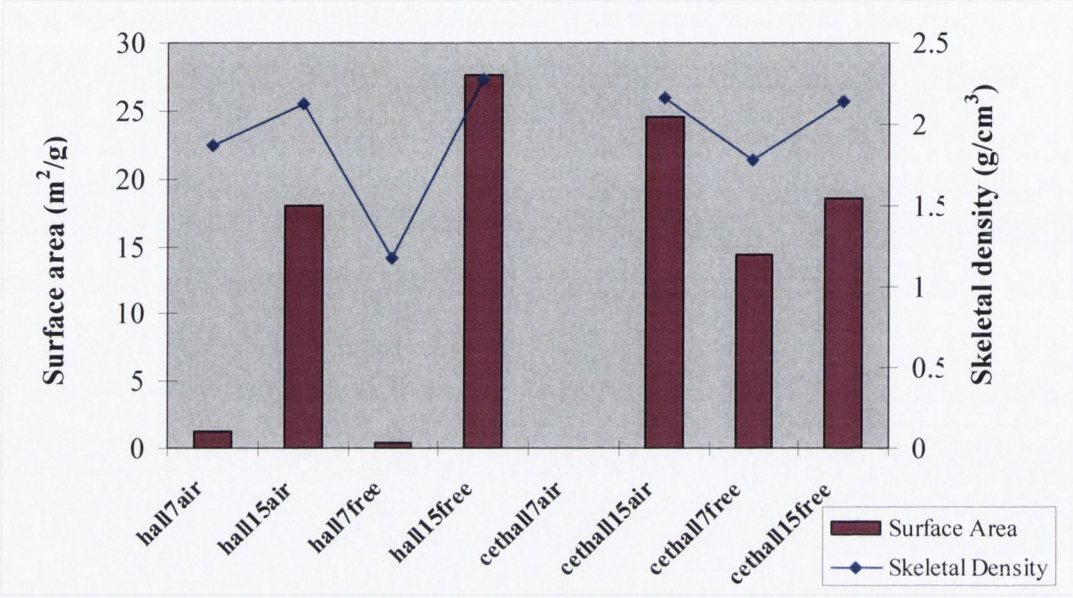

Key: h = halloysite; cethall = cetrimide coated halloysite; 7 = 7.5% w/w halloysite concentration; 15 = 15% w/w halloysite concentration; air = air/oven dried method and free = freeze-dried method.

Figure 7.6.2a Comparison of the surface area and skeletal density of non-drug beads prepared under different drying conditions.

Figure 7.6.2b is an extension of Figure 7.6.2a. The surface area values for each sample formulation are compared based on the grade of halloysite used. A 2 sample t-test for each of the samples groups listed on the x-axis, e.g. 15% air-dried or 7.5% freeze-dried was conducted. It was used to confirm that the grade of halloysite used impacted significantly on the surface area, which is the impression from Figure 7.6.2b. The null hypothesis was tested based on existence of no difference between the mean surface areas values for each of the sample groups. The significance level for the test was 95%. The p values for the 2 sample t-tests were 0.000, 0.000 and 0.002 for the 15% air-dried, 7.5% freeze-dried and

15% freeze-dried sample groups respectively. The surface areas for each of the sample groups were significantly different as the p value was < 0.05 in all cases.

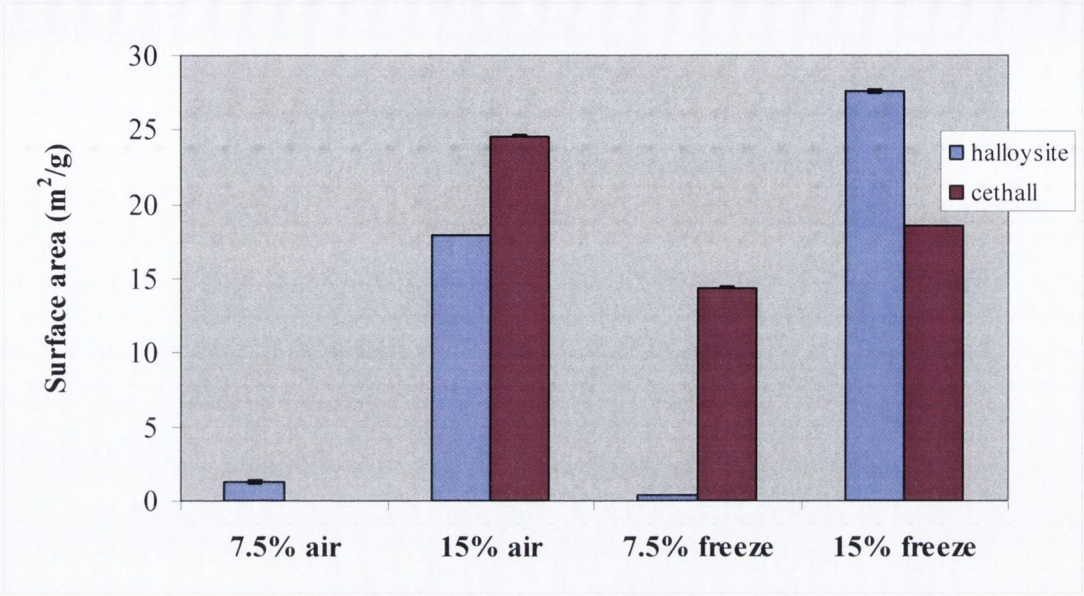

Key h = halloysite; cethall = cetrimide coated halloysite; 7 = 7.5% w/w halloysite concentration; 15 = 15% w/w halloysite concentration; air = air/oven dried method and freeze = freeze dried method.

Figure 7.6.2b Comparison of the surface area of non-drug beads prepared with halloysite and cetrimide coated halloysite and dried using two different methods.

A 2-sample t-test was also conducted on the surface area values for freeze-dried cetrimide halloysite beads. The variable investigated was solid content. The increase in cetrimide halloysite from 7.5% to 15% had a significant effect on the surface area of this sample group. It had a p value of 0.005. The test again had a confidence interval of 95%.

7.6.3 SEM Analysis

The microscopic appearance of the bead formulations was examined using SEM. Figures 7.6.3a-d depict SEM images of the bead formulation containing 7.5% halloysite dried using the air-oven dry method. It can be seen from Figure 7.6.3a that the typical diameter of a bead sample is in the region of 1.5 mm. The surface of the beads at low magnification appears quite roughened but the bead nonetheless has a spherical morphology. The vertical aspect appears elongated; it has a length of 1.4 mm. The bead has a width of 1.3 mm. It is highlighted in Figure 7.6.3a that the sample has fissures on the surface of the bead. These fissures are magnified in Figure 7.6.3b. The fissures are parallel cracks that form a ring around the bead. The ring is not continuous in all cases. This may have arisen due to shearing forces when the bead was extruded from the needle. It might also have formed as the bead dried out and the alginate gel contracted. The rapid loss of water during drying was proposed by Hills *et al.* (2000) as an explanation for crack and fissure formation. The authors proposed air or vacuum drying at low temperatures to overcome this problem. In the present study it was noted that beads were smaller and collapsed if they were subject to a particular drying method immediately after preparation, hence an air drying phase was introduced prior to the oven or freeze-drying methods.

The presence of halloysite can be seen on the bead surface at higher magnification, Figure 7.6.3c. The distinctive tubular structure is evident in clusters and enmeshed with the calcium alginate. The presence of fine pores is also evident. This is expected because beads prepared by the method employed are usually porous (Mukhopadhyay *et al.*, 2005). They appear in a random cluster formation. They are typically less than 0.1-0.2 μm in diameter. The appearance of these pores is further magnified in Figure 7.6.3d.

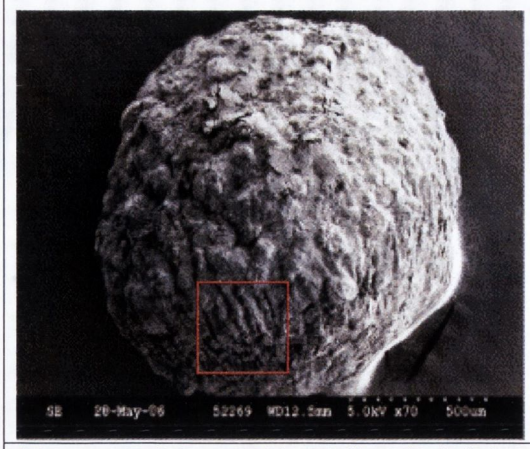

Figure 7.6.3a 7.5% Halloysite/Alginate air-dried. (Magnification x 70)

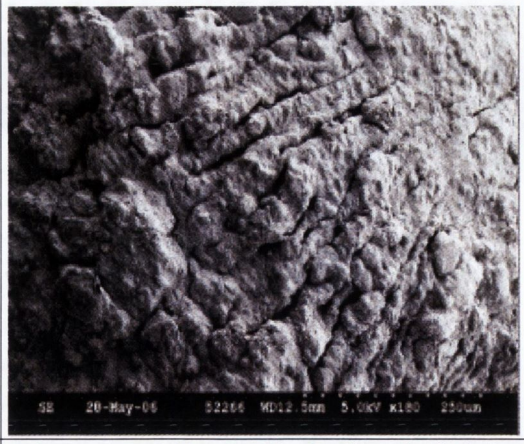

Figure 7.6.3b 7.5% Halloysite/Alginate air-dried. (Magnification x 180)

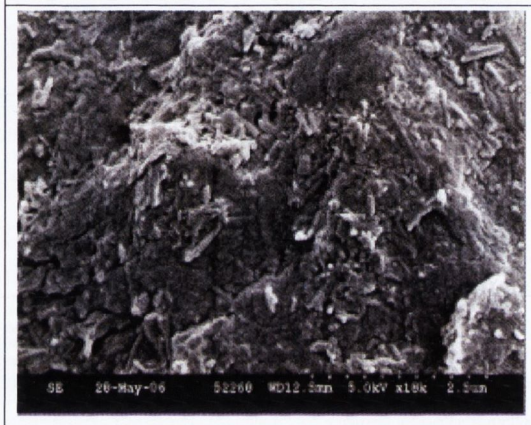

Figure 7.6.3c 7.5% Halloysite/Alginate air-dried. (Magnification x 18,000)

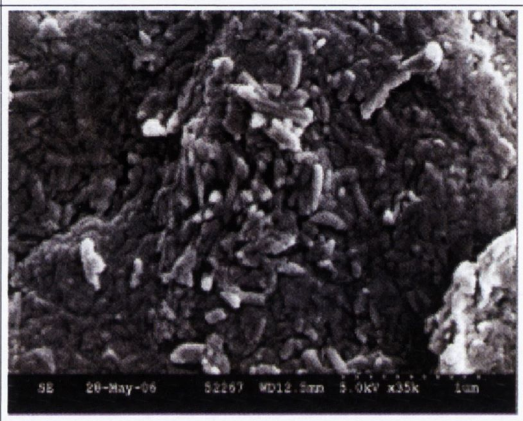

Figure 7.6.3d 7.5% Halloysite/Alginate air-dried. (Magnification x 35,000)

Figure 7.6.3e is a depiction of a bead formulation containing 15%; dried using the air-oven drying method. The presence of fissures observed in Figure 7.6.3b is again evident on the bead surface. The parallel furrows are approximately 400 μm in length. Figures 7.6.3f-h depict SEM images for the 7.5% halloysite, freeze-dried formulation. The diameter of the bead was measured from various points on the circumference of the image. The diameter is in the range 1.43-1.45 mm indicating that it is more spherical than that in Figure 7.6.3a. The presence of pores on the bead surface is just about visible. The existence of pores in this formulation is confirmed in Figure 7.6.3g. They have a diameter range of 1-2 μm, but some larger pores, which are up to 5 μm in diameter, also exist. The pore structure is magnified in Figure 7.6.3h. The appearance of the pores is different to that seen with the air-dried sample. The difference in pore structure is attributable to the freezing of water

crystals in the bead structure prior to drying; this results in relatively larger pores being formed. It can be seen that the pore extends from the surface towards the interior. The pores were produced by a number of mechanisms. The presence of the solid inclusions and also the surfactant led to the entrainment of air bubbles in the formulation during shearing (Byrne, 2004), these factors contribute to pore formation. The viscous nature of the formulations entrapped the air bubbles, which manifest after drying as pores. Bodmeier and Paeratakul (1989) produced chitosan and calcium-alginate pellets by a similar method and made similar observations. Sepulveda and Binner (1999) enhanced porosity in ceramic products by using foaming clay mixtures. This has important consequences for sample wetting and drug release studies because the enhanced pore network will aid the dissolution medium to intrude the bead structure more rapidly.

Figure 7.6.3i is a depiction of the 15% halloysite sample dried using the freeze-drying procedure. The image highlights that there are some undulations on the surface. Pores with diameters up to 2 μm are also present over the surface. It was seen in section 7.6.2 that this sample had the highest surface area and skeletal density. The high solid content of this contributes to the high density. The external surface area of each bead is increased because the beads are larger due to the increase in the content of solid inclusions, however the open pore network leading to the surface also contributes to the surface area. Figure 7.6.3j depicts the surface of a bead prepared using 7.5%, air-dried cetrimide coated halloysite sample. There is no apparent difference due to the presence of the cetrimide coating. The presence of pores on the sample surface is extensive. The formation of the pore network in this sample was enhanced by air entrainment due to the presence of the surfactant. This contributes to increased sample wetting. In tandem with this there is an increase in sample wetting inherent in the formulation that contains the surfactant. The impact of the combined factors on sample wetting is examined in swelling studies in Section 7.6.5.

Figure 7.6.4e 15% Halloysite/Alginate air-dried. (Magnification x 200)

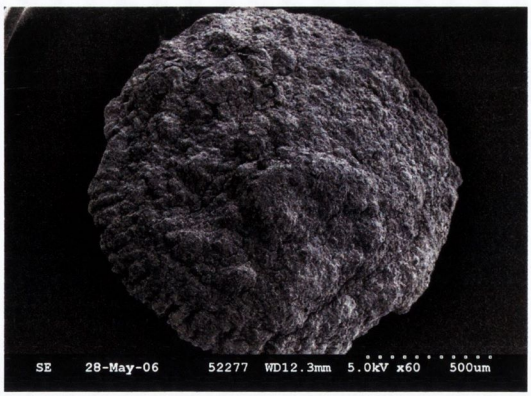

Figure 7.6.4f 7.5% Halloysite/alginate freeze-dried. (Magnification x 60)

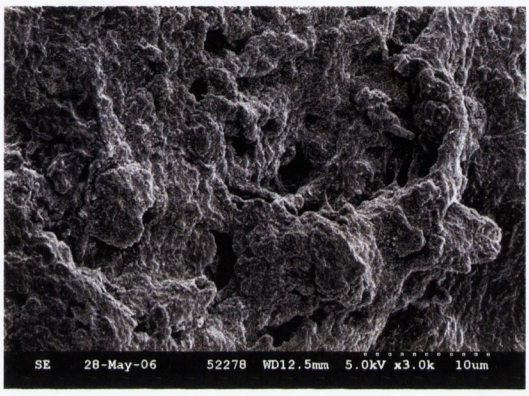

Figure 7.6.3g 7.5% Halloysite/alginate freeze-dried. (Magnification x 3,000)

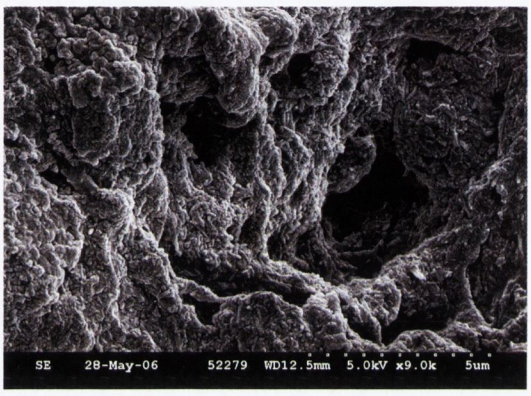

Figure 7.6.3h 7.5% Halloysite/alginate freeze-dried. (Magnification x 9,000)

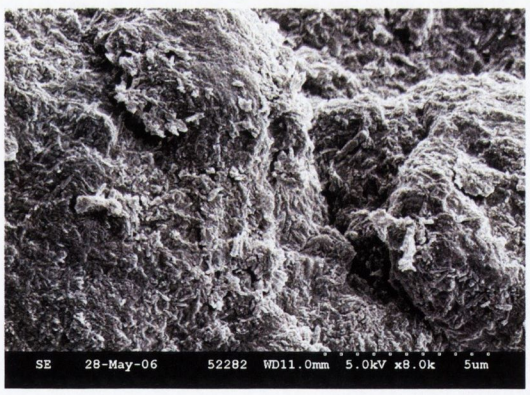

Figure 7.6.3i 15% Halloysite/Alginate freeze-dried. (Magnification x 8,000)

Figure 7.6.3j 7.5% Cet-halloysite/alginate air-dried. (Magnification x 3,500)

7.6.4 Bead Sphericity Analysis

The sphericity of the samples was determined using Winseedle® analysis. A digitised image of the pellets was obtained using a scanner. Using this image the software calculates parameters such as pellet length; width, average curvature and average projected perimeter. The ratio of pellet width to length is used as an indication of pellet sphericity. The closer the ratio to 1, the more the sample approximates to sphericity.

Table 7.6.4a illustrates the length width ratio for the non-drug bead formulations prepared. The presence of a cetrimide coating on the clay causes an increase in sphericity relative to the corresponding uncoated sample, with the exception of the 15% w/w samples that were air-dried. The presence of the cetrimide reduced the surface tension in the sample so the spherical morphology was assumed more readily. However it was observed using rheological evaluation in Section 7.5.4 that the 15% halloysite air-dried sample was the most viscous formulation, whereas the other formulations had similar apparent viscosities. The pellets formed using this formulation were deformed less by air currents as they were discharged from the needle and dropped vertically into the gelation medium and also by viscous drag effects as the samples were stirred in the gelation medium. Hence this sample has a ratio of 0.9411, which is the closest approximation to unity. With the exception of this sample and its freeze-dried equivalent, the freeze-dried samples have lower sphericity indices than the air-dried samples. Freeze-drying the samples involves freezing them in liquid nitrogen prior to the procedure. The bead contains water which contributes to pore formation, this water is removed by sublimation and vacuum effects resulting in beads with a more irregular morphology. However the air-drying procedure, which enabled water loss equally in all directions prior to the final morphological structure being determined, resulted in a more uniform sphere.

Table 7.6.4a Sphericity index of non-drug bead formulations.

Sample	Halloysite	Concentration (% w/w)	Drying method	Average length/width ratio
1	Halloysite	7.5	Air-Oven Dry	0.8421
2	Cet-halloysite	7.5	Air-Oven Dry	0.8944
3	Halloysite	15.0	Air-Oven Dry	0.9411
4	Cet-halloysite	15.0	Air-Oven Dry	0.8834
5	Halloysite	7.5	Freeze Dry	0.8207
6	Cet-halloysite	7.5	Freeze Dry	0.8779
7	Halloysite	15.0	Freeze Dry	0.8407
8	Cet-halloysite	15.0	Freeze Dry	0.8714

7.6.5 Swelling Studies

The aim of this study was to assess the swelling behaviour of non-drug bead formulations. The swelling ability of the beads was assessed in McIlvaine buffer 5.5 as it simulates the likely wound environment better than water. The buffer is also superior to water for the studies because it contains sodium ions. Sodium ions are a primary component of simulated wound fluid (Thomas and Loveless, 1998). The dynamic weight change of the beads with respect to time was calculated according to Equation 3.2 in Section 3.15.4. Figure 7.6.5a illustrates the swelling behaviour of non-drug beads. The samples were examined over 24 hr but had typically reached equilibrium after 6 hr. The bead sample formulated using uncoated halloysite 7.5% and oven dried displayed the greatest increase in weight (395%), followed by oven dried, uncoated halloysite 15% sample (302%). Of the samples which did not disintegrate over the time period, halloysite 7.5% freeze-dried beads had the smallest increase in weight (226%). The freeze-dried samples appeared to float on the swelling medium. This is due to the high degree of porosity in these samples. The water in these samples acted like a pore forming agent which was then removed by sublimation of ice from the frozen samples as the sample was freeze-dried. A porous network remained after the ice was removed (Byrne, 2004). The swelling behaviour is due to the tendency of the beads to absorb water in order to fill the inert pore regions of the polymer network of the dehydrated beads until they reach equilibrium hydrated state

(Hoffman, 2002). Swelling behaviour is influenced by the alteration of the cross-linking bonds associated with the polymer network in the presence of the osmotic pressure of the liquid medium. When these two forces are equal, no further water uptake by the beads is observed (Pasparakis and Bouropoulos, 2006).

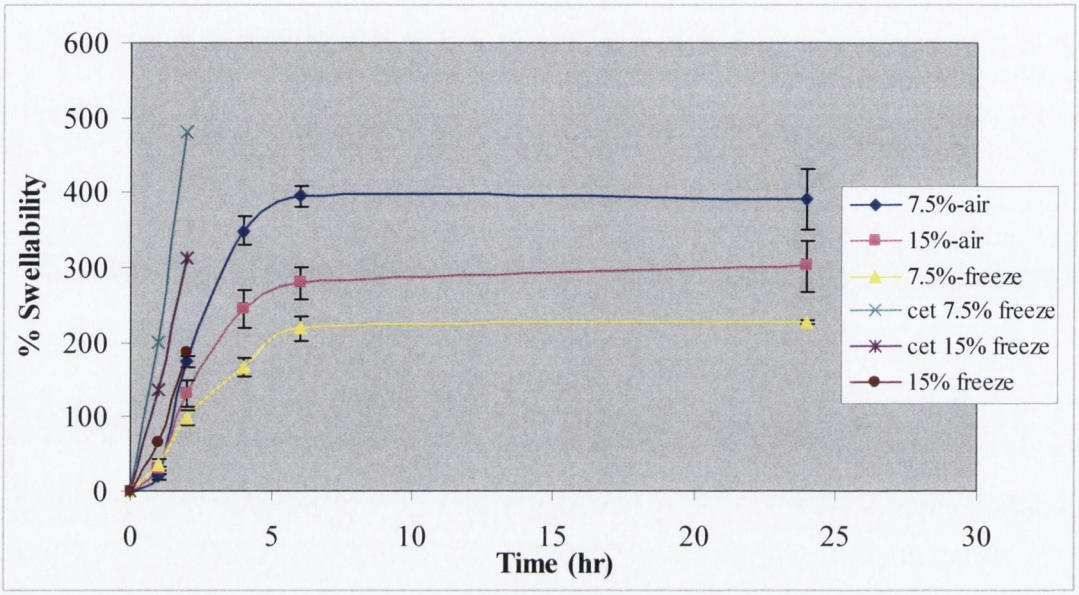

Key: cet = cetrimide coated halloysite; 7.5% = 7.5% w/w halloysite concentration; 15% = 15% w/w halloysite concentration; air = air/oven dried method and freeze = freeze- dried method.

Figure 7.6.5a Swelling ratios of non-drug beads formulated using different quantities and grades of halloysite and dried using two different methods.

Figure 7.6.5a also illustrates swelling behaviour for samples prepared with cetrimide coated halloysite. Despite relatively rapid disintegration, the rate and extent of swelling was greater in the case of the cetrimide coated samples (cetrimide coated halloysite samples 7.5% and 15%, dried using the freeze drying procedure) displayed in Figure 7.6.5a. The swelling of cetrimide coated halloysite, 7.5% sample prepared by freeze-dying displayed the greatest increase in swelling behaviour after two hours (483%). This compared to 174%, at an equivalent time period for the halloysite 7.5% sample, which displayed the greatest increase in volume per weight of the intact samples. The cetrimide coated samples were more fragile and disintegrated during handling. They remained intact in the buffer medium but on contact and gentle blotting of the excess medium, they broke

up. It was expected that the presence of the surfactant would increase sample wetting and hence sample disintegration. The air-dried cetrimide coated samples also disintegrated rapidly; the swelling values are not depicted.

Figure 7.6.5b depicts the swelling behaviour of air-dried beads containing halloysite 7.5% and coated with Eudragit® E PO. The swelling profile is different to that observed for those samples in Figure 7.6.5a. Over the initial two hr period the weight only increases by a mere 17%. The weight increases to 191% after 6 hr and peaks to 307% after 24 hr. The coating material covers the pores and fissures, thus reducing buffer imbibition. The bead begins to swell as the medium permeates the coating and reaches the interior of the bead. The methacrylic acid copolymer is soluble in media up to pH 5; above this value it is expandable and permeable (Röhm Pharma).

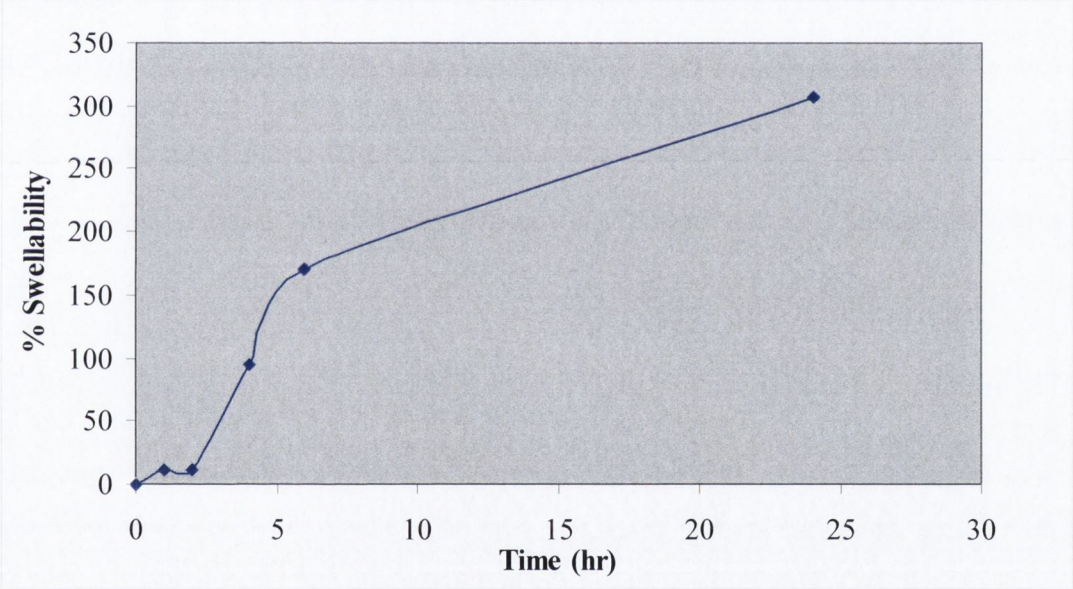

Figure 7.6.6b Swelling ratio of non-drug beads formulated to contain halloysite 7.5% w/w, air dried and coated with Eudragit® E PO.

7.7 PREPARATION AND CHARACTERISATION OF METRONIDAZOLE BEADS

7.7.1 Introduction

Calcium-alginate beads devoid of active drug were characterised in Section 7.6. The study was undertaken to ascertain the optimum conditions for bead formulation. The halloysite grade was used for the preparation of metronidazole containing beads as the cetrimide grade disintegrated too rapidly despite displaying enhanced swelling characteristics. It was decided to include halloysite at a concentration of 7.5% w/w because this formulation produced the optimum increase in weight during the swelling studies conducted in Section 7.6.5. It also displayed a low surface area but a high density, Figure 7.6.2a. This indicated it had a high halloysite content, which existed as part of a closed pore network which contributed to the high particle density but relatively low surface area. This is important from an absorption perspective. The low external surface area implies that there will be a relatively slower release of the active compared to samples with high external surface areas. The samples were prepared using the air/oven drying method as the samples produced using this method were less brittle than those prepared by the freeze-drying method.

Preliminary experiments involved the production of beads using halloysite that had been loaded with metronidazole using different vehicles. The release profiles for the metronidazole loaded halloysite grades were examined in Section 7.3. However due to the poor encapsulation of metronidazole, the small quantity of metronidazole present had leached out during the preparation. It was decided to prepare metronidazole beads, which incorporated the raw drug dissolved in the alginate halloysite system. The formulation of drug loaded samples was also subject to some modification. Four sub categories were considered. The first section examines the production of beads using needles of two different external diameters. The impact of solution thermodynamics is also investigated. The second category examines the coating of bead samples with some coating materials. Category three shows the effect of a change in the gelation medium used to cross-link alginate/halloysite/drug complex. The use and the incorporation of chitosan in formulations is considered in the final category.

Beads were produced using halloysite 7.5% w/w and were air/oven dried. The samples were produced using a needle with an external diameter of 0.8 mm, the needle was coloured green and it was referred to as "green needle" in the study. All the samples were produced using a green needle unless otherwise specified. The metronidazole concentration in the final formulations was 2% w/w. This formulation was used as a reference, to which all others were compared. The concentration was increased to a level above the saturation solubility because the metronidazole content in previous samples prepared with a concentration of 1% w/w was found to deplete considerably during the preparation process. It was postulated that the thermodynamics were unfavourable during the gelation process because the $CaCl_2$ solution had a volume of 50 ml. This large volume acted as a release medium for metronidazole from the concentrated environment of the bead. It was found that increasing the metronidazole concentration above the saturation solubility together with decreasing the rate and duration of agitation minimised the problem of metronidazole depletion.

7.7.2 Formulation Variables

7.7.2.1 Introduction

As noted above the samples were produced using a needle with an external diameter of 0.8 mm. The size of the needle orifice impacts on the size of the bead diameter and hence on the surface area. The surface area has consequences for sample release. Beads were also prepared using a needle with a smaller external diameter of 0.5 mm. These samples are termed "orange needle". The impact of needle bore diameter on bead morphology was considered initially when it became increasingly difficult to extrude some of the formulations. It was thought that some formulations were too viscous to be produced using particular needle sizes. This prompted rheological evaluation of bead formulations, the results of which are discussed in Section 7.5.4.

Metronidazole was included at a concentration above its saturation solubility to rectify the problem of metronidazole depletion in the gelation medium. It was decided to investigate the presence of metronidazole in both the alginate/halloysite dispersion and in the gelation medium. The aim was to ascertain if the presence reduced the movement of metronidazole due to an inequilibrium between the halloysite/alginate complex and the gelation medium.

7.7.2.2 Needle Orifice Diameter

The release profile for the reference sample, titled "green needle" is depicted in Figure 7.7.2.2. Release is almost complete by the 1 hr time period, 89% of the encapsulated active had been released. The samples had disintegrated by the 6 hr time period, however fragments of the beads were still visible in the basket apparatus. It was thought that the agitation, at a rotation speed of 50 rpm was too vigorous. However, this level of agitation would not be encountered in a wound environment, hence the samples would not disintegrate as quickly. The encapsulation of metronidazole for the green needle formulation is displayed in Table 7.7.2.2. The bead formulation encapsulated 5.94 +/- 0.03 g of metronidazole per 100 g of bead formulation. This represents a significant improvement in encapsulation potential compared to the loading and spray-dry methods. As elucidated in Section 3.14.1 the beads were produced using a needle attached to a syringe. The pointed tip of the needle allowed the production of droplets with a narrow size distribution (Byrne, 2004; Buchmuller and Weyermans, 1989; Knoch, 1994).

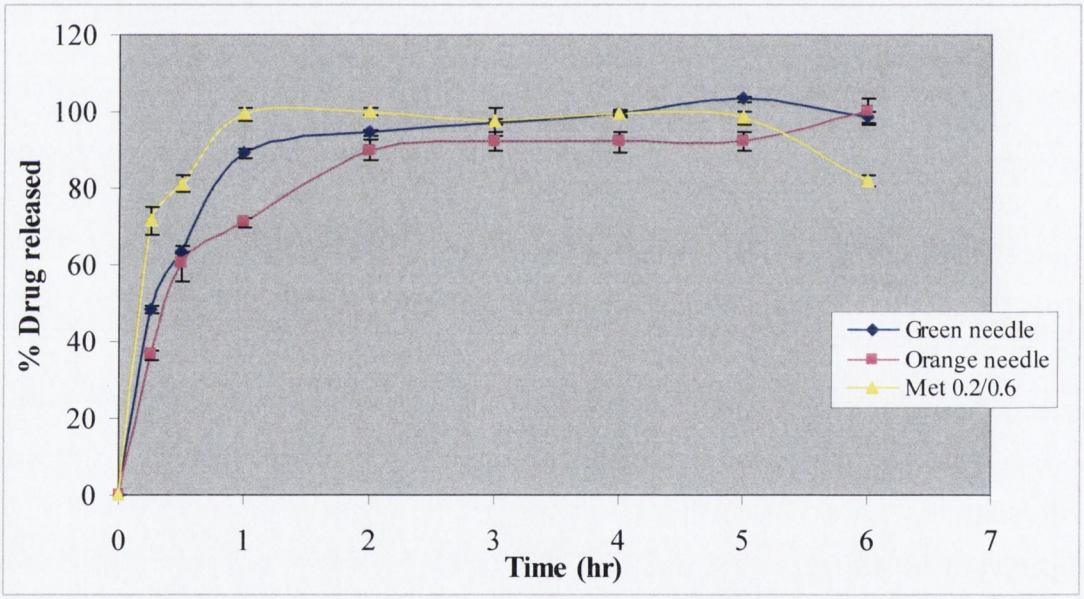

Figure 7.7.2.2 Metronidazole release from bead formulations produced using different needle diameters and metronidazole concentrations.

Beads were also produced using a needle with a smaller exterior diameter than the green needle that was employed to produce the remaining formulations. The exterior diameter of the needle used to produce the sample referred to as "orange needle" was 0.5 mm, this was measured using a micrometer. The resultant sample had a smaller bead diameter. This was

not surprising, as it would be expected that a reduction in needle diameter would produce a smaller droplet size. The droplet size is an important determinant of the final bead size (Byrne, 2004). Other authors found that changing the orifice size had similar effects on particle diameter (Buxton and Peach, 1984; Buchmuller and Weyermanns, 1989; Chong-Kook and Eun-Jin, 1992).

The release profile for the sample titled "orange needle" is evident in Figure 7.7.2.2. The particle size of the orange needle sample is decreased compared to that produced using the green needle; the diameter of a random sample of each type was measured with a ruler. Consequently the surface area per unit weight would increase. The ramifications for a larger surface area are an increase in active release. However, the release rate decreased. The orange needle formulation displayed 71% release after a 1 hr period, this rose to 89% after 2 hr. The release is less than the 89% and 94% observed for the green needle sample at equivalent time points. The narrower orifice produces beads subject to relatively higher shear forces; this may lead to a decrease in sample porosity. This manifests as a decrease in the rate of release. The % encapsulation for the "orange needle" formulation is 4.49 +/- 0.14% w/w, Table 7.7.2.2. This value is less than that for the "green needle" formulation. This is attributable to the smaller droplet having an decreased surface area available for cross-linking resulting in a decreased encapsulation. The contribution of the matrix is decreased with time and the release profiles appear approximately similar.

Table 7.7.2.2 Encapsulation efficiency of metronidazole in bead formulations.

Sample	Encapsulation efficiency (% w/w)	St. dev. (+/-)
Green needle	5.74	0.03
Met 0.2/0.6	3.24	0.03
Orange needle	4.49	0.14

7.7.2.3 Metronidazole Concentration

The effect of metronidazole concentration in the bead formulation was further investigated by adding metronidazole to the alginate complex at a concentration level equivalent to its saturation solubility. Metronidazole was also added to the gelation medium, at a concentration slightly in excess of its saturation solubility. The intention was to create an

equilibrium in the thermodynamics between the two systems during the complexation procedure. The release profile for the sample is depicted in Figure 7.7.2.2. The sample is referred to as Met 0.2/0.6, this is indicative of the quantity of metronidazole (0.2 g) in the halloysite/alginate complex and the 0.6 refers to the quantity of metronidazole (0.6 g) in the gelation medium. The profile indicates that the release rate is higher for this sample; this is to be expected as the overall drug concentration was doubled. There was an increased possibility of drug deposition at the surface, resulting in an augmentation of the burst release effect. After a time period of 1 hr, 99% of the active was released, this compared to 89% for the "green needle" sample at an equivalent time period.

This method of production resulted in an encapsulation of 3.24 +/- 0.03 % w/w. This value is less than that of the reference sample. It is suggested that the presence of metronidazole in the gelation medium reduced the activity of $CaCl_2$ in the formulation; hence the encapsulation was less efficient. It may have shielded the electrostatic attraction between the polyionic substances or it may have complexed to some extent with the calcium ions, thus reducing the polycation availability for matrix formation.

7.7.3 Sample Coating

7.7.3.1 Introduction

Coating is a commonly encountered process in drug delivery especially oral drug delivery. Possible applications include taste masking, component stability and the controlled delivery of the active constituent. It is the latter function that is considered here. The halloysite/alginate/metronidazole bead complex referred to as "green needle" resulted in 89% release after 1 hr. The bead complex conferred an improvement in metronidazole encapsulation but not with regard to modulation of metronidazole release. The aim of this section was to control the release of metronidazole by coating beads produced using a number of established coating materials. However it would be expected that the procedure might contribute to the burst release effect as some of the active is dissolved and released during the coating procedure, it may become entrapped in the sample coating resulting in a contribution to the burst release effect. It may also weaken the coating on the sample. The coating process may also result in a decrease in % encapsulation due to the release from the bead during the coating process. The release of metronidazole from coated formulations is compared to the green needle formulation in Figure 7.7.3.2.

7.7.3.2 Eudragit® E PO

The effect of coating the sample with the methacrylic acid copolymer, Eudragit® E PO is first considered. The release profile is depicted in Figure 7.7.3.2a. The rate and quantity released are less for the coated sample. The % active release for the Eudragit coated and uncoated sample were statistically analysed at each time point using a t-test, with a significance level of 0.05. The % release for the samples is significantly different at all time points except for the 1 hr time period. After 1 hr, 89.13% and 80.9% of the active has been released from the green needle and Eudragit® coated samples respectively. After the 6 hr period of analysis, 84% of the active had been released, this compares to 100% release for the green needle sample over the same time period. The nature of the Eudragit® material was alluded to in Section 7.6.5, in which the swelling behaviour of a coated bead was examined. The coating material resulted in a lag phase in the swelling profile. The Eudragit® material is soluble up to pH values of 5; above this value it is permeable and expandable (Röhm Pharma). These features help modulate the release from the bead. However it is possible because the pH of the buffer is close to 5, that some of the coating material is soluble. A mixture of coating materials, with varying solubility characteristics at other pH levels, such as Eudragit® S could be beneficial. It is soluble at pH values greater than 7 (Röhm Pharma). The % encapsulation is decreased to 5.4% compared to 5.94% for the reference "green needle" sample, Table 7.7.3.2. This is attributable to release of some of the active during the coating process.

SEM analysis conducted on pellet formulations in Section 7.6.3 revealed the presence of pores and fissures on the bead surface. It was also evident from Figure 7.6.3h that these pores were not just confined to the surface but protruded from the interior. The cluster arrangement of these pores results in a complex matrix formation on the interior. It is by this network that liquid medium may intrude, with the result that the bead hydrates and swells. However, by covering the exterior of the bead with a coating material, these pores and fissures become occluded and the inlet possibility for liquid media is reduced.

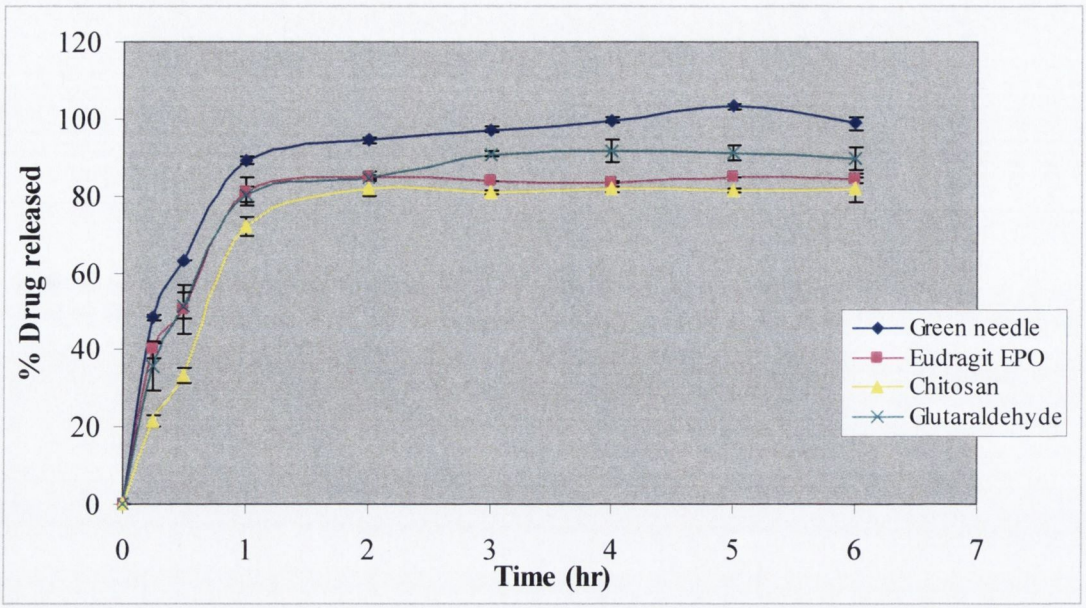

Figure 7.7.3.2 Metronidazole release profiles from reference bead sample and coated samples.

Table 7.7.3.2 Encapsulation of metronidazole in the reference bead formulation and in bead formulations coated using a number of coating materials.

Sample	Encapsulation (% w/w)	St. dev. (+/-)
Eudragit® EPO coated	5.4	0.17
Chitosan coated	5.5	0.16
Glutaraldehyde coated	4.19	0.02
Green needle	5.94	0.03

7.7.3.3 Glutaraldehyde

The second substance employed is the cross-linking agent, glutaraldehyde. Levis (2000) employed glutaraldehyde to control the release of diltiazem hydrochloride from modified halloysite. He observed that an optimum concentration existed for obtaining controlled release of the formulation. Doubling the concentration from 10 to 20% w/w resulted in a rigid structure, which failed to retard drug release. Glutaraldehyde is biodegradable, but also serves as a good cross-linking agent (Lee *et al.*, 1981). Sriamornsak *et al.* (2005) employed glutaraldehyde at a concentration of 2% v/v to harden calcium pectinate beads

and prolong the release of metronidazole from the matrix. The release profile for the glutaraldehyde coated sample, Figure 7.7.3.2a overlaps that of the Eudragit® coated sample up to the time period of 2 hr, beyond this release continues to increase with 91.6% released over the analysis period. Coating the bead with the cross-linking agent, glutaraldehyde did not appear to confer any advantage on the release profile. A large alteration in the burst release for this formulation and Eudragit® coated sample relative to the reference sample was not observed, this may be due to the dissolution of some of the active during the coating process. Hence, some of the active is incorporated at the surface; it is rapidly released and contributes to the burst release effect. The method resulted in an encapsulation of 4.19 +/- 0.02% w/w, Table 7.7.3.2.

7.7.3.4 Chitosan

The use of the polycation, chitosan, as a coating material affected the greatest control of metronidazole release. Statistical analysis of metronidazole release from the green bead and chitosan coated formulation was conducted using the t-test method. A 95% confidence interval for differences in means of the % released for each formulation at all time points was used. The % release from the samples was calculated to be significantly different at all time points. Coating with a chitosan solution of 0.8% w/w resulted in a decrease in the burst release effect, Figure 7.7.3.2a. After 0.25 hr release from the chitosan coated sample was 21.6% compared to 48.4% for green needle sample. The % release at the 1 hr time period was 33.3 for the coated sample and 63.2 for the reference sample. Release from the coated sample was 81.6% over the time interval examined.

7.7.4 Gelation Medium

7.7.4.1 Introduction

Drug alginate matrices are prepared by spraying or dropping an alginate drug aqueous dispersion into a bath of calcium chloride (Aoki, *et al.*, 1993; Aslani and Kennedy, 1996; Kikuchi *et al.*, 1997). This was the approach employed to produce beads in this Chapter. However modifications were considered as the method used did not result in adequately controlled drug release. The cross-linking of alginate and calcium entraps the active but it can also encapsulate $CaCl_2$. This can make the beads hygroscopic (Mukhopadhyay *et al.*, 2005) which has implications for bead stability.

7.7.4.2 Incorporation of Glutaraldehyde in the Gelation Medium

The role of the cross-linker, glutaraldehyde in the gelation medium was also assessed. It was included at a concentration of 10% v/v. The release profile for the sample illustrated in Figure 7.7.4.2 is similarly shaped to that for the reference sample. It did not confer an improvement in release modulation; there is evidence of an enhanced burst release effect. The % release at a time period of 0.25 hr is 61.5, this is significantly greater than the 48.4% attributable to the reference sample, "green needle" at the same time point.

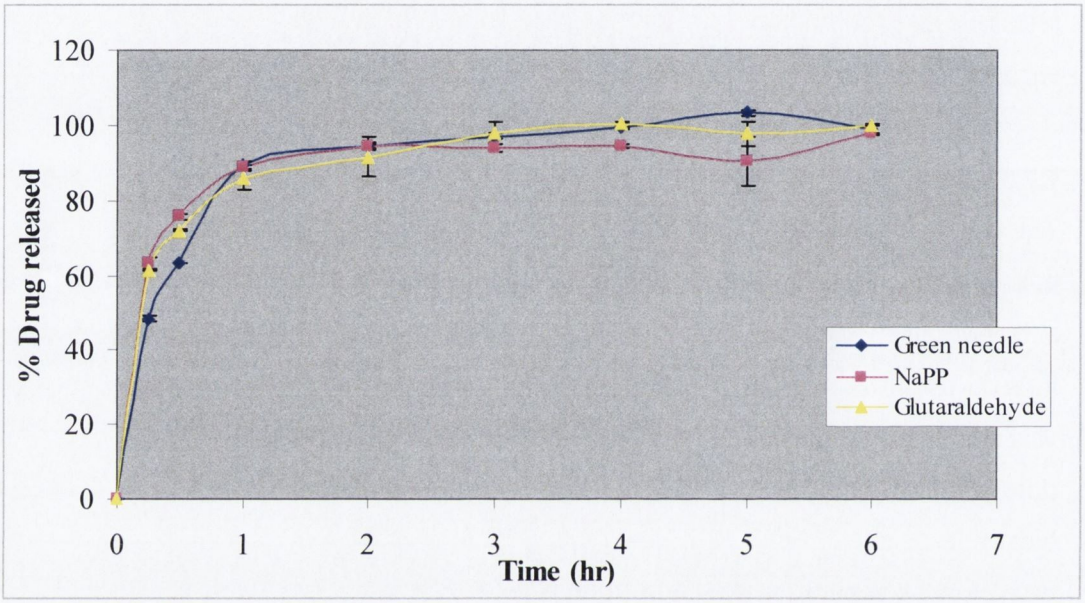

Figure 7.7.4.2 Metronidazole release from beads produced using different gelation media.

The encapsulation of metronidazole in formulations with different gelation media is depicted in Table 7.7.4.2. The encapsulation of metronidazole decreased as a result of the inclusion of glutaraldehyde in the medium (3.24 +/- 0.03% w/w). The encapsulation is less than that observed for the glutaraldehyde coated sample (4.19% w/w), Table 7.7.3.2. This indicates that the glutaraldehyde medium is less effective at encapsulating metronidazole compared to the reference formulation.

Table 7.7.4.2 Encapsulation of metronidazole in bead formulations, expresses as a % of metronidazole release per 100 g of bead formulation.

Sample	Encapsulation (% w/w)	St. dev. (+/-)
Glutaraldehyde	3.24	0.03
Green needle	5.94	0.03
NaPP	4.88	0.14

7.7.4.3 Increasing Concentration of Sodium Polyphosphate (NaPP) in the Gelation Medium

The effect of increasing the concentration of the polyanion sodium polyphosphate (NaPP) from 0.5 to 2.5% w/w was investigated. NaPP was included in the complexation system in all formulations. It was increased here to ascertain if the polyionic cross-linking process could be enhanced. Polyphosphate is frequently employed in bead preparation (Shu and Zhu, 2000). These authors noted that its use with chitosan resulted in beads with a reduced mechanical strength, which limits the use of this combination pharmaceutically. Films cross-linked with triphosphate (tripolyphosphate) and calcium chloride were found to be insoluble but permeable to water vapour. Drug permeability varies with pH and the extent of cross-linking (Remunan-Lopez and Bodmeier, 1997).

The presence of the NaPP does not improve the sustained release capacity of the formulation; the release profile is similar to that for gelation modification due to the presence of glutaraldehyde, Figure 7.7.4.2. It also has an enhanced burst release effect compared to the green needle sample. The % release is equivalent and 97.7% is released over the time period. This is not significantly different from the reference sample value of 100%. However it should be noted from Table 7.7.4.2 that the presence of NaPP resulted in an increase in encapsulation, 4.88 +/- 0.14% w/w compared to the samples prepared using glutaraldehyde. However the encapsulation was less than that observed with the reference "green needle" formulation.

7.7.5 Chitosan Containing Formulations

7.7.5.1 Introduction

Chitosan is used either as a means of coating alginate beads in order to alter the diffusion rate of the encapsulated substances (Anal *et al.*, 2003) or as an additive for the bulk modification of the bead's structure (Lin *et al.*, 2005; Gotoh, *et al.*, 2004). The interaction between chitosan and alginate has been exploited to produce different biomaterials in the form of microcapsules, hydrogels, films, sponges and foams (Polk *et al.*, 1994; Liao *et al.*, 2005; Lai *et al.*, 2003). Alginate chitosan beads are prepared by ionic interaction between the carboxyl residues of alginate and the amino terminals of chitosan. Complexation of alginate with chitosan reduces the porosity of the alginate beads and decreases the leakage of the encapsulated drugs (Sezer and Akbuğa, 1995; Huguet *et al.*, 1996). In addition, chitosan acquires a higher level of mechanical strength with the support of the alginate gel mass (Wong *et al.*, 2002). Murata *et al.* (1993) treated alginate beads with chitosan in order to overcome gel erosion problems associate with sodium alginate beads. The authors found that chitosan suppressed the gel erosion of alginates.

7.7.5.2 Preliminary Studies

The bead formulations in this Chapter were produced using a dropping method. The gelation medium used was again varied. In this section chitosan and calcium chloride was the medium chosen. Chitosan was prepared as a 1% w/v solution and was further diluted to produce the requisite concentration. It was found that a chitosan concentration of 1.0% w/v was too viscous. This was deduced from the resultant morphology of the beads. The approximately spherical bead was dropped into the medium and its morphology was altered as it was agitated in the chitosan solution. The viscous solution created a drag effect; the resultant bead morphology had a characteristic comet appearance. Half the bead was spherical; the other was roughly cone shaped. It was the intention to optimise the concentration of chitosan in the gelation medium without adversely affecting the spherical morphology of the bead. Hence it was deemed necessary to conduct rheological evaluation on chitosan solutions.

7.7.5.3 Rheological Evaluation of Chitosan Solutions

Rheograms for chitosan solutions with concentrations of 0.2, 0.6 and 1.0% w/v are illustrated in Figure 7.7.5.3. It can be seen from the rheological depiction for lowest chitosan solution concentration (0.2% w/v) that the flow curve is approximately linear (R^2 = 0.9887). This is indicative of a Newtonian substance with a constant viscosity under the experimental conditions examined. As the concentration increased from 0.2 to 0.6 and finally to 1.0% w/v the linear appearance was less pronounced. The R^2 values were 0.9646 and 0.9465 for the 0.6 and 1.0% w/v concentrations respectively. This corresponds to an increase in pseudoplastic behaviour. The apparent viscosity for the solutions at an approximate shear rate value of 1000 s^{-1}, increases from 13.80 to 43.76 and finally to 81.80 mPa.s as the concentration of chitosan increases from 0.2 to 0.6 and finally 1.0% w/v. It was decided that concentrations of 0.6 and 0.8% w/v would be employed for the gelation medium because the 1.0% w/v sample was too viscous.

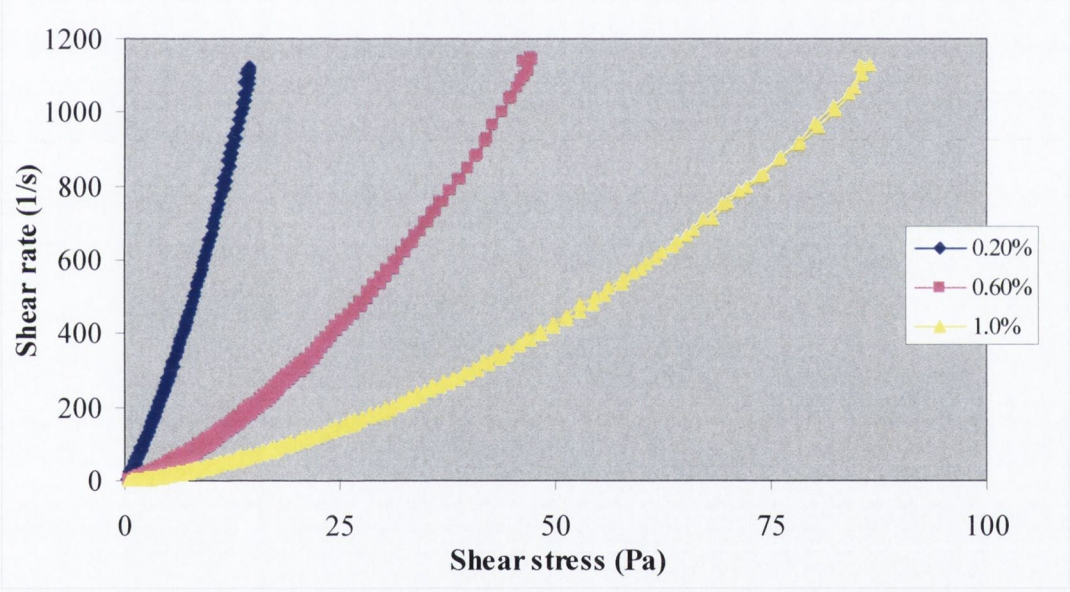

Figure 7.7.5.3 Rheological profiles of different concentrations of chitosan solutions.

7.7.5.4 Release Profiles

The role of chitosan was examined from two perspectives. Its role as a coating material was elucidated in Section 7.7.3.4. The polycation, chitosan was also used to form the polyionic complex with alginic acid. The effect of its concentration in the gelation medium at two levels 0.6 and 0.8% w/v on its ability to encapsulate and modify drug release were assessed. Chitosan is frequently reacted with sodium tripolyphosphate (NaPP) in the

preparation of beads. However, it was noted previously in this section that the mechanical strength of these chitosan beads is low (Shu *et al.*, 2000). However, NaPP has another function. Due to the adhesive properties of chitosan, the beads tend to agglomerate (Lim *et al.*, 1997; Murata *et al.*, 1999). A solution of NaPP was employed to wash the beads as it hardened the coat and thus prevented the adhesion of beads during drying (Wong *et al.*, 2002). It was considered that this washing process might have leached some of the drug resulting in lower % encapsulation.

It was noted that encapsulation was reduced when chitosan was used as the gelation medium, Table 7.7.5.4. It was possible to produce spherical beads using chitosan at a concentration of 0.8% w/v but not using the higher 1.0% w/v. The production of beads using a chitosan concentration of 0.6% w/v was also assessed. Formulation of beads using chitosan as the gelation medium resulted in a decrease in encapsulation to 2.45% w/w compared to the reference "green needle formulation". The decrease in chitosan concentration further adversely affected the encapsulation. The metronidazole content decreased from 2.45 +/- 0.35% to 1.4 +/-0.1% w/w as the chitosan concentration was decreased from 0.8 to 0.6% w/v.

Table 7.7.5.4 Encapsulation of metronidazole in chitosan bead formulations, expresses as a % of metronidazole release per 100 g of bead formulation.

Sample	Encapsulation (% w/w)	St. dev. (+/-)
Chitosan 0.6%	1.4	0.10
Chitosan 0.8%	2.45	0.35
Chitosan coated	5.5	0.16
Green needle	5.94	0.03

The release profile for the chitosan 0.6% w/v sample is comparable to the reference sample, green needle, except that it has a higher burst release component, Figure 7.7.5.4. After 0.25 hr, 67.7% is released; this is significantly greater than the 48.38% release from the green needle sample. An increase in chitosan concentration to 0.8% significantly altered the release profile. The % released at 0.25 hr dropped to 45.68%, whilst this is comparable to the reference sample it must be noted that the release at the remainder of the

time points is significantly different. At time points of 1, 3 and 5 hr, the % release from chitosan 0.8% is 64.1%, 78.00% and 82.67% respectively. The % release for the reference sample at equivalent times is 89.1%, 97% and 100%. Chitosan alginate beads have smaller pores, which accounts for the retardation of the active through a reduction in diffusion capability. However it is through chitosan coating that the most favorable release profile and encapsulation is achieved.

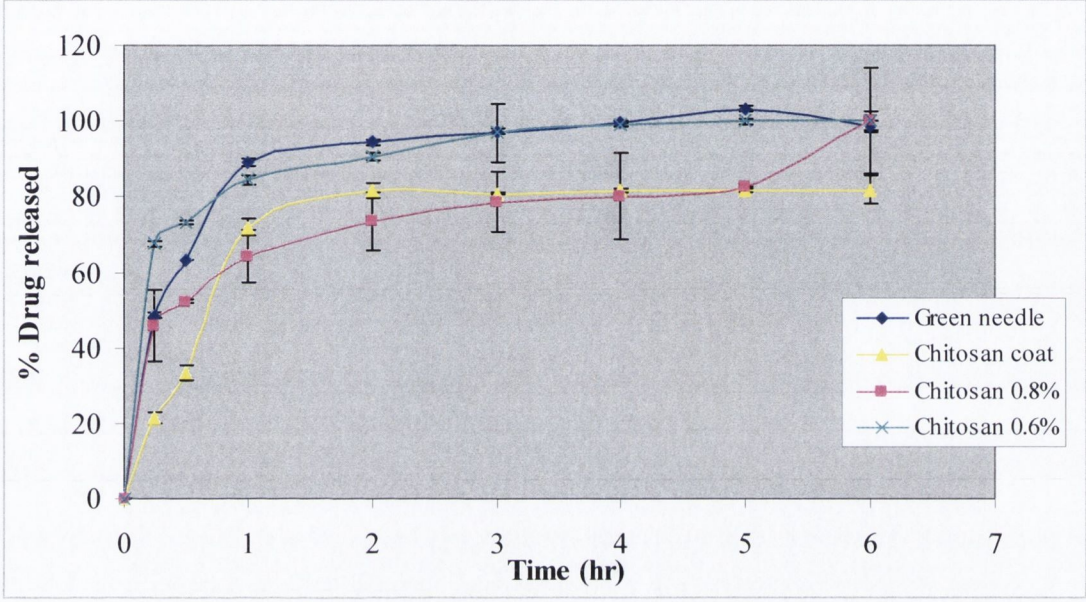

Figure 7.7.5.4 Release of metronidazole from beads formulated with chitosan or calcium-alginate beads coated with chitosan compared to control.

7.8 METRONIDAZOLE RELEASE FROM ROZEX® GEL

A principal treatment available for the topical infections associated with ulcers includes a metronidazole gel formulation. Various proprietary brands exist, the brand considered here is Rozex®, which contains metronidazole at a concentration of 0.75% w/w. It is applied to the wound and covered with a secondary dressing. The type of dressing is dependent on the amount of exudate produced. In the case of small cavity wounds, they may be filled with gel but larger wounds should be packed with gauze impregnated with the gel. However, careful use is advised as indiscriminate use can lead to the development of resistance (Cundell *et al.*, 2002).

The incorporation of metronidazole in a halloysite bead formulation fulfills the role of gel formulation as above, with the added benefit of the adsorbent capacity. The bead formulation also aims to control the release of the active in the heavily exudating wound environment. This may prove less possible in the case of the metronidazole gel. The release of metronidazole from a gel formulation across a synthetic membrane, Silastic® was assessed using a Franz cell. The method does not take account of the presence of exudates diluting the gel formulation. Figure 7.8 depicts the cumulative release of metronidazole from the Rozex® formulation per unit area of the membrane over a five hour period. The release is uniform and approximates that observed for an infinite dose application even though it would be deemed a finite dosage form (Williams, 2003). The reason for this is the quantity of application; it exceeds that which produces a finite release profile. The square root of time release of the sample was also examined. It was found that the profile was linear and conformed to the Higuchi model; the linear regression coefficient R^2 (fit to Equation 6.2) was 0.9842. Over the time period examined, it was calculated that 56.9 mg of metronidazole was released per g of formulation. This quantity equates with that encapsulated in the chitosan coated bead formulation, 5.5 +/- 0.16% w/w. The samples were not compared directly as they were examined using different approaches. However, this highlights another advantage of the bead formulations as a potential delivery approach for metronidazole because an equivalent drug loading is achievable.

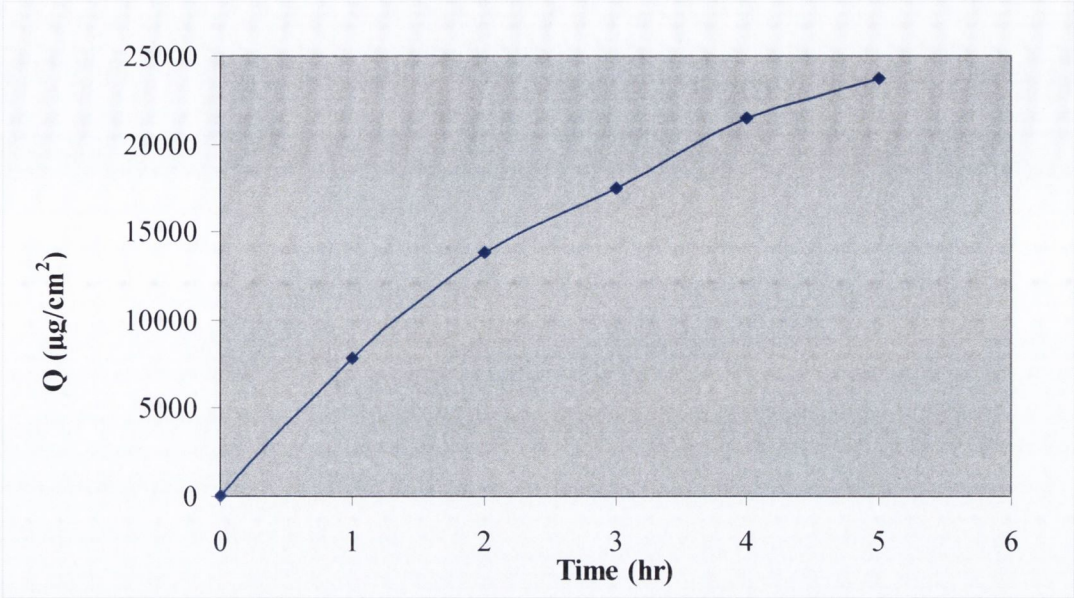

Figure 7.8 Cumulative release (Q) of metronidazole from Rozex® gel formulation using a Franz cell apparatus.

7.9 CONCLUSIONS

The preparation of metronidazole halloysite complexes using a vacuum loading method resulted in a very low encapsulation of metronidazole (0.27-0.47 g per 100 g of complex) with no sustained release capacity. Preparation of complexes with a sufficient quantity of metronidazole encapsulated was inhibited by the poor aqueous solubility of metronidazole. Alternative systems were investigated as loading solutions. Halloysite and cetrimide coated halloysite samples prepared using an ethanol/water co-solvent system displayed a difference in the amount released. However the samples prepared using a vehicle containing ascorbic acid did not because the metronidazole was ionised to a greater extent due to the lower acidic environment of the ascorbic acid vehicle. The ionised sample could not integrate with the hydrophobic cetrimide coated halloysite surface; hence it offered no advantage in increasing the encapsulation and prolonging metronidazole release. The release profile was equivalent for the halloysite and cetrimide coated sample. Halloysite metronidazole complexes were prepared which encapsulated a sufficient quantity of metronidazole which could affect release equivalent to a proprietary preparation. The co-spray-dried complex incorporating metronidazole, halloysite and chitosan resulted in an increase in metronidazole encapsulation relative to the vacuum loaded samples but it was

still very low. The release from the sample was dependent on the medium pH; release was greater at neutral pH, 7.4 compared to an acidic pH of 4.0 due to the insolubility of chitosan at the higher pH. Hence at an increased pH the polyionic interaction which is responsible for entrapping the drug is reduced.

The formulation of a metronidazole halloysite bead complex was an effective method for encapsulating the antibacterial agent. Non-drug formulations were produced first in order to determine an optimum formulation. This was decided based on characterization studies. SEM analysis highlighted the presence of pores on the bead surfaces, the extent of the pore network and the difference between the closed and open pores contributed to the differences in surface area observed between the samples. The surface area was increased as expected in samples, which had a higher concentration of halloysite (15% compared to 7.5% w/w). The drying method and presence of the surfactant, cetrimide, also impacted on the surface area, the contributions made by these formulation variables are greater in the samples which contained 7.5% halloysite. The skeletal density of samples prepared using the freeze-drying procedure was lower due to the high degree of porosity present in these samples as a result of the removal of water (in the form of ice) from the samples. These samples were seen to float in swelling studies due to presence of the porous network, but also they were more fragile as the mechanical strength of the beads was reduced due to the weaker structural support. The 7.5% halloysite sample showed the greatest degree of swelling because the structure was less rigid than the sample which contained 15% halloysite. The rigidity of this sample accounts for it displaying the most spherical morphology. It was the most viscous formulation, hence the spherical droplet was deformed to a lesser extent as the bead was dropped into and stirred in the gelation medium.

The air dried sample with a 7.5% halloysite concentration was chosen as the formulation in which to incorporate metronidazole because air dried samples had a higher mechanical strength and displayed the greatest swelling property. The samples were produced with needles of two different orifice sizes. The sample produced with an external diameter of 0.8 mm resulted in enhanced encapsulation and release because the potential for polyionic complexation between the components was greater in the sample with a larger bead surface area. It was noted that increasing the metronidazole concentration above the saturation solubility value in the halloysite/alginate complex was sufficient to arrest its depletion

from the bead sample. The creation of a thermodynamically equivalent environment by adding metronidazole to the gelation medium as well as the halloysite/alginate complex did not confer any improvement in encapsulation or release.

Coating the sample with Eudragit and glutaraldehyde caused a decrease in the % release of metronidazole at all time points compared to the reference formulation. The release was retarded to the greatest extent by coating the beads with chitosan. The % encapsulation decreased in all the coated samples. This was due to metronidazole release from the bead during the coating process. The impact of the gelation medium used to cross-link the halloysite/alginate/metronidazole complex on the % encapsulation and release was also investigated. A decrease in the % encapsulation was observed for the alternative gelation media. The release profiles were similar to the reference sample, but with a slightly greater burst release effect attributable to the glutaraldehyde and NaPP cross-linking agents compared to the reference. Chitosan was examined as a cross-linking agent at two levels, 0.6 and 0.8% w/v. It was not possible to increase the chitosan concentration in the gelation medium because it was very viscous and resulted in deformed bead morphologies. The use of chitosan resulted in a decrease in the % encapsulation. The % encapsulation of metronidazole was 1.4 and 2.45% per 100 g of bead formulation for systems produced using chitosan cross-linking concentrations of 0.6 and 0.8% w/v respectively. This represents a considerable decrease from the 5.94% achieved using the $CaCl_2$ reference sample. However the % release was decreased relative to the reference sample. Coating the samples with chitosan had the largest contribution to decreasing the % burst release because the chitosan covered the surface pores, restricting entry of the dissolution medium and hence altering the diffusion rate of the encapsulated substances (Anal *et al.*, 2003).

Release of metronidazole from the proprietary preparation, Rozex® gel was examined using a Franz cell. An equivalent amount of metronidazole was released from the preparation compared to the chitosan coated bead formulation per unit weight over an equivalent time period. The gel formulation would not produce uniform release in the wound environment due to the presence of exudates, which would dilute it and cause it to be removed from the wound environment. A standardised release profile from the bead in the presence of a large volume of fluid has been produced. The bead formulation also has the advantage of displaying swelling and sorptive capacities.

Chapter 8

GENERAL DISCUSSION

The research presented in this thesis focused on the potential applications of a novel excipient halloysite in topical and transdermal drug delivery. Halloysite is a microtubular aluminosilicate clay material. The use of halloysite for the controlled delivery of drugs and other chemicals in a number of applications has been elucidated by various authors. Entrapment of the active material within the tubular lumen is the primary focus point for the encapsulation of the active material. Levis and Deasy (2002) used mercury porosimetry to distinguish between interparticulate and intraparticulate void space, which was representative of the space between individual tubules and aggregates, and that which existed through the individual mineral particles, respectively. The authors determined that the available volume for entrapment was 0.246 ml/g. A secondary characteristic of the clay mineral which enhances drug loading is the presence of a negative charge along the tubule surface (Tari *et al.*, 1999) and a positive charge at the tubule ends. It is possible that the surface charge may be used to adsorb the active depending on the pH of the drug loading solution and the pK_a of the active material.

Levis and Deasy (2003) investigated halloysite for the controlled delivery of diltiazem HCl and propranalol. It was observed that simple entrapment without the aid of a polymer or coating material resulted in poor drug retardation, 90% release was observed within 1 hr. However coating of the drug loaded systems with cationic polymers such as chitosan and lipid materials including Precirol AT05 resulted in the retardation of drug release. Kelly (2002) utilised halloysite for the controlled delivery of the antibiotic, tetracycline base in order to formulate a product for the treatment of periodontitis. The author created a sustained release complex by coating the drug loaded halloysite with chitosan. Controlled release of the active over a period of 63 days was observed. Salter (2003) examined halloysite for the controlled release of pesticide preparations. The author formulated two delivery systems, a pellet formulation and a suspension concentrate for the delivery of cypermethrin and chlorpyrifos respectively.

A range of active materials commonly encountered in topical and transdermal drug delivery were provisionally considered. Some of the actives originally considered were fusidic acid, clindamycin hydrochloride, erythromycin and coal tar. Preliminary studies were conducted on coal tar in order to improve the cosmetic appearance and odour which are the primary factors for patient non-compliance with regard to coal tar products. The drug loaded product was qualitatively assessed. Despite a reduction in the pungency compared to the raw material, advanced studies were not undertaken due to assay difficulties with the complex and variable composition of coal tar solution. It was decided to pursue investigation into three active materials which were representative of drug compounds used to treat a wide array of topical conditions. Urea, salicylic acid and metronidazole were also chosen based on the ease of quantitation. Also the pure form of some of the antibiotics listed above was extremely expensive.

It was considered rational to examine halloysite for potential applications in transdermal and topical drug delivery because it is chemically similar to kaolin which has established uses in oral and topical pharmaceutical preparations (Handbook of Pharmaceutical Excipients, 2005). Therapeutically kaolin has been in oral anti-diarrhoeal preparations (Sweetman, 2005). In topical preparations kaolin has been used in poultices and as a dusting powder (Handbook of Pharmaceutical Excipients, 2005). It was hoped that halloysite could be employed to treat conditions which would benefit from its adsorbent properties. It was also considered that it would augment the keratolytic properties of topical drug materials through the exfoliate capacity of the microtubular clay mineral. Kaolin is used in a number of cosmetic preparations for this purpose. The superior adsorptive capacity of halloysite compared to kaolin has been demonstrated by a number of authors (Evicm and Barr, 1955; Barr and Arnista, 1957). The authors observed that halloysite was a better adsorbent of the alkaloids strychnine, atropine and quinine by a factor of approximately two. This increase in sorption capacity is related to the greater surface area of halloysite compared to kaolin (Theng, 1995).

Kaolin is also used in protective creams (Viseras *et al.*, 2006). It is used to provide a mechanical barrier to dry dust irritants (Alexander, 1973). It is included at a concentration of 20% w/w for protective purposes in a water miscible barrier preparation, recommended by the Barrier Substances Subcommittee of the BP Codex (Sweetman, 2005). Halloysite has the added advantage that it has a tubular morphology which offers a potential reservoir

for drug entrapment compared to that of the plate-like morphology of kaolin. It was hoped that the halloysite excipient would perform a number of functions in the formulation. Inherent in controlling drug delivery is the need for a prolonged residence time on the surface. Also the halloysite is used to impart enhanced structural integrity to semi-solid formulations. Prior to commencement of the work in this thesis the safety and non-irritancy of halloysite for application to the skin was considered. Halloysite was incorporated in two ointment bases, WSP and Plastibase® and was applied on the forearm of two subjects for three consecutive days. The ointment/halloysite system was occluded with a dressing. No irritation or adverse reaction was noted in either subject, indicating that despite its short tubular shape (< 1 μm), it did not pose any potential irritancy issues.

Halloysite from different sources has been characterised by Levis (2000) and Salter (2003). Halloysite deposits have been exploited in Japan, France and Korea with the largest commercial deposits in New Zealand. Halloysite is the product of soil mineral weathering; therefore the indigenous environment dictated the formation, morphology and appearance of the halloysite sample. Two grades of halloysite were initially investigated. Halloysite G from New Zealand was available in an extracted state, with an apparently high tubule content as judged from SEM analysis. A crude sample of halloysite containing rock from the Balekisir region of Turkey was also considered. The Balekisir halloysite sample was investigated because it had a flesh-like colour. This characteristic could prove advantageous due to its similarity to natural skin tone. The Balekisir grade was extracted using an autogeneous grinding process and was qualitatively assessed using SEM. The tubules were shorter (< 0.5 μm) than the halloysite G (0.5 - 1 μm) sample and adulteration was also present. Hence it was decided to concentrate on the halloysite G because it was available in an extracted form and the longer tubule length afforded an enhanced reservoir capacity. Chemical modification was undertaken initially as a means of purification and investigation of the structural and compositional factors affecting the halloysite morphology. It is accepted that halloysite has adulterants on the surface in the form of iron oxides and calcium salts (Takahashi *et al.*, 2001). A deferration procedure, which removes surface Fe, resulted in the removal of the bulk of Fe from the samples. However a small quantity remained after the process indicating that this was intrinsic to the halloysite structure. This Fe had substituted for aluminium in the octahedral sheet (Soma *et al.*, 1992). The Fe content in the Balekisir sample (9569 ppm) was significantly higher than in the halloysite G (2045 ppm) sample. The flesh colour of the Baleksir sample is attributed

to its high Fe content. The deferration process results in a decrease in surface area and skeletal density values. This is attributed to the removal of Fe and calcium, which coordinate with the negative tubule surface. The removal of the cations results in a denser packing tubular network due to electrostatic attraction of the positive ends with the negative tubule surface. The exposed surface area is decreased. Despite the particles exhibiting an increased packing density, the skeletal density appears lower because the ability of the helium atom to penetrate into the aggregate is restricted. The structural build-up in halloysite has been referred to as a "house of cards" structure (van Olphen, 1977).

Chemical modification was also conducted to enhance the properties of halloysite that were considered desirable in topical drug delivery. Theng and Wells (1995b) examined the potential of halloysite to decolourise and refine oil and butterfat. The authors noted that the capacity was increased when the halloysite was activated with acid prior to use. Fahn (1979) attributed the increased adsorption capacity to increases in specific surface area, mesopore volume, surface acidity of the clay samples, together with the formation of amorphous colloidal silica. The surface area of the halloysite G sample almost doubled as a result of the acid washing process. The treatment process results in a halloysite grade with an increased adsorptive capacity and a concomitant decrease in adulterate substances. The increase in surface area results from the dissolution of Al at the tubule edge. The supernatant from the washing process displayed a bright yellow colour and the resulting clay material was whiter in appearance.

Surfactant adsorption on the clay mineral was first considered in relation to the Balekisir extraction process. It was considered that a tubular enriched material with substantially less adulteration could be obtained using deflocculation studies. This led to the concept of the formulation of an organo-halloysite grade. Commercial products Bentone® and Baragel® have been formulated by adsorption of quaternary ammonium and benzalkonium surfactant derivatives on the surface of the aluminium silicate clay, bentonite. They are employed as gelling agents in non-polar organic solvents in a wide array of topical products including anti-perspirants, lotions, suntan products, nail lacquers and lip products (Viseras *et al.*, 2006). The quaternary ammonium bromide surfactant, cetrimide was chosen to form the organo-halloysite grade. A cationic surfactant was used, as it would result in optimal complexation due to electrostatic interaction with the negative tubule surface. Cetrimide was also chosen because it possessed innate antiseptic properties (Handbook of

Pharmaceutical Excipients, 2005). The cetrimide coated grade displayed improved flow properties compared to the uncoated grade.

The nature and extent of surfactant – clay adsorption was investigated using a solution depletion method. It is important to characterise surfactant binding because the extent of binding dictates the final characteristics of the complex. It is also important in scale-up and production to assess the exact quantities required because too much may result in a reversal of the desirable characteristics, hence incurring unnecessary expense. The investigation of the deflocculating power of different surfactants highlighted that halloysite could be deflocculated most successfully in terms of quantity required to cause deflocculation using the anionic surfactant sodium lauryl sulphate (SLS). The positive tubule ends comprise a relatively smaller surface area. Hence the adsorption of the negative surfactant inhibited structural build-up and the tubules remained deflocculated. Larger quantities of cationic surfactants were required to produce a similar effect due to the larger negative tubule surface area. SLS systems remained deflocculated after a period of 72 hr.

Surfactant adsorption is complex and is influenced by surface pre-treatment, surfactant structure and the presence of electrolytes in the system. The presence of electrolytes does not alter the surface charge on the clay mineral but it does alter the surface potential by compression of the electrical double layer (van Olphen, 1977). The electrolyte causes an increase in surfactant adsorption due to closer aggregate packing as a result of a reduction in mutual head-group repulsion. Surfactant isotherms produced using the acid washed halloysite grade highlighted two important variables. Surfactant adsorption was equivalent in halloysite G and acid washed sample because the acidic environment of the system counteracted the contribution made to adsorption by the increased surface area of the acid washed clay. An alteration of surfactant structure also impacted on the adsorption profile. The BP (2007) defines cetrimide as primarily being composed of the 14 hydrocarbon structure. Isotherms were also constructed using the 16 hydrocarbon structure in the trimethylammonium bromide compounds. The isotherms conformed to these expected from literature sources. Equivalent quantities were adsorbed at lower equilibrium concentrations and an increase in surface excess was observed. Similar observations were made in the isotherms of the alkyl pyridinium surfactants. The impact of surfactant structure was further elucidated using surfactants that have a benzene ring intrinsic to their composition. A sharp rise in adsorption was observed in the region of the bulk solution

CMC. Plateau values were not generally observed in this region. It is considered that this region in all profiles corresponded to region III of the "two-step" and "four-region" model. The isotherms examined appear to be the product of features of both models but more closely resemble the "two-step model". This is in keeping with observations that materials such as halloysite, which have constant surface charges as a result of isomorphous substitutions in the crystal structure, display adsorption isotherms that conform to the "two-step model". An expected decrease in adsorption was observed in the case of anionic surfactants (SDBS).

Microbiological assay highlighted that the antiseptic integrity of cetrimide was maintained in the cetrimide coated grade. The cetrimide coated grades were prepared by adding cetrimide (0.2 g) per gram of halloysite. However it was determined that approximately 60% of the added amount was bound to the halloysite clay surface.

Urea was chosen because of its low molecular weight and high water solubility. Hence the molecule could be loaded into the tubular lumen and the release would not be hindered by poor aqueous solubility. Urea – halloysite topical complexes are formulated to encapsulate and modulate urea release for potential use as a humectant or as a keratolytic. The halloysite might enhance the keratolytic role of urea but it might counteract the humectant properties of urea through its sorptive capacity. However halloysite could be employed in barrier formulations similar to kaolin (Sweetman, 2005) and hence reduce transepidermal water loss. Halloysite was loaded with urea using a vacuum loading method. Large quantities of urea were encapsulated both intra-tubularly and inter-tubularly. Initial process and formulation investigations highlighted that loading solution volume and pH, the frequency of loading and the presence of a cetrimide coat were important variables. The cetrimide coated grade significantly increases encapsulation efficiency. Urea crystallises in a channel formation permitting the enclosure of the hydrocarbon chains of the surfactant molecule (Martin, 1993).

A spray-drying procedure was employed to produce uniform particles. Co-spray-dried halloysite/urea complexes were formulated with lecithin. It was intended to produce emulsion formulations with this complex but time constraints did not allow this. The ratio of the formulation components was held constant except for one sample in which the lecithin concentration was reduced. The morphology of the co-spray-dried particles was

dependent on the concentration of lecithin in the formulation. The appearance of the samples with higher lecithin concentrations was gelatinous-like with the urea and halloysite tubules enmeshed in the emulsifier. This was not as evident with decreasing lecithin concentration. Urea encapsulation is affected by the concentration of urea. When lower concentrations are used in the formulations, the grade of lecithin appears to have an impact on urea encapsulation. Release was not modulated from these formulations.

Formulation of salicylic acid (SA)/halloysite complexes were also investigated. SA acts as a keratolytic (British Pharmacopoeia, 2007). It was hoped that halloysite complexes would enhance this activity through their exfoliate activity and its role as an adsorbent. Preliminary investigations were conducted into the effect of vacuum loading of halloysite with SA solutions. A factorial design was employed; the model response factor was SA encapsulation. It was affected by halloysite grade, loading solution volume and frequency. Encapsulation was greater with the cetrimide coated grade. The surfactant aids co-adsorption of SA at the surface during the loading study, hence increasing the encapsulation. The results were considered in the construction of a further factorial design. It was hoped that a SA/halloysite complex with a modulated release action would be formed, however this was not achieved. SA release at 1 and 8 hr intervals was not significantly different in the case of the uncoated samples. The study highlighted that despite a decrease in loading solution by a factor of 8, the release was reduced by only a factor of 5 between the samples which displayed the highest encapsulation in both studies. Therefore an optimal loading solution concentration exists in order to maximise SA encapsulation. The quantity released was statistically investigated using ANOVA. All the factors considered interact with each other, hence the results must be considered in tandem with each other.

Spray-dried complexes were prepared incorporating halloysite, SA and cetrimide. The porous samples produced displayed pores which intruded to the sample interior. Spherical particles were evident which showed fracturing and blow-holes due to internal pressure in the particle which arose due to air entrainment in the liquid feed (Oakley, 1997). The concentration of SA in the formulations and the solvent medium used impacted on SA encapsulation. Encapsulation was also enhanced when the solid concentration in the liquid feed is reduced. Ethanol was employed as the loading medium or in co-solvent systems because poor aqueous solubility limited the preparation of drug solutions with an adequate

SA concentration. The halloysite and surfactant concentrations also were important factors in the physical properties of the co-spray-dried complexes. Higher halloysite concentrations produced denser particles with a greater surface area. An increased surfactant concentration resulted in samples with lower skeletal density and surface area values, this being indicative of a greater degree of closed porosity. This has important implications for formulation of the spray-dried components in topical formulations.

Prior to formulation of topical products, the effect of halloysite on the rheological and textural qualities of halloysite and the cetrimide coated grades in two ointment bases, WSP and macrogol ointment was examined. Shear flow rheometry highlighted that the apparent viscosity of WSP samples increased with increasing solid concentration, however this was not observed when the sample was coated. The surfactant conferred a hydrophobic quality on the clay surface, the result of which was enhanced flow in the WSP base. However non-destructive dynamic oscillatory tests using the macrogol ointment base, showed that the solid component, G' increased when the cetrimide coated sample was added. This is exacerbated by increasing the solid content in the ointment base. This was confirmed using measures of sample hardness. The test was also used as an indication of spreadability. It was decided that a halloysite concentration of 20% would not adversely affect speadability, formulation aesthetics and patient acceptability. Preliminary studies were conducted on Plastibase® ointment systems containing halloysite at different concentrations. However sample bleeding was observed during rheological evaluation, hence this base was not used in further studies.

Three co-spray-dried complexes were chosen for incorporation into topical vehicles. The samples chosen represented a range of formulation variables including halloysite and cetrimide concentration, and they also displayed varying physical features. Preliminary studies examined the release of SA from the co-spray-dried complexes incorporated in WSP. Minimal release was observed because the presence of halloysite in the co-spray-dried matrix created a more tortuous diffusion pathway; hence SA release was slower compared to the raw drug in WSP alone. This prompted the examination of raw SA from various topical vehicles and a proprietary product Diprosalic®. Cumulative SA release is influenced by the vehicle type and the grade of WSP used (Kneczke *et al.*, 1996).

It was decided to examine SA release from the spray-dried complexes from two topical cream formulations, Aqueous Cream and Cetrimide Cream. The release from the samples was analysed using the Higuchi square root of time release model. The rate of release was influenced by the surfactant concentration included at the spray-drying step. The SA in the topical formulation was also important. The rate and extent of SA release was lower in the Cetrimide Cream vehicle because it was more viscous.

Byrne (2004) produced pellets using halloysite and kaolin. The author observed controlled release of the active material from the halloysite formulations. He provided the first conclusive evidence that the microtubular structure entrapped the active and extended release unlike the plate structure of kaolin. The ability of the halloysite structure to control the release of metronidazole in a calcium alginate matrix was assessed for potential application in a wound dressing. Non-drug formulations were prepared in order to optimise bead formulations. They were characterised in terms of surface area, skeletal density, SEM, sphericity and swelling analysis. The halloysite concentration was an important determinant in the surface area and skeletal density of the samples. Beads prepared using the surfactant coated grade disintegrated more readily as expected. The freeze-dried samples were less dense when the lower concentration of halloysite was used, they were observed to float on the swelling medium. In preliminary studies glucose was included as a cryoprotectant in freeze-dried formulations in order to maintain the spherical structure which tended to collapse in some samples, however the samples produced using glucose were excessively brittle. Hence it was not used in further formulations. A control formulation containing metronidazole was produced; other modified samples were prepared and compared to this. Metronidazole was included at a concentration above its saturated solubility to compensate for the loss of metronidazole from the bead during the gelation process. Alternative gelation media were investigated but encapsulation and release modulation were not as good as the control formulation. Coating the reference formulation with chitosan caused the greatest retardation of drug release because the chitosan covered the pores on the surface of the bead and impeded the buffer medium intruding to the bead interior. Release from this formulation was equivalent to an equivalent weight of a proprietary gel preparation. The bead formulation has the advantage that it has a sorptive capacity and will maintain the active in the wound site for a prolonged period of time compared to the gel formulation.

The research presented in this thesis focused on the fundamental use of halloysite in topical and transdermal drug delivery. It aims to examine a number of areas where the clay could be utilised. The present study could be further extended to include the formulation of beads using the acid washed grade. The silver cation which has applications in wound treatment could be adsorbed to the clay surface prior to application into the bead complex. However, broader applications for the use of halloysite may include the use of the drug loaded clay as dusting powders in the treatment of athlete's foot, where the sorptive capacity of the clay would be beneficial in tandem with drug release from the tubule lumen. The concept of clay alginate matrices could be extended to include clays, which have greater surface areas and swelling capability. Examples of alternative clays include bentonite which is widely used in topical preparations and also sepiolite. The pharmaceutical applications of sepiolite are currently being investigated by Barry (2006).

In conclusion the research presented highlights that the novel excipient halloysite has potential application in the field of topical and transdermal drug delivery. Halloysite alone did not adequately control the release of the actives examined but sufficient drug sample could be encapsulated within and between the tubules to justify its inclusion in topical formulations. In conjunction with this the clay also has a number of advantageous properties including sorptive capacities. Halloysite can also be applied to other areas by simple modification such as surfactant adsorption at the solid interface. The research examines fundamental applications and constitutes formative work in the area of the role of halloysite in extended topical and transdermal drug delivery. It is believed that no other work has been conducted to date in this area. Further work is needed to examine other topical and transdermal applications and to extend the research to examine the in-vivo applications to assess the performance of these formulations.

REFERENCES

Abounassif, M.A., Mian, M.S., Mian., N.A.A., (1994),
Salicylic acid, In: *Analytical Profiles of Drug Substances and Excipients*, Brittain, H.G., (Ed.), Vol. 23, Academic Press, pp. 422-470.

Aglietti, E.F., Porto Lopez, J.M., Pereira, E. (1988),
Structural alterations in kaolinite by acid treatment, *Appl. Clay Sci.*, **3**, 155-163.

Ahmed, M., Enever, R.P., (1981),
Formulation and evaluation of sustained released paracetamol tablets, *J. Clin. Hosp. Pharm.*, **6**, 27-38.

Alexander, L.T., Faust, G.T., Hendricks, S.B., Insley, H., McMurdie, H.F., (1943),
Relationship of the clay minerals halloysite and endellite, *Amer. Mineral.*, **28**, 1-18.

Alexander, P., (1973),
Harry's Cosmeticology. The Principles and Practice of Modern Cosmetics, Vol. 1, 6th edition., Harry, R.G., (Ed.), Leonard Hill Books, London.

Allwood, M.C., (1986),
Metronidazole topical gel, *Pharm. J.*, **236**, 158.

Anal, A.K., Bhopatkar, D., Tokura, S., Tamura, H., Stevens, W.F., (2003),
Chitosan-alginate multilayer beads for gastric passage and controlled intestinal release of protein, *Drug Dev. Ind. Pharm.*, **29**(6), 713-724.

Andreola, F., Castellini, E., Manfredini, T., Romagnoli, M., (2004),
The role of sodium hexametaphosphate in the dissolution process of kaolinite and kaolin, *J. Eur. Ceramic Soc.*, **24**, 2113-2114.

Anonymous, (1974),
Lecithin: it's composition, properties and use in cosmetic formulations, *Cosmet. Perfum.*, **89**, 31-35.

Anonymous (1991),
Intranasal insulin formulation reported to be promising, *Pharm. J.*, **247**, 17.

Aoki, S., Ando, H., Tatsuishi, K., Uesugi, K., Ozawa, H., (1993),
Determination of the mechanical impact force in the in-vitro dissolution test and evaluation of the correlation between in vivo and in vitro release, *Int. J. Pharm.*, **95**, 67-75.

Aomine, S., Miyauchi, N., (1963),
Age of the youngest hydrated halloysite in Kyushu, *Nature*, ***199***, 1311-1312.

Ashford, R.F.U., Plant, G.T., Maher, J., (1980),
Metronidazole in smelly tumours, *Lancet*, (i), 874-875.

Aslani, P., Kennedy, R.A., (1996),
Effect of gelation conditions and dissolution media on the release of paracetamol from alginate gel beads, *J. Microencapsul.*, **13**, 301-614.

Atkin, R., Craig, V.S.J., Wanless, E.J., Biggs, S., (2003a),
The influence of chain length and electrolyte on the adsorption kinetics of cationic surfactants at the silica-aqueous solution interface, *J. Coll. Interface. Sci.*, **266**, 236-244.

Atkin, R., Craig, V.S.J., Hartley, P.G., Wanless, E.J., Biggs, S., (2003b),
Adsorption of ionic surfactants to a plasma polymer substrate, *Langmuir*, **19**, 4222 4227.

Atkin, R., Craig, V.S.J., Wanless, E.J., Biggs, S., (2003c),
Mechanism of cationic surfactant adsorption at the solid-aqueous interface, *Adv. Colloid Interface Sci.* **103**, 219-304.

Atkin, R., Craig, V.S.J., Biggs, S., (2001),
Adsorption kinetics and structural arrangements of cetylpyridinium bromide at the silica-aqueous interface, *Langmuir*, **17**, 6155-6163.

Atkin, R., (2004),
Personal Communication

Atkins, B., (2004),
Phenomenox, Personal Communication

Attwood, D., Florence A.T., (1983),
Surface activity, In: *Surfactant Systems: Their Chemistry, Pharmacy and Biology,* Chapman and Hall, London, pp. 1-39.

Attwood, D., Florence A.T., (2006),
Surfactants, In: *Physicochemial Principles of Pharmacy,* 4th Edition, Pharmaceutical Press.

Attwood, D., Patel, H.K., (1989),
Composition of mixed micellar systems of cetrimide and chlorhexidine digluconate, *J. Colloid Interface. Sci.*, **49**, 129-134.

Aulton, M.E., (2002),
Pharmaceutics; The Science of Dosage Form Design, 2nd Edition, Churchill Livingstone, Edinburgh.

Bailey, S.W., (1990),
Halloysite-A Critical Assessment, *Proc. 9th Int. Clay Conf., Strasbourg*, 89-98.

Ball, B., Fuerstenau, D.W., (1971),
Thermodynamics and adsorption behaviour in the quartz/aqueous surfactant system, *Discuss. Faraday Soc.*, **52**, 361-371.

Barnes, H.A., Hutton, J.F. and Walters, K., (1989),
An Introduction to Rheology, Elsevier, New York.

Barnes, H.A., (2000),
The flow of suspensions, In*: A Handbook of Elementary Rheology,* Institute of Non-Newtonian Fluid Mechanics, University of Wales, (119-140).

Barr, M., Arnista, E.S., (1957),
Adsorption studies on clays. I. The adsorption of two alkaloids by activated attapulgite, halloysite and kaolin, *J. Am. Pharm. Assoc.*, **46**, 486-489.

Barry, B.W. (1974),
Rheology of Pharmaceutical and Cosmetic Semisolids. In: *Advances in Pharmaceutical Science,* Bean H.S., Beckett A.H., Carless J.E., (Eds.), vol. 1, Academic press New York and London, pp.1-72.

Barry, B.W. (1983),
Rheology of Dermatological Vehicles, In: *Drugs and the Pharmaceutical Sciences, Dermatological Formulations - Percutaneous Absorption*, Marcel Dekker, New York, pp. 351-396.

Barry, B.W., (1987),
Mode of action of penetration enhancers in human skin, *J. Control. Rel.*, **6**, 85-97.

Barry, B.W., (2002),
Transdermal drug delivery, In: *Pharmaceutics; The Science of Dosage Form Design*, 2nd Edition, Aulton, M.E., (Ed.), Churchill Livingstone, Edinburgh, pp. 499-533.

Barry, A., R., (2006),
Current Research, unpublished, Trinity College Dublin.

Barry, B.W., Morrision , J.C., Russell, G.F.J., (1970),
Prediction of the critical micelle concentration of mixtures of alkyltrimethylammonium salts, *J. Colloid Interf. Sci.*, **33**, 554-561.

Barry, B.W.,Grace, A.J., (1970),
Grade variation in the rheology of white soft paraffin B.P.,*J. Pharm. Pharmacol.*, **22**, 147S-156S.

Barry, B.W., Grace, A.J., (1971a),
Structural, rheological and textural properties of soft paraffins, *J. Texture Studies*, **2**, 259-279.

Barry, B.W., Grace, A.J., (1971b),
Rheological properties of white soft paraffin, *Rheol. Acta*, **10**, 113-120.

Barry, B.W.,Grace, A.J., (1972),
Grade variation in the rheology of white soft paraffin B.P., *J. Pharm. Sci.*, **61**, 335-341.

Barry B.W. and Meyer, M.C., (1973),
Sensory assessment of spreadability of hydrophilic topical preparations, *J. Pharm. Sci.*, **62**, 1349-1354.

Bashir, S.J., Dreher, F., Chew, A.L., Zhai, H., Levin, C., Stern, R., Maibach, H.I., (2005),
Cutaneous bioasssy of salicylic acid as a keratolytic, *Int. J. Pharm.*, **292**, 187-194.

Bates, T.F., Hildebrand, F.A., Swineford, A., (1950),
Morphology and structure of endellite and halloysite, *Am. Mineral.*, **35**, 463-485.

Bates, T.E., (1971),
The kaolin minerals. In *The Electron Optical Investigations of Clays*, Gard, J.A., (Ed.), Mineralogical Society, London, pp. 109-157.

Baveja, S.K., Rao, A.V.R., (1973),
Kinetics of metronidazole hydrolysis, *Indian J. Technol.*, **11**, 311-312.

Becher, P., Clifton, N.K., (1959),
Nonionic surface-active agents : II. Time dependence of micellar breakdown,
J. Colloid Sci., **14**, 519-523.

Billany, M., (2002),
Suspensions and emulsions, In: *Pharmaceutics*; *The Science of Dosage Form Design*, 2nd Edition, Aulton, M.E., (Ed.), Churchill Livingstone, Edinburgh, pp. 359.

Bergman, H.D., (1999),
Diarrhoea and its treatment, *Commun. Pharm.*, **3**, 31-35.

Beringer, P., Hendrickson, R., (Eds.), (2005),
Gastrointestinal and liver drugs, In: *Remington: The Science and Practice of Pharmacy,* 21st Edition, Beringer, P., Hendrickson, R., (Eds.), Lippincott, Williams and Wilkins, Philadelphia, pp. 1313.

Bijsterbosch, B.H., (1974),
Characterization of silica surfaces by adsorption from solution. Investigations into the mechanism of adsorption of cationic surfactants, *J. Colloid Interface Sci.*, **47**, 186-198.

Bodmeier, R., Paeratakul, O., (1989),
Spherical agglomerates of water insoluble drugs, *J. Pharm. Sci.*, **78**, 964-967.

Bond, J.R., Barry, B.W., (1988),
Limitations of hairless mouse skin as a model for in vitro permeation studies through human skin: hydration damage, *J. Invest. Dermatol.*, **90**, 486-489.

Brindley, G.W., 1961,
Kaolin, serpentine and kindred minerals. In *The X-ray Identification and Crystal Structures of Clay Minerals.* Brown, G., (Ed.), 2nd Edition Mineralogical Society, London, pp. 51-131.

Brindley, C.W., Brown, G., (1980),
Crystal structures of clay minerals and their X-ray identification, 1st Edition, Mineralogical Society, London.

British National Formulary, (2004),
British National Formulary, 47th Edition, British Medical Association and the Royal Pharmaceutical Society of Great Britain, The Pharmaceutical Press, London.

British Pharmacoepia (2007), *British Pharmacopoeia, Volumes I & II*, The Pharmaceutical Press, London.

British Pharmacoepia (1998),
British Pharmacopoeia, Volumes I & II, The Pharmaceutical Press, London.

Brittain, H.G., (2003),
X-ray diffraction of pharmaceutical materials, In: *Analytical Profiles of Drug Substances, Excipients, and Related Methodology*, Florey, K., (Ed.), Elsevier Academic Press, London, New York, pp. 274-319.

Bronaugh, R.L., Maibach, H.I., (1999),
Percutaneous Absorption Drugs - Cosmetics – Mechanisms - Methodology, 3rd Edition, Marcel Dekker, New York.

Broze, G., (1995),
Solubilization and detergency, In*: Solubilization in Surfactant Aggregates,* Christian, S.D., Scamehorn, J.F., (Eds.), Surfactant Science Series (55), Dekker, New York, pp. 496.

Buchmuller, J., Weyermanns, G., (1989),
Device for the controlled freezing of viscous liquids, U.S. Patent 4, 829, 783.

Bury, R., Favoritti, P., Treiner, C. (1998),
Specific interactions between salicylate derivatives and cetylpyridinium chloride both at the silica/water interface and in solution: A calorimetric investigation, *Colloids Surf. A*, **139**, 99-107.

Buxton, I.R., Peach, J.M., (1984),
Process and apparatus for freezing a liquid medium, U.S. Patent 4, 470, 202.

Byrne, R.S., (2004),
Thesis, Trinity College, Dublin.

Camp, R.W., Stanley, H.D., (1991),
Advances in measurement of surface area by gas adsorption, *American Laboratory*, **9**, 34-36.

Carr, R.L., (1965),
Evaluating flow properties of solids, *Chem. Eng.*, **72**, 163-168.

Carson, C.D., Kunze, G.W., (1970),
New occurrence of tabular halloysite, *Soil Sci. Soc. Amer. Proc.*, **34**, 538-540.

Chander, S., Fuerstenau, D.W., Stigter, D., (1983),
Adsorption of Polymers, In: *Adsorption from Solution,* Ottewill, R.H., Rochester, C.H., (Eds.), Academic Press, London, New York, pp. 197.

Chandar, P., Somasundaran, P., Turro, N.J., (1987),
Fluorescence probe studies on the structure of the adsorbed layer of dodecyl sulfate at the alumina - water interface, *J. Colloid Interface Sci.*, **117**, 31-46.

Cherkaoui, I., Monticone, V., Vaution, C., Treiner C., (1998),
Surface modification of silica particles by a cationic surfactant: adsolubilization of steroids from aqueous solutions, *Int. J. Pharm.*, **176**, 111-120.

Cherkaoui, I., Monticone, V., Vaution, C., and Treiner C. (2000),
Coadsorption of the sodium salts of two steroid molecules at a silica/interface as induced by the adsorption of a cationic surfactant, *Int. J. Pharm.*, **201**, 71-77.

Chien, Y.W., (1984),
Solubilization of metronidazole by water-miscible multi-cosolvents and water-soluble vitamins, *J. Parenter. Sci. Technol.*, **38**(1), 32-36.

Chong-Kook, K., Eun-Jin, L., (1992),
The controlled release of blue dextran from alginate beads, *Int. J. Pharm.*, **79**, 11-19.

Chorro, M., Chorro, C., Dolladile, O., Partyka, S., Zana, R., (1999),
Adsorption mechanism of conventional and dimeric cationic surfactants on silica surface: effect of the state of the surface, *J. Colloid Interf. Sci.*, **210**, 134.

Churchman, G.J., Payne, D., (1983),
Mercury intrusion porosimetry of some New Zealand soils in relation to clay morphology and texture, *J. Soil Sci.*, **34**, 437-451.

Churchman, G.J., Theng, B.K.G., (1984),
Interactions of halloysites with amides: mineralogical factors affecting complex formation, *Clay Miner.*, **19**, 161-175.

Churchman, G.J., Theng, B.K.G., (1994),
Interactions of halloysite with amides: mineralogical factors affecting complex formation, *Clay Miner.*, **20**, 241-246.

Churchman G.J., Davy, T.J., Aylmore, L.A.G., Gilkes, R.J., Self, P.G., (1995),
Characteristics of fine pores in some halloysites, *Clay Miner.*, **30**, 89-98.

Clarke, G.H., (1985),
Special clays, *Ind. Miner.*, **216**, 25-51.

Clarke, C., (2004),
How to choose a suitable emollient, *Pharmaceutical Journal*, **273**, 351-353.

Cohen, S., Lobel., E., Trevgoda, A., Peled, Y., (1997),
A novel in-situ forming drug delivery system from alginates undergoing gelation in the eye, *J. Control. Release,* **44**, 201-208.

Cooper, E., (1984),
Increased skin permeability for lipophilic molecules, *J. Pharm. Sci.*, **73**, 1153-1156.

Craig, D.Q.M., Tamburic, S., Buckton, G., Newton, M.J., (1994),
An investigation into the structure and properties of Carbopol 934 gels using dielectric spectroscopy and oscillatory rheometry, *J. Control. Rel.*, **30**, 213-223.

Crank, J. (1975),
The Mathematics of Diffusion, 2nd Edition, Clarendon Press, Oxford.

Cross, S.E., Roberts, M.S., (1993),
Subcutaneous absorption kinetics of interferon and other solutes, *J. Pharm. Pharmacol.*, **45**, 606-609.

Cullum, D.C. (1994),
Basic Techniques, In: *Introduction to Surfactant Analysis*, Blackie Academic and Professional, Glasgow, Chapman and Hall, London, pp. 42-76.

Cundell, J., Donnelly, J., Gill, D., Witherow, A., Bradley, L., (2002),
Evidence-Based Wound Management, Northern Ireland Centre for Postgraduate Pharmaceutical Education and Training, Queen's University, Belfast.

Daniels, R. and Rupprecht H., (1985),
Adsorption and chemical stability of a cationic aggregating ester – propantheline bromide on silica surfaces in aqueous dispersions, *Pharm. Res.*, 170-175.

Daniels, R., Kerstiens, B., Tiscinger-Wagner, H. and Rupprecht H., (1986),
The stability of drug adsorbates on silica, *Drug Dev. Ind. Pharm.,* **12**, 2127-2156.

Davis, S.S. (1969),
Viscoelastic properties of pharmaceutical semi-solids 1: ointment bases, *J. Pharm. Sci.* **58**, 412-418.

Deem, D.E., (1985),
Surfactant analysis in cosmetic preparations, In: *Surfactants in Cosmetics,* Rieger, M.M., (Ed.), Surfactant Science Series, Vol 16, Marcel Dekker, New York, Basel, pp. 103-131.

Denkbas, E.B., Seyyal, M., Piskins, E., (1999),
5-Fluorouracil loaded chitosan microspheres for chemoembolization, *J. Microencapsul.*, **16**, 741-749.

de Keizer, A., van der Ent, E.M., Koopal, L.K., (1998),
Surface and volume charge densities of monodisperse porous silicas, Colloid Surf. A., ***142**, 303-313.*

Diamond, S., (1970),
Pore size distribution in clays, *Clays Clay Miner.*, **18**, 7-23.

Dick, S.G., Fuerstenau, D.W., Healy, T.W., (1971),
Adsorption of alkylbenzene sulfonate (A.B.S.) surfactants at the alumina-water interface, *J. Colloid Interface Sci.*, **37**, 595-602.

Dijt, J.C., Cohen Stuart, M.A., Fleer, G., (1994),
Reflectometry as a tool for adsorption studies, *Adv. Colloid Interface Sci.*, **50**, 79-101.

Dixon, J.B., McKee, T.R., (1974),
Internal and external morphology of tubular and spheroidal halloysite particles, *Clay Miner.*, **22**, 233-249.

Drajet, K.I., (2000),
Alginates, In: *Handbook of Hydrocolloids,* Philips, G.O., Williams, P.A., (Eds.), Woodhead Publishing, UK, pp. 379-395.

Drug Information Full Text, (2006),
Drug Information Full Text, American Society of Hospital Pharmacists, Maryland, USA.

Du Plessis, J., Pugh, W.J., Judefeind, A., Hadgraft, J., (2002),
Physico-chemical determinants of dermal drug delivery: effects of the number and substitution pattern of polar groups, *Eur. J. Pharm. Sci.*, **16**, 107-112.

El Tayar, N., Tsai, R-S., Testa, B., (1991),
Percutaneous penetration of drugs; a quantitative structure-permeability relationship study, *J. Pharm. Sci.*, **80,** 744-749.

Elias, P.M., (1981),
Epidermal lipids, membranes and keratinisation, *Int. J. Dermatol.*, **20**, 1-9.

Epton, S.R., (1948),
A new method for the rapid titrimetric analysis of sodium alkyl sulfates and related compounds, Trans. Faraday Soc., **44**, 226-230.

Esezobo, S., (1989),
Disintegrants: effects of interacting variables on the tensile strengths and disintegration times of sulfaguanidine tablets, *Int. J. Pharm.*, **56**, 207-211.

Esumi, K., Sugimura, A., Yamada, T., Meguro, K., (1992),
Adsorption of dioctadecyldimethylammonium chloride on silica, *Colloids Surf.*, **62**, 249-254.

Evcim, N., Barr, M., (1955),
Adsorption of some alkaloids by different clays, *J. Am. Pharm. Assoc.*, **44**, 570-573.

Fahn, R., (1979),
Acid activated clays and their adsorption properties, Proc. Soc. Mining Engineers, AIME, Tuscon, Arizona, **328**, 1-13.

Fan, A., Somasundaran, P., Turro, N.J., (1997),
Adsorption of alkyltrimethylammonium bromides on negatively charged alumina, *Langmuir,* **13**, 506.

Farmer, V.C., Russell, J.D., (1966),
Effects of particle size and structure on the vibrational frequency of layer silicates, *Spectrochimica Acta.*, **22**, 389-398.

Farmer, V.C., Smith, B.F.L., Tait, J.M., (1979),
The stability, free energy and heat of formation of imogilite, *Clay Miner.*, **14**, 103-107.

Favoritti, P., Monticone, V., Treiner C. (1996),
Coadsorption of naphthalene derivatives and cetyltrimethylammonium Bromide on alumina/water, titanium dioxide/water and silica/water interfaces, *J. Colloid Interface. Sci.,* **179**(1), 173-180.

Fernandez-Hervas, M.J., Holgado, M.A., Fini, A., Fell, J.T., (1998),
In vitro evaluation of alginate beads of a diclofenac salt, *Int. J. Pharm.*, **163**, 23-34.

Few, A.V., and Ottewill, R.H., (1956),
A spectrophotometric method for the determination of cationic detergents, *J. Colloid Sci.,* **11**, 34-48.

Foreman, M.I., Clanachan, I., Kelly, I.P., (1978),
The diffusion of nandrolone through occluded and non – occluded human skin, *J. Pharm. Pharmacol.*, **30**, 152-157.

Fox, C., (1985),
Surfactants in cosmetic suspensions, In: *Surfactants in Cosmetics,* Rieger, M.M., (Ed.), Surfactant Science Series, Vol 16, Marcel Dekker, New York, Basel, pp. 401-429.

Fripat, J.J., (1957),
Proprietes de surface des alumino-silicates, Bull, Groupe Franc. Argiles., **9**, 23-45.

Frost, R.L., Tran, H.T., Kristof, J., (1997),
FT-Raman spectroscopy of the lattice region of kaolinite and its intercalates, *Vibrational Spectroscopy*, **13**, 175-186.

Fuerstenau, D.W., (1956),
Streaming potential studies on quartz in solutions of aluminium acetates in relation to the formation of hemimicelles at the quartz-solution interface, *J. Phys. Chem.*, **60**, 981-985.

Fuerstenau, D.W., (1970),
Interfacial processes in mineral/water systems, pure and applied chemistry, *Pure Appl. Chem.*, **24,** 135-168.

Fuerstenau, D.W., Wakamatsu, T., (1975),
The effect of pH on the adsorption of sodium dodecyl sulfonate at the alumina/ water interface, *Faraday Discuss. Chem. Soc.*, **59**, 157-168.

Fuerstenau, D.W., Jia, R., (2004),
The adsorption of alkylpyridinium chlorides and their effect on the interfacial behaviour of quarz, *Colloids Surf.* A., **250**, 223-231.

Führer, C., (1982),
The classification of agents used in dermatology, In: *Dermal and Transdermal Absorption*, 1st International Symposium, Munich, (Eds.), Brandau, R., Lippold, B.H., Wissenschaftliche Verlagsgesellschaft mbH Stuttgart 1982, pp. 14-26.

Ganza-González, A., Anguiano-Igea, S., Otero-Espinar, F.J., Blance-Mendez, J., (1999),
Chitosan and chondroitin microspheres for oral administration controlled release of metoclopramide, *Eur. J. Pharm. Biopharm.*, **48**, 149-155.

Gao, Y., Du, J., Gu, T., (1987),
Hemimicelle formation of cationic surfactants at the silica gel-water interface, *J. Chem. Soc. Faraday Trans.* 1, **83**, 2671-2679.

Gaudin, A.M., Fuerstenau, D.W., (1955),
Streaming potential studies - quartz flotation with cationic collectors, *Trans.* AIME., **202**, 958-962.

Genta, I., Perugini, P., Pavanetto, F., (1998),
Different molecular weight chitosan microspheres: influence on drug loading and drug release, *Drug Dev. Ind. Pharm.*, 24, 779-784.

Ginn, M.E., (1970),
Adsorption of cationic surfactants on mineral substrates, In: *Cationic Surfactants*, Jungerman, E., (Ed.), Marcel Dekker, New York, pp. 341-367.

Goloub, T.P., Koopal, L.K., Bijsterbosch, B.H., (1996),
Adsorption of cationic surfactants on silica. Surface charge effects, *Langmuir,* **12**, 3188-3194.

Goloub, T.P., Koopal, L.K., (1997),
Adsorption of cationic surfactants on silica. Comparison of experiment and theory, *Langmuir,* **13**, 673-681.

Gombotz, W.R., Wee, S.F., (1998),
Protein release from alginate matrices, *Adv. Drug Del. Reviews*, **31**, 267-285.

Gotoh, T., Matsushima, K., Kikuchi, K.I., (2004),
Preparation of alginate-chitosan hybrid gel beads and adsorption of divalent metal ions, *Chemosphere,* **55**, 135-140.

Gozalez, L., Ibarra, L.M., Rodriguez, A., Moya, J.S., Valle, F.J., (1984),
Fibrous silica gel obtained from sepiolite by HCl attack, *Clay Miner.*, **19**, 93-98.

Gregg, S.J., Sing, K.S.W., (1982),
Adsorption, Surface Area and Porosity, Academic Press, London.

Greenland, D.J., Quirk, J.P., (1963),
Determination of surface areas by adsorption of cetylpyridinium bromide from aqueous solution, *J. Phys. Chem.*, **67**, 2886-2887.

Greenwood, F.G., Parfitt, G.D., Picton, N.H., Wharton, D.G., (1968),
Adsorption and wetting phenomena associated with graphon in aqueous surfactant solutions, In: *Adsorption from Aqueous Solution*, Gould, R.F., (Ed.), Advances in Chemistry Series, 79. American Chemical Society, Washington D.C., pp. 135-144.

Grim R. E., (1953),
Clay Minerology, McGraw-Hill, New York, N.Y.

Grit, M., Zuidam, N.J., Underberg, W.J.M., Crommelin, D.J.A., (1993),
Hydrolysis of partially saturated egg phosphatidylcholine in aqueous liposome dispersions and the effect of cholesterol incorporation on hydrolysis kinetics, *J. Pharm. Pharmacol.*, **45**, 490-495.

Hadgraft, J., (1983),
Percutaneous absorption: possibilities and problems, *Int. J. Pharm.*, **16**, 255-270.

Handbook of Pharmaceutical Excipients, (2005),
Handbook of Pharmaceutical Excipients, Rowe, R.C., Sheskey, P.J., Owen, C.O., (Eds.), *5th Edition*, American Pharmaceutical Association, Pharmaceutical Press, London and Chicago.

Harrison, J.L., Greenburg, S.S., (1962),
Dehydration of fully hydrated halloysite from Lawrence County, Indiana, *Clays and Clay Miner.*, **9**, 374-377.

Harvey, C.C., (1996),
Halloysite – For high quality ceramics, In: *Industrial Clays*, 2nd Edition, Kendall, T., (Ed.), London: Industrial Minerals Information Ltd., 71-73.

Haug, A., (1964),
Composition and properties of alginates, Ph.D. thesis, Norges tekniske hoyskole, Trondheim, Norway.

Hausner, H.H.., (1967),
Friction conditions in a mass of metal powder, Ìnt. J. Powd. Metall., **3**, 7-13.

Heller, J., Lin-Shu, L., Ng, S., Duncan, R., Richardson, S., (1996),
Alginate/Chitosan microporous microspheres for the controlled release of proteins and antigens, *Proc. Int. Symp. Control. Release Bioact. Mater.*, (23), 269-270.

Heller, J., (1987),
Use of polymers in controlled release of active agents, In: *Controlled Drug Delivery; Fundamentals and Applications*, 2nd Edition, Marcel Dekker, Inc., pp. 179-212.

Hendersen, N.L., Meer, P.M., Kostenbauder, H.B., (1961),
Approximate rates of shear encountered in some pharmaceutical processes, *J. Pharm. Sci.*, **50**, 788-791.

Hendricks, S.B., (1938),
On the crystal structure of the clay minerals: Dickite, halloysite and hydrated halloysite, *Am. Mineral.*, **23**, 295-301.

Henriksen, I., Sminstad, G., Karlsen, J., (1994),
Interactions between chitosans and liposomes, *Int. J. Pharm.*, **101**, 227-236.

Hesselink, F. TH., (1983),
Adsorption of polyelectrolytes from dilute solution. In: *Adsorption from Solution at the Solid/Liquid Interface*, Parfitt, G.D., Rochester, C.H. (Eds.), Academic Press, New York.

Hiemstra, T., De Wit, J.C.M., Van Riemsdijk, W.H., (1989),
Multisite proton adsorption modeling at the solid/solution interface of hydroxides: A new approach: II. Application to various important hydroxides *J. Colloid Interface Sci.*, **133**, 105-117.

Hiemstra, T., Van Riemsdijk, W.H., (1991),
Physical chemical interpretation of primary charging behaviour of metal hydroxides, *Collids Surf.*, **59**, 7-25.

Higuchi, T., (1961),
Rate of release of medicaments from ointment bases containing drugs in suspension, *J. Pharm. Sci.*, **50**, 874-875.

Higuchi, T., (1963),
Mechanism of sustained action medication: theoretical analysis of rate of release of solid drugs dispersed in solid matrices, *J. Pharm. Sci.*, **52**, 1145-1149.

Higuchi, T., (1982),
In vitro drug release from ointments and creams, In: *Dermal and Transdermal Absorption, 1st International Symposium, Munich,* (Eds.) Brandau, R., Lippold, B.H., Wissenschaftliche Verlagsgesellschaft mbH Stuttgart, 1982, pp. 90-100.

Hills, B.P., Godward, J., Debatty, M., Barras, L., Saturio, C.P., Ouwerx, C., (2000),
NMR studies of calcium induced gelation. Part II. The internal bead structure, *Magn. Reson. Chem.*, **38**, 719-728.

Hirano, S., Seino, H., Akiyama, Y., Nonaka, I., (1988),
Biocompatibility of chitosan by oral and intravenous administration, *Polym. Eng. Sci.*, **59**, 897-901.

Hofman, U., Weiss, A., Koch, G., Mehler, A., Scholz, A., (1956),
Intracrystalline swelling, cation exchange, anion exchange of minerals of the montmorillionite group and kaolinite, *Clays, Clay Minerals*, **4**, 273-287.

Hofmann, A.S., (2002),
Hydrogels for biomedical applications, *Adv. Drug Deliv. Rev.*, **43**, 3-12.

Horsch, W., (1984),
Transportmechanismen und einflußfaktoren in den systemen salbe/haut und arzneistoff/salbengrundlage, *Pharmazie*, **39,** 598-605.

Hough, D.B., Rendall, H.M., (1983),
Adsorption of Ionic Surfactants, In: *Adsorption from Solution at the Solid/Liquid Interface*, Parfitt, G.D., Rochester, C.H. (Eds.), Academic Press, New York.

Hughes, I.R., (1966),
Mineral changes of halloysite on drying, *N.Z.J. Sci.*, 67, 1599-1606.

Huguet, M.L., Neufeld, R.J., Dellacherie, E., (1996),
Calcium-alginate beads coated with polycationic polymers: comparison of chitosan and DEAE dextran, *Process Biochem.*, **31**, 347-353.

Idson, B. (1975),
Percutaneous absorption, *J. Pharm. Sci.*, **64**, 901-923.

ICH online,
www.ich.org

International Federation Societies of Cosmetic Chemists (1997),
An Introduction to Rheology, (IFSCC) Monograph number 3, Micelle Press, Dorset, England.

Jones, D.S., Woolfson, A.D., Djokic, J., Coulter, W.A., (1996),
Development and mechanical characterisation of bioadhesive, semi-solid, polymeric systems containing tetracycline for the treatment of periodontal diseases, *Pharm. Res.*, **13**, 1734-1738.

Jones, D.S., Woolfson, A.D., Brown, A.F., (1997),
Textural analysis and flow rheometry of novel, bioadhesive antimicrobial oral gels, *Pharm. Res.*, **14**, 450-457.

Joseph, I., Venkataram, S., (1995),
Indomethacin sustained release from alginate-gelatin or pectin-gelatin coacervates, *Int. J. Pharm.*, **125**, 161-168.

Kelly H. M., 2002,
Thesis, Trinity College Dublin.

Kelly H. M., Deasy P.B., Claffey, N., (2004),
Formulation and preliminary in vivo dog studies of a novel drug delivery system for the treatment of peridontitis, *Int. J. Pharm.*, **274**, 163-183.

Kikuchi, A., Kawabuchi, M., Sugihara, M., Sakurai, Y., Okano, T., (1997),
Pulsed dextran release from calcium-alginate gel beads. *J. Control. Release*, **47**, 21-29.

King, A.H., (1983),
Brown seaweed extracts (Alginates). In: *Food Hydrocolloids*,
Glicksham, M., (Ed.), Vol. 2, CRC Press, Boca Raton, pp. 116-154.

Kirkman, J.H., (1975),
Clay mineralogy of some tephra beds of Rotorua area, North Island, New Zealand, *Clay Miner.*, **10**, 437-449.

Kirkman, J.H., (1977a),
Halloysite disks and cylinders, *Clay Miner.*, **12**, 199-216.

Kirkman, J.H., (1977b),
Possible structure of halloysite disks and cylinders observed in some New Zealand rhyolitic tephras, *Clay Miner.*, **12**, 199-216.

Kodama, H., Oinuma, K., (1963),
Identification of kaolin minerals in the presence of chlorite by X-ray diffraction and infrared adsorption spectra, In: *Clays and Clay Minerals*. Proc. 11th Nat. Conf. Clays Clay Minerals Natl. Acad. Sci. Natl. Res. Council, pp. 236-249.

Kneafsey, B., O'Shaughnessy, M., Condon, K.C., (1996),
The use of calcium alginate dressings in deep hand burns, *Burns*, **22**, 3-40.

Kneczke, M., Landersjö, L., Lundgren, P., Fuhreer, C., (1986),
In vitro release of salicylic acid from two different qualities of white petrolatum, *Acta Pharm. Suec.*, **23**, 193-204.

Knoch, A., (1994),
Cryopelletization, *Multiparticulate Oral Drug Delivery*, Ghebre-Sellassie, I., (Ed.), Marcel Dekker, Inc., New York, pp. 35-50.

Koopal, L.K., (1993),
In: *Coagulation and Flocculation, Theory and Application*, Dobias, B., (Ed.), Surfactant Science Series, vol. 47, Dekker, New York, pp. 101.

Koopal, L.K., Lee, E.M., Böhmer, M.R., Lajtar, L., Narkiewicz-Michalek, J., Rudzinski, W., (1993),
A new theoretical approach to adsorption of ionic surfactants at water/oxide interfaces: effects of oxide surface heterogeneity, *Langmuir,* **9**, 3174-3190.

Koopal, L.K., Lee, E.M., Böhmer, M.R., (1995),
Adsorption of cationic and anionic surfactantants on charged metal oxide surfaces, *J. Colloid Interface Sci.*, **170**, 85-97.

Koopal, L.K., Goloub, T., de Keizer, A., Sidorova, M.P., (1999),
The effect of cationic surfactants on wetting, colloid stability and flotation of silica, *Colloids Surf.* A., **151**, 15-25.

Koopal, L.K., Goloub, T., Davis, T.A., (2004),
Binding of ionic surfactants to purified humic acid, *J. Colloid Interface Sci.*, **275**, 360-367.

Kulkarni, A.R., Soppimath, K.S., Aminabhavi, T.M., Rudzinski, W.E., (2001),
In-vitro release kinetics of cefadoxril-loaded sodium alginate interpenetrating network beads, *Eur. J. Pharm. Biopharm.*, **51**, 127-133.

Kunze, G.W., Bradley, W.F., (1964),
Occurrence of tabular halloysite in Texas soil, In: *Clays and Clay Minerals, Proc. 12th Natl. Conf., Atlanta, Georgia,* 1963, Bradley, W.F., (Ed.), Pergamon Press, New York, pp. 523-527.

Lampe, M.A., Burligame, A.L., Whitney, J., (1983),
Human stratum corneum lipids: characterisation and regional variations, *J. Lipid Res.*, **24**, 120-130.

Lashmar, U.T., Beesley, J., (1993),
Correlation of the rheological profile of an oil-in-water emulsion with manufacturing procedures and stability, *Int. J. Pharm.*, **91**, 59-67.

Lazarev, A.N., (1974),
The dynamics of crystal lattices, In: *The Infrared Spectra of Minerals*, Farmer, V.C., (Ed.), Mineralogical Society, London, pp. 69-86.

Lee, T.K., Sokalaski, T.D., Royer, G.P., (1981),
Serum albumin beads: an injectable, biodegradable system for the sustained release of drugs, *Science*, **213**, 233-235.

Lee, E., Koopal, L.K., (1996),
Adsorption of cationic and anionic surfactants on metal oxide surfaces: surface charge adjustment and competition effects, *J. Colloid Interface Sci.*, **177**, 478-489.

Levis, (2000),
Thesis, Trinity College Dublin.

Levis, S.R., Deasy, P.B., (2002),
Characterisation of halloysite for use as a microtubular drug delivery system, *Int. J. Pharm.*, **243**, 125-134.

Levis, S.R., Deasy, P.B., (2003),
Use of coated microtubular halloysite for the sustained release of diltiazem hydrochloride and propranolol hydrochloride, *Int. J. Pharm.*, **253**, 145-157.

Lai, H.L., Abu'Khalil, A., Craig, D.Q.M., (2003),
The preparation and characterisation of drug-loaded alginate and chitosan sponges, *Int. J. Pharm.*, **251**, 175-181.

Liao, I.C., Wan, A.C., Yim, E.K., Leong, K.W., (2005),
Controlled release from fibres of polyelectrolyte complexes, *J. Control. Release*, **104**, 347-358.

Lin, Y.H., Liang, H.F., Chung, C.K., Chen, M.C., (2005),
Physically crosslinked alginate/N,O-carboxymethyl chitosan hydrogels with calcium for oral delivery of protein drugs, *Biomaterials*, **26**, 2105-2113.

Lim, L.Y., Wan, L.S.C., (1995),
Heat treatment of chitosan films, *Drug Dev. Ind. Pharm.*, **21**, 839-846.

Lim, L.Y., Wan, L.Y.L., Thai, P.Y., (1997),
Chitosan microspheres prepared by emulsification and ionotropic gelation, *Drug Dev. Ind. Pharm.* **23**, 981-985.

Lipoid® Product Information,
Lipoid® GMBH, Germany.

Liu,Y., Kalen, A., Risto, O., Wahlstrom, O., (2002),
Fibroblast proliferation due to exposure to a platelet concentrate in vitro is pH dependent, *Wound Repair Regen.*, **10**, (5), 336-340.

Longwell, J., Maniece, W.V., (1955),
Determination of anionic detergent in sewage effluents and river water, *Analyst,* **80**, 167-171.

Longworth, A.R., French, J.D., (1969),
Quality control of white soft paraffin, *J. Pharm. Pharmac.*, **21**, 1S-5S.

Loth, H., Rugge-Wolff, I., Schäfer, U., (1984),
Freisetzung aus suspensionssalben und korngröße, *Acta Pharm. Technol.*, **30**(2), 161-169.

Lowell, S., Shields, J.E., (1991),
Density Measurement, In: *Powder Surface Area and Porosity*, 3rd Edition., Scarlett, B., (Ed.), Chapman and Hall, London, pp. 227-234.

Luckham, P.F., Rossi, S., (1999),
The colloidal and rheological properties of bentonite suspensions, *Adv. Colloid Interface Sci.*, **82**, 43-92.

Machluf, M., Regev, O., Peled, Y., (1997),
Characterisation of microencapsulated liposome systems for the controlled delivery of liposome associated macromolecules, *J. Control. Release,* **43**, 35-45.

Malcolm, K., (1995),
A basic guide to the Higuchi equation (Equation invasion), UKICRS newsletter, Vol. 10, 2005.

Martin A.N., Banker, G.S. and Chun A.H.C. (1964),
Advances in Pharmaceutical Science, Bean H.S., Beckett A.H., Carless J.E., (Eds.), Vol. 1, Academic Press, New York and London, pp. 1-85.

Martin, A., (1993),
Colloids, In: *Physical Pharmacy*, 4th edition. Williams and Wilkins, Baltimore, Philadelphia, Hong Kong, London, Munich, Sydney, Tokyo, pp. 393-422.

Mazzo, D.J., Obetz, C.L., Shuster, J., (1994),
Diltiazem hydrochloride, *Analytical Profiles of Drug Substances and Excipients, Volume 23*, Brittain, H.G., (Ed.), Academic Press Inc., London, pp. 53-98.

McDermott, D.C., Lu, J.R., Lee, E.M., Thomas, R.K., Rennie, A.R., (1992),
Study of the adsorption from aqueous solution of hexaoxyethylene glycol monododecyl ether on silica substrates using the technique of neutron reflection, *Langmuir*, **8**, 1204.

McGuire, J.L., Gendimenico, G.J., Cauwenbergh, G., Mezick, J.A., (2000),
Drugs used in dermatology, In: *Pharmaceuticals, Classes, Therapeutic Agents, Areas of Application*, Vol. 4, McGuire, J.L, (Ed.), Wiley-VCH, New York, pp. 1713-1733.

Mellor, J.W., (1908),
A note on the nomenclature of clays, *Trans. Eng. Cer. Soc.*, **8**, 23-30.

Mendelovici, E., Yariv, S., Villalba, R. (1979),
Iron bearing kaolinite in Venezuelen laterites: I. Infrared spectroscopy and chemical dissolution evidence, *Clay Minerals*, **14**, 323-333.

Moore, D. M., Reynolds, R.C., (1989),
X-ray Diffraction and the Identification and Analysis of Clay Minerals, Oxford University Press, Oxford and New York.

Monticone,V., Treiner, C., (1995),
Effect of pH and ionic strength on the adsorption of cetylpyridinium chloride and the coadsorption of phenoxypropanol at a silica/water interface, *Colloids Surf. A.*, **104**, 285-293.

Morgan, D.A., Shaw, D.B., Sidebotton, M.I., Soon, T.C., Taylor, R.S., (1985),
The function of bleaching earths in the process of palm, palm kernel and coconut oils, *J. Am. Oil Chem. Soc.*, **62**, 292-299.

Mortazavi, S.A., Carpenter, B.G., Smart, J.D. (1993),
A comparative study on the role played by mucus glycoproteins in the rheological behaviour of the mucoadhesive/mucosal interface, *Int. J. Pharm.* **94**, 195-201.

Moriyama, N., (1975a),
Stability of aqueous ferric oxide suspension, *J. Colloid Interface Sci.*, **50**(1), 80-88.

Moriyama, N., (1975b),
The stability of aqueous ferric oxide suspensions and its relation to the chemical composition of anionic surfactants, *J. Colloid Interface Sci.*, **52**(2), 303-307.

Mukhopadhyay, D., Reid, M., Saville, D., Tucker, I.G., (2005),
Cross-linking of dried paracetamol alginate granules, Part 1. The effect of the cross-linking process variables, *Int. J. Pharm.*, **299**, 134-145.

Mullins E., (2003),
In: *Statistics for the Quality Control of the Chemistry Laboratory,* Royal Society of Chemistry, Cambridge.

Murata, Y., Miyamoto, E., Kawashima, S., (1993),
Prepartaion of chitosan reinforced alginate gel beads - effects of chitosan on gel matrix erosion, *Int. J. Pharm.*, **96**, 139-145.

Murata, Y., Miyamoto, E., Kawashima, S., (1996),
Additive effect of chondroitin sulfate and chitosan on drug release from calcium-induced alginate gel beads, *J. Control. Release*, **38**, 101-108.

Murata, Y., Toniwa, S., Miyamoto, E., Kawashima, E., (1999),
Preparation of alginate beads containing chitosan nicotinic acid salt and the functions, *Eur. J. Pharm. Biopharm.*, **48**, 49-52.

Murata, Y., Sasaki, N., Miyamoto, E., Kawashima, E., (2000),
Use of floating alginate gel beads for stomach-specific drug delivery, *Eur. J. Pharm. Biopharm.*, **50** (2), 221-226.

Nagasawa K., Noro H., (1987a),
An electron spin resonance study of halloysites, *Clay Science*, **6**, 261-268.

Nagasawa K., Noro H., (1987b),
Mineralogical properties of halloysites of weathering origin, *Chemical Geol.*, **60**, 145-149.

Nagasawa, K., Karube, K., (1975),
Clay mineral formation in a volcanic ash layer in the Seto group, Central Japan,
Contributions of Clay Mineralogy-Dedicated to Professor Toshio Sudo, on the occasion of his retirement, 80-184.

Nakano, M., Patel, N., (1970),
Release, uptake and permeation behaviour of salicylic acid in ointment bases, *J. Pharm. Sci.*, **59**, 985.

Napper, D.H, Netschey, A., (1971),
Studies of the steric stabilization of colloidal particles *J. Colloid Interface Sci.*, **37** (3): 528-535.

Nash, T., (1959),
Thermodynamic barrier to micelle formation and breakdown: I. Cetyltrimethyl ammonium salts, *J. Colloid Sci.*, **14** (2), 59-73.

Neal, M., Worrall, W.E., (1977),
Minerology of fireclays: part 1. The crystalinity of kaolinite in fire clays, Transactions of the British Ceramic Society, **76**, 57-61.

Neubert, R.H.H., Schmalfuß, U., Huschka, C., Wohlrab, W.A., (1988),
Neuere Entwicklungen auf dem Gebiet der dermalen Wirkstoffapplikation. *[Recent Developments in the Field of Dermal Drug Application. In German). Pharm. Ind.*, **60**, 2.

Newman, R.H., Childs, C.W., Churchman, G.J., (1994),
Aluminium coordination and structural disorder in halloysite and kaolinite by ^{27}Al NMR spectroscopy, *Clay Miner.*, **29**, 305-312.

New Zealand MIA, (2001),
Case Study: Halloysite Clay [Online].http.//www.minerals.co.nz

New Zealand China Clay, (2001),
Halloysite [Online].http.//www.nzcc.co.nz

Nicoli, S., (2004),
"Introduction to Transdermal Delivery", Socrates Intensive Course on Innovative Therapeutics: from Molecules to Medicines, Parma, 27 June-7 July 2004.

Nielsen, P., (1983),
A double blind study of 1% metronidazole cream versus systemic oxytetracycline therapy for rosacea, *B. J. Dermatol.*, **109**, 63-65.

Noro, H., Yamada, K., Suzuki, K., (1981),
An application of electron probe microanalysis for clay minerals, *J. Mineral. Soc. Japan*, **23**, 149-158.

Noro, H., (1986),
Hexagonal platy halloysite in an altered tuff bed, Komaki City, Aiche Prefecture, Central Japan, *Clay Miner.*, **21**, 401-415.

Novak, E., Osbourne, D.W., Matheson, L.E., (1991),
Evaluation of cefmetazole rectal suppository formulation, *Drug Dev. Ind. Pharm.*, **17** (3), 373-389.

O'Donnell, C. (2004)
Waters HPLC specialists.

O'Connor, R.E., Schwartz, J.B., Felton, L.A., (2005),
Powders, In: *Remington: The Science and Practice of Pharmacy,* 21st Edition, Beringer, P., Hendrickson, R., (Eds.), Lippincott, Williams and Wilkins, Philadelphia, pp. 702.

O'Haver, J.H., Lobban, L.L., Harwell, J.H., O'Rear III, E.A., (1995),
Solubilization in Surfactant Aggregates, Christian, S.D., Scamehorn, J.F., (Eds.), Surfactant Science Series (55), Dekker, New York, pp. 277-295.

Oakley, D.E., (1997),
Produce uniform particles by spray drying, *Chem. Eng. Progress*, **10**, 48-54.

Orienti, I., Aiedeh, K., Gianasi, E., Bertasi, V. and Zecchi, V., (1996),
Indomethacin loaded chitosan microspheres. Correlation between erosion process and release kinetics, *J. Microencap.*, **13**, 463-472.

Ostrenga, J., Steimetz, C., Poulsen, B.J., (1971),
Significance of vehicle composition II: prediction of optimal vehicle composition, *J. Pharm. Sci.*, **60**, 1175-1183.

Pabst, W., Kuneš, K., Havrda, J., Gregorova, E., (2000),
A note on particle size analyses of kaolin and clays, *J. Eur. Ceramic Soc.*, **20**, 1429-1437.

Parfitt, G.D., Rochester, C.H., (1983),
Adsorption from Solution at the Solid/Liquid Interface, Academic Press, New York.

Pasparakis, G., Bouropoulos, N., (2006),
Swelling studies and in vitro release of verapamil from calcium alginate and calcium alginate-chitosan beads, *Int. J. Pharm.*, **323**, 34-42.

Pauling, L.C., (1930),
The structure of micas and related minerals, *Nat. Acad. Sci. Proc.*, **16**, 123-129.

Peña, M.A., Reíllo, A., Escalera, B., Bustamante, P., (2006),
Solubility paramter of drugs for predicting the solubility profile type within a wide polarity range in solvent mixtures, *Int. J. Pharm.*, **321**, 155-161.

Peper, H., Taylor, E.G., (1963),
Slow equilibration of micellar detergent solutions, *J. Colloid Sci.*, **18**, 4, 318-327.

Polk, A., Amsden, B., Yao., K.D., Peng, T., Goosen, M.F., (1994),
Controlled release of albumin from chitosan-alginate microcapsules, *J. Pharm. Sci.*, **83**, 178-185.

Prescott, L.M., Harley, J.P., Klein, D.A., (2005),
In: *Microbiology*, 6th Edition, McGraw Hill, New York, London, pp. 104.

Price, R.R., Gaber, B.P., Lvov, Y., (2001),
In vitro release characteristics of tetracycline HCl, khellin and nicotinamide adenine dinucleotide from halloysite; a cylindrical material, *J. Microencapsulation*, **18**(6), 713-722.

Pugh, W.J., (1999),
Relationship between H-bonding of penetrants to stratum corneum lipids and diffusion, In: *Percutanious Absorption; Drugs-Cosmetics – Mechanisms -Methodology*, Bronaugh R. L., Maibach, H.I., (Eds.), 3rd Edition, Marcel Dekkar, New York.

Pugh W.J., Roberts, M.S., Hadgraft, J., (1996),
Epidermal permeability-penetrant structure relationships 3: the effect of hydrogen bonding interactions and molecular size on diffusion across the stratum corneum, *Int. J. Pharm.*, **138**, 149-167.

Pye, R.J., Burton, J.L., (1976),
Treatment of rosacea by metronidazole, *Lancet,* (i), 1211-1212.

QuantiChrom™ urea assay kit (DIUR-01K),
Product information leaflet, BioAssay Systems, USA.

Quantin P., Herbillion A.J., Janot C., Stiefferman, G., (1984),
L'halloysite blanche riche en fer de Vate (Vanuata). Hypothese d'un edifice interstratifie halloysite-hisingeroite, *Clay Minerals*, **19,** 629-643.

Radebaugh, G.W., (1996),
Rheological and mechanical properties of dispersed systems, In: *Pharmaceutical Dosage Forms: Disperse Systems*, 2nd Edition, Lieberman, H.A., Rieger, H.M., Banker, G.S., (Eds.), Dekker, New York, pp. 153-209.

Radoslovich, E.W., (1963),
The cell dimensions and symmetry of layer-lattice silicates. VI. Serpentine and kaolin morphology. *Am. Miner.*, **48**, 368-378.

Rasmussen, M.R., Snabe, T., Petersen, L.H., (2003),
Numerical modelling of insulin and amyloglucosidase release from swelling Ca-alginate beads, *J. Control. Release*, **91**, 395-405.

Reiger, M.M., (1989),
Surfactants, In: *Pharmaceutical Dosage Forms: Disperse Systems,* (Eds.) Lieberman, H.A., Rieger, M.M., Banker, G.S., Marcel Dekker, New York, pp. 211-286.

Remunan-Lopez, C., Bodmeier, R., (1997),
Mechanical, water uptake and permeability properties of crosslinked chitosan glutamate and alginate films, *J. Control. Rel.*, **44**, 215-225.

Rendall, H.M., Smith, A.M., (1979),
In: *Surface Active Agents*, Society of Chemical Industry, London, pp. 37.

Rendon, J.L., Serna, C.J., (1981),
IR spectra of powder hematite: effects of particle size and shape, *Clay Minerals*, **16**, 375-382.

Rennie, A.R., Lee, E.M., Simister, E.A., Thomas, R.K., (1990),
Structure of a cationic surfactant layer at the silica-water interface, *Langmuir*, **6**, 1031.

Roberts M.S., Pugh W.J., Hadgraft J., Watkinson, A. C., (1995),
Epidermal permeability-penetrant structure relationships: 1. An analysis of methods of predicting penetration of monofunctional solutes from aqueous solutions, *Int. J. Pharm.*, **126**, 219-233.

Roberts, M.S., Pugh W.J., Hadgraft J., (1996),
Epidermal permeability-penetrant structure relationsips. 2. The effect of H-bonding groups in penetrants on their diffusion through the stratum corneum, *Int. J. Pharm.*, **132**, 23-32.

Rogers, A.F., (1917),
A review of the amorphous minerals, *J. Geol.*, **25**, 515-541.

Rohm Pharma, Weiterstadt, Germany,
Eudragit ® Product Information

Rosen, M.J.and Nakamura, Y. (1977),
The relationship of structure to properties in surfactants 6. The adsorption of α, ω-Bis(sodium p-sulfophenoxy)alkanes on alumina. *J. Phys. Chem.*, **81**, 873-879.

Rosen, M. J., (1989),
Adsorption at Interfaces: Electric Double Layer, In: *Surfactants and Interfacial Phenomen,* 2nd edition. John Wiley and Sons, New York.

Rossi, S., Luckham, P.F., Tadros, Th.F., (2002),
Influence of non-ionic polymers on the rheological behavior of Na^+-montmorillonite clay suspensions - I Nonylphenol-polypropylene oxide-polyethylene oxide copolymers, *Colloids Surf. A.*, **201**, 85-100.

Rupprecht, H.J., (1972),
Influence of solvents on adsorption of ionic surfactants on highly dispersed silicas,*J. Pharm. Sci.*, **61**, 700-702.

Ryu, D.Y., Free, M.L., (2003),
The use of electrochemical quartz crystal microbalance and surface tension measurements for the determination of octylamine and cetylpyridinium chloride adsorption in sodium chloride solutions, *Colloids Surf. A*, **226**, 17-23.

Saihan, E.M., Burton, J.L., (1980),
A double blind trial of metronidazole versus oxytetracycline therapy for rosacea, *Br. J. Dermatol.*, **108**, 327-332.

Salter A.E., 2003,
Thesis, Trinity College Dublin.

Scamehorn, J.F., Schechter, R.S., Wade, W.H., (1982),
Adsorption of surfactants on mineral oxide surfaces from aqueous solutions: I: Isomerically pure anionic surfactants, *J. Colloid Interface Sci.*, **85**, 463.

Scheuplein, R.J., (1967),
Mechanisms of percutaneous absorption. II. Transient diffusion and the relative importance of various routes of skin penetration, *J. Invest. Dermatol.*, **48**, 79-88.

Scheuplein R.J., Blank, I. H., Brauner, G.J., Macfarlane, D.J., (1969),
Percutaneous absorption of steroids, *J. Invest. Dermatol.*, **52**, 63-70.

Sepulveda, P., Binner, J.G.P., (1999),
Processing of cellular ceramics by foaming and *in situ* polymerisation of organic monomers, *J. Eur. Ceram. Soc.*, **19**, 2059-2066.

Serna, C.J., Rendon, J.L., Iglesias, J.E., (1982),
Infrared surface modes in corundum-type microcrystalline oxides, *Spectrochemica Acta*, **38A**, 797-802.

Sezer, A.D., Akbuğa, J., (1999),
Release characteristics of chitosan treated alginate beads II. Sustained release of a low molecular weight drug from chitosan treated alginate beads, *J. Microencapsul.*, **16**, 687-696.

Shah, V.P., Eikins, J.S., William, R.L., (1999),
Role of in vitro release measurement in semi-solid dosage forms, In: *Percutaneous Absorption Drugs – Cosmetics – Mechanisms - Methodology*, 3rd Edition, Bronaugh, R.L., Maibach, H.I., (Eds.), Marcel Dekker, New York, pp. 555-570.

Shaw, B.T., Humbert, R.P., (1941),
Electron micrographs of clay minerals, *Soil Sci. Soc. Am. Proc.*, **6**, 146-149.

Sherman, P., (1970),
Industrial Rheology, Academic Press, London and New York.

Shinoda, K., Tamamushi, B., Nakagawa, T., Isemura, T., (1963),
Colloidal Surfactants, Academic Press, New York, London.

Shore, P.A., Brodie, B.B., Hogben, C.A.M. (1957),
The gastric secretions of drugs: a pH partition hypothesis, *J. Pharmacol. Exp. Ther.*, **119**, 361-369.

Shotton, E., Leonard, G.S., (1976),
Effect of intragranular and extragranular disintegrating agents on particle size of disintegrated tablets, *J. Pharm. Sci.*, **65**, 1170-1174.

Shu, X.Z., Zhu, K.J., (2000),
A novel approach to prepare tripolyphosphate/chitosan complex beads for controlled release drug delivery, *Int. J. Pharm.*, **201**, 51-58.

Sigma Product Information Sheet,
Cetrimide.

Sing, K.S.W., Everett, D.H., Haul, R.A.W., Moscou, L., Pierotti, R.A., Rouquerol, J., Siemieneiwska, T., (1985),
Reporting physisorption data for gas/solid systems with special reference to the determination of surface area and porosity, *Pure & Appl. Chem.*, **57**, 603-619.

Singh, D.K., Ray, A,R., (1999),
Controlled release of glucose through modified chitosan membranes, *J. Membrane Sci.*, **155**, 107-112.

Smith, J.M., (1968),
Kinetics of adsorption, In: *Adsorption from Aqueous Solution*, Gould, R.F., (Ed.), Advances in Chemistry Series, 79. American Chemical Society, Washington D.C., pp. 8-22.

Smith, A.R.W., Lambert, P.A., Hammond, S.M., Jessup, C., (1975),
The differing effects of cetyltrimethylammonium bromide and cetrimide B.P. upon growing cultures of *Escherichia coli* NCIB 8277, *J. Appl. Bact.*, **38**, 143-149.

Smith, E.W., Surber, C., Maibach, H.I., (1999),
Topical dermatological vehicles, a holistic approach, In: *Percutaneous Absorption Drugs – Cosmetics - Mechanisms - Methodology*, 3rd Edition Bronaugh, R.L., Maibach, H.I., (Eds.), Marcel Dekker, New York, pp. 779-787.

Soil Survey, (1984),
Procedures for collecting soil samples and methods of analysis for soil survey,
Soil Survey Investigations Rep. 1, USDA-SCS Agricultural Handbook, U.S. Government Print Office, Washington DC.

Somasundaran, P., Healy, T.W., Fuerstenau, D.W., (1964),
Surfactant adsorption at the solid-liquid interface - dependence of mechanism on chain length. *J. Phys. Chem.*, **68**, 3562-3566.

Somasundaran, P., Fuerstenau, D.W., (1966),
Mechanisms of alkyl sulfonate adsorption at the alumina - water interface,*J. Phys. Chem.*, **70,** 90-96.

Soma, M., Churchman, G.J., Theng, B.K.G., 1992,
X-ray photoelectron spectroscopic analysis of halloysites with different composition and particle morphology, *Clay Mineral*, **27**, 413-421.

Sriamornsak, P., Thirawong, N., Puttipipatkhachorn, S., (2005),
Emulsion gel beads of calcium pectinate capable of floating on the gastric fluid: effect of some additives, hardening agent or coating on release behaviour of metronidazole, *Eur. J. Pharm. Sci.*, **24**, 363-373.

Strnadnova, M., Leimbach, J., Rupprecht, H., 1995,
Adsorption of codeine on hydrophilic silica and silica surface modified by hydrophobic groups in the presence of electrolytes, *Coll. Polym. Sci.*, **273**, 687-692.

Sweetman, S.C., (2005),
Martindale. The Complete Drug Reference, 34th Edition, Sweetman, S.C., (Ed.), Pharmaceutical Press, London.

Tadros, Th. F., (1995),
Surfactants in Agrochemicals, Marcel Dekker, New York.

Takahashi, T., Dahlgren, R.A., Theng, B.K.G., Whitton, J.S., Soma, M., (2001),
Potassium-selective halloysite rich soils formed in volcanic materials from northern California, Soil Sci. Soc. Am. J., **65**, 516-526.

Takeshi, H., Kato, C., (1969),
Montmorillionite minerals, In: *The Clays of Japan*, Geological Survey of Japan, Toyko, pp. 103-120.

Tamamushi, B., (1963),
Colloidal Surfactants: Some Physiochemical Properties, Shinoda, K., (Ed.), Academic Press, London.
Tari, G., Bobos, I., Gomes, C.S.F., Ferreira, J.M.F., (1999),
Modification of surface charge properties during kaolinite to halloysite 7Å transformation, *J. Colloid Interface Sci.*, **210**, 360-366.

TA-XT2 Application Study (2000),
Petroleum jelly, Stable Micro Systems Ltd., Surrey, UK.

Tazaki, K., (1979),
Micromorphology of halloysites produced by weathering of plagioclase in volcanic ash, P*roc. Int. Clay Conf. Oxford*, pp. 415-422.

Tazaki, K., (1981),
Analytical electron microscopic studies of halloysite formation processes – morphology and composition of halloysite, *Proc. Int. Clay Conf. Bologna-Pavia*, pp. 573-584.

The Merck Index, (1998),
12th Edition, Chapman and Hall, London.

The Pharmaceutical Codex, (1994),
The Pharmaceutical Codex. Principles and Practice of Pharmaceutics, 12th Edition, Wade, A., (Ed.), The Pharmaceutical Press, London.

Theng, B.K.G., (1974),
The Chemistry of Clay-Organic Reactions, Adam Hilger, London.

Theng, B.K.G., Russell, M., Churchman, G.J., Parfitt, R.L., (1982),
Surface properties of allophane, halloysite and imogolite, *Clays Clay Miner.*, **30**, 143-149.

Theng, B.K.G., Wells, N., (1995a),
The flow characteristics of halloysite suspensions, *Clay Miner.*, **30**, 99-106.

Theng, B.K.G., Wells, N., (1995b),
Assessing the capability of some New Zealand clays for decolourising vegetable oil and butter, *Applied Clay Sci.*, **9**, 321-326.

Theng, B.K.G. (1995),
On measuring the specific surface area of clays and soils by adsorption of *para*-nitrophenol: use and limitations. *In*: *Clays Controlling the Environment: Proceedings of the 10th International Clay Conference, Adelaide, Australia 1993,* (Eds.), Churchman, G.J, Fitzpatrick, R.W. Eggleton, R.A., Melbourne, CSIRO Publishing, pp. 304–310.

Thomas, S., Loveless, P., (1998),
Odour absorbing dressings: a comparative laboratory study,
www.worldwidewounds.com

Tombácz, E., Libor, Z., Illés, E., Majzik, A., Klumpp, E., (2004),
The role of reactive surface sites and complexation by humic acids in the interaction of clay mineral and iron oxide particles, *Organic Geochem.*, **35**, 257-267.

Tonnesen, H.H., Karlsen, J., (2002),
Alginate in drug delivery systems, *Drug Dev. Ind. Pharm.*, **28** (6), 621-630.

Torn, L.H., de Keizer, A., Koopal, L.K., Lyklema, J., (2003),
Mixed adsorption of poly(vinylpyrrolidone) and sodium dodecylbenzenesulfonate on kaolinite, *J. Colloid Interface Sci.*, **260**, 1-8.

Treiner, C., Monticone, V., (1995),
Porosity effects on the adsorption of cationic surfactants and the coadsorption of 2-naphthol at various silica-water interfaces, ACS Symposium meeting, Washington DC.

United States Pharmacopeia, (2006),
United States Pharmacopeia, 29th Edition, The National Formulary, 24th Edition, United States Pharmacopoeial Convention, Inc., USA.

USP online,
www.usp.org

van der Marcel, H.W., Beutelspacher, H., (1976),
Clay and related minerals, In: *Atlas of Infrared Spectroscopy of Clay Minerals and their Admixtures,* Elsevier, New York, pp. 65-198.

van Doorne, H., (1990),
Interaction between preservatives and pharmaceutical components, In: *Guide to Microbiological Control in Pharmaceutics,* Denyer, S.P., Baird, R.M., (Eds.), Ellis Horwood, New York, London, pp. 274-291.

van Olphen, H., (1977),
An Introduction to Clay Colloid Chemistry: For Clay Technologists, Geologists and Soil Scientists, 2nd Edition., Wiley, New York.

van Olphen, H., (1987),
Dispersion and flocculation, *Chemistry of Clays and Clay Minerals*, Newman, A.C.D., (Ed.), Longman Scientific & Technical, Harlow, England, pp. 203-224.

Vatier, J., Vallot, T., Farinotti, R., (1996),
Antacid drugs: multiple but too often unknown pharmacological properties, *J. Pharm. Clin*, **15**, 41-51.

Velegol, S.B., Fleming, B.D., Biggs, S., Wanless, E.J., Tilton, R.J., (2000),
Counterion effects on hexadecyltrimethylammonium surfactant adsorption and self-assembly on silica, *Langmuir*, **16**, 2548.

Verwey, E.J.W., Overbeek, J. Th., G., (1948),
Theory of the Stability of Lyophobic Colloids, Elsevier, Amsterdam.

Viseras, C., Aguzzi, C., Cerezo, P., Lopez-Galindo, A., (2006),
Use of clay minerals in semi-solid healthcare and therapeutic products, Appl. Clay Sci., Article in press.

Wada, S., Mizota, C., (1982),
Iron-rich halloysite (10 Å) with crumpled lamellar morphology from Hokkaido, Japan, *Clays and Clay Minerals*, **30** (4), 315-317.

Wakamatsu, T., Fuerstenau, D.W., (1968),
The effect of hydrocarbon chain length on the adsorption of sulfonates at the solid/water interface In: *Adsorption from Aqueous Solution*, Gould, R.F., (Ed.) Advances in chemistry series, 79. American Chemical Society, Washington D.C. pp. 161-172.

Wallhauser, K.H., (1995),
Surfactants and the preservation of cosmetic preparations, In: *Surfactants in Cosmetics*, Rieger, M.M., (Ed.), Surfactant Science Series, Vol 16, Marcel Dekker, New York, Basel, pp. 211-250.

Ward, R.K., Hubbard, A.W., Sulley, H., Garle, M.J., Clothier, R.H., (1998),
Human keratinocyte cultures in an in vitro approach for the assessment of surfactant-induced irritation, *Toxicology in Vitro,* **12**, 163-173.

Wangnerud, P., Olofsson, G., (1992),
Adsorption isotherms for cationic surfactants on silica determined by *in situ* ellipsometry, *J. Colloid Interface Sci.*, **153**, 392-398.

Wanless, E., (2004),
Personal communication.

Waters Product Information Guide,
Troubleshooting HPLC, Waters Corporation.

Wearley, L.L., Anthony, G.D., (1976),
Metronidazole, In: *Analytical Profiles of Drug Substances and Excipients*, Florey, K., (Ed.), Vol. 5, Academic Press, New York, San Francisco and London.

Welin-Berger, K., Neelissen, J.A.M., Bergenståhl, B., (2001),
The effect of rheological behaviour of a topical anaesthetic formulation on the release and permeation rates of the active compound, *Eur. J. Pharm. Sci.*, **13**, 309-318.

Wells, J., (2002),
Pharmaceutical preformulation: the physicochemical properties of drug substances, In: *Pharmaceutics*; *The Science of Dosage Form Design*, 2nd Edition, Aulton, M.E., (Ed.), Churchill Livingstone, Edinburgh, pp. 113-138.

Wilkes, G.L., Brown, I.A., Wildnauer, R.H., (1973),
The biochemical properties of skin, *CRC Crit. Rev. Bioeng.*, 453-495.

Williams, A.C., (2003),
Transdermal and Topical Drug Delivery, Pharmaceutical Press, London, pp. 1-82.

Wilson, M.J., (1994),
Identification and Characterisation, In: *Clay Minerology: Spectroscopic and Chemical Determinative Methods,* Chapman and Hall, New York, pp. 18-21.

Woodford, R., Barry, B.W., (1974),
Comparative bioavailability of proprietary topical corticosteroid preparations: vasoconstrictor assays on 30 creams and gels, *Br. J. Dermatol.*, **991**, 323-338.

Wong, L.P., Gilligan, C.A., Li Wan Po, A., (1992),
Preparation and characterisation of sustained release ibuprofen-cetostearyl alcohol spheres, *Int. J. Pharm.*, **83**, 95-114.

Wong, T.W., (1994),
Influence of counterions on properties of chitosan beads, Honours year thesis, National University of Singapore.

Wong, T.W., Chan, L.W., Shyan, B.K., Heng, P.W.S., (2002),
Design of controlled-release solid dosage forms of alginate and chitosan using microwave, *J. Control. Release,* **84**, 99-114.

Yamamoto, H., Takeuchi, H., Hino, T., Kawashima, Y., (2000),
Mucoadhesive liposomes: Physicochemical properties and release behaviour of water soluble drugs from chitosan-coated liposomes, *S.T.P. Pharma Sciences*, **10**, 63-68.

Yao, J., Strauss, G., (1992),
Adsorption of cationic surfactants on medical polymers: effect of surfactant and substrate structures, *Langmuir,* **8**, 2274-2278.

Yuan, J., Murray, H.H., (1997),
The importance of crystal morphology on the viscosity of concentrated suspensions of kaolin, *Applied Clay Sci.*, **12**, 209-219.

Zimmer, A.K., Maincent, P., Thouvenot, P., Kreuter, J., (1994),
Hydrocortisone delivery to healthy and inflamed eyes using a micellar polysorbate 80 solution or albumin nanoparticles, *Int. J. Pharm.*, **110**, 211-222.

Zografi, G., Patel, P.R., Weiner, N.D., (1964),
Interaction between orange II and selected long chain quaternary ammonium salts,
J. Pharm. Sci., **53**, 544-549.

APPENDICES

Appendix 1

Calibration curves used to determine the concentration of drugs in solution

(1) Tetradecyltrimethylammonium bromide in water – dye method

Analytical wavelength: 486 nm

Concentration (g/L) = (Absorbance – 2.9451) / 295.97

$R^2 = 0.9996$

(2) Tetradecyltrimethylammonium bromide in water containing NaBr (150 mM) – dye method

Analytical wavelength: 486 nm

Concentration (g/L) = (Absorbance – 2.156) / 303.92

$R^2 = 0.9953$

(3) Hexadecyltrimethylammonium bromide – dye method

Analytical wavelength: 486 nm

Concentration (g/L) = (Absorbance) / 395.34

$R^2 = 0.9633$

(4) Tetradecyltrimethylammonium bromide in water – HPLC method

Analytical wavelength: 205 nm

Concentration (g/L) = (Peak area – 68,945) / 5 x 10^7

R^2 = 0.9994

(5) Tetradecyltrimethylammonium bromide in water containing KCl (10 mM) HPLC method

Analytical wavelength: 205 nm

Concentration (g/L) = (Peak area – 107,086) / 5 x 10^7

R^2 = 0.9996

(6) Hexadecyltrimethylammonium bromide in water – HPLC method

Analytical wavelength: 205 nm

Concentration (g/L) = (Peak area – 44,962) / 5 x 10^7

R^2 = 0.9995

(7) Benzalkonium chloride in water

Analytical wavelength: 262 nm

Concentration (g/L) = (Absorbance – 0.0477) / 7.6856

R^2 = 0.9910

(8) Dodecylpyridinium chloride in water

Analytical wavelength: 256 nm

Concentration (g/L) = (Absorbance – 0.0261) / 140.03

R^2 = 0.9999

(9) Dodecylpyridinium chloride in water containing KCL (10 mM)

Analytical wavelength: 259 nm

Concentration (g/L) = (Absorbance – 0.0289) / 136.52

$R^2 = 0.9998$

(10) Cetylpyridinium chloride in water

Analytical wavelength: 259 nm

Concentration (g/L) = (Absorbance – 0.0173) / 80.662

$R^2 = 0.9981$

(11) Sodium dodecylbenzene sulphate in water

Analytical wavelength: 224 nm

Concentration (g/L) = (Absorbance – 0.0749) / 226.11

$R^2 = 0.9912$

(12) Sodium dodecylbenzene sulphate in water containing KCL (mM)

Analytical wavelength: 224 nm

Concentration (g/L) = (Absorbance – 0.0144) / 247.4

$R^2 = 0.9912$

(13) Urea in water

Analytical wavelength: 492 nm

Concentration (mg/L) = (Absorbance – 0.1093) / 0.0083

$R^2 = 0.9969$

(14) Urea in McIlvaine buffer pH 5.5

Analytical wavelength: 492 nm

Concentration (mg/L) = (Absorbance – 0.0236) / 0.0103

$R^2 = 0.9959$

(15) Salicylic acid in water

Analytical wavelength: 295.5 nm

Concentration (g/L) = (Absorbance – 0.0409) / 226.71

$R^2 = 0.9989$

(16) Salicylic acid in McIlvaine buffer pH 5.5

Analytical wavelength: 295.5 nm

Concentration (g/L) = (Absorbance + 0.0313) / 254.67

$R^2 = 0.9998$

(17) Salicylic acid in PBS 7.4

Analytical wavelength: 295.5 nm

Concentration (mg/L) = (Absorbance – 0.01199) / 0.02826

$R^2 = 0.99822$

(18) Salicylic acid in ethanol

Analytical wavelength: 304 nm

Concentration (g/L) = (Absorbance + 0.0.0113) / 261.06

$R^2 = 0.9981$

(19) Metronidazole in water

Analytical wavelength: 320 nm

Concentration (g/L) = (Absorbance – 0.0214) / 568.81

$R^2 = 0.9999$

(20) Metronidazole in a water / ethanol co-solvent system (75:25)

Analytical wavelength: 320 nm

Concentration (g/L) = (Absorbance – 0.0663) / 579.68

$R^2 = 0.9959$

(21) Metronidazole in McIlvaine buffer pH 5.5

Analytical wavelength: 320 nm

Concentration (mg/L) = (Absorbance – 0.02081) / 0.52876

$R^2 = 0.9998$

Appendix 2

Chromatogram for parabens standards obtained using UV detection at 254 nm.

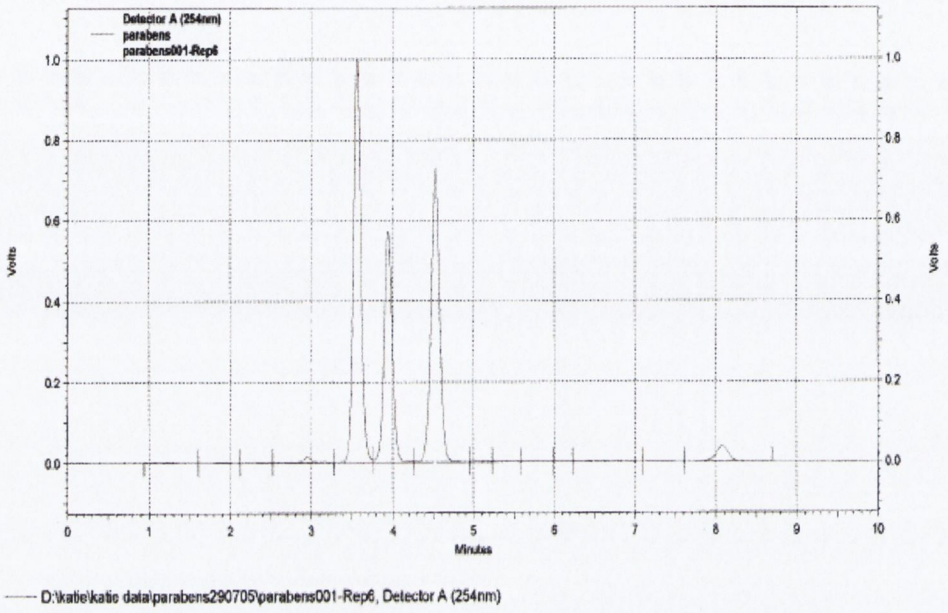

Appendix 3

Chromatogram for tetradecyltrimethylammonium bromide obtained using UV detection at 205 nm.

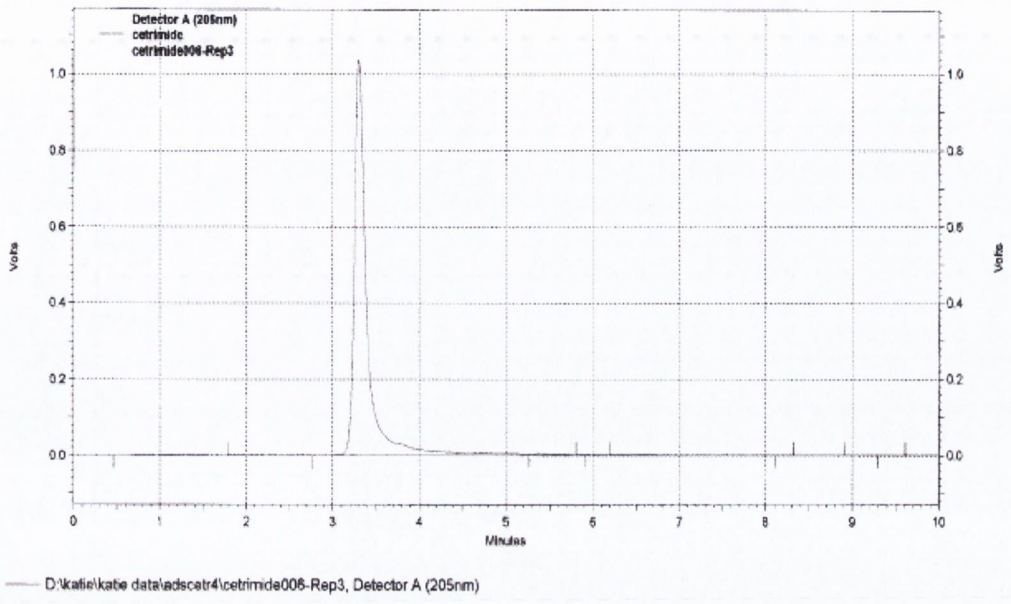

Appendix 4

Chromatogram for hexadecyltrimethylammonium bromide obtained using UV detection at 205 nm.

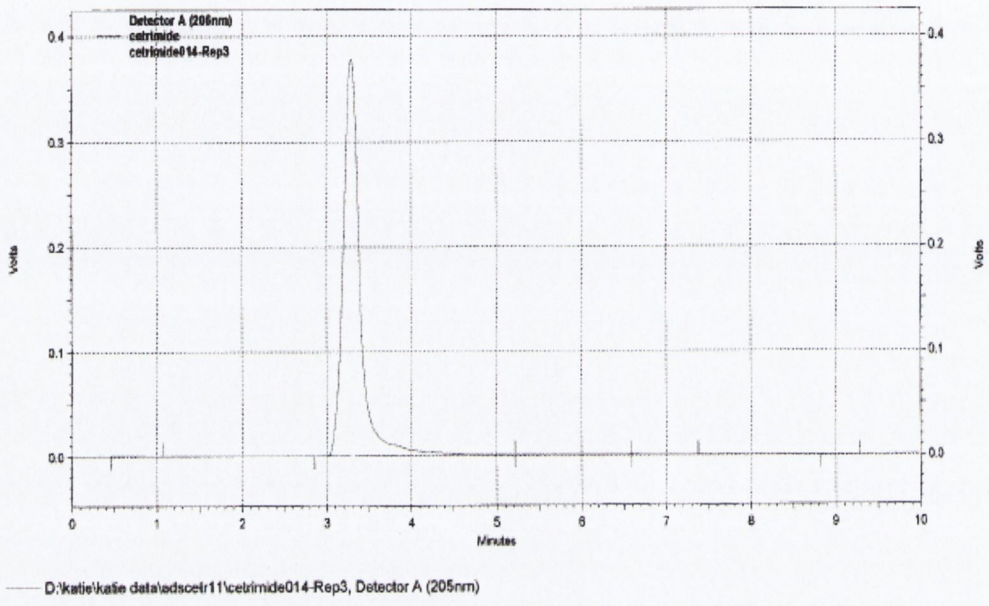

Appendix 5a

Main effects plot for the loading of halloysite with urea using a fractional factorial, 2^{4-1} design.

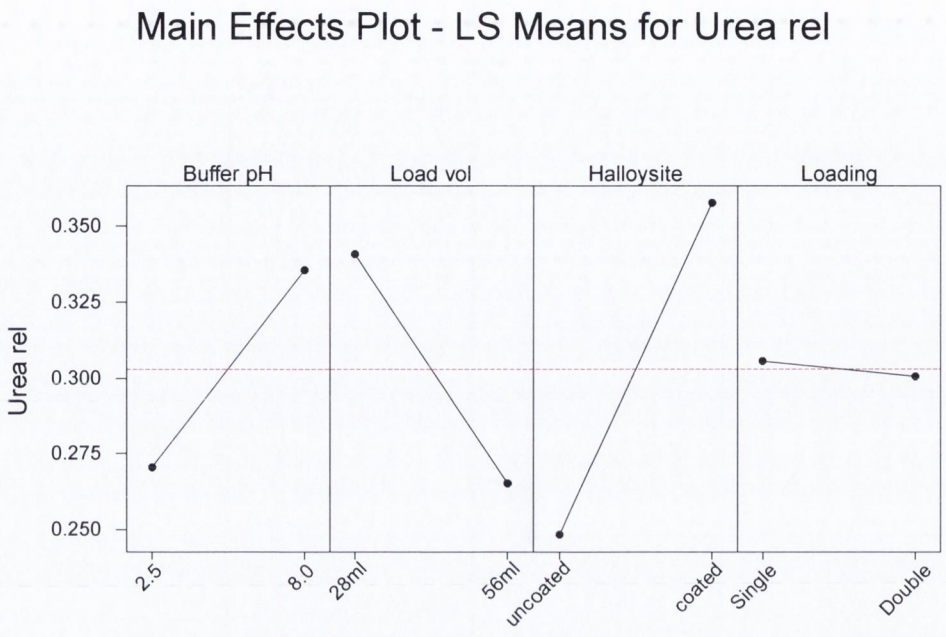

Appendix 5b

Interaction plot for the loading of halloysite with urea using a fractional factorial, 2^{4-1} design.

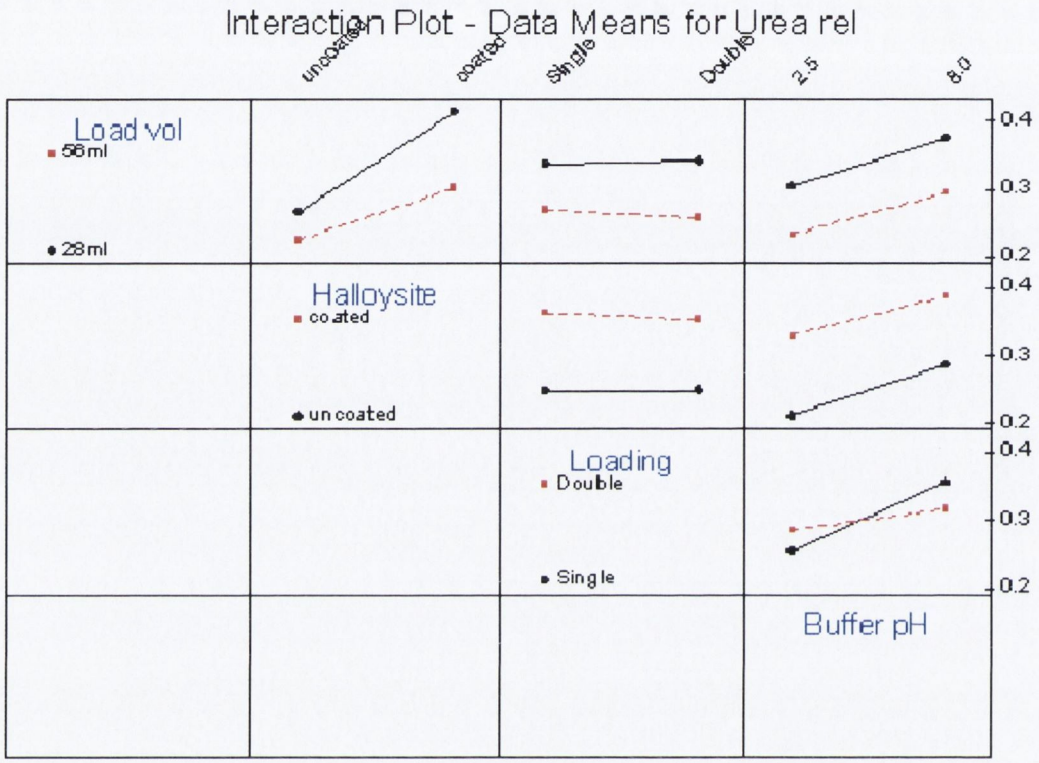

Appendix 6
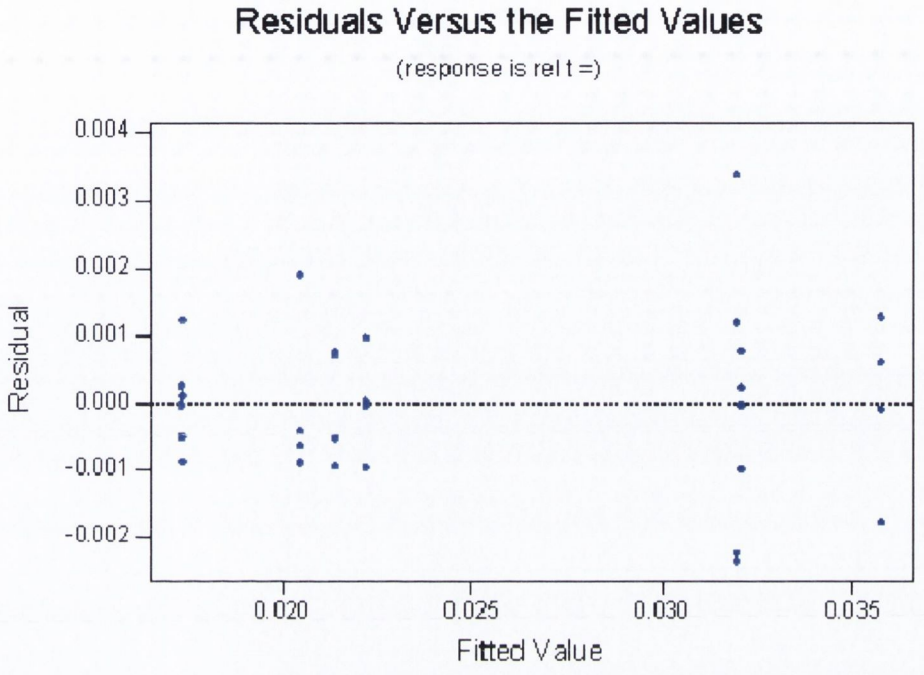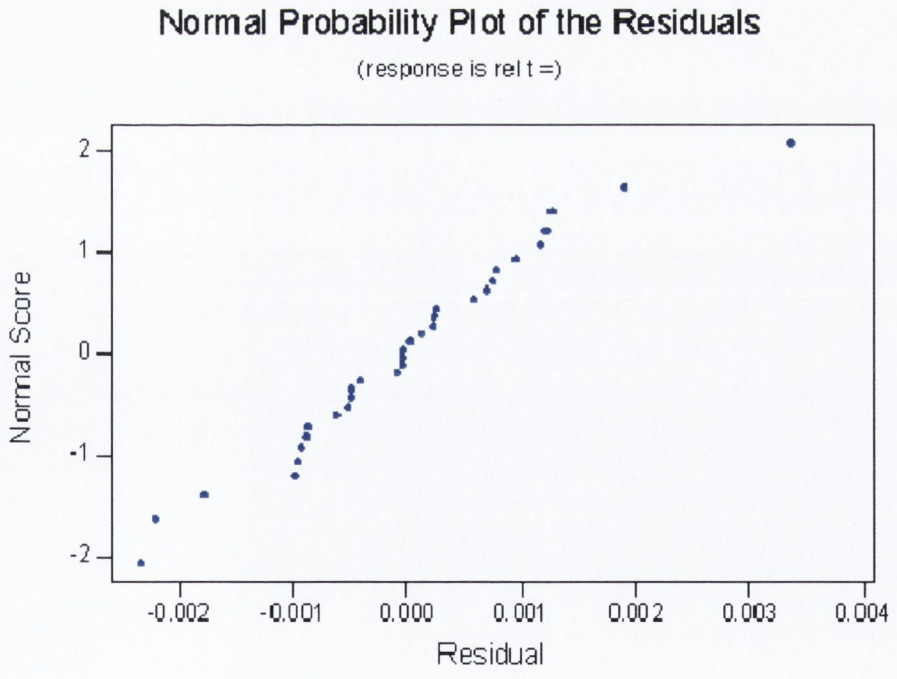
Residual plot for release of salicylic acid from halloysite at t = 8 hours – advanced study.